REFERENCE ONLY

UNIVERSITY OF LONDON THESIS

Degree PhD Year 2006 Name of Author WATSON S.T

RAR

NDON

U

SOLUTE TRANSPORT AND HYDRODYNAMIC CHARACTERISTICS IN THE CHALK AQUIFER AT TILMANSTONE, KENT

BY

SALLY JAYNE WATSON

A thesis submitted for the degree of Doctor of Philosophy
of the
University of London

Department of Earth Sciences
University College London
Gower Street
London
WC1E 6BT

2005

ProQuest LLC
789 East Eisenhower Parkway
P.O. Box 1346
Ann Arbor, MI 48106-1346

ABSTRACT

Research on the hydrodynamic characteristics of the Chalk aquifer is described in relation to the timescales and spatial extent of solute transport, focussing on the Tilmanstone – Eastry valley in east Kent. Groundwater contamination occurred there over a 70-year period as a result of coalfield brine infiltrating from surface lagoons. The resulting contamination is used as a large-scale, long-term conservative solute transport experiment, within which a series of geological and hydrogeological observations, and tracer tests, are used to investigate the transport properties of the Chalk. The objective is to consider appropriate methodologies for application to groundwater contamination investigations in the Chalk and characterisation of Chalk groundwater bodies in the context of the requirements of the EU Water Framework Directive.

The geology and hydrogeology of the Tilmanstone area are reassessed in the light of recent work on Chalk lithostratigraphy, using available hydrological data and employing a regional groundwater flow model, coupled with a solute transport model utilising a first order mass transfer coefficient dual porosity approach. Field tests are analysed in terms of aquifer properties pertinent to solute transport at a scale of metres to tens of metres. Vertical profiles of hydraulic conductivity, groundwater velocity, fracture aperture and effective porosity are developed. A profile of chloride concentration in porewater is interpreted in the light of this work to develop a hydrostratigraphy for the area.

A 1-D dual porosity model employing Fickian diffusive exchange is used to compute chloride concentration of fracture water and matrix porewater over time. This provides predictions for comparison with observations and the results of the mass transfer coefficient approach in the 3-D regional model. The combined results from the 1-D and 3-D models are used to direct development of a conceptual model of contaminant transport in the Chalk. Emphasis is placed on the effects of diffusive exchange between porewater and fracture water and the effects of the solute exchange approach adopted at different times in the plume history. Results are used to judge the applicability of methods for investigating contaminated groundwater and characterising groundwater bodies in the dual porosity Chalk aquifer.

Acknowledgements

I am indebted to a number of people who have provided me with help, advice and support throughout the course of my research. I would like to acknowledge and thank the following for their input over the past five years:

My supervisors: Dr Willy Burgess for his support, encouragement and enthusiasm throughout the research; Professor John Barker for providing routes to think about the concepts and maths supporting hydrogeology in a new way; and Dr Denis Peach who has been an ongoing source of support and inspiration throughout my hydrogeological career. I would also like to thank Professor Tim Atkinson for his enthusiasm, help and advice with tracer testing and warming ginger wine during cold winter fieldwork.

Although this PhD was mostly self-funded, the UCL Graduate School generously awarded me a 6 month Fellowship, through the recommendation of Prof. Alan Lord. I would like to thank both Alan Lord for proposing this and the UCL Graduate School Grants committee for awarding me the money.

While at UCL I have been extremely fortunate to meet some fantastic people who have been great fun. Especially fun and fantastic are: Aidan Foley, Gerd van den Daele, Tim Wright, Nicky Robinson and Ben Fretwell who all had the misfortune to share an office with me; Caroline Davis, Sophie Des Clers who shared the same building; and Sudeep Kanungo, Ranna Patel, Karen Tingay, Pantea Lotfian, Charlie Rendall and Paul Walker, with whom I shared some great moments during UCL Graduate School facilitation work.

Many people at BGS Wallingford provided help, advice and very importantly two new boreholes, and I would particularly like to thank Ann Williams, John Bloomfield, Dave Buckley, Ian Gale, Mike Bird and Kate Griffiths for this. I would also like to thank Mike Packman and Terry Keating at Southern Water who were both generous with their time and help with data provision.

Finally, I thank my partner Ben, formatting king, for being so supportive, chivviing me along and believing I would finish.

Abbreviations, units and measures

1D; 2D; 3D	1 dimension(al); two dimension(al); three dimension(al)
^{13}C	Carbon thirteen
ADE	Advection dispersion equation
AGK	Institute fur Angewandte Geologie Karlsruhe Universitat
BGS	British Geological Survey
BGU	Ben Gurion University of the Negev, Israel.
BH	Borehole
CCTV	Closed circuit television
Cl	Chloride
d	Day
DEFRA	Department for Environment Food and Rural Affairs
DEM	Digital elevation model
DP1D	Dual porosity in one dimension
EA	Environment Agency of England and Wales
EC	European Commission
EC	Electrical conductivity, also SEC, specific electrical conductivity
EEA	European Environment Agency
EPM	Equivalent porous media
EU	European Union
FD	Finite difference
FDWC	Folkestone and District Water Company, also Folkestone and Dover Water Company
FE	Finite element
Fracflow	Fracture flow in rocks – EU funded project under 5th Framework programme
GEUS	Danish and Greenland Geological Survey
GPZ	Groundwater protection zone
GRP	Glass reinforced plastic
GTU	Groundwater Tracing Unit, University College London
GW Vistas	Groundwater vistas. Pre and post processor software produced by Environmental Simulations Inc. in Shrewsbury, UK
HUJ	Hebrew University of Jerusalem

ID	Internal diameter
IGS	Institute of Geological Sciences (precursor to British Geological Survey)
KBr	Potassium bromide
km	Kilometres
L	Litre
LiBr	Lithium bromide
LiCl	Lithium chloride
LVI	Lower Venson Farm inclined borehole
LVV	Lower Venson Farm vertical borehole
m	Metres
m aOD	Metres above Ordnance Datum
m bGL	Metres below ground level
mg	Milligram
Ml	Megalitre (1,000,000 litres or 1000 m^3)
mm	Millimetres
MODFLOW	Modular flow model fortran coded groundwater flow software produced by the United States Geological Survey
MS	Member States
MSc	Master of Science
MSci	Degree awarded following four years of undergraduate science studies
MT3DMS	Mass transport in three dimensions multi-species. Solute transport software produced by Papadopoulos in the USA
MTC	Mass transfer coefficient
NaCl	Sodium Chloride (common salt)
NO_3	Nitrate
NRA	National Rivers Authority (precursor to Environment Agency)
ppb / ppm	Parts per billion / parts per million; equivalent to micrograms per litre and milligrams per litre respectively
PWS	Public Water Supply
QSS	Quasi steady state
Ramsar	Denotes wetland site designated under the Ramsar (Iran) agreement

SAC / cSAC	Special area of conservation cSAC denotes the site is put forward as a candidate, but has not been confirmed
SP	Stress period
SSSI	Site of special scientific interest
SWA	Southern Water Authority
SWIFT	Sandia Waste flow and transport
UCL	University College London
WFD	Water Framework Directive
WRc	Water Research centre
WWTW	Waste water treatment works

CONTENTS

TABLES

FIGURES

APPENDICES

1 Introduction

1.1 Objectives and scope of work

The main objective of this research is to investigate the extent to which observations of solute transport in the Chalk might be linked at a variety of scales, and hence the extent to which short-term, small scale observations are related to larger-scale, longer term outcomes of interest for environmental management and assessment of groundwater contamination events.

Within this main objective, specific research aims are to:

- Evaluate the hydraulic properties of the Chalk at scales of 1 to 10 m at sites in the Tilmanstone - Eastry valley, Kent UK, using conventional field investigation techniques augmented by tracer tests;
- Re-evaluate the development of the long term pollution of groundwater by NaCl brine in the Tilmanstone - Eastry valley, at scales of 10 m to 10 km, through field studies and mathematical modelling;
- Establish the relevant application of specific data types to the prediction of solute transport in the Chalk aquifer.

The work focuses on particular features of the Chalk aquifer that may dominate solute movement at different temporal and spatial scales, for example:

- The detailed Chalk stratigraphy and associated hydrostratigraphy;
- The density, orientation and style of fracturing – at the local and regional scale;
- The significance of diffusive exchange.

This work is particularly concerned with the Chalk aquifer in south-east England, focussing on the Tilmanstone-Eastry valley in north-east Kent for the acquisition of field data.

1.2 Context of research: Overview

On 23 October 2000, Directive 2000/60/EC of the European Parliament and Council establishing a framework for Community action in the field of water policy was finally adopted (European Commission, 2000). Commonly known as the EC Water Framework Directive (WFD), the Directive is a comprehensive piece of legislation that

sets out quality objectives for all waters in Europe. It prescribes a high level of aquatic ecosystem protection and hence it requires the integration of water resource management with the protection of the natural ecological state and functioning of the aquatic environment. The water needs of terrestrial ecosystems are included in the scope of the WFD, as are the aquatic ecosystems directly dependent on wetlands. In order to achieve the level of protection aspired to by the WFD, Member States are required to integrate water quality and water quantity management as well as surface and groundwater management. Measures to control pollution are integrated with environmental quality objectives. A summary of the scope and aims of the WFD is presented in Appendix 1.

Under the Directive, EC Member States are required to identify groundwater bodies (Common Implementation Strategy, 2003), in order to provide assessments of their quantitative and chemical status, and implement monitoring programmes to establish groundwater body status trends in order to prevent further deterioration of, and protect and enhance the status of aquatic ecosystems. Where that status is found to be poor or deteriorating due to anthropogenic activities, member states are required to draw up plans for halting and reversing that deterioration. The WFD does not provide explicit guidance on how groundwater bodies should be delineated. *Article 2.12* of the WFD provides the definition of a ***body of groundwater*** as a distinct volume of groundwater within an aquifer or aquifers. Within the Common Implementation Strategy (2003) it is noted that the delineation of bodies of groundwater must ensure that the relevant objectives of the WFD can be achieved. The delineation should be in such a way as to enable an appropriate description of the quantitative and chemical status of groundwater.

For the Chalk aquifer these requirements pose particular difficulties. The highly porous, low permeability Chalk matrix is pervaded by a network of interconnected fractures, which provide a high secondary permeability but have a low storage. The primary matrix porosity and the secondary fracture porosity thus give the Chalk aquifer two very different regimes for solute transport and provide it with its so called dual porosity character. The matrix pore space provides storage for approximately 95% of the water in the aquifer, but this water is essentially immobile. The high permeability of the aquifer is provided by the fractures and the solute or pollutant load of the water in these

is moderated through diffusive exchange with the immobile water in the matrix. Over time considerable quantities of solute or pollutant can be stored in the matrix, but normal sampling from monitoring wells will only sample the flowing water in the fractures, possibly giving no direct indication of the stored pollutant concentrations. Conventional pumped groundwater samples alone cannot provide adequate information on the status of the groundwater body as a whole or for making predictions of trends in water quality.

The Environmental Protection Act 1990 (UK Government 1990), The Environment Act 1995 (UK Government 1995), The Water Resources Act 1991 (UK Government 1991a) and The Groundwater Regulations 1998 (UK Government 1998) require the Environment Agency of England and Wales (EA) to consider the impacts of substances and activities on all environmental media and to monitor the extent of pollution in controlled waters. This includes groundwater. The majority of groundwater quality sampling in the UK is currently undertaken at Public Water Supply (PWS) boreholes. These were not designed to provide the type of data required by the WFD. The focus of monitoring at PWS's means that spatial coverage of data is limited and groundwater supporting aquatic ecosystems may not be monitored.

1.3 Use of a plume at Tilmanstone, Kent for understanding long-term monitoring and contaminant migration

Over the period from 1905 to 1974 the National Coal Board used surface lagoons at the Tilmanstone colliery to dispose of millions of litres of mine waters with high concentrations of chloride (Headworth *et al.* 1980). The high chloride waters penetrated to a depth of approximately 100 m, contaminating 3.75 x 10^9 m^3 of rock and groundwater volume, based on the 200 mg/L Cl contour in 1974 (Figure 1-1). It is estimated (Headworth *et al.* 1980) that 318,000 tonnes of chloride was discharged onto the Chalk aquifer. Investigations during the 1970s (Section 2.7.2) provide a snapshot of the chloride plume that resulted from the mine water disposal and subsequent data collection means that the chloride plume development has been tracked and can be treated as a large scale tracer test. The Tilmanstone chloride plume and its associated dataset illuminate solute transport processes over time and distance scales not normally available for study. Most importantly, the long term distribution of the chloride in the Chalk aquifer provides evidence for groundwater flow paths and the relationship of

those flow paths to Chalk lithology and may be used to highlight the most significant parameters for predicting future trends of groundwater quality in the Chalk aquifer.

The chloride plume in the Tilmanstone-Eastry valley effectively provides a large scale, long-term (conservative) tracer test. Data from monitoring of groundwater are available at various times over a 50 year period and new borehole core (drilled in 1999) from the Tilmanstone – Eastry valley allows an updated matrix porewater profile to be constructed. This provides a new basis for improved conceptual model development and calibration of mathematical models. In addition recent development in understanding and classification of Chalk stratigraphy and lithology in south-east England (Bristow *et al.* 1997) (Section 3.2.3) provides a new framework for conceptual model development, particularly with reference to contaminant transport (Mortimore 1990). Advantage has been taken to use the available borehole infrastructure for additional research, including borehole dilution and tracer tests, reported in this thesis (Chapter 4). The historical contamination of the Tilmanstone-Eastry valley has precluded the development of the valley's groundwater resources and this creates additional benefit for tracer testing as there is a considerable distance to the nearest public water supply borehole (Figure 3-19). Having a relatively isolated valley within which to undertake tracer tests allows scope for the use of higher tracer concentrations. This is particularly beneficial where there is uncertainty over groundwater flow directions or where borehole infrastructure is not ideally located in combination with fracture orientation. The Tilmanstone-Eastry valley, and its associated groundwater contamination, is therefore considered to provide an ideal field location in which to explore the applicability of using effective transport parameters, derived from small scale tracer tests, in larger scale regional models.

The new legislative requirements of the WFD coupled with the opportunity afforded by the large scale of the chloride plume in the Tilmanstone - Eastry valley provide a context for the research presented in this thesis. This thesis is intended as a contribution to the debate on how best to implement aspects of the WFD to the UK's most important aquifer.

1.4 Approach

The main objective of the research, as set out in Section 1.1, was approached by undertaking an assessment of the hydraulic and solute transport properties of the Chalk

aquifer using hydrogeological field investigations. Data from field studies, i.e. short term tests, were used to guide the choice of parameter values for a semi-analytical dual porosity model, and modelling results have been compared with matrix porewater concentrations observed in Chalk core extracted from within the area of the contaminant plume. Existing approaches to diffusive exchange in fractured porous media are considered and assessed through 3D regional solute transport modelling for the particular case of the Chalk aquifer. This provides short term observations to guide the parameter values used in numerical models which can then be used to make predictions over the longer term. As the Tilmanstone – Eastry valley has such a long term dataset these numerical model predictions can then be compared to the known long term development of the groundwater plume.

The specific research aims are addressed through the use of field investigation techniques which have been used to provide insight into and observations of aquifer properties at scales ranging from 1 to 10 m; Tracer tests and analysis of solute breakthrough curves and borehole dilution curves, at scales of 1 to 10 m, were used to evaluate transport characteristics and behaviour of the dual porosity Chalk system directly; The long term pollution of groundwater in the Tilmanstone – Eastry valley was re-evaluated by analysing the observations from short-term tracer and other field investigations in the context of recent developments in the description and classification of Chalk stratigraphy and lithology. The results have been compared to findings and modelling predictions from previous investigations of the development of the contaminant plume in the area studied. This has led to new insights into the hydrogeology, thus allowing an updated conceptual model of the area to be proposed. The hydrogeological field investigation techniques used during the research have been assessed in order to reveal the most relevant data for the prediction of solute transport in the Chalk aquifer.

The particular features of the Chalk aquifer that may dominate the movement of solute at different temporal and spatial scales are examined by both field investigations and the numerical modelling work. The detailed Chalk stratigraphy and associated hydrostratigraphy is revealed through borehole core and geophysical logging in combination with analysis of Chalk matrix porewater; the density, orientation and style of fracturing is examined by field observations of fracture frequency and measurements

of orientation, as well as by tracer testing; the significance of diffusive exchange is examined during the tracer testing and by numerical modelling.

1.5 Structure of thesis

Following this introductory chapter, Chapter 2 provides background and literature reviews of the key elements forming the framework for the research: the Chalk aquifer, transport processes, investigative and modelling approaches. Chapter 3 describes the geology and hydrogeology of the area studied. The hydrogeology presented at this stage is that known from previous studies. Consideration is given to the hydrogeological uncertainties. Chapter 4 presents the fieldwork undertaken and data collected during the course of the current research. This includes tracer testing, hydraulic testing, borehole drilling and borehole geophysics. Chapter 5 presents an analysis and discussion of these field data. This reinterpretation provides a modified hydrogeological conceptual model for the area. Modelling requirements and model selection for solute transport modelling are discussed in Chapter 6, and model development and results are described. Chapter 7 discusses the approaches adopted and addresses the effectiveness of the different field techniques. It considers the insights provided by the mathematical modelling undertaken in the context of monitoring well location and the design of groundwater sampling programmes for the Chalk aquifer. The use of data sets for the prediction of groundwater quality and the setting of remediation targets is discussed. Conclusions are drawn from the research. Chapter 8 makes recommendations and suggestions for future work in the area based on the findings of the research.

1.6 Links to MSc research and other studies

1.6.1 MSc research at UCL

Three MSc research projects were supervised by the author during the period of the research described in this thesis. These MSc research projects were designed as preliminary explorations of particular aspects of the main body of research presented in the current thesis. Topics for the MSc research included trialling of field techniques, initial tracer tests to establish borehole to borehole connections and tracer quantities and the relationship between recharge and groundwater level response in hydrostratigraphic horizons. Fieldwork was carried out jointly between the MSc student and the author.

The three MSc projects are summarised here with the outcomes identified that were taken forward by the research described in this thesis.

In the initial MSc project (Hazell 1998) a hydrochemical survey was undertaken to update the information relating to the extent of the groundwater plume and the first set of single borehole dilution tests were carried out. The project allowed the injection and monitoring method for the tracer solution to be developed. Information from the rates of decay of the tracer in the boreholes was then taken forward by the current research for further analysis and to link with the results from other field investigations such as geophysical logging and borehole to borehole tracer tests.

The second MSc project (Chahinian 1999) investigated recharge mechanisms on the Chalk through statistical approaches. No significant link between recharge and groundwater level response was revealed and there was no further development of the work.

The final MSc project (Quinn 2000) undertook a borehole-to-borehole tracer test at Lower Venson Farm. A single borehole dilution test was also carried out at BHE. The borehole to borehole tracer test allowed the development of the bailer string sampling method to be developed as well as providing information relating to which boreholes the tracer travelled to and the quantity of injected tracer required for detection at the observation boreholes. This information was used and refined by the author of the current thesis when planning the final combined borehole to borehole tracer test and single borehole dilution tests undertaken in 2001.

In addition an MSci student participated in the fieldwork for the final borehole to borehole tracer test, wrote up the approach and undertook some basic analysis of the observations for the MSci project.

1.6.2 Other studies

Mutual benefit was sought between the research described in this thesis and a European funded programme entitled Pollutant transport, monitoring techniques and remediation strategies in cross European fractured chalk (FRACFLOW) Contract number: ENV4-CT97-0441. The project was funded by the European Commission under the Environment and Climate 1994-1998 programme and involved researchers from five

institutions: Geological Survey of Denmark and Greenland (GEUS), Ben-Gurion University of the Negev (BGU), British Geological Survey (BGS), Institut für Angewandte Geologie, Karlsruhe Universität (AGK), and the Hebrew University of Jerusalem (HUJ).

The objective of FRACFLOW was to characterise the flux and transport of inorganic and organic pollutants through fractured chalk systems in Europe, and to identify generic monitoring and remediation strategies for various pollutant and hydrogeological scenarios in fractured Chalk across Europe. The Lower Venson Farm site was chosen for investigation for a number of reasons including the existing information that had been collated by research at UCL and also the availability of sites for further borehole drilling. As part of the FRACFLOW project two boreholes were drilled at Lower Venson Farm in the Tilmanstone – Eastry valley. The additional information provided by these two boreholes benefited the research described in this thesis and the investigations carried out as part of the research described in this thesis provided benefit to the FRACFLOW project.

Where relevant, data collected for the FRACFLOW project were made available for further analysis and interpretation in the research described in this thesis, and tracer tests undertaken for the research described in this thesis during the period of the FRACFLOW programme are included in FRACFLOW reporting (FRACFLOW, 1999). Although not leading the investigations undertaken for the FRACFLOW project the author of this thesis actively participated in data acquisition for the FRACFLOW programme at Lower Venson Farm, including borehole drilling, packer testing, geophysical logging and water sampling.

Fieldwork undertaken during the research described in this thesis and for the FRACFLOW programme is presented in Chapter 4 where the author had a direct involvement in it. Further, relevant, fieldwork undertaken by FRACFLOW personnel is described in Chapter 5, where fieldwork results are discussed in full.

1.6.3 Timescale

Fieldwork took place over three main summer field seasons as well as additional work through some winter months. Table 1-1 provides a summary of when the various field

investigations occurred, who carried it out and where specific reporting of the activity can be found.

Table 1-1 Diary of field investigations.

Date	Nature of investigations	Undertaken by	Relevant documentation
Summer 1998	Hydrochemical sampling Single borehole dilution tests	S. J. Watson S. Hazell	Hazell, S. 1998 Unpublished MSc thesis, UCL
Summer 1999	Borehole drilling (BGSV and BGSI at Lower Venson Farm); Geophysical logging; Lithological logging; Packer testing; Core porewater sampling; Fracture density measurements; detailed water level monitoring	British Geological Survey Hebrew University of Jerusalem S.J. Watson	Bird *et al.*, 1999 BGS Technical Report WD/99/42
Winter 1999	Geophysical logging Natural gradient tracer test	S.J. Watson T.C. Atkinson	Phase two, test one. UCL internal report. FRACFLOW 2nd annual progress report. ENV4-CT97-0441
Summer 2000	Single borehole dilution tests Natural gradient tracer test	S.J. Watson S. Quinn	Quinn, S. 2000. Unpublished MSc thesis, UCL
Summer 2001	Single borehole dilution tests Natural gradient tracer test	S.J. Watson W.G. Burgess C. Warren D. Cartwright V. Coy R. Patel	Patel, R. 2002. Unpublished MSci thesis, UCL.

1.7 Groundwater protection in the UK

This introductory chapter concludes with a summary of the development of groundwater protection in the UK. It provides a guide to the routes by which EU legislation has been transposed into UK law and summarises the Water Framework Directive, its aims and approach and how it is likely to impact the way that monitoring of groundwater in the UK is carried out.

UK groundwater legislation is not a modern invention. Early recognition of the links between public health and decaying organic matter and the first laws concerning the subsurface environment can be traced at least as far back as the Cemeteries Clauses Act of 1847 (UK Government 1847). Over the 150 years since then, water resources protection legislation has evolved and undergone several refinements. UK water legislation has followed a progression leading from water resources development for economic gains and improvements in human health through the early part of the 20th century, to pollution control measures in the 1980's and 1990's. Finally it moved onto ecosystem sustainability and holistic approaches at the start of the 21st century, in response to a sustainable development agenda. Most recent protection legislation has come about through the transposition of EC Directives into UK law.

A summary of the evolution of EC and UK legislation and guidance relating to the protection of groundwater is provided in Figure 1-2.

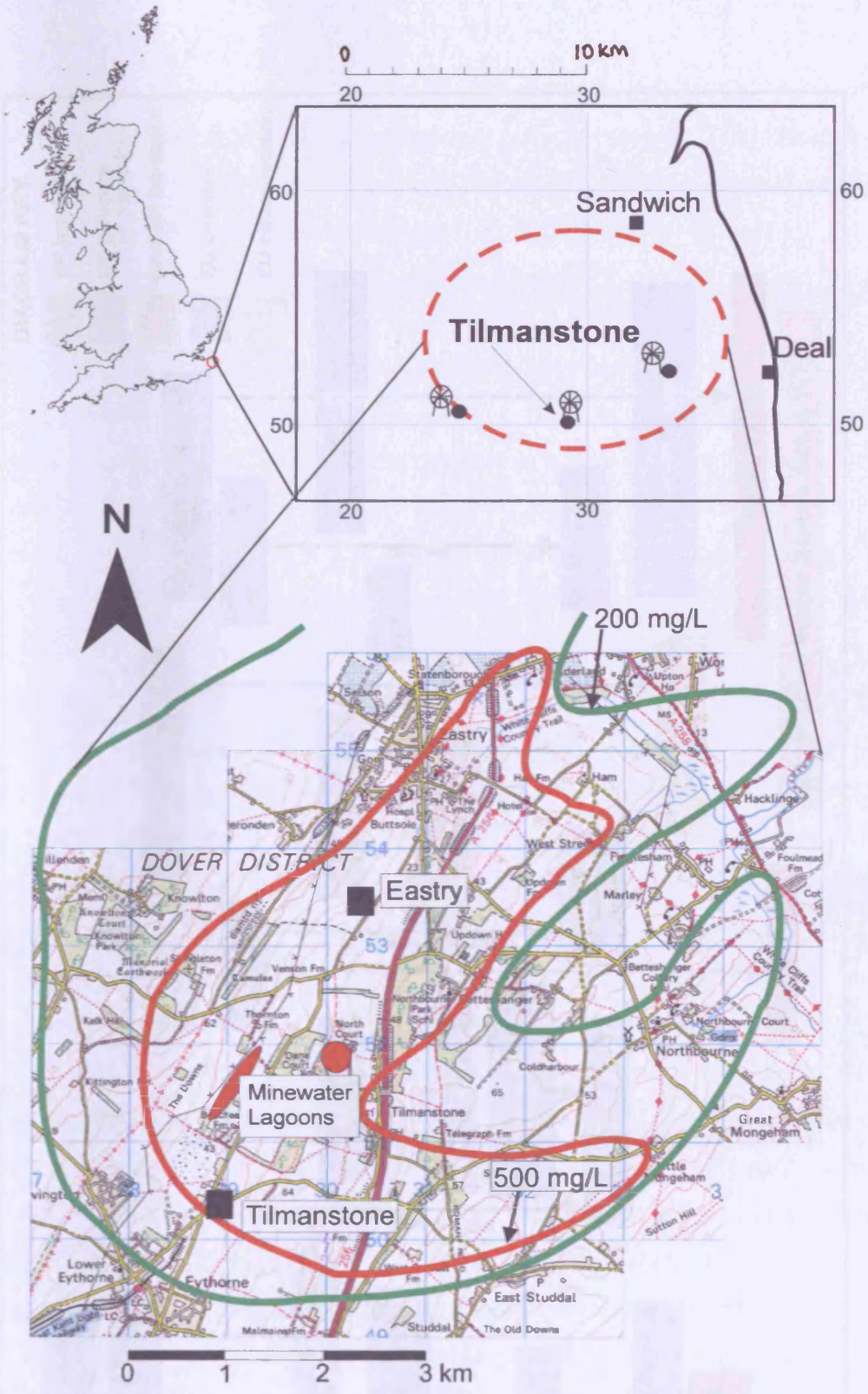

Figure 1-1 Location of the Tilmanstone - Eastry valley and the extent of the mine water plume from hydrochemical sampling in 1974.

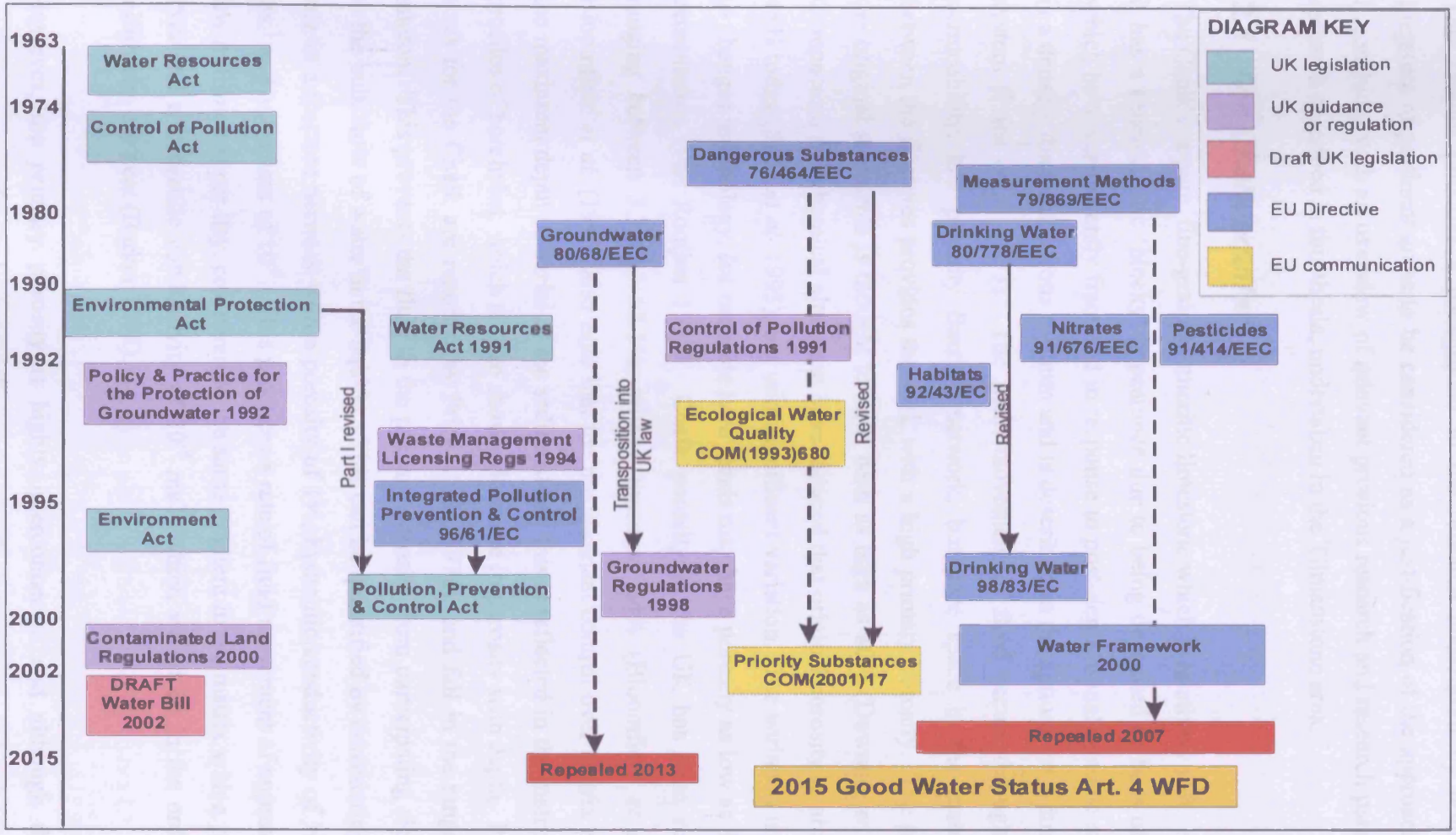

Figure 1-2 Summary of EU and UK groundwater protection legislation and guidance.

2 Background and literature reviews

This chapter provides a background to the research undertaken by reviewing the literature of pertinent areas to be considered as a justification of the approach adopted. It concludes with an overview of relevant previous research and research parallel to the research described in this thesis, undertaken in the Tilmanstone area.

2.1 The Chalk aquifer

The Chalk is a pure, fine-grained, micritic limestone which is relatively soft. At outcrop it has a characteristic 'blocky' appearance due to being deposited as beds of sediment which have subsequently fractured in response to post-depositional tectonic stresses. It is a densely fractured porous medium and is described as the epitome of a dual porosity system (Price *et al.* 1993). The main movement of fluid occurs through the high permeability, low porosity fracture network, but pore space in the matrix blocks between the fractures provides the rock with a high primary porosity. The porosity of the original sediments is thought to have been as high as 80% (Downing *et al.* 1993). Compaction and chemical alteration have reduced that original porosity to around 20 to 45% today (Price *et al.* 1993), but with significant variation. The variation is attributed to changes in lithology, for example hard bands may have porosity as low as 8%, due to cementation (van Rooijen 1993). Chalk porosity in the UK has been reported as ranging between 3.3 and 55.5%, with a mean of 34% (Bloomfield *et al.* 1995). Bloomfield *et al.* (1995) also note that the predominant control over matrix porosity is the maximum depth of burial of the sediment and this is reflected in the matrix porosity profiles of boreholes, which tend to show a decrease in porosity with depth. Pore-throat sizes for the Chalk are reported by Price *et al.* (1976), and fall in the range 0.1 to 1 micron. This prevents the fluid in the primary porosity from participating significantly in the bulk flow of water in the aquifer. This can be quantified by considering the flow rate in a fracture network with a porosity of 1%, hydraulic conductivity of 10^{-7} to 10^{-5} ms^{-1} and a gradient of 10^{-3}. This produces a rate of fluid movement of approximately a few millimetres per day, compared to the same gradient in the matrix with a porosity of 35% and a hydraulic conductivity of 10^{-8} ms^{-1}, which would be in the order of one millimetre per year (Barker 1993).

However, the primary porosity is highly interconnected and although the matrix porewaters are effectively immobile, transport of contaminants and solutes can take

place by diffusion within them (Barker 1993). The water stored in these pore spaces constitutes 95% of the volume of water stored in the rock (Downing *et al.* 1993) and hence porewater in the Chalk provides a large storage reservoir for pollutants. The matrix blocks therefore store essentially immobile water and are described as having immobile or matrix porosity (θ_{im} or θ_m) and permeability (k_{im} or k_m), (Price *et al.* 1993, Bibby 1981). The fractures contain the moving fluid in the system or aquifer and so are described as having a mobile or fracture porosity (θ_{mo} or θ_f) and permeability (k_{mo} or k_f).

The Chalk has long been described as having high permeability associated with valleys (Ineson 1962). Price *et al.* (1993) suggest transmissivity values of around 2500 $m^2 d^{-1}$ for the central valley area of unconfined Chalk, reducing to around 15 - 20 $m^2 d^{-1}$ or less beneath interfluves. In general, the upper 50 m of the Chalk is regarded as the main aquifer. Evidence for this is provided by flow logging in boreholes (Owen and Robinson 1978) and is related to the base level of erosion and to Pleistocene base levels, (Jones and Robins 1999). A decrease in permeability with depth is attributed to reductions in fracture density and aperture. However some strata at greater depths, for example the Melbourn Rock and the Chalk Rock (Price *et al.* 1977, 1982; Jones and Robins 1999), are known to be particularly productive, a feature attributed to increased fracturing observed in hardbands. Younger (1989) proposed a model that accounts for low permeability 'putty chalk' encountered in the Thames Valley at the boundary between Quaternary river gravels and the upper zone of the Chalk aquifer. Younger's model proposes that during the Devensian glaciation, freeze-thaw action in seasonal taliks, or unfrozen zones, caused the formation of putty chalk at the interface between the river gravels and Chalk. Furthermore, permafrost beneath the seasonal taliks acted to restrict dissolution and this resulted in a zone of low permeability.

2.1.1 Importance of the Chalk as an aquifer and for aquatic ecosystems

In the UK, the Chalk has been used extensively as an aquifer for water supply since the 1800s. In the south of England it provides approximately 70% of the water for supply (based on data available from Digest of Environmental Statistics, DEFRA 2002).

As well as its significance for public water supply, groundwater from the Chalk is also critical for providing baseflow in many Chalk rivers and streams, and thus maintaining the health of aquatic ecosystems. The sustainability of this system is dependant on the protection of both water quantity and quality.

2.1.2 Chalk vulnerability to pollution

The Chalk works well as an aquifer because its fracture network allows the ready transmission of water. However, its fractured nature coupled with an often thin or absent soil and drift cover at outcrop make it particularly vulnerable to pollution. Furthermore, its location in the south and east of England, which has the highest population density in the UK coupled with industrial and extensive agricultural land-use has provided for many potential sources of pollutants, both point and diffuse (Foster 1993). These include nitrates (Foster *et al.* 1986), pesticides (Lawrence and Foster 1987), landfill (Davey *et al.* 1998), hydrocarbons (Burgess *et al.* 1998), and volatile organics (Chilton *et al.* 1989, Rivett *et al.* 1990).

Once pollutants have entered the aquifer they may then be subject to rapid transport, potentially affecting large volumes of rock. The dual porosity nature of the rock means that these pollutants can diffuse into the matrix, resulting in a long-term reservoir of pollution in the immobile porewater. The diffusive exchange works to reduce the peak of a pollutant load, where there is still capacity in the matrix for sorption or storage of pollutant. This can provide an opportunity for degradable pollutants to break down or decay before reaching a receptor such as a public water supply or ecological habitat. However, as diffusion into the rock matrix retards the movement of pollutant, it also prolongs the presence of persistent pollutants in the aquifer system.

2.1.3 Chalk aquifer groundwater flow models with particular reference to southeast England

Much attention has been given to numerical modelling of groundwater flow in the Chalk aquifer. The principal feature of interest has been the variation of hydraulic conductivity or transmissivity with depth (Rushton *et al.* 1989, Taylor and Hulme 2000). Models were constructed by Oakes and Pontin (1976), Connorton and Hanson (1978) and Morel (1980) in order to understand and manage groundwater resources in the Chalk aquifer of the Berkshire Downs. However, it is noted by Rushton *et al.* (1989), that these did not account for variation in transmissivity with saturated depth and did not represent the intermittent nature of certain springs and rivers.

Rushton *et al.* (1989) focus on the variability of transmissivity with depth and also its relationship to geomorphology. High values of transmissivity are used for river valleys (500 – 1000 m^2d^{-1}) with up to an order of magnitude reduction for the interfluve areas

(100 m^2d^{-1}). A similar distribution was also adopted for the specific yield. Values ranged from 0.003 for the interfluves to more than 0.05 close to some rivers.

The other key process focussed on by Rushton *et al.* is the relationship between rivers and groundwater. Four conditions are recognised and these are sketched and described in Figure 2-1.

Rushton *et al.* report that the variation in transmissivity with saturated depth and geomorphology resulted in good model calibration to the observed patterns of groundwater hydrographs, spring discharge and river flow. The numerical model was used to test various operational conditions for the Thames Groundwater Scheme (a river augmentation scheme) and assess the impact on groundwater levels and river flows.

The approach of Rushton *et al.* (1989) was also used by ACER (1991) for East Kent. This is discussed further in Section 2.7.4.

The principal interest that remains in modelling the Chalk aquifer relates to our ability to model solute transport and to use models of solute movement in the Chalk to predict the risks to downstream aquatic ecosystems and groundwater abstractions as well as to investigate options for remediation or containment of contaminants.

2.2 Monitoring groundwater quality

Everett (1980, cited in Chilton and Milne 1994) defines monitoring as a scientifically-designed surveillance system of continuing measurements and observations, which includes evaluation procedures. A hierarchical approach may be adopted where the monitoring is undertaken at various time and spatial scales in order to provide different levels of information. These scales are likely to be:

Spatial: National, regional, local
Temporal: Monthly, annual, decadal
Information users: institutions, regulators, planners, Government, private individuals

Current monitoring of groundwater in the UK is undertaken in order to fulfil responsibilities imposed by a range of legislature, as outlined in Chapter 1. The Environment Agency has a statutory duty under Section 84 of the Water Resources Act

(1991) *"to monitor the extent of pollution in controlled waters"*. This includes groundwaters. Other drivers for monitoring of the UK's groundwaters include the Groundwater Regulations (1998), which complete transposition of the EC Groundwater Directive (European Commission 1980a), and place a duty on the Environment Agency to prevent pollution of groundwater by List II substances. The EC Nitrate Directive (European Commission 1991b) requires monitoring of groundwaters to determine areas requiring designation as nitrate vulnerable zones. The Environment Agency also has a long term objective of managing the UK's water resources in a sustainable way (Environment Agency 2001). The Royal Commission on Environmental Pollution (1992) endorsed the need for improved monitoring of groundwater in order *"to give a representative picture of the state of groundwaters in aquifers throughout the country"*.

The European Commission requires that member states implement a National Monitoring Programme for groundwater through the Groundwater Action Programme and the Eurowaternet initiative (EEA, 2003). Most recently the EU Water Framework Directive (European Commission 2000) requires an integrated approach to ensure that aquatic ecosystems are protected and enhanced through implementation of River Basin Management Plans. Under this directive groundwater bodies must be defined and statutory monitoring and reporting is required.

Chilton & Milne (1994) note that it is important to recognise that the UK's aquifers tend to be small and often locally fault-bounded. Some, as in the case of the Chalk, display a dual porosity nature. The combination of these factors gives rise to very complex flow and transport regimes, which do not easily lend themselves to statistical distributions of monitoring points, as developed for the more extensive, porous aquifers such as exist in the USA and concerning which much of the statistical work has been undertaken. However, as assessment objectives require both spatial and temporal data, the sampling locations and the sampling frequencies need to be specified and this does mean that two areas suitable for statistical analysis can be identified:

1. Optimisation of the monitoring network to ensure adequate representation of hydrogeological complexity and quality variables.
2. Guidance for the required sampling frequency required to detect changes in mean concentration of a determinand over time (Clarke 1992).

2.2.1 UK groundwater monitoring strategy

Chilton and Milne (1994) provided the National Rivers Authority (NRA, now the Environment Agency) with a national strategy for groundwater quality assessment. The work was undertaken to aid the NRA in its ability to provide the necessary level of protection to comply with its statutory requirements. Five primary objectives for the NRA's national quality assessment monitoring strategy are interpreted from the general duty under their legal requirement '*to monitor the extent of pollution in controlled waters*' (UK Government, The Water Resources Act, 1991). These are:

- Trends
- Baseline for future issues
- Spatial distribution
- Early warning
- Monitoring of nitrate

The strategy proposed a target monitoring network of 3000 sampling points with a mean density of 1 per 25 km^2 to 1 per 50 km^2 of aquifer. This is then divided according to the following criteria:

- One sample point per 25 km^2 for outcrops of major aquifers;
- One sample point per 35 km^2 for confined areas of major aquifers;
- One sample point per 50 km^2 for the outcrop and confined areas of the minor aquifers.

A regular grid design for the monitoring network is not recommended. Instead variation should be allowed in order to accommodate:

- Increased density of monitoring in recharge areas for the early warning of diffuse impacts;
- Small and/or sinuous, elongated aquifer outcrops;
- Landuse variation;
- Distribution of licensed and actual groundwater abstraction;
- Local considerations/regional requirements e.g. saline intrusion, security of quality in confined aquifers, rising groundwater levels.

It is also recommended that the monitoring network is restricted to sampling points where both construction details and hydrogeological conditions in combination provide the best depth control over the sample origin. So samples will always be representative of a known horizon which is in good hydraulic contact with the groundwater flow system in the aquifer and so representative of the groundwater quality in the aquifer at

the sampling point. Thus the authors envisage that this will restrict a national network to the following installations:

- Existing abstraction boreholes which provide adequate depth control;
- Existing observation boreholes which provide or can be modified to provide good depth control;
- New observation boreholes designed and constructed so as to provide good depth control;
- Major springs if they provide good control over sample origin.

2.2.2 Groundwater quality monitoring in the Chalk

Monitoring of groundwater has two main requirements. Firstly, a need to characterise the current situation and secondly, to guide long-term protection of the resource for various receptors, for example for drinking water and for aquatic ecosystems.

Adequate characterisation of the fracture network is clearly one of the most important requirements when trying to make predictions of where and how fast a pollutant may move in the Chalk. However, in characterising the pattern of pollution in a dual porosity system, the interaction between the fractures and matrix may be the more significant factor. In order to quantify pollution in the Chalk, sampling of both the mobile and immobile water is necessary (Headworth *et al.* 1980, Headworth 1994). Particular considerations for monitoring groundwater quality in the Chalk aquifer include:

- Standard monitoring well design will only sample the main body of flowing groundwater, immobile water in the matrix will not routinely be sampled.
- Sampling at PWS wells means that when a pollutant is detected it may be too late – the borehole may need to be removed from supply.
- The existing network is focussed on PWS and these PWS boreholes tend to be located in the main axes of valleys, limiting coverage.
- PWS's will tend to dilute concentrations due to the volume of the abstraction.
- Following the recommendations of Chilton and Milne (1994) will require a large commitment to constructing new monitoring and characterisation points. This needs to be carried out with careful consideration of the dual porosity nature of the aquifer.

2.3 Fractured media

Fractured geological formations occur throughout the world and are of interest in many different contexts. These include exploitation for petroleum products, exploitation for water supply, applications in geotechnical engineering including tunnels and other subsurface structures. Fractures range in extent from a few microns to many kilometres and throughout this range they are of interest for the way in which they control flow and transport of fluids (Berkowitz, 2002).

2.3.1 Fracture geometry

Within the hydrogeological and engineering geology literature a variety of terms are found to describe planar partings in aquifers. The terms 'fracture' and 'fissure' are used interchangeably (Bloomfield 1999). The term fracture has been described as referring to a discrete discontinuity which may be natural or induced (Barker 1993). Bloomfield (1999) specifies fractures as having accommodated strain by brittle failure. Initially the mode of formation may seem irrelevant. However, if it is possible to correlate a type of discontinuity with, for example a tectonic phase or type of lithology or combination of the two, then it may be possible to predict styles and types of fracturing and geometry (Gillespie *et al.* 1993; Bloomfield 1996). Table 2-1 is taken from Fracflow (1999) and is the terminology adopted by the current research.

Table 2-1 Definitions of terms used for fractured media (*after* Fracflow 1999)

Term	Definition
Discontinuity	General term for a planar fabric feature, either sedimentological or structural
Fracture	Discontinuities that have accommodated strain by brittle failure
Bedding fracture	Fractures located at discrete sedimentological boundaries or parallel to these boundaries
Joint	Fractures with no shear displacement
Fault	Fractures with shear displacement at the scale of observation
Fracture set	A group of sub-parallel fractures
Fracture network	All fractures in the rock mass

A survey of fracturing in the Chalk undertaken by Bevan and Hancock (1986) identifies three different types of joints: vertical extension; conjugate steeply inclined; and conjugate vertical (Figure 2-2).

The frequency of fracturing varies from many per metre of rock to less than one per metre. Bloomfield (1996) reports that fracture frequency tends to decrease exponentially with depth. Huang and Angelier (1989) report tension tectonic joints showing a gamma distribution and suggest that negative exponential distributions (reported by others) are due to lack of resolution in data collection; Ladeira and Price (1981) suggest there is a relationship between fracture spacing and bed thickness or the nature of adjacent beds. They find that where adjacent layers are relatively thick the fractures in the more competent layers are more widely spaced than when the adjoining incompetent layers are thin.

It is only because of the fracturing in the Chalk that it functions as an aquifer (Crampon *et al.* 1993). Price *et al.* (1993) have calculated theoretical hydraulic conductivities for the Chalk (Figure 2-3).

They assumed the fractures to form a regular array with constant apertures. In reality the fracture spacing, size and aperture are distributed parameters (Bloomfield 1999). Fracture spacing, b (m), and fracture density, N (m^{-1}) are related by Nb = 1.

Fracturing often displays a dominant orientation and this results in significant anisotropy (Barker, 1993). The connectivity of a fracture network influences the size of dispersive effects (Smith and Schwartz, 1984), see Section 2.4.

Porosity

The porosity of a rock, n, can be defined as the ratio of the total volume of the voids, V_V to the volume of rock, V_T, hence $n = V_V/V_T$. The effective porosity, n_e, is usually defined as the portion of the rock or media through which the transport of solutes occurs or that portion of the media that contributes to flow (Fetter 1992, Domenico and Schwartz 1990). It is recognised that the effective porosity is less than the total porosity as not all water-filled pores or fractures are interconnected or contribute to flow. Luckner and Schestakow (1991) equate effective porosity and mobile water content. In fractured media there are two domains which can contribute to the total porosity. The

open fractures through which the majority of flow occurs co-exist with the pore space within the matrix blocks, which contribute relatively insignificantly to flow, but are important for solute transport problems. Both of these domains have an effective porosity. Matrix effective porosity values are relatively straightforward to measure from rock cores and are well documented for the UK Chalk by Bloomfield *et al.* 1995. Representative values of the effective matrix porosity for the Chalk in East Kent are presented in Table 2-2.

Table 2-2 Representative values for effective matrix porosity of the Chalk in the Thames and Chilterns Region of Bloomfield *et al.* (1995), which includes the area of East Kent.

	Upper Chalk	Middle Chalk	Lower Chalk
Mean	38.8	31.4	26.6
Minimum	5.6	9.5	11.6
Maximum	48.9	52.6	39.5
Standard deviation	5.8	6.6	6.6
Number of samples	724	356	158

In Chalk aquifers it is often assumed that the specific yield may be interpreted as representing the fracture effective porosity for solute transport (Bibby 1981, Little *et al.* 1996). Within the groundwater literature there is inconsistency in the use of the terms specific yield and effective porosity (Dassargues *et al.* 1991, Little *et al.* 1996, Suzuki *et al.* 1996). It is useful to consider the implications of the use of specific yield parameter values for the effective porosity of fractures. Within the realm of water resources, the specific yield is defined as the volume of water released from storage in an unconfined aquifer per unit surface area of aquifer per unit decline in the water table (Freeze and Cherry 1979). Bear (1972) defines effective porosity as the drainable porosity or total porosity minus field capacity. He goes on to indicate that for homogeneous soils and deep water tables, specific yield and effective porosity are identical. It is likely that this is where the inconsistencies have arisen. Bear (1972) is referring to these parameters in the context of free draining soil; however it seems that Bear's equality of the parameters under limited circumstances has been carried through to the hydrogeology literature. Indeed, Bear (1972) specifically cautions against confusing effective porosity pertaining to transport with that pertaining to drainage and capillary processes. It is therefore

likely that using values of specific yield for the effective porosity for solute transport in fractures will be inappropriate. This is because specific yield values are usually derived through hydraulic testing and the fluid volumes released due to the stresses applied during hydraulic testing may be unrepresentative of the volume of water through which solute transport occurs. This is similar to the differences between hydraulic and mass balance methods to determine fracture aperture values discussed in Section 2.3.2. Stephens *et* al. (1998) assess a sedimentary sequence and compare effective porosity calculated from tracer tests with effective porosity values derived by a variety of methods, including calibration of solute transport models using values typical of pumping test specific yield. They find that tracer derived effective porosity values are 50 to 90% smaller than those derived by alternative methods.

Yeh *et al.* (2000) use a tracer method to calculate hydraulic conductivity and effective porosity in a column experiment. They consider the hydraulic conductivities derived through this method to be more precise than those derived through more conventional flow-meter methods. Furthermore they argue that effective porosities derived through hydraulic methods will tend to be over-estimated due to mistaking total pore volumes for the effective pores.

Values for effective porosity in a fractured rock can be determined if the Darcy velocity or flux, q, and average linear velocity, v, are known, through the relationship $n_e = q/v$.

2.3.2 Fracture aperture

Fracture apertures in the Chalk are generally only up to a few millimetres in width, but there is a range from relatively tight fractures to solution-enlarged karstic-type openings (Price *et al.* 1993; Banks *et al.* 1995). Price (1987) suggests a mechanism for preferential enlargement of fractures through concentration of flow due to topography and thinning of drift cover. Lloyd (1990, 1993) and Younger (1989) consider the influence of flow concentration to discharge points following the last glaciation.

The early description of fractures and apertures relied on a model of smooth, parallel plates with a constant separation or aperture. More realistic representation of the natural systems requires that fracture walls are rough and that aperture varies. The aperture variation is described by an aperture density distribution. This aperture density distribution is defined by an equivalent aperture for a fracture (Moreno *et al.* 1988;

Witherspoon *et al.* 1980). Different equivalent apertures have been defined depending on the type of measurement employed and three alternative definitions are commonly found in the literature. These are the:

1. Mass Balance Aperture (δ_m);
2. Frictional Loss Aperture (δ_l); and
3. Cubic Law Aperture (δ_c) (Tsang 1992).

A further definition is found through the characteristic time for diffusion (t_{cf}) within a fracture of aperture, a, Barker (1985b):

$$t_{cf} = \frac{\left(a/2\phi\right)^2}{D_A}$$

Equation 2-1

Where D_A is the apparent diffusion coefficient (see Section 2.4.3) and ϕ is the matrix porosity.

Some confusion has arisen in the literature over the mass balance aperture, frictional loss aperture and cubic law aperture and this is unravelled by Tsang (1992), who demonstrates that Brown's (1987) ranking of:

$$\delta_m \geq \delta_c \geq \delta_l$$

Equation 2-2

is correct. This is due to the relationship between the equivalent apertures measured and their being an expression of the arithmetic or geometric means of the parameter being measured. A brief explanation of the relationship between the equivalent apertures, based on Tsang's (1992) summary, is provided here. The estimation of the equivalent aperture is carried out through tracer and / or hydraulic testing and the method of testing chosen gives rise to a number of different parameter measurements. The Mass Balance Aperture (δ_m) is derived through tracer transport. It is derived from measurable quantities which rely only on mass balance physical laws and is related directly to the pore volume of the fracture. This means that it relates to the arithmetic

mean of all the aperture values in the flow paths of the tracer transport process. The Frictional Loss Aperture (δ_f) is a function of the permeability of a pair of plates (with constant aperture) and the transport velocity. The equivalent permeability is shown by Dagan (1979) to be well approximated by a geometric mean. The arithmetic mean of a dataset is larger than its geometric mean so this accounts for the first and third terms in the relationship of Equation 2-2. The Cubic Law Aperture (δ_c) is shown to be a multiplicative average of the other two, hence its location in the middle position of the relationship. Tsang (1992) considers the Mass Balance Aperture the most worthy of being an equivalent aperture since it captures the average aperture along the flow path of the tracer transport.

The direct measurement of fracture aperture is problematic. If direct measurements are made of fracture apertures at the ground surface the fracture aperture may have been subject to stress release and weathering and is therefore likely to be unrepresentative of the fracture aperture at the depth in the aquifer at which groundwater flow is occurring. Bloomfield (1996) has made direct measurements of fracture aperture in Chalk at a quarry. The range of fracture aperture measured was less than 0.5 mm to 23.5 mm.

2.3.3 Channelling

Barker (1991) notes that channelling in fractures has important impacts on flow and transport, recognising three key effects:

- It determines effective porosities and velocities
- The amount of sorption and / or diffusion into the matrix is controlled by the contact area
- Flow interaction between intersecting fractures is sensitive to channel density

2.3.4 Fracture skin effects

It is observed that some fractures or sections of fractures have altered porosity immediately behind the fracture wall adjacent to the aperture space (Bloomfield, 1999). This takes the form of increased porosity with increased pore throats immediately behind the fracture wall, followed by a decreased porosity due to cementation. Porosity variation adjacent to fractures has important implications for exchange of solutes between fractures and matrix.

2.4 Flow and transport in dual porosity media

In a dual porosity medium two domains exist with quite different characteristics in terms of flow and solute transport: the fracture network is responsible for the regional transport of fluid and solutes and the porous matrix acts as a locally interacting storage / release reservoir for solutes (Barker 1985a). Due to the local storage effect of the matrix porewater the effects of fracture – matrix interaction tend to be more significant for solute transport than for fluid flow (Berkowitz, 2002).

2.4.1 Conceptual developments

Lapidus and Amundson (1952) formulated the convective (advection) dispersion equation (CDE or ADE), Equation 2-3 for one-dimensional flow in a homogeneous, isotropic porous media.

$$\frac{\partial C}{\partial t} = D\frac{\partial^2 C}{\partial z^2} - v_e \frac{\partial C}{\partial z}$$

Equation 2-3

Where C is solute concentration, t is time, D the dispersion coefficient, z distance and v_e groundwater velocity. They argue that with the velocities normally encountered in flow through porous media, instantaneous equilibrium of the solute within the fluid filled pore space cannot be assumed. Diffusion (dispersion) has to be considered as it will have a pronounced effect on the arrival time of solute flowing through a porous system. For instantaneous injection of solute into a steady flow field, Equation 2-3 produces nearly sigmoid or symmetrical concentration distributions for the solute arriving at an observation point (Figure 2-4).

Early approaches to flow and transport in porous media use the velocity profile observed in capillary tubes, as proposed by Taylor (1953) and expanded on by Aris (1956), to account for the observed variation in arrival times of solute at an observation point. However, although symmetrical concentration distributions for solute arrival at an observation point have been reported (Coats and Smith 1964; Gershon and Nir 1969) many authors also reported strongly non-sigmoid and asymmetrical distributions (Scheidegger 1961; Biggar and Nielsen 1962; Kay and Elrick 1967; Coats and Smith 1964; Passioura 1971) (Figure 2-4). This asymmetrical solute distribution is often referred to as 'tailing'. One explanation for the observed asymmetry of arrivals used the

concept of a variable velocity profile within a pore but this was further developed for groups or bundles of macropores, utilising a skewed porewater velocity distribution and was known as the capillary bundle model (Turner 1958; Haring and Greenkorn 1970; Lindstrom and Boersma 1971). Other proposals explaining the tailing were made on the basis of distinct mobile and immobile regions within the porous medium. Several experimental conditions were suggested that would produce this tailing effect:

Unsaturated flow (Nielsen and Biggar 1961), producing immobile water (Turner 1958; Deans 1963; De Smedt *et al.* 1981) which prevents or restricts solutes in the immobile region from participating in the flow process;

Aggregated media which provides slow moving or immobile water in which displacement is dependant on diffusion. In large aggregates the amount of immobile water decreases and the diffusion pathway becomes longer resulting in long tails on the breakthrough curve (Biggar and Nielsen 1962; Green *et al.* 1972; McMahon and Thomas 1974; Nkedi-Kizza *et al.* 1983);

Porewater velocity (or mobile water velocity). Experimental studies indicated pronounced tailing occurs with decreases in velocity and propose this is due to more time available for diffusion (Biggar and Nielsen 1962; Skopp and Warwick 1974).

2.4.2 Non conformity with theoretical predictions of ADE

The asymmetry observed in the tracer breakthrough illustrates a non-normal travel time distribution for the systems considered. Various systems have been proposed to account for the asymmetry of breakthrough timing (Figure 2-5).

Coats and Smith (1964) describe a system with dead-end pores in which immobile water is trapped, allowing transported solute to diffuse into the dead-end pore volume and be stored, until it can diffuse back into the mobile domain. Passioura (1971) describes a system in which flow is occurring through macropores and solute is diffusing into soil aggregates. Skopp and Warwick (1974) describe solute moving with the mobile water in the macropores but diffusing into a 'halo' of immobile water that surrounds the inactive soil grains.

Early research into non-ADE behaviour was undertaken in chemical engineering (Van Deemter *et al.* 1956, Aris 1975). Most charged components in soil systems or artificially packed beds interact with the solid phase. Chemical engineering and analytical chemistry studies recognised that the differences in this interaction between different components provided a way of separating the components by displacement techniques. An early application is found in chromatography where the identification and quantification of substances is based on the different transport velocities of the substances in a particular media. However, within hydrogeology, a crucial early conceptual leap that attributed observed flow behaviour in fractured porous media to flow and interaction processes in two different domains (i.e. dual porosity media) was formulated by Barenblatt *et al.* (1960) and Warren and Root (1963) then introduced the concept into the US petroleum literature. Most of the early experimental work to understand non-ADE behaviour was undertaken on soils, or aggregated porous media, to look at leaching of chemicals through soil horizons and salinisation effects from irrigation. The systems were described by macropores and aggregates, as shown in Figure 2-5, but Barenblatt *et al.* recognised that fractured porous media are an extreme case of aggregated porous media. The fracture and matrix block domains co-exist and for non-steady state flow, the rate of transfer of fluid (and hence solute) between the two must be accounted for. They recognised a characteristic time for delay, τ, in the transient pressure response observed in a fractured porous medium. This characteristic time is described by $\tau = \eta/\kappa$, where η is the ratio of the fracture permeability to the rate of transfer of fluid between the fractures and matrix blocks and κ is described as the coefficient of piezo-conductivity of the fractured rock which for flow corresponds to the porosity and compressibility of the matrix blocks, but for solute transport the compressibility of the blocks is replaced by the tortuosity and constrictivity of the matrix block (see Section 2.4.3 and Appendix 2) . The exception to the necessity for explicit account of the transfer between the two domains is that if the characteristic time for the process under consideration, e.g. change in rate of abstraction, change in concentration of a solute, is long compared to the characteristic delay time, then the system can be described as a porous medium. The application of the dual porosity concept was extended, being noted by Foster (1975) as a mechanism to explain the observed movement of tritium in the Chalk aquifer and used by Young *et al.* (1976) to describe nitrate distribution in the Chalk. The two domains of the dual porosity system are described separately. Flow occurs through the interconnected fracture network and

the matrix blocks provide storage and interconnect locally with the fractures to exchange fluid, solute, heat etc (Figure 2-6). Movement of solute into the rock matrix is controlled by the porosity and diffusivity of the rock and where reacting species are present their concentrations are influenced by the rates and equilibria of the reactions.

Dual porosity systems should not be confused with dual-permeability systems. In the case of dual permeability, layers of permeable rock alternate with layers of lower permeability. Flow occurs in all layers, but at different rates, dependant on the permeability.

2.4.3 System description

The dual porosity and heterogeneous nature of the Chalk complicates predictions of contaminant transport and procedures for monitoring groundwater quality. The following section outlines the dominant processes operating in dual porosity systems and provides the basic equations that can be used to describe flow and solute transport in the Chalk.

Flow in fractures

Darcy's law is valid in fractures which have linear-laminar flow (when the Reynolds number is inversely proportional to the friction factor). The transition from linear to turbulent flow in fractures occurs at a Reynolds number of around 2300 (Louis 1974, reported in de Marsily 1986).

Where Darcy's law is valid, a transmissivity can be calculated for a fracture, T_f, using the cubic law (Snow 1968; Witherspoon *et al.* 1980). Assuming that the fracture is planar, with a constant aperture, a, and with smooth surfaces, then;

$$T_f = \frac{ga^3}{12\upsilon}$$

Equation 2-4

v is the kinematic viscosity of the water (or fluid) and g is the acceleration due to gravity.

For groundwater at around 10 °C, an approximate relation between aperture, a, hydraulic conductivity, K, and fracture density, N, is given by:

$$K\,[\mathrm{md}^{-1}] \approx 50N\,[\mathrm{m}^{-1}]\,a\,[\mathrm{mm}]^3$$

Equation 2-5

Flow in fractures is extremely sensitive to the aperture: T_f for an aperture of 1 mm is 10^{-3} m^2s^{-1} and 1 m^2s^{-1} for an aperture of 1 cm (approximately 86 and 86400 m^2d^{-1} respectively), (Barker 1993).

A hydraulic diffusivity, D_h, for the mobile flow system can be defined by:

$$D_h = K/S_s$$

Equation 2-6

Where S_s is the specific storage. This is relevant where a dual porosity system is considered as an equivalent porous medium, with respect to modelling flow, see Section 2.5.1.

Dispersion

Spreading of transported solutes by variations in the fluid flow velocity is termed hydrodynamic dispersion. It is generally accepted to occur at a microscopic scale due to flow variation around grains, causing dispersion in the order of centimetres and also at a macroscopic scale due to macroscopic heterogeneities within the porous medium, causing dispersion in the order of metres. In porous media, dispersion is normally represented in the Advection Dispersion Equation (ADE Equation 2-3) as the characteristic dispersion coefficient, D_L, i.e. longitudinal dispersion, when considering movement in the direction of groundwater flow (D_T and D_V are used for horizontal transverse and vertical transverse dispersion respectively and the relationship between them is usually $D_L > D_T > D_V$). The coefficient is considered to increase in proportion to the value of the velocity such that $D_L = \alpha_L v$, where α_L is the longitudinal dispersivity [L]. In fractured media, dispersion occurs due to the heterogeneity of velocities within the fracture as well as the variation in velocity due to moving between fractures with different aperture and also due to the intersection of fractures with different orientations.

Much has been written about the scale-dependency of dispersion. A review of dispersivity data is provided by Gelhar *et al.* (1992), and stochastic methods to describe scale effects are suggested by Dagan (1982) and Gelhar and Axness (1983). An alternative perspective on the matter is given by Molz *et al.* (1983) who consider that

the scale effect is not real, but appears as a result of the increasing uncertainty in parameter values that occurs with distance and hence travel-time from a measurement point. In general there are two ways in which macrodispersion is included in solute transport models:

1. The heterogeneity of the modelled domain is lumped into a macrodispersion term. The dispersivity coefficients are not physically consistent, but statistically they represent the general behaviour of the contaminant with the mean advective flow. This is advantageous in that it is unnecessary to know the detail of small scale heterogeneities, but it is problematic to vary the scale from that at which the values were originally derived.

2. The known heterogeneities of the system are accounted for through variation in the hydraulic conductivity or effective porosity values. The dispersivity values obtained at a local scale do not need to be scaled up since they can be considered as representative at the scale used in the model.

An overview of dispersion in the Chalk is provided by Barker (1993). Barker (1993) demonstrates that in the Chalk, dispersion can often be ignored as its effect on solute dilution is negligible in relation to the effect of matrix diffusion for most times and distances of interest in contaminant transport.

Matrix diffusion

Studies of groundwater flow in fractured media emphasise the dominating influence of fractures on the effective permeability of the rock mass (Grisak and Pickens 1980). The fractures are the main paths for groundwater flow and solute transport but the matrix surrounding the fracture heavily influences the overall transport process. Diffusive exchange of solute between fracture and matrix water impacts solute concentration in the fractures (Figure 2-7).

The effect of this process is to slow down the advance of solutes or contaminants and to reduce the size of the concentration peak observed, but to prolong the persistence of contaminants in the fracture system (Foster 1975, Barker and Foster 1981, Gooddy and Lawrence 1994).

Diffusive exchange occurs between matrix porewater and mobile groundwater in fractures at the sub-metre scale: the kinematic porosity, fracture and matrix porosities, and the diffusion coefficient of the saturated matrix are the key parameters (Barker *et al.* 2000; Fretwell *et al.* 2000).

A characteristic time for diffusion over a distance, x, can be defined as x^2/D, where D is the diffusivity (diffusion coefficient divided by porosity) (Barker 1993). Using this relationship quantifies the timescale that needs to be considered for matrix diffusion. Figure 2-8 shows the characteristic time for diffusion against increasing matrix block-size for the reported range of diffusion coefficients for chloride in Chalk (Hill 1984, Gooddy *et al.* 1995). Chalk blocks near the ground surface are of the order of 10 to 50 cm and it can be seen from Figure 2-8 that times for diffusion across blocks of this size range from 77 days to 3 years (10 cm block size) and 5 to 60 years (50 cm block size). This provides a guide to the timescale required for clean-up of contaminated Chalk.

Molecular diffusion

The laws used to describe diffusion into immobile water are Fick's first and second laws and the process is represented by a diffusion coefficient. Several different diffusion coefficients are necessary to describe the diffusive process and this has led to some confusion in the literature. For clarity, the relationship between the three diffusion coefficients used in tracer studies in porous media is given in Appendix 2 along with reported values from experimental work.

Fick's second law is of greatest interest to solute transport in dual porosity media. It is used to describe **time-dependant** diffusion in a porous medium:

$$\frac{\partial C}{\partial t} = D_A \frac{\partial^2 C}{\partial x^2}$$

Equation 2-7

Where D_A is the apparent diffusion coefficient, as described in Appendix 2. Typical values of D_A for chloride in the Chalk range from 5.5 to 8.8 x 10^{-10} m^2s^{-1} (Gooddy *et al.* 1995).

Another approach that has been used to account for the movement of solute between mobile and immobile water uses a rate limited mass transfer coefficient (van Genuchten and Dalton 1986, Sudicky and Frind, 1982, Haggerty and Gorelick, 1995). This is also described as a quasi-steady state approach by Barker (1985a), see Section 2.5.3 and Chapter 6.

2.4.4 Scale of measurements

Field investigations are generally applied at boreholes, leaving considerable uncertainty about aquifer parameters between boreholes. The transport of solutes depends to a large degree on the heterogeneity of the parameters that control transport in the subsurface. For non-reacting solutes, the spreading of a solute plume will be dominated by the spatial structure and connectivity of the hydraulic conductivity field. Limited knowledge of the variations in fracture density, geometry and connectivity and of matrix porosities restricts the ability to predict pollution migration at the field scale. Transport parameters are very sensitive to internal aquifer geometry and so even reasonable estimates of fracture geometry can cause misleading errors in predictions of contaminant movement. Mean aquifer parameters are not very useful for predicting contaminant transport at small to medium scales.

2.5 Modelling solute transport in dual porosity media

Barker (1993) identifies several models in use to simulate flow and transport in fractured systems such as the Chalk. The most appropriate use of these models is based on an understanding of the fracture system and the time-scale of the transport processes. A brief summary of these timescales and models is adopted from Barker (1993) below:

2.5.1 Equivalent porous medium (EPM) models

In these models the complexities of the fracture/matrix systems are represented by values for storage and transport parameters for the combined system. This type of model is considered to be most appropriate for regional water resources studies where the time-scale of any significant changes is likely to be long in comparison to the time for pressure changes to propagate across a matrix block. This condition is never likely to be satisfied for solute transport models due to the very long time needed for the diffusive transport of solutes (Section 2.4.3).

2.5.2 Diffusive dual (or double) porosity (DP) models

The solute concentration in a matrix block is considered as being controlled by the equivalent value in the fractures and the relevant diffusive parameters in the matrix block. Darcy's law is treated as a diffusion of heads into the matrix block and diffusion of solutes is described using Fick's law. There are two cases considered:

1) If the time-scale of interest is a small fraction of the time for diffusion across a matrix block, then only the fracture/matrix contact area per unit volume of rock is important and the simplifying assumption of an infinite matrix can be made. E.g. 1-D TALBOT.

2) If the time-scale of interest is similar to the time for diffusion across a matrix block, then the sizes and shapes of the matrix blocks become important (Barker 1985b). E.g. RADIAL TALBOT which considers aquifer block thickness.

A common assumption, made to simplify mathematical representation of the fractures, is that the fracture network comprises a set of equally spaced parallel channels (Grisak and Pickens 1980; Sudicky and Frind 1982; Barker 1982).

2.5.3 Quasi-steady state (QSS) models

In this type of model the diffusive model described in Section 2.5.2 is treated approximately. The matrix is regarded as having a single value of head or solute concentration and a diffusive exchange (often termed mass transfer) with the fractures is calculated as being proportional to the difference in concentration/head between the fracture and the matrix (Barker 1985a). This type of model is relevant where changes in the fractures are slow compared to the time required for diffusive equilibrium within a matrix block. This approach has been extended into a multi-rate model by Haggerty and Gorelick (1995) and Harvey and Gorelick (2000) whereby the mass transfer relationship has a distribution of rate coefficients.

2.5.4 Aquifer heterogeneity and stochastic versus deterministic approaches

For a dual-porosity aquifer, such as the Chalk, it can be demonstrated that matrix diffusion, rather than advective dispersion, dominates the solute transport process (Barker 1993). This is because the diluting effect of matrix diffusion on a dissolved solute is much greater than the diluting effect attributable to dilution within a fracture.

However, the diffusive process is strongly affected by the fluid velocity which controls the time available for diffusion to occur. The fluid velocity field in a dual-porosity medium is a function of the fracture aperture and heterogeneity of the medium through which the fluid is flowing. This heterogeneity is uncertain and measurements of aquifer properties at one location and scale may be of limited use at a larger scale. Two different approaches are generally adopted to approach the problem of heterogeneity of aquifers within numerical models. Stochastic methods treat aquifer heterogeneity as a random field and stochastic methods to describe aquifer heterogeneity have been applied (Sudicky and Huyakorn 1991, Yeh 1992) to make predictions about the transport of solute in aquifers. However, the stochastic approach relies on an adequate representation of the random field for a representative elementary volume and a fundamental question remains as to whether stochastic methods are applicable under field conditions, particularly for fractured media (Dassargues *et al.* 1996, Robinson 2002). As an alternative, a fully deterministic approach to solute transport modelling requires that all the variability in the heterogeneity of the aquifer is accounted for explicitly. This is usually impractical as the acquisition of the variability information required to provide a deterministic description would probably result in the destruction of the aquifer. However, the use of tracer tests to directly determine effective transport parameters overcomes the uncertainty about heterogeneity, thus both reducing the need for the potentially large number of aquifer parameter measurements necessary to provide a stochastic representation of aquifer properties and overcoming the difficulties of a deterministic approach.

Dassargues *et al.* (1996) consider that in practical cases it is difficult to apply geostatistically based methods to scale up groundwater flow and transport parameters. Instead they suggest the use of local geological data, to obtain a subjective geological interpretation, to which are added measurements of aquifer parameters that indicate spatial variability and heterogeneity in hydraulically distinct layers, such that the flow and transport parameters required for a regional scale numerical model can be inferred or extrapolated. Combining geological data with field based measurements of transport parameters accounts for macrodispersivity by including the detail of the geology. The uncertainty of the variability of microdispersivity is accounted for through the analysis of tracer tests that have sampled the range of microdispersivity along the flowpath taken by the tracer.

2.5.5 Numerical solute transport models in the Chalk

Very few numerical models representing solute movement in the Chalk account for its dual porosity character. Modelling approaches tend to accommodate the attenuating effect of the matrix porewater storage by simply retarding the solutes. Models that explicitly characterise the Chalk as a dual porosity system are reviewed here.

Bibby (1981) describes a dual porosity model developed to represent the evolution of the contaminant plume from the Tilmanstone colliery in Kent: the subject of this current study. The model incorporates diffusion from a constant concentration boundary into a two-dimensional transport model. The paper notes that often the controlling influences on the transport of solutes in groundwater are, what Bibby terms as, 'secondary processes' such as adsorption, reaction and diffusion, rather than primary mechanisms such as convection and dispersion. Because the Chalk's fractures are narrow, separating relatively large, highly porous blocks, mass transport is dominated by the molecular diffusion of solutes between the mobile fracture water and the water in the block pores. During the modelling process Bibby found it necessary to iterate between the flow and transport models to obtain a transmissivity distribution with which both historical water level and chloride concentration data could be reproduced. The transport model was very sensitive to the velocity field and hence to the choice of transmissivity and therefore was difficult to calibrate. The values of dispersivity which are used are very large, although similar values are noted as having been used by Robertson and Barraclough (1973) for other aquifers at a regional scale. It is concluded that the model is not, in any case, very sensitive to changes in dispersivity when the values required are so large. Bibby remarks that the only surprising parameter value used in the modelling is the effective saturated thickness of the fractured zone transporting the pollutants, which is only 10 m, assuming a matrix block porosity of 0.35.

The prediction by Bibby's model of future changes in the contamination concentration in the aquifer indicated that by 2008 there would still be 30% of the original 318,000 tonnes of chloride, discharged from the Tilmanstone colliery, in the aquifer.

Brettmann *et al.* (1993) modelled results from tracer tests carried out in a fractured chalk. They used a three-dimensional finite difference model for flow and transport. The model was developed as a dual porosity continuum model. Advection was

assumed to occur only in the fractures and the matrix water was assumed to be static. Solute exchange between the fractures and matrix occurred according to the local concentration difference between the mobile and immobile phases. Observed breakthrough curves from a two-well tracer test were reproduced, but the tails of the curves were not well represented. Modelling was also carried out with the model set up as a single porosity model with advection and dispersion only in the fractures and no solute exchange with the porous matrix. The models provided a poor simulation of the observed data, greatly overestimating the observed concentrations and showing little tailing effect in the falling limb. The authors conclude that modelling of flow and transport in the chalk cannot be undertaken with a single porosity model, and when dealing with contaminant transport in the chalk, and similar systems, a fractured and porous domain must be represented.

Moench (1995) uses a model incorporating fracture skin to analyse a tracer test undertaken by Garnier *et al.* (1985) in densely fractured chalk near Béthune, France (see Section 2.6.2). The test was undertaken in fractured chalk beneath an argillaceous till. Instantaneous injection of four tracers was made into a steady flow regime with the injection well 10.22 m from the monitoring well. Use of multiple tracers in a tracer test should reveal estimates of dual porosity aquifer parameters which are independent of the tracer used (providing linear, reversible adsorption can be assumed). The same dispersivity, fracture porosity, matrix-block dimension and matrix porosity should be revealed through the analysis of the individual tracer breakthrough curves. Moench found it necessary to include a fracture skin in the model in order to achieve such results. The fracture skin acted to provide some resistance to diffusion into the rock matrix and the advective arrival times, independent of the tracer used, mass recovery rates, consistent with measured values, and relative values of effective diffusion coefficients, consistent with free water diffusion coefficients for the separate tracers, were obtained.

Little *et al.* (1996) use FEPOLL (Shapiro, 1984, *cited in* Muller 1987) to model the contamination by chloride of a large area of Chalk near Royston, Cambridge. The Chalk is characterised as a dual porosity system with lateral advection and hydrodynamic dispersion being dominant in the fractures and molecular diffusion being dominant in the matrix. The fracture model is coupled to the surrounding porous matrix

by the analytical solution for one-dimensional diffusion. The original FEPOLL code is used and extended in the manner described by Bibby (1981) to simulate matrix diffusion. The Chalk is conceptualised as a stack of homogeneous isotropic plates of Chalk matrix separated by horizontal fractures. This horizontal plate model for the Chalk is acknowledged as potentially naive but stands up well to comparison with Huyakorn and Pinder (1983) which uses more complex geometries (equal sized porous spheres). It is concluded that the potential inaccuracies have more to do with the concept that the blocks are of equal shape and size than with their geometry. A good agreement between field data for the average matrix block size and the porous plate thickness inferred by calibration was obtained, suggesting that fracture spacing data from scanline surveys can usefully support the development of a dual porosity transport model for the Chalk.

Biver (1994) uses a dual porosity finite element code (LAGAMINE – developed at the University of Liège) to model the breakthrough of tracer for two tests over approximately 20 m in the chalk aquifer at Bertrée, Belgium. The tests are undertaken in a converging groundwater flow regime, for a regional, unstressed flow regime. A good match between observed and modelled data is obtained. The test is described further in Section 2.6.2.

2.6 Tracer tests

In the previous sections the Chalk as a dual porosity system has been described and important features that control solute transport highlighted. These features or parameters (aperture, groundwater velocity, fracture connectivity, hydraulic conductivity, porosity etc) need to be attributed values in order to utilise the equations presented that describe solute transport. This, as in many areas of hydrogeology, presents tremendous challenges due to the variable nature of geological media. Tracer testing offers an approach that provides a way to overcome the difficulties faced by incomplete or absent knowledge about the geometry of fractured systems. Tracer tests cut across the uncertainties of the system geometry, determining effective transport parameters directly. The need to define aquifer and transport heterogeneities is side-stepped. However, tests are usually (due to logistical and financial constraints) small-scale (tens of metres) and may not provide useful information for longer-term predictions of contaminant movement and planning for removal / remediation. The

exhaustive studies undertaken at Borden (Sudicky, 1986) and Cape Cod (Hess *et al.* 1992), for example, are rarely feasible.

A tracer test is basically a physical/chemical field method for obtaining data to describe advection, dispersion and diffusion in an aquifer. Ideally the tracer used should be conservative so that no interaction between it and the medium through which it is flowing, for example by sorption, occurs. Tracer tests may be undertaken for a variety of reasons, including to (Ward *et al.* 1998):

- establish hydraulic connections;
- determine groundwater flow directions; and
- calculate groundwater velocities.

Three main classes of test have been identified (Jakobsen *et al.* 1993):

1) single-well test,
2) two-well test, and
3) natural gradient test.

However a more appropriate separation may simply be between forced gradient and natural gradient tests as single-well tests include forced and natural gradient types and two, or multiple, well tests may also be under forced or natural gradient conditions. A comprehensive review of tracer testing with particular application in the UK is given by Ward *et al.* (1998). Jakobsen *et al.* (1993) note that the reliability of the results from many tracer tests carried out are questionable due to difficulties such as ill-defined input functions, inaccurate monitoring or inappropriate models used to analyse data. The dimensionality of the study is also recognised as an important issue. Field observations have generally shown that the vertical mixing of a contaminant plume in groundwater is very small, i.e. the plume is often restricted to a limited vertical range.

Local site conditions in the Tilmanstone – Eastry valley (borehole construction, difficulties associated with disposal of contaminated groundwater etc, see Section 4.3) preclude the use of pumping which is necessary for forced gradient tracer tests. Hence only natural gradient tests are reviewed here.

2.6.1 Single-well tests

A natural gradient single-well test is usually described as a single-borehole dilution test. The aim of this method is to obtain a direct measurement of the specific discharge (Darcy velocity) (Halevy *et al.* 1967).

Theory

A tracer is injected into the saturated borehole column, or an isolated interval, such that a uniform concentration of tracer is achieved. The subsequent dilution of the tracer should be exponential with a time constant related to the specific discharge (Darcy velocity of groundwater in the vicinity of the borehole). The change in tracer concentration is caused by flow of groundwater across the borehole and by diffusion. The 'decay' or dilution of the tracer is monitored either by detectors in the borehole or by careful sampling. The natural hydraulic regime should not be disturbed. The test is only valid for measuring the Darcy velocity if dilution due to head differences, density currents, flow due to artificial mixing and flow other than due to horizontal movement of groundwater are eliminated or accounted for (Halevy *et al.* 1967). Halevy *et al.* therefore consider the single borehole dilution technique to be best suited to homogeneous and isotropic formations with results obtained in fractured or cavernous rock only being considered to provide qualitative profile information. In summary, the following conditions must be met (Ward *et al.* 1998):

- *"The concentration within the borehole remains uniform and equal to the concentration leaving the borehole;*
- *The concentration at time zero is instantaneously raised to* c_i*;*
- *Water enters the borehole from an aquifer thickness equal to the screened or open length of the borehole – i.e. there is no vertical flow in the aquifer;*
- *Water upstream of the borehole is at a uniform background concentration of* c_b*; and*
- *The flow is steady state."*

If these assumptions are met the change in tracer mass in the borehole over a time interval t, will be equal to the mass fluxes into and out of the borehole:

$$\pi R^2 L_{sat} \Delta C = q L_{scrn} \alpha D (c_b - c_i) \Delta t$$

Equation 2-8

where

R borehole radius

L_{sat} saturated depth of borehole

ΔC change in borehole concentration

q Darcy velocity in the aquifer

L_{scrn} open length of the borehole

α ratio of the width of the aquifer contributing flow to the borehole to the borehole diameter (see Figure 2-9)

D borehole diameter (2R)

c_b background aquifer concentration of tracer (often zero)

c_i borehole concentration at time zero

Δt change in time

Parameters measured

The Darcy velocity, q, is determined directly from Equation 2-8 and if the hydraulic conductivity (K), gradient (i) or kinematic porosity (n_e) of the system is known then other parameters can be derived through the following relationships:

$$q = -Ki$$

Equation 2-9

$$v = q/n_e$$

Equation 2-10

where v is groundwater velocity.

Examples

Ward and Williams (1995) undertook a series of single borehole dilution tests in a borehole in the Chalk in order to identify and quantify major flow horizons. Dilution of tracer in the borehole was very rapid, with concentrations returning to background levels in less than 20 hours. A single major flow horizon was found to dominate the flow in the borehole.

Lewis *et al.* (1966) used single borehole dilution techniques to obtain hydraulic conductivity values in fractured rocks. They found a good agreement between hydraulic conductivity values obtained through this method and those obtained through pumping tests. They also note that the single borehole dilution approach is more economical from the point of view of time, cost and repeatability than pumping tests.

2.6.2 Multiple well tests

Multiple well tests under natural gradient conditions involve the addition of tracer into a borehole (either the entire open section or part of it, isolated by packers). The introduction of the tracer should not cause any change to the natural hydraulic conditions. The movement and / or dilution of the tracer is then monitored at other boreholes. This type of tracer test is particularly difficult when conducted between two boreholes as the capture zones of the boreholes under natural gradient conditions are limited to αD, as shown in Figure 2-9. Boreholes need to be positioned along the line of flow or within the region in which the tracer disperses (Ward *et al.* 1998). In a fractured aquifer this may not be directly down-gradient of the injection borehole due to the orientation of the fractures.

Theory

Analytical solutions for the ADE (Equation 2-3) have been found for a number of initial and boundary conditions. A summary of solutions of particular application to solute transport studies is provided by Fetter (1992). The solutions require a simple geometry and a homogeneous aquifer (Fetter 1992). The solutions presented include:

For the case of one-dimensional step change in concentration, where water is flowing at a steady state through, e.g. a column of a porous medium. Tracer is then used to replace the flow of water. The tracer in the water exiting the column is analysed and the ratio of the tracer concentration, C (at time t), over C_0, the injected tracer concentration, is plotted against time, t. The breakthrough of the tracer is predicted to appear as in Figure 2-10.

For the initial conditions

$C(x, 0) = 0 \quad x \geq 0$

And boundary conditions

$C(0, t) = C_0 \quad t \geq 0$

$C(\infty, t) = 0 \quad t \geq 0$

The solution to Equation 2-3 for these conditions is given by Ogata and Banks (1961) as

$$C = \frac{C_0}{2}\left[erfc\left(\frac{L - v_x t}{2\sqrt{D_L t}}\right) + \exp\left(\frac{v_x L}{D_L}\right) erfc\left(\frac{L + v_x t}{2\sqrt{D_L t}}\right)\right]$$

Equation 2-11

Where L is the flow distance in direction x at time t, and *erfc* represents the complementary error function (Freeze and Cherry 1979 Appendix V).

Other types of concentration boundary conditions include:

exponential decay of the source term

$C(0, t) = C_0 t^{-it}$

where i is a decay constant; and

pulse loading, where a constant concentration occurs for a fixed period of time, followed by a period of time with another concentration. One particular example of this is where the concentration is C_0 for times from 0 to t_0 followed by 0 for all times greater than t_0 *i.e.*:

$C(0, t) = C_0 \quad 0 < t \leq t_0$

$C(0, t) = 0 \quad t > t_0$

Parameters measured

Natural gradient tracer tests provide qualitative information such as connectivity, as well as quantitative information on travel times, groundwater velocity and dispersion.

Analysis of tracer tests in fractured porous media such as the Chalk need to be undertaken with care as the effect of matrix diffusion may be important. Ward *et al.* (1998) identify four regimes based on the time-scale for molecular diffusion and these can be used to determine the extent to which a tracer test will be diagnostic of aquifer transport parameters. The regimes are summarised in Figure 2-11.

Examples

Allen *et al.* (1997) in the BGS Chalk Aquifer Study review permeability and fractures in the English Chalk, citing several tracer studies that have been carried out in the Chalk. Most of these have been carried out to examine known karstic features e.g. Morris and Fowler 1937, who looked at swallow holes at Water End in Hertfordshire. Test results established velocities of up to 5500 md^{-1}. Atkinson and Smith (1974) undertook a tracer experiment in the Havant-Bedhampton area and established travel times of 62.5 hours for peak concentration at a spring 5.75 km from the injection point. This corresponds to a velocity of 2200 md^{-1}.

Calculations using the quantities of flow and hydraulic gradient led Atkinson and Smith to compare the flows observed to those in a pipe of 0.74 m diameter. Price (1987) suggested that an idealised fracture of only 4.5 mm width with a transmissivity of 5000 m^2d^{-1} would provide the necessary flow.

Banks *et al.* (1995) report a tracer test in Berkshire between a swallow hole and a spring 4.7 km apart. Velocities observed were 5800 md^{-1} for peak concentration and 6800 md^{-1} for breakthrough. These are the highest values reported for the Chalk. Using the method of Price (1987) Banks *et al.* calculate that the fracture system could be represented by a single fracture of 5.4 mm aperture.

Allen *et al.* (1997) note that little work has been carried out where no known karstic features exist. An exception is provided by Price *et al.* (1992) where tracer studies were carried out to look at the routes taken by water entering soakaways beside a motorway, only 3 km from a public water supply (PWS). Results indicated that some tracer moved rapidly to the PWS, with velocities of up to 2400 md^{-1}. Tracer recovery was very low and this was attributed to significant amounts of the tracer moving through very small fractures.

Ward (1989) undertook a series of tracer tests in conjunction with pumping tests to determine hydraulic characteristics. Ward and Williams (1995) undertook natural gradient tracer tests between boreholes in dry valleys in the Chalk of East Yorkshire. Groundwater flow connections and velocities were established through passive monitoring for fluorescein and photine CU tracers. Groundwater velocities of 50 – 280 md^{-1} were measured in the valleys.

Garnier *et al.* (1985) undertook tracer tests using Uranine (disodium fluorescein), ^2H_2O (deuterium), I^- (iodide) and $H_2{}^{13}CO_3$ in fractured chalk in France. Moench (1995) reanalyses the data using a dual porosity model which incorporates a diffusion limiting skin on the fracture surfaces (see Section 2.5.5).

Black and Kipp (1983) describe the fieldwork for and analysis of a tracer test using ^{82}Br at an experimental site in the Lower Chalk. The plot was instrumented with boreholes and irrigated to cause saturation of the unsaturated zone down to the water table, an

approximate thickness of 11 m. The results are modelled and parameters are derived by fitting to 3 dimensionless parameters: the ratio of small to large pores; the dispersivity; and the average pore length over which diffusive interaction occurs. They find that dispersivity can be related to the average size of blocks in dual porosity media.

Biver (1994) reports two tracer tests in Chalk in Belgium. The Chalk occurs under a cover of Tertiary and Quaternary deposits, approximately 25 m below ground level. Laboratory work established a mass transfer coefficient between mobile and immobile water of 10^{-6} s^{-1}. Tests using NO_3^- in a regional flow field and Uranine in a converging flow field were undertaken. Transport coefficients used to calibrate a numerical model are given in Table 2-3.

Table 2-3 Transport coefficients used in model calibration by Biver (1994)

Transport coefficient	Regional flow	Converging flow
Longitudinal dispersivity (α_L), m	4	4
Transverse dispersivity (α_T), m	1	-
Mass transfer coefficient, for mobile to immobile region transfer of solute, s^{-1}	0.9×10^{-6}	1.5×10^{-6}
Effective porosity (fractures), %	7	7.5
Immobile, matrix porosity, %	15	40

Jakobsen *et al.* (1993) describe a two-well tracer test conducted in the Chalk of eastern Denmark. Tracer (lithium chloride) injected into a well was monitored arriving at a discharge well 25 m away from the input point. The monitoring took place at five different intervals vertically. The results indicated a rapid flow route affected by advection and dispersion in the fractures as well as processes other than these, assumed to be the influence of diffusion into the porous matrix.

Dassargues *et al.* (1996) describe a series of tracer tests undertaken in a fractured Carboniferous limestone aquifer in Belgium. The effective transport parameters resulting from the tracer tests are then scaled up and used in a regional groundwater flow model to produce groundwater protection zones. Dassargues *et al.* use the transport parameters derived from the tracer testing directly in the regional modelling. They argue that as they have a relatively detailed knowledge of the geology, the

expected scale effect on the dispersivity (Gelhar *et al.* 1992) is considered explicitly through a deterministic representation of the heterogeneity.

The tracer test and solute transport literature reviewed has tended to fall into two areas;

- Tracer tests are carried out and modelling of the solute breakthrough is undertaken to derive transport parameters (Biver 1994, Garnier *et al.* 1985, Black and Kipp 1983) ;
- Flow and solute transport modelling is undertaken at a regional scale. The model is calibrated to a large scale contaminant plume, from which transport parameters are derived (Little *et al.* 1996, Bibby 1981).

Although Dassargues *et al.* (1996) go some way to linking the two areas noted above, by undertaking tracer tests to derive effective transport parameters, and then using these values at a regional scale, they do not have the benefit of a large scale plume to compare their regional model results to. Bibby (1979) reports tracer tests in the Tilmanstone-Eastry area (described in Section 3.3.7) but, the majority of these tests were unsuccessful. For the single, successful test, undertaken under pumped conditions over 25 m, a dispersivity of 2.2 m is calculated. This tracer-test derived dispersivity can be compared to Bibby's final calibrated model values for longitudinal dispersivity of 120 m and a transverse dispersivity of 60 m. It would appear that Bibby's results confirm the scale dependency of dispersion discussed by Gelhar *et al.* (1992). However, the approach adopted by Dassargues *et al.* (1996) suggests that tracer testing in combination with detailed representation of the geology at the regional scale may provide a way to overcome the expected scale dependency of dispersion.

2.7 Previous and parallel research in the Tilmanstone area

Figure 1-1 shows the location of Tilmanstone in east Kent. There is a long history of interest in the quality of the groundwater in the Tilmanstone area. The practice in the Kent area of disposing of coalfield minewater to lagoons on the surface of the Chalk for rapid infiltration alerted a number of workers throughout the early 1900's, including Buchan (1962). Increases in chloride concentrations at the nearby Wingham PWS, due to disposal of minewater from Snowdown colliery, provoked early action and a pipeline was constructed to take the minewater to the Little Stour river. The Tilmanstone – Eastry valley did not have an existing PWS to provoke such action however, and disposal of minewaters to lagoons continued until 1974.

2.7.1 The British Geological Survey

Concerns over the pollution of the Tilmanstone - Eastry valley were addressed in the 1950s and 1960s by the Institute of Geological Science (now the British Geological Survey, BGS). Two sets of water samples were taken and analysed (Anon 1953, Harvey 1962). Assessment of the resource was also reported on by Downing (1956).

2.7.2 Kent River Board / Southern Water Authority/ Southern Water & Southern Science

Most of the early research carried out on the Tilmanstone-Eastry plume was undertaken by the Kent River Board, later to become part of the Southern Water Authority. Aspects of this work are documented in internal working reports as well as in reports from consultants. These consultants included the Water Research Centre (WRc), who undertook numerical modelling work and porewater extraction from borehole core, BGS who completed geophysical borehole logging and Hunting Surveys who undertook resistivity surveys in the area. The investigations and modelling are summarised in Headworth *et al.* (1980), Bibby (1981) and Headworth (1994). A brief overview is provided here.

The delineation of the extent of chloride pollution began in 1948 when 40 private wells in the area were sampled. Sampling continued until the 1970's and while sampling from open wells is often of questionable accuracy it established the extent of the plume as 27 km^2 (using the 200 mg/L isochlor). The chloride contours for 1974 are presented in Figure 2-12.

In 1973 a surface resistivity survey was commissioned from Huntings Surveys. This defined the plume as extending along two dry valleys running towards the North and South Streams as shown in Figure 2-13. An area of 10 km^2 was delineated, taking the 30 ohm-m contour as the definition of the saline plume. This is more restricted than the area established by the well sampling and is a function of the parameters taken for the delineation. Headworth (1994) considers the well sampling gives the better overall representation of the surface extent of the pollution plume.

The following details of drilling in the Tilmanstone area investigations are noted by Headworth (1994):

- eight boreholes were drilled at three sites down-gradient of the mine soakage ditches, to depths of 50, 100 and 150 m at each site.
- U100 coring was employed (not successful below the water-table, GRP lining also unsuccessful).
- three additional 150 m deep continuously cored boreholes at 100 mm diameter were drilled. Cores were crushed, centrifuged and analysed for chloride at one metre intervals. Major ion analysis was performed at 6 m intervals. This provided the most valuable information from the investigation (Headworth 1994).

Figure 2-14 shows the vertical distribution of chloride in the Chalk aquifer proposed by Headworth *et al.* (1980) based on a compilation from the investigations undertaken in the 1970's.

In spite of scant data about mine pumping activities and water quality, Headworth *et al.* (1980) and SWA (1976a) estimate that between 1907 and 1974 approximately 187×10^6 m^3 of water was disposed to the Chalk and that this contained 318,000 metric tonnes of chloride (Figure 2-15). Until 1952 the quantities abstracted were variable and the chloride content was below 500 mg/L. In 1952 the Milyard seam was opened and both the quantity of water and the chloride content rose. At this stage chloride concentration was 1500 mg/L, but from 1965 this increased to 3000 mg/L and the amount pumped rose to 11 Ml/d. It is clear that had the disposal to the Chalk been stopped as late as 1960, the extent of groundwater pollution would have been significantly less severe.

Analysis of the sampling of the North and South Streams (SWA 1976a) indicated only 47,000 tonnes of the chloride (15% of that discharged from the mine) had discharged from the aquifer at springs draining to these boundary streams. The feasibility of remediating the aquifer by pumping was considered. Pumping from the Eastry PWS borehole took place for fifteen months, to assess the impact of a longer term removal of water. The results showed that pumping to remediate would be a long and costly process.

The final contribution to the study at that stage came from two models developed by Bibby (1979). A transient Finite Element model of the groundwater flow regime was

constructed and calibrated, and this was linked to a diffusion-dispersion model of solute transport. The model confirmed the results produced by the test pumping, showing that 87% of the discharged chloride still remained in the aquifer in the mid 1970s. The model predicted that it would take thirty years for chloride in groundwater at Eastry PWS to reduce to 200 mg/L. The model also demonstrated the futility of trying to rehabilitate the aquifer artificially. This was attributed to the groundwater abstracted at Eastry being predominantly from the fractures and this groundwater would discharge naturally into the North and South Streams within a year or two. As the majority of the chloride was stored in the matrix blocks, pumping could only advance the clearance by a small amount by helping to reduce the chloride concentration in the fractures and marginally accelerating the rate of exchange between matrix and fracture water.

Some additional testing was undertaken at one of the Eastry observation boreholes in 1991 by Southern Science (Southern Science 1991). Chloride concentrations were recorded as 830 mg/L, rising to 1070 mg/L then falling to 1020 mg/L after five hours pumping. These observations compare to model predictions of 770 mg/L by Bibby (1979). So the natural rehabilitation of the aquifer has not advanced as rapidly as predicted by the original modelling.

Mott MacDonald (1998) used in-house software to develop a two layer, surface water-groundwater interaction model of the Eastry valley for Southern Water. It was developed to look at the effect on stream flow of abstracting from the Eastry borehole. The model has a monthly time step and utilises recharge calculated from Theissen polygons at three locations within the modelled area. There is a strong correlation of rainfall with elevation. Definition of permeability is essentially taken from the 1991 model, ACER (1991). It was found that to calibrate the model to available stream flow data and groundwater levels satisfactorily the top layer of Chalk could be no more than 40 m thick. This correlates well with the information gathered during the aquifer investigation undertaken by Headworth *et al.* (1980).

The main difficulty that arose with the Mott MacDonald model was that stream data relate to water level rather than flow and there is little useful information regarding spring elevations and stream profiles, so these had to be included in the model relatively inaccurately. Localised run-off from the area around the North and South streams was

excluded and this may be quite important as the marsh areas are on alluvial deposits so storage would be expected to occur in this area, with release of water during the summer months. The model indicated relatively rapid changes in stream flow when abstracting from Eastry PWS at the licensed rate during the summer months. It also showed a rapid decline of flow in the streams once the main recharge season had finished, an implication of the fairly shallow nature of the active horizon and low storage capacity of the Chalk.

2.7.3 Environment Agency Southern Region

The EA (Southern Region) has developed a steady state groundwater flow model using MODFLOW which extends approximately from Dover to the River Great Stour. It uses the valley pattern developed by University of Birmingham / ACER (1991) for the East Kent aquifer model but cannot incorporate the variation in transmissivity with water table elevation. Recharge is applied as an annual average.

2.7.4 Folkestone and Dover Water / University of Birmingham / ACER consultants

During the 1980's, Acer Consultants undertook an investigation for Folkestone and District Water Company (now Folkestone and Dover WC) to assess the potential for utilisation of new water resources in the region. The study included the development of a large numerical model, by the University of Birmingham, covering the area from Canterbury across to the coast at Dover (ACER 1990b). The model had a fairly coarse grid of 1 km to assess water resources availability and consider optimisation of abstraction.

Cross *et al.* (1995) discuss the response of the East Kent aquifer during the 1988-92 drought and the ability of the model developed by the University of Birmingham (ACER 1990b) to reproduce the observed hydrographs. A full explanation of the model is given in the Water Resources Study of East Kent Aquifer (ACER 1991). The model covers the area from the groundwater divide to the west of the River Great Stour, eastwards to the coast at Deal and south to Dover and Folkestone. The northern boundary is taken as the area where groundwater quality deteriorates under the Tertiary cover, and it is assumed that this indicates a region of no-flow. The southern boundary is taken as the groundwater divide observed along the high point of the North Downs.

An important feature which is included in the model is the ability to represent varying transmissivity with elevation of the water table as a hydraulic conductivity varying with depth is incorporated. Generally satisfactory agreement is achieved between observed and simulated groundwater heads, although the north eastern area of the model domain, in the vicinity of Hacklinge Marsh, approximately 3 km east of Eastry (see Figure 1-1), is less accurately represented. It is thought that this may be due to the influence of mine subsidence and that an improved understanding of surface water-groundwater interaction is necessary.

2.7.5 University College London

Research has been carried out in the Tilmanstone area at University College London since the early 1980s. Oteri (1981) undertook PhD research, using the area as a field site for geophysical resistivity technique investigations. This was followed by MSc research by Peedell (1994) who updated knowledge of the extent of the pollution by undertaking a hydrochemical survey. MSc research by Carniero (1996) undertook an assessment of the original model predictions and parameter values, compared to the updated field measurements of the pollution development. During the period of the current PhD research, and under the supervision of the author, MSc projects have been undertaken by Hazell (1998), focussing on single borehole dilution tests; Chahinian (1999), analysing the relationship between recharge and groundwater levels; and Quinn (2000), undertaking further single borehole dilution tests and a borehole to borehole natural gradient tracer test.

2.7.6 Fracflow project

In 1999 a site within the Tilmanstone-Eastry valley was also utilised by a European Union funded research project: FRACFLOW (2001). This was a pan-European Research project with partners from the UK, Denmark, Germany and Israel with the objective of investigating ways to characterise flow and contaminant transport in fractured chalk. Research sites were established in Israel, the UK and Denmark. The British Geological Survey was the UK partner. At the UK site in the Tilmanstone-Eastry valley (the Lower Venson Farm site originally established by SWA in the 1970s) two cored boreholes were drilled, one vertical and one at 30° from the vertical. These were geophysically logged and packer tested. The vertical borehole had samples taken from the core, from which porewater was extracted and analysed. Analysis of the geological structure of the area was undertaken from digital elevation data and cliff and

quarry sections as well as by televiewer logging of the boreholes. Interpretation of regional structures likely to be influential on hydraulic behaviour, and the relationship between fracture frequency and depth was made. A two-dimensional vertical 'slice' model using the SWIFT dual porosity software (Reeves *et al.* 1986) was developed to assess the impacts of the interpreted hydraulic controls. Full details of field and laboratory investigations are given in a series of reports: FRACFLOW 1st to 3rd annual progress reports and FRACFLOW 1997-2001 Final Report.

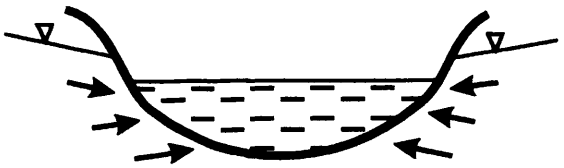

Increased groundwater head results in increased flow to the river.

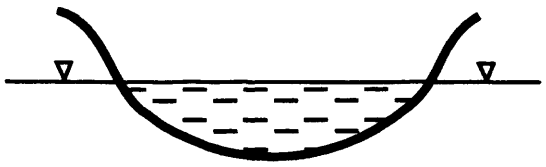

Groundwater head equals river level, no flow between river and aquifer.

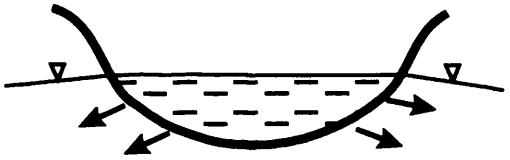

Groundwater head is below river level, water flows from the river to the aquifer, providing sufficient water is present in the river.

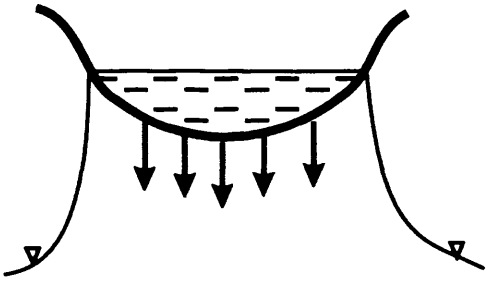

The flow from the river to the aquifer reaches a limiting value.
Further decline in groundwater level results in no increase in loss from the river.

Figure 2-1 Sketch of different representations of river - groundwater interaction, *after* Rushton *et al.* (1989).

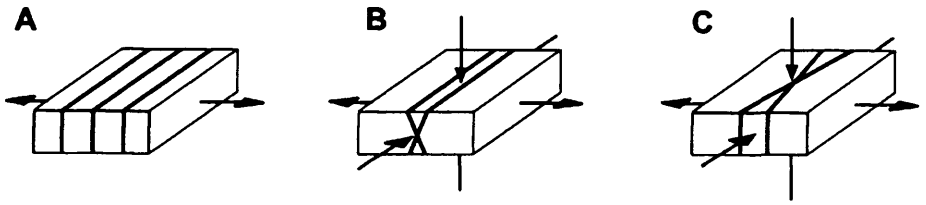

A single set vertical extension joints; **B** conjugate steeply inclined joints; **C** conjugate vertical joints.
The arrows indicate the inferred directions of the principal stress axes.

Figure 2-2 Joint Types. Block diagrams of joint types (*after* Bevan and Hancock 1986).

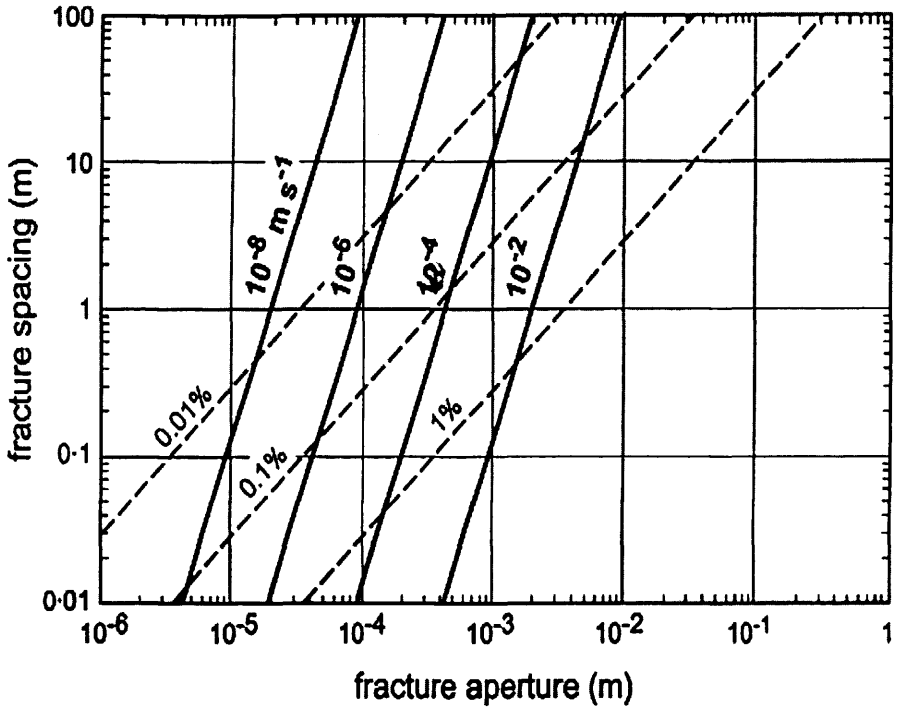

Figure 2-3 Aperture spacing, hydraulic conductivity and porosity relationship, (*after* Price *et al.* 1993).

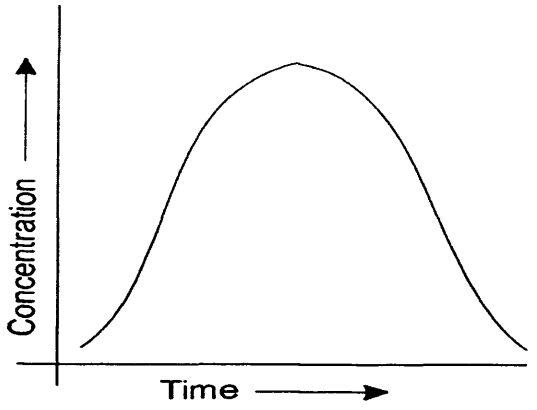

Typical tracer breakthrough for single porosity media.

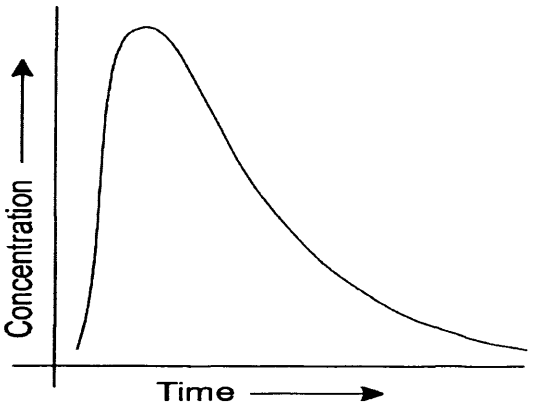

Typical tracer breakthrough for dual porosity media. Note long tailing effect attributed to diffusion from matrix porewater.

Figure 2-4 Symmetrical concentration breakthrough predicted by Eqn 2-3 and asymmetrical breakthrough demonstrating 'tailing' effect.

Conceptual models for observations of non-ADE solute arrival times

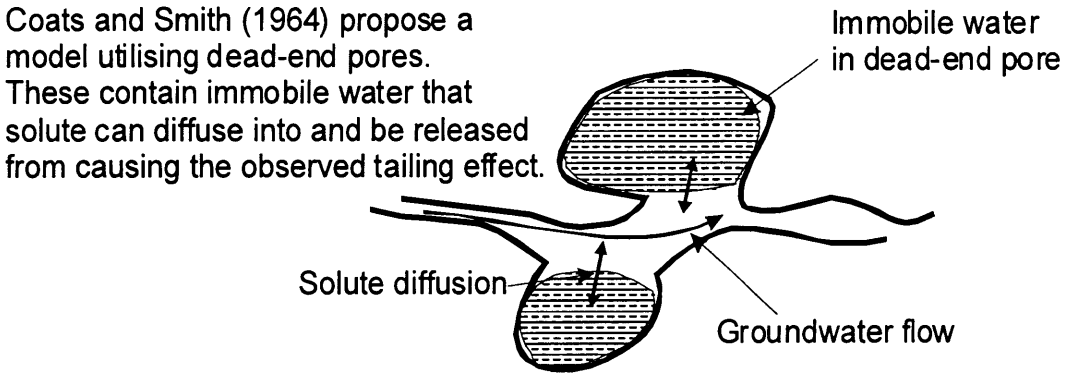

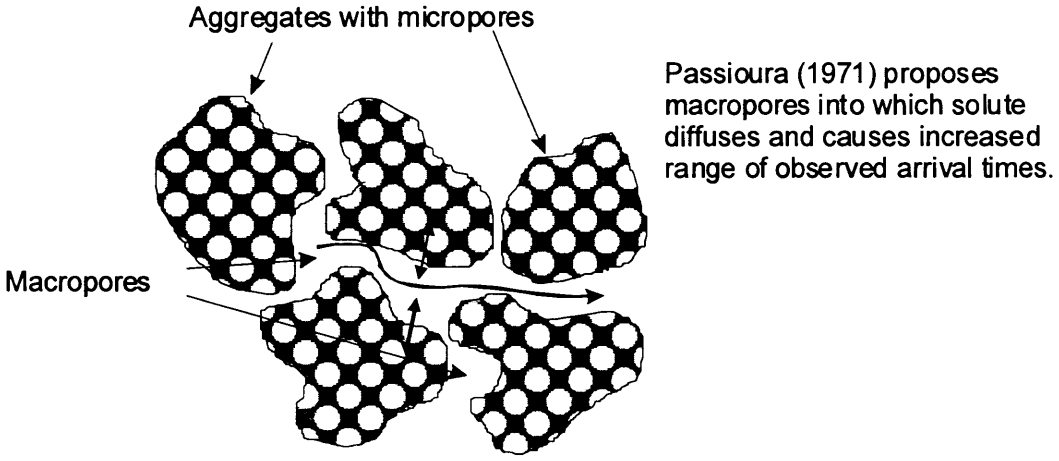

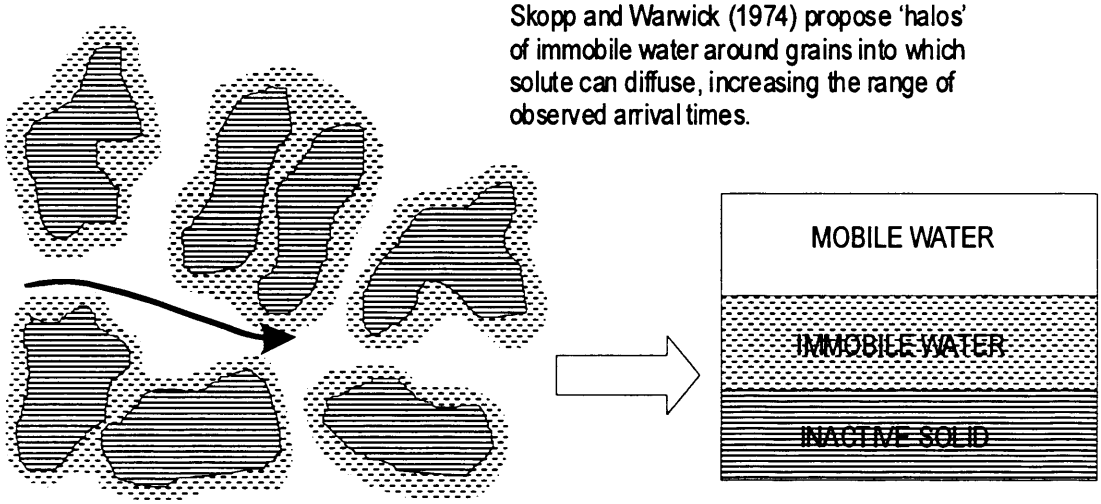

Figure 2-5 Conceptual models to describe ADE and non-ADE breakthrough.

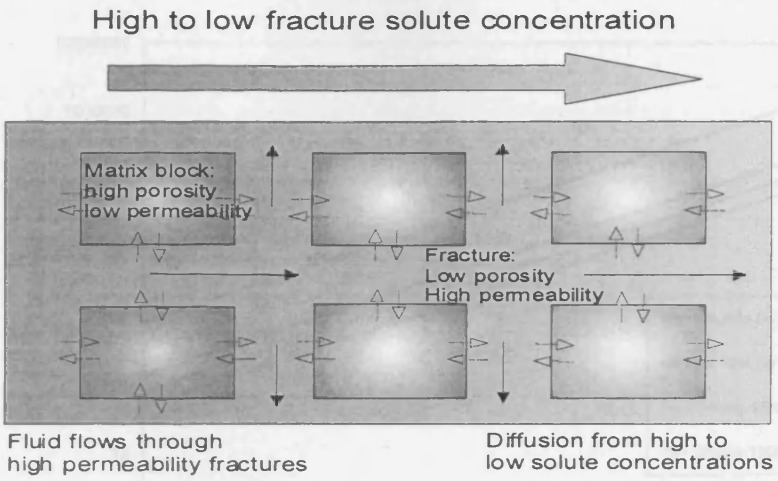

Figure 2-6 Solute exchange in dual porosity media.

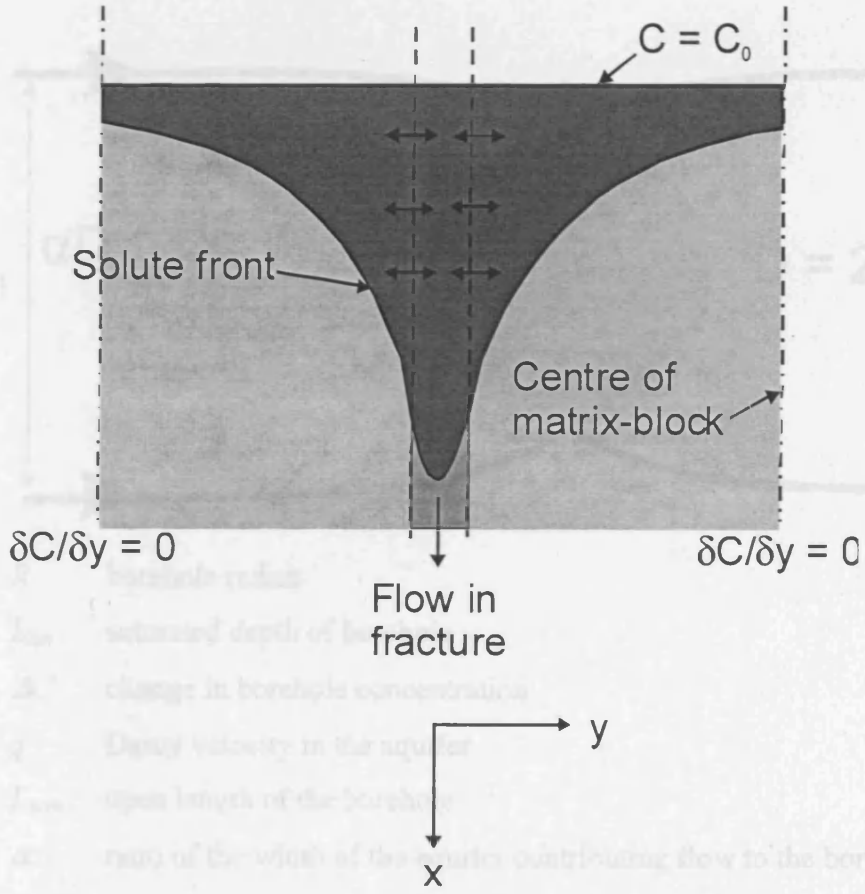

Figure 2-7 Change in solute concentration in fracture due to diffusive exchange with matrix water.

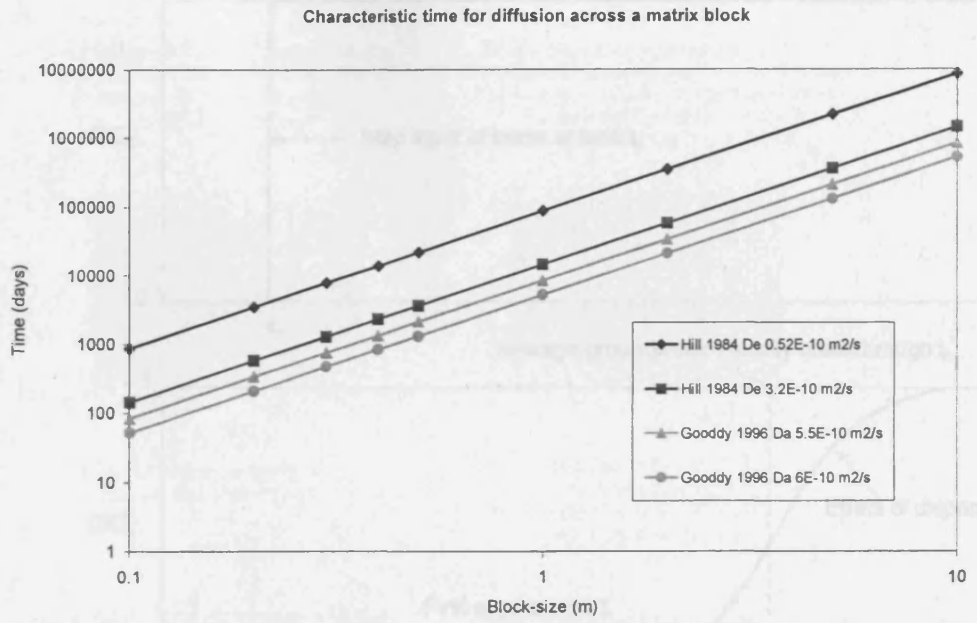

Figure 2-8 Time for diffusion across matrix blocks in the Chalk.

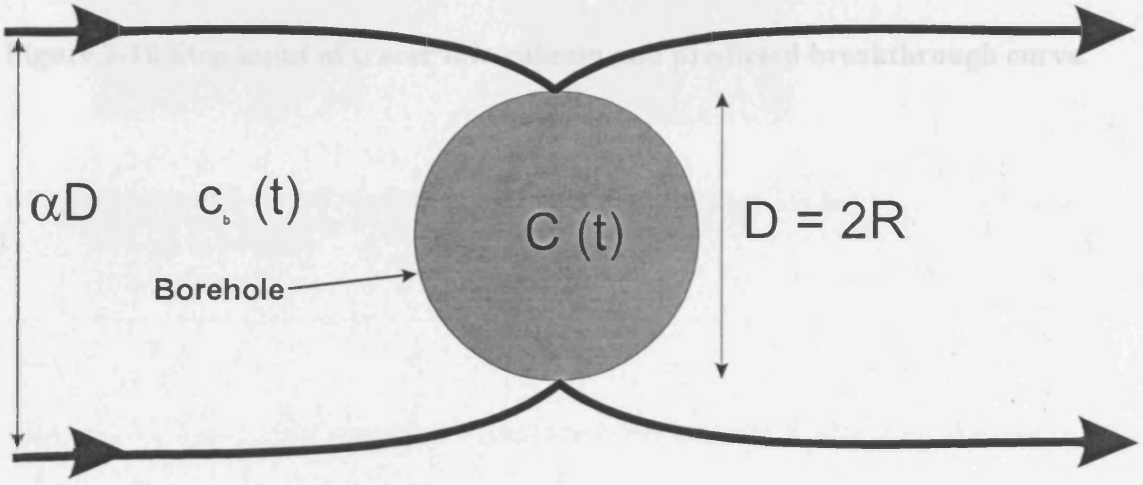

R borehole radius

L_{sat} saturated depth of borehole

ΔC change in borehole concentration

q Darcy velocity in the aquifer

L_{scrn} open length of the borehole

α ratio of the width of the aquifer contributing flow to the borehole to the borehole diameter

Figure 2-9 Width of aquifer contributing to flow to the borehole.

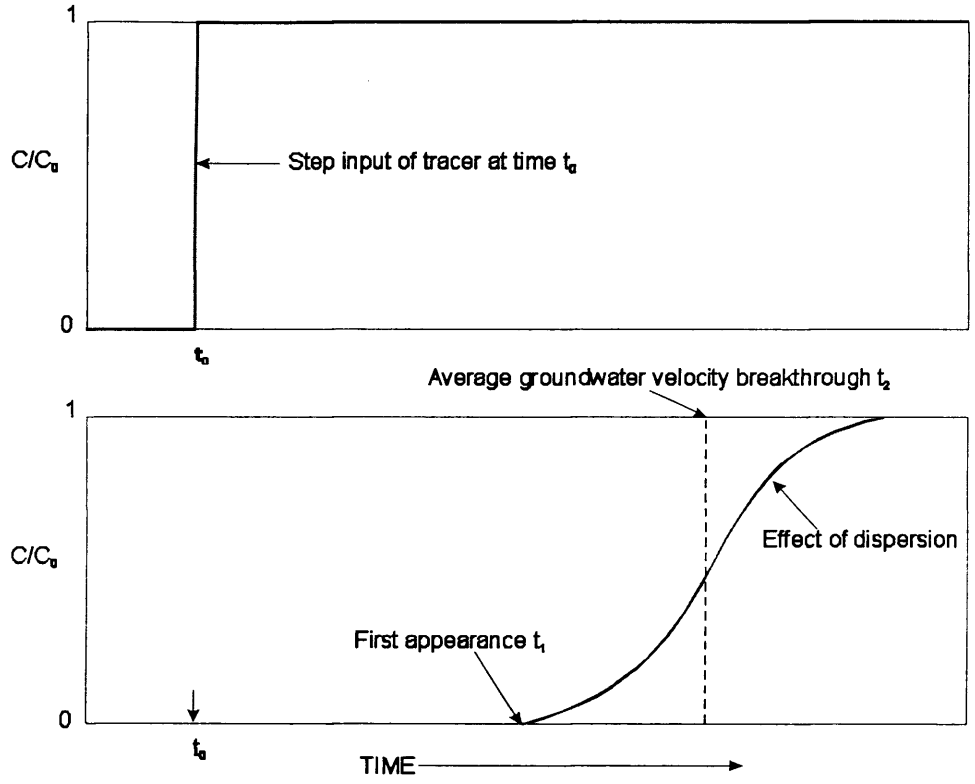

Figure 2-10 Step input of tracer into column and predicted breakthrough curve.

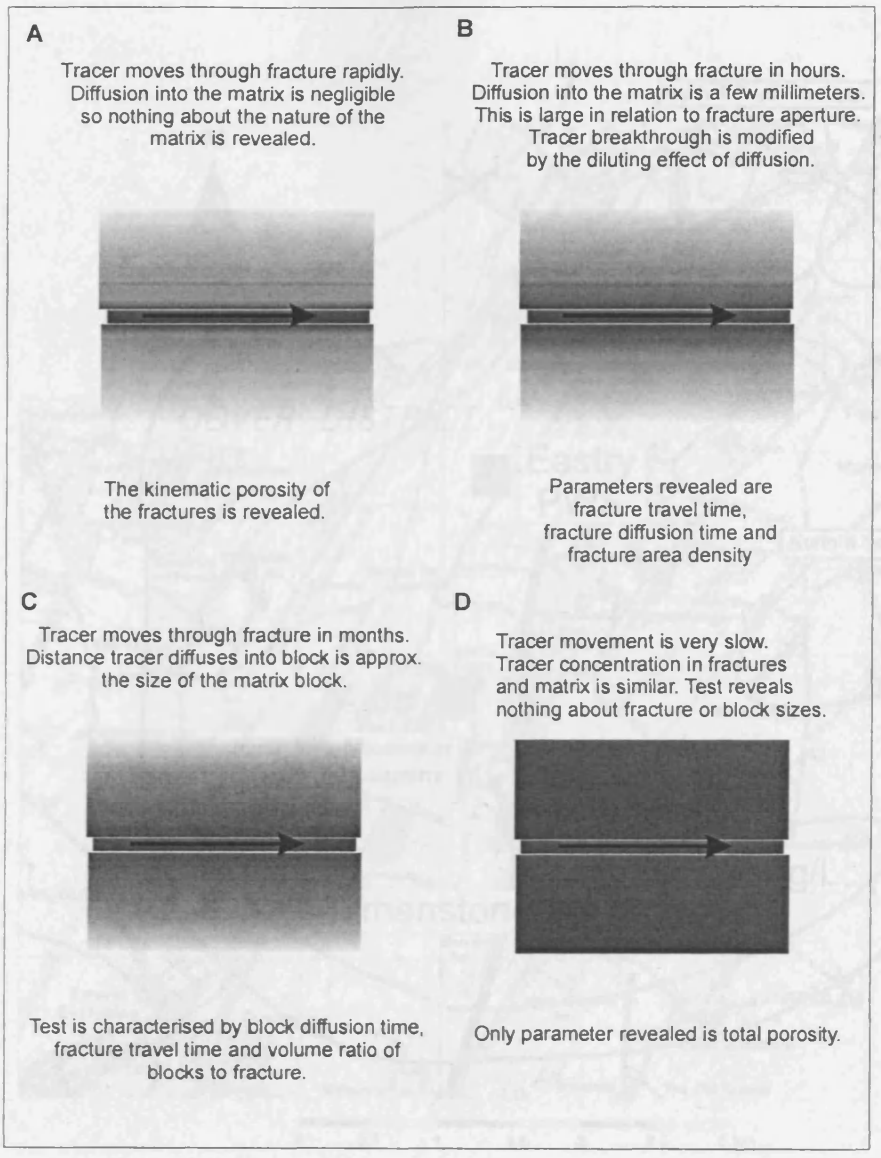

Figure 2-11 Tracer test regimes in fractured media, *after* Ward *et al.* (1998).

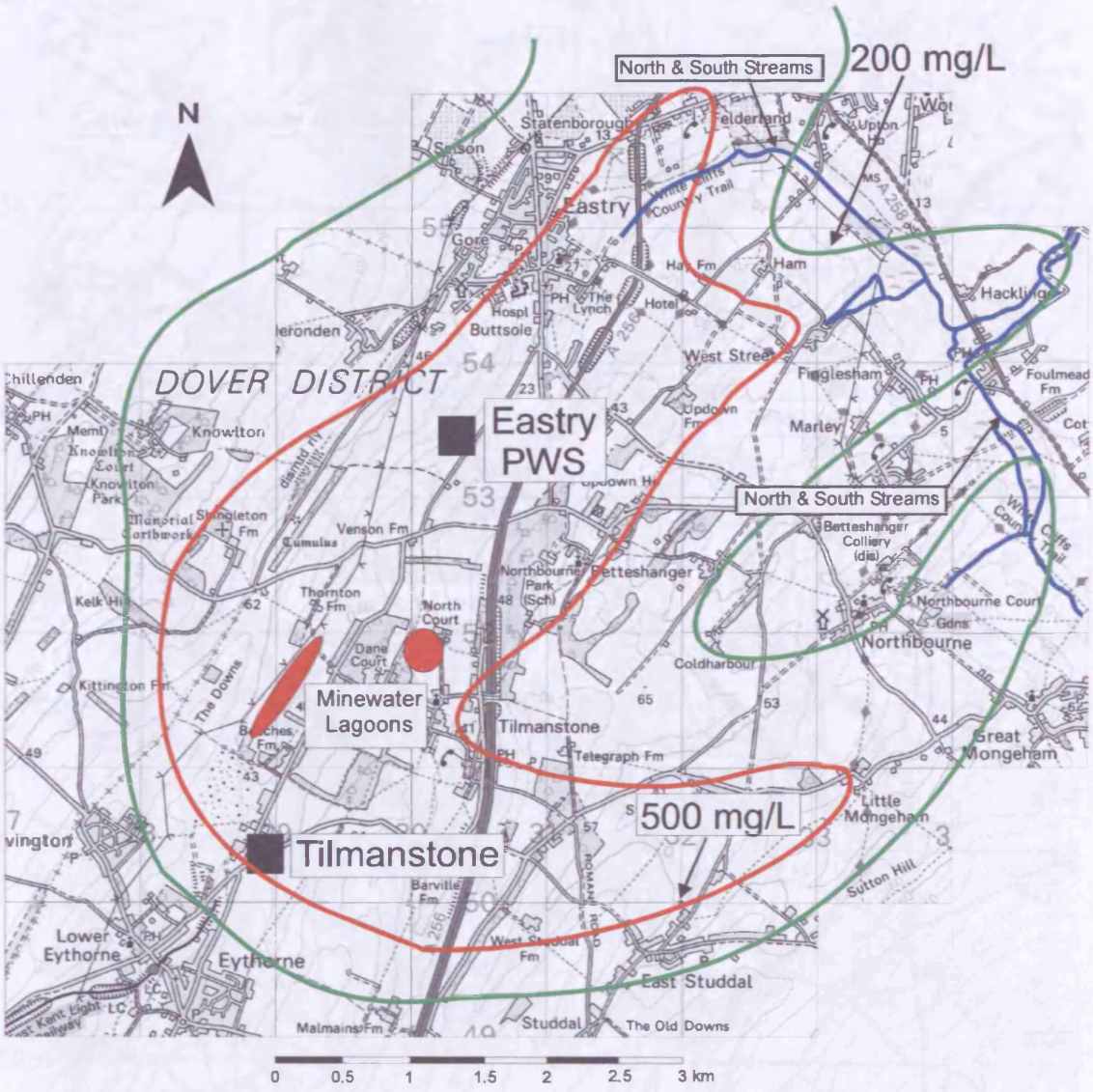

Figure 2-12 Chloride concentration contours demonstrating the extent of high chloride groundwater in 1974.

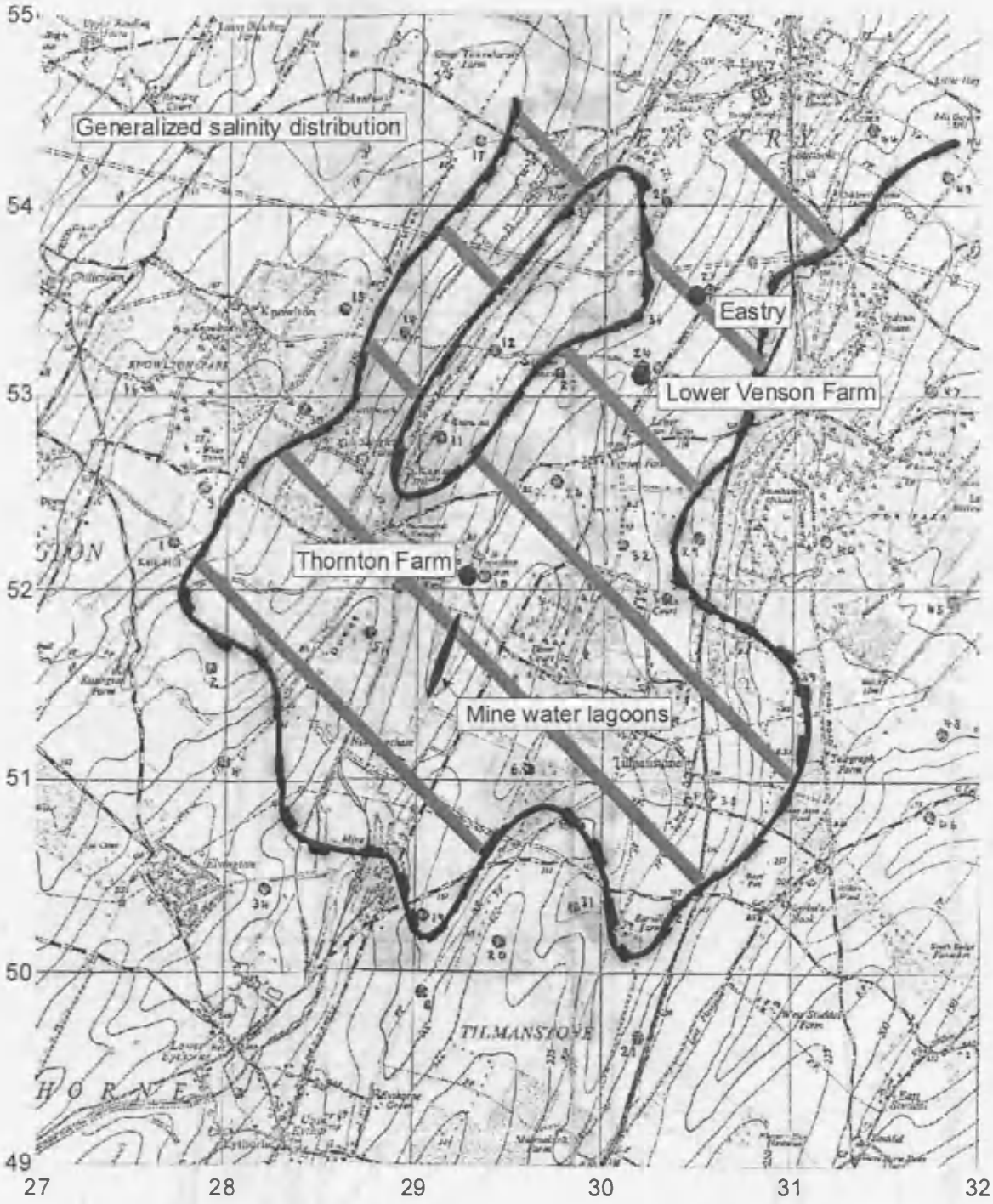

Figure 2-13 Tilmanstone resistivity survey 1973.

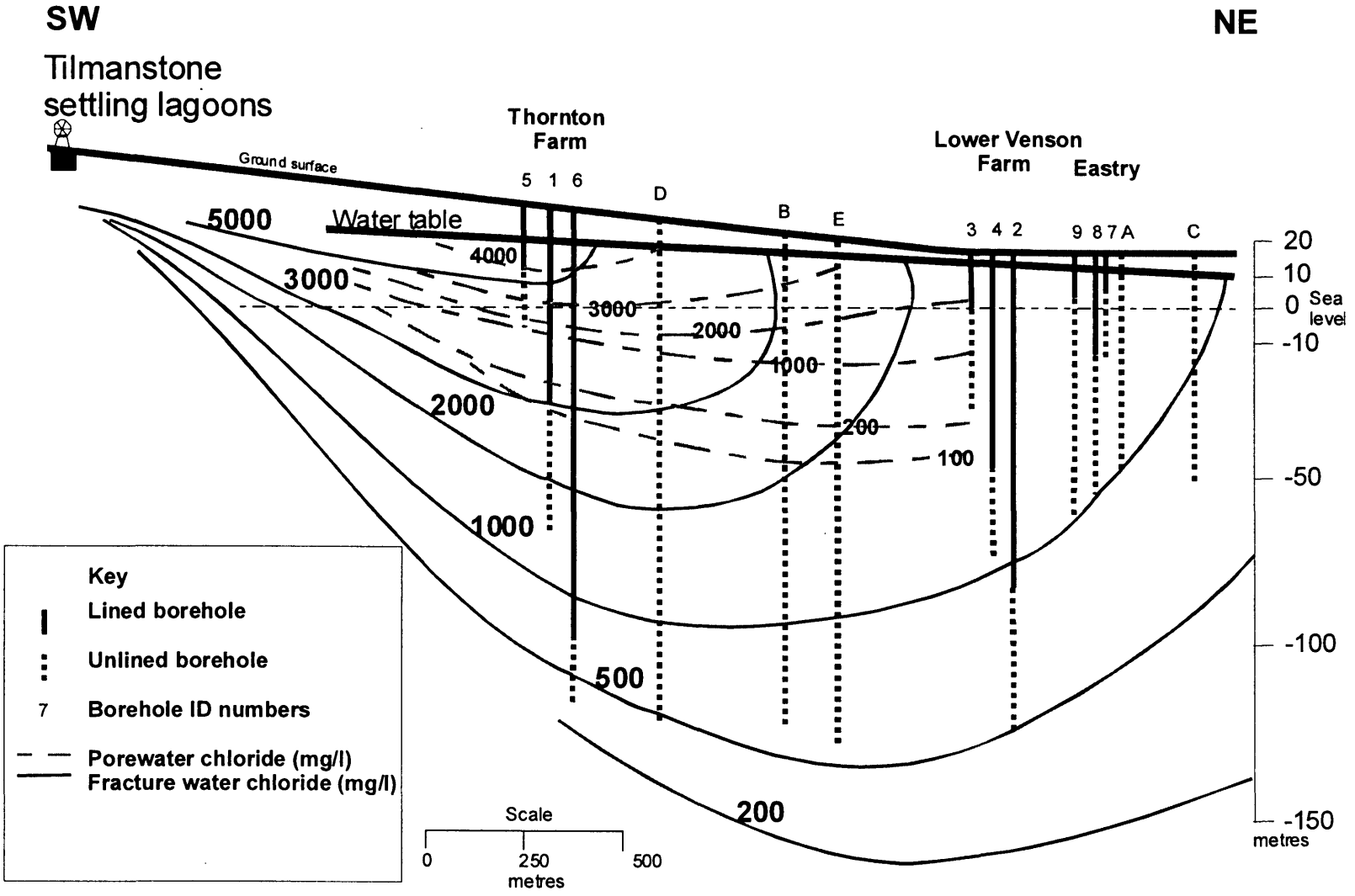

Figure 2-14 Interpretation of chloride distribution from 1970s investigations *after* Headworth *et al.* (1980).

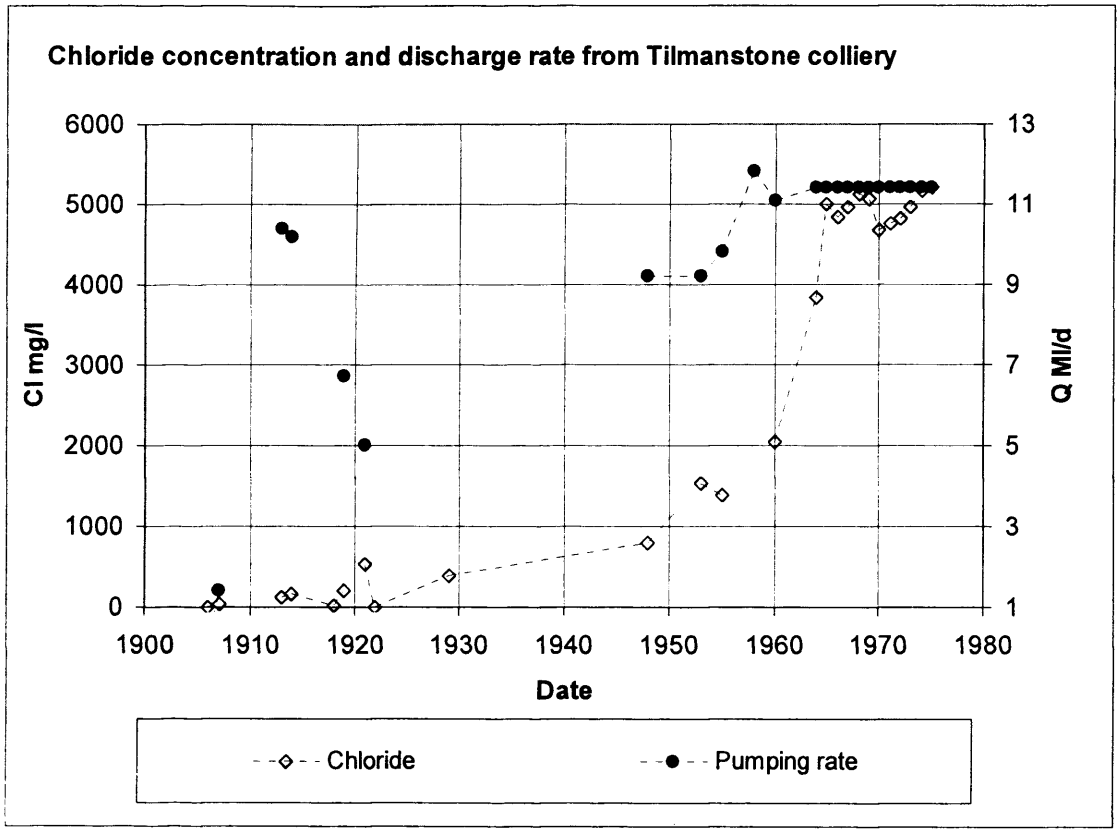

Figure 2-15 Quantity and quality of disposed minewater (*after* Headworth *et al.* 1980).

Note the majority of high chloride concentration and high quantity infiltration occurs after the mid 1950's.

3 Geology and Hydrogeology

The aim of this chapter is to review the geological and hydrogeological framework of the study area. Subsequent chapters will interpret data from field investigations and consider them in the context of this framework.

The chapter describes the stratigraphy and structure of the study area from the Carboniferous Limestone to the Cretaceous Chalk Group. It reviews in more detail the tectonic setting, stratigraphy, lithology and structure of the Chalk Group that is encountered by the boreholes constructed within the Tilmanstone - Eastry valley. Pertinent hydrogeological data for the study area are reviewed.

3.1 General

The area studied is located on the dip slope of the North Downs, to the south-east of Canterbury and north of Dover, in the south-east of the UK, Figure 3-1. The area is now predominantly agricultural, with some light industry. From 1900 to approximately 1980 the area had extensive coal mining operations, with pit-heads located at Chislett, Tilmanstone, Betteshanger and Snowdown. The landscape is classic chalk lowland, having dry valleys terminating with springs and chalk streams. Much of the area from the springs of the North and South Streams to the coast is designated as a Site of Special Scientific Interest (SSSI), Special Area of Conservation (SAC) and protected under the Ramsar Treaty (http://ramsar.org/key_sitelist.htm, accessed 20.09.2002). Most of these conservation measures are to protect bird populations attracted by the marshy areas of Hacklinge Marsh and further to the north, at Minster Marshes and Pegwell Bay. Management agreements between landowners and English Nature exist to maintain summer water levels in the North and South Streams through reducing over-abstraction. The coast-line is formed by the high white cliffs of the Chalk at Dover, which fall with the dip of the Chalk along the coast to the north where dune deposits, for example at the Royal Cinque Golf course, near Sandwich, provide a coastal barrier.

3.2 Geology

Table 3-1 details the strata proven in the area.

Table 3-1 Stratigraphic sequence (*after* BGS 1988)

PERIOD	FORMATION	
PALAEOCENE & EOCENE	Oldhaven Beds (up to 1.5 m)	
	Woolwich Beds (up to 9 m)	
	Thanet Beds (31 m) Bullhead Bed	
CRETACEOUS	UUUUUUU Unconformity	
	Upper Chalk (up to approximately 116 m)	
	Middle Chalk (approximately 70 m)	
	Lower Chalk (approximately 64 m)	
	Gault (30 to 48 m)	
	Lower Greensand (10 to 26 m)	
	Wealden (0.5 to 18 m)	
JURASSIC	UUUUUUU Unconformity	
	Corallian (0 to 34 m)	
	Oxford Clay (0 to 41 m)	
	Kellaways Beds (0 to 16 m)	
	Cornbrash (0 to 8 m)	
	Forest Marble (0 to 6 m)	
	Great Oolite (0 to 31 m)	
	UUUUUUU Unconformity	
	Lias (0 to 6 m)	
CARBONIFEROUS	UUUUUUU Unconformity	
	Upper Coal Measures (up to 732 m)	
	Middle Coal Measures (110 to 152 m)	--M---M-- Marine Bands
	Lower Coal Measures (61 to 85 m)	
	UUUUUUU Unconformity	
	Carboniferous Limestone (up to 48 m)	

A geological map is provided in Figure 3-2, showing the distribution of solid and drift deposits across the area studied.

3.2.1 Carboniferous

Carboniferous Limestone

The oldest rocks proven in the area are from the Carboniferous Limestone. No complete drilled section exists, hence their thickness is unknown. It is, however, estimated that up to 300 m of rock of Dinantian age exists and geophysical evidence

suggests a slight eastward thickening (BGS 1988). The rocks include calcite-mudstones, oolitic limestones and bioclastic limestones. Thin interbeds of mudstone, siltstone or sandstone have also been noted. Possible dolomitisation has been recorded and some of the darker limestones are carbonaceous. Some limestones have small sparry calcite lined cavities with apparent oily inclusions. Calcite veins and stylolite sutures are commonly developed in the limestones on joints and tension gashes. In some cores the limestone surfaces are fissured and infilled by overlying sediments to a few metres.

Coal Measures

Unconformably overlying the Carboniferous Limestone sequence, the Coal Measures comprise mudstones, silty mudstones, siltstones and sandstone with coal seams and seat earths. Fourteen coal seams are recognised in the sequence in Kent. It was the Coal Measures that were the source of the brine that currently pollutes the groundwater of the Tilmanstone- Eastry valley. The Coal Measures lie in an elongated WNW-ESE synclinal basin. The basin limits are not well defined and may be partly faulted. Boreholes suggest that the basin may comprise two subsidiary troughs that are separated by an anticlinal structure located to the south-west of the former Tilmanstone colliery. The deepest part of the northern trough lies between Waldershare and St Margaret's-at-Cliffe, where at least 860 m of Coal Measures have been drilled through.

3.2.2 Jurassic

A wedge of relatively thin Jurassic strata sits unconformably over the Carboniferous sequence. It thins northwards over the London-Brabant massif. Many of the borings undertaken for the coal mining provide information on the Jurassic geology and hydrogeology. The series comprises Liassic limestones, clays and shales followed by the oolitic and sandy limestones of the Great Oolite. This is overlain by dark mudstones and hard limestones of the Forest Marble formation. More limestones from the Cornbrash follow, usually capped by a marly clay. These levels produced considerable quantities of water and caused problems with the operation of the coalmine due to water ingress into the shafts. Above the Cornbrash are the Kellaways Beds, a sequence of sandstones and clays and 40 m of Oxford Clay. This is followed by the Corallian sequence of limestones sandwiched between clays and marls.

3.2.3 Cretaceous

At the base of the Cretaceous sequence the Wealden Formation unconformably overlies the Jurassic. Reactivation of older faults in the late Jurassic produced a block-faulted terrain in the area that was substantially eroded prior to deposition of the earliest Cretaceous rocks. Up to 18 m of coarse pebbly Hastings beds and Weald Clay of the Wealden and up to 26 m of Atherfield Clay, Sandgate Beds and Folkestone Beds of the Lower Greensand have been proven. The Wealden and Lower Greensand beds are separated from the Chalk Group by the intervening Gault, which comprises up to 48 m of mudstones.

The Chalk: Recent advances in stratigraphic research

Throughout the 1980's a new stratigraphy for the Cretaceous Chalk in the UK was proposed. Initially two separate sequences were suggested for the South Downs (Mortimore 1986a) and North Downs (Robinson 1986). However, key marker horizons for both sections were recognised and the Upper Cretaceous Chalk in the North and South Downs was reconciled into one stratigraphy (Mortimore 1987; 1997; Bristow *et al.* 1997). This new stratigraphy also links southern England's Chalk sequence to that occurring elsewhere in Europe, and to some extent world-wide (Mortimore and Pomerol 1987).

Individual flint bands and marls seams have been traced over hundreds of kilometres and geophysical logging can be used to identify these layers (Barker *et al.* 1984; Mortimore 1986b; Mortimore and Pomerol 1987). Table 3-2 summarises the detailed lithostratigraphy for the Chalk Group encountered in the study area (after Mortimore 1997 and Bristow *et al.* 1997).

Tectonic setting for chalk deposition

The Chalk in north Kent is at the edge of the Anglo-Paris Basin / London Brabant Massif. The period of chalk deposition was one of tectonic stability. The two main controls that allowed the massive development of chalk were the rise in sea level and the lack of erosion on the land, which meant that terrigenous input was progressively reduced (Hancock, 1993). This second condition is demonstrated in the Lower Chalk where a reduction in clay content is seen from 30% at the base to 10% at the top of the formation.

Chalk deposited in basinal regions is thicker than that deposited over stable platforms. Jefferies (1963) recorded examples of rapid lateral changes in unit thicknesses across single basins by examining the Plenus Marls. Over the 45 km from Beachy Head to Steyning in Sussex the thickness of the Plenus Marls halves. The extent of these differential vertical movements within basins has been revealed by the detail of chalk lithostratigraphy provided by Mortimore and Pomerol (1987, 1991).

Table 3-2 Chalk stratigraphic units (*after* Mortimore 1997 and Bristow *et al.* 1997)

FORMATION	MEMBERS/BEDS		KEY BOUNDARY MARKERS
Upper Chalk	Seaford Chalk	Haven Brow	
		Cuckmere	*Bedwell's Columnar Flint*
		Belle Tout	*Seven Sisters Flint Band*
	Lewes Nodular Chalk	Shoreham	
		Beachy Head	*Shoreham Marls*
		Light Point	
		Beeding	
		Hope Gap	
		Cliffe	
		Navigation	*Navigation Marls*
		South Street	*Dover Top Rock*
		Kingston	*Dover Chalk Rock*
		Ringmer	*Bridgewick Marl & flints*
		Caburn	*Caburn Marl*
		Glynde	*Southerham Marl* *First nodular chalk*
Middle Chalk	New Pit Chalk Member		*Glynde Marls*
	Holywell Nodular Chalk Member		*Gun Gardens Main Marl*
	Melbourn Rock		*Foyle Marl*
Lower Chalk	Plenus Marls Zig Zag Chalk		*Tenuis Limestone*
	West Melbury Marly Chalk Glauconitic Marl		

It is likely that there has been significant reactivation along underlying (Variscan) tectonic features such that lateral variations in lithology correspond to underlying tectonic structures. Mortimore and Pomerol (1991) examined this variability in the South Downs. They used seismic sections that reveal the deep tectonic structure beneath the Chalk. Where they had detailed knowledge of the overlying Chalk they

were able to reconcile major changes in lithology and thickness with the position of underlying tectonic lines or deep faults (Mortimore *et al.* 1996). Comparing isopachyte and lithofacies data to structure contours indicates key hinge-lines across which thickness changes abruptly and unusual lithologies, including hardgrounds and channel scours, are located. These ancient tectonic faults and thrusts, generated in the basement rocks, influenced sedimentation by creating local basins and highs as well as by controlling the position of marginal platforms. This has a strong influence on the position of soft and hard chalks (Mortimore 1990, Hancock 1993).

Chalk stratigraphy and bed characteristics

The Chalk Group encountered by cored boreholes within the study area range from the Cenomanian New Pit Chalk Member to Coniacian Seaford Chalk (Table 3-2). A brief description of the various units relevant to the present research is given below.

Lower Chalk - overview

The formation is approximately 80 m thick near to Dover and consists of dark grey marly chalk overlain by greyish white, more massive chalk. The Foyle Marl at the boundary between the Plenus Marls and the Melbourn Rock marks its upper limit.

Chalk Members and Beds proven in the Tilmanstone - Eastry valley Lower Chalk: Plenus Marls

The sequence of marl bands forming the Plenus Marls is the lowest horizon intersected by a borehole in the research area (Lower Venson Farm BH2). They are relatively incompetent, thick greyish green marls sandwiched between more competent chalk (the Zig Zag Chalk and the Melbourn Rock).

Middle Chalk

Melbourn Rock

This is a very hard, extensively fractured rock. The base of it forms the boundary marker for the base of the New Pit Chalk Member and the Lower Chalk / Middle Chalk Formation boundary. The transition from Cenomanian to Turonian is marked by the top of the unit. The Melbourn Rock is considered to be a good water producing horizon and this is most likely related to the combination of fracturing and to the presence of underlying low permeability horizons. The fracturing produces well-connected

pathways, able to collect water from the overlying horizons and, as it is prevented from travelling through the underlying deposits, it becomes channelled towards boreholes within the Melbourn Rock.

Holywell Nodular Chalk Member

The top of this sequence is marked by the Malling Street Marls. Lithological marker bands in the Melbourn Rock and Holywell Nodular Chalk Member recognised in the South Downs are absent from the North Downs due to condensation (Mortimore, 1987).

New Pit Chalk Member

These are massive beds with conspicuous marl seams. A characteristic feature of the beds is the intense, steeply inclined fracturing which dissipates along the marl seams. The marls are thick and plastic with a brittle texture. The chalk of both the Holywell Nodular and New Pit Chalk Members is very soft to medium hard.

Upper Chalk

Glynde Marl

The Glynde Marls comprises black, plastic clays, typically 0.05 to 0.1 m thick. The first Glynde Marl (GM1) is overlain by chalk with marl seams. Wray (1995) shows that many of the key marker marl seams originated as volcanic ash-fall tuffs (for example the Glynde 1, Southerham 1, Caburn and Bridgewick 1 Marls).

Lewes Nodular Chalk

The base of the Lewes Nodular Chalk is now taken at the base of the first nodular layer, rather than the Glynde Marl 1 (Mortimore, 1997; 1986a). The formation is marked by regular seams of nodular chalk and flint. This is a distinct lithological change from the New Pit Chalk Member. Typically, bands of red, iron-stained nodular layers are also seen.

Southerham Marl

The basal surface of the marl marks the Glynde / Caburn Beds boundary. It is a plastic marl with underlying flint horizons.

Caburn Marl

The basal surface of this defines the Caburn / Ringmer Beds boundary. There is a sequence of nodular beds and flints. The flints are typically pink, small and carious.

Bridgewick Marls and flints

The basal surface of the first marl marks the Ringmer / Kingston Beds boundary.

Dover Chalk Rock (Kingston Hardgrounds)

The Chalk Rock sequence in the East Kent area consists of approximately 1m of nodular lumpy chalk with bands of large flints at its upper and lower surface. Smaller flints occur in between. This sequence of hardgrounds is typically fractured, due to being more brittle, and this tends to produce a higher permeability than the softer chalks.

Dover Top Rock (Navigation Hardgrounds)

The Dover Top Rock is an approximately 0.5 m thick band of yellowish nodular chalk with an upper hardground surface.

Navigation Marls

The base of the first marl in this sequence marks the Turonian / Coniacian boundary. The marls are seen at outcrop at the southern end of St Margarets Bay and comprise two marls, flints and hardgrounds.

Shoreham Marls

This is a persistent marker bed throughout much of southern England. It is well defined in geophysical logs, producing a distinctive response on gamma and resistivity logs, demonstrated for example in Figure 3-3. The upper marl marks a major change in chalk sedimentation. The conspicuous iron-stained nodular chalks are replaced by homogenous, pure white chalks with prominent flint seams.

Seaford Chalk

The Lewes Nodular Chalk / Seaford Chalk boundary is taken at the top surface of the upper Shoreham Marl. These white, more pure, chalks produce a uniform development of joint systems and fracture frequency due to the lithology change. Two, regular, close-spaced (60 - 200 mm) to medium-spaced (200 - 600 mm) joint sets produce a characteristic blocky appearance. The chalk is soft to medium hard and this, combined with its high purity, produces a greater tendency for karstic or solution feature development than in softer chalks.

Belle Tout Beds

These form the basal beds of the Seaford Chalk. They are marked by three marl bands.

Seven Sisters Flint Band

This is a very prominent semi-tabular flint band seen clearly running across St Margarets Bay, as well as many other locations along the coast. It is 0.25 to 0.3 m thick and the top surface of it is taken as the Belle Tout / Cuckmere Beds boundary.

Cuckmere Beds

The Cuckmere Beds form the uppermost bed of the Seaford Chalk seen in the Tilmanstone area.

Structural features in the Chalk

Hercynian structures occur throughout southern England (Hancock 1993) and structural development following older Hercynian structures continued to affect sedimentation of the Chalk throughout the Cretaceous. East-west structures are controlled by northwest - southeast strike slip shears, i.e. the east-west structures are terminated by the northwest-southeast structures, see Figure 3-4. These structures are catalogued in oil company records, which are not generally available (Mortimore, 1999 *pers comm.* Geological Society, South-East Regional group meeting).

In the Tilmanstone – Eastry area the beds dip gently to the northeast at 0.5 to 1°. Sub-horizontal joints are common in the marly layers whereas vertical joint sets are more prevalent in the harder chalk bands. The marl bands, due to their more plastic nature, have tended to dissipate stresses sub horizontally. This has caused fractures in any overlying hard rock to open as a result of tension, for example in the Melbourn Rock overlying the Plenus Marls.

Weathering of Chalk

The degree to which chalk breaks down or disintegrates is controlled by its lithology. Harder chalk layers retain a blocky structure, and marls and sheet flints have tended to act as breaks to the degree of weathering. Heave structures have been produced by freeze-thaw action during periglacial conditions throughout the Quaternary acting on fully saturated chalk. This has reduced blocky chalk to a soft paste (putty chalk). Putty chalk is not uniformly present due to its lithological control and also other factors that

may have influenced the extent of weathering. Where found it is commonly around 1 – 2 m thick. High porosity chalk is very susceptible to frost action and disintegrates to a silty grain size during freeze-thaw cycles.

3.2.4 Tertiary

The Tertiary sequence is dominantly marine. Sediments were deposited in a marine to marginal marine environment in a basin that now includes south-east England, the Paris Basin and part of Belgium. The sequence comprises the Palaeocene Thanet Beds, Woolwich Beds and Oldhaven Beds overlain by the Eocene London Clay. The Thanet Beds commence with the clear marker of the Bullhead Bed comprising green patinated flints up to 0.3 m in diameter. The sequence generally comprises sands, often with flint pebbles, clays and marls.

3.3 Hydrogeology

The main aquifer for the area is the Chalk. It forms the higher ground of the North Downs, dipping gently to the north-east at approximately 0.5 – 1° (BGS 1988). The aquifer is unconfined over much of the area, becoming confined towards the north-east by Tertiary deposits. Groundwater flow from the aquifer supports baseflows in three main stream / river systems: the North and South Streams, the Nailbourne / Little Stour and the Wingham Stream. Water is abstracted for public supply at ten wells over approximately 210 km^2, of which Wingham has the largest licensed volume (25 Ml/d) and also has an extensive adit system. The area is extensively licensed for agricultural abstraction, although this is predominately for surface waters. Surveys conducted in the 1970s, using infra-red techniques, indicated little or no outflow from the aquifer at the coastal boundary (SWA 1976c). Disposal of water from coal mining impacted groundwater in the Snowdown – Wingham valley, as well as the Tilmanstone - Eastry valley. The chloride concentration at Wingham started to rise in 1925 – 1926, peaking in 1936 and falling rapidly once disposal practices were altered (Bibby 1979). The region was considered in need of increased supply for public consumption for many years (ACER 1990a). Proposals for a reservoir at Broad Oak were made as along ago as the 1970s (Kent County Council 1976), but the proposals were shelved. The droughts in 1991 – 1992 brought the deficit into sharp focus again and Southern Water developed plans to bring Eastry PWS online using desalinisation to reduce the chloride concentrations (The Guardian, 1996). European and UK legislation and regulation intervened however, and environmental protection became the underlying driver for

policy. Southern Water eventually surrendered their license for abstraction at Eastry PWS, becoming one of the first water companies in the UK to do so under the conditions imposed by the Habitats Directive.

3.3.1 Recharge

In order to formulate a water balance for an aquifer it is necessary to quantify the volume of water entering the system through rainfall recharge (Ward and Robinson, 1989; Rushton and Ward 1979). Not all rainfall will become recharge so it is necessary to identify the features that will affect recharge estimation. In this section different approaches to estimate recharge, undertaken by previous workers for the Tilmanstone area, are reviewed.

The Kent River Authority Section 14 survey uses the simple relationship:

average rainfall – average actual evaporation = average infiltration

744 mm – 474 mm = 272 mm

This value was used by WRc when modelling the Tilmanstone plume (Bibby 1979).

ACER (1991) used a conventional soil moisture balance approach (Rushton and Ward 1979) for a groundwater flow model of the East Kent aquifer, but recognised that the estimation of recharge should reflect the effects of drift cover and elevation on the availability of recharge to the aquifer. The soil moisture balance was therefore modified according to the type of aquifer or drift cover and elevation. Three elevation zones were identified, as the intensity of rainfall varies with elevation:

Zone 1: elevations less than 70 m aOD
Zone 2: elevations between 70 and 130 m aOD
Zone 3: elevations greater than 130 m aOD

Four aquifer / drift cover types were identified; Head, Clay with Flints, Alluvium and Chalk. Table 3-3 gives the average annual recharge calculated for the zones and cover types.

Table 3-3 Average annual recharge (mm a^{-1}) for East Kent model (*after* ACER 1991)

Zone	Head	Clay-w-flints	Alluvium	Chalk
Zone 1 <70 m	267	279	267	277
Zone 2 70 – 130 m	298	309	298	308
Zone 3 >130 m	335	346	335	345*
* note that for the current area modelled no Chalk outcrop is found for Zone 3				

For the low lying Chalk there is very little difference between the recharge values used by ACER and the Kent River Authority. The differences arise for the areas with drift cover, and at higher elevations. It should be noted that the recharge from the clay-with-flints is greater than that for the exposed Chalk. This is because the clay-with-flints is assumed to allow recharge throughout the year, at a steady rate of 0.1 mm d^{-1}. Figure 3-5 shows the current area studied with the 70 m and 130 m aOD contours being used to define the change in the recharge zone value for a particular cover type.

Three recharge cover types are marked (alluvium and head are combined as the average annual recharge is the same for both) and the cover type changes colour where the elevation zone changes. Table 3-4 gives the areas covered by each cover type for each elevation zone.

Table 3-4 Area covered by cover type, in each elevation zone

	Head & Alluvium	Clay-w-Flints	Chalk
Zone 1 <70 m	4×10^7 m^2	3.13×10^5 m^2	6.13×10^7 m^2
Zone 2 70 – 130 m	2.38×10^7 m^2	9.63×10^6 m^2	4.62×10^7 m^2
Zone 3 >130 m	3.75×10^5 m^2	3×10^6 m^2	
Total	6.42×10^7 m^2	1.3×10^7 m^2	1.08×10^8 m^2

The volume of recharge attributable to each cover type is given in Table 3-5.

Table 3-5 Volume of annual recharge attributable to each cover type (m^3)

	Head & Alluvium	Clay-w-Flints	Chalk
Zone 1 <70 m	1.07×10^7	8.72×10^4	1.7×10^7
Zone 2 70 – 130 m	7.1×10^6	2.97×10^6	1.42×10^7
Zone 3 >130 m	1.26×10^5	1.04×10^6	
Total	1.8×10^7	4.1×10^6	3.12×10^7
Grand Total	5.32×10^7 m^3		

As a comparison, for the same area, the Section 14 survey value of 272 mm would produce 5.02×10^7 m^3 of recharge, which is 2.99×10^6 m^3 less.

Table 3-6 gives the ratio of the average annual recharge to the average annual rainfall for each cover type and elevation zone (Head and Alluvial deposits combined).

These ratios are used in the numerical modelling in Chapter 6 to calculate recharge from annual rainfall data, as the data necessary to calculate recharge at the detail recommended (Jackson and Rushton, 1987), for example rainfall and evapotranspiration at daily or 10 daily frequency, were not available.

Table 3-6 Average annual recharge to average annual rainfall ratio

	Head & Alluvium	Clay-w-Flints	Chalk
Zone 1 <70 m	0.36	0.38	0.37
Zone 2 70 – 130 m	0.38	0.4	0.39
Zone 3 >130 m	0.41	0.42	No Chalk outcrop in current model at this elevation

The approach adopted in the current research is therefore a compromise between applying a blanket value for recharge and incorporating distributed recharge into the numerical modelling.

3.3.2 Surface water

An understanding of the surface water flow regime is required for water balance calculations and in order to provide calibration targets for groundwater modelling.

Surface water courses in the Tilmanstone – Eastry area rely for a large component of their flow on discharging groundwater. The main surface water features in the area are the North and South streams, the Nailbourne and the Wingham River. The lower reaches of the Nailbourne become the Little Stour at Wickhambreau (NGR 6221 1586) and the Wingham Stream joins the Little Stour approximately 1.5 km below this point.

As shown in Figure 3-6, the North and South streams are located at the north-eastern end of the Tilmanstone – Eastry valley. The spring lines and upper reaches of the streams form a line running north-west to south-east along the edge of the Tertiary outcrop. After rising from a series of small springs they interconnect with a complex series of drainage ditches and aqueducts. At some points the streams flow over the top of each other, contained in concrete or brick channels. Downstream of this, in the area of Hacklinge Marshes (Figure 3-6), the streams flow below Ordnance Datum. The stream and ditch network join at Roaring Gutter and are raised to above sea level by pumping, before flowing along a drainage canal or dike to join Sandwich Haven and flow out to sea. The Coal Board previously ran this control pumping as the area has been affected by subsidence associated with mining activities. No records of the quantity of water pumped were kept. More recently the pumping has been taken under the control of the Environment Agency. They maintain a record of hours of pump operation and this can be converted to volumes pumped.

The North and South Streams are heavily licensed for water abstraction for agriculture. The entire Hacklinge Marsh area is farmed, much of it with high water demand salad crops. As well as the control on the flow of water in these streams created by the pumping at Roaring Gutter, the upper reaches have wooden baffles or weirs across them. Farmers can raise and lower these to control water during the summer months in order to ensure a supply of water for irrigation. These controls on the system make accounting for the water difficult. A stage-discharge relationship is impossible to establish. The Environment Agency maintains gauging stations at points along the system and undertakes flow measurement. A summary of data obtained from the Environment Agency for the period 1972 to 1992 for the Hacklinge gauging point is presented in Figure 3-7. For clarity only monthly totals for October, January, April and July are presented. The location of the Hacklinge Station is shown on Figure 3-6 and

the station represents the combined flows for the northern branch of the North and South Streams.

The data show a declining trend in stream volumes. However it is not clear what may be causing this. Management of the drainage network is complex as license holders operate a wooden baffle dam system to ensure adequate storage of water. Since the early 1990s English Nature have established a number of management agreements aimed at maintaining summer water levels throughout the marsh area to support aquatic ecosystems. It is not clear what the impact of these management agreements has been, although they might be expected to lead to raised water levels in the downgradient reaches of the system and lowered water levels in the upper reaches, which might appear as a relative increase in flows from upper reaches to lower reaches. At the same time, the Environment Agency manages the lower area of the Hacklinge Marshes as a winter holding area for storm water, to prevent flooding of Sandwich. From a management point of view their ideal situation would be to have the marshes drained as low as possible for the start of the winter to maximise their storage potential – the opposite aim of the English Nature agreements. Some of the decline in streamflow is likely to be as a result of the cessation of input into the system from the mine water lagoons. There is also a large variability in the monthly flows between years.

The Environment Agency have undertaken a water balance calculation for the Hacklinge Marshes, for the period April 1997 to September 1997, in order to determine if the resource is over-licensed. The results of their analysis are summarised as monthly totals in Table 3-7. These data represent the combined flow of the northern and southern branches of the North and South Streams at the Roaring Gutter pumping point.

Table 3-7 Flow at Roaring Gutter April – September 1997

	April	**May**	**June**	**July**	**August**	**September**
Approx. monthly total (m^3)	8.7 x 10^5	7.66 x 10^5	8.22 x 10^5	1.04 x 10^6	7.56 x 10^5	9.58 x 10^5
Average daily flow over period ($m^3 d^{-1}$) 2.88 x 10^4 (28.8 Ml d^{-1})	Average weekly flow over period ($m^3 w^{-1}$) 2.01 x 10^5					Total flow over period (m^3) 5.43 x 10^6

SWA calculated a water balance for the area during the investigations undertaken in the 1970s. For the period 1963 – 1974, a flow of 36.29 Ml d^{-1} is calculated for the North and South Streams, see Figure 3-8 for annual data. These data were obtained through regular flow gauging, since 1962, at Hacklinge Road and Adelaide Bridge gauging points. These data are probably a best estimate for outflow from the valley, but it is important to remember that over the record period the flows would have been enhanced due to the additional input from the mine drainage lagoons. SWA deduct 11.35 Ml d^{-1} from the average value to remove the effects of the mine-water input. They then add 10% to allow for surface runoff from the surrounding area, giving an average flow of 27.43 Ml d^{-1}. The addition of 10% to the flow calculation is probably not unreasonable, given that much of the land immediately surrounding the North and South Streams comprises alluvial sediments.

Flow in the Wingham River is also gauged by the Environment Agency. Inspection of the gauging station at Durlock (NGR 6275 1576) revealed a rather under-sized structure and at high flows water over-tops the sides of the engineered channel. This will considerably reduce the accuracy of any stage-discharge relationship developed for the Durlock gauging station at higher flows. Flows reported by Southern Water during the 1970s investigations, and used by Bibby (1979) for groundwater flow model calibration indicate a flow of 0 – 40 000 m^3 d^{-1}. Acer (1991) also modelled groundwater flow in the region using a stream flow of 5000 to 25 000 m^3 d^{-1} for the Wingham River and 4000 to 27 000 m^3 d^{-1} for the Well Chapel Springs (which flow into the Wingham River).

Flow in the Nailbourne River generally only occurs below Bishopsbourne (NGR 6189 1526). The river is marked on the OS map as far as Lyminge, but the upper reaches remain dry except in exceptionally wet years.

3.3.3 Groundwater levels and gradients

The Environment Agency Southern Region provided the data used to assess water-level variation and regional hydraulic gradients for the area studied. A complete set of the EA's observation borehole records up to 1999 for Kent was made available. A sub-set of these observations, from boreholes relevant to the area studied, has been assessed for length of record, reliability of record, location of observation borehole, usual range of

water level recorded in the observation borehole and periods of particularly high or low water level.

Regional overview

The earliest usable, continuous water-level records in the dataset date from 1949. Two records of observations exist for 1927 and 1928 but the water-levels bear no relation to the later observations recorded at the sites, so the early observations have been ignored. The borehole with the longest continuous record is at Knowlton by Dower House (NGR 2790 5340) and the observations start in 1954, continuing until 1999. Observation boreholes have been grouped according to the length of record and Figure 3-9 shows the spatial coverage of observation boreholes for those temporal groupings. After the mid to late 1980s several records display a decrease in the frequency of monitoring. Some boreholes may have been removed from the observation network due to e.g. the phreatic surface falling below the base of the borehole during the summer period.

Groundwater levels in the area range from approximately 60 m aOD in observation boreholes located towards the crest-line of the North Downs to 1 m aOD in boreholes located in the lowland valleys.

Observation boreholes demonstrate seasonal water level fluctuations varying from 10 m in boreholes located towards the North Downs to approximately 2 m in boreholes located in the north east of the area, around the lower reaches of the Nailbourne and Hacklinge Marshes. Drought periods can be picked out in many of the groundwater records, notably for the years 1989 and 1992.

Water-level observations are now described in more detail by dividing the area studied into sub-regions where the groundwater response can be characterised by the records from a few observation boreholes within each sub-region. Figure 3-10 indicates the sub-regions and the locations of the observation boreholes assessed.

The regional hydraulic gradient along the Tilmanstone – Eastry valley is reported by Peedell (1994) as being 0.005, although from measurements of groundwater head from EA data the gradient appears to be 0.0035.

Sub-regional assessments

Area 1

Near to the Nailbourne river. Observation boreholes: Old Palace Bekesbourne (1936 5554); Bramling Bottom (2180 5530); Old Forge Bishopsbourne (1891 5261); Woolton Farm (1867 5682) and Lee Priory (2115 5667), see Figure 3-11. The nearest PWS to Old Forge is Barham (approximately 2km away) and to Bramling Bottom is Wingham (approximately 3 km away).

The observations span 1950 to 1994 (Bramling Bottom); 1968 to 1999 (Old Forge); 1970 to 1999 (Old Palace); (Woolton Farm) and 1973 to 1983 (Lee Priory), see Figure 3-11.

The records have gaps in the observations and examples of the water-level falling below the base of the borehole in dry summers (Old Palace and Old Forge). The observation record indicates declining water-levels through the late 1960s/early 1970s. At Bramling Bottom this trend seems to stop around 1973 and water-levels stabilise. However, from 1988 to 1991/92 water-levels again decline. The observation record from 1950 to 1952 at Bramling Bottom shows a fall in the water-table from approximately 14 m aOD to approximately 12.5 m aOD. This corresponds to a period of increasing abstraction at Wingham PWS (approximately 12000 m^3d^{-1} to 14500 m^3d^{-1}), see Figure 3-12, (historical abstraction for Wingham, Flemings and Woodnesborough), however water-levels observed in the late 1960s are at approximately 13.5 m aOD and this is a period of maximum abstraction (22000 m^3d^{-1}) at Wingham. The record from the observation borehole at Lee Priory demonstrates a slight increase in water-levels over the period 1973 to 1984. The record at Woolton Farm is quite different to the other observation boreholes in this area. The borehole is further from the river and the water-level response observed may be influenced by drift cover. The general range in water-level for this group of observation boreholes is 2 to 3 m.

Area 2

To the south-east of the Nailbourne river. Observation boreholes: Soles Farm Nonnington (2537 5001) and Ackholts Cottages Snowdown (2420 5150), see

Figure 3-13. The topography is higher (ground elevations are approximately 70 to 100m aOD) with steeper valleys.

Both observation boreholes are at the heads of dry valleys. The data are of reasonable quality. Soles Farm is very good from the start of the record in 1971 until 1983, after this the frequency of monitoring reduces, but is still adequate to maintain a good representation of seasonal fluctuation. In contrast the record at Ackholts Cottages is sparse from the start of its record in 1967 until 1981 and is not even adequate to provide a representation of the seasonal fluctuation in the water-table. Following 1981 the frequency of monitoring increases and the record is very detailed through to 1987. The monitoring frequency then decreases, but the record is still very good and seasonal fluctuations are well represented. An overall decline in water-levels is observed in both boreholes over the entire length of their records. Both sets of observations indicate water-level lows in 1972/73; through most of the 1980s; and an exceptional low in 1991/92, following a decline from a water-level high observed for 1987/88. The normal water-level variation is 3 m but exceptionally 5 m is observed.

Area 3

Further downslope, towards the main valley upstream of Wingham PWS. Ground elevations are lower, approximately 40 to 60 m aOD. Observation boreholes: Off Licence Adisham (2250 5340); Ratling Court Aylesham (2399 5372); Whittakers Shop Goodnestone (2550 5450) and Old Court Farm Cottages (2440 5310), see Figure 3-14.

Off Licence and Ratling Court have periods of patchy observations over the record e.g. Ratling Court 1983 to 1987 and Off Licence from 1977 to 1985. A decrease in the frequency of observation occurs at Ratling Court after 1983 but the record of seasonal variation is preserved. The period 1985 to 1996 shows an increased frequency of observation at Off Licence. Both observation boreholes have similar ranges of 19 to 24 m aOD (seasonal range of 5 m). 1991/1992 is a period of exceptionally low water-level. Whittakers Shop and Old Court have continuous records from 1967 to 1983, with a seasonal fluctuation of approximately 2 to 3 m. The records indicate a slight decline in water-levels from 1967 to 1973, but after this time the water-levels seem to stabilise.

Area 4

Eastern part of region studied. The topography is flat and the ground elevation is low, generally 5 to 30 metres above sea-level. The observation boreholes are located in the Chalk but close to the edge of the overlying Tertiary deposits. The main drift deposit in the area is Head, associated with the dry valleys. The nearest PWS is at Sutton (Figure 3-19). The records commented on are for observation boreholes at Ripple Nurseries (3490 4960, record 1967 to 1998); Pixwell Great Mongeham (3460 5100, record 1967 to 1998); Cottington Court (3500 5334, record 1871 to 1998); Updown End Betteshanger (3205 5395, record 1971 to 1998) and Worth Mill (3290 5560, record 1968 to 1981), see Figure 3-15.

The records for Ripple, Pixwell and Updown End display a general decline in the water-level over the period of the observations. The record for Cottington Court however shows a very distinct rise in water-level after 1983. This also coincides with the start of a decreased frequency of monitoring. The most obvious reason for the shift in the hydrograph would be a change in the datum used for measuring the water-level, which is then not accommodated by the database record, or a change locally in abstraction regime. There is no information to shed further light on this, so the data should be treated with caution. The record at Pixwell indicates that the borehole regularly dries in summer months. The shape of the hydrograph at Worth Mill is less spiky than the others considered in this area and this is likely to be due to the presence of overlying drift deposits. The observation boreholes have a range in water-level from approximately 0.25 m aOD to approximately 12.75 m aOD. The seasonal fluctuation observed is in the order of 1 to 5 m.

Area 5

Central area of the region studied. Observation boreholes: Coldblow Nonnington (2730 5240, record 1971 to 1998) and Kittington Cottages (2750 5190, record 1967 to 1983), see Figure 3-16.

The Coldblow observation borehole is located on an interfluve. There is one extremely low water-level recorded in 1985. The observations demonstrate a steady decline in the water-table over the length of the record. The decline appears to be more rapid after 1982. The seasonal fluctuation is approximately 4 to 5 m. The observation borehole at Kittington Cottages is located in a dry valley. The seasonal fluctuation is approximately

3 - 4 m. The record from Kittington Cottages shows a rapid decline in water-levels in 1971/72, which is followed by an apparent increase then decrease in water-levels through the 1970s and early 1980s. This may be a response to the cessation of the mine-water lagoons.

Area 6

This is the dry valley running south-west from Flemings (see Figure 3-19, NGR 2960 5670) and Woodnesborough (NGR 3010 5660) PWSs. The five observation boreholes located in this dry valley: Upper Selson Farm (3020 5540); Hammil Cottages (2900 5530); Walnut Tree Cottage (2850 5510); Rowling Cottages Aylesham (2770 5443) and Knowlton by Dower House (2790 5340)) all have records that show a decline in water-levels from around 1970, see Figure 3-17. The seasonal fluctuation observed is approximately 3 m.

Summary

The groundwater level records from the observation boreholes in the area studied demonstrate seasonal fluctuations typical of a Chalk aquifer. The observation coverage, both spatially and temporally, provides adequate information to characterise groundwater level gradients and fluctuations. Variability in response is seen between observation boreholes located in low-lying areas, those located in upland areas, boreholes located in valleys and those located on the interfluve areas of the region studied. The effect of variation in groundwater abstraction is observed in some groundwater level records as is the change in groundwater level due to cessation of infiltration from the mine-water disposal lagoons at Tilmanstone.

Limitations of the data include the use of boreholes drilled for domestic boreholes as observation boreholes. It is seen that these are often inadequate in years when particularly low groundwater levels occur, arguably the most important time to be able to monitor groundwater levels. The use of these boreholes also tends to under-represent groundwater level changes in interfluves areas. Variation in the water-table due to valleys and interfluves is not well represented by the data.

The observations are useful for providing calibration data for regional groundwater flow models although the models should also be calibrated to flow data.

Carneiro (1996) undertook detailed analysis of groundwater gradients, concluding that no significant change has occurred in the hydraulic gradient since at least 1978 and that changes reported by Peedell (1994) were due to reductions in the numbers of boreholes sampled and reliance on automated contouring of water levels. However, reductions in groundwater levels in observation boreholes close to the mine water lagoons indicate that the recharge mound created by the mine discharge water infiltration gradually dissipated over approximately 5 years and this would have influenced the hydraulic gradient locally.

3.3.4 Mine-water discharge

Saline mine-water, which was pumped from the working coal levels, was discharged to disposal areas. These disposal areas included ditches, ponds and lagoons. Figure 3-18 indicates the location of these discharge areas.

The disposal areas are all located directly on the Chalk aquifer. No lining of the lagoons is reported and the main concern was that fines would settle on the base, reducing the infiltration capacity. The largest area is formed by the lagoons immediately to the south of Thornton Farm. The quantity and chemistry of the waters discharged to the lagoons is not well documented. The quantity and quality of the water pumped from the mine varied according to the levels that were being worked.

Table 3-8 provides the estimated quantity of mine-water discharged to the lagoons and ponds as presented to the Public Inquiry into the groundwater pollution from the coal-mine activities (Southern Water Authority 1976a).

Table 3-8 Minewater discharge *after* SWA Paper C prepared for Public Inquiry into groundwater pollution from mine drainage at Tilmanstone, Kent (SWA 1976a).

Period	No. of days	Q Ml d^{-1}	Total discharged Ml
1906 – 1913	2557	5.1	13040.7
1913 – 1918	1826	10.5	19173
1918 – 1922	1461	7.5	10957.5
1922 – 1948	9497	4.8	45585.6
1948 – 1953	1826	9.2	16799.2

Period	No. of days	Q Ml d^{-1}	Total discharged Ml
1953 – 1955	730	9.5	6935
1955 – 1958	1096	10.9	11946.4
1958 – 1960	731	11.4	8333.4
1960 – 1964	1461	11.2	16363.2
1964 – 1965	365	11.4	4161
1965 – 1973	2922	11.4	33310.8
		Grand Total (Ml)	179105.8

A graphical summary of the mine water discharge and chloride concentration of the discharge waters is presented in Figure 2-15 (after Headworth *et al.* 1980).

3.3.5 Groundwater abstraction

The groundwater from the Chalk aquifer across the region has been extensively exploited for water supply. This is through large public water source (PWS) wells, boreholes for agricultural irrigation and smaller domestic wells. Figure 3-19 shows the location of the public supply sources in the area. Most are located near to the north eastern coastal region, although the largest supply in the area is at Wingham, licensed for 9129 Mla^{-1}. The coastal PWSs are managed to minimise the risk of saline intrusion from the coast (Headworth 1994). Figure 3-12 details the historical abstraction regimes for the PWSs in the area studied. The sources for the data are summarised in Table 3-9. The biggest decline in abstraction occurs at Wingham where the annual volume abstracted has fallen from approximately 8000 Ml to approximately 4000 Ml. Some PWSs demonstrate increases in abstraction, for example at Ringwould (approximately 250 Ml in 1982 to 1000 Ml in 2000) and Martin Gorse (approximately 1270 in 1977 to approximately 1800 Ml in 2000).

Table 3-9 Source of data for historical abstraction summary

Date	PWS		Data source	Comments
1926 – 1976	Wingham		Bibby (1979) WRc Report: A numerical model of contamination by mine drainage water of the chalk aquifer, Tilmanstone, Kent	Report Table 2 provides $m^3 d^{-1}$ abstraction rates – these have been converted to annual Ml volume
1980 – 1990	Kingsdown St Margarets Lighthouse Woodnesborough Flemings	Wingham Deal Ringwould Martin Mill Martin Gorse Sutton Betteshanger	ACER (1991) Water resources study of the east Kent aquifer: Mathematical model of the Chalk aquifer by Birmingham University School of Civil Engineering	Annual abstraction Ml values provided
1991 - 1996	Ringwould Sutton Flemings Martin Mill	Martin Gorse Woodnesborough Deal Wingham	Southern Water Plc	Daily data – converted to annual volume
1997 - 2000	Ringwould Sutton Flemings Martin Mill	Martin Gorse Woodnesborough Deal Wingham	Southern Water Plc	Annual volume Ml

3.3.6 Summary of the water balance

From the data presented in the preceding sections, the daily water balance over the period 1960 to 1974 is estimated as:

Inflows:

Recharge - 145734 m^3d^{-1}

Infiltration from lagoons – 11400 m^3d^{-1}

Total in = 157134 m^3d^{-1}

Outflows:

Surface water

North & South Str – 36290 m^3d^{-1}

Wingham River – 20000 m^3d^{-1}

Well Chapel Spr – 15000 m^3d^{-1}

Nailbourne River – 40500 m^3d^{-1}

111790 m^3d^{-1}

Abstraction - 35000 m^3d^{-1}

Total out = 146790 m^3d^{-1}

In-Out = 10344 m^3d^{-1}

% discrepancy = 3.4%

This relatively small error in the water balance suggests that the flows in the area are adequately understood and accounted for and that these flow volumes can be used as guides for developing and calibrating a groundwater model.

3.3.7 Aquifer characterisation

A review of existing data is provided here to characterise the distribution of aquifer properties for an initial conceptual model.

Information from pumping test data

Pumping tests have been carried out in the area for assessment of water resources and also during the SWA Tilmanstone investigations in the early 1970s (Headworth *et al.* 1980). Available transmissivity data calculated from these tests are summarised in Table 3-10.

Table 3-10 Summary of transmissivity data available for area studied. N.B. superscript numbers refer to superscripts on Figure 3-20

Pumping well / strata	Calculated transmissivity m^2d^{-1}	Location of well / borehole	Data source
Worlds Wonder[1] (Chalk)	510 – 570	Upper reaches of Nailbourne.	Report on test pumping of Worlds Wonder BH 1980 (SWA 1980).
Coombe Farm (Chalk)	500	Dry valley	ACER 1990b review of data.
Kingsdown[3] (Chalk)	1100	Dry valley near coast.	Exploratory drilling and test pumping 1984.
Otty Bottom[4] (Chalk)	450	Dry valley near coast.	
Lighthouse[5] (Chalk)	210	Cliffs above St Margaret's at Cliffe.	
Ringwould[6] (Chalk)	600	NE trending dry valley near coast.	
Lwr Venson Fm BH3[7] Chalk upper zone (20 – 50 mbgl)	62	Tilmanstone-Eastry valley, NE trending dry valley, 8km inland from coast.	Short term pumping tests (SWA 1976b). Report on the test pumping of observation BH's Oct 1975 – Jan 1976 Tilmanstone investigation.
Lower Venson Fm BH4[8] Chalk middle zone (60 – 100 mbgl)	1250		
Lower Venson Fm BH2[9] Chalk deep zone (100 – 150 mbgl)	0.9		
Eastry[10]	790 - 1550		Headworth *et al.* 1980.
Lower Venson Farm BH4[11] (Chalk middle zone)	115		Carneiro 1996. Reinterpretation of SWA (1976b) short term tests Oct 1975 – Jan 1976 using Warren and Root method.
Thornton Farm BH1[12] (Chalk middle zone)	120		

Figure 3-20 indicates the distribution of the pumping test locations and the parameter values calculated.

Water level responses in boreholes at Lower Venson Farm during the pumping test at Eastry are also commented upon by Bibby (1979). A rapid response in all three levels intercepted by the observation boreholes at Lower Venson Farm was recorded and Bibby interprets this as indicating that at sufficiently large distances (300 m from Eastry to Lower Venson Farm) these layers in the aquifer are connected. Bibby (1979) also suggests that this anisotropic behaviour indicates mainly horizontal fissuring.

Information from tracer test data

Several tracer tests were run during the SWA Tilmanstone investigations in 1975-76, but only limited details remain available. Tests and results are summarised in Table 3-11.

Table 3-11 Summarised tracer testing - Tilmanstone investigations (Bibby 1979)

Injected tracer	**Test input and monitoring points**	**Results**
Rhodamine WT	Injected 25 m from a pumping well (no details of exact location or depth)	No response. Attributed to too low a pumping rate and local heterogeneity.
A 'cocktail' of tracers	Injected into three observation boreholes at Lower Venson Farm and monitored for at pumping well at Eastry (300 m away)	No response. Attributed to molecular diffusion between mobile water in fractures and immobile water in matrix blocks.
Alcohol	Into borehole 25 m from pumping well (no location mentioned, but possibly Eastry)	60% recovery, see Figure 3-21 D_L = 2.2 m, but no molecular diffusion allowed for.

Figure 3-21 presents a successful tracer test breakthrough curve for the final test listed in Table 3-11, using alcohol 25 m from a pumping borehole.

Information from core data

Details of matrix porosity, derived from core material collected during the SWA Tilmanstone investigations, are presented in Figure 3-22. A mean interconnected porosity of 44.5% for Upper Chalk data and 38.3% for Middle Chalk data have been calculated, although these should be treated with caution as they are calculated from digitised data and the location of the Upper / Middle Chalk boundary cannot be conclusively determined. Chloride concentration data determined from the core material are also presented in Figure 3-22.

3.3.8 Controls on the distribution of aquifer characteristics in the Tilmanstone - Eastry valley

The characteristics of the Chalk aquifer are commonly found to demonstrate a distribution linked to vertical and horizontal variations of the medium (Ineson 1962, Bloomfield 1996). The following section assesses the information available to determine this variability for the Tilmanstone – Eastry valley.

Information from geophysical data (logs and surface)

Geophysical logging of the boreholes drilled during the SWA investigations in the 1970's was undertaken for both formation and fluid parameters. The extent of borehole geophysical investigations is summarised in Table 3-12. Further discussion of borehole geophysical logging from the 1970s investigations and more recently is provided in Section 4.4.2.

In addition to borehole geophysics, surface resistivity surveys were undertaken throughout the investigations in the 1970s. The extent of the saline plume delineated in this way is shown in Figure 2-13.

Table 3-12 Summary of all geophysical logging data available for the Tilmanstone-Eastry valley from work prior to the current research.

Borehole	Type of log	Logged by & date	Available data and format
BH 2	Caliper; Gamma Ray;16" resistivity; 32" resistivity; Single point resistivity; Fluid temperature; Differential temperature	R. Brereton, 26/07/1973 15/08/1973 12/12/1973	Paper copies of logs

Borehole	Type of log	Logged by & date	Available data and format
Eastry 79 m borehole	16" resistivity; Fluid resistivity; single point resistivity	R. Brereton, 15/08/1973	Paper copies of logs
Thornton Farm 100 m borehole	Caliper; 16 & 64 Resistivity; Self Potential	R. Brereton, 27/03/1974	Paper copies of logs
Thornton Farm 150 m borehole	Caliper; 16 & 64 Resistivity; Self Potential	R. Brereton, 1973	Paper copies of logs
Eastry BH 7 & 8	CCTV	Southern Science, 1991 (now Water Resources Section of Southern Water plc)	Video of CCTV

Lithological controls

Of particular significance to the hydrogeology is the improved detail provided by the new stratigraphy. Traditional stratigraphic divisions of the Chalk in the Anglo-Paris Basin were very broad. Zones or stages were typically 60 – 100 m thick. Hydrogeological studies tended to apply parameter values according to the broad divisions of Upper, Middle and Lower Chalk. However, these divisions do not necessarily correspond with lithologies of importance to hydrogeology, such as regular seams of flints and nodular chalk. The traditional breadth is also of limited use in contaminant transport studies (Mortimore 1990). The new stratigraphy recognises that lithological variation has caused the sediments to respond in different ways to tectonic stresses, for example. This has produced lithostratigraphic horizons that have significantly affected the way in which water flows through the rock and this allows individual chalk beds or members to be categorised according to their fracture characteristics and their potential as aquifers to become clearer. An example of this is the tendency for marl seams to produce inclined conjugate joint sets, and these combined with horizontal fractures, provide a route for vertical groundwater flow and solute movement at the marl seam 'barrier'. This is further demonstrated in Table 3-13.

Table 3-13 Chalk Group fracturing and aquifer potential (*after* Mortimore *et al.*, 1990)

Chalk Group Bed/Member	Hardness	Fracture characteristics	Aquifer potential
Seaford Chalk	Very soft to medium hard	Medium spaced regular joints	High

Chalk Group Bed/Member	Hardness	Fracture characteristics	Aquifer potential
Lewes Nodular Chalk	Alternating very soft to very hard, some massive bands	Nodular chalk fracturing and widely spaced conjugate joints	Mixed; low except on faults
Holywell Nodular Chalk	Very soft to medium hard	Medium spaced conjugate joints	Locally good where well fractured
New Pit Chalk Beds	Very soft to medium hard	Intense steeply inclined fractures dissipating along marl seams	Solution widened features along marl seams
Melbourn Rock	Hard	Medium spaced conjugate sets	High
Plenus Marls	Medium hard	Poorly fractured	Low

It is well documented (Ineson 1959) that groundwater hydrographs vary depending upon their location in interfluves or valleys, recharge or discharge areas and the observation borehole hydrographs presented here for the Tilmanstone – Eastry area indicate spatial controls on groundwater level response which generally comply with this expected distribution. The surface geophysics undertaken in the 1970s indicates that the saline plume from the mine-water lagoons has moved preferentially along the valleys, as would be predicted by generally accepted Chalk conceptualisation and hydraulic property distributions (Ineson 1959, Price *et al.* 1993). However, the detailed lithostratigraphy of the Chalk coupled with fracture characteristics of the specific horizons (Mortimore *et al.* 1990) suggests that, superimposed on the interfluve / valley break-down of characteristics and hydraulic behaviour, there are additional features that provide important control over fluid flow and solute transport within the Chalk aquifer.

3.4 Summary and discussion

This chapter has described the relationship between lithology, fracturing and the resulting water bearing potential within the rocks of the Chalk Group. Basement faults and thrusts have influenced sedimentation of the Chalk through the creation of local basins and highs. There is a distribution of fractures that relates to the lithologies associated with these sedimentation settings. Sandwiches of soft-hard-soft chalks or hard-clay-hard rocks, e.g. the hard beds either side of the Plenus Marls, have particular fracture distributions. Marls and clays have accommodated stresses horizontally whereas harder formations have tended to fracture vertically. Water bearing horizons occur on top of relatively unfractured thick marls, such as the Glynde Marl. Traditional

divisions within the Chalk Group did not correspond to lithologies of particular importance to hydrogeology such as marl bands, flint horizons and hardgrounds. Geophysical logs can help to identify these layers, and can be used to develop conceptual models for the area, to be tested through field investigations and groundwater modelling.

3.4.1 Summary of conceptual model

The more detailed definition of the Chalk lithostratigraphy described by Bristow *et al.* (1997) provides a new framework within which to develop a hydrogeological conceptual model for the Tilmanstone-Eastry valley. Similarly the influence of large scale structural features and smaller scale structures associated with the same tectonic episodes (Mortimore and Pomerol 1991) suggests that investigation of these may provide new insights into controls on aquifer hydraulics. The vertical limits of observation boreholes provide an improved resolution of hydraulically important horizons and the variability of aquifer water level response. This revised framework leads to the need for a more detailed assessment of hydraulic parameters, and in particular of their vertical variability.

The development in understanding between lithology, fracture frequency and fracture style (Mortimore *et al.* 1990) has important implications for both flow and solute transport. Improved understanding of this relationship is necessary in order to make predictions about preferential flow and hence solute movement. The failure to observe tracer at monitoring points for several of the reviewed SWA tracer tests, highlights the unexpected control that fracture orientation can have over directions of fluid flow and solute transport at the local scale and serves to emphasise the importance of investigating this aspect of the Chalk in solute transport studies.

The conceptual model of the hydrogeology of the area around the Tilmanstone-Eastry valley is one of a gently dipping, multi-layered Chalk aquifer. Marl horizons and hardgrounds that are present in the Chalk sequence can be identified on geophysical logs and traced across the region. These features appear to influence groundwater flow. The Chalk is unconfined across most of the region, becoming confined beneath the Tertiary cover to the north. Recharge occurs across the aquifer, directly where the Chalk is exposed and indirectly through superficial deposits where present. Rainfall volume is related to elevation and recharge is controlled both by elevation and surficial

cover type. Chalk groundwater discharge supports baseflow in the streams and rivers. The region is heavily exploited for water resources, both through abstraction from the Chalk aquifer and small scale abstraction from surface water courses.

3.5 Hydrogeological data gaps

This final section of Chapter 3 comments on the usefulness of available hydrogeological data for interpretation and conceptual model development as well as for numerical model calibration.

Although there are a number of long term hydrographs in the area, water level data are limited in that they focus on the central valley areas with little or no data available for the interfluves. Due to the use of abandoned domestic wells for water level monitoring, the water table falls below the base of some boreholes during drought periods. Other observation boreholes are designed with an open section that cuts across several different Chalk lithologies, producing an observed water level which is an average between all the levels. This will compromise use of the hydrograph for model calibration where the model is divided into layers that do not correspond to the same intervals open to the observation borehole.

Many of the pumping tests carried out during previous investigations have been short duration and at low flow rates. It was often not possible to monitor water levels in the same horizon of the aquifer from which water was being pumped. Observation boreholes drilled for the SWA (1976b) investigations were designed to sample vertically discrete sections of aquifer. This means that when one borehole at each of the investigation locations (Thornton Farm; Lower Venson Farm and Eastry) was pumped, the observation boreholes were open over different intervals. Parameter values derived from pumping tests in these boreholes must therefore be used with caution.

Hydrochemical sampling was generally undertaken from shallow domestic boreholes and it was later realised (Headworth *et al.* 1980), that the chloride concentrations were unrepresentative of the fracture water chloride for specific horizons. Instead an averaged value was measured. Matrix porewater concentration data from the SWA investigation are available for BHB only. Other data have not been preserved and all that remains is the conceptual model presented by Headworth *et al.* (1980). The conceptual model appears to simplify the distribution of porewater chloride

concentration whereas the data at BHB suggest that specific horizons were important for solute movement. This limits the usefulness of the historical chloride concentration data, both for fracture and porewater samples, in undertaking solute transport model calibration.

Hydraulic parameters vary both between Chalk layers and laterally between valley and interfluve. The frequency of fracturing appears to be controlled by both lithology and depth and the style may vary depending on the lithology. The fracture orientation influences fluid movement and this is seen in local scale tracer tests conducted by SWA. In terms of understanding the framework that controls solute transport, there is no direct information about fracture aperture, fracture style and groundwater velocity, nor dispersion parameters.

The construction details for the observation borehole infrastructure located in the Tilmasntone – Eastry valley are provided in Table 3-14 and Figure 3-23.

Table 3-14 Tilmanstone - Eastry valley observation borehole design for boreholes installed during 1970s investigations, *after* Oteri (1980), see also Figure 3-23.

Location	Grid Reference	Infrastructure originally installed	Infrastructure remaining	Information available
Thornton Farm	^{6}2930 ^{1}5200	3 boreholes BH1: datum 31.57 m aOD, 100 m depth, cased to 55 m. BH5: datum 31.57 m aOD, 39 m depth, cased to 24 m. BH6: datum 31.52 m aOD, 150 m depth, cased to 130m. Cased diam. 100 mm/4"; open-hole diam 200 mm/8" for all boreholes in group.	BH5 accessible BH1 and BH6 are both partially collapsed and / or blocked.	Geophysical logs Water levels Groundwater chemistry changes during pumping Calculated transmissivity from short term pumping tests
BHB	^{6}2964 ^{1}5266	Datum unknown. Cored borehole to 150 m.	Borehole collapsed	Porewater concentrations 1974 Porosity values Geophysical logs (poor quality)
BHE	^{6}3005 ^{1}5268	Datum 22.54 m aOD. Borehole drilled to 79 m. Borehole diameter 200 mm / 8"	Accessible	Water levels
Lower Venson Farm	^{6}3020 ^{1}5310	3 boreholes BH2: datum 18.05 m aOD, 150 m depth, cased to 100m. BH3: datum 18.43 m aOD, 46 m depth, cased to 20 m. BH4: datum 18.13 m aOD, 90 m depth, cased to 65 m. Cased diam. 100 mm/4''; open-hole diam. 200 mm/8'' for all boreholes in group.	All accessible to drilled depth	Geophysical logs Water levels Groundwater chemistry changes during pumping Calculated transmissivity from short and longer term pumping tests
Eastry	^{6}3040 ^{1}5338	5 boreholes BH7: datum 16.8 m aOD, 75 m depth, cased to 55 m. Cased diam. 100 mm/4''; open-hole diam. 200 mm/8''. BH8: datum 16.98 m aOD, 30 m depth, approx. 7 m casing.	All accessible to drilled depth. BH9 no longer readily accessible as it is located in a locked	

		Borehole diam. 200 mm/8''. BH9: datum 16.95 m aOD, 76 m depth cased to 30 m. Cased diam. 610 mm/24''; open-hole diam. 840 mm/33''. BHA: 18.94 m aOD, c. 50 m depth, unknown casing details. Borehole diam. 200 mm/8". BHC: datum unknown. Located away from main cluster, approximately 100 m further down valley. 15 m deep.	building.	

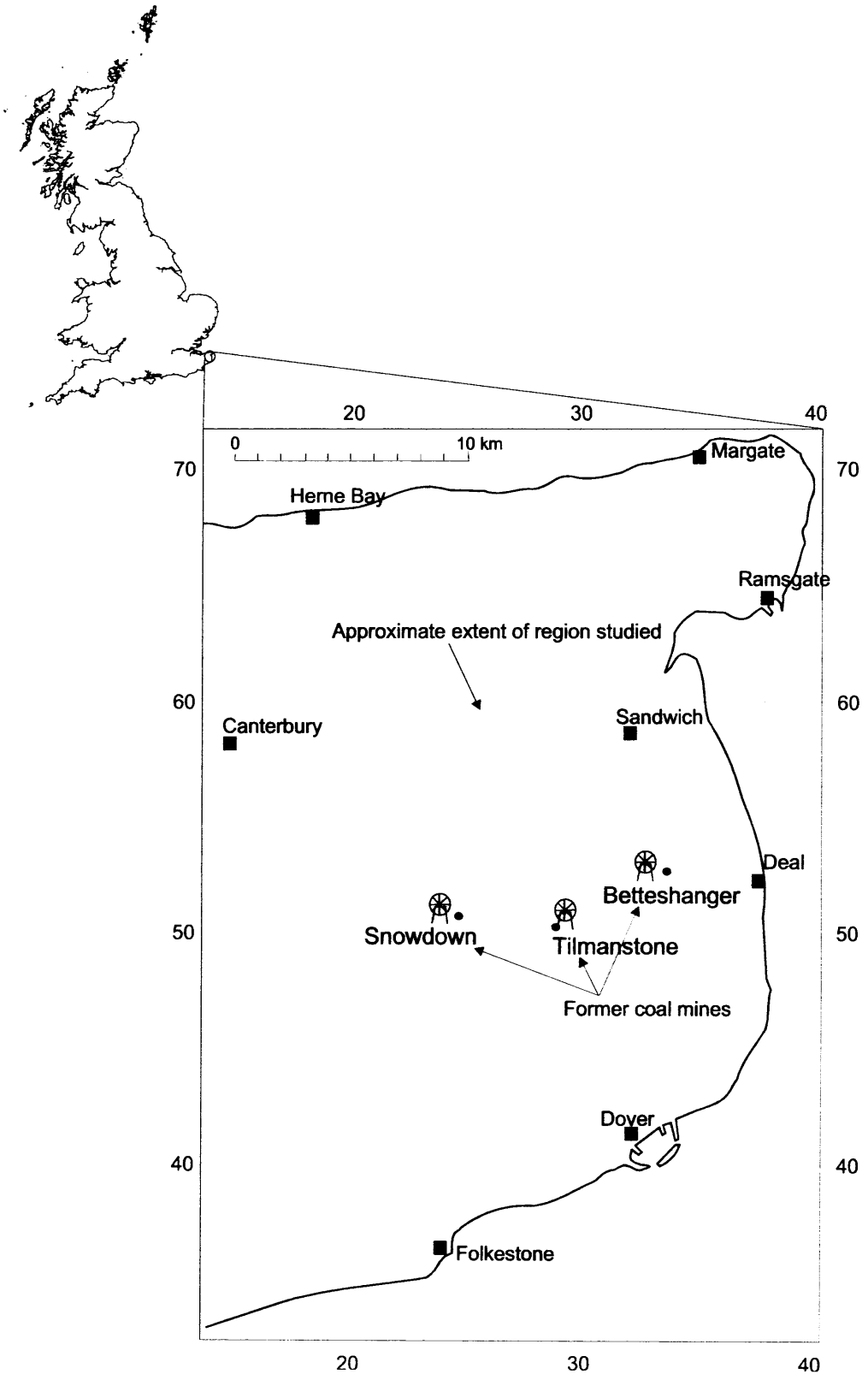

Figure 3-1 Location map of region studied.

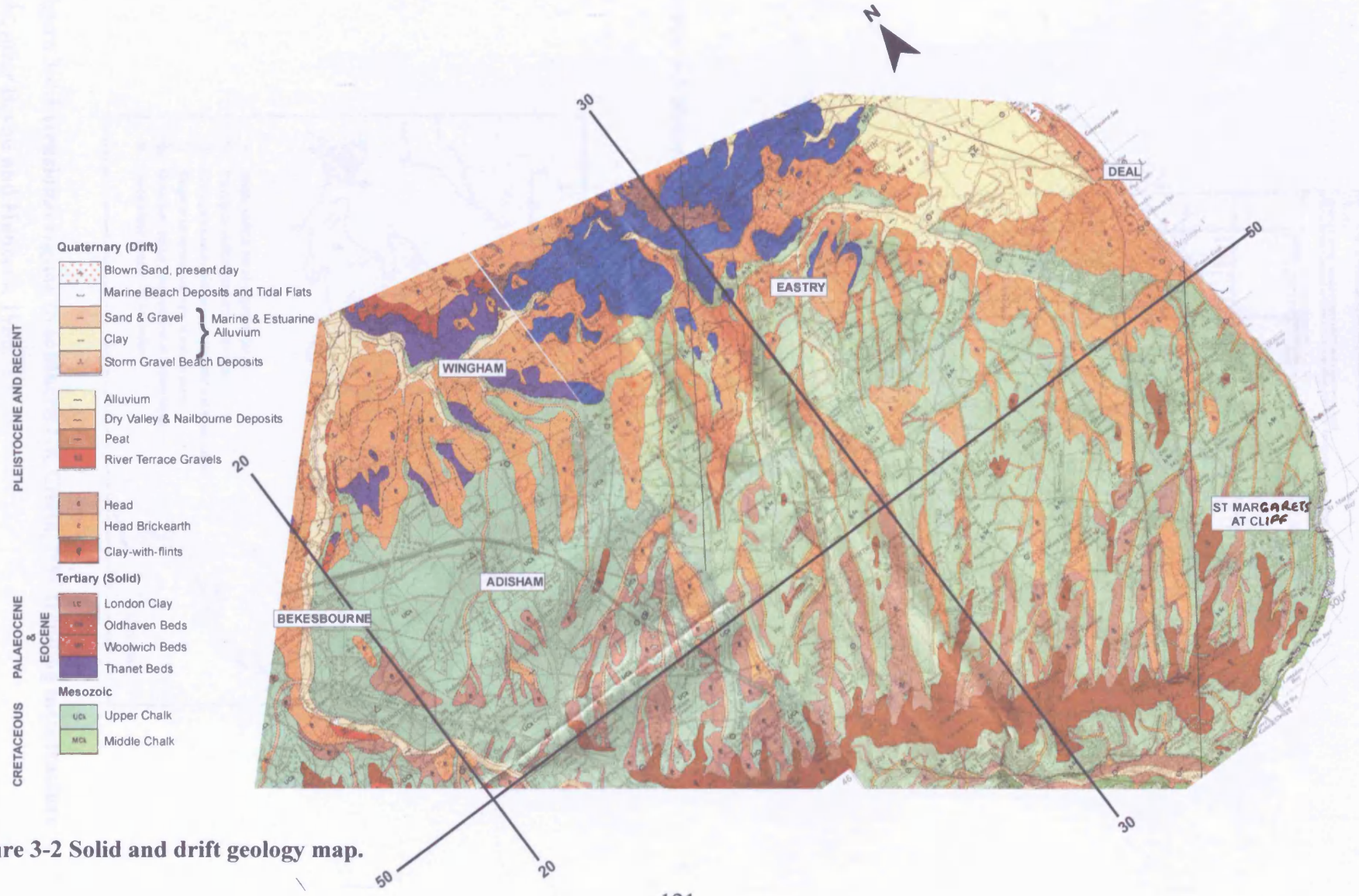

Figure 3-2 Solid and drift geology map.

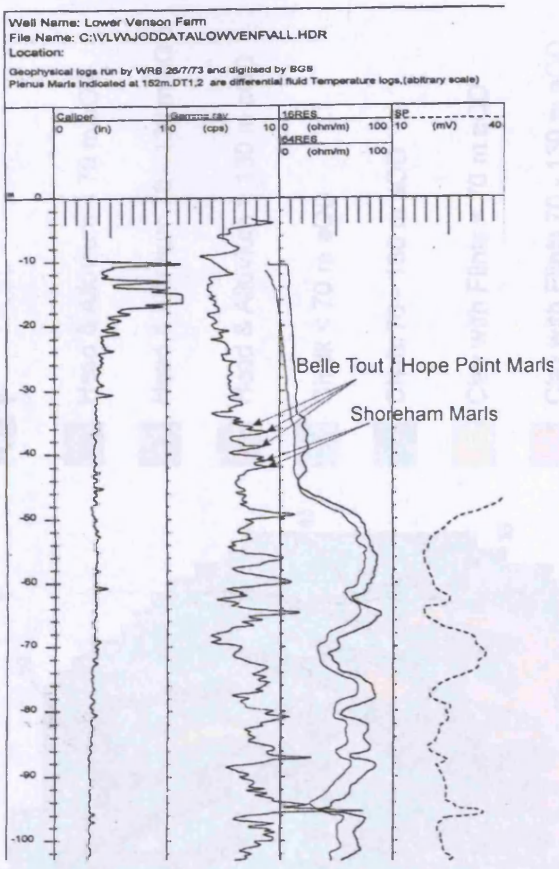

Figure 3-3 Shoreham and Belle Tout Marls on gamma log.

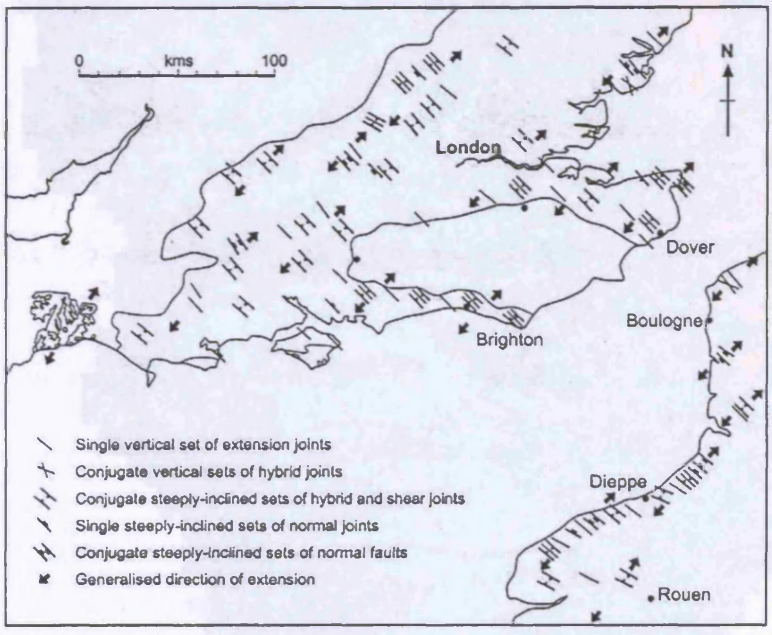

Figure 3-4 Extensional regime in southern UK Chalk, NW trending mesofracture sets, *after* Bevan and Hancock 1986.

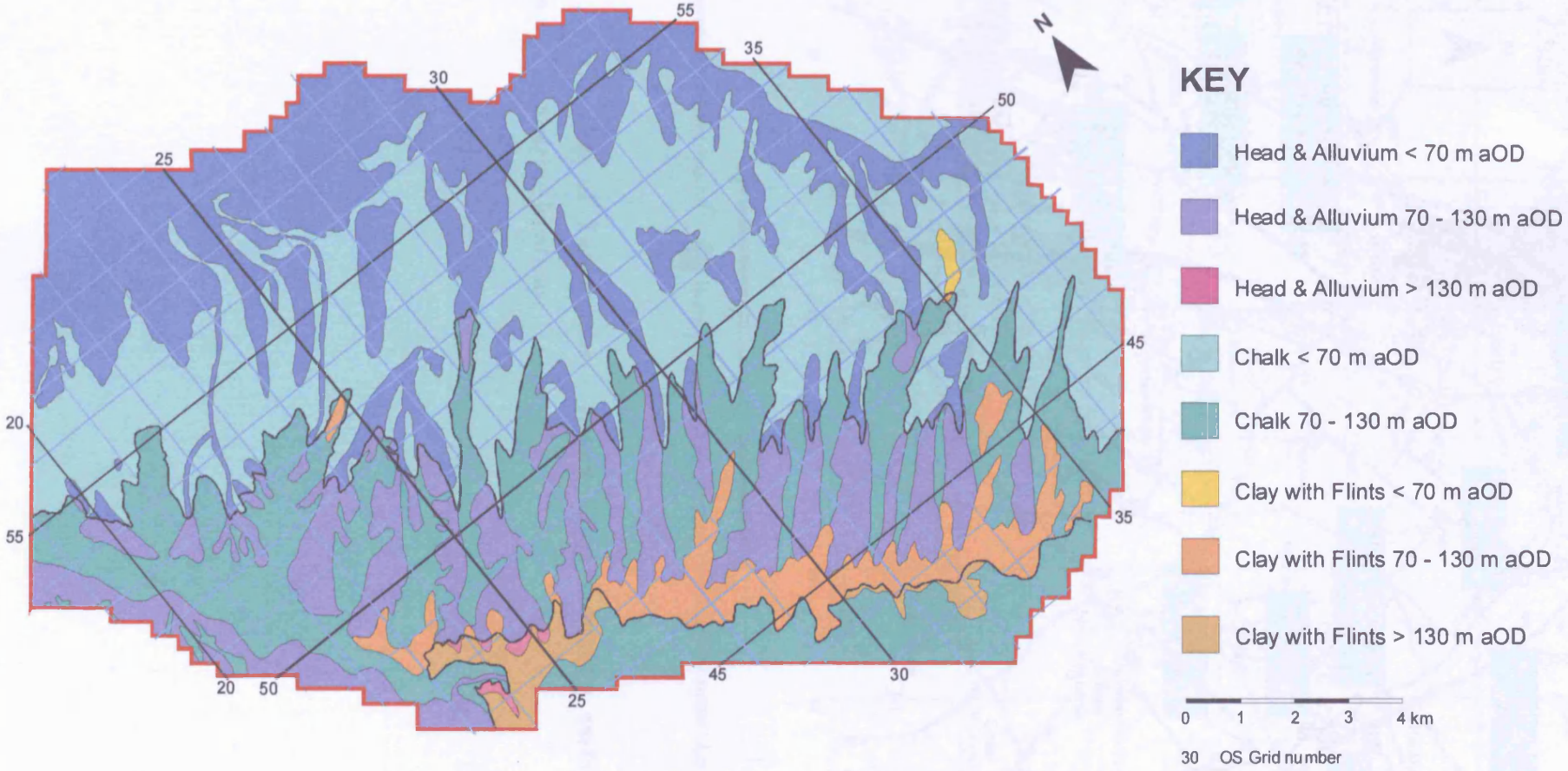

Figure 3-5 Recharge zones.

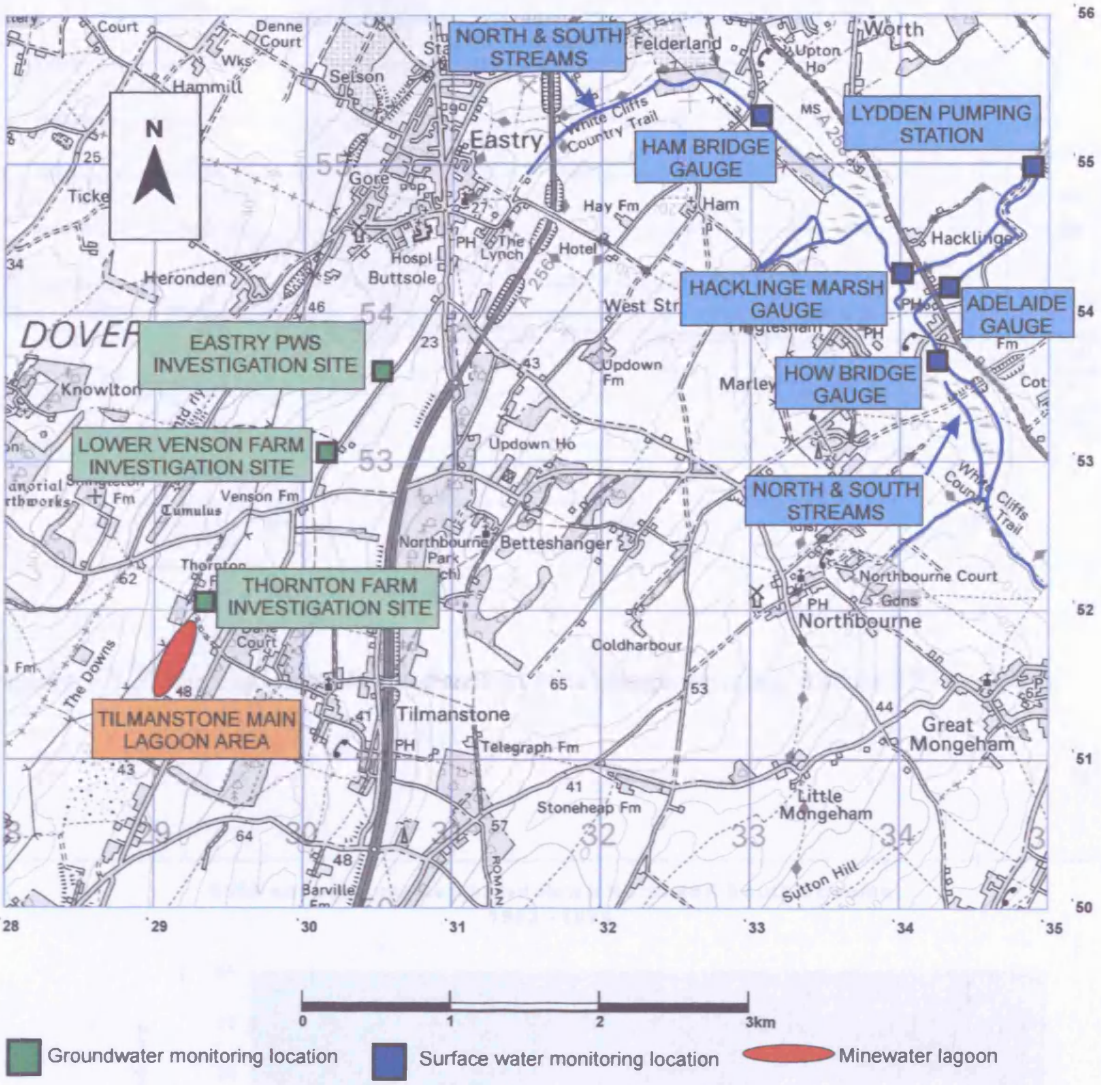

Figure 3-6 OS map of Tilmanstone - Eastry valley indicating surface and groundwater monitoring locations.

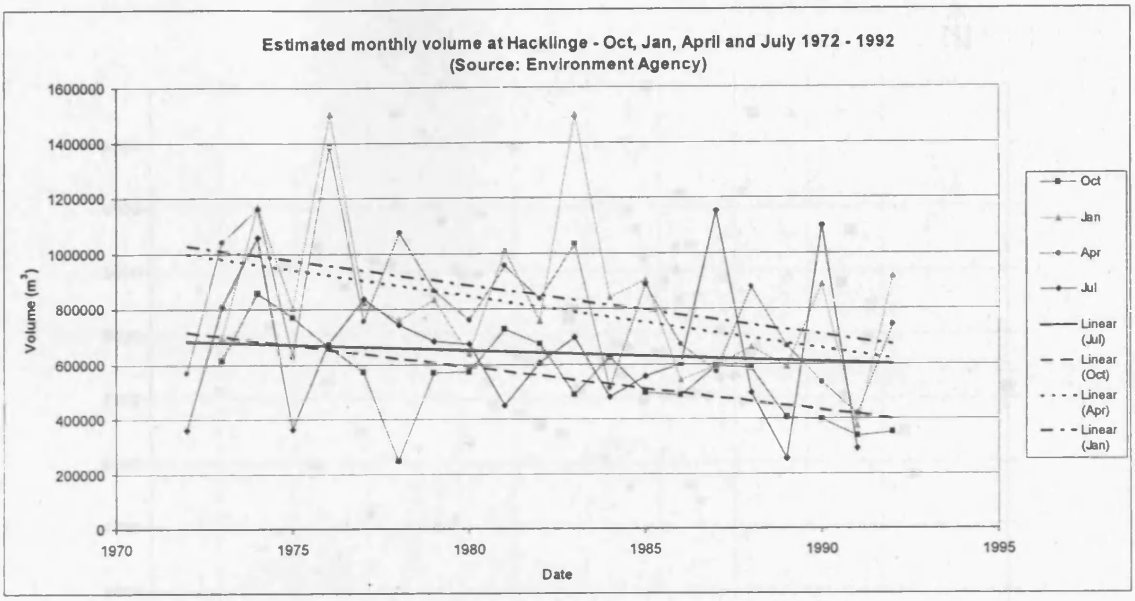

Figure 3-7 Estimated monthly volume at Hacklinge gauging station 1972 – 1992.

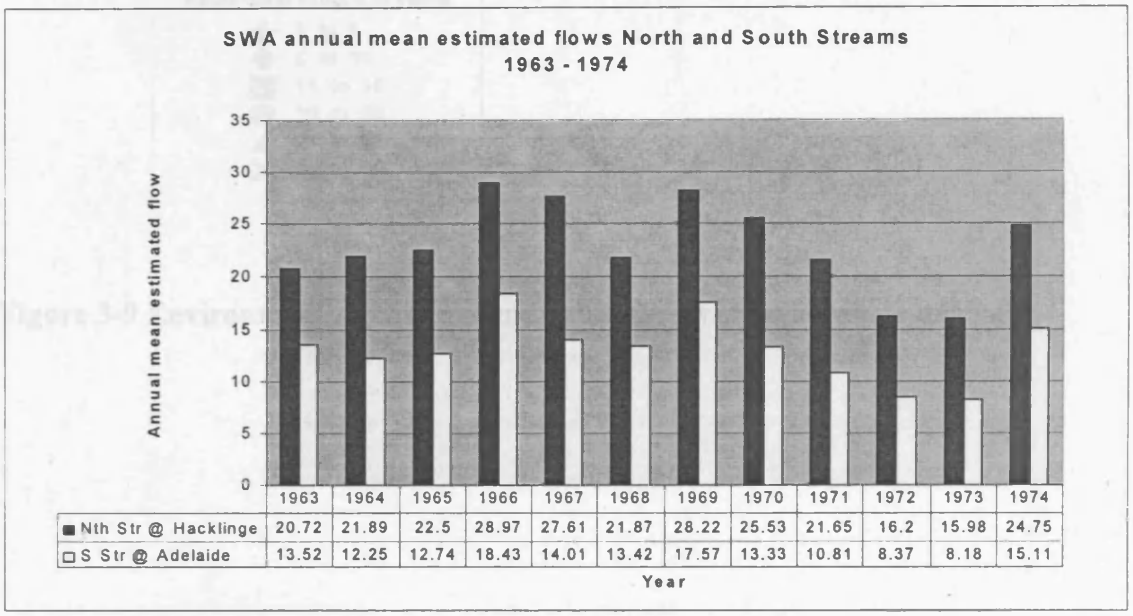

Figure 3-8 SWA mean estimated flows for North and South Streams (SWA 1976a).

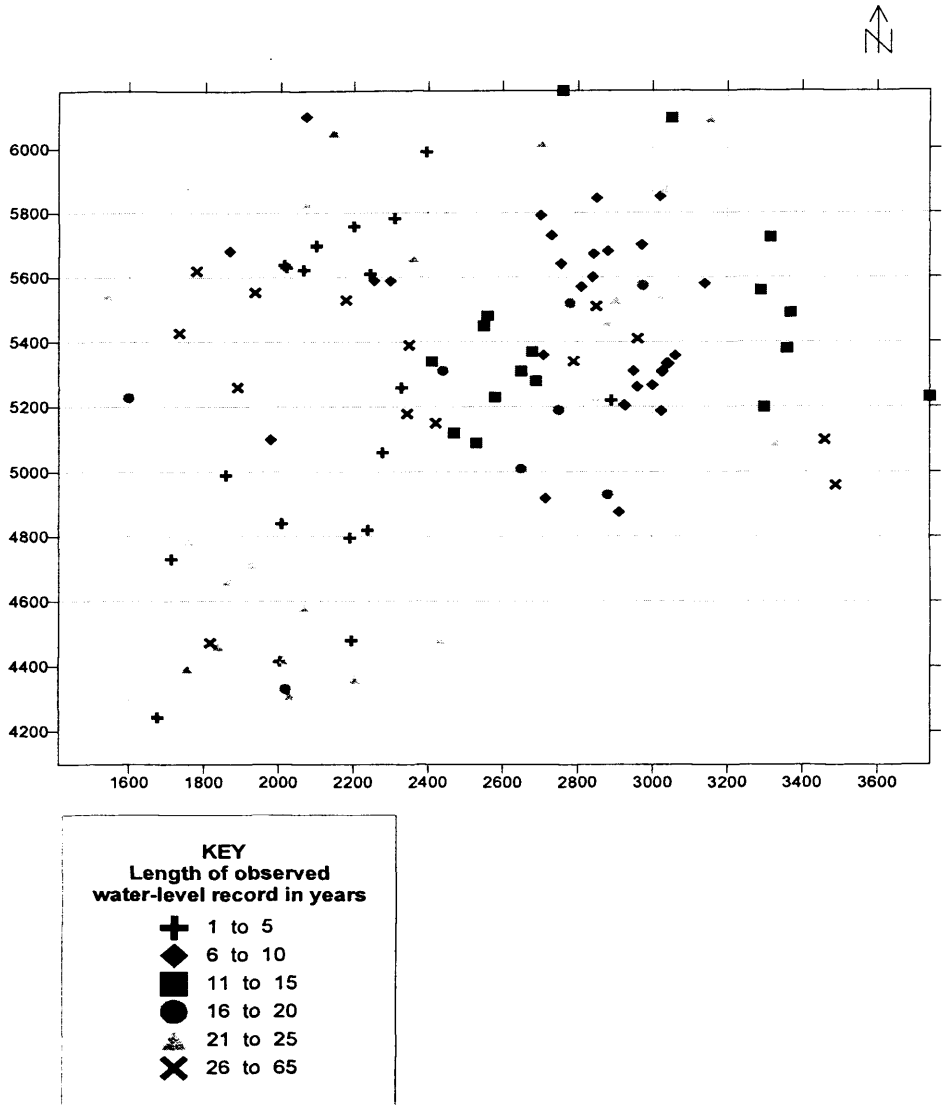

Figure 3-9 Environment Agency groundwater observation borehole network.

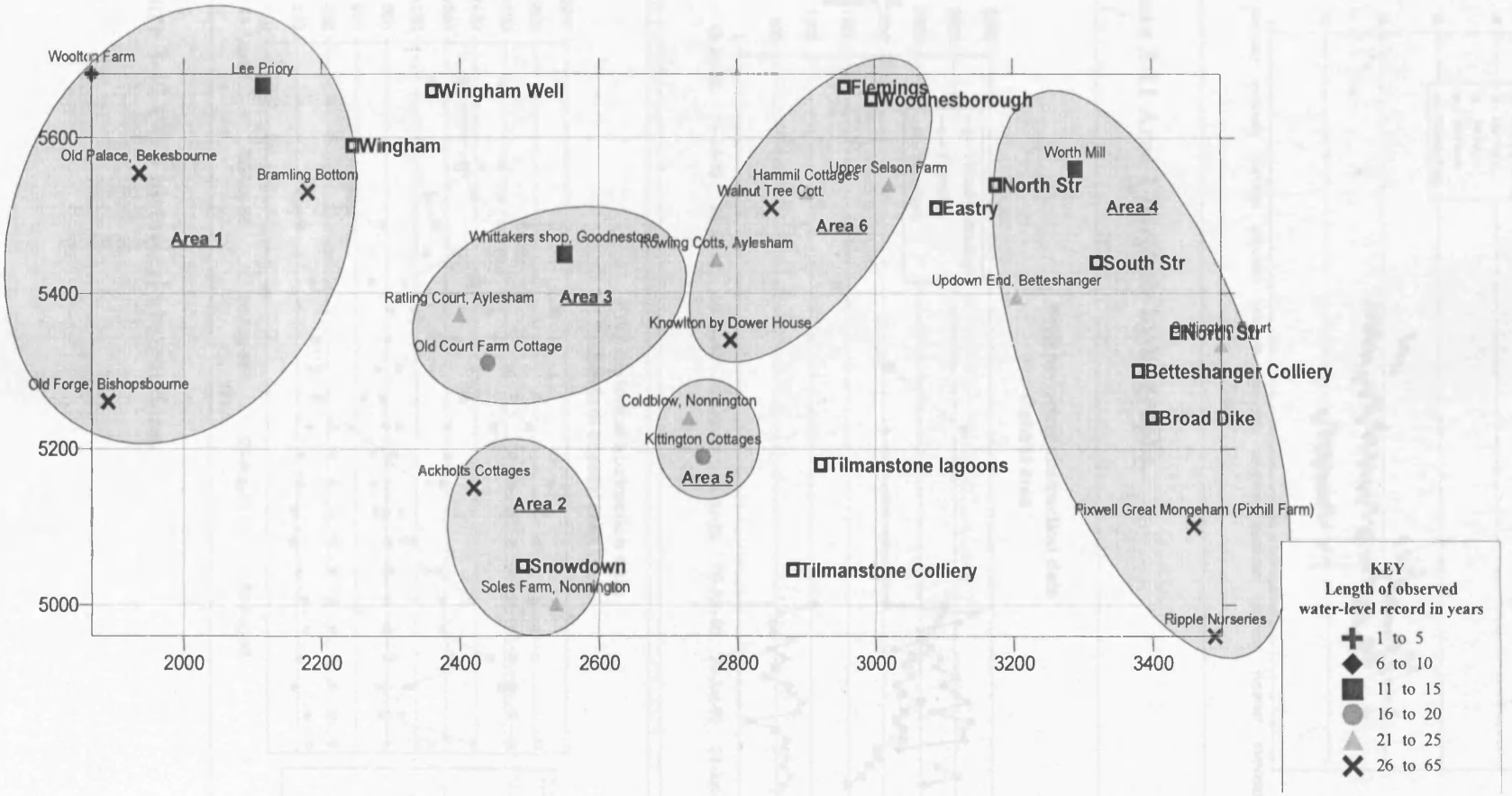

Figure 3-10 Observation borehole area groupings.

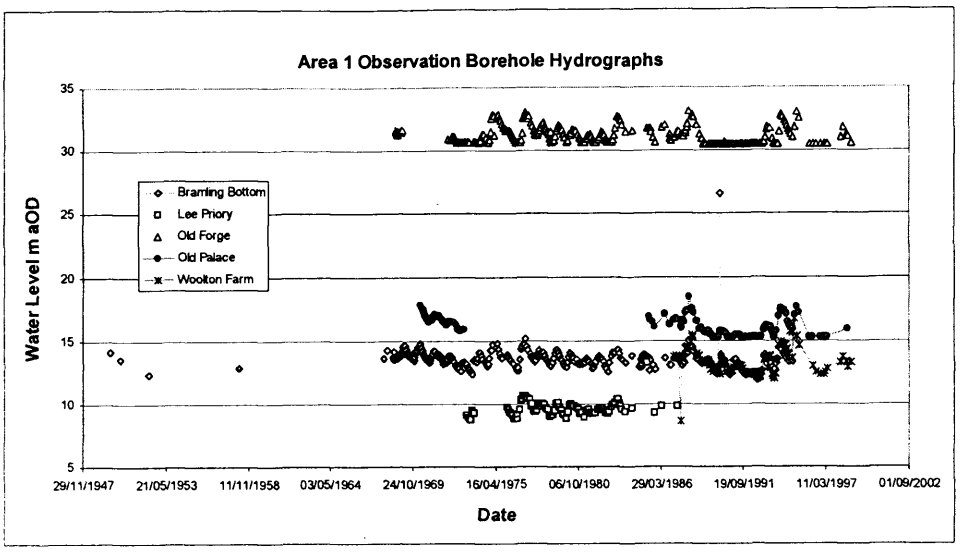

Figure 3-11 Area 1 borehole hydrographs.

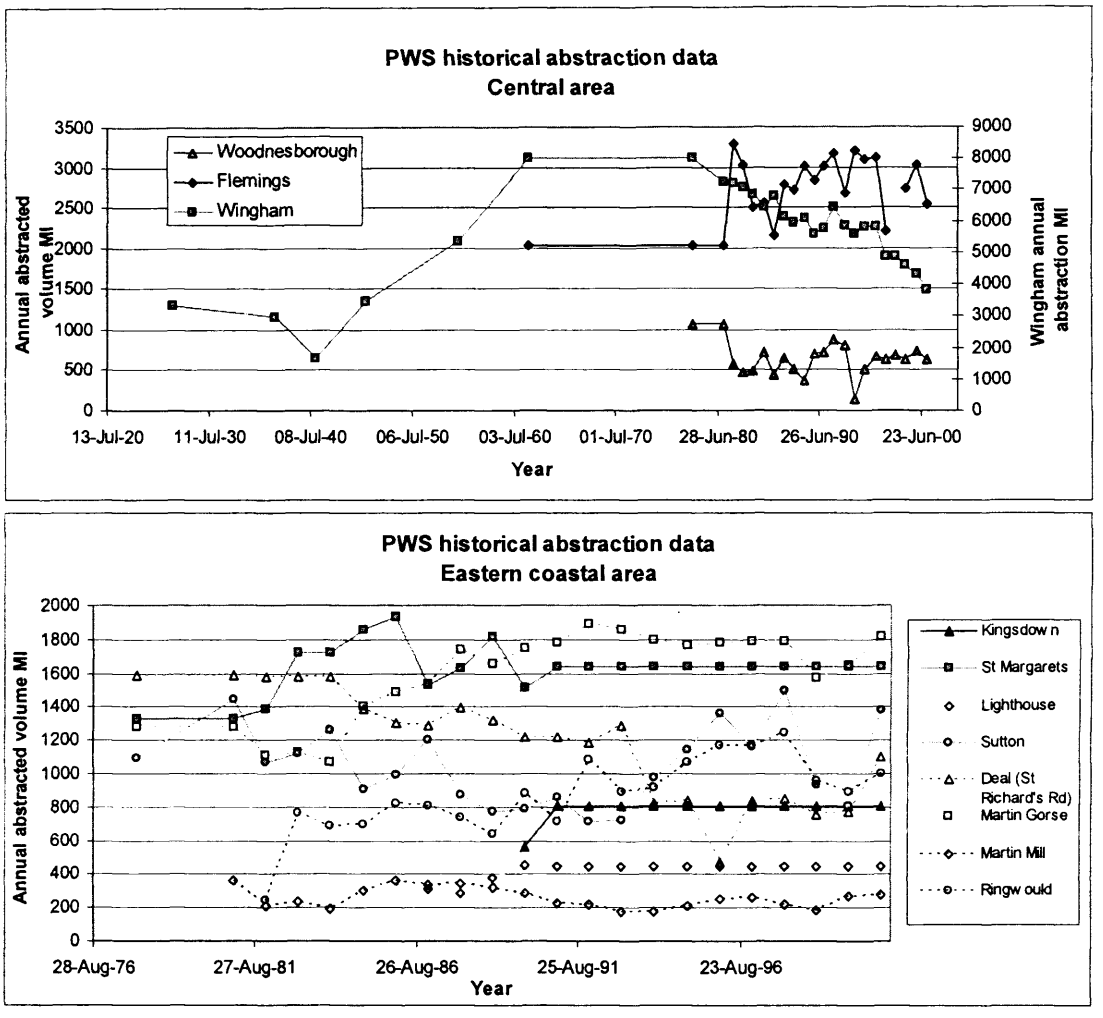

Figure 3-12 PWS historical abstractions.

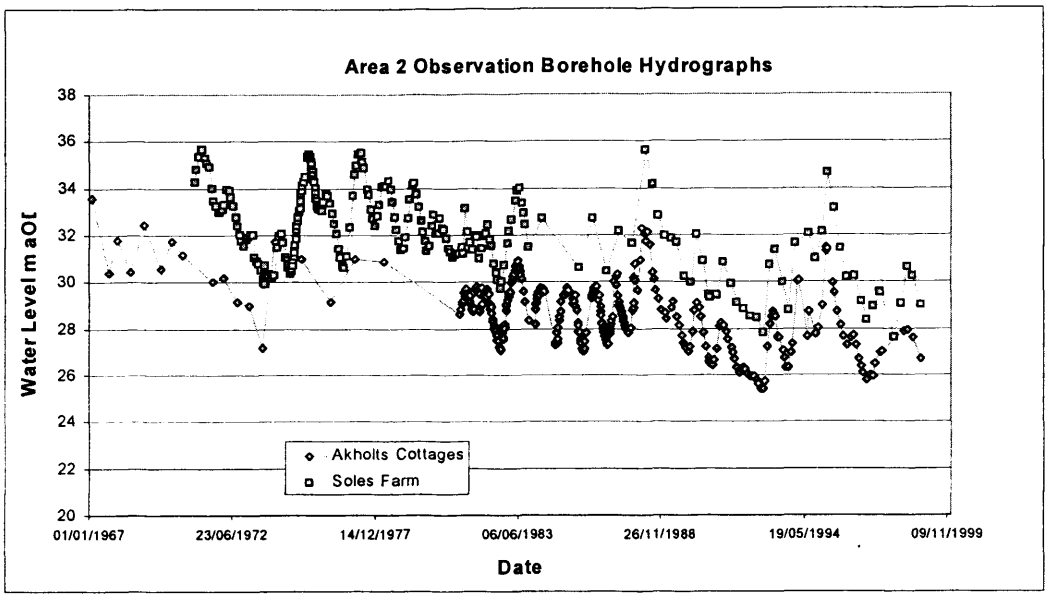

Figure 3-13 Area 2 borehole hydrographs.

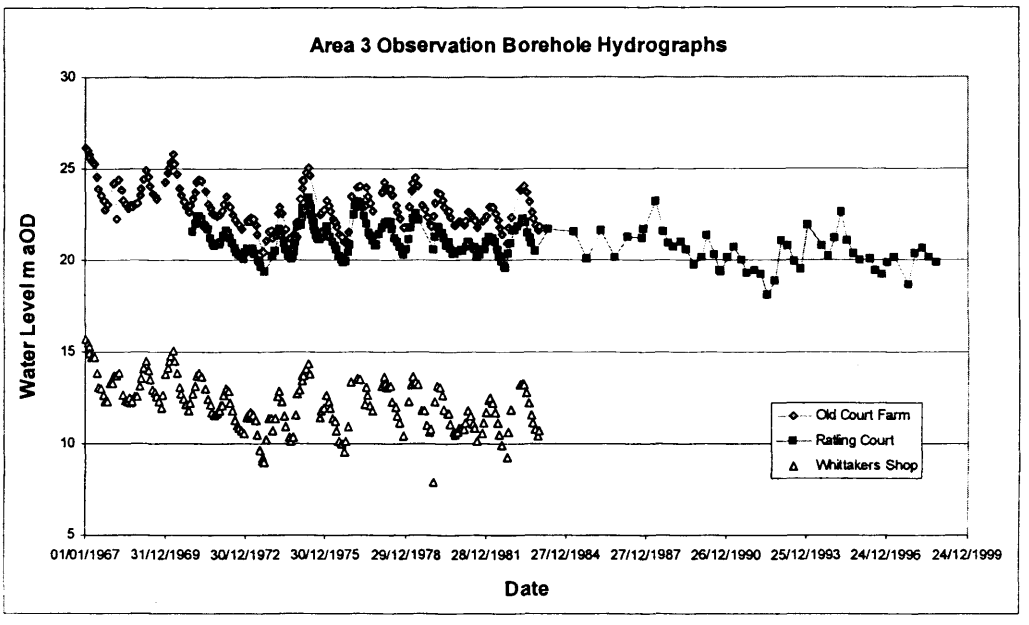

Figure 3-14 Area 3 borehole hydrographs.

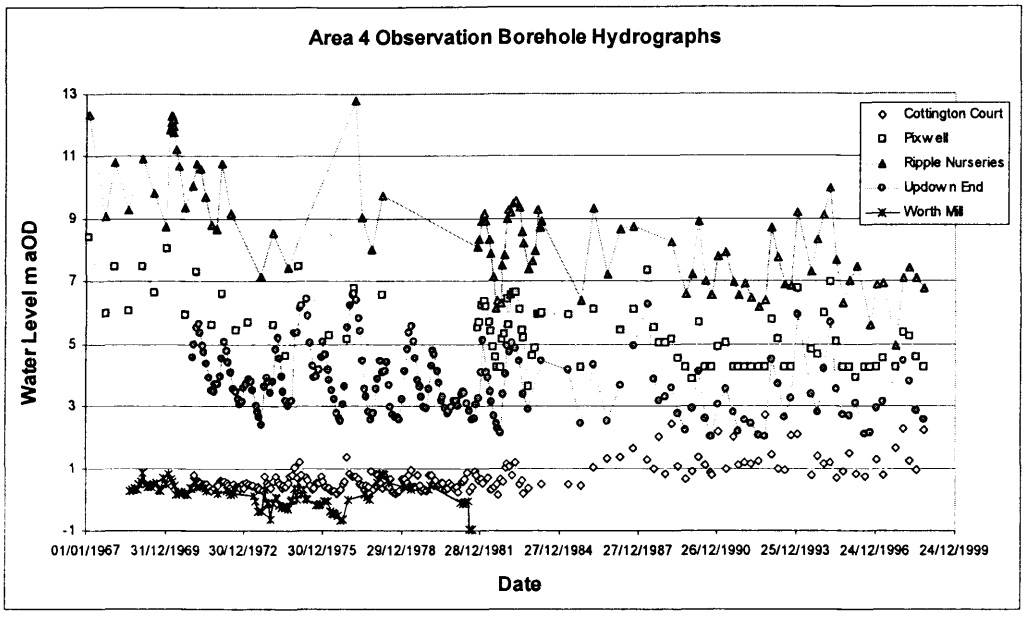

Figure 3-15 Area 4 borehole hydrographs.

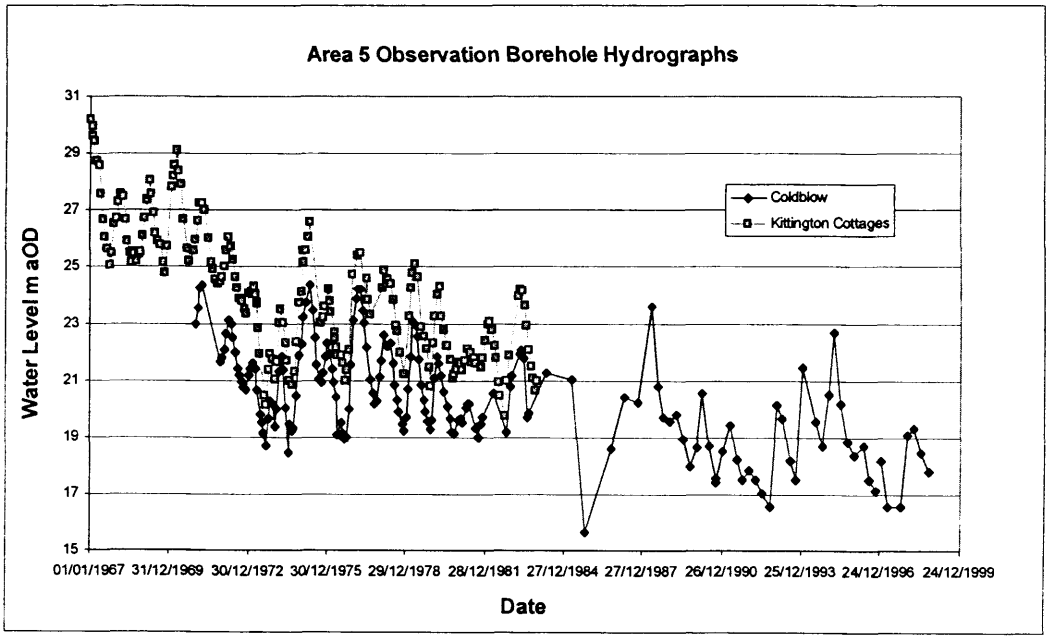

Figure 3-16 Area 5 borehole hydrographs.

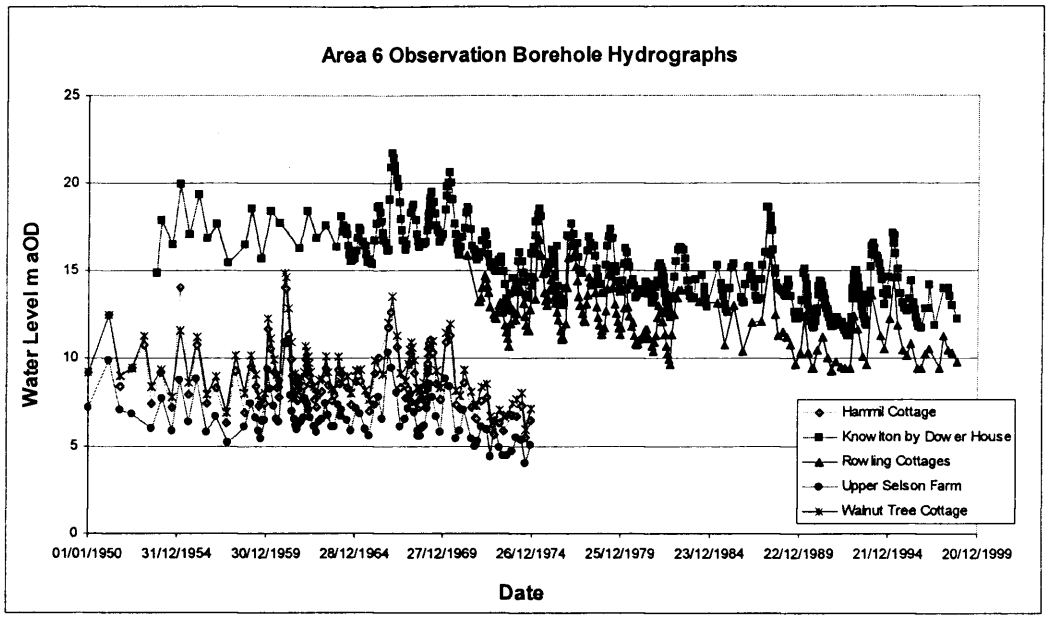

Figure 3-17 Area 6 borehole hydrographs.

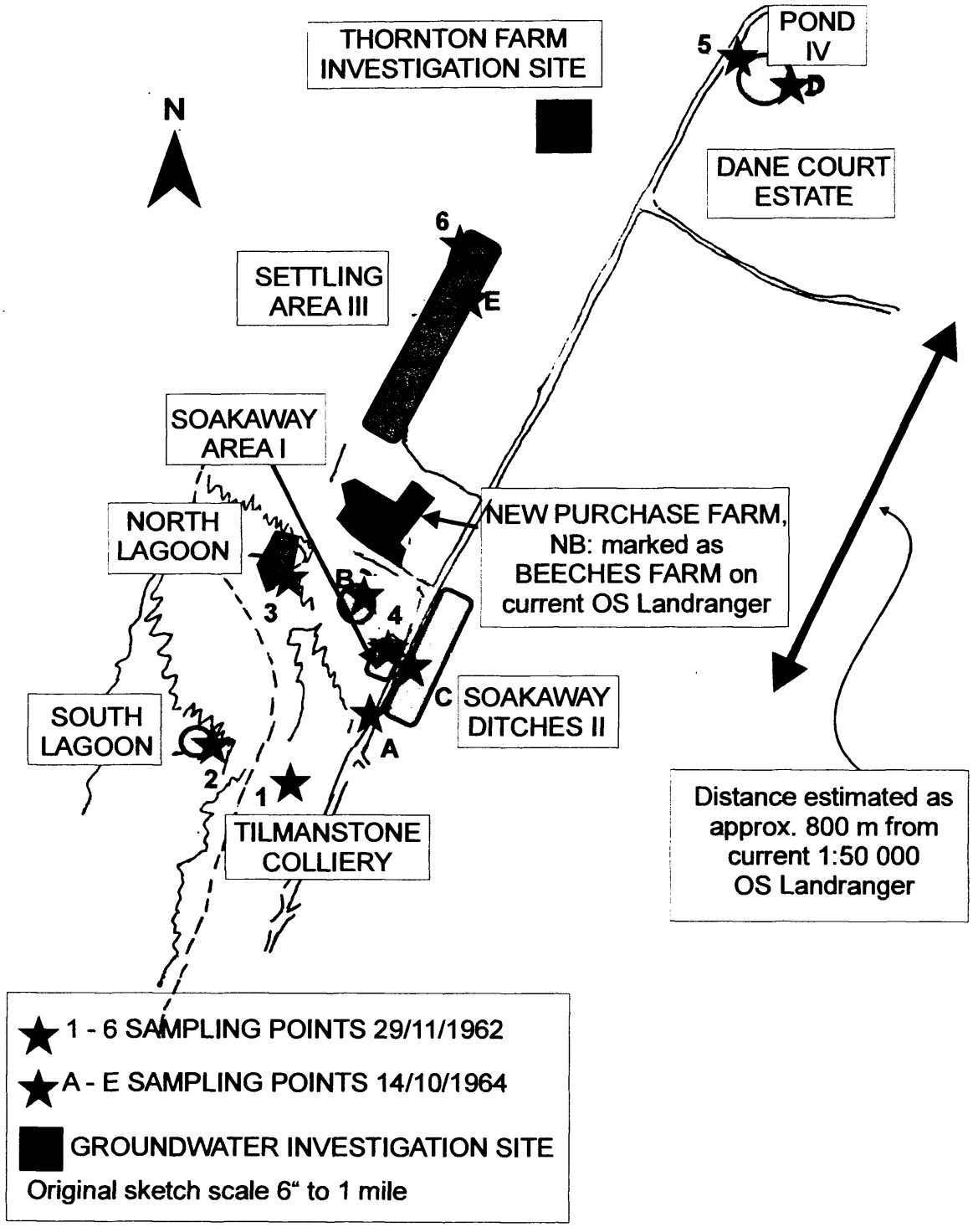

Figure 3-18 Location of mine-water discharge areas at Tilmanstone colliery.

Redrawn from a copy of an original sketch held by BGS.

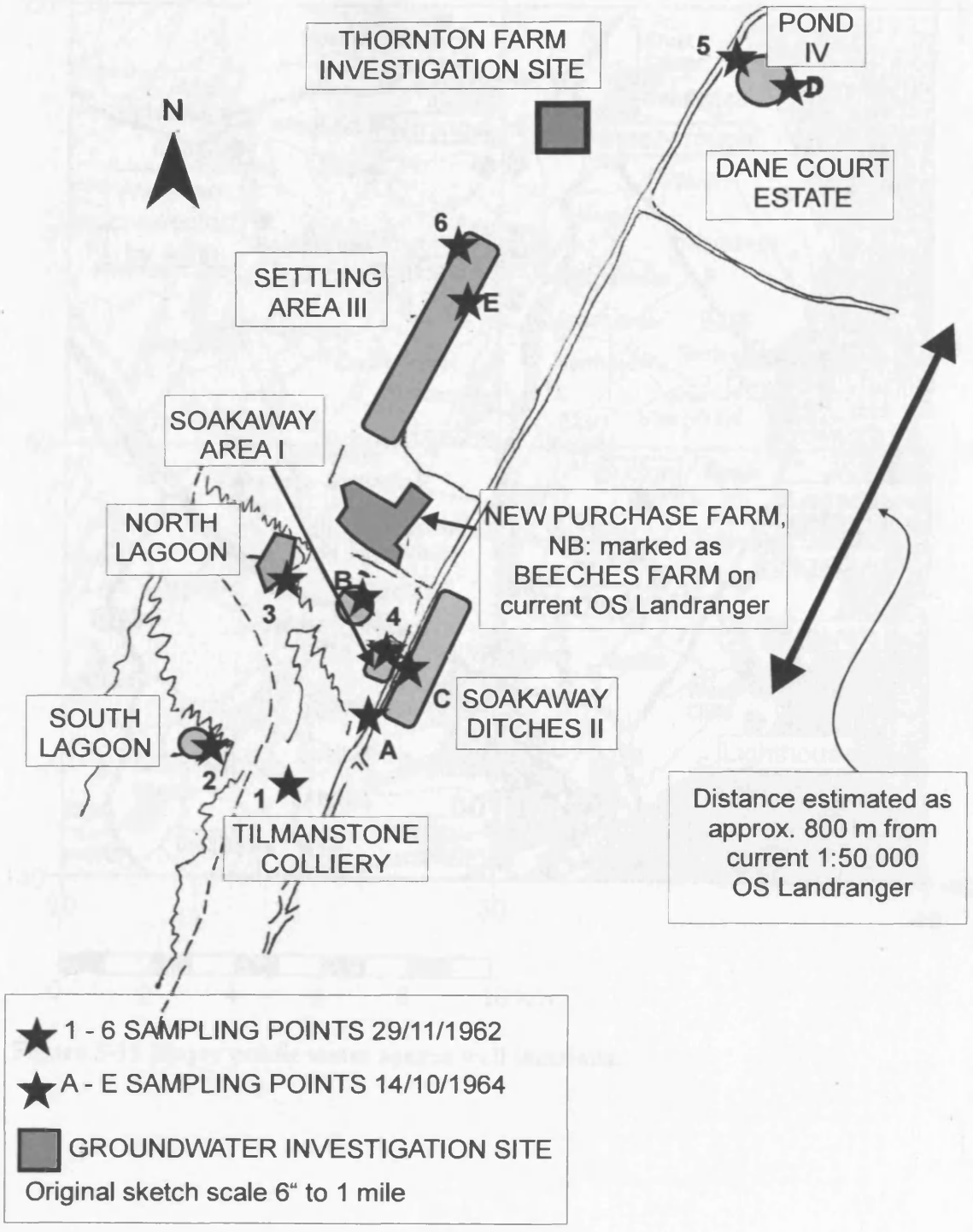

Figure 3-18 Location of mine-water discharge areas at Tilmanstone colliery.

Redrawn from a copy of an original sketch held by BGS.

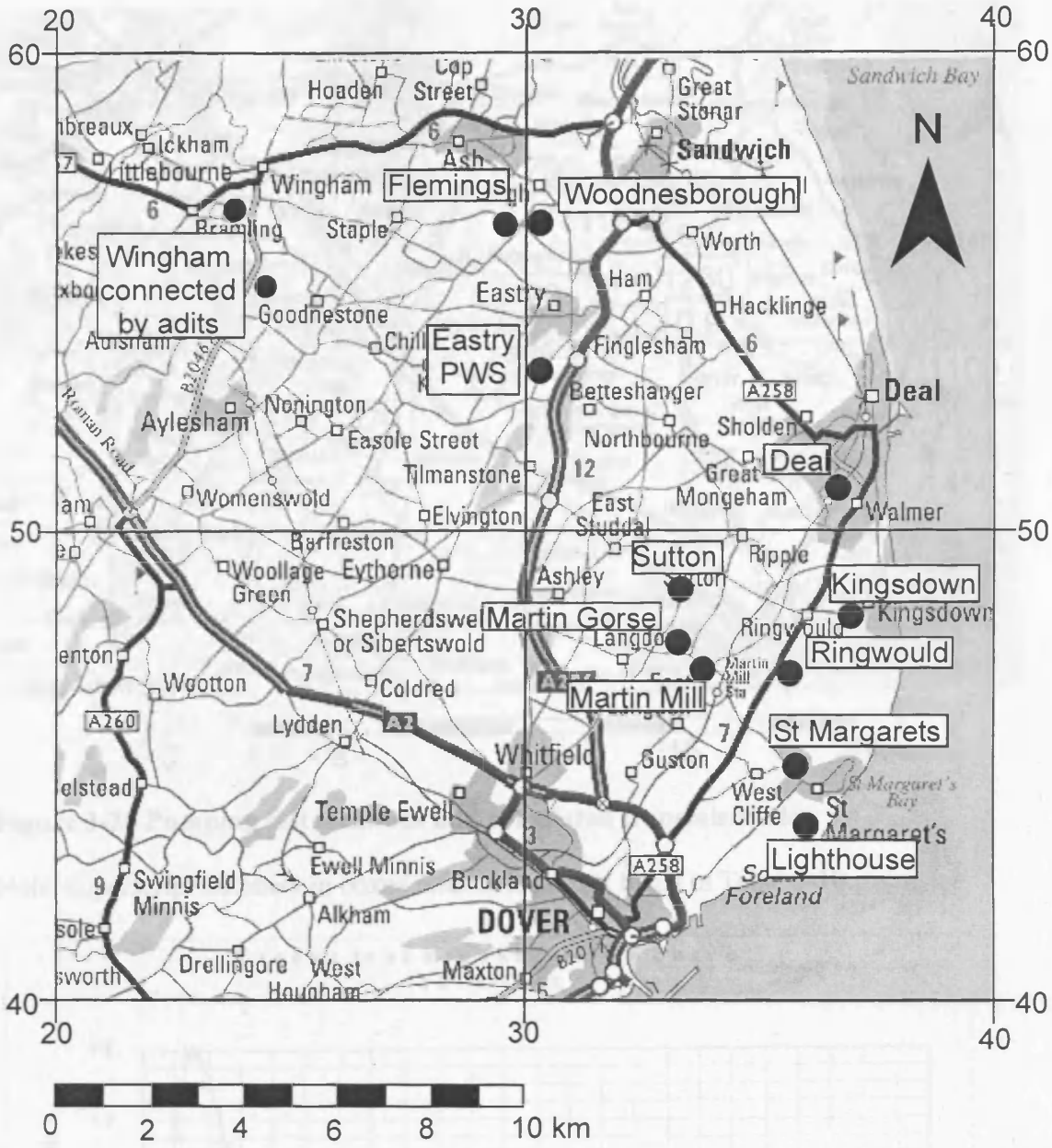

Figure 3-19 Major public water source well locations.

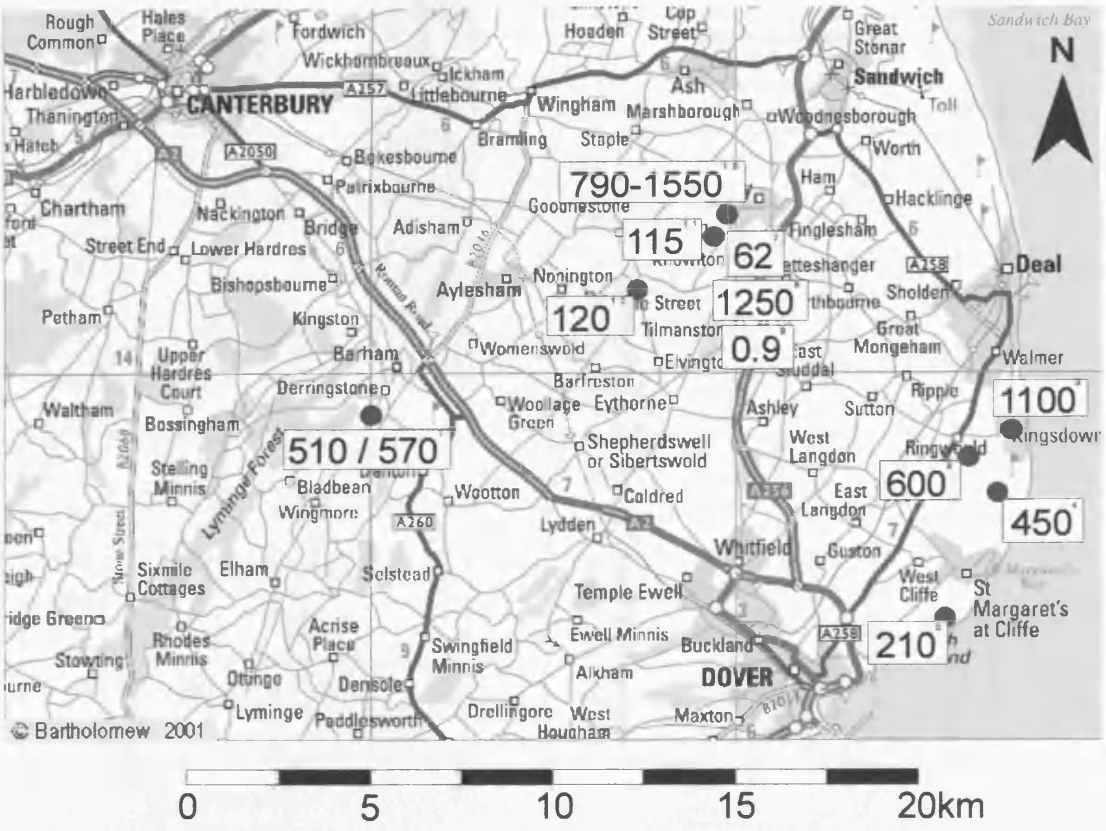

Figure 3-20 Pumping test locations and calculated transmissivities.

Note: superscript numbers in boxes refer to locations listed in Table 3-10.

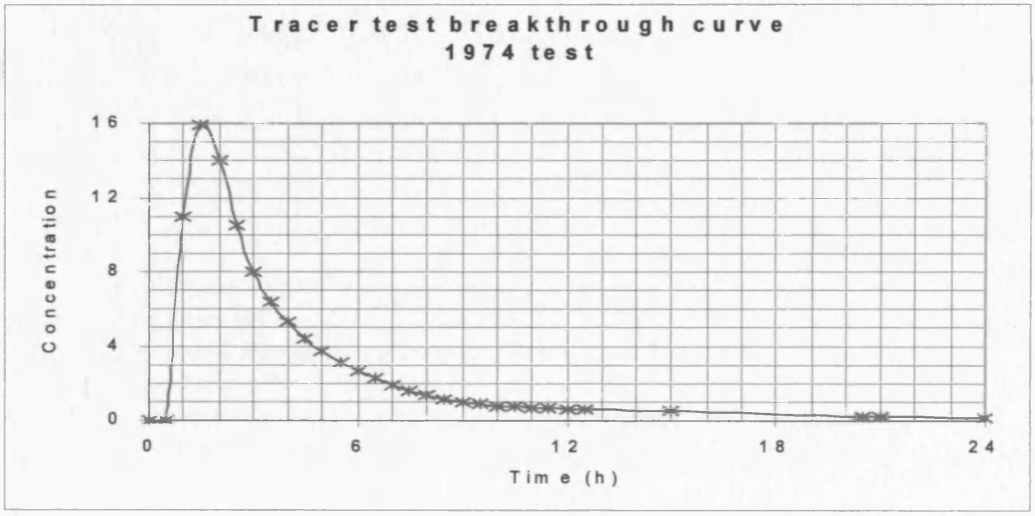

Figure 3-21 Digitised tracer test breakthrough curve (*after* Bibby 1979).

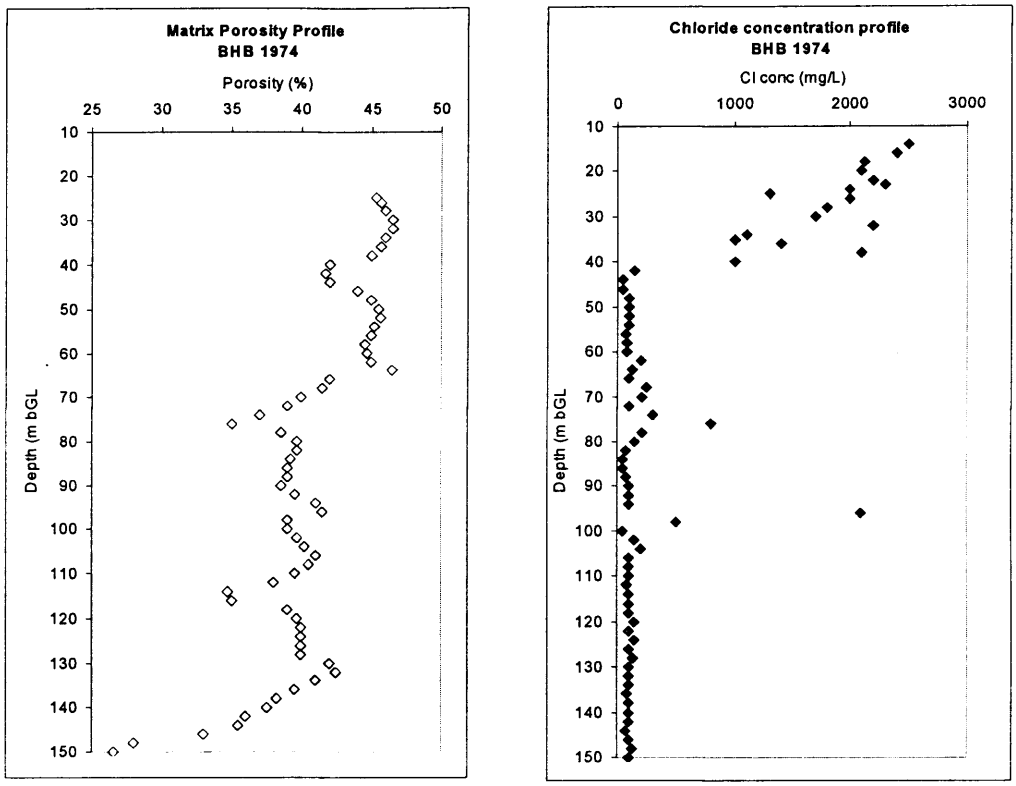

Figure 3-22 Digitised matrix porosity and porewater chloride concentration data (*after* Bibby 1979).

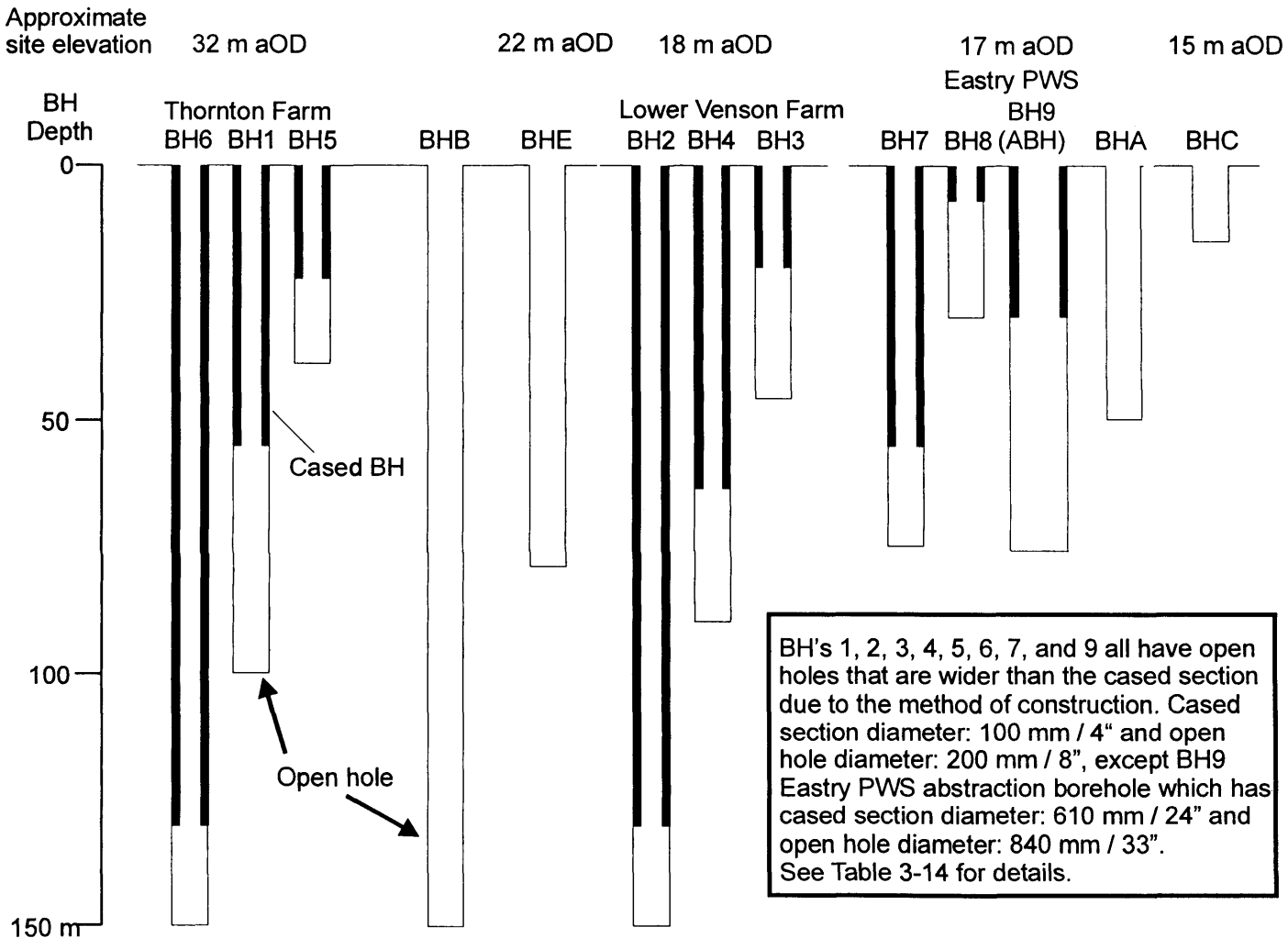

Figure 3-23 Construction details for observation borehole infrastructure in the Tilmanstone - Eastry valley.

4 Fieldwork and data collation

4.1 Overview

This chapter describes the field investigations undertaken during the period of the research by the author that are used to understand the framework and determine values for the parameters relevant to solute transport. It also draws on investigations undertaken in parallel with this current research, and those undertaken previously during investigations into the pollution of the Tilmanstone - Eastry valley. The subsequent chapter presents interpretations and draws together these investigations to provide the framework for understanding solute transport in the Chalk aquifer in the Tilmanstone – Eastry valley.

For clarity the components of the physical framework and the related hydraulic and solute transport properties, discussed in Chapter 2, are listed here:

Physical framework	**Hydraulic and solute transport properties**
Geological strata	Hydraulic conductivity
Structural boundaries	Groundwater head and gradients
Fracture connectivity	Groundwater flux
Fracture orientation /style	Fracture aperture
Fracture frequency / matrix block size	Fracture porosity
Matrix porosity	Diffusion coefficient
	Dispersivity

The fieldwork undertaken for the study has involved a range of hydrogeological investigative techniques such as borehole drilling, water level monitoring, packer testing, single borehole dilution tests and natural gradient tracer tests. These techniques have been employed in order to investigate the hydraulic regime and geological framework in the study area and assess the ways in which this regime and framework influence the transport of dissolved solutes. The fieldwork has sought to address the variety of scales, both in distance and time, at which the hydraulic regime and geological framework may influence the transport of dissolved solutes.

4.2 Fieldwork objectives

The aim of the fieldwork was to provide further hydrogeological characterisation of the Tilmanstone-Eastry valley and the associated groundwater pollution from the mine-water disposal. This expands on the investigations undertaken during the 1970s by the SWA and provides data for interpretation in the light of the more detailed lithostratigraphical understanding provided by Bristow *et al.* (1997). The fieldwork objectives are summarised as:

- To undertake detailed hydrogeological characterisation at the Lower Venson Farm site.
- To determine effective transport properties of the Chalk aquifer in the Tilmanstone - Eastry valley from tracer tests at different sites and scales.
- To consider the regional structural and lithological framework within which the hydraulic regime operates.
- To determine parameter values for hydraulic conductivity, Darcy velocity, fracture porosity, matrix porosity, dispersivity, aperture size and matrix block size.

4.3 Constraints

As with most field-based investigations, planned work met with a number of constraints. Although the plume in the Tilmanstone - Eastry valley affords us the opportunity to undertake research on a large, long-term, conservative pollutant plume, this in itself provides a constraint on the fieldwork that can be undertaken. Any contaminated water removed from the aquifer requires disposal. This essentially precludes undertaking pumping tests (due to the cost of pumped water disposal and limits of access for large tankers to the site) and provides difficulties where forced gradient i.e. pumped, tracer tests might be proposed. Part of the importance of the Tilmanstone - Eastry valley was that there was a history of investigations that had left borehole infrastructure in place. Unfortunately, after an initial review of the infrastructure, it became apparent that the borehole design had resulted in boreholes being completed at different depths within the aquifer (Figure 3-23). This does not lend itself as a set-up for borehole-to-borehole tracer tests. Also, although it does reveal information on vertical gradients within the aquifer, it does not provide suitable data to calculate horizontal gradients at individual sites for tracer test planning. Existing boreholes at the Thornton Farm and Lower Venson Farm sites were completed with the

cased section of the borehole at 100 mm diameter. This restricts the diameter of pumps and other sampling equipment that can be used down the boreholes.

Two new boreholes were drilled as part of another project running during the period of the current research (EU Fracflow, see Section 2.7). The data from the drilling of these boreholes and the subsequent infrastructure were available to this research project, however the timing of drilling and borehole location were restricted to fit in with the Fracflow project and availability of land and co-operation of landowners in the valley. Landowner co-operation became a problem at Thornton Farm and subsequent to the summer 1998 fieldwork, access to this site became problematic.

Finally, severe restrictions on movement in the UK countryside were imposed following the Foot and Mouth disease outbreak during Winter 2000 / 2001. This coincided with the planned timing of the final tracer test and the test had to be postponed until summer 2001.

4.4 Geological framework

4.4.1 Borehole drilling

Two air-flush rotary cored boreholes were drilled at the Lower Venson Farm site. The locations of all boreholes drilled during previous investigations in the area as well as those drilled during the course of this research are shown in Figure 4-1. The locations of the new boreholes relative to the existing boreholes at the Lower Venson Farm site are shown in Figure 4-2. The drilling programme and completion details are described in Bird *et al.* (1999). Relevant details for the current research are summarised here.

Both boreholes are 100 m in length. BGS LVI (inclined borehole) is drilled at an angle of 30 degrees to the vertical, resulting in the end of the borehole being at 86.6 m below ground level (bGL) (Figure 4-3). 700 mm of 205 mm ID steel casing is grouted in from the surface. The borehole is then cased from ground level to 26.26 m (a vertical depth of 22.69 m bGL) with 141 mm ID plastic casing. This casing is grouted to approximately 2 m bGL, above a rubber retaining ring forced down the annulus. The grout was installed to support the borehole walls. It is unlikely to provide an effective seal to prevent rapid movement of solutes from the ground surface into the borehole as it does not fully case out the unsaturated zone.

The second borehole drilled at the Lower Venson Farm site is BGS LVV (vertical borehole). This is sited 30 m along the drilled line of BGS LVI. Again, 700 mm of 205 mm ID steel casing was installed with 14.56 m of 141 mm ID plastic casing inserted inside and grouted to approximately 2 m bGL.

4.4.2 Geophysical logging

Borehole geophysical logging has been undertaken at various sites in the Tilmanstone - Eastry valley throughout the history of investigations in the area. Table 3-12 in Chapter 3 summarised the extent of the historical geophysical logging.

A brief description of the main benefits of undertaking geophysical logging in fractured chalk aquifers is given here. Further detail on the application of geophysical logging in hydrogeological investigations is given in Tate *et al.* (1970); Price *et al.* (1977); Driscoll, (1986); Howard, (1990); Vernon *et al.* (1993); Paillet, (1995).

Caliper logs: the diameter of uncased boreholes is measured using a tool with several extendable arms that are forced out onto the borehole wall. As the tool is raised up the borehole, changes in the borehole diameter cause the arms to move in and out, with the minimum reading being the drilled diameter. Changes in the diameter of a borehole may be indicative of features of hydrogeological interest. An increase in diameter may suggest the presence of fracture zones, where preferential enlargement has occurred. Care must be taken with this interpretation however as it could also mean, for example, that unconsolidated sediments have collapsed into the borehole during drilling. The log does not give any indication about the direction of an enlargement and small vertical features are unlikely to be registered by the tool.

Formation electrical logs: these tools measure changes in the electrical resistivity of the rock mass and its associated porewaters. Measurements are related to changes occurring up to a few millimetres into the rock from the borehole wall. An open fracture containing conducting groundwater should show up as a low resistivity reading compared to the rock matrix, but the technique is very sensitive to borehole geometry and formation fluid properties so in the pollution plume under investigation here, where porewater also has a high EC, it is likely that only limited information can be gleaned from this log.

Gamma logs: these tools measure the gamma rays emitted as naturally occurring radiation in the materials encountered by the borehole. The radiation recorded is used as a qualitative guide for stratigraphic correlation and permeability. Elements such as potassium, uranium and thorium are strong gamma emitters and these are associated with clay minerals. In chalk sequences this is particularly useful for detecting marl horizons which contain clay minerals and therefore are recorded on a gamma log as a peak in the signal (as indicated on Figure 3-3). Marl horizons tend to be of low permeability so are of hydrogeological interest as they may act as barriers to vertical movement of water and solutes. They are also known to be traceable over large areas, making them useful as stratigraphic marker horizons for correlation purposes (Barker *et al.*, 1984; Mortimore and Pomerol, 1987). Gamma logs are also useful for detecting lithological changes associated with bedding plane fractures. Deposition of uranium, which is very mobile, may occur in fractures and the gamma log may also detect this. Care must be exercised when interpreting the logs, however, as coarse sandstones may produce a similar response to marl horizons due to the presence of potassium feldspar, another high gamma emitter. Interpretation difficulties also arise where caving of the borehole has occurred. The larger borehole diameter means that the tool is further away from the emitter. In this case it will appear that a formation with lower gamma emissions has been encountered where actually the change is due to borehole diameter variation.

Fluid logs: Fluid logs measure properties of the fluids contained in and entering the borehole, as opposed to the properties of the material the borehole has been drilled in. Standard logs include fluid electrical conductivity (EC), temperature and flow. EC and temperature logs are very useful for indicating fluid inflow through changes in EC and temperature and this is often associated with fracture zones. Fluid flow logs are used to indicate vertical flow within the borehole as well as flow from fluid entering the borehole. There are two types of flow meter – impeller and thermal. Measurements may be taken under natural or pumped conditions (either pumping of the borehole being logged or of adjacent boreholes). By flow logging and identifying changes in velocity, taking into account borehole diameter changes through caliper logging, fluid inflows can be located and the relative magnitude of inflows determined (Paillet, 1993).

Borehole TV logs: these are run using a CCTV set-up with a powerful light source to illuminate the borehole walls. A direct image of the borehole walls is produced. Clear fluid is required in the borehole for the log to be useful and if the borehole diameter is too large it may be necessary to run several logs with the camera moved to be close to the borehole wall. Where fracturing is observed it may also be possible to gain a qualitative indication of fluid flow if particles can be seen moving across the image. This may prove useful when deciding on specific locations for fluid flow logs or locating horizons for packer testing.

It is unlikely that any one type of geophysical log can provide a unique answer and in general it is necessary to run as many different types of logs as possible in order to aid hydrological interpretation. Geophysical logging of the new boreholes was undertaken 4 days after completion of drilling at BGS LVI and 1 day after drilling finished at BGS LVV. In both cases this was before the plastic casing was installed. Standard suites of geophysical logs were run by BGS including caliper, gamma, resistivity, magnetic susceptibility, temperature, SP, fluid conductivity and flowmeter logs. In addition to the new boreholes, BGS undertook geophysical logging of LVF BH2, BH3 and BH4. Geophysical logs for BH2 (1973) and BGS LVV (1999) are presented as figures within this chapter (Figure 4-4 and Figure 4-5). Copies of all other geophysical logs, including from work predating the current research are provided in Appendix 4.

Further geophysical logging was also undertaken for the current research in LVF BH2, BH3 and BH4 approximately four months after the borehole completion. Portable geophysical logging equipment, loaned by the University of East Anglia, was utilised to run fluid logs (temperature, conductivity and heat-pulse (flow) logs), electrical and gamma logs. Table 4-1 summarises the most recent geophysical logging, indicating which logs were run in each borehole.

Table 4-1 Summary of geophysical logging undertaken at Lower Venson Farm during the period of the research 1998 – 2001.

Borehole	Type of log	Logged by & date	Available data and format
BH 2	Caliper, fluid (temp & conductivity), natural gamma, resistivity (point and induction),	D. Buckley BGS 29/06/1999	Digital data (held by BGS) & paper copies (Appendix 4)

Borehole	Type of log	Logged by & date	Available data and format
	magnetic susceptibility, SP		
BH 3	Caliper, fluid (temp & conductivity)	D. Buckley BGS 1999	Digital data (held by BGS) & paper copies (Appendix 4)
BH 4	Caliper, fluid (temp & conductivity)	D. Buckley BGS 1999	Digital data (held by BGS) & paper copies (Appendix 4)
BGS LVI	Caliper; Gamma Ray; Focused resistivity; Induction resistivity; magnetic susceptibility; Fluid temp & Fluid conductivity	D. Buckley BGS 1999	NB two sets of logs exist, one, which is inclined, and one, which has been converted to the vertical. The caliper log is suspect as the arms don't touch the BH wall properly.
BGS LVV	Caliper; fluid flow; Gamma Ray; Focused resistivity; Induction resistivity; magnetic susceptibility; Fluid temp & Fluid conductivity	D. Buckley BGS 1999	Digital data (held by BGS) & paper copies (Appendix 4)
BH 2	Fluid (temp & conductivity); Heat pulse at various depths.	S. J. Watson & T.C. Atkinson 14/10/1999	Paper print outs, digital data on floppy disk
BH 3	Fluid (temp & conductivity); Heat pulse at various depths.	S. J. Watson & T.C. Atkinson 12/10/1999	Paper print outs, digital data on floppy disk
BH 4	Fluid (temp & conductivity); Heat pulse at various depths.	S. J. Watson & T.C. Atkinson 12&13/10/1999	Paper print outs, digital data on floppy disk

Geophysical log description

A general description of the geophysical logs run in the boreholes in the Tilmanstone – Eastry valley is undertaken here with regard to features relevant to flow and pollutant transport in a fractured Chalk aquifer. Where logging of a borehole has been undertaken at different times, relevant changes in the logged response are noted.

BH2: The geophysical log from 1973 is provided in Figure 4-4. The caliper log run prior to installation of casing indicates the larger diameter of the borehole from ground level to approximately 30 m bGL, suggesting a more heavily fractured region with marked fissuring from 10 to 16 m bGL. A large deflection in the log also occurs at 122 m bGL. This is also observed in the log run in 1999. In the 1973 logs there is a slight flattening of the temperature profile associated with this fissure, but nothing marked. In the 1999 logs there is a decrease in conductivity with a step rise in conductivity around the feature. The temperature log shows a steep rise above the fracture with a flat gradient across it, followed by a gentle increase in gradient below it.

During the 1999 geophysical logging of this borehole a grab sample was taken from the end of the borehole where there is a marked increase in EC. Analysis of the sample reveals high Cl and Li concentrations, and it is suggested that LiCl was used as a tracer during the 1970's investigations and it has remained at the bottom of the borehole, moving only by diffusion. During the drilling of BGS LVV some of the water produced during drilling was disposed of to BH2. Only approximately 6 m^3 was disposed of in this way as the water level in BH2 did not fall rapidly enough to take water at the rate BGS LVV produced it. The water produced from BGS LVV had a higher EC than that observed in BH2. Geophysical logging of BH2 subsequent to the disposal indicated that the high EC water now filled most of the BH2 borehole column except for a slight decrease in EC associated with the fracture feature at 120 m.

In summary:

- Original logging of the borehole in 1973 indicated a higher salinity water body overlying relatively fresher water (Brereton 1973).
- The borehole was used during tracer testing in the late 1970s and high conductivity seen today at the bottom of the borehole is related to LiCl tracer which has not dispersed.
- Borehole logging undertaken subsequent to the disposal of higher EC water from BGS LVV indicates a slow reduction in conductivity, particularly centred around a fracture feature observed on the caliper logs from 1973 and 1999.

BH3 log (30.6.99 BGS)

Caliper log indicates a fracture at 27 m bGL. There are also fractures indicated above this at 25 and 22 m bGL. The induction resistivity log shows an increase from 27 m bGL. There is a peak in the fluid conductivity at 22 – 24 m bGL, which decreases to a minimum at 36 m bGL, before increasing again, to the base of the borehole.

BH4 (30.06.99 BGS)

The caliper log suggests possible fracturing / borehole widening at 68 m bGL and 72 m bGL. The fluid conductivity log shows a step in EC at 71 m bGL. EC increases then follows a gradual decline to the base of the borehole. The average EC is 3125 µS/cm, the peak is 3140 µS/cm, which then declines to 3050 µS/cm at the base of the borehole.

BGS LVV (8.7.99 BGS)

The geophysical logs run in BGS LVV are provided in Figure 4-5. The caliper log indicates fractures at 19, 23 and 26m bGL. There is possibly some enlargement of the borehole at 68 to 70 m bGL and BGS LVI has flint rubble returned in the core from approximately this depth. The natural gamma log has notable peaks in the log at 28, 38, and 46 m bGL, a cluster of peaks at 49, 50 and 51 m bGL and additional peaks at 56, 59, 64, 76, 79, 81, 87 and 95 m bGL. An interpretation of these peaks is provided in Chapter 5. Peaks in the magnetic susceptibility log at 34 and 46 m bGL may indicate the presence of flints. The fluid conductivity log indicates a small decrease in fluid conductivity at 25 m bGL. The heat-pulse flowmeter log indicates some interesting water movement in the borehole. Readings were taken in the borehole while pumping at 16.3 m^3/h (drawdown = 0.66 m). The reading at 91 m indicates downward flow despite pumping at this rate. 17% of the total discharge is contributed to the borehole from the upper 20 m of the borehole; 48% of the total discharge comes from the zone 69 – 77 m bGL and 35% from the zone 77 – 85 m bGL. Below this horizon water appeared to be leaving the borehole, despite pumping.

Televiewer and optiviewer logs

In addition to the standard geophysical logs, Robertson Geologging undertook acoustic televiewer logging of both boreholes. This technique produces a continuous image of the acoustic response of the borehole wall. Open fractures produce contrasting features to the matrix and so provide details of fracture location. The fluid in the fractures conducts the sound wave more slowly than the rock matrix. The processing produces a virtual core for the borehole: fractures appear on the log image as dark lines, with the matrix as a paler background (Figure 4-6). Fracture orientation can also be determined from the tool orientation. Any intersection of the borehole by a planar dipping fracture will appear as a sinusoidal image and from this azimuth and dip can be determined (Zemanek *et al.* 1970, Paillet 1995).

Optiviewer logging is a relatively new technique to be used in hydrogeology in the UK. It uses a digital image video camera to record the borehole wall features, producing an extremely high-resolution image of the borehole wall. This can then be interpreted to define fractures and with good resolution, aperture size. In some cases it has produced images that can be used to produce virtual lithological logs, because the resolution is so good. Its advantage over acoustic televiewer logging is that it can operate both above

and below the water table, whereas the televiewer log requires fluid to act as a transporting medium. Unfortunately the optiviewer logging undertaken at Lower Venson Farm did not produce good quality images and the interpretation of them proved difficult. The acoustic televiewer logging produced the most useful data. A summary of additional logging undertaken by Robertson Geologging is provided in Table 4-2.

Table 4-2 Summary of Robertson Geologging geophysical logging at Lower Venson Farm.

Borehole	Type of log	Logged by & date	Available data and format
BGS LVI	Optiviewer log – digital video log	Robertson Geologging 1999	CD-ROM with data and viewing programme
BGS LVV	Optiviewer log – digital video log	Robertson Geologging 1999	CD-ROM with data and viewing programme
BGS LVI	Televiewer – acoustic log	Robertson Geologging 1999	Colour prints of log and interpretation
BGS LVV	Televiewer – acoustic log	Robertson Geologging 1999	Colour prints of log and interpretation

The acoustic televiewer software interprets the logged readings and produces an image of the interpretation as a virtual core of rock with the fractures marked on the core. Depth of fracture, angle of dip and direction of dip for the televiewer log of BGS LVV are presented in Table 4-3.

Table 4-3 Acoustic televiewer results for BGS LVV providing interpreted fracture with direction and degree of dip.

Depth (m)	Azimuth (degrees)	Dip (degrees)
21.54	65	12.9
24.24	96	12.5
24.27	301	14.1
24.85	231	14.6
24.91	342	15.2
25.45	299	9.4
25.95	125	18.4
28.09	150	75.2
28.27	288	4
31.46	61	41.8

Depth (m)	Azimuth (degrees)	Dip (degrees)
35.31	1	11.5
35.37	352	14.8
36.13	76	30.3
45.61	205	25.9
45.67	359	12
49.86	253	22.5
52.56	292	9.9
53.41	131	7.5
53.42	55	4
54.22	139	24.7
54.37	47	31.4
55.77	41	17.1
58.6	243	43.2
62.38	252	2
63.79	42	17.2
68.34	241	8.9
68.47	60	8.7
70.93	17	16.2
76.3	29	56.2
76.42	28	50.3

4.4.3 Structural assessment

Geological mapping at coastal and quarry sections, combined with analysis of core material and geophysical formation logs provides an integrated approach to forming a conceptual model of the physical framework of the aquifer. Assessment of changes in surface topography using digital elevation models (DEMs) can provide information from a local to a regional scale on structures that may exert control over the groundwater flow regime. Fracture mapping in quarries, road cuttings and at coastal exposure as well as geophysical acoustic televiewer logging can be used to build datasets of fracture set orientation and also fracture frequency. Establishing a relationship between fracture frequency and depth or lithology provides important information on matrix block size.

Catchment conceptual model of geological structure:

BGS developed a catchment scale conceptual model of the geological structure for the Tilmanstone area. This was done utilising digital elevation models (DEM's) to identify lineament patterns. Figure 4-7 details the model developed for Tilmanstone.

The DEM and interpreted structures have been overlain on a digital topographic map. The land surface aspect is then used to provide an indication of the structure. A number of structural scales are identified by BGS. These are:

- **Bounding structures**: interpreted as the largest faults, folds or monoclines in a catchment.
- **Within-block structures**: smaller structural lineaments that may indicate fault zones or zones of disturbance.
- **Local zones**: of folding and more diffuse deformation, not cross-cutting larger features.

Fracture sets and orientation:

There are three main joint sets in the Tilmanstone area. Two sub-vertical and one sub-horizontal. The two sub-vertical sets strike at 030 and 210 degrees and the sub-horizontal set is oriented parallel to the regional bedding which dips between 0.5 and 1 degree to the north east. The contoured pole plots of all fracture orientation data for the Tilmanstone area collected during the BGS Fracflow investigation are presented in Figure 4-8, after FRACFLOW (1999).

Fracture density depth relationship:

As part of the FRACFLOW investigations BGS undertook scanline surveys (Priest and Hudson, 1981; Priest 1993) in the area around the Tilmanstone - Eastry valley. The sites surveyed included the coastal outcrop cliffs of St Margarets Bay (NGR 6368 1442), a small chalk pit / road cutting (NGR 6300 1505) to the east of the Tilmanstone colliery and Rowlings Quarry (NGR 6284 1553). The fracture profiles produced from the televiewer and optiviewer logging were also assessed. Fracture intensity in the Chalk is known to vary with depth (Allen *et al.* 1997) and a fracture density depth relationship was established for the area, described by the equation:

Log fracture density [1/m] = -1.685 x Log depth [m bGL] + 2.5365
(Bloomfield *et al.* 2000).

This relationship is used to plot the points in Figure 4-9, which shows the number of fractures per metre along with the corresponding matrix block sizes, at Lower Venson Farm.

The form of the relationship is of a negative exponential decline in fracture frequency with depth. This fracture-density-depth relationship is unsurprising given the findings of Hudson and Priest (1979). They combine three fracture spacing distributions; negative exponential, normal and uniform, which when taken in combination are considered by the authors to be likely to approximate any in-situ fracture spacing distribution.

The *negative exponential distribution* characterises fracture spacings associated with randomly positioned fractures along a scanline or borehole. This implies mutual independance between fracture positions. A *uniform distribution* occurs where all fracture spacing values, up to a limiting value, have an equal probability of occurring. A *normal distribution* has a mean fracture spacing of the most commonly occurring value. The occurrence of a fracture is related to the position of adjacent fractures and reflects the original formation process.

Hudson and Priest's results from the combination of distributions are dominated by the negative exponential distribution with an exception occurring only when a normal distribution makes an 80% contribution. Mixed fracture spacing distributions tend to converge to a negative exponential distribution. A combination of at least two of the three fracture spacing distributions is likely to be encountered in the field as most fracturing occurs as a result of a number of geological and mechanical factors in combination, hence it is likely that a fracture-density depth relationship will have a negative exponential form.

4.5 Hydraulic regime and hydraulic properties

4.5.1 Water level monitoring

Monitoring of water levels in the Tilmanstone – Eastry valley is undertaken by the Environment Agency. The groundwater hydrographs are typical of those for boreholes in fractured chalk, displaying a spiky response to rainfall, indicative of low storage. Water levels generally rise rapidly with the onset of winter recharge around October followed by an exponential recession curve. This recession reflects the ease of drainage of upper, more highly fractured levels within the aquifer, slowing down as lower less fractured and hence less readily drained levels are reached. Figure 4-10 gives the water levels monitored during the period of current research.

The datum levels for BH2, BH3, BH4 and BHE were re-surveyed during the period of the research after concerns were raised about the labelling of the boreholes at the Lower Venson Farm site by the Environment Agency and the datum recorded for BHE on Environment Agency records. After levelling the borehole datum and reviewing borehole construction records (SWA 1976a) and original files it is concluded that the Environment Agency records are incorrect with the labels for BH3 and BH4 being switched at some point. The water level records for these two boreholes have been amended in the light of this finding.

The hydrographs indicate that water levels in the middle part of the aquifer, monitored in BH4 (at Lower Venson Farm) are slightly higher than those in the upper part of the aquifer (monitored by BH3 at Lower Venson Farm). This suggests that some of the lithologies present in the lower part of the Seaford Chalk / upper part of the Lewes nodular Chalk are able to act as semi-confining layers, at least locally. The monitoring network in the valley is not adequate to estimate how extensive the confining layer may be.

4.5.2 Packer tests

Packer testing of aquifers is usually undertaken to obtain a measure of bulk hydraulic conductivity for a discrete section of a borehole. A summary of packer testing theory and approach is presented here followed by the results from testing undertaken at the Lower Venson Farm site.

A packer test is generally carried out for several sections in the borehole in order to make a quantitative assessment of the contribution of each section to the overall transmissivity of the aquifer in the vicinity of the borehole (Brassington and Walthall 1985). It is usually assumed that steady state conditions have been achieved during each stage of the test and the Hvorslev (1951) method is then used to calculate the hydraulic conductivity for the test section. Hvorslev (1951) provides a number of pre-determined shape factors for various piezometer and packer arrangements.

Where l/r exceeds 10 (or $l > 5r$, Price *et al.* 1982) then the Hvorslev formula can be simplified to:

$$K = \frac{Q}{2l\pi H} Ln\left(\frac{l}{r}\right)$$

Equation 4-1

where

K – hydraulic conductivity

l – length of test section

r – radius of borehole at test section

Q – volumetric flow rate

H – drawdown in the test section

Sources of error

Sources of error in packer testing include:

- poor sealing of packers and short circuiting - this is checked for by using stepped injection rates and checking that a linear response is observed. The injection rate is stepped up in 3 stages (equilibrium is established at each stage) then stepped down via the same stages. Ideally the pressures recorded for the upward and downward steps should be identical;
- non-saturation of the test zone;
- fracture development due to use of excessive injection pressure head;
- fracturing due to packer inflation; and
- analysis of non-steady state conditions

Approach

Packer testing of BGS LVV was undertaken on 13 and 14 July and 17, 18 and 19 August 1999. Table 4-4 gives details of dates and the intervals tested.

Table 4-4 Diary of packer testing undertaken at BGS LVV, Lower Venson Farm.

Date	Test number	Packered interval (m bGL)
13/07/99	1	30.18 to 33.05
13/07/99	2	45.48 to 48.37
14/07/99	3	75.80 to 78.85
17/08/99	4	35.7 to 38.58

Date	Test number	Packered interval (m bGL)
17/08/99	5	39.25 to 42.13
17/08/99	6	49.46 to 52.33
19/08/99	7	57.20 to 60.07
19/08/99	8	61.76 to 64.64
18/08/99	9	65.5 to 68.38
18/08/99	10	76.09 to 78.96
18/08/99	11	81.29 to 84.16
18/08/99	12	82.28 to 85.15

Figure 4-11 shows the packer rig layout.

The testing methodology followed that set out in Price and Williams (1989). The procedure is summarised as:

1. Packer string lowered to appropriate depth.
2. Water level in borehole measured and monitored for duration of test.
3. Transmitter used to measure water level in the test interval (water level in test interval initially at equilibrium with borehole water level).
4. Packers inflated slowly (pressure required calculated as approximately 6 bars above pressure in test interval).
5. Monitoring of transmitter readings, water level and inflation pressure during inflation. (Dipper left in borehole, just above water table to give warning if inflation failed and gas began airlifting water).
6. Sealing of packers usually gives a small but significant change in transmitter, water level and inflation pressure readings.
7. When readings were stable, pumping commenced and the water level, transmitter reading and flow meter were continuously monitored. Movement of water level in the borehole indicates packer leakage.
8. When stable flow rate and transmitter readings were achieved, the data were noted and the pump rate changed. This step was repeated a number of times.
9. Pumped water was sampled immediately before pump shutdown.
10. Pressure readings and water level were monitored after final pump shutdown and when readings had stabilised the packers were deflated and the packer string moved to a new interval.

Choice of test interval

Test interval locations were constrained by the presence of flint horizons. Inflated packers are susceptible to puncture by sharp flints and so cannot be set over a flint horizon. To a certain extent this may have led to a bias in intervals chosen such that the packers straddle flint horizons and preferentially test those features. Flint horizons may act as a barrier to the downward migration of fluids and develop preferential flow horizons above them. Testing of such a feature will produce a higher than average hydraulic conductivity for that interval and this must be considered when interpreting the results.

The in-situ pressure head (in metres) with depth, as calculated from the observed pressure transducer readings, for each sealed packer interval is provided in Figure 4-12 A. There is an increase in pressure head with depth.

The hydraulic head calculated for each packered interval for the tests undertaken in the period 17 to 19 August 1999 is provided in Figure 4-12 B. The August period is chosen as this was when the majority of measurements were made. The hydraulic head is the sum of the pressure head and elevation head. The elevation head is taken as the elevation in metres above Ordnance Datum of the midpoint of the packered interval. The measurements indicate a general decline in hydraulic head with depth, with head minima at -32.7 m aOD (50.9 m bGL), -48.8 m aOD (67 m bGL) and -65.5 m aOD (83.7 m bGL). An interpretation of the head minima in relation to the geophysical logging is provided in Section 5.3.2.

Calculated hydraulic conductivities are presented in Table 4-5.

Table 4-5 Hydraulic conductivity calculated from packer testing in BGS LVV, Lower Venson Farm. Interval length is 2.87 m, radius 0.09 m.

Test number & interval (m bGL)	Flow rate (m^3/day) & drawdown (m)		Calculated hydraulic conductivity (m/d)
30.18 – 33.05	Q = 64.37 Q = 16.85	Δs = 0.09 Δs = 0.03	137 106
35.70 – 38.58	Q = 35.28 Q = 37.44	Δs = 0.108 Δs = 0.145	63 49
39.25 – 42.13	Q = 25.92 Q = 31.68	Δs = 0.08 Δs = 0.104	62 59

Test number & interval (m bGL)	Flow rate (m^3/day) & drawdown (m)		Calculated hydraulic conductivity (m/d)
45.48 – 48.37	Q = 23.76 Q = 63.36	Δs = 0.09 Δs = 0.33	52 37
49.46 – 52.33	Q = 48.96 Q = 47.52 Q = 33.12	Δs = 0.52 Δs = 0.51 Δs = 0.28	18 18 22
65.5 – 68.38	Q = 43.2	Δs = 0.08	101
75.98 – 78.83	Q = 63.64	Δs = 0.07	164
76.09 – 78.96	Q = 50.4	Δs = 0.06	172
81.29 - 84.16	Q = 17.28 Q = 14.4 Q = 12.96 Q = 21.6	Δs = 1.32 Δs = 4.55 Δs = 1.01 Δs = 0.66	3 1 2 6
82.28 – 85.15	Q = 16.56	Δs =1.82	2

4.5.3 Matrix porosity

Porosity measurements were carried out by BGS on the core samples from BGS LVV using liquid resaturation porosimetry as described by Bloomfield *et al.* (1995). Figure 4-13 shows the results plotted against depth. A profile of digitised data for BHB (NGR 6296 1526) from the investigations undertaken in 1974 (previously presented in Figure 3-22) is also provided in the figure for comparison.

A summary of the porosity of BGS LVV is given here and a fuller analysis and interpretation of BGS LVV and BHB is presented in section 5.2.3. The porosities measured from the BGS LVV core show a decline in value from approximately 45% to 40% between 8 and 60 m bGL. Higher porosity is measured at approximately 17 (48%), 21 (53%) and 28 to 32 (46%) m bGL and lower values at approximately 37 (39%) and 60 (37%) m bGL. Below 70 m bGL there is a marked change in the profile with much lower porosity values being measured notably at 74 (27%), 82 to 84 (26%) and 88 (34%)m bGL. The average porosity for the total BGS LVV core is 42%, and splitting it at the Seaford Chalk, Lewes Nodular Chalk boundary gives an average porosity of 44.5% for the upper 42 m of the core and 40% for 44 to 98 m bGL. Taking a boundary at the Chalk Rock gives a porosity of 43% for the Upper Chalk and 38% for the Middle chalk. These average values are slightly higher than those reported by Bloomfield *et al.* (1995) for the area they describe as Thames and Chilterns, which is the relevant area for Tilmanstone. Bloomfield *et al.* report a mean of 38.8% for Upper Chalk and 31.4% for the Middle Chalk for the Thames and Chilterns area.

4.6 Solute transport regime

4.6.1 Single borehole dilution tests

Single borehole dilution tests were undertaken during summer 1998 at Thornton Farm, Lower Venson Farm and Eastry (Hazell 1998). The methodology followed was that detailed in Ward *et al.* (1998). A quantity of tracer solution is introduced into the borehole such that the concentration of the chosen tracer is raised to 100 to 1000 times background levels. The tracer is introduced via a length of hosepipe. The hosepipe has a weight attached to the lower end and a funnel inserted at the top, with a small gap to allow air to escape. Tracer solution is introduced slowly into the hosepipe such that water inside the piping is displaced by the tracer solution. Once the hosepipe is full of the tracer solution, it is slowly withdrawn, allowing the tracer solution to enter the borehole as a line source. Figure 4-14 shows the hosepipe injection arrangement. Sampling of the borehole water containing the tracer is then undertaken at intervals until concentrations return to background.

It is often convenient and cost effective to use a salt as the tracer solution as it is then straightforward to measure the change in electrical conductivity (EC) of the borehole water directly using an EC probe, and either to correlate this with the salt concentration or to use the EC readings directly for the test analysis. The most convenient and cost effective salt to use is NaCl, due to its ease of availability. This was the approach initially adopted for the single borehole dilution tests that were run during summer 1998, but a number of difficulties arose. These were mainly associated with the existing background concentrations of NaCl in the aquifer from the saline mine waters and the problem of achieving a large enough increase in EC, without running into problems associated with density of the tracer solution.

Single borehole dilution testing undertaken in subsequent field seasons (summer 2000 and 2001) utilised either a bromide salt solution (KBr or LiBr) or fluorescent tracer dyes (sodium fluorescein, Rhodamine WT and photine). The fluorescent tracer used during summer 2000 was analysed using the spectrofluorometer at the School of Environmental Sciences, University of East Anglia (Quinn 2000). The fluorescent tracer solutions have the advantage that much smaller quantities of tracer need to be introduced for concentrations to be raised 1000 times above background levels. However the approach required the development of a sampling methodology that

minimised disturbance to the water column, but allowed a sample to be collected from regular intervals within the borehole. The method developed utilises a string of self-sealing bailers set at intervals along a weighted line. As the line is lowered through the water column water flows into and through each bailer (Figure 4-15). At the required depth the movement is halted, allowing the bailers to settle, then the line is steadily withdrawn. The upward movement causes each bailer's non-return valve to seal, capturing a sample from the relevant depth. As each bailer reaches the surface its contents are transferred to a sample bottle for later analysis. Only the middle part of the sample is retained. A single transfer tube is used between bailers and between runs so the lower part of the bailed sample is flushed through the tube to remove the effect of previous samples. The upper section of the bailer contents is also discarded to reduce the impact of pollution of the bailer sample with borehole water from a different level due to interaction at the top opening of the bailer tube.

Analysis of the fluorescent samples from the summer 2001 testing was undertaken in the laboratory using the UCL Groundwater Tracing Unit's Perkin-Elmer LS55 Luminescence Spectrometer. Analysis of the Rhodamine WT samples from the single borehole dilution test in BGS LVV 2001 proved difficult due to that tracer needing to be of high concentration as it was used for a borehole to borehole natural gradient test, see section 4.6.2. All samples were therefore diluted by a factor of 100 in the laboratory using a 0.1 ml epindorff pipette and 10 ml flask prior to running through the fluorometer.

The analysis procedure is straightforward. Having calibrated the machine by running a set of the appropriate standards through it, the diluted samples are then poured into clear plastic cuvettes. Calibration plots for fluorescein and Rhodamine WT are given in Figure 4-16. The samples are inserted into the cuvette holder located in the front door of the instrument, the door is closed and the machine takes a reading which is then stored in the computer file for that session. Occasional blanks and standards were also run through to check machine calibration. Samples for the single borehole dilution tests were analysed in reverse order such that the higher concentration, early samples were analysed last. This reduces the chance of introducing errors by contaminating later, lower concentration samples with solution from higher concentration samples.

Examples of the results obtained for two of the boreholes tested are given in Figure 4-17, Figure 4-18 and Figure 4-19. All other results and analyses are collated in Appendix 4.

Figure 4-17 to Figure 4-19 show typical responses measured in the boreholes during the single borehole dilution testing. The difficulty of evenly distributing tracer in the borehole is demonstrated in Figure 4-17 at 0 m aOD where a high concentration spike is observed in all the sample runs. The tracer concentration achieved is only double background levels, rather than the 100 to 1000 times recommended by Ward *et al.* 1998. This does not seem to invalidate the test as it is still possible to take several readings to give a time series of EC measurements along the borehole profile.

The EC observations at the top of the borehole indicate an increase in concentration over time in the normalised profile in Figure 4-17. This is thought to be due to tracer being released within the cased section of the borehole and the tracer then diffusing from the cased section into the open section of the borehole. The calculated Darcy velocity at the top of the borehole should be ignored. BH3 at Lower Venson Farm was the only borehole to have a repeat test undertaken, the two resulting profiles are those presented in Figure 4-17 and Figure 4-18. The tests were undertaken at similar times of the year: June 1998 and July 2001, however the water level, tracers used and the sampling methodologies were different. The water level was approximately 4.5 m higher in 2001 compared to 1998. The 1998 test used NaCl and the EC depth probe, whereas the 2001 test used sodium fluorescein and the bailer string sampling method. The profile for the bailer string sampling method Figure 4-18 is smoother compared to that from the EC depth probe (Figure 4-17). This reflects the stronger mixing effect of running the bailer string up and down the borehole water column, compared the EC depth probe. The initial profile (Co) for the 2001 test is also smoother than the 1998 profile and this is probably due to a reduction in the rate of removal of the injection hose. Care was also taken to ensure no tracer was injected within the cased section of the borehole and this appears to have been successful.

Most of the borehole profiles show a steady decay in either EC or concentration over time. In some of the tests particular horizons show more rapid decay, such as -7 to -8 m

aOD in the normalised plot for Figure 4-19. This may be indicative of horizons with a greater degree of fracturing.

Overall the single borehole dilution tests show some interesting results. For the tests undertaken in the upper part of the aquifer (broadly BH3, BH8, BHE and BGS LVV) no horizons with particularly rapid loss of tracer are identified. Instead the flow in the aquifer appears to be relatively evenly distributed. However in the test undertaken for the middle part of the aquifer (BH4) specific horizons appear to be more important for flow within an overall low flow zone.

Care needs to be taken when interpreting data where there appeared to have been some influence on the observations due to tracer diffusing out of the cased section of the borehole. The bailer string method tends to smooth the distribution of tracer in the water column so is a less suitable method where an aquifer is subject to high flow horizons. The single borehole dilution test approach has been successful in the Tilmanstone-Eastry valley in spite of the high background chloride concentrations and has proved to be a relatively low cost and rapid method for measuring Darcy velocity and enabling calculation of spatial distribution of hydraulic conductivity. Undertaking the testing at different times of the year would readily provide data on the temporal variation of Darcy velocity.

4.6.2 Natural gradient tracer tests

An initial natural gradient tracer test was undertaken over winter 1999 / 2000. This involved injecting 40 g of Diphenyl Brilliant Flavine 7GFF (also known as Direct Yellow) dissolved in 11 L of tap water into BGS LVV. The injection method was via the weighted hosepipe in the same way as the single borehole dilution tests. Monitoring in BH's 2, 3 and 4 was undertaken by attaching unbleached cotton wool wads to weighted monofilament fishing line and suspending this arrangement in the borehole. The tracer dye sorbs to the cotton wool and can be detected by fluorescence under ultra-violet light as small yellow spots on the cotton wool. This type of test can only be used to give qualitative results. The cotton-wool detector lines were changed at intervals after the injection. Full details of the test results are given in Appendix 4; the inferred pathways are presented in Figure 4-20.

In spite of tracer being injected through the entire open length of the borehole, there was only a positive detection of tracer appearance in BH3. The water levels between boreholes show that there is a vertical hydraulic gradient from BGS LVV to BH2 and BH3, indicating that movement of tracer from BGS LVV to both BH3 and BH2 is possible. The water level in BGS LVV is 0.19 m higher than in BH3 and 0.68 m higher than in BH2. The test suggests that BGS LVV is providing a short circuit to the aquifer system, allowing water flowing at deeper levels approximately 65 to 90 m bGL at Lower Venson Farm (the interval open to BH4) to move up into shallower levels which BH3 is open to. The possible positive at BH2 is feasible, given the movement of groundwater detected within BGS LVV by the heat-pulse flowmeter measurements (Section 4.4.2), but no further interpretation of this result is justified given the uncertainty of the markings on the cottonwool.

Following from the results of this first test, a second natural gradient test was designed. 37.74 L of 318 mg/L bromide solution was injected into the upper section (15 – 46 m bGL) of BGS LVV (Quinn 2000), approximately the same open interval as BH3. Sampling was undertaken in BH3 using the bailer string method as described in section 4.6.1. For the bromide solution, an ion-specific electrode was used to monitor samples in the field (Quinn 2000). The ion-specific electrode was loaned by BGS and calibrated prior to sampling and at the end of each day, to check for instrument drift.

Figure 4-21 shows the measured bromide concentration over time and depth. Only very low concentrations of KBr were detected. It is likely that this is due to the monitoring borehole not being located directly down gradient of the injection borehole.

Approximately 1% of the injected solution was recorded at the monitoring borehole. Peaks in concentration are observed at –2.5 and –23 m aOD 17.75 hours after injection and at –7 m aOD after 20.95 hours after injection. The entire profile shows an increased bromide concentration after 24.67 hours after injection. Unfortunately, due to the extremely low concentrations observed at the monitoring borehole, the sampling was undertaken too infrequently so these results do not provide adequate detail to calculate travel times for individual fracture pathways, although the results do suggest that tracer is taking more rapid pathways at some horizons in the aquifer than at others. A much higher tracer concentration was expected, therefore the rise in concentration that did

occur did not trigger the necessary increase in frequency of sampling. It was therefore decided to re-run the test using more responsive, fluorescent dyes and to design the test such that two single borehole dilution tests were run at the same time. This allows the flux leaving the injection borehole to be compared with the groundwater flux entering the monitoring borehole.

This second natural gradient testing from BGS LVV to BH3 took place in summer 2001. Separate teams carried out injection and sampling in order to ensure that no cross pollution occurred between the two boreholes. 195 g of 21.3% active ingredient Rhodamine WT was injected into BGS LVV, having been dissolved in 4 litres of tap water. This resulted in a concentration in the borehole after injection of approximately 43 mg/L. 50 ml samples were collected in brown screw-cap bottles and stored in the dark. See section 4.6.1 for the laboratory fluorometer instrument details and analysis method. Field analysis also took place using a Turner Instruments 10-AU Field fluorometer hired from ENTEC Ltd. This provided a field check that tracer solution was being detected and enabled the initial, detailed sampling to be terminated once a peak, steady concentration was reached.

The results for this 2001 natural gradient tracer test suggest at least two possibilities for the approach that could be taken to interpret them. The tracer arrives at individual levels at different times in the early-time data (Figure 4-22 and Figure 4-23) and this suggests that tracer is following pathways either of differing lengths or at differing velocities. Variation in velocity could be caused by fracture aperture variability. However it is arguable that the individual tracer peaks on the early data are not real tracer breakthrough peaks but are experimental error or variability as they are generally only represented by one data point. The longer-term data (Figure 4-24 and Figure 4-25) show a build up in tracer concentration to a high concentration maintained over several days.

Summary discussion of tracer tests

The results from the tracer testing, both single borehole dilution and natural gradient, demonstrate the difficulty of undertaking tracer tests in the Chalk. The natural gradient tracer tests in particular highlight the importance of understanding the fracture orientation and groundwater gradients at a very local level when designing tracer tests. BGS LVV and BH3 are only 28 m apart and have a 0.2 m head difference, suggesting a

component of groundwater flow is from BGS LVV to BH3, but only approximately 1% of injected tracer is recovered in BH3, suggesting it is located at the edge of the tracer plume or is bypassed by more transmissive fracture channels. It is also important to consider what effect pumping may have in over-riding the natural flow directions and routes, and how interpretations based on pumped tracer tests may not provide an understanding of the natural, unstressed system.

4.7 Plume characterisation

4.7.1 Hydrochemical sampling

Sampling in and around the Tilmanstone – Eastry valley has been undertaken sporadically since the early 1900s. Initially the aim was to ascertain the effects of the mine water disposal technique. More recently the aim of the sampling has been to delineate the extent of the pollution plume and to track its movement. Sampling of boreholes in and around the Tilmanstone – Eastry valley was undertaken during summer 1998 (Hazell 1998). This survey updated previous chemical sampling undertaken in the area in 1994 (Peedell 1994), 1977 (SWA) and 1949 (Buchan 1962). It proved impossible to locate or gain access to several of the boreholes used for sampling in previous surveys, making direct comparison between years difficult at individual sampling locations. Samples were recovered using a pump borrowed from Kent area Environment Agency (EA) or directly from storage tanks or in-situ pumps where access for the EA's pump was restricted. A summary of the analyses from the 1998 survey is given in Appendix 4 and reported on by Hazell (1998). Figure 4-26 provides contoured chloride concentrations from the surveys undertaken in 1949, 1977 and 1994.

Water samples were collected during packer testing of BGS LVV. Results of analyses are provided in Table 4-6.

Table 4-6 Chloride concentration of fracture water samples collected during packer testing of BGS LVV.

Date	Depth range	Cl conc (mg/L)
13 - 14 July 1999	30.18 to 33.05	860
	45.5 to 48.37	860
	75.8 to 78.67	840
16 - 19 August 1999	25.7 to 38.58	880
	39.23 to 42.13	850

Date	Depth range	Cl conc (mg/L)
	49.46 to 52.33	900
	65.5 to 68.34	850
	65.5 to 68.34	860
	76.09 to 78.96	830
	82.28 to 85.15	540

For comparison, data from sources in valleys adjacent to the Tilmanstone – Eastry valley, and thought to be unaffected by mine water pollution, are provided in Figure 4-27.

The data presented in Figure 4-27 suggest that the PWS boreholes at Woodnesborough and Flemings, although located in a valley adjacent to the Tilmanstone-Eastry valley (see Figure 3-19) may be drawing high chloride water in from the Tilmanstone plume. However the boreholes are also located close to the Tertiary cover and it is likely that water drawn from this area may have elevated chloride levels. Further consideration of these boreholes is beyond the scope of the current research.

4.7.2 Porewater sampling

The Chalk core produced from the drilling of BGS LVV was taken to BGS at Wallingford and sampled approximately every 0.5 m. The sampled core was crushed and centrifuged and the liberated porewater was then analysed by BGS. The full set of analytical results is given in Appendix 4. Figure 4-28 shows the porewater SEC and chloride concentrations against depth.

During sampling of the core no particular attention was paid to selecting core material close or nearer to a fracture. This was due to the poor quality of the core, which was very broken and so it was difficult to distinguish between natural and drilling-induced fractures. The porewater chloride concentration is very smooth across the upper part of the borehole (0 to 40 m bGL), indicating that porewaters within the matrix blocks have had time to reach very similar concentrations. The porewater chloride concentration decreases very rapidly at approximately 45 m bGL, and then rises again at 60 m bGL before decreasing again at approximately 80 m bGL. Figure 4-28 also indicates the fracture water chloride concentrations from samples taken during the packer testing. Samples obtained from horizons at 50 m and 82 m below ground level show a large difference in fracture water and porewater chloride concentrations. For comparison with a dissolved contaminant from a different source, Figure 4-29 shows a plot of nitrate

concentrations against depth as well as chloride concentrations for BGS LVV porewater.

There is a clear difference in the styles of the profiles due to the contaminant source. The chloride has managed to penetrate a considerable depth into the aquifer, probably due to the driving head that existed during the mine water lagoon operation. The nitrate concentration peaks at 10 m bGL, below which the concentration is fairly uniform at 4 - 5 mg/L to 80 m bGL. Below this the nitrate concentration decreases sharply to 2 mg/L.

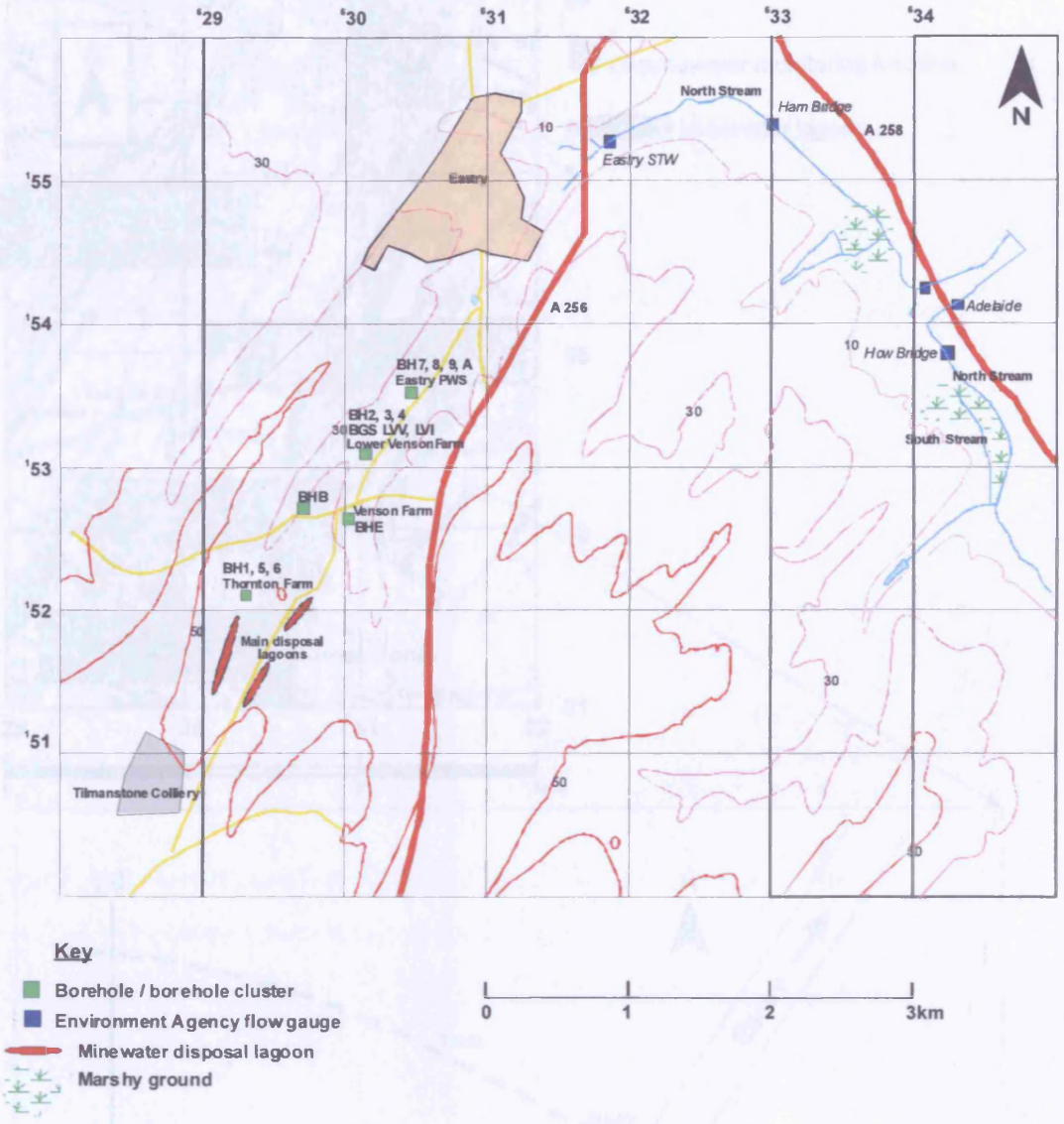

Figure 4-1 OS map of Tilmanstone – Eastry valley showing borehole locations.

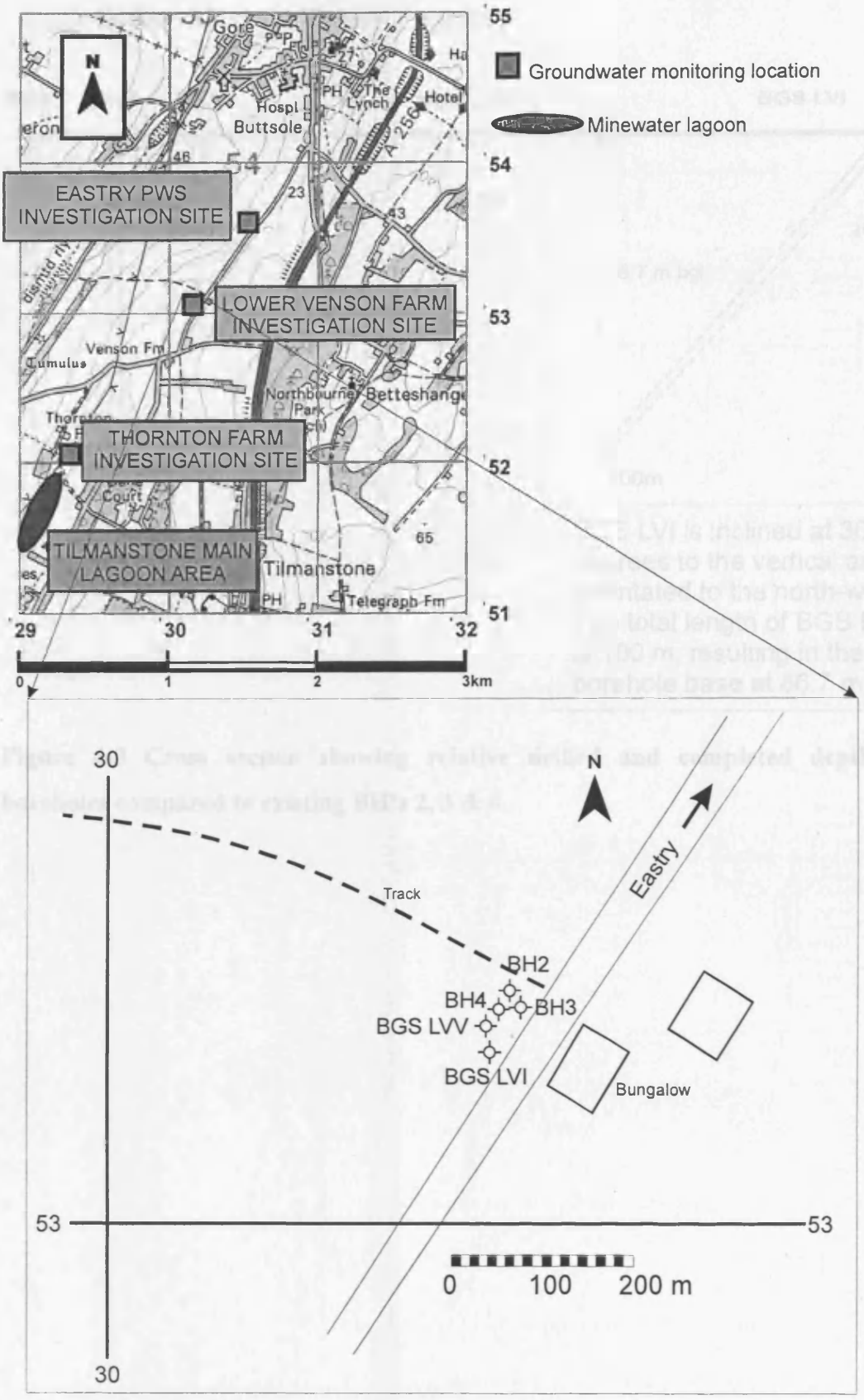

Figure 4-2 Location of observation borehole sites in the Tilmanstone-Eastry valley and site plan for Lower Venson Farm with new boreholes BGS LVV and BGS LVI located.

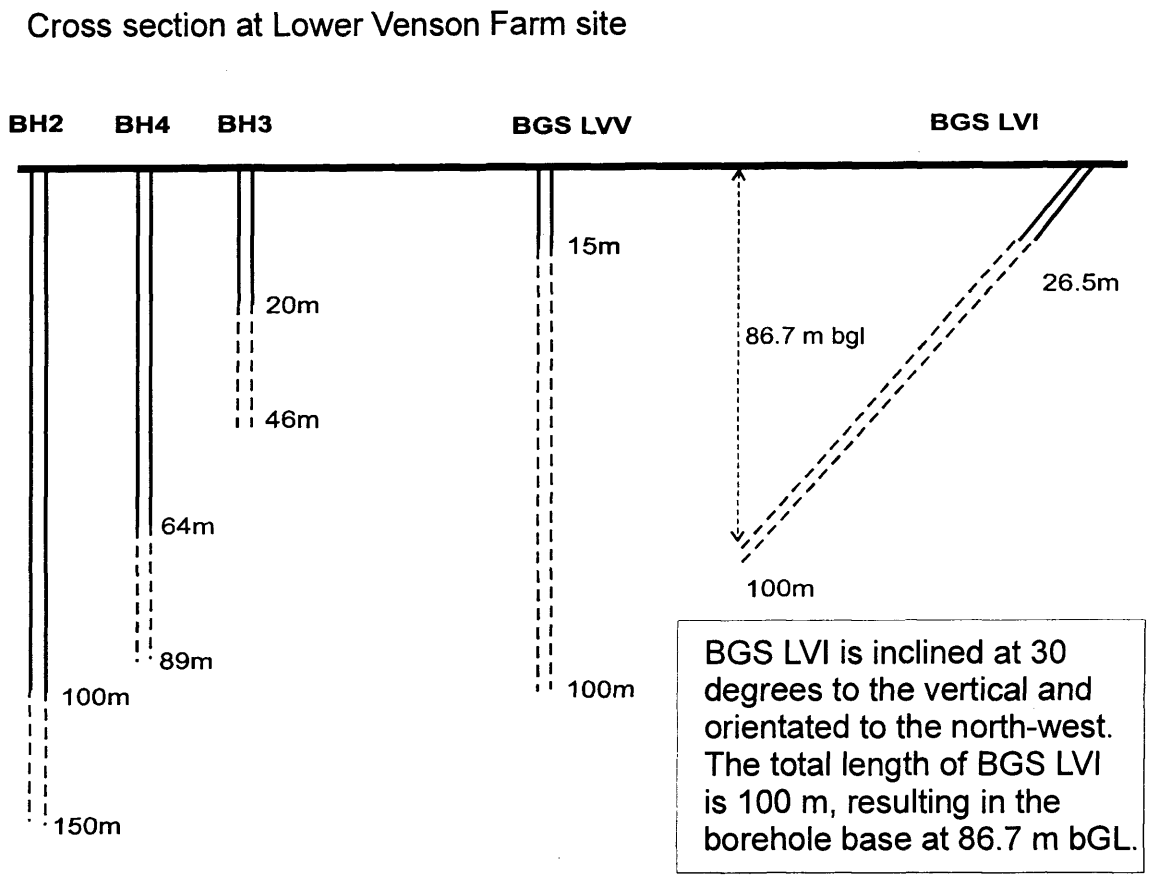

Figure 4-3 Cross section showing relative drilled and completed depths of boreholes compared to existing BH's 2, 3 & 4.

DATUM = 18.047 m OD

Well Name: Lower Venson Farm
File Name: C:\VLWJODDATA\LOWVENFALL.HDR
Location:

Geophysical logs run by WRB 26/7/73 and digitised by BGS
Plenus Marls indicated at 152m.DT1,2 are differential fluid Temperature logs,(abitrary scale)

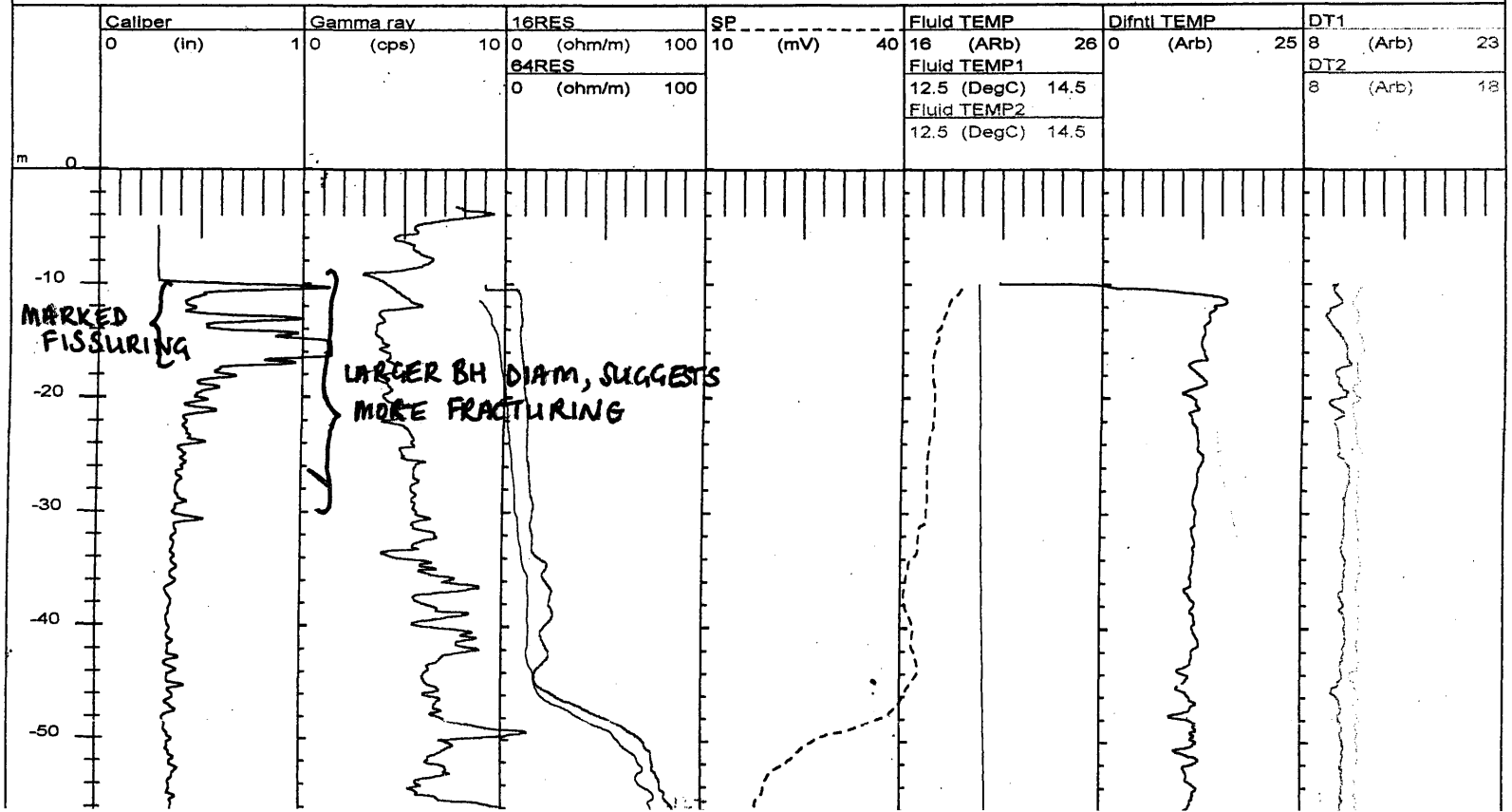

Well Name: Lower Venson Farm-vertical
File Name: C:\VLW\RGL\VENFARMV\ALL.HDR
Location:

Geophysical logs run by BGS 8/7/99.log datum is GL (0.1m below temporary steel casing top).
SWL:8.54mbd.Borehole was completed previous day and stood for only 18hrs max.
Borehole was pumped and pumped fluid logs are suffixed 'Q'.pumping rate was 16.8m3/h, PWL:9
Heat-pulse flowmeter measurements made when pumping at 10,11.5,13,18,24.7,28.5,35,75,80,9
Vertical bars in ac-Flowmeter track are 17,65 and 100% of total discharge (MSUS log suspected

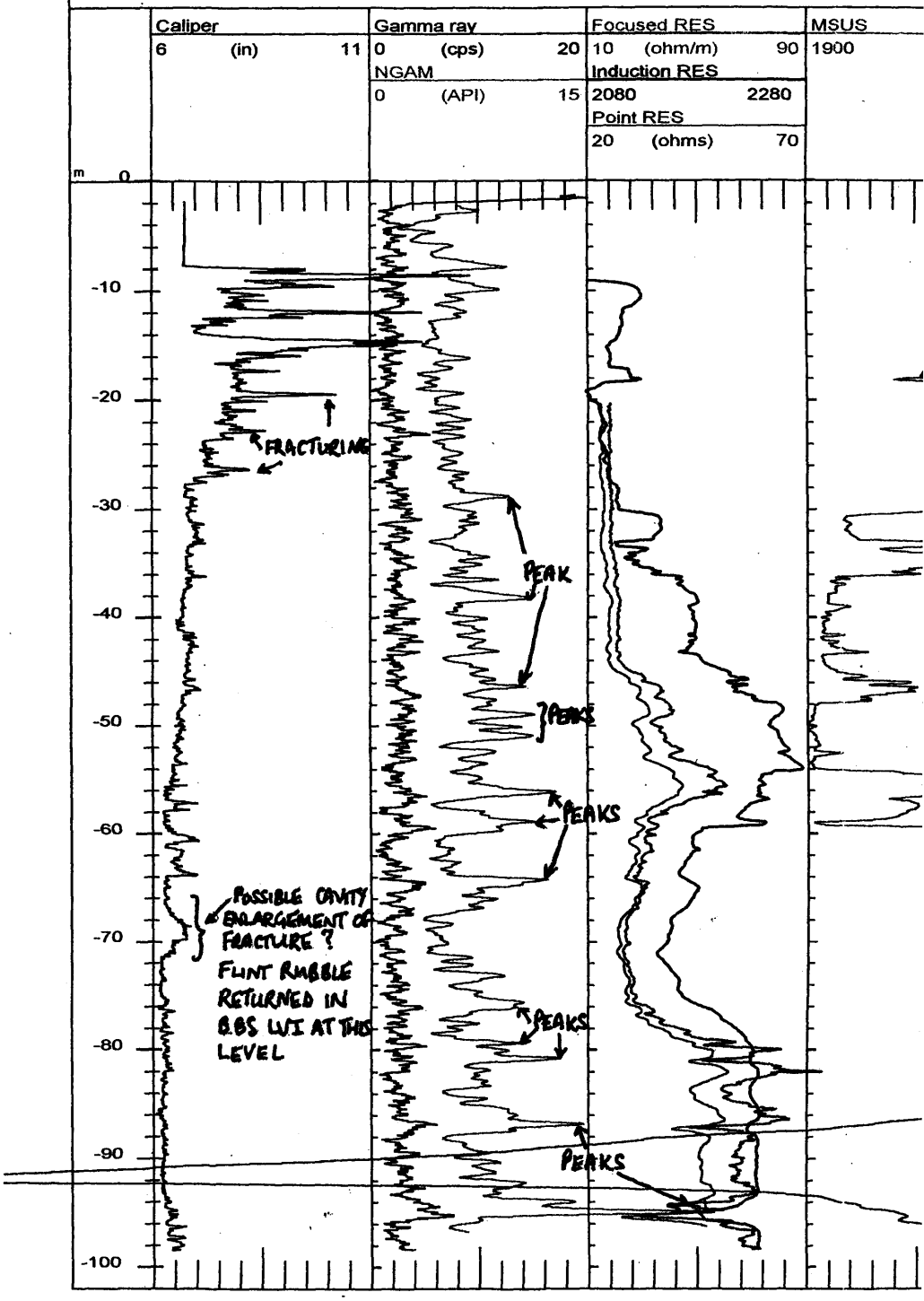

Figure 4-6 Acoustic televiewer logging image for BGS LVV (depth interval 23 to 28 m bGL)

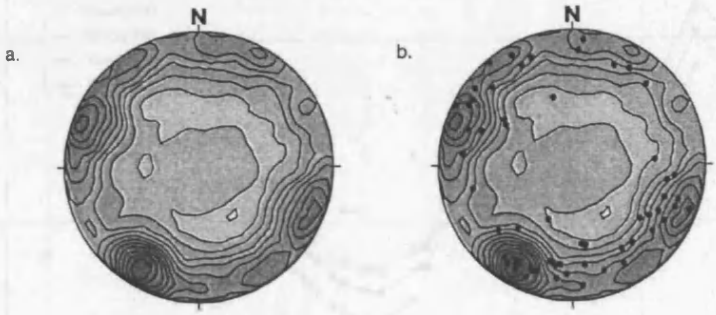

Figure 4-8 Contour plot of poles to fractures for all fracture orientations measured in the Tilmanstone area, *after* BGS (FRACFLOW 1999).

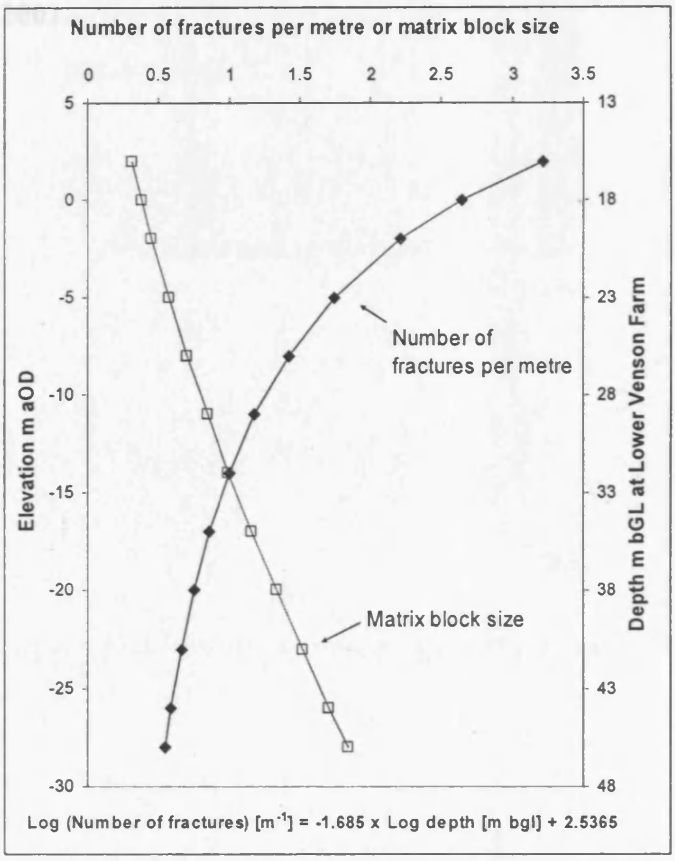

Figure 4-9 Fracture-density depth relationship and corresponding matrix block size at Lower Venson Farm.

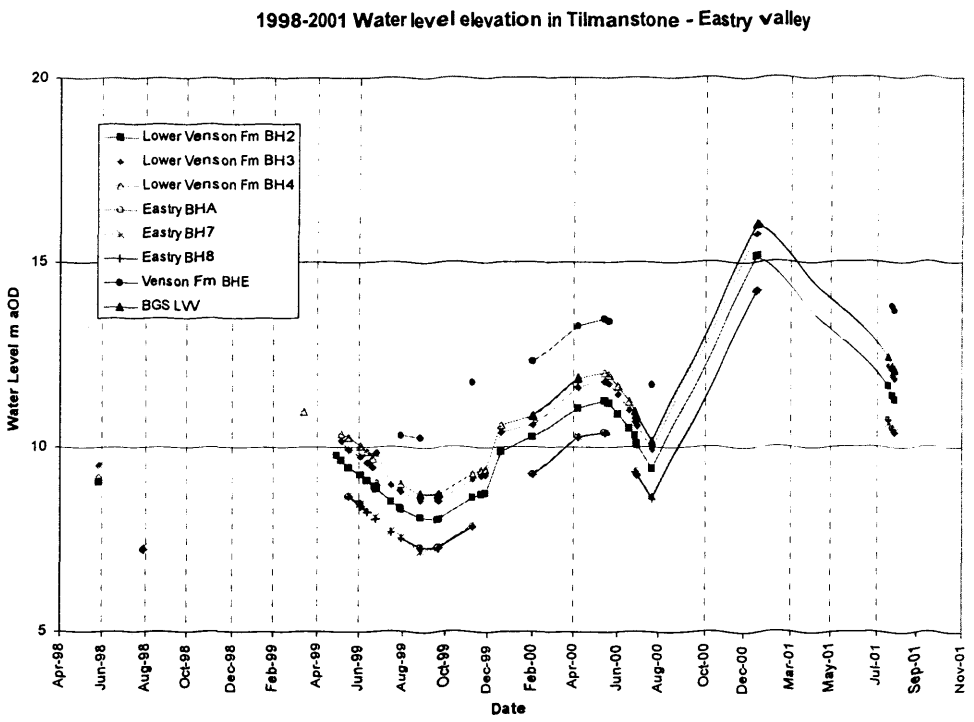

Figure 4-10 Hydrographs for boreholes in the Tilmanstone - Eastry valley 1998 – 2001.

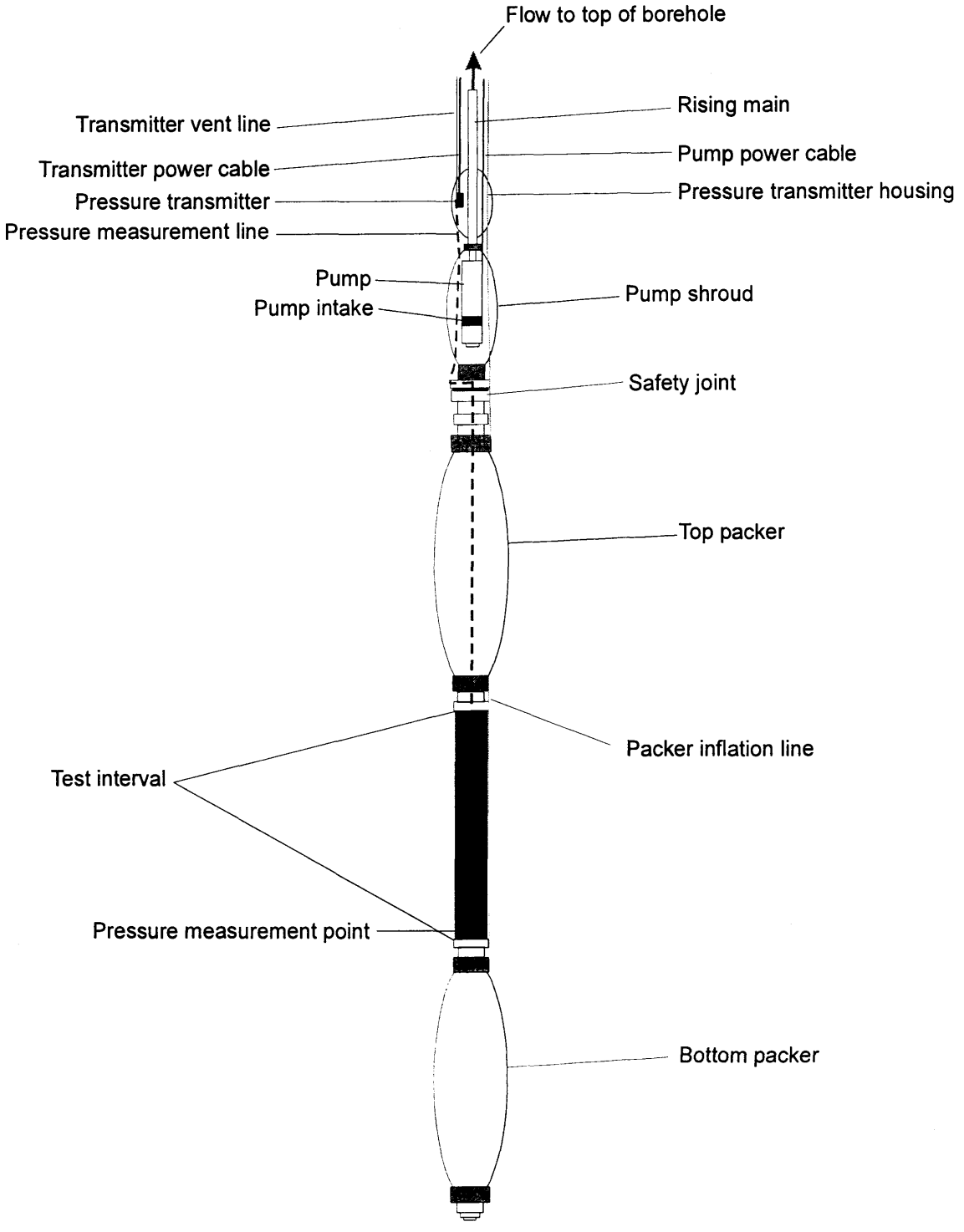

Figure 4-11 Packer rig layout, *after* Price and Williams (1989).

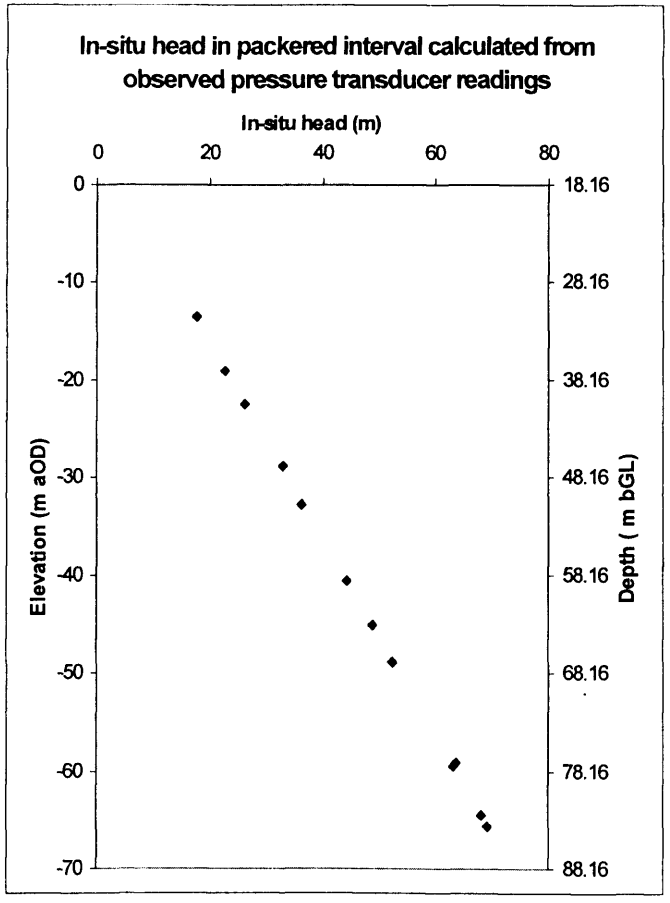

A

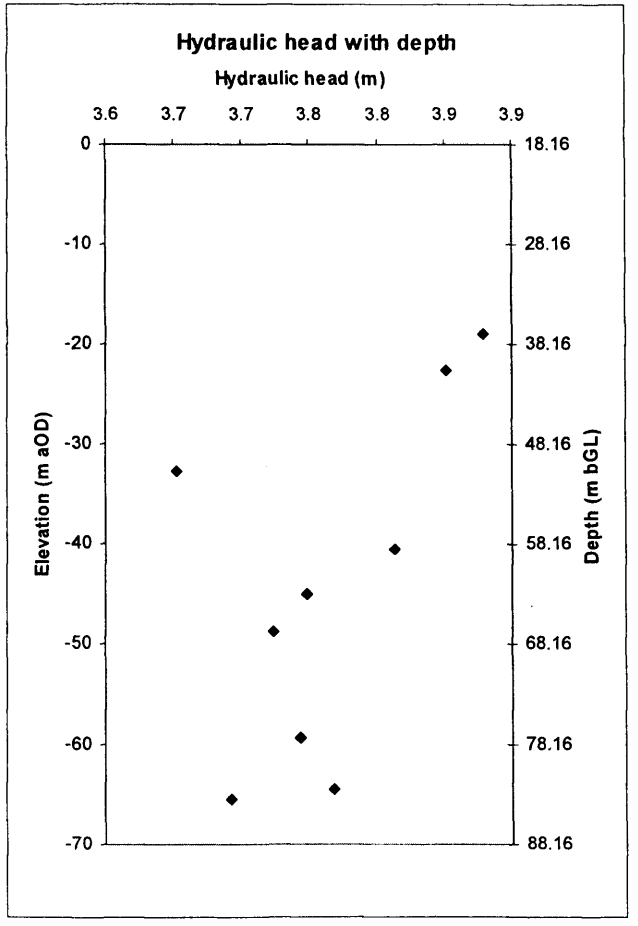

B

Figure 4-12 Groundwater pressure heads (A) and hydraulic head (B) observed in packered intervals during packer testing .

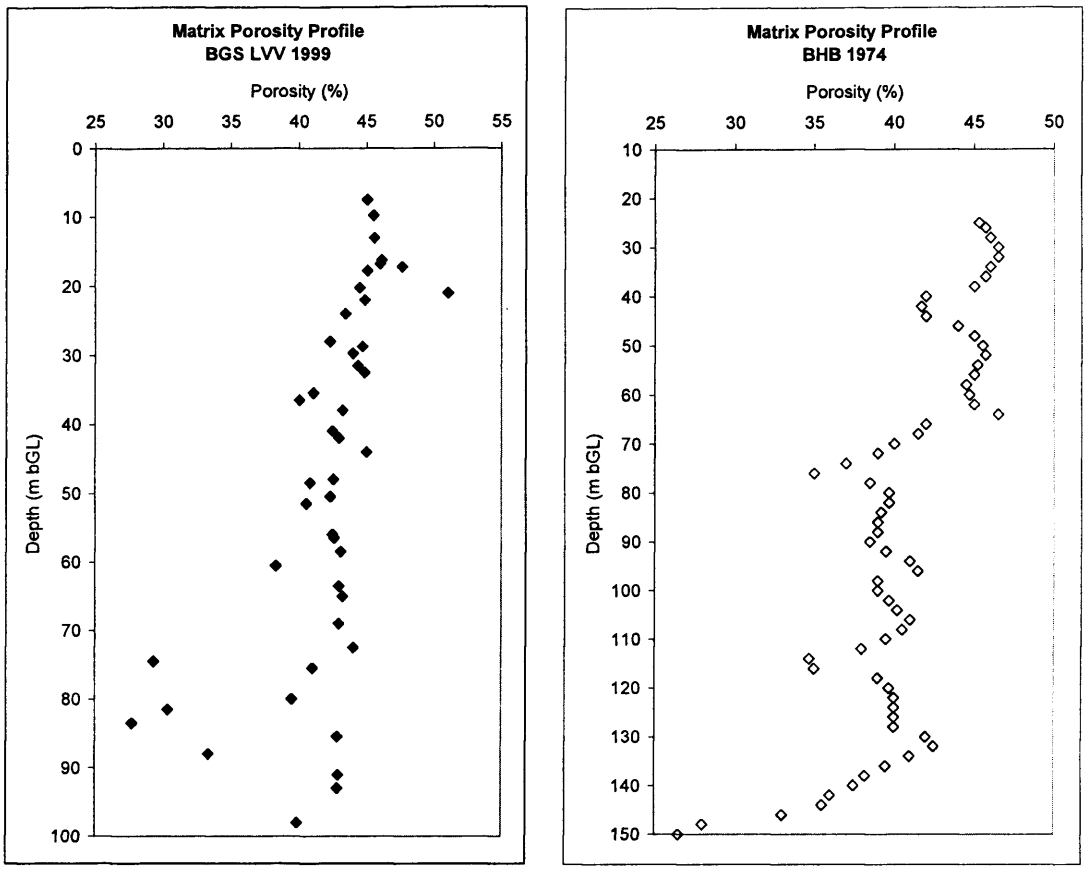

Figure 4-13 BGS LVV Chalk core porosity, as determined by BGS by liquid resaturation porosimetry, and BHB core porosity (data digitised from results presented by SWA (1976a), testing method unknown).

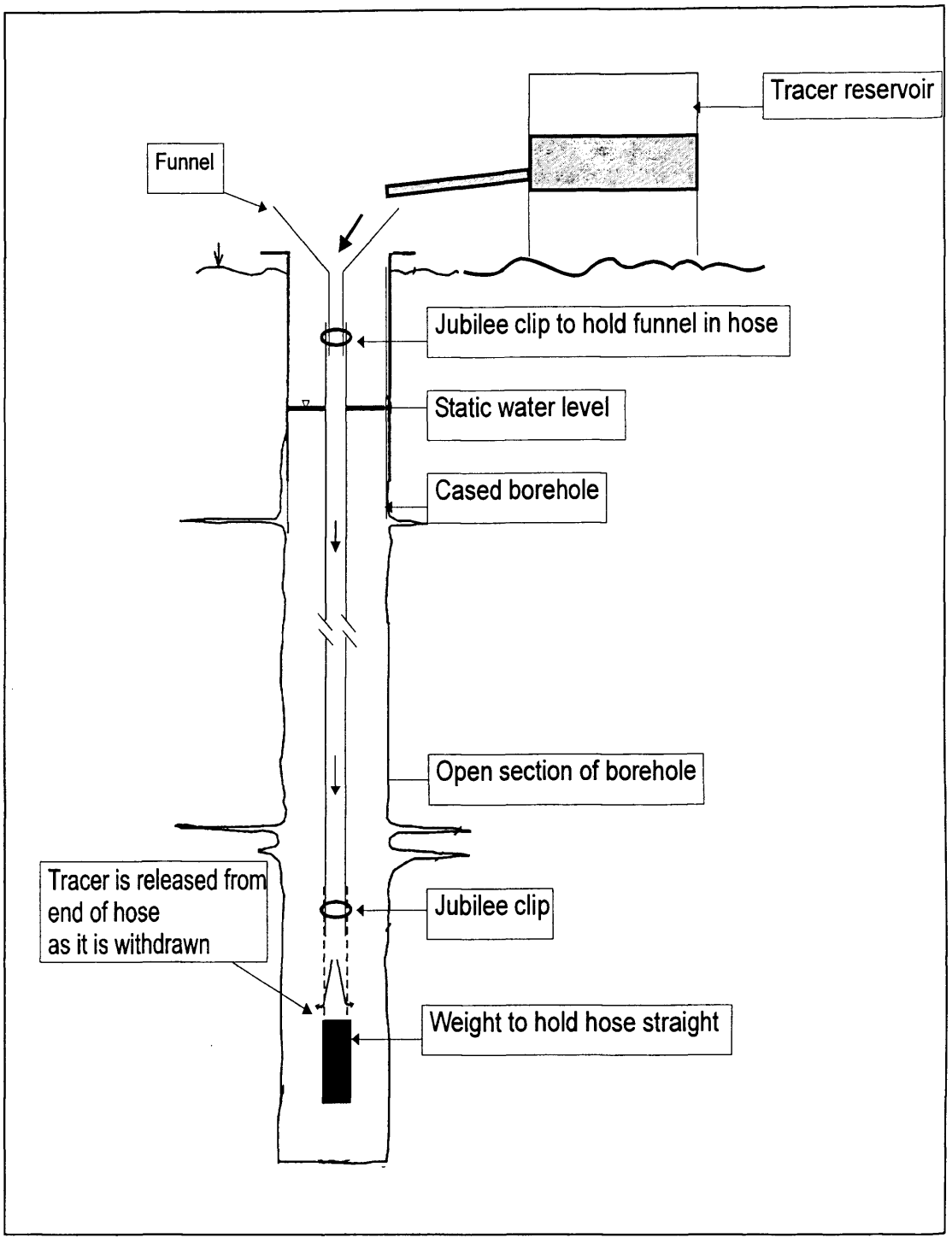

Figure 4-14 Single borehole dilution test tracer injection hosepipe arrangement.

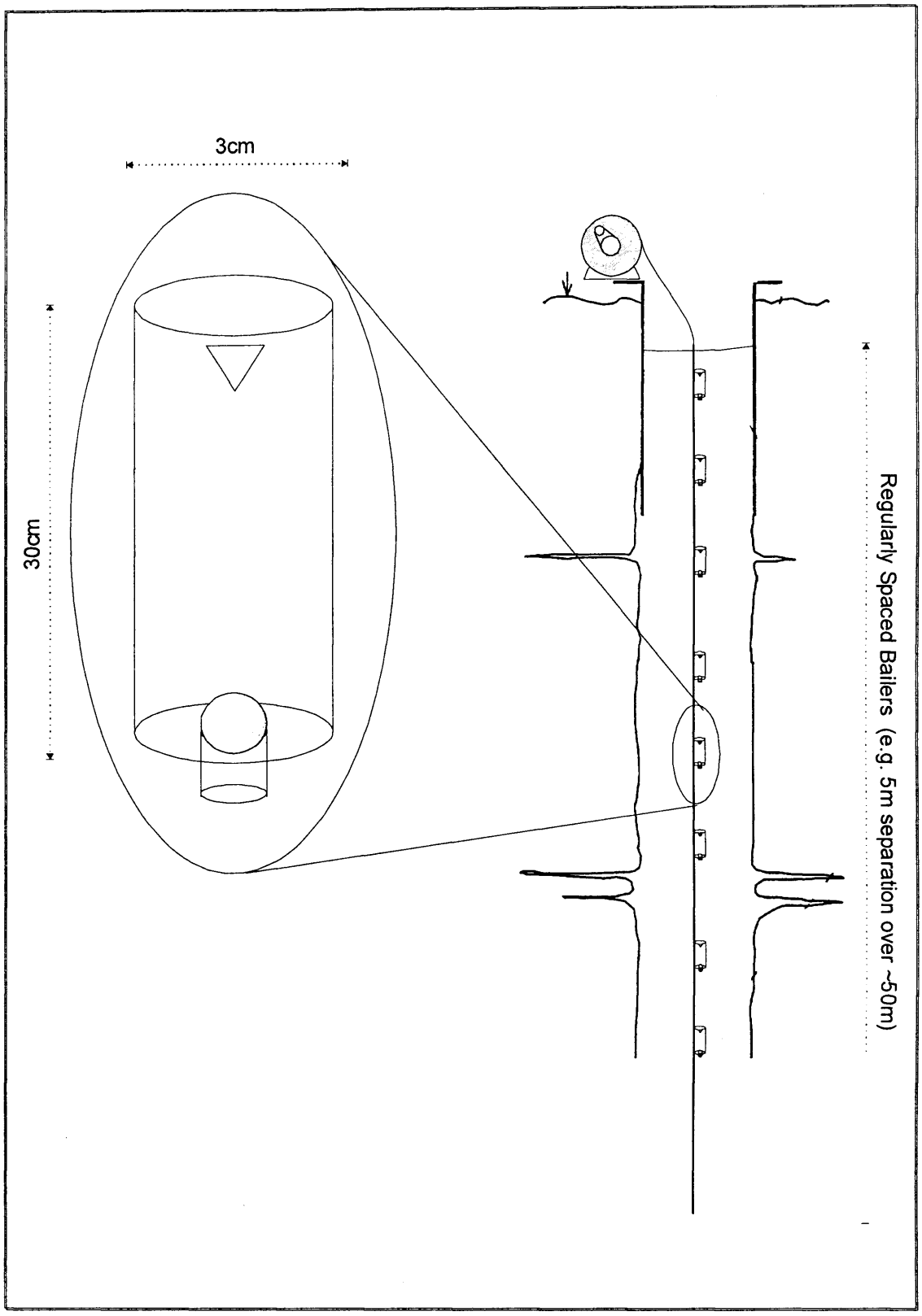

Figure 4-15 Single borehole dilution test bailer string sampling arrangement.

Fluorescein standard machine calibration

Standard	Conc ppb	Intensity
1	50	53.977
2	100	108.964
3	300	325.515
4	600	596.214
5	1000	860.295

Excitation wavelength (nm)	491
Emission wavelength (nm)	513
Excitation slit (nm)	15
Emission slit (nm)	2.5
Integration time (s)	2
Emission filter	430 nm cut-off

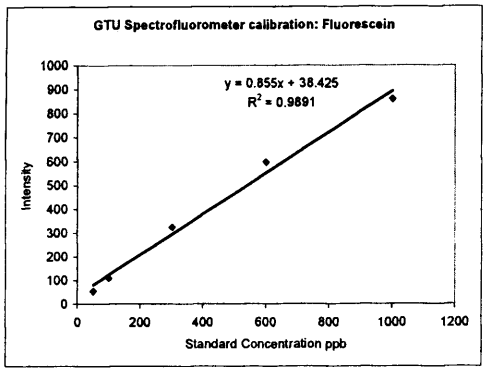

Rhodamine standard machine calibration

Standard	Conc ppb	Intensity
1	0.5	1.198
2	3	7.288
3	6	14.466
4	50	119.862
5	100	232.667
6	300	647.936

Excitation wavelength (nm)	545
Emission wavelength (nm)	590
Excitation slit (nm)	10
Emission slit (nm)	5
Integration time (s)	2
Emission filter	430 nm cut-off

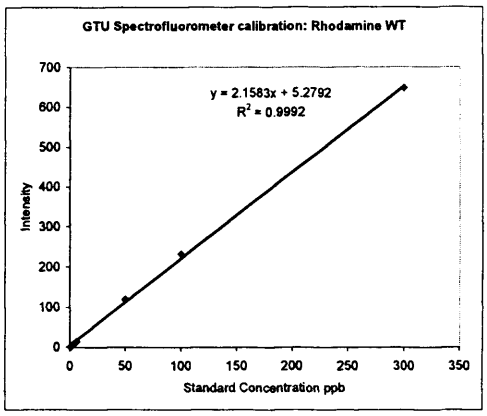

Figure 4-16 Spectrofluorometer calibration plots for fluorescein and Rhodamine WT for 2001 single borehole dilution test and natural gradient tracer test in BGS LVV and BH3 at Lower Venson Farm.

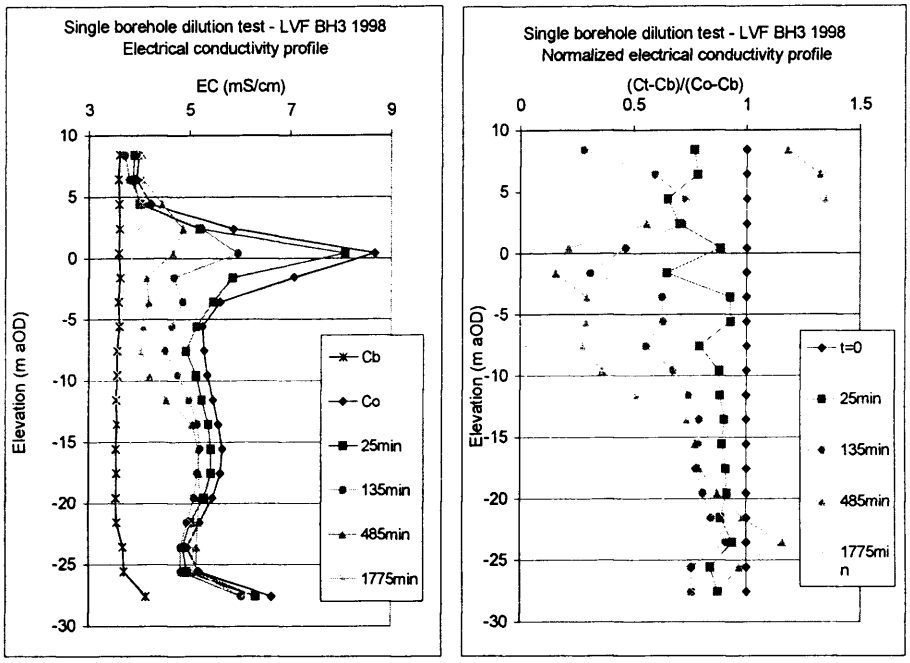

Figure 4-17 Single borehole dilution test results: Lower Venson Farm BH3 1998.

The plot on the left shows actual EC readings taken over time and the plot on the right shows a normalised profile.

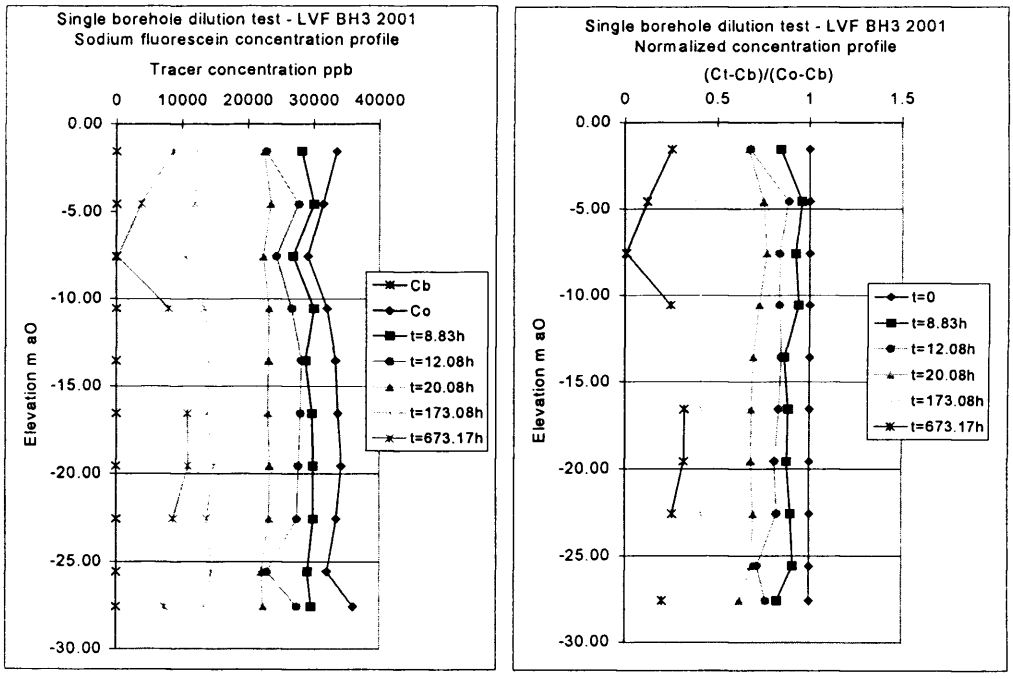

Figure 4-18 Single borehole dilution test results: Lower Venson Farm BH3 2001.

The plot on the left shows sodium fluorescein concentrations changing over time and the plot on the right shows the normalised profile over time.

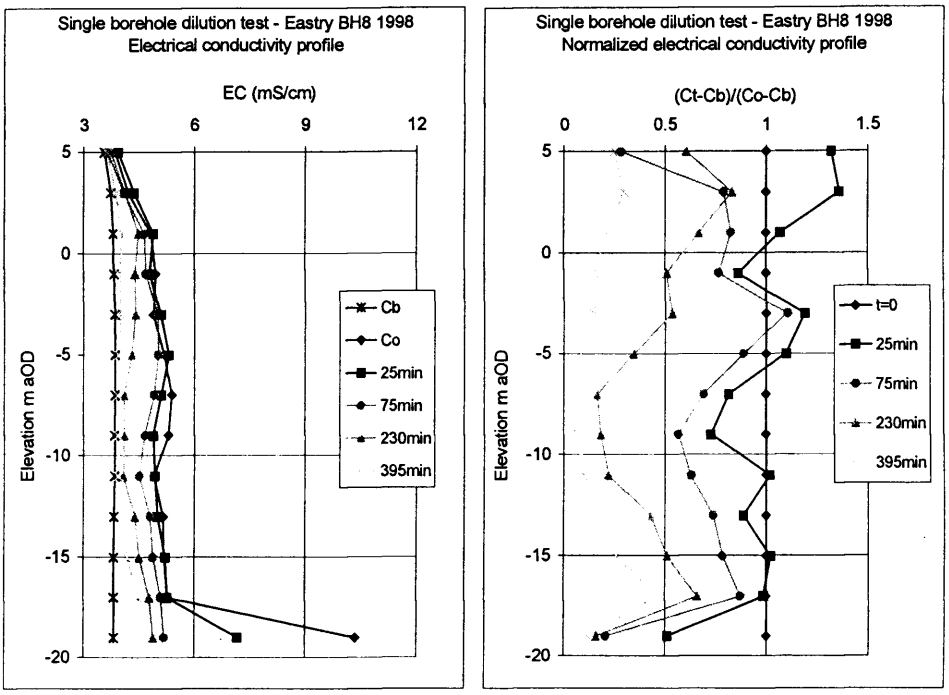

Figure 4-19 Single borehole dilution test results: Eastry BH8 1998.

The plot on the left shows the EC readings over time and the plot on the right shows the normalised data.

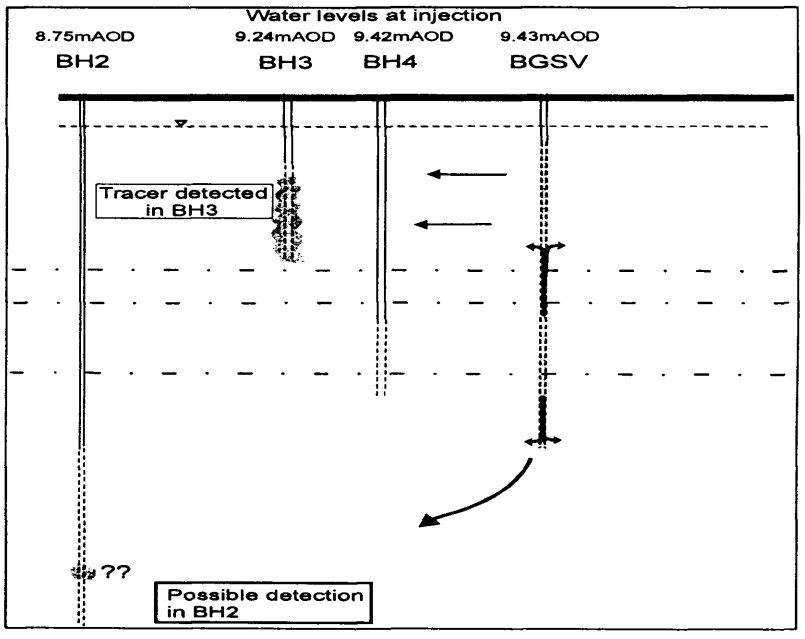

Figure 4-20 Summary sketch of results of BGS LVV natural gradient tracer test using Direct Yellow.

The only clear positive results were observed in BH3. There was a possible detection in BH2. Dashed lines indicate possible marl horizons.

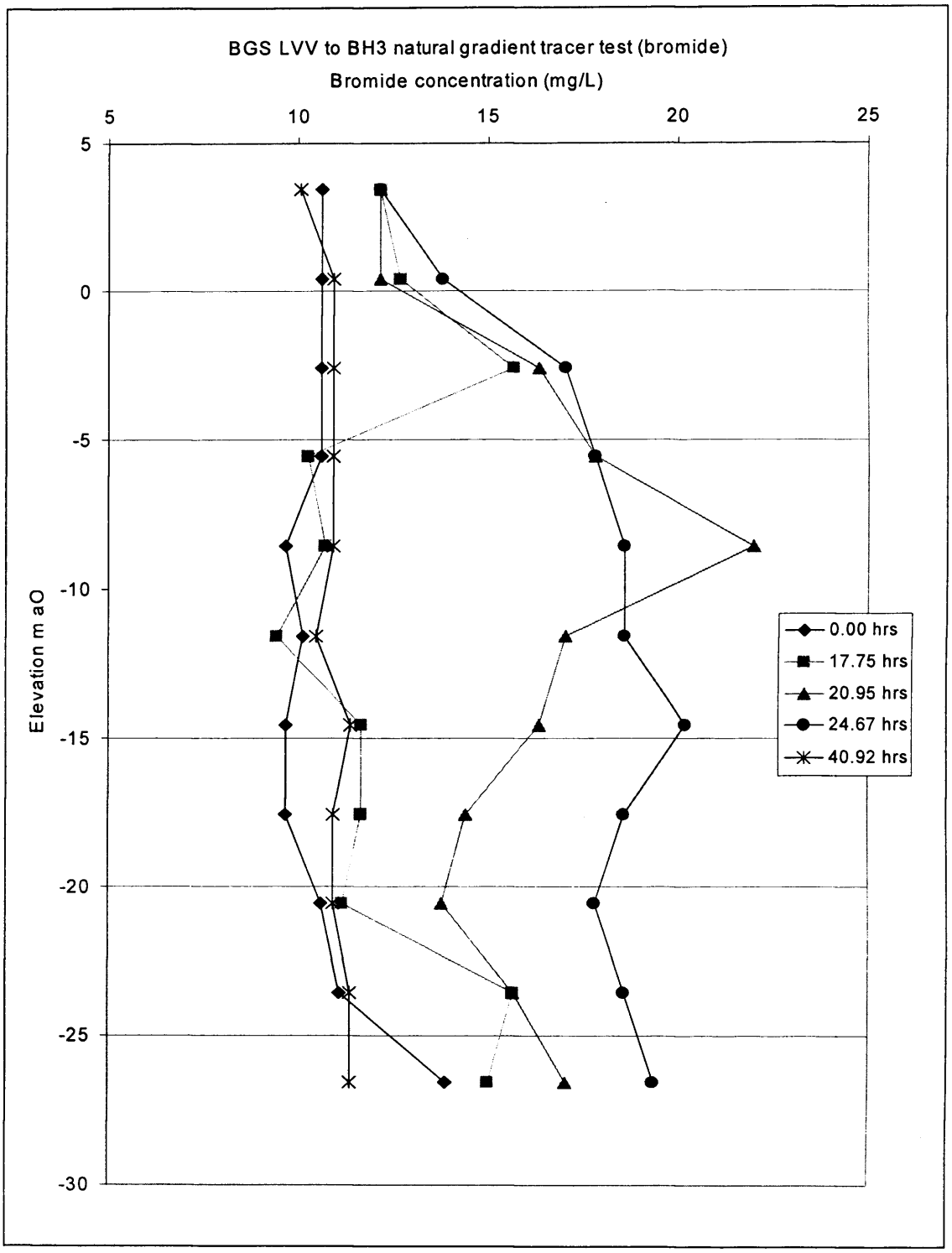

Figure 4-21 BGS LVV to BH3 natural gradient tracer test using bromide (*after* Quinn 2000).

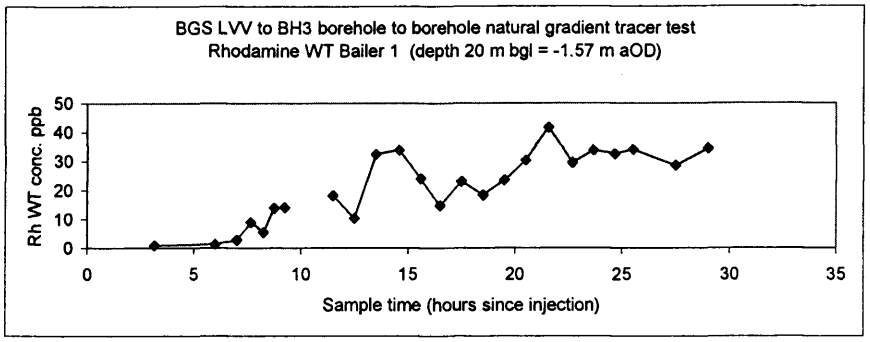
BGS LVV to BH3 borehole to borehole natural gradient tracer test
Rhodamine WT Bailer 1 (depth 20 m bgl = -1.57 m aOD)
Rh WT conc. ppb
0
10
20
30
40
50
0
5
10
15
20
25
30
35
Sample time (hours since injection)

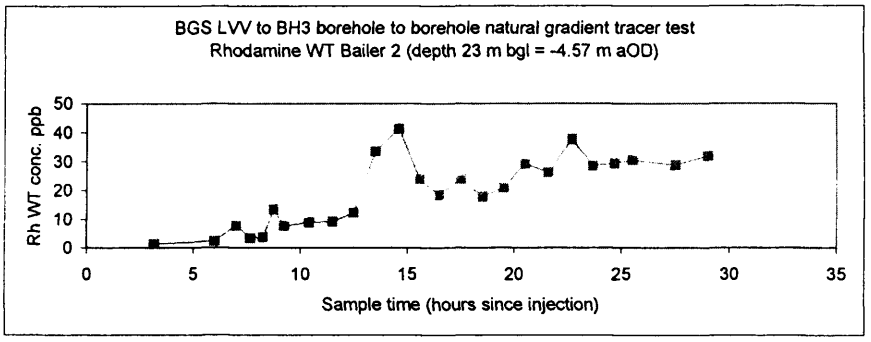
BGS LVV to BH3 borehole to borehole natural gradient tracer test
Rhodamine WT Bailer 2 (depth 23 m bgl = -4.57 m aOD)
Rh WT conc. ppb
0
10
20
30
40
50
0
5
10
15
20
25
30
35
Sample time (hours since injection)

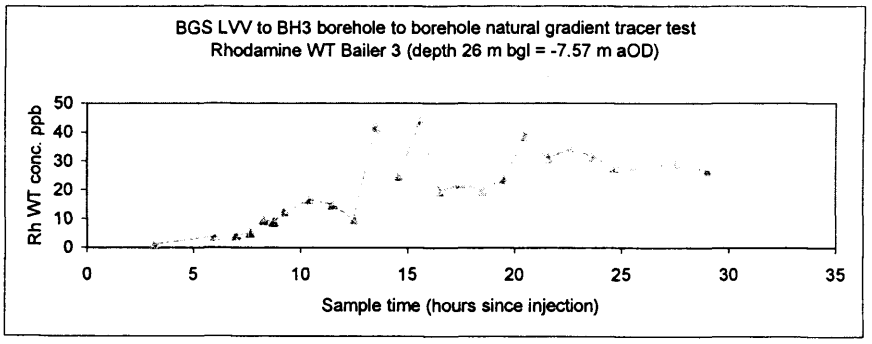
BGS LVV to BH3 borehole to borehole natural gradient tracer test
Rhodamine WT Bailer 3 (depth 26 m bgl = -7.57 m aOD)
Rh WT conc. ppb
0
10
20
30
40
50
0
5
10
15
20
25
30
35
Sample time (hours since injection)

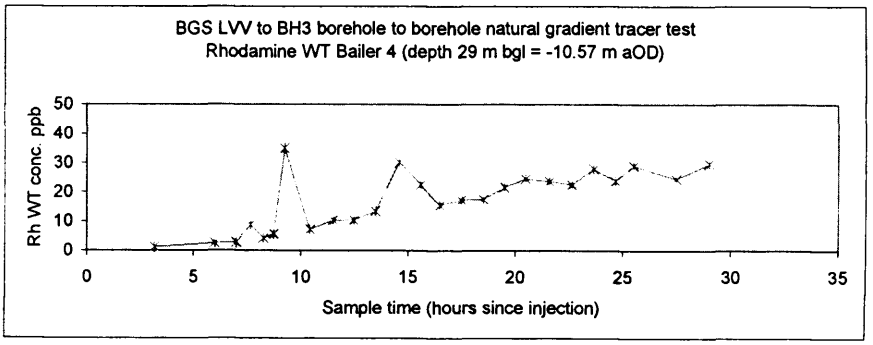
BGS LVV to BH3 borehole to borehole natural gradient tracer test
Rhodamine WT Bailer 4 (depth 29 m bgl = -10.57 m aOD)
Rh WT conc. ppb
0
10
20
30
40
50
0
5
10
15
20
25
30
35
Sample time (hours since injection)

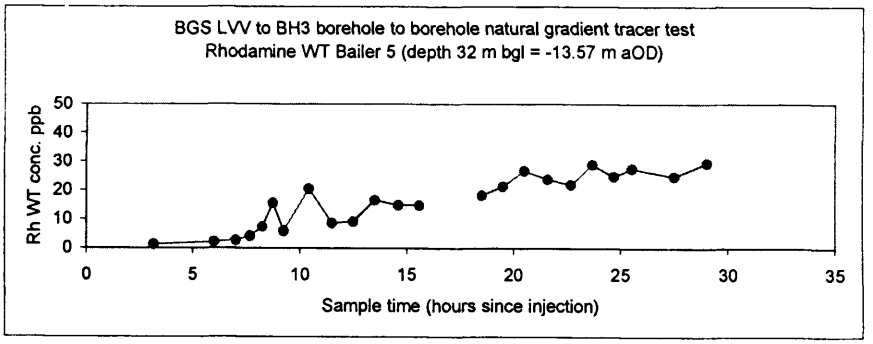
BGS LVV to BH3 borehole to borehole natural gradient tracer test
Rhodamine WT Bailer 5 (depth 32 m bgl = -13.57 m aOD)
Rh WT conc. ppb
0
10
20
30
40
50
0
5
10
15
20
25
30
35
Sample time (hours since injection)

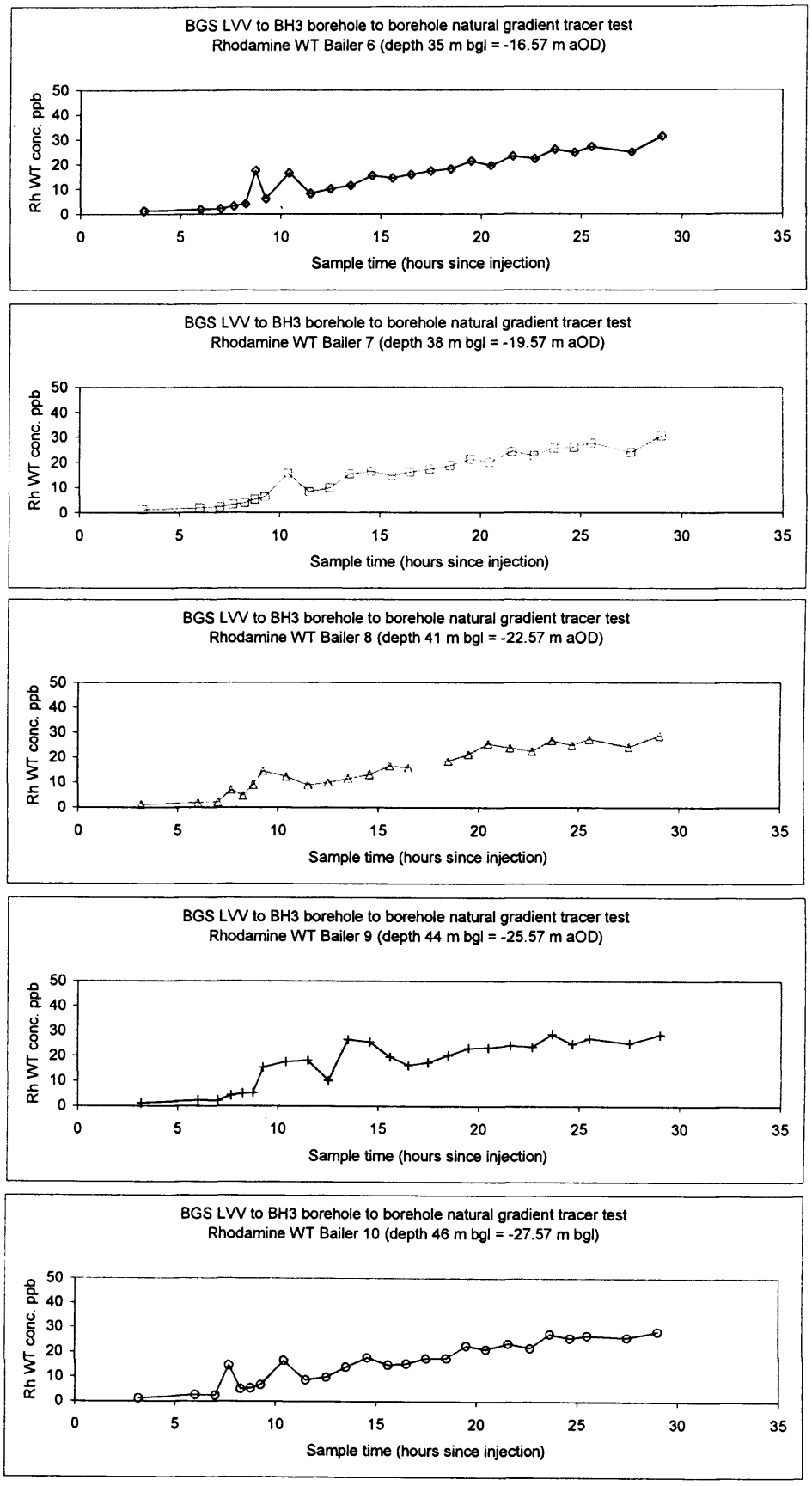

Figure 4-22 BGS LVV to BH3 natural gradient tracer test: Early time observations for bailers 1 to 10.

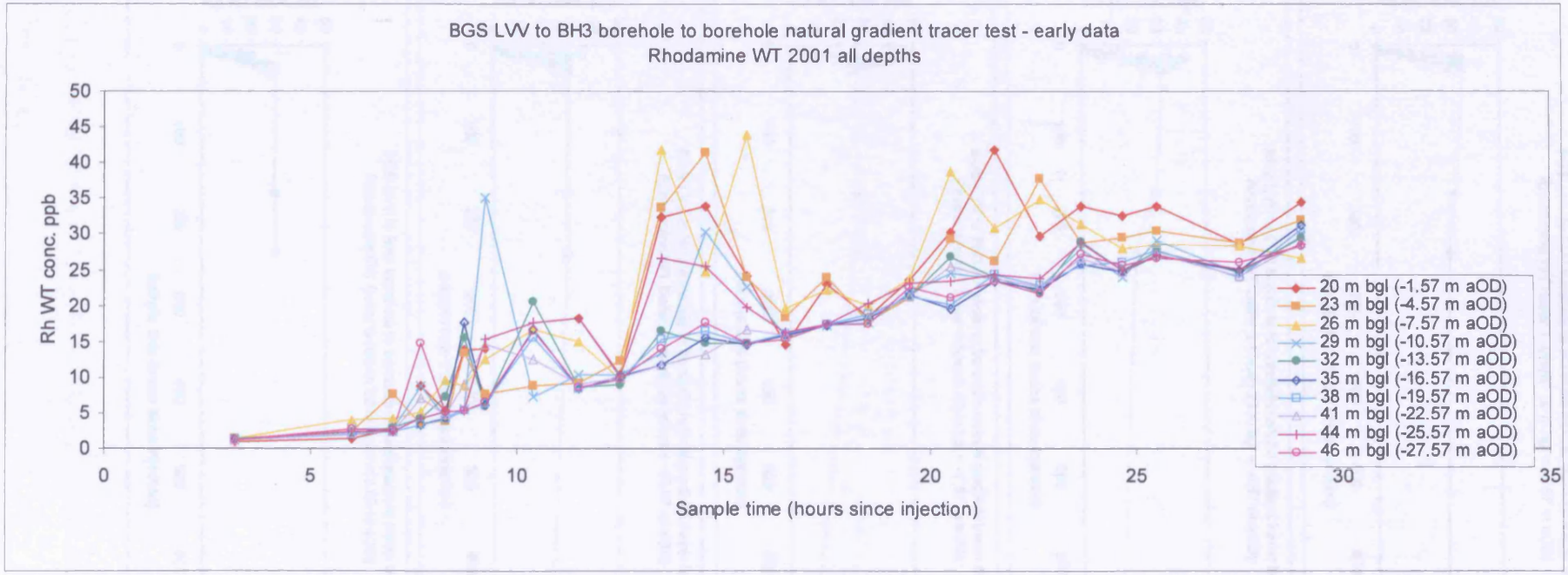

Figure 4-23 BGS LVV to BH3 natural gradient tracer test: Summary plot of all early time data.

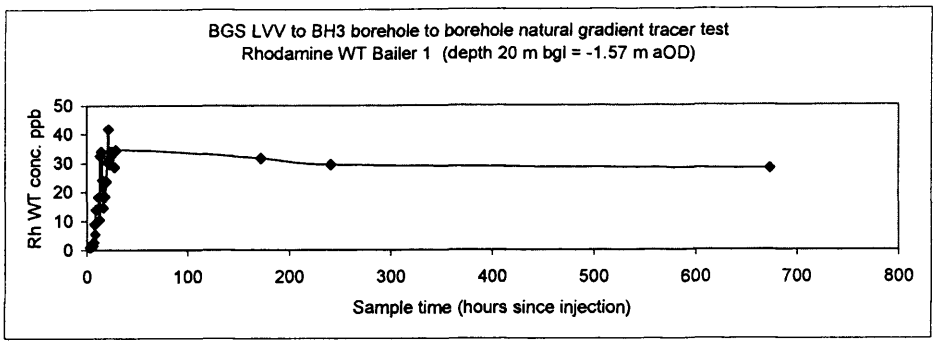
BGS LVV to BH3 borehole to borehole natural gradient tracer test
Rhodamine WT Bailer 1 (depth 20 m bgl = -1.57 m aOD)
Rh WT conc. ppb
0
10
20
30
40
50
0
100
200
300
400
500
600
700
800
Sample time (hours since injection)

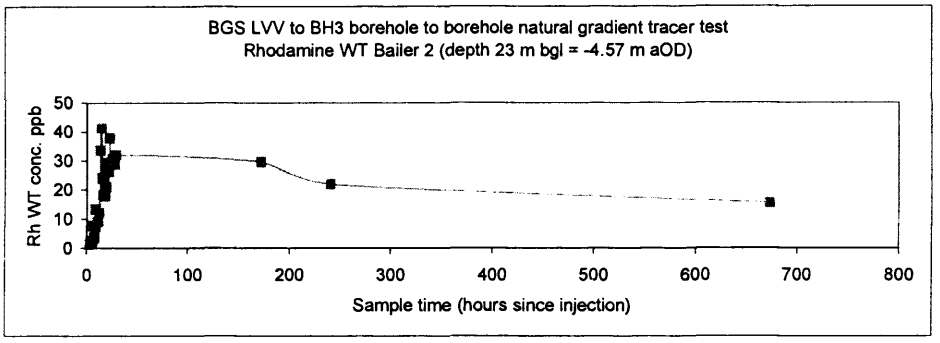
BGS LVV to BH3 borehole to borehole natural gradient tracer test
Rhodamine WT Bailer 2 (depth 23 m bgl = -4.57 m aOD)
Rh WT conc. ppb
0
10
20
30
40
50
0
100
200
300
400
500
600
700
800
Sample time (hours since injection)

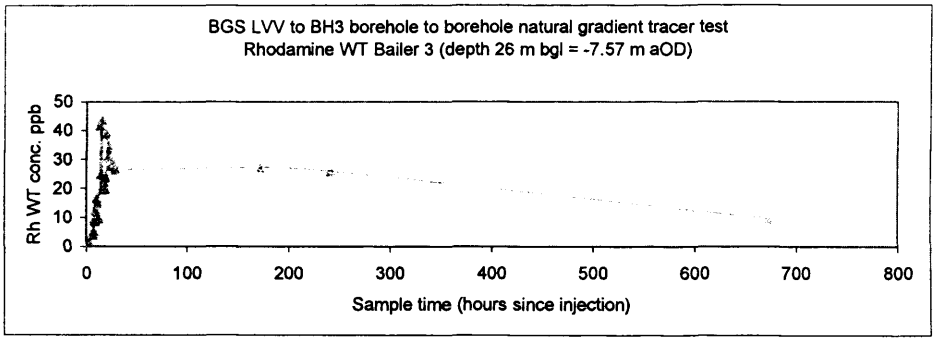
BGS LVV to BH3 borehole to borehole natural gradient tracer test
Rhodamine WT Bailer 3 (depth 26 m bgl = -7.57 m aOD)
Rh WT conc. ppb
0
10
20
30
40
50
0
100
200
300
400
500
600
700
800
Sample time (hours since injection)

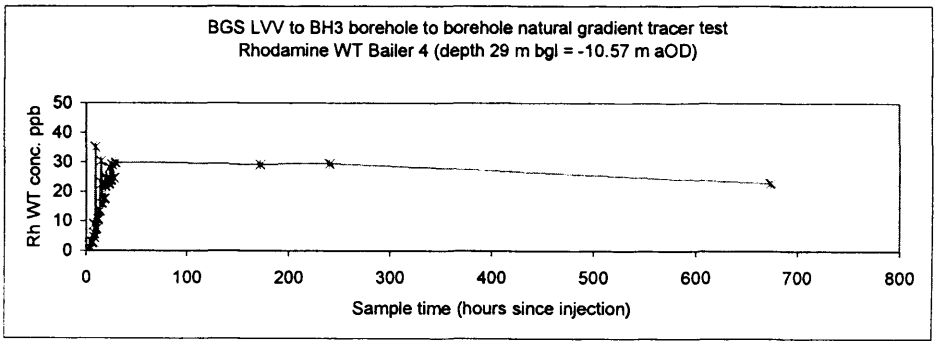
BGS LVV to BH3 borehole to borehole natural gradient tracer test
Rhodamine WT Bailer 4 (depth 29 m bgl = -10.57 m aOD)
Rh WT conc. ppb
0
10
20
30
40
50
0
100
200
300
400
500
600
700
800
Sample time (hours since injection)

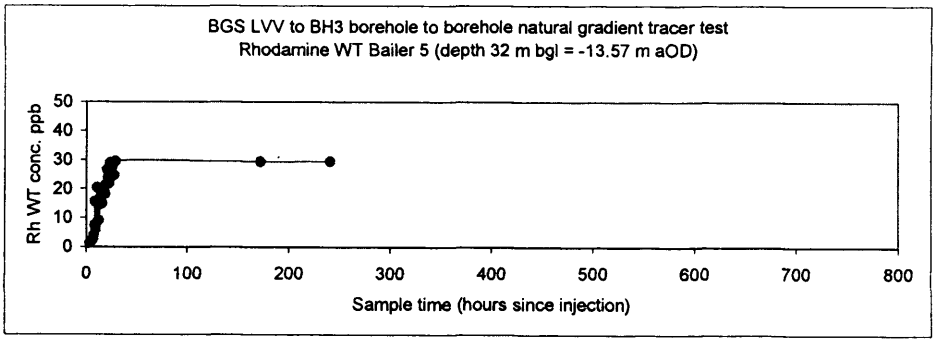
BGS LVV to BH3 borehole to borehole natural gradient tracer test
Rhodamine WT Bailer 5 (depth 32 m bgl = -13.57 m aOD)
Rh WT conc. ppb
0
10
20
30
40
50
0
100
200
300
400
500
600
700
800
Sample time (hours since injection)

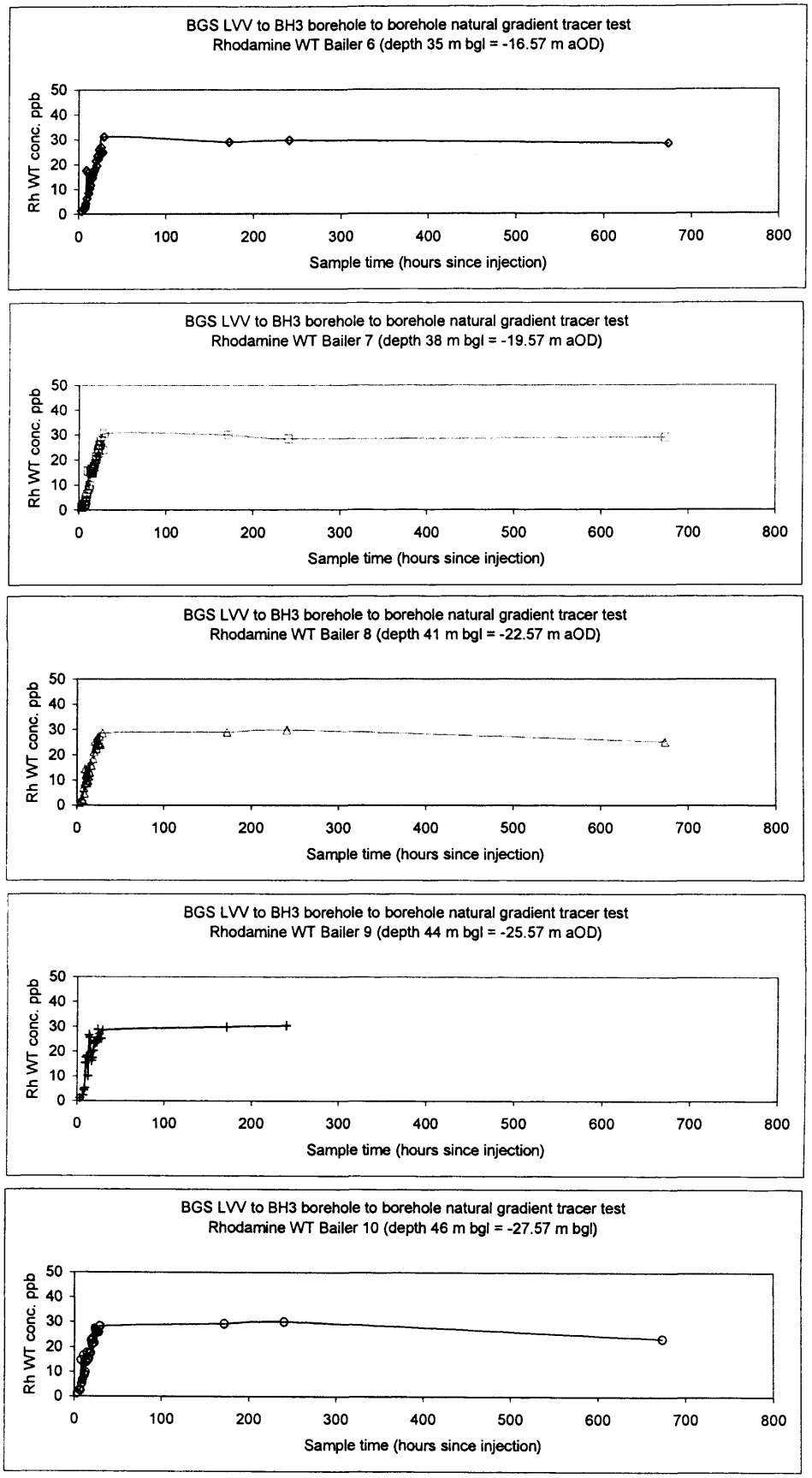

Figure 4-24 BGS LVV to BH3 natural gradient tracer test: All observations for bailers 1 to 10.

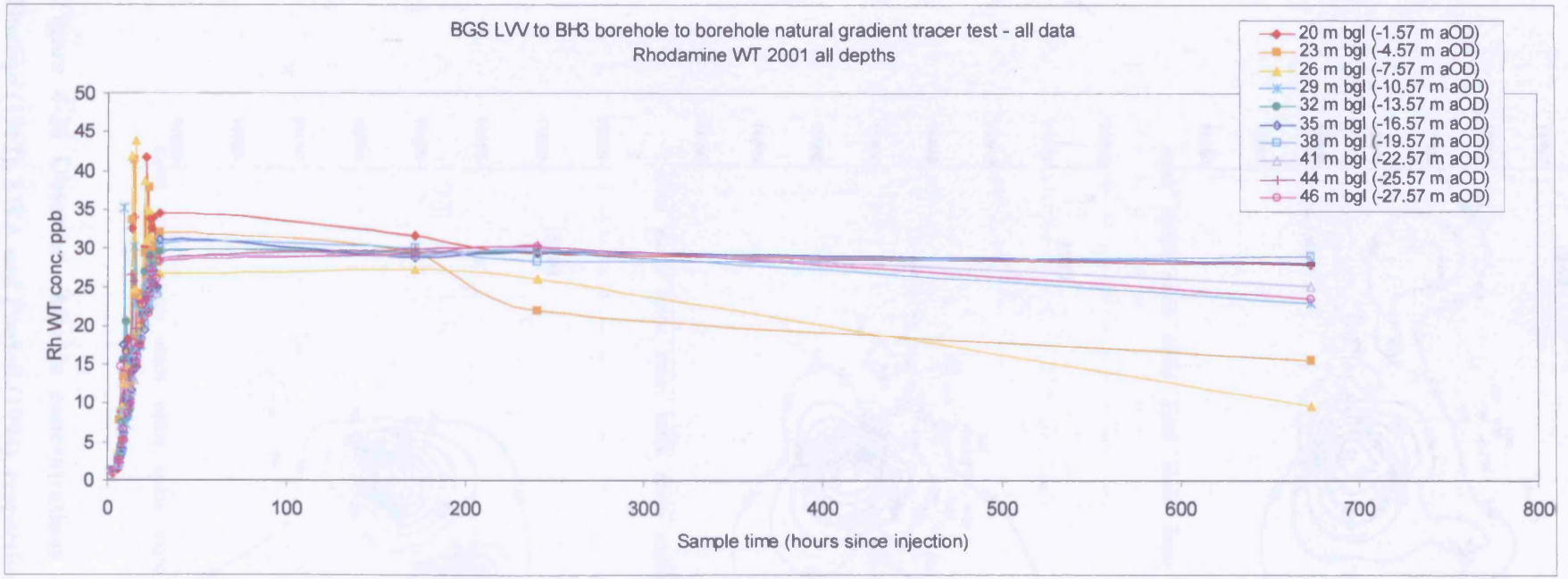

Figure 4-25 BGS LVV to BH3 natural gradient tracer test: Summary plot of all observations.

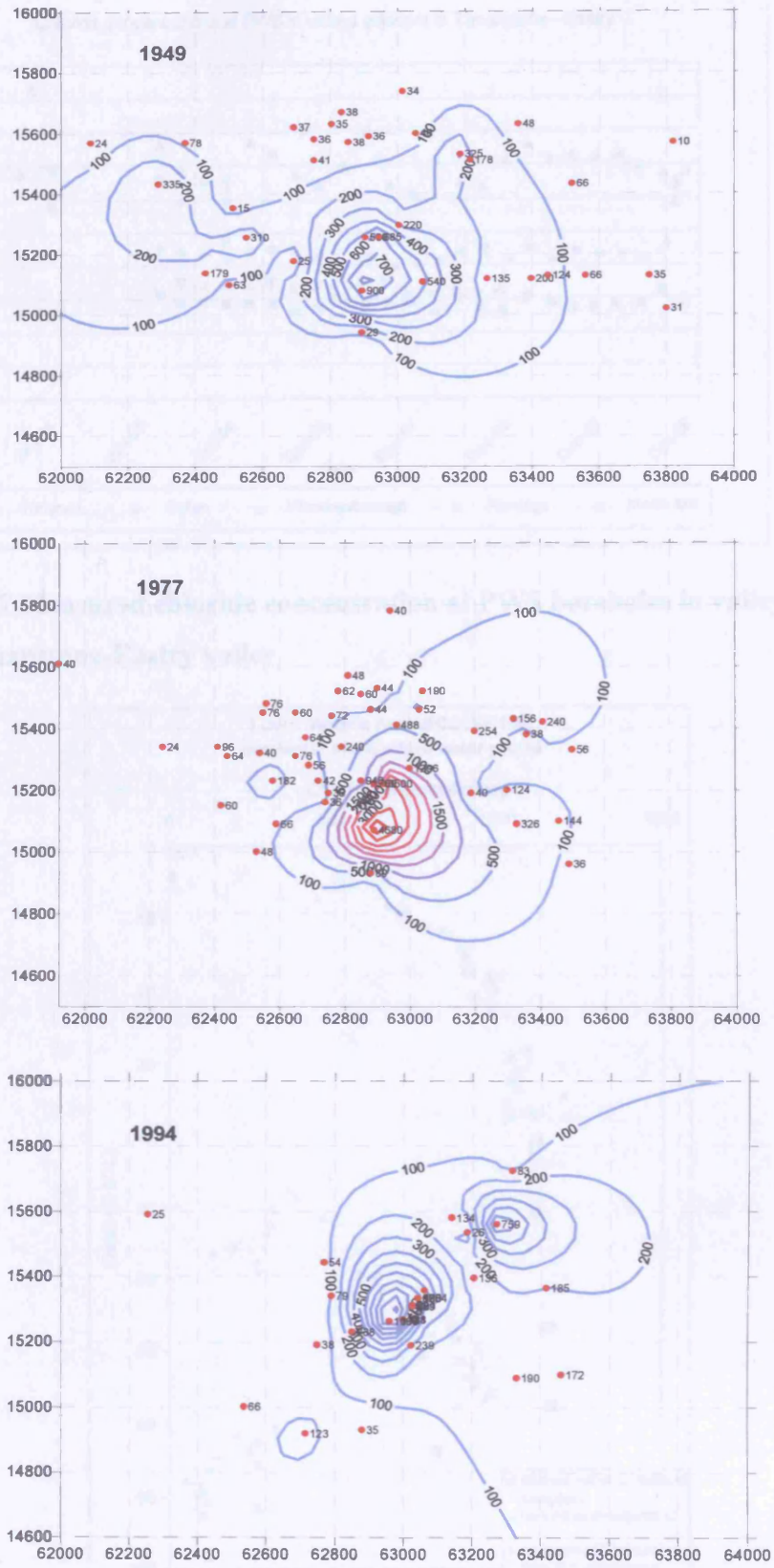

Figure 4-26 Observed chloride concentrations in 1949, 1977 and 1994 (*after* Buchan (1962), SWA and Peedell (1994), respectively).

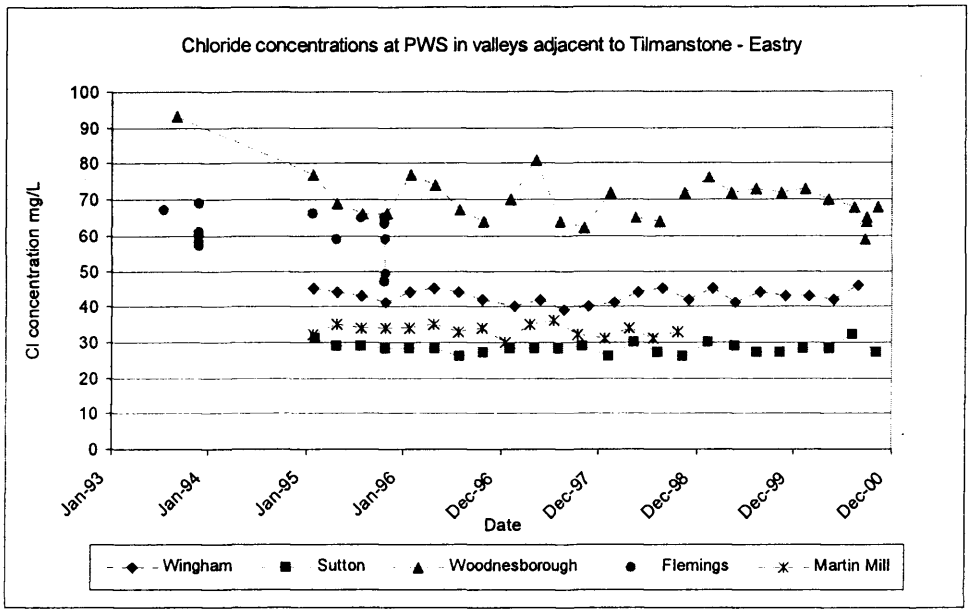

Figure 4-27 Measured chloride concentration at PWS boreholes in valleys adjacent to the Tilmanstone-Eastry valley

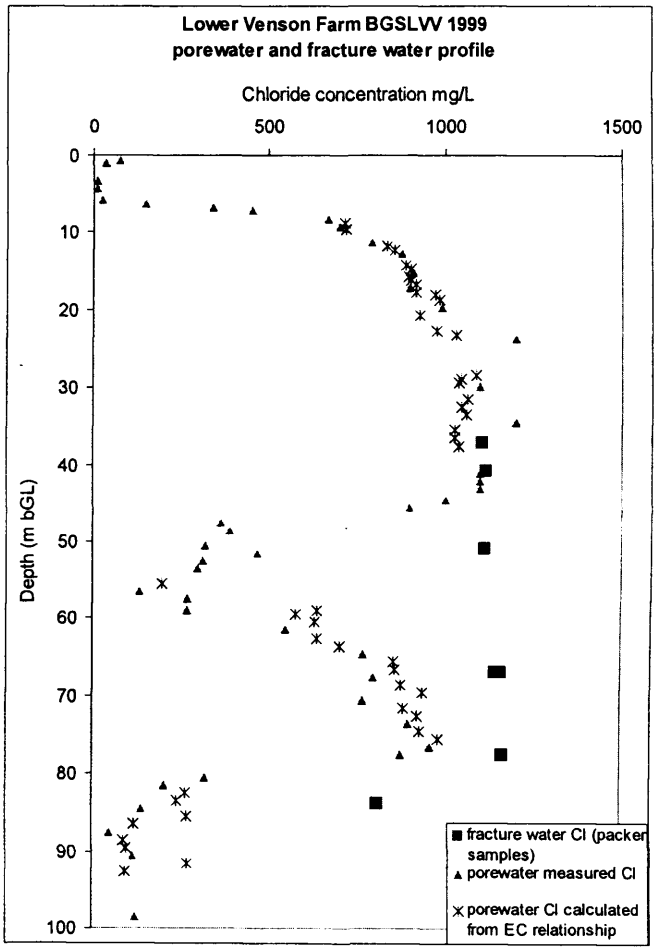

Figure 4-28 BGS LVV core porewater profile: Measured EC and chloride concentration for porewater and fracture water. The plot also includes chloride concentration calculated from EC:Cl correlation.

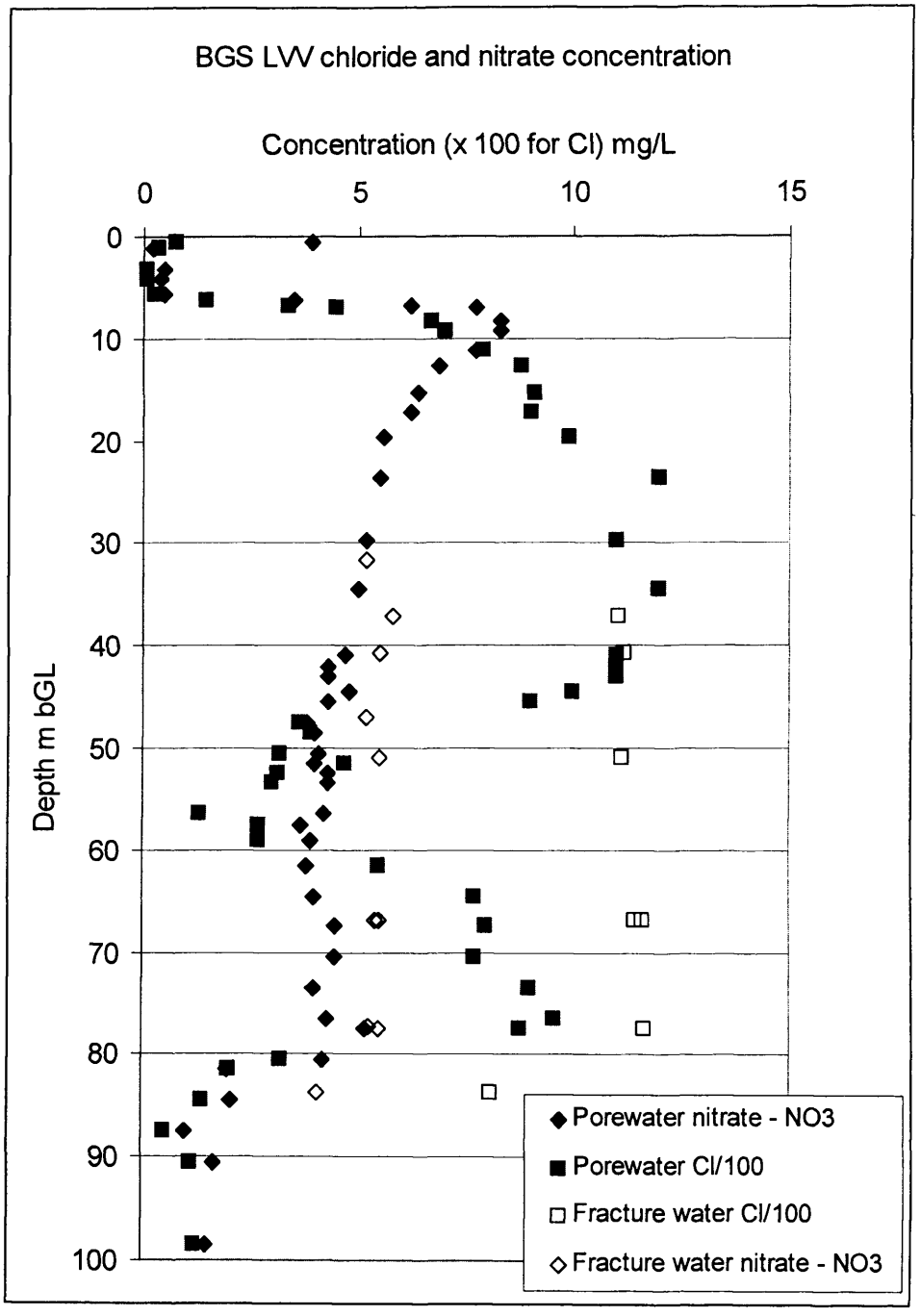

Figure 4-29 BGS LVV chloride concentration profile compared to nitrate concentration.

5 Analysis and interpretation of fieldwork results and development of a conceptual model

5.1 Overview

This chapter contains the analysis and interpretation of the results from the various field techniques described in the previous chapter. In addition it contains interpretation of results from other relevant fieldwork. The aim of the chapter is to compare parameter values derived from the different field techniques and to integrate them in order to improve on the existing conceptual hydrogeological model for the area.

5.2 Geological framework

The geological framework of the Tilmanstone – Eastry valley is considered by drawing together evidence for lithological variation, structural setting and lithologically-controlled response to post-depositional tectonic events.

5.2.1 Lithostratigraphy

As described in Chapter 3 (Geology and Hydrogeology), the lithology of the Chalk Group exhibits variations that arise from the range of depositional environments existing in the tectonic setting of the Cretaceous. Lithologies commonly encountered include hardgrounds, marl horizons and fine-grained, pure limestones.

Analysis and interpretation of the core logging undertaken by BGS at Lower Venson Farm (BGS LVV and BGS LVI) combined with the geophysical logging of the boreholes at this site, both from 1999 and from the 1970's investigations, provides detailed evidence of lithological variation. It is possible to correlate marker horizons identified by Mortimore (1997) in the coastal section of the Chalk Group to those encountered further inland at Lower Venson Farm, as well as other boreholes in the Tilmanstone – Eastry valley. The most useful data are from the 1973 geophysical logging of BH2 (gamma and resistivity logs), the gamma log of BGS LVV and BGS LVI and the core logging of the latter two boreholes. The annotated geophysical logs for BH2 (1973) and BGS LVV (1999) showing marker marl, flint and hardground horizons are provided in Figure 5-1 and Figure 5-2.

As previously indicated (Chapter 4), gamma logs are particularly useful for identifying marly horizons in the Chalk due to the higher clay content in this lithology. Assessment of the gamma logs with the core logs from the BGS boreholes indicates that the gamma log also responds markedly to the hardgrounds that occur at the top of the Lewes Nodular Chalk. Resistivity logs are also very useful as indicators of hardgrounds and marl horizons. Lower resistivity values indicate marl seams and higher resistivities indicate hardgrounds (Mortimore 1990). Figure 5-3 provides an interpretation of the lithostratigraphy from the geophysical logging for BH2 (1973), BGS LVV and BGS LVI (1999) and the core logging of BGS LVV and BGS LVI (1999). The log of the coastal section at Langdon Stairs (NGR 6345 1425) by Mortimore (1997) is also provided, as Figure 5-4, for comparison.

The boreholes encounter lithologies from the upper part of the Chalk Group sequence detailed in Mortimore (1997) and Bristow *et al.* (1997). From ground level to approximately 40 m bGL (-21.84 m aOD) the boreholes encounter chalk from the Seaford Chalk member. A small deflection in the gamma logs for BH2 (1973), BGS LVV and BGS LVI (1999) at 40 to 41 m bGL (-21.84 to -22.84 m aOD) is taken to mark the upper of the two Shoreham Marls. Marls are also noted in the core log for BGS LVI at this level. This small deflection occurs below the much larger response which is taken as being caused by the lowest of the Belle Tout / Hope Point Marls. The Shoreham Marl 2 marks the transition from the Seaford to the Lewes Nodular Chalk. From 42 m to approximately 65 m bGL (-23.84 to -46.84 m aOD) the Lewes Nodular Chalk has a sequence of hardgrounds (Light Point; Beeding; Hope Gap and Cliffe) which are well picked out both by the geophysical logs and are also visible in the core from BGS LVV and BGS LVI. The top of the Dover Top Rock is picked out by the two uppermost Navigation Marls and the Navigation Hardground. Occasional (unnamed) marls are visible in the core in the 10 m between this and the Dover Chalk Rock sequence. The Dover Chalk Rock is represented in the core as a series of hardgrounds and marls between approximately 75 and 79 m bGL (-56.84 to -60.84 m aOD). Immediately below the Dover Chalk Rock are the two Bridgewick Marls and the broken flints at 80 m (-61.84 m aOD) observed in BGS LVV may represent the Bopeep Flints. The marls produce strong responses in the gamma logs. Broken flints at 83.5 m bGL (-65.34 m aOD) observed in the BGS LVI and BGS LVV core are likely to represent the Bridgewick Flints. Deflections in the gamma log can be picked out for the Caburn

Marl and Southerham Marl in BH2 and BGS LVV. The longer log of BH2 continues to 150 m bGL (-131.95 m aOD) at which point the Plenus Marls provide a clear response on the gamma log.

Figure 5-5 extends this lithostratigraphic interpretation along the length of the Tilmanstone – Eastry valley to incorporate the geophysical logs from Thornton Farm (BH6 and BH1) and Eastry (BHA and BH7). Also marked are the locations of faults in the basement rock, as indicated on the BGS geological map Dover (Sheet 290 Solid and Drift), and the large syncline inferred from structure contours on strata encountered by boreholes in the colliery workings.

5.2.2 Geological structure and fracturing

During the post-Cretaceous structural development of the area, variations in lithology resulted in differential development of fracturing and hence of groundwater flow characteristics. The structural development of the area further contributes to the framework within which groundwater flow and transport operates. The hierarchy of structural development proposed by Bloomfield *et al.* (2000) is linked at the largest scale to basement tectonic movement and results in the creation of low permeability bounding structures. Bloomfield *et al.* suggest that there is limited groundwater flow across these features, and the result is a semi-autonomous, fault-bounded Chalk block. The location of the North and South Streams may be due to one of these bounding structures at the northern limits of the area and so may the Nailbourne River to the west. Within the block there are further structural features, which may also be linked to basement tectonic controls as suggested by Mortimore and Pomerol (1991). These 'in-block' structural features may create hydraulic baffles, but their actual effect is unclear (Bloomfield *et al.* 2000). Faults are recorded in Carboniferous deposits directly below the Tilmanstone – Eastry valley in several places (Figure 5-5). This may indicate tectonic reactivation on old lines of movement, causing bed thinning or lithological changes as suggested by Mortimore (1990), and resulting in a reduction in hydraulic conductivity of the sediments. Different lithologies have responded differently to these tectonic movements as seen in the fracturing development and hydraulic conductivities measured in the area. The hydraulic gradient between Thornton Farm and BHE (see Figure 4-2 for locations) is steeper than that between Thornton Farm and Eastry. This may be related to an in-block feature or a reflection of the topography. However the topography may itself be an expression of underlying tectonic features. Further

investigation, such as through surface geophysics, may be useful to clarify the geological structure in this area.

Variation in fracturing with depth and lithology

Fractures picked out by the Televiewer logging are detailed on a lithological profile for BGS LVV in Figure 5-6.

The block sizes calculated from the fracture density depth relationship established by Bloomfield *et al.* (2000) are also indicated. The time to reach diffusive equilibrium as, described by Barker (1993), across the range of block sizes, is provided in Table 5-1.

Table 5-1 Time to reach diffusive equilibrium for the block sizes calculated from Bloomfield *et al.* (2000) fracture density depth relationship.

Depth (m bGL)	Block size (m)	Time for diffusion*
10	0.14	123 days
20	0.45	3.5 years
30	0.9	13.6 years
40	1.46	36 years
50	2.12	76 years
60	2.89	141 years
70	3.74	237 years
80	4.69	372 years
90	5.72	553 years
100	6.83	788 years

*assumes time for diffusion = $(\text{block-size})^2/D_A$
where D_A = diffusivity = Apparent Diffusion Coefficient = 4.69×10^{-10} m^2s^{-1}, Barker (1993).

Mortimore (1990) notes that the purer, more homogeneous Seaford Chalk tends to be intensely fractured with orthogonal joint sets, compared to the underlying Lewes Nodular Chalk. This is reflected in the fracture-density versus depth relationship established by Bloomfield *et al.* (2000). However, this contrast in fracturing is associated with the lithology of the particular Chalk units rather than the depth at which they occur, so using fracture-density versus depth as a guide to describe profiles of hydraulic conductivity may be misleading.

5.2.3 Porosity

Porosity variations have important implications for the time taken to reach diffusive equilibrium between fracture and porewater solute concentrations, through their control

of diffusivity, and for the volume of solute or pollutant stored in the rock matrix. The apparent diffusion coefficient, D_A, is proportional to the total connected porosity, so a higher porosity means that diffusion across a matrix block can proceed faster and that, ultimately, more solute can be stored in the matrix pore space.

It is difficult to attribute porosity values to specific lithologies in BGS LVV as extensive core-loss occurred during drilling. There may therefore be a discrepancy between the level at which a lithology causes a response on the geophysical log and where it is recorded in the core log. However, bearing this in mind, an attempt is made to assess the porosity data in the context of the lithologies encountered. Figure 5-7 overlays porosity data with lithostratigraphy derived from geophysical logging and core inspection.

Interesting points on the porosity profile are seen at 21 m bGL (-2.84 m aOD) where a notably high porosity of 51% is measured in the shelly debris beds of the Seaford Chalk. The low porosity of 40% at 36.5 m bGL (-16.84 m aOD) may be associated with the Belle Tout / Hope Point Marls. No specific lithology change is recorded in the core log for this level, but orange staining of the chalk is noted. A decrease in porosity may also be associated with the Shoreham Marls at 41 m bGL (-22.84 m aOD). The low porosity values of 41% recorded at 48.5 and 51.5 m bGL (-30.34 and -33.34 m aOD) may be influenced by the Light Point Hardgrounds. However, no such low values are recorded at the levels of the Beeding or Hope Gap Hardgrounds, although a low value of 38% is recorded at 60.5 m bGL (-42.34 m aOD). Reference to the core log indicates that marls are observed at this level. No low porosities are recorded in association with the Cliffe Hardground, Navigation Hardground / Marls or Dover Top Rock sequence. A very low porosity of 29% at 74.5 m bGL (-56.34 m aOD) is likely to be related to the hardgrounds of the Dover Chalk Rock sequence. Lower porosities are recorded between 80 and 84 m bGL (-61.34 and -65.34 m aOD) and these seem to be associated with the Bridgewick Marls and a grey siliceous band observed in the core. The porosity increases to a relatively high value of 43% at 85.5 m bGL (-67.34 m aOD) before decreasing again to 33% at 88 m bGL (-69.34 m aOD). These two data points may fall either side of the Caburn Marl, which is thought to occur at 87 m bGL (-68.34 m aOD), although it is possible that the low value represents the porosity of the marl or associated marly horizons.

A profile of porosity data from BHB, obtained when it was first drilled, is available from Bibby (1979), Figure 3-22. These porosity measurements were derived from core obtained through U100 sampling of the borehole. This method produced more cohesive lengths of core (Headworth, 1994) than the drillings of 1999. Unfortunately, a lack of geophysical logs for this borehole makes it difficult to relate porosity changes to lithology variations. In order to try to relate particular horizons in BHB to those in BGS LVV some assumptions have been made. These are that the top of BHB is at 32 m aOD (as estimated from the 1: 10 000 OS map of the area) and that the strata are dipping at approximately 1° to the north-east. This suggests that the lower porosity values observed between 38 and 46 m bGL (-6 and -14 m aOD) in BHB may be related to the Belle Tout / Hope point and Shoreham Marls. It is also likely that the porosity reduction observed between 54 and 70 m bGL (-22 and -38 m aOD) is related to the sequence of hardgrounds between the Light Point Hardgrounds and the Dover Top Rock. The low porosity value observed in BHB at 76 m bGL (-44 m aOD) may indicate the same lithology represented in BGS LVV by the low porosity value at 74 m bGL (-55.84 m aOD). Similar porosity values are seen in both boreholes for the Dover Chalk Rock. A slight increase in porosity just below the level of the Caburn Marls may represent the Caburn Sponge Beds, although there is no note of this horizon in the core from BGS LVV. The next notable decrease in porosity in BHB is observed at approximately 114 m bGL which may relate to the Glynde Marls. The higher porosity values observed at approximately 130 m bGL may be indicative of the Melbourn Rock in which case the gradual decrease in porosity below this would relate to the Plenus Marls and the Lower Chalk below.

In summary, comparison of the porosity profile for BGS LVV with the lithostratigraphy does not indicate any strong correlation of porosity with lithology type, although a limited relationship is apparent. The porosity profiles from BHB and BGS LVV both show a trend of decreasing porosity with depth (in accordance with observations elsewhere, Bloomfield *et al.* (2000). The BHB profile displays a marked change from a porosity of 40 – 47 % to a depth of approximately 67 m bGL, decreasing to 35 – 40% below this level. The BGS LVV porosity averages 44% for the Seaford Chalk samples and 39% for the Lewes Nodular Chalk samples. No evidence for low porosities for hardgrounds was recorded, although this may be due to poor core recovery.

5.3 Hydraulic regime

5.3.1 Groundwater heads and hydraulic gradients

Decadal changes (i.e. between 1970 and 1980 and 1990) in water-levels have been plotted and are presented in Figure 5-8 and Figure 5-9. Changes for both winter (usually using February observations) and late summer (usually using early October observations) have been plotted. These months were chosen because most sites had observations for these months. Changes have been calculated automatically by subtracting the 1970 contour plot from the later (1980 or 1990). This means that a relative rise in the water-table between the two dates produces a positive value and a relative fall produces a negative value. Not all observation boreholes had water-level records for both periods. Observation boreholes are labelled on the contour plots and where there is only one name at the borehole marker this indicates only one of the periods is represented in the data-set for that borehole. Water-level variations of 1 to 1.5 metres are unlikely to be significant. The antecedent conditions have not been analysed, so the difference may simply reflect a wetter or dryer period just before the water-level observation was made. Changes in water-level of several metres are likely to be related to stress changes to the groundwater regime. These stresses may include changes in abstraction regime and cessation of infiltration from mine-water disposal lagoons.

Variation 1970 to 1980

Both winter and summer contours (Figure 5-8 A and B) indicate a rise in water-level around Tudor House Nurseries, close to Wingham PWS. Winter and summer contours indicate a large (approximately 4 to 8 m) fall in the water-table associated with Barham PWS in the south-west of the region. Winter and summer contour plots indicate a significant fall in the water-table around the Tilmanstone Colliery (approximately 4 to 8 m). This decline is seen to dissipate radially from the disposal lagoon area so that at the distance of the North and South Streams the water-level change is less than 1 m.

Variation 1970 to 1990

Over the longer 20-year period (Figure 5-9 A and B) a fall in the water-table of approximately 10 m has occurred due to the cessation of infiltration from the mine-water lagoons. The water-level decline caused by Barham PWS is still evident. A slight decline in water-level is observed around Wingham PWS for the summer comparison but a very large rise in water-level (approximately 10 m) is observed around

the same area for the winter levels. There is a decline in abstraction at Wingham over this period from approximately 22000 m^3d^{-1} to approximately 15800 m^3d^{-1} (see Figure 3-12), but it is unclear if such a large rise in water-level could be attributable to this.

Since the minewater lagoons ceased to operate, relatively large changes in groundwater level are observed, but this does not seem to have produced a major impact on groundwater gradients. Groundwater hydraulic gradients have been calculated between Thornton Farm and Venson Farm BHE and Thornton Farm and Eastry for both historical and modern groundwater levels. The results are summarised in Table 5-2.

Table 5-2 Comparison of modern and historical groundwater hydraulic gradients for the Tilmanstone - Eastry valley.

	Location	Hydraulic gradient
Modern Gradient		
'Summer' 1992	Thornton Farm to BHE	0.0051
	Thornton Farm to Eastry	0.0041
'Winter' 1990	Thornton Farm to BHE	0.0055
	Thornton Farm to Eastry	0.0044
Historical Gradient		
'Summer' 1970	Thornton Farm to BHE	0.0045
	Thornton Farm to Eastry	0.0045
'Winter' 1970	Thornton Farm to BHE	0.0053
	Thornton Farm to Eastry	0.0046

The calculated hydraulic gradients are slightly surprising as the continuous infiltration from the minewater lagoons might have been expected to reduce the variation between summer and winter groundwater levels. This does not appear to be observed as the difference between the summer / winter gradient for the historical case is 0.0001 (Thornton Fm – Eastry) and 0.0008 (Thornton Fm – BHE) and for the modern case 0.0003 (Thornton Fm – Eastry) and 0.0004 (Thornton Fm – BHE). So the modern gradient difference is greater over the longer distance (Thornton Farm to Eastry), which conforms to the anticipated effect but the shorter distance (Thornton Farm to BHE) had a greater summer / winter hydraulic gradient difference during minewater operations.

Given that the water levels used for the historical hydraulic gradient calculation are estimates from the groundwater contour map (from ACER 1990) these variations may be attributable to poor data. The main effect of interest to the present study is to alter

the groundwater velocity during the main minewater infiltration period compared to the present day. Using the relationship: *velocity* = $(Ki)/n_e$, groundwater velocities of between 400 and 500 md^{-1} are calculated from the modern and historical hydraulic gradients presented in Table 5-2. This assumes a hydraulic conductivity, K, of 100 md^{-1} (from packer testing Section 4.5.2) and effective porosity, n_e, of 0.1% (from tracer tests, discussed further below). These velocities are high in comparison to those observed during tracer tests (discussed below).

5.3.2 Groundwater flow

The flow log run in BGS LVV (1999) (Figure 4-5 and Figure 5-2) indicates a horizon that appears to be important for groundwater flow at approximately 20 m bGL (-1.8 m aOD). The log suggests that 15 to 20% of the flow in the borehole is associated with this level (*pers. comm.* D. Buckley). Similar results have been obtained for the Seven Sisters Flint Band in the South Downs (Jones and Robins 1999), but the interpolation from the coastal section at Langdon Stairs to BGS LVV suggests that the Seven Sisters Flint Band is a few metres below 20 m bGL in BGS LVV, so the inflow observed at 20 m bGL may be related to the Cuckmere Flints or another flint horizon. The EC log measured in BGS LVV during pumping shows a small increase in EC (approximately 10 μScm^{-1}) at 19 m bGL (-0.84 m aOD), approximately 1 m above this flow horizon. At 25 m bGL (-6.84 m aOD), approximately 1 m above the level of the Seven Sisters Flint Band, the EC log records a decrease in EC (approx. 15 μScm^{-1}) indicating an influx of fresher water, but no such response is observed on the unpumped log. These EC fluctuations are small in comparison to the electrical conductivity of the fluid in the aquifer at this level, but they may be more significant than their magnitude first suggests as it requires a considerable EC contrast from any inflowing water to impact the EC measured in the borehole by the logging probe. The next major water inflow below this is at approximately 69 m bGL (-50.83 m aOD), which is a few metres below the Dover Top Rock, and where a fractured horizon is suggested by the presence of flint rubble in the core of BGS LVI. Below this at approximately 77 m bGL (-58.84 m aOD), in the Dover Chalk Rock sequence, another large increase in flow is recorded. The Televiewer log also indicates a fracture around this level. A large deflection in the fluid logs (both pumped and unpumped) also occurs at this level. Below this, small outflows are associated with the Caburn Marl (approximately 86 m bGL / -67.84 m aOD) and Southerham Marl (approx. 92 m bGL / -73.84 m aOD).

The hydraulic features of the fracture indicated on the caliper log of BH2 were investigated in 1999 using a heat-pulse flow meter on the unpumped borehole. The results were inconclusive, with the logs indicating both minor upward and downward flow.

The head minima noted for the packered intervals (Section 4.5.2) at -32.7 m aOD (50.9 m bGL), -48.8 m aOD (67 m bGL) and -65.5 m aOD (83.7 m bGL) indicate levels of groundwater flow, and comparison with the geophysical logs suggests that these lie at the Light Point Hardgrounds, the Dover Top Rock and between the Bridgewick and Caburn Marls respectively. The flow log recorded water leaving the open borehole at -65.5 m aOD (i.e. between the Bridgewick and Caburn marl) even during pumping.

Observations described thus far indicate that in the part of the aquifer formed by the Seaford Chalk groundwater flow is rather evenly distributed, but some variability is introduced by hardgrounds and marl horizons. Lower in the succession, in the Lewes Nodular Chalk, groundwater flow in the aquifer is more strongly associated with fractured hardground sequences.

5.3.3 Hydraulic conductivity variation

Remnant tracer test from 1970s

Geophysical logging of BH2 at Lower Venson Farm in 1999 revealed a very high fluid electrical conductivity at the base of the borehole. A groundwater sample obtained from this level had very high concentrations of chloride (5100 mg/L) and lithium (1105mg/L) (I. Gale *pers. comm.*). It is reported (Bibby 1979) that during the original investigations in the area, WRc undertook groundwater tracing tests. Bibby (1979) notes that a '*cocktail of tracers*' were injected at three boreholes drilled to different depths at Lower Venson Farm. The aim of the test was to detect the tracers at Eastry. Details are not given of the substances injected. From the analysis of the sample collected in 1999 it is suggested that lithium chloride was used in BH2 in the 1970s and that there is so little flow in this part of the aquifer that it is still present in the borehole approximately 25 years later. This is supported by the heat-pulse flowmeter readings described in 5.3.2

Tracer tests

Single borehole dilution tests and natural gradient tracer tests were undertaken in the Tilmanstone-Eastry valley (Section 4.6). Both these types of tracer test can provide evidence of spatial variation in the hydraulic regime of the aquifer. A combined interpretation of the results of tests presented in Chapter 4 is developed below.

Single borehole dilution tests

Figure 5-10 presents a summary of the Darcy velocity determinations from all the single borehole dilution tests. The Darcy velocity calculated through single borehole dilution testing can be converted to a hydraulic conductivity value if the local hydraulic gradient is known. In the Tilmanstone - Eastry valley the calculation of hydraulic gradient is complicated by borehole completion over different, and non-overlapping, depth intervals at each site. The hydraulic gradient used for the hydraulic conductivity calculation is therefore taken from the entire length of the valley from the Thornton Farm boreholes to the Eastry boreholes as the detail at different aquifer horizons is not known. On this basis the calculated hydraulic conductivities are given in Figure 5-11.

Two general trends are evident:

- An apparent reduction in hydraulic conductivity with depth
- An apparent increase in hydraulic conductivity down the hydraulic gradient.

The magnitude of the apparent increase in hydraulic conductivity moving down-gradient may not be an entirely natural effect as the large diameter borehole at the Eastry site was acidised after construction. It is not clear how far from an acidised borehole fracture enlargement may occur, although reported gas escape of up to 50 metres away from acidised boreholes elsewhere indicates that acid may also be able to penetrate to this distance (Banks *et al.* 1993). However as the greatest effect of acidisation is to remove drilling slurry from the borehole walls (Banks *et al.* 1993) it is unlikely that much increase in local hydraulic conductivity could be attributed to the acidisation. In addition, the Eastry borehole, which is the most down-gradient point of the sites tested, is also more centrally located in the main Tilmanstone - Eastry valley compared to Lower Venson Farm, so it is not surprising to see a larger Darcy velocity associated with this site. The single borehole dilution tests are assessed individually below, starting at the most up-gradient site in the valley, and then the findings from all the sites are drawn together.

Thornton Farm BH5

At Thornton Farm, Figure 5-12, the initial observations indicate a steady increase in Darcy velocity with depth to 6.6 m aOD (from 0.12 to 0.15 md^{-1}). The Darcy velocity then decreases, reducing to a 0.11 md^{-1} which is observed to -0.4 m aOD. The last two points (at approximately -3.4 and -4.4 m aOD) have a markedly lower Darcy velocity (0.03 and 0.06 md^{-1}).

Venson Farm BHE

At Venson Farm BHE, the bailer sampling method was used and it seems that this may have smoothed out the variability that is recorded by the electrical conductivity method of sampling, see Figure 5-13. The observed Darcy velocities are in the range 0.05 to 0.11 md^{-1}. The trend of the observations is a general increase in Darcy velocity with depth.

Lower Venson Farm BH2, BH3, BH4, BGS LVV

Lower Venson Farm is the next site in a down-gradient direction. Here BH2, BH3, BH4 and BGS LVV were all tested using the single borehole dilution technique. BH3 was tested using both the EC probe (1998) and bailer string (2001) method for comparison. The results for BH2 were impossible to analyse as most samples collected showed an increase in fluorescein concentration over time. It is not clear how this could happen and instrumental error seems likely (Quinn 2000). The results are not considered further.

BH3 is open across the uppermost section of the aquifer at this site. The observations show a decreasing Darcy velocity with depth, declining from 0.2 to 0.01 md^{-1} Figure 5-14.

One observation indicates a slightly higher Darcy velocity of 0.24 md^{-1} at -5.57 m aOD. This first test, undertaken in 1998, used NaCl as a tracer and measured the decrease in electrical conductivity with an EC probe on a long cable. A second dilution test was run in BH3 in 2001. This test used fluorescein as the tracer and the bailer string method for sampling.

The plotted data from this test, Figure 5-15, reveal a smooth profile of Darcy velocity, probably due to the mixing effect of running the bailer string repeatedly through the

water column. The style of the profile matches that from the 1998 test, but the average Darcy velocity from the 1998 test is 0.12 md^{-1} whereas the average from the 2001 test is 0.06 md^{-1}, half that derived by the probe and cable method of sampling. The tests were both conducted during summer fieldwork in July (2001) and August (1998). There was a difference between tests in water levels of approximately 4.50 m. During the single borehole dilution test in 1998 the water level at Lower Venson Farm BH3 was approximately 7.60 m aOD whereas in 2001 the water level in BH3 was 12.18 m aOD. However the hydraulic gradient along the valley was approximately the same for both years. The difference between the results is probably not significant as they are both of the same order of magnitude, rounding up or down gives 0.1 md^{-1} for both tests. The variation in the results is attributed to the difference between the sampling methods.

The data for BH4 indicate a section of the aquifer with a low Darcy velocity (range 0.01 to 0.02 m/d) except at -51.87 and -53.87 m aOD where the Darcy velocity increases to 0.07 m/d, see Figure 5-16

BGS LVV was tested at the same time as BH3 in 2001, using Rhodamine WT as the tracer and the bailer string for sampling. The section of the borehole tested is open over the same interval as BH3. The values of Darcy velocity recorded in the borehole are very similar to those recorded in BH3 during the 2001 test, although values below -4.57 m aOD are slightly higher.
Three explanations may be suggested for this:

- BGS LVV is located nearer to the central axis of the valley, where Darcy velocity would be expected to be higher;
- The field conditions may not conform to the assumption of no vertical flow in the borehole. Upward flowing water would cause more rapid dilution of the tracer, producing an apparent increase in Darcy velocity;
- The results may reflect natural variability of Darcy velocity in the Chalk aquifer.

Of these explanations, and given the indication of flow in BGS LVV from the borehole flow logging, it would appear that the second explanation - of upward flow in the borehole - is the most likely. The invalidity of the assumption of no upward flow in the borehole suggests that the results for this test must be treated with caution. As in BH3,

the overall shape of the BGS LVV profile is smoothed, probably due to the mixing effect of the bailer string in the water column during sampling runs.

Eastry BH7, BH8, BHA

BH7 at Eastry is open over a similar interval to BH4 at Lower Venson Farm, between -38.2 and -56.2 m aOD. The plotted data, presented in Figure 5-18, reveal velocities similar to those measured in BH4, and these are generally in the range 0.01 to 0.03 md^{-1}. At -40.2 m aOD a higher value of 0.06 md^{-1} is recorded and at the end of the profile two higher values of 0.06 and 0.05 md^{-1} are recorded at -54.2 and -56.2 m aOD respectively. These seem to correlate well with the higher values recorded in BH4 at -51.87 and -53.87 m aOD (0.07 md^{-1}).

BH8 and BHA both show very similar responses when tested. The upper part of the aquifer, measurable over a similar interval to BH3, shows high Darcy velocities, in the range 0.3 to 0.9 md^{-1} (Figure 5-19 and Figure 5-20). The velocities recorded between -5 to -9 m aOD are particularly high, between 0.5 to 0.9 md^{-1}. This may correlate with the higher value observed in BH3 at -5.57 m aOD. Below -18 m aOD BHA displays a sharp decrease in velocity, generally in the range 0.03 to 0.05 md^{-1}.

Summary of observations from the single borehole dilution tests

Figure 5-10 and Figure 5-11 display the single borehole dilution test results plotted against elevation, but as discussed in previous sections, the strata are dipping at approximately 0.5° to 1° to the north-east, roughly along the line of the Tilmanstone-Eastry valley and hence the line of the borehole sites. Interpretation of the results must therefore allow for this. As already stated, the overall trends observed in the data are an increase in Darcy velocity down-gradient and a decrease in Darcy velocity with depth. It also seems possible to correlate some of the variations seen in the Darcy velocity data with features observed in the lithology logs.

- The marked decrease in Darcy velocity recorded in BH3, BHA and BH8 occurs at approximately the level of the Belle Tout / Hope Point Marls.
- The increase in velocity recorded in BH7 at -40 m aOD is at the approximate level of the Beeding Hardground.
- At approximately -50 and -55 m aOD respectively, BH4 and BH7 indicate slight increases in Darcy velocity. This level is slightly above the Dover Chalk Rock sequence which might be anticipated as a likely higher zone of Darcy velocity.

- The core log for BGS LVI at this level recorded a fracture with flint rubble present in the core. At this level the flow and EC logs for BGS LVV also record an inflow and a step in the logs. These observations together provide strong evidence for water movement at this horizon in the aquifer, despite the fact that no significant lithology change is observed.
- The increase in Darcy velocity observed in BHE below -28 m aOD does seem to occur at approximately the level at which the Beeding, Hope Gap and Navigation Hardgrounds occur in the Chalk sequence.
- The marginally higher velocity recorded in BHE at -23 m aOD may be related to the Light Point Hardground, which occurs at approximately this elevation.

Natural Gradient tests

A series of natural gradient tracer tests were run between BGS LVV, BH3 and other boreholes at Lower Venson Farm which provide data for assessment of parameters such as travel time, fracture aperture and fracture porosity.

The initial natural gradient test, undertaken in 1999, from BGS LVV to the other boreholes at the Lower Venson Farm site provided evidence of measurable connections between boreholes BGS LVV and BH3 and a possible connection to BH2. No positive result was obtained from BH4. This is interesting as BH4 is the closest borehole to the injection borehole (BGS LVV) and, as for BH3 but unlike BH2, is also open over some of the same section of the aquifer as BGS LVV. The results obtained indicate movement of tracer out of the upper part of BGS LVV and across to BH3 and also possibly out of the lower part of the borehole and down to the upper part of the open section of BH2 (Figure 4-20), but not horizontally across to BH4.

The second tracer test, carried out in 2000 from BGS LVV to BH3, built on this initial positive result, but revealed very little as the sampling regime was not frequent enough. The main breakthrough appears to occur after approximately 17.75 hours, see Figure 4-21. A calculation comparing the mass of tracer injected with the concentration measured indicated that less than 1% of the injected tracer was detected at the monitoring borehole. This provided a useful guide for calculating the quantity of tracer to use in the subsequent 2001 test.

The breakthrough curves from the third natural gradient tracer test, between BGS LVV and BH3 in an experiment run in 2001 are given in Figure 4-22 to Figure 4-25 and show an extended peak tracer concentration at different depths in BH3 between 15 hours and more than 30 hours after injection of tracer at BGS LVV. The rising limbs of the tracer arrival curves at each measuring interval also have small peaks, which suggest partial breakthrough of tracer at earlier times. Three horizons show a breakthrough after 9.25 hours, six with a breakthrough after 10.4 hours and the remaining horizon after 14.58 hours, results presented in Figure 4-22 and Figure 4-23. The interpretation of these results is complicated by the arrangement of the injection and observation boreholes. It is not clear whether the boreholes are directly up and down-gradient of each other. The groundwater head difference and observations during previous tests demonstrate the potential for water movement between the boreholes and this is related to the local fracture orientations. However the absence of boreholes completed at the same depths in the immediate vicinity of the test means that triangulation to calculate the direction of the local hydraulic gradient is impossible. Further difficulty is introduced by the possibility of upward and downward flow in the injection borehole, although by injection over the restricted interval 20 to 46 m it was intended to minimise the impact of this. Due to these limitations only a simple interpretation of the observed tracer arrivals is considered appropriate. However, it is to be hoped that future changes to the infrastructure at the Lower Venson Farm site may allow these data to be revisited to undertake further analysis.

The analysis undertaken uses the tracer travel times to calculate an effective porosity. A variety of approaches have been taken to assess the effective porosity from these data. If the small peaks on the rising limb of the breakthrough curve are significant, reflecting rapid transit pathways, then one assumption that may be made is that all the tracer has travelled the same distance and the range of arrival times reflects variations in velocity experienced by the tracer due to variation in effective porosity. Alternatively, the tracer paths may be tortuous and the range of arrivals may be a reflection of the tracer travelling different distances at the same velocity. Taking the first case, assuming the distance travelled is to be the same for all tracer and equal to the most direct route of 28 m from BGS LVV to BH3, a groundwater velocity has been calculated for each interval, as listed in Table 5-3.

Table 5-3 Groundwater velocity, Darcy velocity and effective porosity calculated from first arrivals at each interval in BH3.

Bailer	Depth / Elevation (m bGL) / (m aOD)	Early peak breakthrough time (d)	Groundwater velocity (md^{-1})	Darcy velocity (md^{-1})	Effective porosity
1	20 / -1.57	0.385	72.65	0.07	0.001
2	23 / - 4.57	0.608	46.09	0.07	0.0016
3	26 / -7.57	0.434	64.49	0.08	0.0012
4	29 / -10.57	0.385	72.65	0.05	0.0007
5	32 / -13.57	0.434	64.49	0.05	0.0008
6	35 / -16.57	0.434	64.49	0.05	0.0008
7	38 / -19.56	0.434	64.49	0.05	0.0008
8	41 / -22.57	0.385	72.65	0.04	0.0006
9	44 / -25.57	0.434	64.49	0.04	0.0007
10	46 / -27.57	0.434	64.49	0.05	0.0007

Considering these results along with the Darcy velocity from the single borehole dilution test at each level in BH3 (2001 single borehole dilution test) the kinematic or effective porosity can also be calculated for each interval, also listed in Table 5-3. The values calculated, around 0.1%, are an order of magnitude lower than that usually assumed for effective porosity in the Chalk, adopted from the common value for specific yield obtained from pumping test analysis. This is interesting as other studies of fractured rocks have found that flow occurs in only 10% of the open fracture (Bourke *et al.* 1985 *cited in* Downing and Wilkinson 1991, and Ward 1989). These findings, in combination with the definition of effective porosity and specific yield provided by Bear (1972) indicate that for solute transport studies it is more appropriate to use an effective porosity of 0.1% than one adopted from a specific yield value derived through hydraulic testing.

An alternative analysis may be undertaken which assumes that only the early arrivals have travelled the most direct path of 28 m (i.e. those at Bailer 1, 4 and 8) and the other, later first arrivals indicate longer, less direct, trajectories. The effective porosities from these horizons may be used to derive effective porosities for the other horizons, which are then used to calculate the range of flowpath lengths, as listed in Table 5-4. This yields a measure of the tortuosity for the flow system between the two boreholes BGS LVV and BH3.

Table 5-4 Effective porosities, groundwater velocities, Darcy velocity and distance travelled using effective porosity from adjacent horizons.

Bailer	Early peak breakthrough time (d)	Groundwater velocity (md^{-1})	Effective porosity	Darcy velocity (md^{-1})	Distance travelled (m)	System tortuosity
1	0.385	72.65	0.001	0.07	28	1
2	0.608	84.9	0.0009	0.07	51.6	1.84
3	0.434	100.6	0.0008	0.08	43.7	1.56
4	0.385	72.65	0.0007	0.05	28	1
5	0.434	74.2	0.0006	0.05	32.2	1.15
6	0.434	81.5	0.0006	0.05	35.4	1.26
7	0.434	82.9	0.0006	0.05	36	1.29
8	0.385	72.65	0.0006	0.04	28	1
9	0.434	73.1	0.0006	0.04	31.8	1.14
10	0.434	82.1	0.0006	0.05	35.7	1.28

The tortuosity can be defined as the length of the actual path travelled divided by the direct distance between the two boreholes. The values calculated for each interval are given in Table 5-4. An implication of this analysis is that the calculated groundwater velocities are higher and therefore the effective porosities are lower for the horizons with the later first arrivals.

A third approach to the analysis of the natural gradient tracer test between BGS LVV and BH3 uses the time to reach the constant concentration breakthrough as the travel time, i.e. 29 hours. This analysis results in a further reduction in the groundwater velocity (23 md^{-1}) and an increase in the calculated effective porosity, to 0.003.

As noted in Section 5.3.1 the groundwater velocity calculated from the hydraulic gradient and hydraulic conductivity is high: 400 – 500 md^{-1}. The tracer test groundwater velocities are almost an order of magnitude lower: 23 – 100 md^{-1}.

The effective porosity values allow fracture apertures to be calculated from the block sizes known from the Bloomfield *et al.* (2000) relationship assuming that the product of block width multiplied by the effective porosity gives the fracture aperture. The calculated apertures are listed in Table 5-5.

Table 5-5 Fracture apertures calculated using effective porosity calculated from three different analysis approaches.

Bailer	Depth / Elevation (m bGL) / (m aOD)	Block-size* (m)	Aperture[1] (mm)	Aperture[2] (mm)	Aperture[3] (mm)
1	20 / -1.57	0.45	0.44	0.44	1.39
2	23 / - 4.57	0.57	0.93	0.50	1.84
3	26 / -7.57	0.71	0.85	0.55	2.37
4	29 / -10.57	0.85	0.57	0.57	1.79
5	32 / -13.57	1.00	0.75	0.66	2.10
6	35 / -16.57	1.17	0.94	0.75	2.62
7	38 / -19.56	1.34	1.07	0.84	2.99
8	41 / -22.57	1.52	0.93	0.93	2.92
9	44 / -25.57	1.71	1.16	1.02	3.22
10	46 / -27.57	1.85	1.37	1.08	3.83

* *Log fracture density [1/m] = -1.685 x Log depth [m bGL] + 2.5365* (Bloomfield *et al.* 2000).
[1] Direct pathway derived effective porosity.
[2] Tortuous pathway derived effective porosity.
[3] Peak concentration derived effective porosity.

Further aperture calculations from tracer test data are considered in Section 5.5.2 and compared with these results.

Packer tests

A vertical profile of hydraulic conductivity calculated from the packer testing undertaken in BGS LVV is given in Figure 5-21.

The upper part of the profile shows a good agreement with the trend obtained from the single borehole dilution tests for BH3 (Lower Venson Farm) and BHA (Eastry) (Figure 5-11). The higher values calculated at 70 and 72 m bGL (-51.87 and -53.87 m aOD) in BH4 (Lower Venson Farm) (Figure 5-16) and at 71 and 73 m bGL (-53.23 and -55.23 m aOD) in BH7 (Eastry) (Figure 5-18) from the single borehole dilution testing are also supported with higher values measured by the packer testing at 65.5 to 68.5 m bGL (-47.34 to -50.34 m aOD) hydraulic conductivity of 101 md^{-1} and 76 to 79 m bGL (-57.84 to -60.84 m aOD) hydraulic conductivity of 164 / 172 m d^{-1}. The relationship of hydraulic conductivity to specific lithologies or features observed in the Chalk sequence is noted in Table 5-6.

Table 5-6 Lithology and hydraulic conductivity for packer test data from BGS LVV, Lower Venson Farm.

Depth (m bGL)	Elevation (m aOD)	Lithology, Formation or Feature & comments	Hydraulic Conductivity (md^{-1})
30 to 33	-11.84 to -14.84	Seaford Chalk	106 / 137
35.5 to 38.5	-18.16 to -21.16	Belle Tout / Hope Point Marls	49 / 63
39.5 to 42	-21.34 to -24.34	Shoreham Marls	59 / 62
45.5 to 48.5	-27.34 to -30.34	Lewes Nodular Chalk	37 / 52
49.5 to 52.5	-31.34 to -34.34	Light Point Hardgrounds	18 / 22
65.5 to 68.5	-47.34 to -50.34	Dover Top Rock? Probably just below the level of the DTR and just at the fracture noted in the core log and also the step in EC and flow logs.	101
76 to 79	-57.84 to -60.84	Dover Chalk Rock sequence Large step in EC log.	164 / 172
81.5 to 85	-63.34 to -66.34	Marl horizon Marl noted in core log at 84 m. Difficulties with packer inflation during testing, therefore unlikely to be reliable data.	Range 1 to 6

The Seaford Chalk generally has a high hydraulic conductivity. The marly beds (Belle Tout / Hope Point and Shoreham Marls) that occur towards the base of the Member have a markedly lower hydraulic conductivity. Features such as the possible fracture at approximately 68 m bGL (-49.84 m aOD) are also horizons of high hydraulic conductivity but this does not appear to be related to a change in lithology. The Dover Chalk Rock sequence also has high hydraulic conductivity and this is almost certainly related to the greater degree of fracturing that is associated with this harder, more brittle series of hardgrounds.

The hydraulic conductivity values calculated from the packer testing are larger than those at equivalent levels obtained through the single borehole dilution testing. One reason for this may be found in the methodology adopted. When setting the level of the packers, particularly where flint horizons are known, it is necessary to ensure that the inflated packer is not likely to be punctured by a sharp object, such as the cut face of a flint. Due to the frequent occurrence of flints in the boreholes, the two packers were set straddling flint bands, so that the flint band was located within the pumped interval. Flint bands may be associated with flowing horizons (Mortimore 1990, Jones and Robins 1999) and so the packer testing may have preferentially sampled more transmissive zones. Packer testing also samples a larger volume of aquifer than does a single borehole dilution test and this may also lead to higher values of hydraulic conductivity being obtained.

Fracture apertures can be calculated from these data using the cubic law approximation, where N is fracture density and a is fracture aperture:

$$K_{eff} \approx 50a^3N$$

The fracture apertures calculated in this way are termed cubic law apertures (Tsang 1992) or hydraulic apertures, and are listed in Table 5-7.

Table 5-7 Fracture apertures calculated from packer test hydraulic conductivity results.

Depth / Elevation m bGL / m aOD	K^1 md^{-1}	K^2 md^{-1}	Aperture[1] mm	Aperture[2] mm
31.5 / -13.07	106	137	1.27	1.39
37 / -18.57	49	63	1.08	1.17
41 / -22.57	59	62	1.22	1.24
47 / -28.57	37	52	1.12	1.26
51 / -32.57	18	22	0.92	0.99
67 / -48.57	101	-	1.92	-
77.5 / -59.07	164	172	2.44	2.48
83 / -64.57	1	6	0.46	0.84

Pumping tests

A summary of the results of the pumping tests undertaken in the 1973 – 1979 investigations is provided in Figure 5-22 as a vertical profile of hydraulic conductivity.

The data are presented as hydraulic conductivity values for ease of comparison to other data already presented, in spite of the original data being calculated as transmissivity. The hydraulic conductivity value has been calculated by dividing the original transmissivity value calculated by SWA (1976b), Headworth *et al.* (1980) or Carneiro (1996) by the open section of the borehole concerned. The trend of decreasing hydraulic conductivity with depth observed by packer testing and single borehole dilution testing is largely supported by the pumping test data, although the tests at BH3 (Lower Venson Farm) and at BH7 (Eastry) indicate very low hydraulic conductivity compared to others at similar intervals. The trend of increasing hydraulic conductivity downgradient is also generally supported with BH4 (Lower Venson Farm) indicating a higher hydraulic conductivity than BH1 (Thornton Farm), and BH9 (Eastry) indicating a higher hydraulic conductivity than both BH1 and BH4. At greater depth, BH2 (Lower Venson Farm) indicates a higher hydraulic conductivity than BH6 (Thornton Farm). It is difficult to make clear statements about the pump test data as most of the tests were of very short duration, typically 6-8 hours, and data from the pumped well were analysed, as no observation boreholes were open over the same interval at the various sites, except at Eastry. In contrast, the pumping test in BH9 at Eastry, which indicates the highest hydraulic conductivity, was undertaken over several months as a large-scale pumping

test to determine the transmissivity of the aquifer and the long-term yield of the borehole and also to assess the suitability of pumping as a method to increase the clean-up rate of the aquifer.

The pumping test interpretations of hydraulic conductivity are compared with the single borehole dilution and packer test results in Figure 5-23. Generally, the packer testing produces the largest value for a given interval / elevation. The pumping test interpretations provide an average value across the intervals of the single borehole dilution point measurements. This is likely to be due to most of the transmissivity being provided by a limited number of fractures, so that on averaging as hydraulic conductivity over the open length of the borehole, the values appear to be smaller. As already noted, the pumping test results for BH3 and BH7 are anomalous in the context of the general trend of increasing hydraulic conductivity down-gradient, and their pumping test interpretations are also in disparity with their respective single borehole dilution test results. The hydraulic conductivity calculated for BH9 at Eastry, which is at the same site and open over much of the same interval as BH7, is also much higher. This may be because the upper part of the aquifer is more important for groundwater flow (BH7 is cased over the upper part of the aquifer). It may also be related to the diameter of the borehole (BH7 has a 200 mm diameter and BH9 has a 610 mm diameter) and the number of interconnected fissures intercepted.

5.4 Pollutant source

5.4.1 Location of lagoons, ponds and ditches

Sketch maps in reports from BGS archives on the Kent coalfield suggest that the distribution of lagoons, pond and ditches for disposal of the mine waters was more complicated than outlined by Headworth *et al.* (1980) and Bibby (1981). Figure 3-18 provides mine disposal water sampling locations identified by BGS staff following investigations at the Tilmanstone colliery during 1962 and 1964.

5.4.2 Accuracy of source term

The record of volumes and chloride content of disposed brines given by Headworth *et al.* (1980) (Figure 2-15) effectively describe the pollutant source term. Table 5-8 summarises the results of brine analysis undertaken by BGS in 1962 and 1964.

Table 5-8 Chloride concentration from samples during 1962 and 1964. Refer to Figure 3-18 for sample location.

Sample site (see Figure 3-18)	Chloride concentration Cl mg/L	Date sampled
1	645	29/11/1962
2	725	
3	605	
4	645	
5	4950	
6	1810	
A	408	14/10/1964
B	1850	
C	470	
D	1940	
E	2910	

Anon (1953) reported that discharged mine waters were drunk by sheep and cattle kept at Dane House. Sheep and cattle can tolerate salinity of up to 10 000 mg/L (total dissolved salts) but concentrations above 3000 mg/L tend to cause digestive problems for the animals (University of Florida, 1992) so this may indicate an upper limit on the minewater discharge concentration at this time. This lends support to the data which show that concentrations of chloride did not rise above 2000 mg/L until after 1960.

The confidence that can be placed on the interpretation of the concentration and volumetric data for brine disposal is limited, however. The early data are over 100 years old. There was no systematic collection of concentration or volumetric data or of the routine of use of the discharge locations during this early phase of brine disposal. However the earliest disposals were undoubtedly of lower concentration and volume so would have had less impact than the later higher volume, higher salinity discharges. There is more confidence in the more recent data. It should be noted, however, that the two parties (Southern Water Authority and the National Coal Board) that were reporting

concentration and volumetric data had very different agendas. The Southern Water Authority was undertaking legal proceedings to stop the discharge of the mine water at the Tilmanstone colliery. The National Coal Board was resisting this change to their operations, which would cost them a great deal in pipeline construction costs. It would therefore have been in Southern Water Authority's interests to exaggerate the pollution potential and National Coal Board's to underplay the concentrations and volumes being discharged. Overall therefore this may reduce the confidence that can be placed on the source term interpreted from Coal Board data as given in Headworth *et al.* (1980). Unfortunately there is no evidence, either in data or memo form that can be used to consider this situation. Headworth (1994) reports that the situation between the two parties was very difficult. Fortunately the independent sampling undertaken by BGS, observing a concentration of 4950 mg/L at sample point 5 in 1962, provides evidence to support the source term data provided by the National Coal Board and reported by Headworth *et al.* (1980).

The groundwater pollution in the Tilmanstone-Eastry valley covers a greater lateral extent than would be expected to be produced from the lagoons located at the head of the valley. As outlined in Chapter 2, the hydraulic conductivity in a chalk valley is generally higher along the central axis of the valley and lower across the interfluves (Ineson 1962). This would tend to focus any pollution along the central axis of the valley. Many of the assessments of the developing chloride pollution, for example by Buchan (1962) and SWA (1976a), indicate a much wider extent to the pollution than this. However, these contour plots may be misleading as there are very few sample points located on the interfluves. Also, considering the BGS investigations undertaken to assess the quality of the water entering the Chalk, it is clear that the disposal of mine-water at the Tilmanstone Colliery was not concentrated at one lagoon area, but was more widely dispersed (Figure 3-18). A series of ditches and ponds were in use and this undoubtedly caused a much greater lateral spread of pollution sources. Furthermore, the head created by the recharge mound from the disposal lagoons would have provided a mechanism for lateral spreading of water. If the strata below the lagoons became fully saturated during disposal operations this would increase the head locally by approximately 15 m. In addition Bloomfield *et al.* (2000) propose within-block structural features that may also influence groundwater movement. The general trend of these features is south-east to north-west, at a high angle to the direction of the

Tilmanstone – Eastry valley and therefore such features could produce solute spreading along a south-east north-west axis.

5.5 Solute transport

5.5.1 Porewater concentrations

The porewater chloride concentration profile obtained from the BGS LVV cores is overlain with the lithology and fracturing interpretations in Figure 5-24, and is compared with the earlier porewater chloride observations in the valley in Figure 5-25.

The relatively even concentration recorded in 1999 in BGS LVV (Lower Venson Farm) porewater from approximately 8 to – 27 m aOD (10 to 45 m bGL) is in contrast to the peaky chloride concentration profile recorded in 1974 in BHB 1974 from 18 to -8 m aOD (14 to 40 m bGL). There are, however, difficulties in comparing the two profiles. The datum for BHB is not precisely known. It has been estimated as 32 m aOD from 1:10 000 maps of the area. There are no lithological records for the borehole so it is difficult to locate it stratigraphically. The only geophysical logs reported are so smoothed that it is impossible to pick out any features other than general fracturing to 30 m bGL (2 m aOD), some possible fracturing at 45 to 50 m bGL (-13 to -18 m aOD) and a large fracture at approximately 97 m bGL (-65 m aOD). The formation resistivity log is similarly featureless. Possible increases in resistivity are recorded at 70, 82, 100 and 122 m bGL (-38, -50, -68 and -90 m aOD), but it is difficult to attribute these responses to any particular lithologies with confidence. It has therefore been assumed that there is a dip of 0.75° (BGS map gives 0.5° to 1°) and the porewater profile is offset according to this assumed datum and dip. Figure 5-25 gives the resulting logs.

There is a similarity in the chloride profiles of 1974 and 1999 in that a sudden, rapid decrease in concentration occurs in both at approximately –23 to –27 m aOD. The peaky nature of the 1974 profile in BHB above this level is however quite different to that seen in 1999 in BGS LVV. This is thought to be due to two main reasons:

- BHB (the 1974 profile) is much closer to the source of the pollution and represents an earlier period in its development giving less opportunity (in terms of distance and time) for the chloride concentration to equilibrate through diffusion if particular horizons were preferentially supporting flow.

- The sampling methodology was different. In 1999, BGS LVV was an air-flush rotary cored borehole and core sub-samples for centrifuging were taken from core at 0.5 m intervals. The information for the method of drilling BHB is not available but it is assumed cores were collected by percussion using U4 (now U100) sample tubes, as was stated in water authority reports and memos associated with the original investigations for core from BHs 1, 3, 5 and 6. Sub-samples were then centrifuged to provide porewater for analysis. However there is no record of the position in the U4 core where the centrifuging sample was taken or whether it was a cumulative sample from the entire core length.

The porewater profile obtained at BGS LVV in 1999 is interpreted as an equilibrated solute plume in its upper section. Chloride porewater and fracture water concentrations are approximately equal. This is in contrast to deeper sections of the porewater profile, such as approximately -32 m aOD (50 m bGL) or approximately -48 m aOD (66 m bGL) where porewater and fracture water concentrations are not in equilibrium. The shape of the profile has evolved from the earlier porewater profile obtained at BHB in 1974. Much of the shape of the BHB 1974 porewater profile has been maintained. In particular, the distinctive decrease in chloride concentration observed at BHB in 1974 below approximately -8 m aOD (40 m bGL) is visible as a sharp decrease in porewater chloride concentration at BGS LVV in 1999 at -27 m aOD (45 m bGL). The lithological log of BGS LVV indicates the presence of the Shoreham Marls approximately at this elevation and it is suggested that this feature has acted to limit the extent of any downward migration of the bulk of the solute plume over the length of the Tilmanstone-Eastry valley.

Occasional peaks in porewater chloride concentration recorded at deeper intervals at BHB in 1974, such as at approximately -43 m aOD (75 m bGL) and -66 m aOD (98 m bGL), may be represented in the BGS LVV 1999 porewater profile by the increased porewater chloride concentration observed between approximately -42 and -60 m aOD. It is also possible to relate this increased chloride concentration with a lithological sequence that includes a series of hardgrounds and the Dover Top Rock and Dover Chalk Rock bands.

The two porewater profiles illuminate the hydro-lithology of the Tilmanstone-Eastry valley, indicating preferential flow along fractured sequences and marly sequences restricting downward migration. The BGS LVV 1999 porewater profile demonstrates the state of equilibrium and disequilibrium between fracture water and porewater concentrations. This can be related to a combination of variable fracturing of lithologies, a general decrease in fracture frequency with depth, producing variation in matrix block size and resulting in different times to reach diffusive equilibrium, and the resultant hydraulic conductivity of the strata.

5.5.2 Tracer tests

Fracture orientation may be expected to affect groundwater flow directions. While it is difficult to determine groundwater flow directions at individual sites in the Tilmanstone – Eastry valley, due to boreholes being completed at different intervals, at Lower Venson Farm tracer dye has moved at an angle to the main direction of flow determined from boreholes located along the whole valley. Fracture orientation appears therefore to have played a role in causing extensive lateral spreading of the pollution and this is further evidenced, at a smaller scale, by the results of the tracer testing at Lower Venson Farm.

Using the hydraulic conductivity values from the single borehole dilution tests in combination with the Bloomfield *et al.* (2000) fracture-density relationship and applying an approximation of the cubic law, as in Section 5.3.3, further values of fracture aperture can be obtained. These have been derived for all the boreholes in which single borehole dilution tests have been successfully undertaken. These estimates of fracture aperture along with aperture values derived from values of effective porosity calculated from the tracer test between BGS LVV and BH3 at Lower Venson Farm are presented in Figure 5-26.

The effective apertures calculated from the different approaches are similar. This is not surprising given the basic observations and calculated values that the derivations are based on: the hydraulic conductivity values used in the cubic law approximation come from the Darcy velocity as does the effective porosity, and both approaches use the same fracture-density depth relationship. The relationship between the fracture-density and aperture is shown in Figure 5-27.

Combining all the observations from the single borehole dilution testing at the Lower Venson Farm site from BH's 3, 4 and BGS LVV allows a vertical profile at 10 metre intervals, from 10 to 100 m bGL, of effective transport parameters to be produced. These are presented in Figure 5-28.

The profile is a combination of parameter values from each of the boreholes: the top 50 m of the profile is constructed from a combination of the hydraulic conductivity values derived from single borehole dilution testing at BH3, with the groundwater velocities from the natural gradient test from BGS LVV to BH3 and the fracture density depth relationship of Bloomfield *et al.* (2000). The hydraulic conductivity values are combined with the matrix block size derived from the fracture density depth relationship within the cubic law approximation to produce an aperture value. The groundwater velocities are calculated from the first arrivals and the direct route between the injection and sampling point.

For the effective transport parameters below 50 m, it has been assumed that the effective porosity is 0.001. The groundwater velocity has been calculated by dividing the Darcy velocity calculated from the single borehole dilution test at BH4 with the 0.001 effective porosity value. The aperture value can then be calculated in the same way as for the top 50 m of the profile.

The Lower Venson Farm site is chosen to generate the effective transport parameter profile as it is the only location where both single borehole dilution tests and borehole to borehole tracer tests were undertaken. Furthermore the majority of the data for the fracture density versus depth relationship are derived at this site.

5.6 Comparison of the field techniques

The experience of applying a variety of tests in the Tilmanstone – Eastry valley merits a comparison of the relative value of the techniques applied. Comparisons between parameter values derived from tests undertaken at different scales are made in this section as well as the values derived through applying different test methodology.

5.6.1 Value from scale of application

Ptak and Teutsch (1994) note that hydraulic conductivity values derived for the same alluvial aquifer at a variety of scales vary over four orders of magnitude. For example,

permeameter tests produce smaller values than sieve analysis, and impeller flowmeter methods cannot measure very small discharge rates, so are not sensitive to low hydraulic conductivity values. Ptak and Teutsch (1994) compare the variance of four methodologies. The smallest variance is observed for late drawdown values from pumping tests. This is due to the larger scale of pumping tests which produce long-range averaged values over larger volumes of aquifer materials, whereas the other techniques observe a more local scale and reflect the aquifer heterogeneity.

The field testing undertaken during the current research has predominantly been at two scales: the immediate environs of the borehole and up to tens of metres between two boreholes. The matrix porewater analysis, single borehole dilution testing, geophysical logging and packer testing fall within the former category, and the borehole to borehole natural gradient tracer test falls into the latter. Existing data, examined as part of the research, generally fall into the second and a third category – that of up to hundreds of metres from the borehole. The pre-existing data falling into the second (tens of metres) category include the pumping tests and tracer testing undertaken by SWA (1976a, b). The hydrochemical sampling undertaken by Buchan (1962), during the SWA 1970s investigations and by Peedell (1994) falls into the third (hundreds of metres) category.

5.6.2 Value of non-invasive techniques

The DEM developed by BGS during the FRACFLOW investigations proved to be a rapid technique to provide evidence for bounding features that may have an impact on groundwater flow at the regional scale. Within these larger blocks other structures were also highlighted by the technique. Several of the larger scale features could be linked to proven fault lines and this helped to provide some verification of the analysis. The difficulty arises in knowing how these structural features will impact the groundwater flow; a fault could be more, or less, permeable than the surrounding strata or provide a route for the transfer of groundwater between horizons. Analysis of DEMs can also provide information on the orientation of major vertical fracturing if the groundcover does not obscure the features. This was not done for the Tilmanstone-Eastry area. The development and analysis of DEMs requires specialist software to analyse the images. The more traditional technique of using stereoscopic glasses to analyse stereo pairs of aerial photos requires relatively simple equipment but most of the subtle landform changes higlighted by DEM analysis, and which appear to have significance for groundwater flow and solute transport, are unlikely to be detected using stereo glasses.

The fracture scanline surveys were particularly effective in the Tilmanstone-Eastry area as there was Chalk at outcrop relatively close to the main area studied. Lithological information could be combined with fracturing style and fracture density information. Fracture information from outcrop surveys was combined with down-hole techniques to establish a fracture-density depth relationship that provides valuable information on matrix-block size variation with depth.

The hydrochemical sampling information that was available for the main discharge point in the Tilmanstone-Eastry valley was of limited value. The unknown effect on the solute concentration due to mixing of solute from different lithologies causes difficulty with the interpretation of trends in the data. Also of significance is the effect of changes in location of sampling point and trends in the quality of the output from the Eastry waste water treatment works which is located close to the first sampling point.

Several of the issues associated with the input term from the discharge lagoons have been discussed in Section 3.3.4. It is of great value to have a description of the input term made close to the time during which the input was occurring. This is particularly the case when the prevailing regulation and record keeping did not provide adequate details that could be returned to at a later date. Furthermore, the institutional changes that have occurred in the intervening 30 years since the cessation of lagoon discharge, would have provided myriad opportunities for information to be lost or destroyed, even if it was held in the first place. The differing agendas of the organisations involved in the construction of the input term are an important consideration. However the calculation of the input term close to the time at which the discharge occurred was very valuable to the current research.

5.6.3 Value of invasive techniques using existing infrastructure

Invasive field methods should be used in a phased manner such that they test and advance the conceptual model. The application of invasive methods will generally be to:

- Delineate the source of a contaminant;
- Define stratigraphic, lithological, structural and/or hydraulic controls on the movement of contaminated groundwater;

- Characterise the fluid and fluid-media properties that affect the migration of the contaminated groundwater;
- Estimate or determine the nature and extent of contamination and the rates and direction of contaminant transport; and
- Evaluate exposure pathways.

An important consideration prior to undertaking an invasive field method is the risk of enlarging the zone of contamination through the technique adopted, such as by causing bypass routes through hydraulically isolating strata. The invasive activities may increase the risks to receptors, generate misleading data leading to a flawed conceptual model, and increase the difficulty and cost of site remediation (USEPA 1992).

The most valuable outcomes from undertaking borehole geophysics were two-fold Firstly the technique provided information, through resistivity logging, which enabled lithologies such as marl bands and hardgrounds to be correlated. This was limited to correlation between boreholes at one site, rather than along the length of the Tilmanstone- Eastry valley. Secondly, the heat-pulse flowmeter was used to indicate whether there was vertical flow in the boreholes used for single borehole dilution testing. A lack of vertical flow is a key assumption for single borehole dilution testing, so to be able to confirm the absence of vertical flow is valuable to provide confidence in the calculated values of Darcy velocity. The digital opti-viewer technique, although not providing useful information in the Tilmanstone-Eastry valley, has been used successfully elsewhere (*pers. comm.* D. Buckley, BGS) and provided valuable information on lithology and strata from existing boreholes which would be at a fraction of the time and cost of drilling new boreholes.

Borehole geophysical logging can be quite slow. It takes approximately 1 to 1½ days to undertake a complete suite of logs in a 100 m borehole. If pumped flowmeter logs are required there may be problems or additional expense incurred in disposing of the abstracted water. Expensive specialist equipment is required to carry out borehole geophysics and the availability of digital opti-viewer in particular, is limited in the UK.

Packer testing may be of limited use in existing Chalk boreholes where properties of specific lithological features are of interest and there is no detailed log of the borehole

available or obtainable from geophysics. Additionally there are potential problems inflating packers over flint horizons as these can puncture the packer. Packers must therefore be located so as to avoid flint horizons and this may result in a bias towards the measurement of flint horizons as these will tend to be located within the measurement interval between the packers. Flint horizons have been associated with greater groundwater flow in some locations and may have a higher hydraulic conductivity associated with them. However where lithological detail for the borehole is available packers can be carefully located and can provide detailed hydraulic conductivity measurements for features or lithologies of interest. Packer testing may also provide an opportunity to obtain fracture water samples from discrete intervals and indicate differentiation of the plume between lithology or strata. However, if there is a hydraulic gradient within the borehole it is likely that any differentiation of the contaminant plume will have been destroyed or confused by the movement of groundwater within the borehole. The isolation of intervals by packers provides an opportunity to make discrete measurements of groundwater head and this may indicate the potential for fluid movement between horizons.

Packer testing is relatively expensive. Specialist equipment is required and usually a drilling rig is needed to lift the packer assembly. Gas canisters are required to inflate the packers and somewhere to dispose of abstracted water is also necessary.

Single borehole dilution testing can be undertaken in existing infrastructure and, as long as there is no vertical hydraulic gradient in the borehole, the Darcy velocity can be obtained. If the hydraulic gradient is known the hydraulic conductivity can be derived. If detailed down hole measurement can be taken horizons with a greater Darcy velocity and hence hydraulic conductivity can also be determined. The technique is relatively rapid as tests can be run in several boreholes simultaneously if they are close enough to each other to allow sampling to be undertaken in rotation. However care should be taken if this is done as there is potential for cross-contamination between boreholes. The equipment required for injection is low-cost and readily available. The most expensive item would be a down hole EC probe for ionic tracers. The cost increases considerably if fluorescent tracers are used. Cross-contamination risks increase and possibly prevent simultaneous borehole testing, a down hole fluorimeter or laboratory analyses will also increase costs and complexity of the testing. However, the simplicity of single borehole

dilution testing and the information it provided in the Tilmanstone-Eastry valley, this is considered to be an extremely valuable field technique for deriving effective transport parameters.

Borehole to borehole tracer tests can be undertaken in existing infrastructure and under natural gradient conditions if the boreholes are close enough and appropriately orientated relative to fracture orientation and groundwater flow direction. Natural gradient tracer tests can provide an ideal range of information on hydraulic conductivity and effective porosity, if the test is combined with single borehole dilution testing to provide a Darcy velocity. It is advisable to take a progressive approach, establishing links between boreholes initially with a 'yes-no' test, such as that described in Section 4.6.2, which does not require excessive expense for monitoring and analysis. Borehole to borehole dilution testing may be problematic in the Chalk if using ionic tracers, as described in Section 4.6.2, and where fluorescent tracers are used costs are incurred for field fluorimeters and sample analysis. The issue of cross-contamination may also mean that tracer testing is relatively labour intensive during the early part of the test. However, as this testing provided key information on effective porosity it was invaluable during the current research.

5.6.4 Value of invasive techniques using new infrastructure

Chalk core from drilling two new boreholes provided confirmation of stratigraphy and lithology. This was of key importance to the research as it provided a framework within which to develop the understanding of plume movement along the Tilmanstone-Eastry valley. However it is often not necessary to have new core to do this. Borehole geophysics may be available and able to provide adequate information to allow lithological detail to be derived. Also, as already discussed, digital opti-viewer logging has been used successfully to determine lithological detail from existing boreholes.

The core provided some indication of fracturing, although it was not particularly valuable as much of the core was fractured during drilling. Although it is usually possible to differentiate between drilling induced fractures and in-situ fracturing, at Lower Venson Farm this was often impossible due to damage, or milling, of the fracture surfaces. The televiewer logging undertaken in the borehole provided more useful information on fracturing than the new core, and a new borehole was not necessary for the televiewer logging.

The porewater extracted from the core provided key information on the distribution of solute. This was valuable as it demonstrated that stratification of the solute plume had been maintained over approximately 2000 m and four decades, and that this could be related to lithology and hydrostratigraphy. It was intended that porewater would be sampled with depth into the matrix from a fracture. However the difficulty of obtaining suitably intact core precluded this. Samples were taken every 0.5 m along the length of the core and analysed for EC. Some samples were also analysed for chloride and the EC and chloride data were correlated to produce a profile of matrix porewater chloride concentration with depth. Particular issues that should be considered with this method include the influence of drilling fluid on the porewater concentrations. This can be managed by removing the outer few millimetres of core prior to sampling (Fretwell 1999). The potential for fluid migration within the core once at the surface and exposed to different pressure conditions, as well as the potential for loss of volatile contaminants needs to be considered when collecting core for porewater analysis. These problems can usually be accommodated by freezing the core or sampling rapidly and storing in sealed containers.

Drilling produced a considerable quantity of water which, due to the high chloride concentration, was problematic to dispose of. Fortunately at Lower Venson Farm it could be returned to the aquifer overnight via the new borehole. The other disposal option was to tanker the water to a waste water treatment works and this would have been prohibitively expensive.

The completed vertical borehole (BGS LVV) was extremely valuable as it provided infrastructure that allowed the borehole to borehole natural gradient tracer test to be undertaken. The potential for undertaking this type of test was previously extremely limited due to the lack of boreholes open over the same interval at each of the sites in the Tilmanstone-Eastry valley. The distance between sites is large, the nearest two sites are 300 m apart, and this probably precludes successful application of natural gradient tracer testing.

The construction of new infrastructure was, however, the most expensive of the field techniques adopted during the research. The information derived from it was invaluable

in developing the links between the plume movement and hydrostratigraphy. However, in terms of providing information on effective transport parameters, the single borehole dilution testing combined with natural gradient tracer testing, is considered to be more useful and cost effective.

5.7 Conceptual model

From the field investigations undertaken as part of this research, in combination with those undertaken previously or in parallel with the current research, the conceptual model for the area originally developed by Headworth *et al.* (1980) and Bibby (1981) may be updated.

A visual representation of the conceptual model is presented in cartoon style in Figure 5-29. Four key elements are identified for the conceptual model. These are indicated on Figure 5-29 by circled numbers. The following section of text describes each numbered element and provides the supporting evidence for it through links to the observations and interpretations presented in Chapter 4 and 5.

Element ①: Geology and structure

The Chalk sequence encountered in the Tilmanstone – Eastry valley can be updated from the simplified Upper, Middle and Lower divisions of Heathcote *et al.* (1980) with the lithological divisions recognised by Mortimore (1997) and Bristow *et al.* (1997). This is indicated on Figure 5-29 by the labelling of the Seaford Chalk, the Shoreham Marl, the Lewes Nodular Chalk, the Hope Gap and Navigation Hardgrounds, the Dover Chalk Rock and the Bridgewick Marls.

This more complex sequence has been identified from the information obtained through recent drilling investigations (Section 4.4.1) and geophysical logging (Section 4.4.2) which has confirmed the presence of the Chalk sequence described at the coastal outcrop (Mortimore 1997, Figure 5-4) for the Tilmanstone – Eastry valley. The elevation of the Shoreham Marl, which divides the Seaford Chalk from the Lewes Nodular Chalk, and the Dover Chalk Rock as well as marker marl seams and hardgrounds have been demonstrated by geophysical logging (Section 5.2.1).

The identification of this more complex Chalk sequence is important in order to allow application of typical hydraulic and geological properties attributed to the lithologies by Mortimore (1990), and which are significant because of their influence over solute movement.

These typical geological and structural properties are marked on Figure 5-29 in grey boxes and are summarised below:

Seaford Chalk
Medium spaced, intense fractures producing a small block size;

Lewes Nodular Chalk
Alternating very soft to very hard bands;
Widely spaced fractures;

Dover Chalk Rock
A significant hardground within the Lewes Nodular Chalk which has few fractures, but where fractured, supports larger apertures;

Lewes Nodular Chalk (at depth)
Larger block sizes.

Structural features have been identified in the Tilmanstone – Eastry valley through the DEM mapping undertaken by BGS (Section 4.4.3, Figure 4-7) and from the geological map for the area (BGS 1977, 1982). The location of faults in the Carboniferous sediments underlying the Tilmanstone – Eastry valley was indicated on Figure 5-5. Vertical fractures are incorporated in the conceptual model within the Chalk sequence in the area above the Carboniferous faulting close to the former minewater lagoon area. Further discussion of this aspect of the conceptual model is undertaken for Element ③.

Element ②: Hydrogeological properties and parameter values

Examination of the Chalk lithology alongside the results from the single borehole dilution and packer testing (Section 5.3.3) demonstrates that specific horizons have a strong influence on groundwater flow within the upper more transmissive 40 – 50 m of

the Chalk aquifer, as well as at greater depths. Single borehole dilution testing has been used successfully to demonstrate a general decrease in hydraulic conductivity with depth, as found elsewhere for the Chalk (Price 1987, Rushton *et al.* 1989, MacDonald and Allen 2001). Results from the single borehole dilution testing are supported by the results from packer testing. However, the results of the field investigations also demonstrate that, at depth, specific horizons such as the Dover Chalk Rock are also important for groundwater flow. The deeper Melbourn Rock is reported as being particularly productive elsewhere (Price *et al.* 1993, Mortimore 1990). These horizons are harder, fractured lithologies which, particularly when adjacent to low permeability marl bands that restrict downward movement of water, are able to transmit relatively large quantities of water. These horizons are also significant for solute transport if the solute is able to migrate down through the aquifer to them. The field results in combination suggest that the changes in hydraulic conductivity are strongly correlated with lithology.

Hydraulic conductivity data from single borehole dilution testing, and independently from packer testing, combined with data from natural gradient tracer tests and a fracture density depth relationship determined for the area, have been used to develop a hydrogeological stratigraphy and a vertical profile of effective transport parameters for the Chalk aquifer in the Tilmanstone –Eastry valley (Section 5.3.3).

Natural gradient tracer testing has been used to demonstrate the effect of fracture orientation on groundwater flow at the tens-of-metres scale.

These properties are included in the grey boxes on Figure 5-29 with the geological properties listed under Element ①and are listed here:

Seaford Chalk

Hydraulic conductivity is in the range of approximately 50 to 100 md^{-1};
Groundwater velocity is approximately 73 md^{-1};
Fracture aperture ranges from approximately 0.4 to 0.7 mm;
Half-block thickness ranges from approximately 0.1 to 0.8 m;

Lewes Nodular Chalk (above the Dover Chalk Rock)

Low hydraulic conductivity, approximately 1 md^{-1}, except along hardground horizons which have higher hydraulic conductivity and groundwater velocity, demonstrated by single borehole dilution testing (Section 5.3.3);

Groundwater velocity ranges between approximately 16.5 md^{-1} (bulk of deposit) and 65 md^{-1} (hardgrounds);

Fracture aperture ranges from approximately 0.6 to 0.8 mm;

Half-block thickness ranges from approximately 1.1 to 1.9 m;

Dover Chalk Rock

Fewer fractures are present but where they occur they tend to have larger apertures providing routes for faster groundwater, and hence solute, movement.

Groundwater velocity approximately 67 md^{-1};

Fracture aperture ranges from approximately 1.1 mm;

Half-block thickness approximately 2 m;

Lewes Nodular Chalk (at depth)

Larger block sizes (calculated through the fracture-density relationship (Section 5.2.2)

Groundwater velocity approximately 9 md^{-1};

Fracture aperture ranges from approximately 0.6 to 0.7 mm;

Half-block thickness approximately 2.9 to 3.4 m;

Element ③: Behaviour of infiltrating minewater brine

Matrix porewater chloride profiles (Section 5.5.1 and illustrated in Figure 5-24 (BGS LVV, 1999) and Figure 5-25 (BHB, 1974)) have demonstrated that the infiltrated minewater has penetrated to depth in the aquifer and is not restricted to the upper 40 m of the Chalk as previously assumed by Bibby (1979). The BGS LVV matrix porewater chloride profile is shown in Figure 5-29 as red and pink rectangles to indicate the changes in chloride concentration with depth. The profile was originally presented in Figure 5-24 and should be read as representing low concentrations on the left, increasing to higher concentrations as the rectangles move further right. The total chloride concentration range represented by the most extreme left and right rectangles is 0 and 1200 mg/L respectively. The movement of chloride at depth appears to be restricted to the Dover Top and Dover Chalk Rock horizons and immediately overlying

hardgrounds and occurs in these strata at relatively high concentration. This is in contrast to the conceptual model proposed by Headworth *et al.* (1980) (reproduced in Figure 2-14) which proposes a relatively even distribution of chloride in fractures and matrix porewaters throughout the Chalk in the Tilmanstone-Eastry valley. The presence of the high matrix porewater chloride concentrations at depth suggests that the infiltrated minewater was not subject to strong attenuation through diffusion. Rather it is indicated that fairly rapid vertical movement of pollutant was possible (indicated by red arrows on Figure 5-29), at least down to the more transmissive horizon at depth. It is presumed (proposed?) that this was possible due to the large heads that developed beneath the disposal lagoons (evidenced by the changes in groundwater heads following closure of the infiltration lagoons, Section 5.3.1).

Element ④: Diffusive exchange

Comparison of the matrix porewater chloride profile for BGS LVV with the chloride concentrations obtained during packer testing, and which are assumed to be broadly representative of fracture water chloride concentration, (Section 5.5.1 and Figure 5-24), indicates variations between the relative concentrations for the mobile (fracture water) and immobile (porewater) domains within the aquifer. The chloride concentrations obtained through packer testing are indicated on Figure 5-29 by blue circles. These are at shallower levels within the Seaford Chalk, porewater and fracture chloride concentrations are similar and this is unsurprising given the time necessary for diffusive equilibrium to occur for these smaller block sizes and the time elapsed since infiltration of the minewater.

Within the Dover Chalk Rock high fracture water concentrations are observed but the matrix porewater chloride concentrations are lower. This suggests relatively high groundwater velocities, supporting rapid groundwater flow and solute transport which reduces the time available for diffusive exchange through this stratum, coupled with a larger block size means that there has not been enough time for diffusive equilibrium between the two domains to occur.

Below the Dover Chalk Rock level it is observed that the difference between fracture and porewater chloride concentrations is even greater and this is again a reflection of the decreasing frequency of fractures and the resultant increase in block-size.

The diffusive exchange characteristics for the Tilmanstone-Eastry valley at different depths within the aquifer are noted on Figure 5-29 in the grey boxes and listed here:

Seaford Chalk

Small block size results in a relatively short time necessary for diffusive equilibrium with a range of approximately 100 to 5000 days.

Dover Chalk Rock

Faster groundwater velocities reduce the time available for solutes to diffuse into the matrix porewater and hence observed solute concentrations are higher than for slower velocity media at the same distance.

Lewes Nodular Chalk (at depth)

Larger block sizes (calculated through the fracture-density relationship (Section 5.2.2) coupled with low hydraulic conductivity and low velocities allow for solute attenuation through diffusive exchange. At this depth within the aquifer, solute movement is dominated by diffusion and the time for diffusive equilibrium is approximately 788 years.

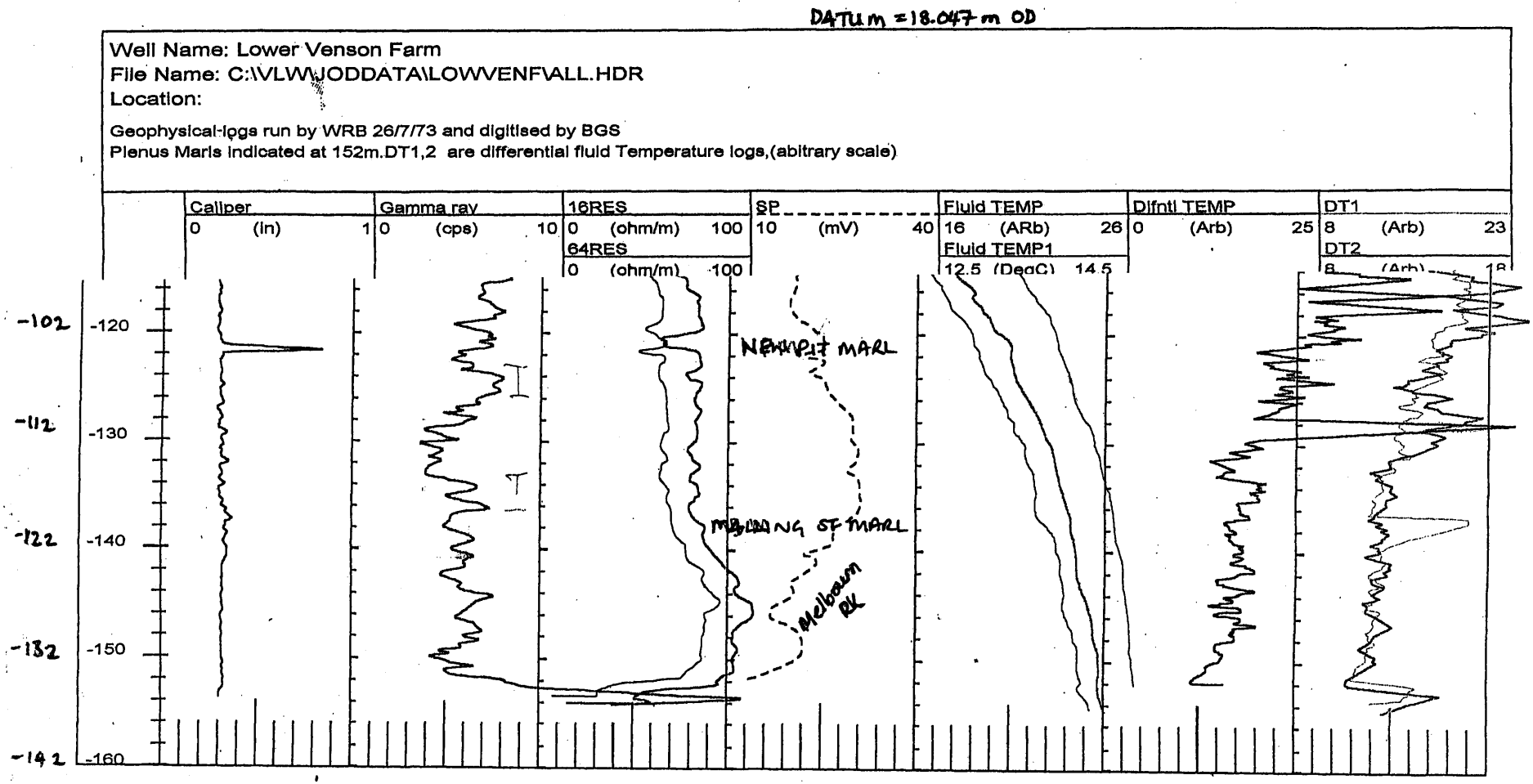

ig for BH2 (1973) indicating lithostratigraphy.

DATUM = 18.047 m OD

Well Name: Lower Venson Farm
File Name: C:\VLW\JODDATA\LOWVENF\ALL.HDR
Location:

Geophysical logs run by WRB 26/7/73 and digitised by BGS
Plenus Marls indicated at 152m.DT1,2 are differential fluid Temperature logs,(abitrary scale)

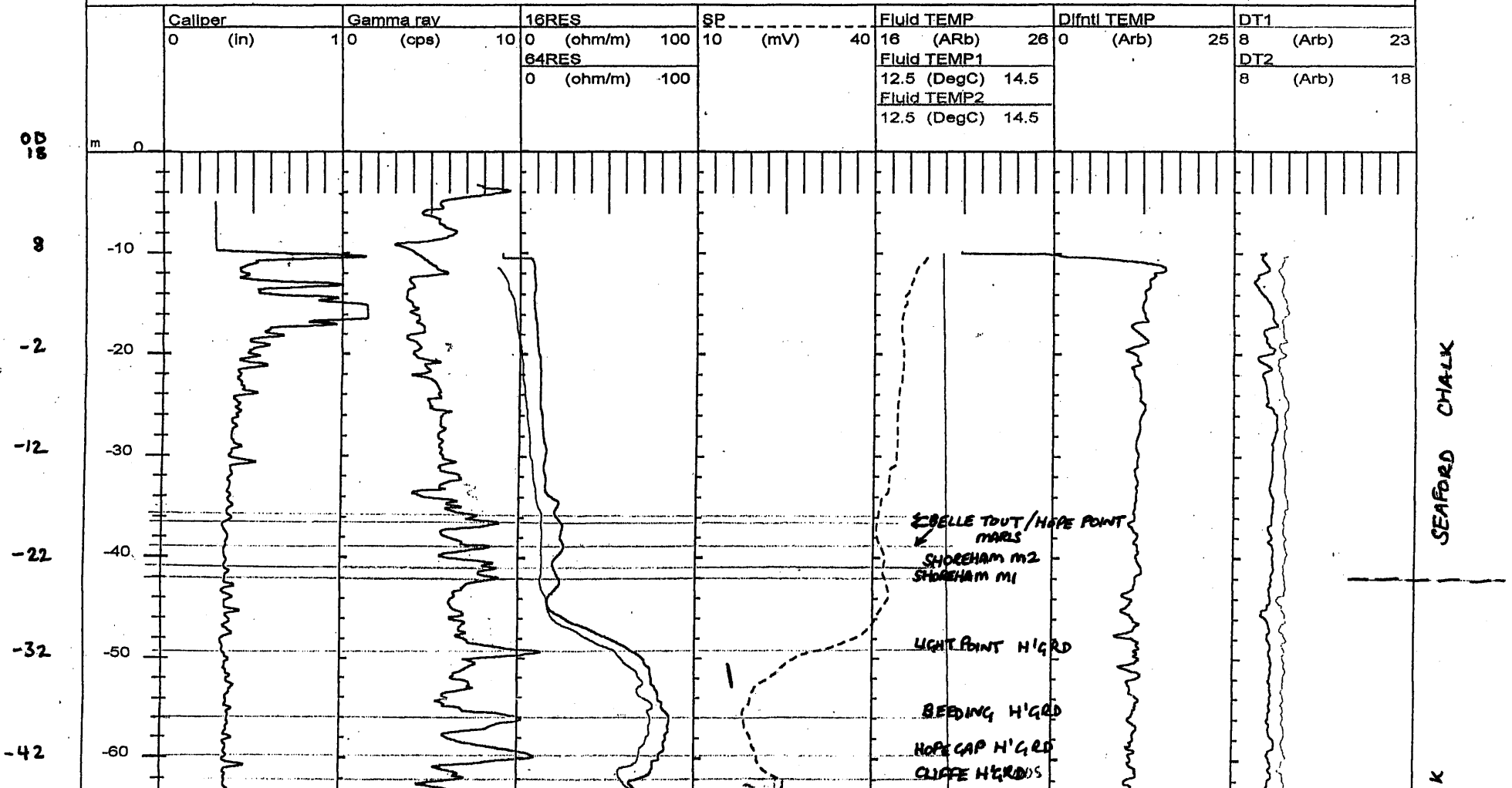

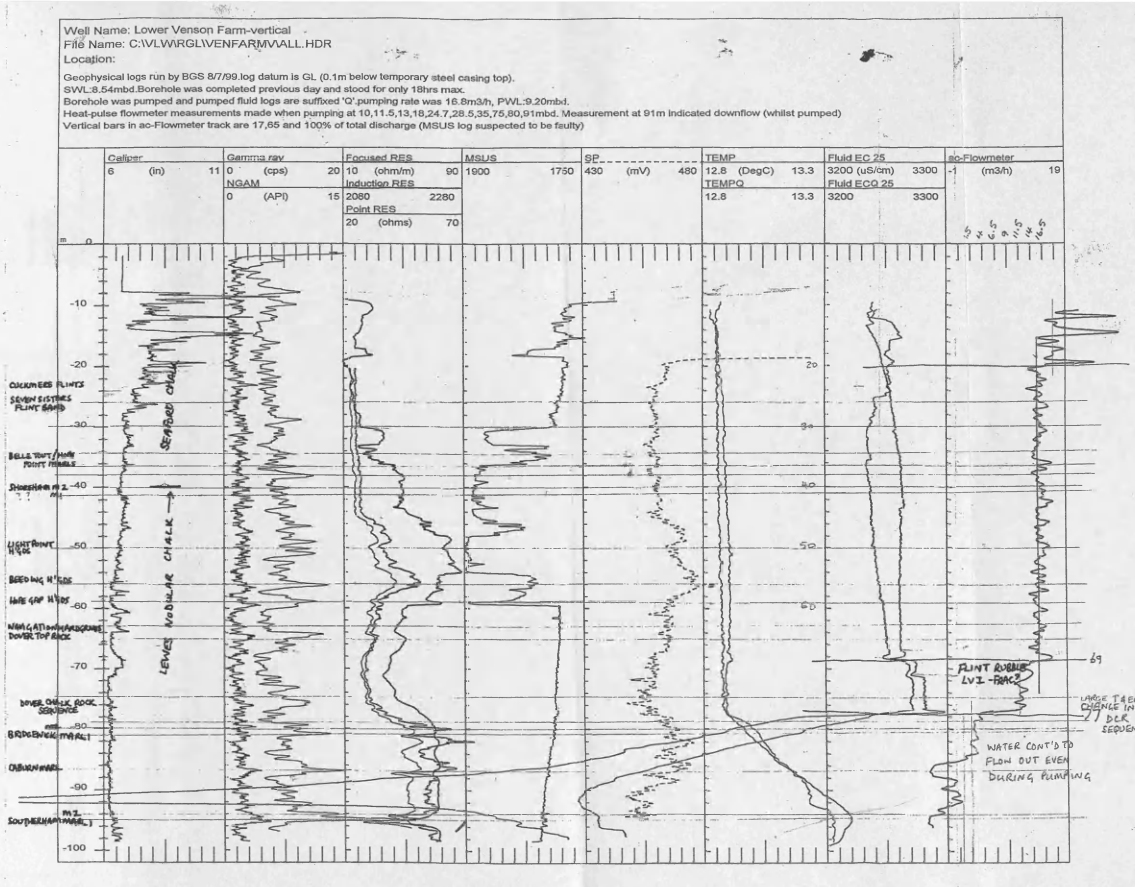

Figure 5-2 Annotated geophysical log for BGS LVV (1999) indicating lithostratigraphy.

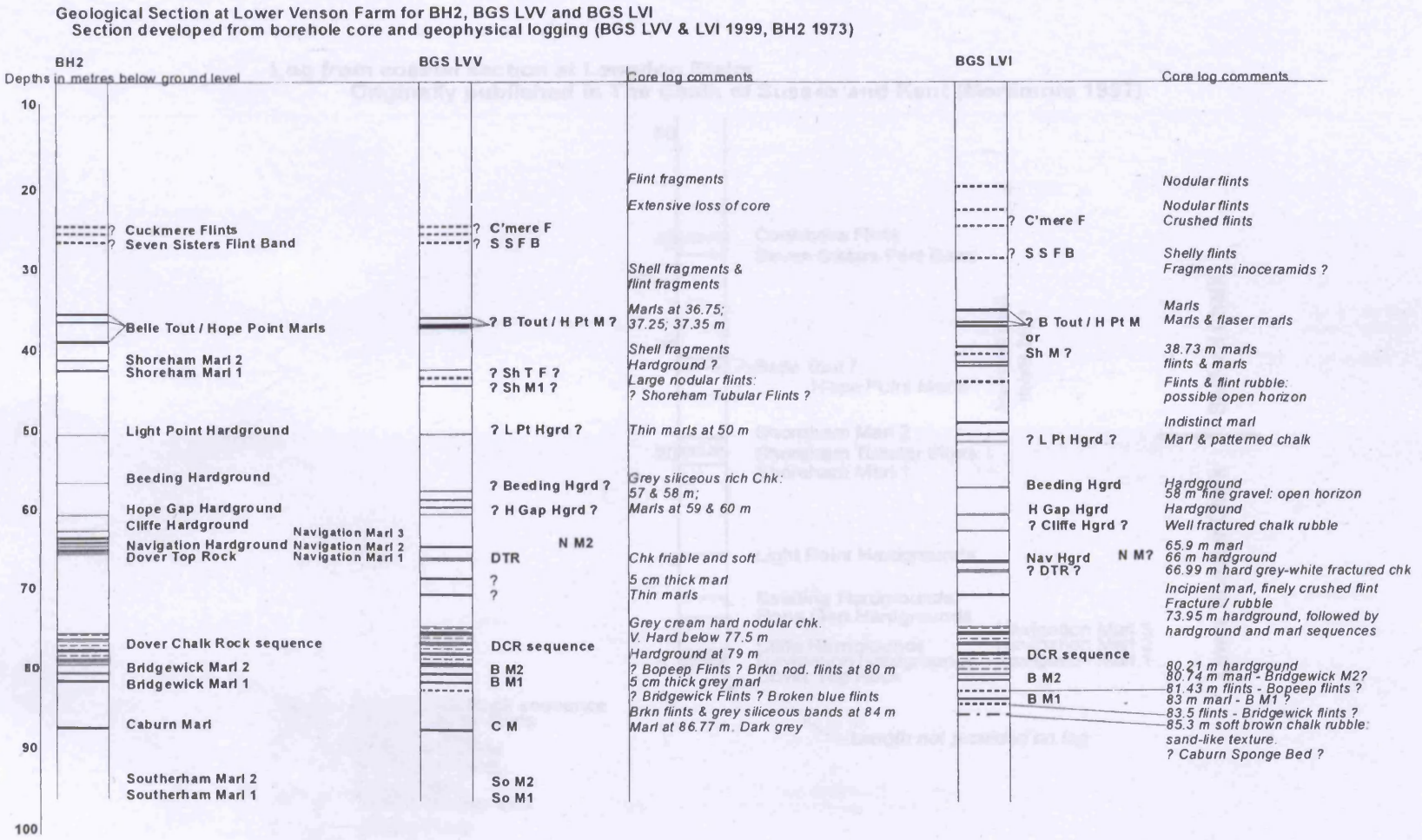

Figure 5-3 Lithological interpretation at Lower Venson Farm.

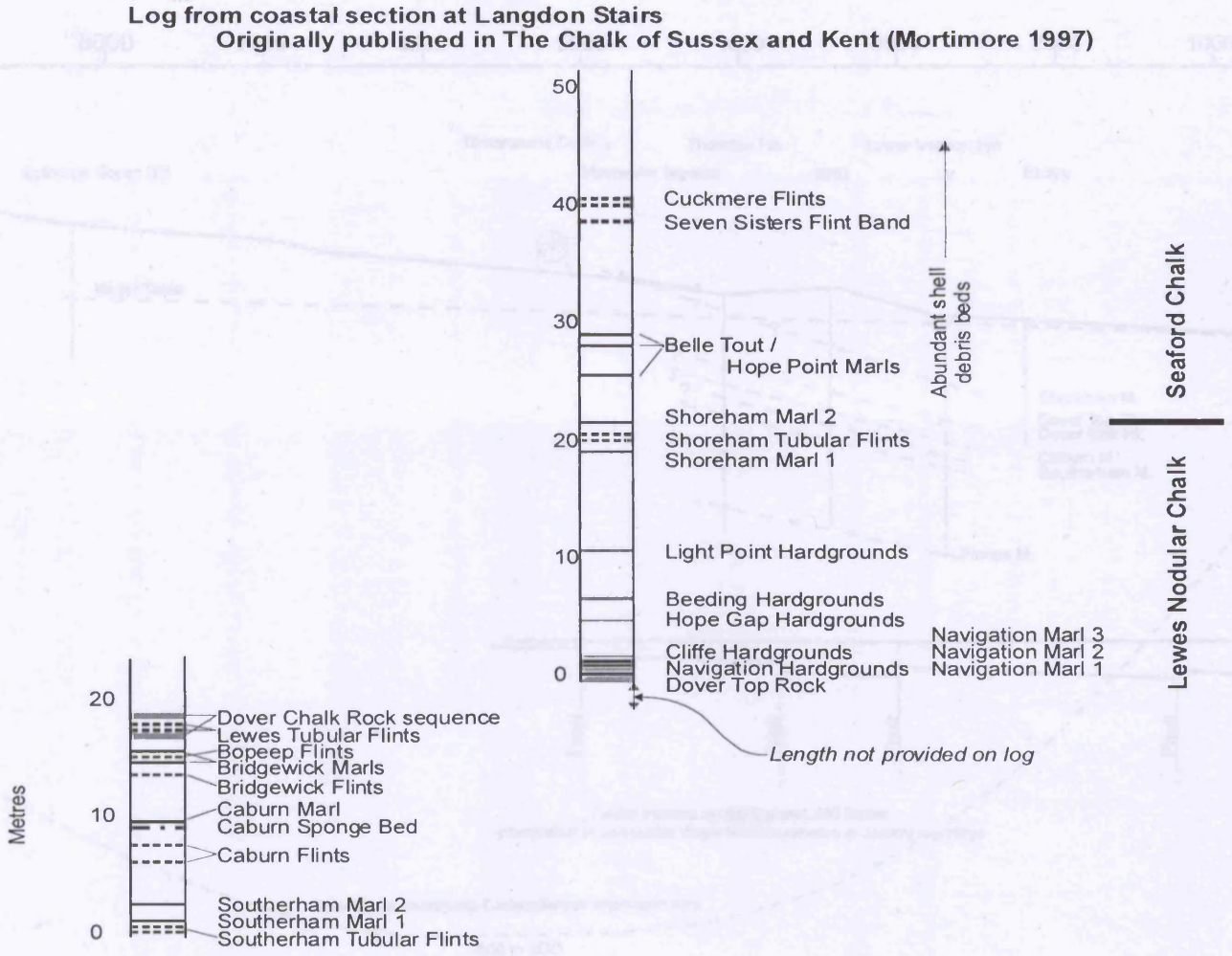

Figure 5-4 Geological log for Langdon Stairs coastal section (*after* Mortimore 1997).

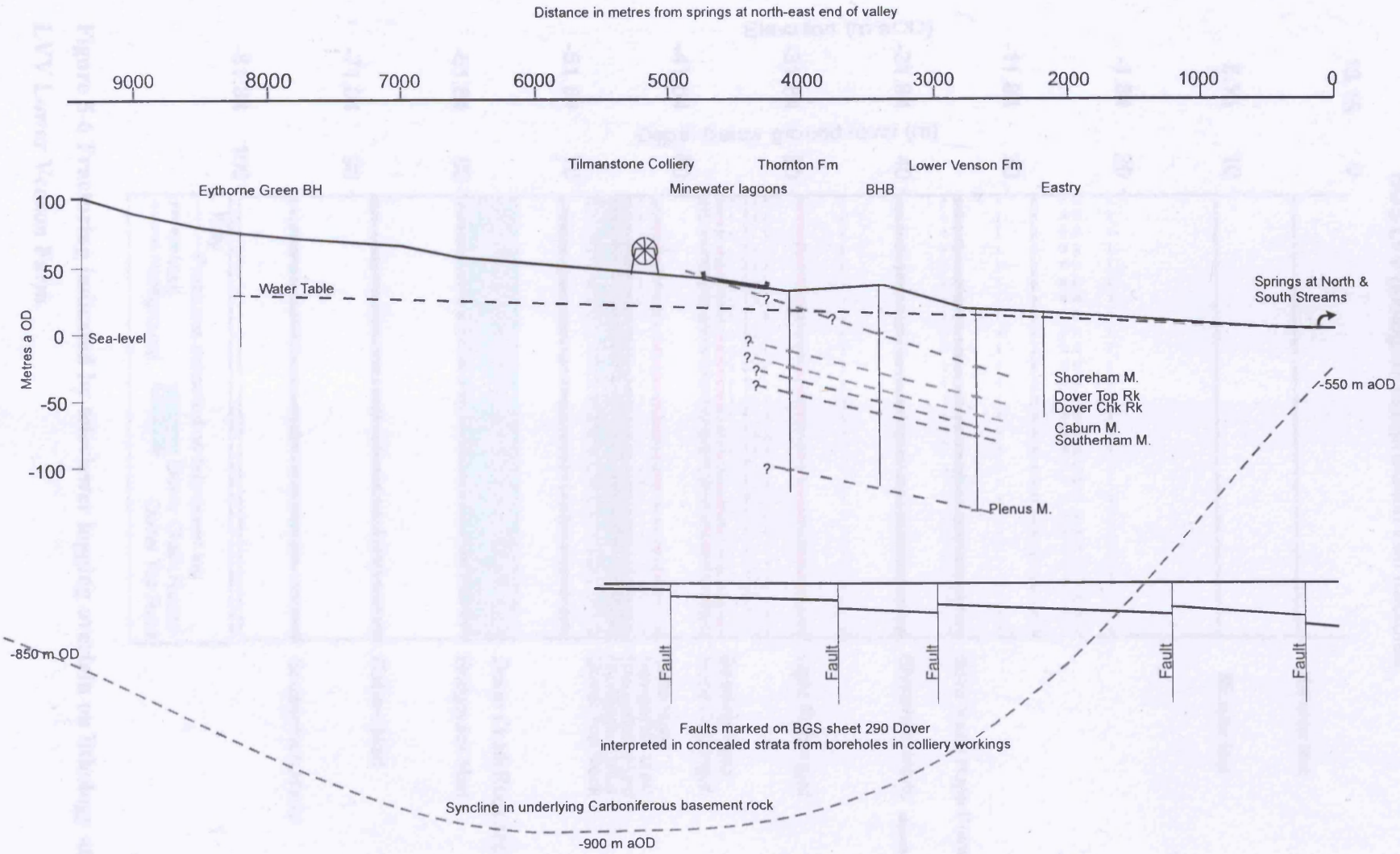

Figure 5-5 Tilmanstone - Eastry valley geological interpretation cross-section.

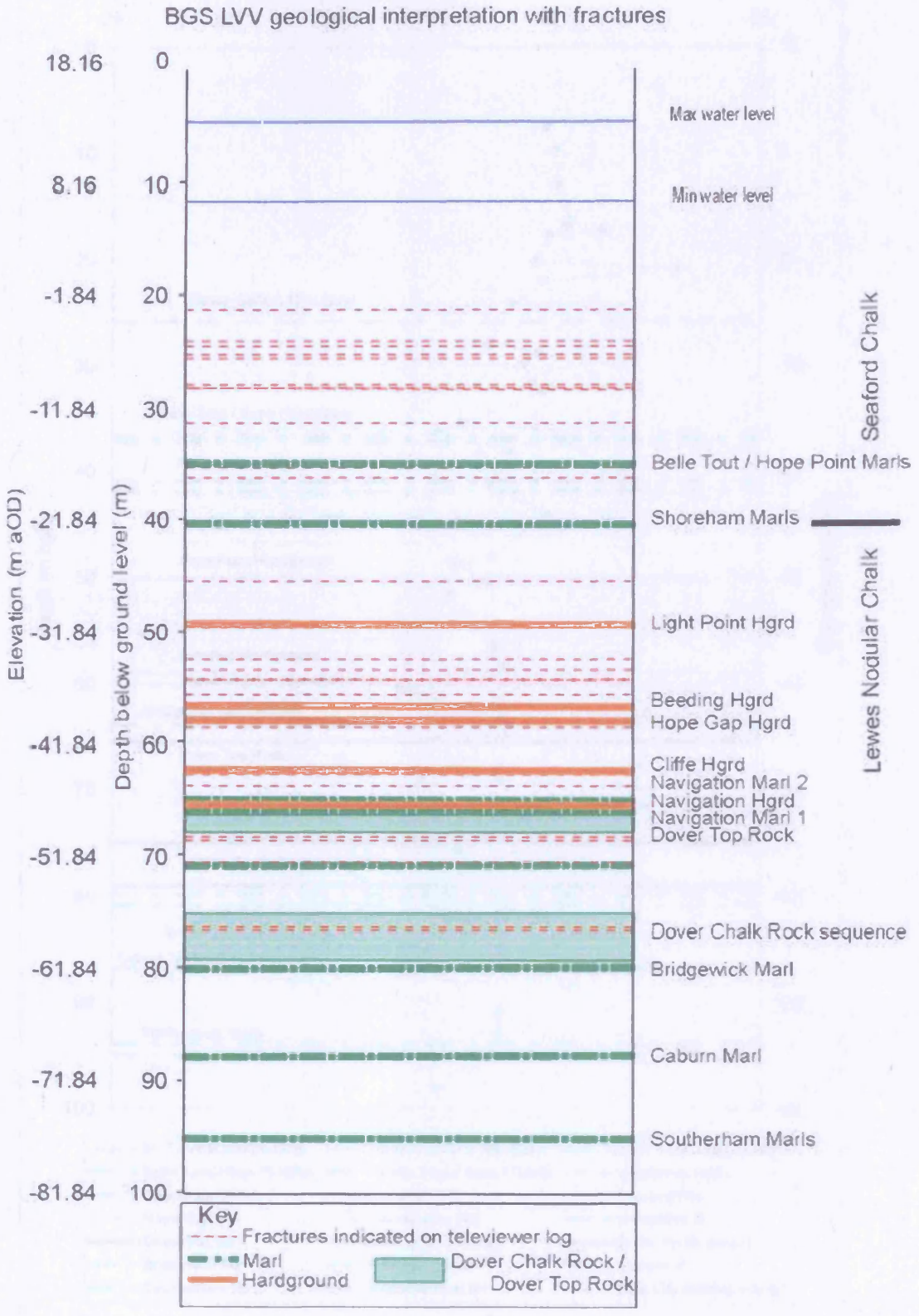

Figure 5-6 Fracturing indicated by televiewer logging overlain on lithology at BGS LVV Lower Venson Farm.

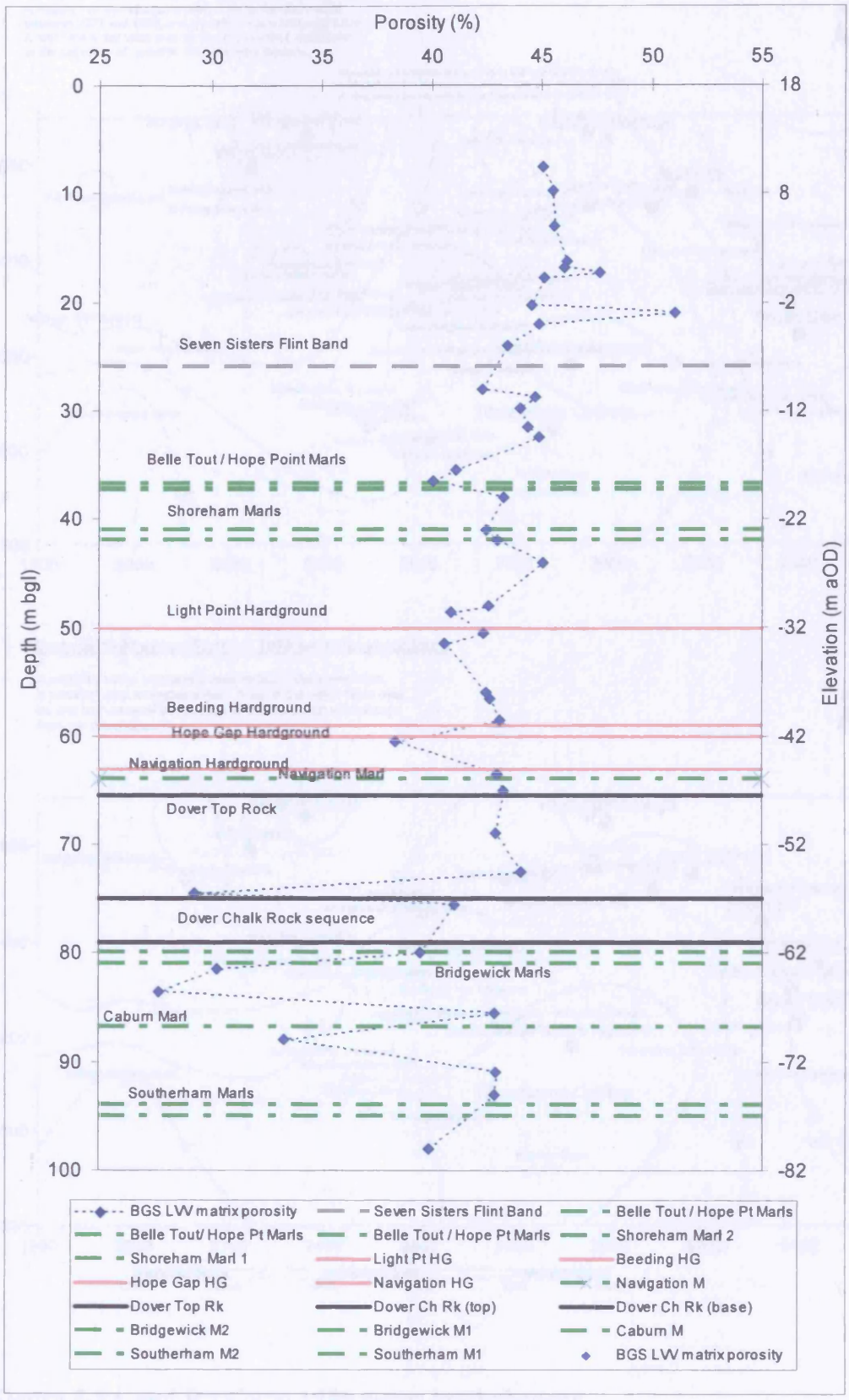

Figure 5-7 Combined geology and matrix porosity profile for BGS LVV.

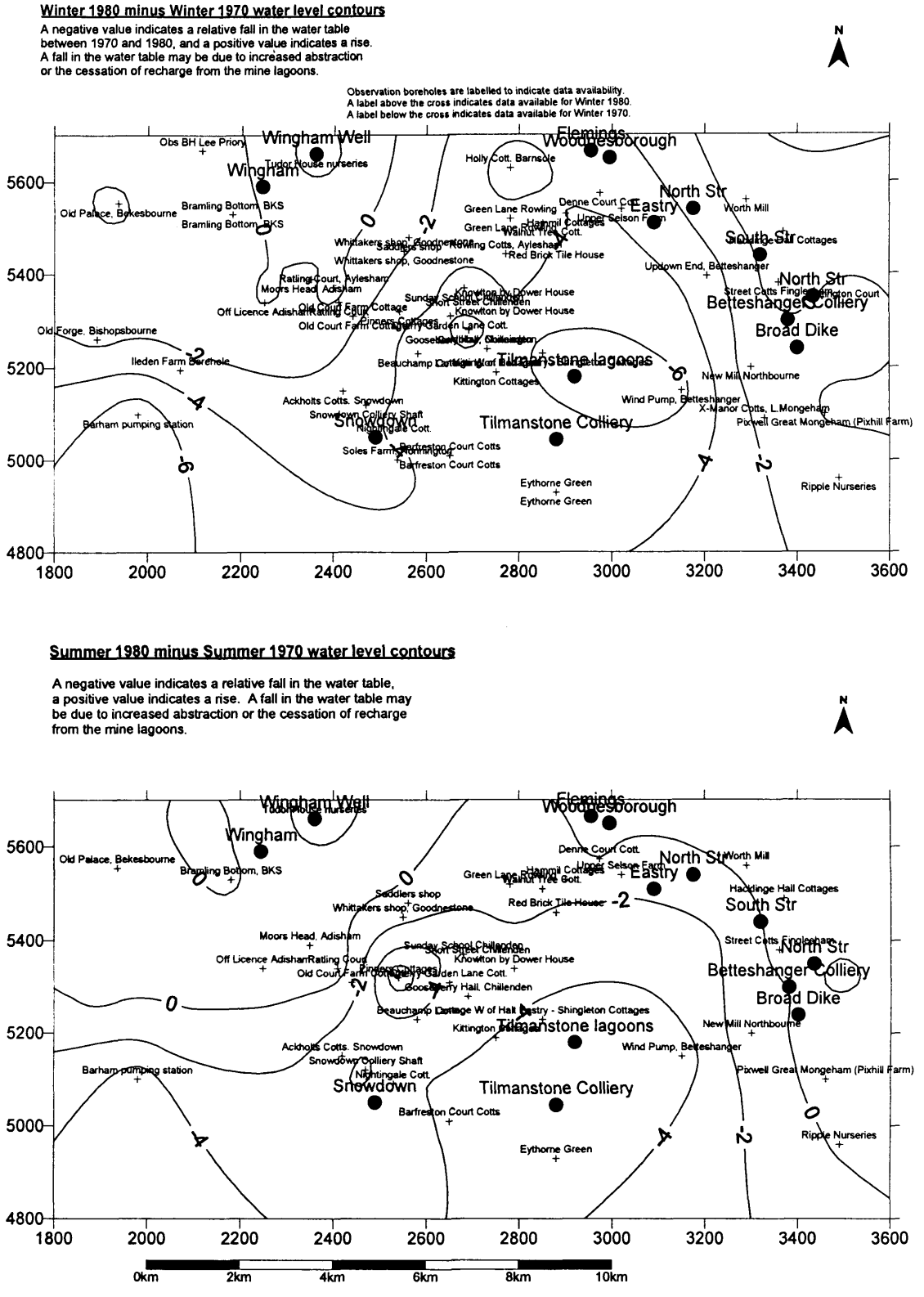

Figure 5-8A and B 1970 to 1980 water level changes.

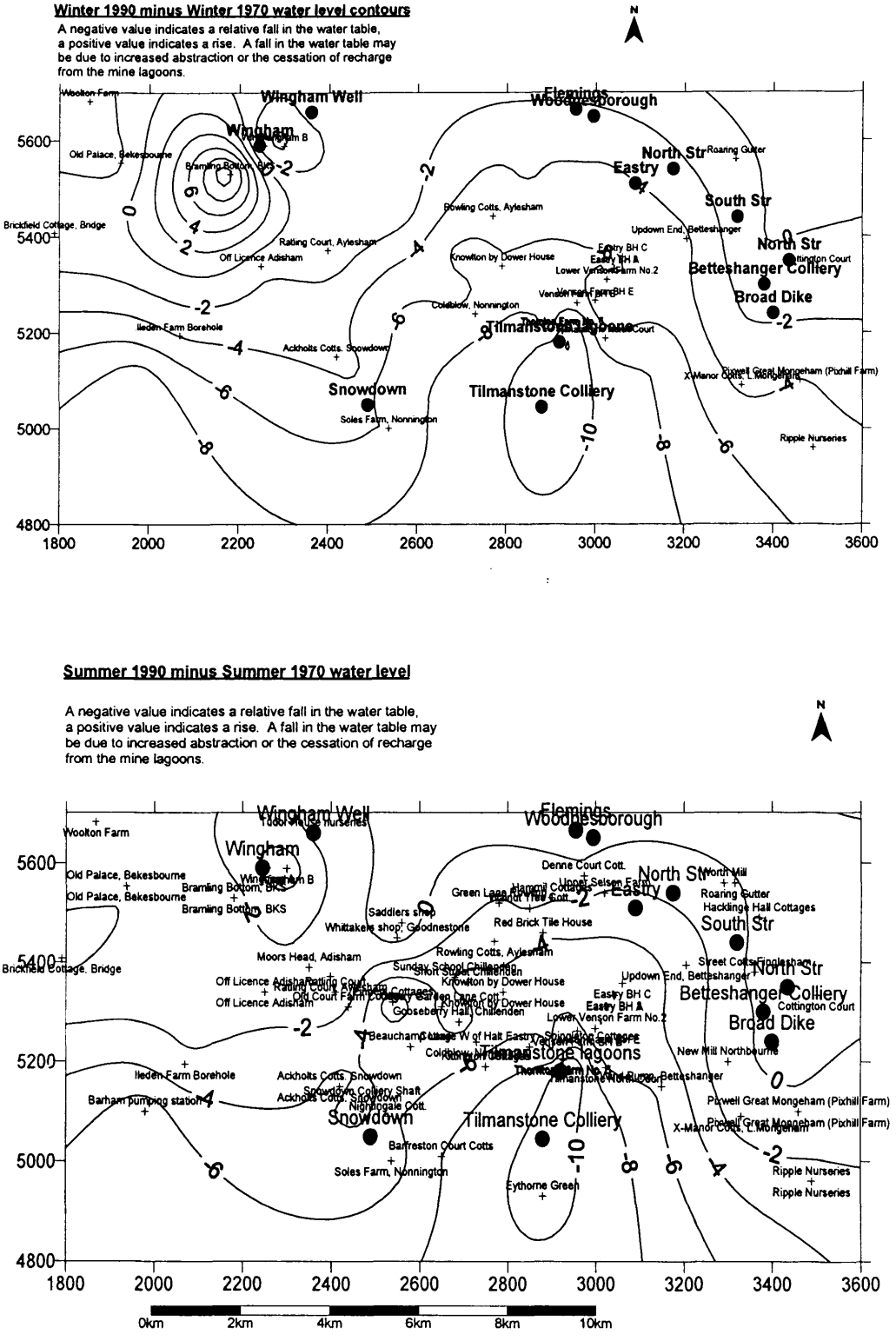

Figure 5-9A and B 1970 to 1990 water level changes.

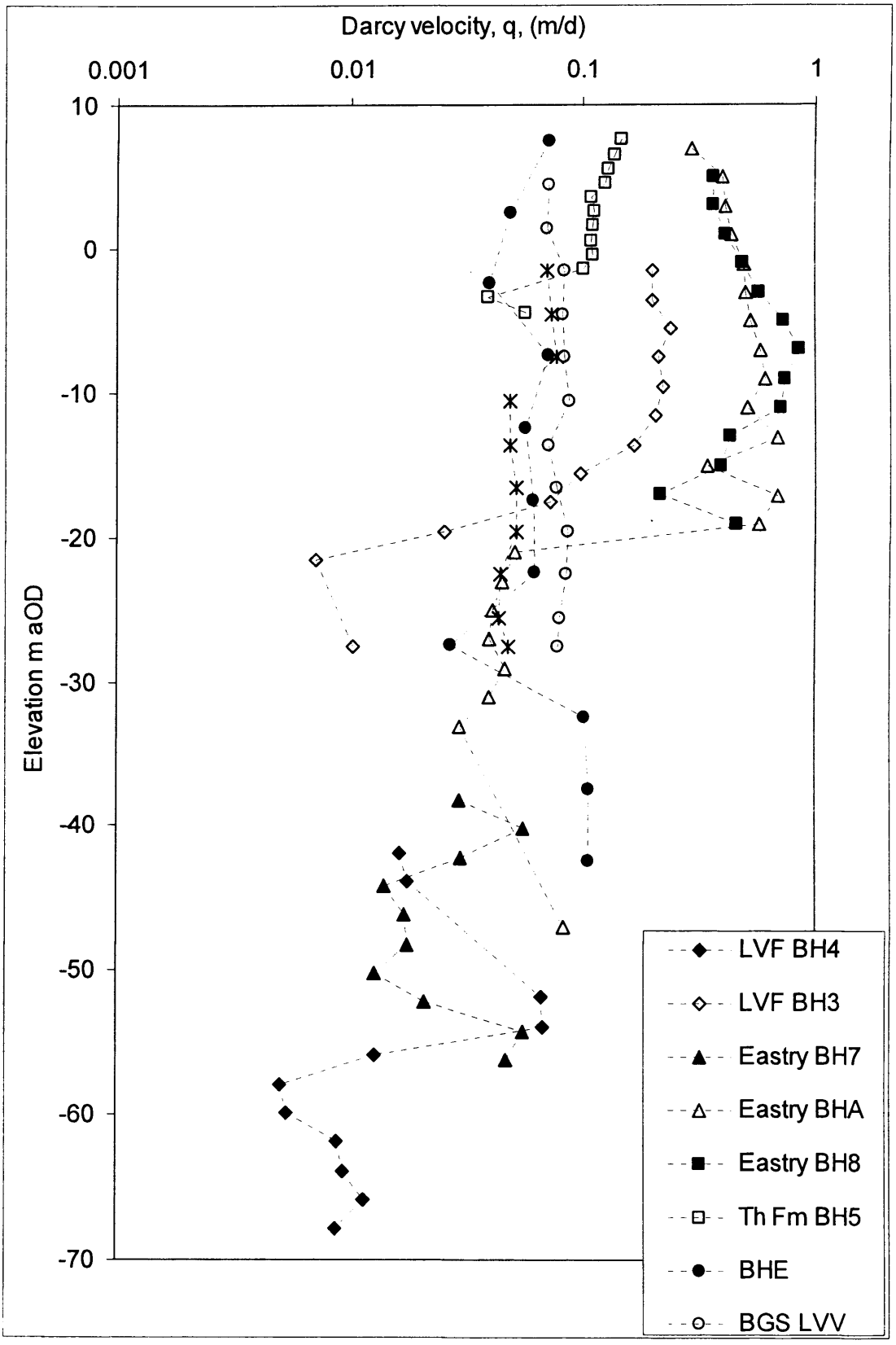

Figure 5-10 Summary of Darcy velocity results for single borehole dilution tests.

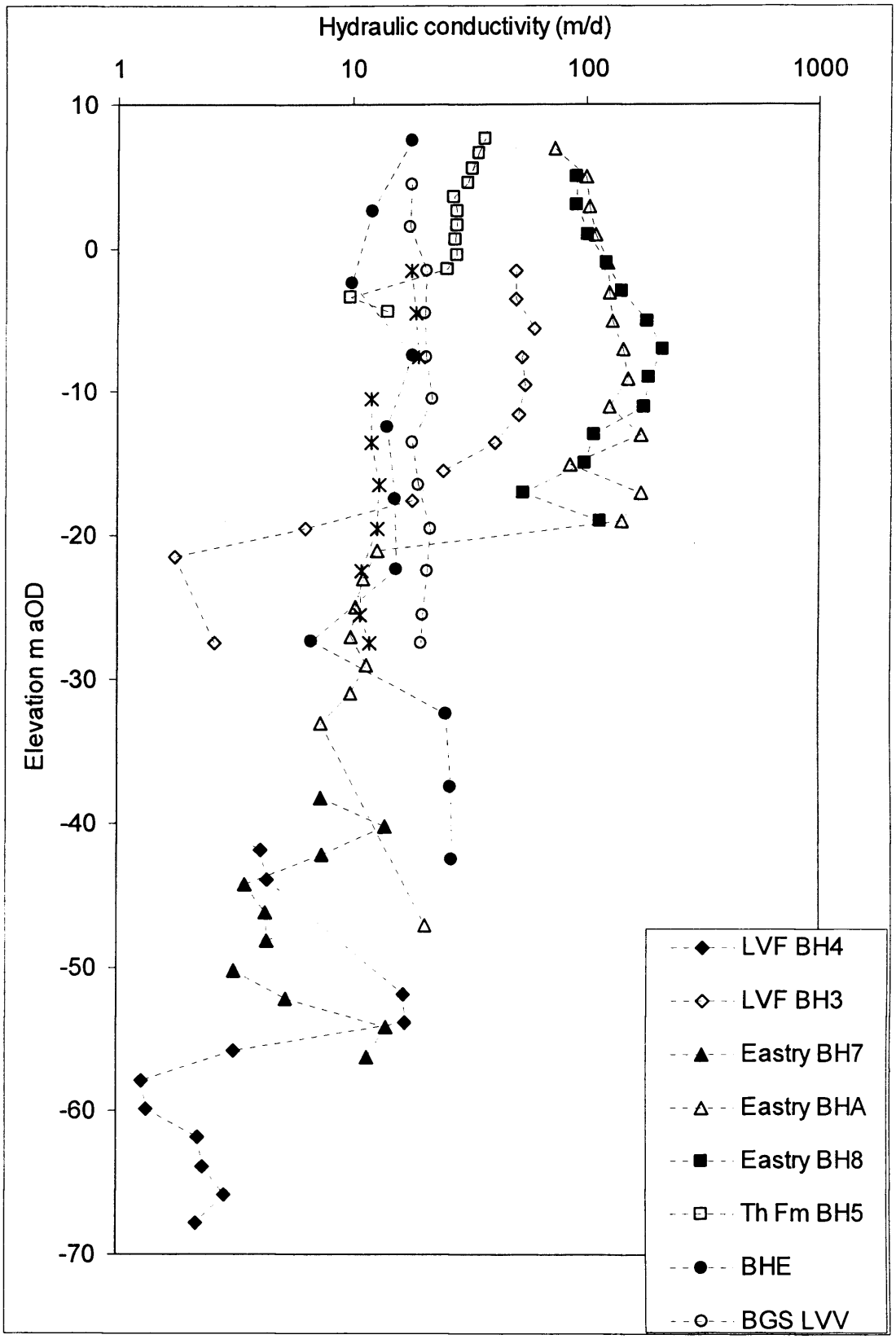

Figure 5-11 Summary of hydraulic conductivity from single borehole dilution tests for Tilmanstone - Eastry valley.

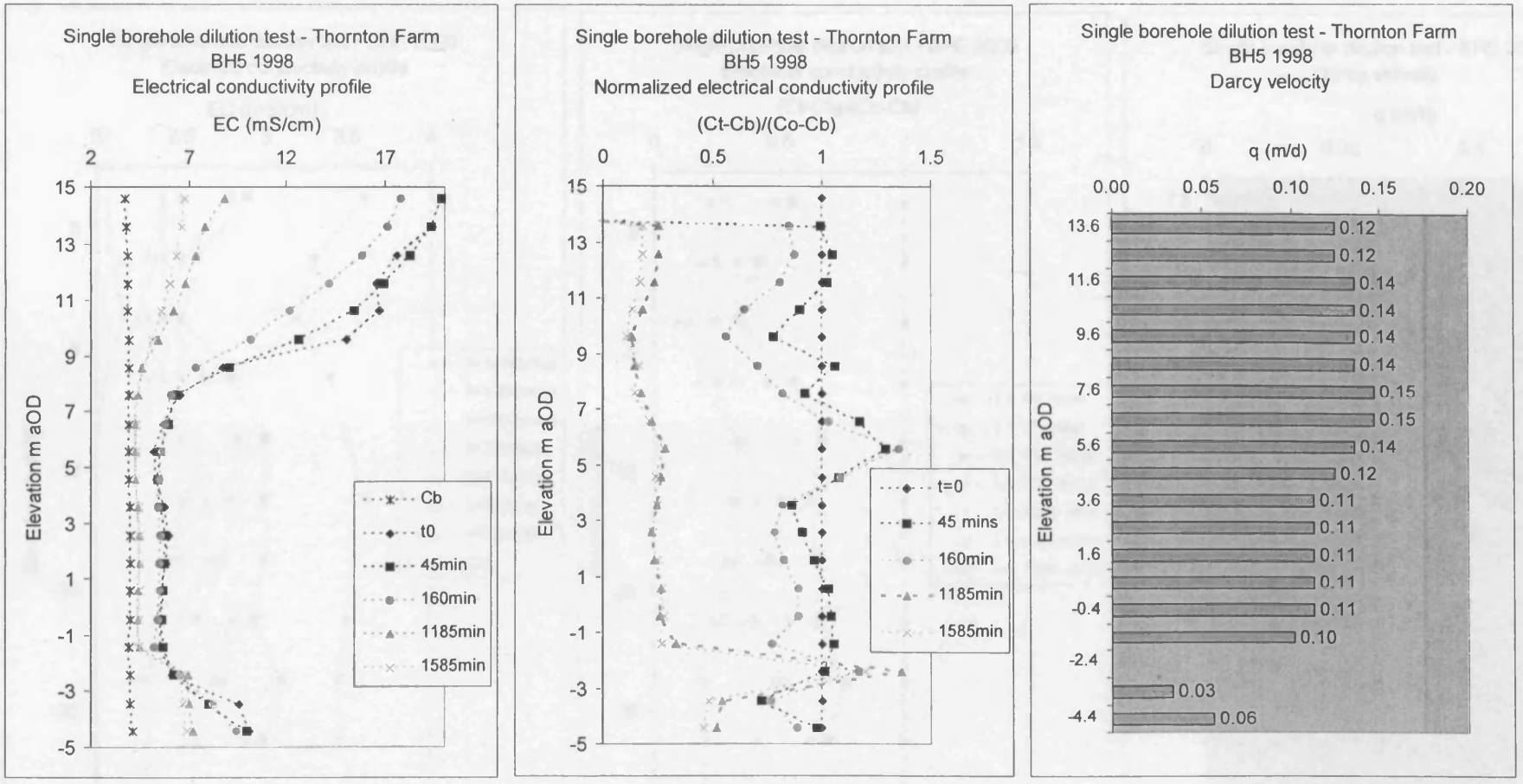

Figure 5-12 Thornton Farm single borehole dilution test results and analysis.

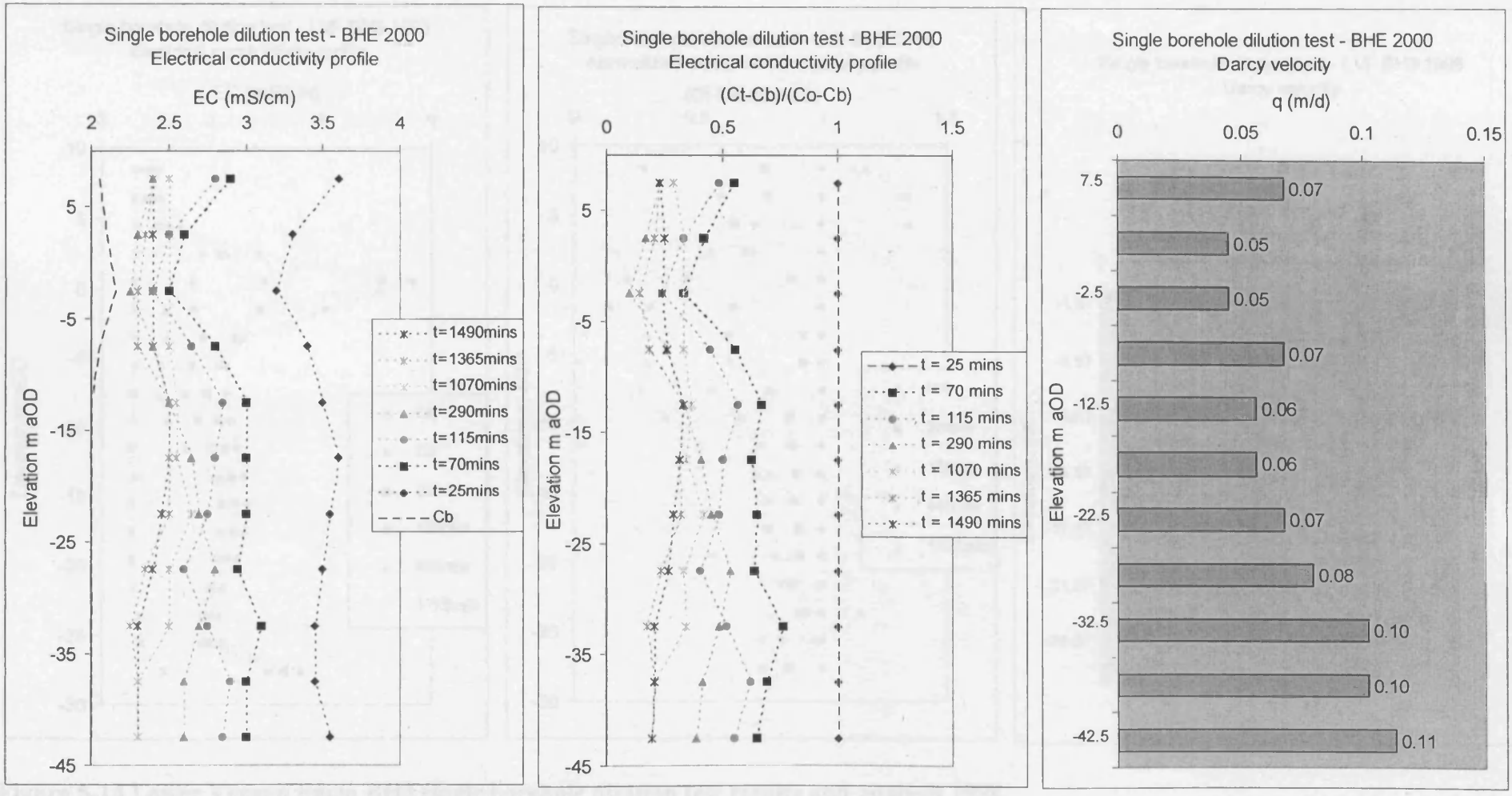

Figure 5-13 Venson Farm BHE single borehole dilution test results and analysis.

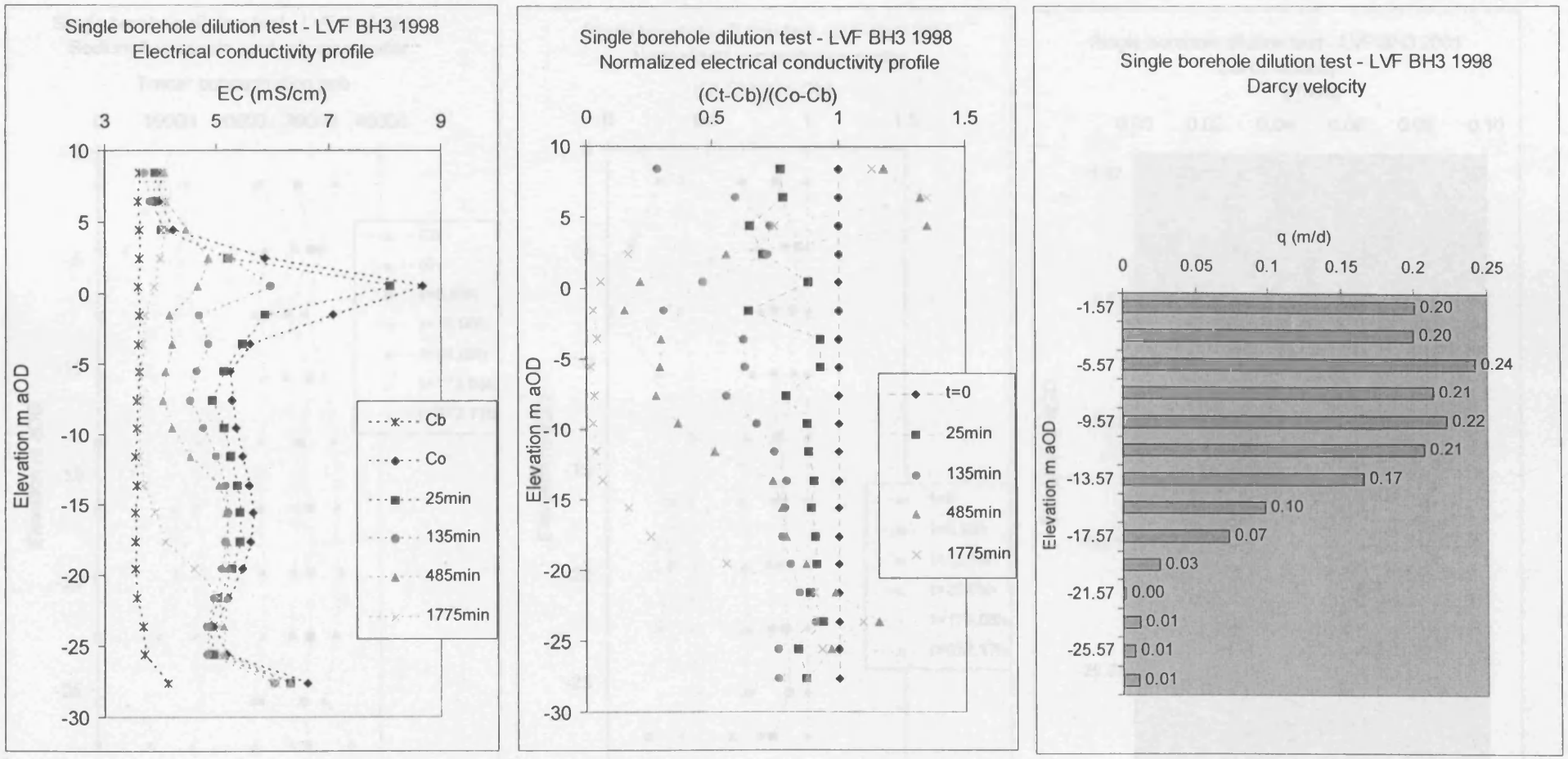

Figure 5-14 Lower Venson Farm BH3 single borehole dilution test results and analysis 1998.

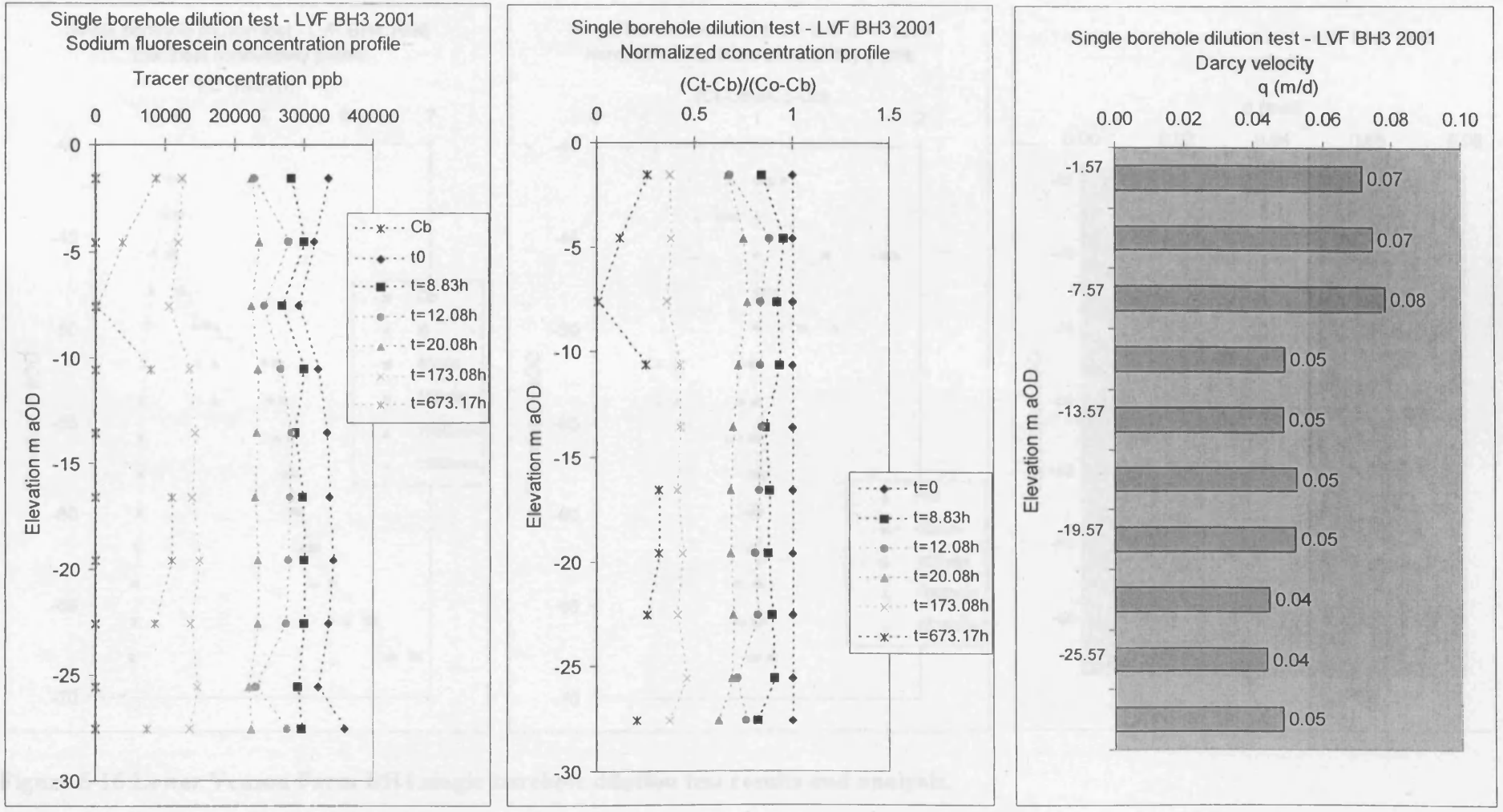

Figure 5-15 Single borehole dilution test results and analysis at Lower Venson Farm BH3 2001.

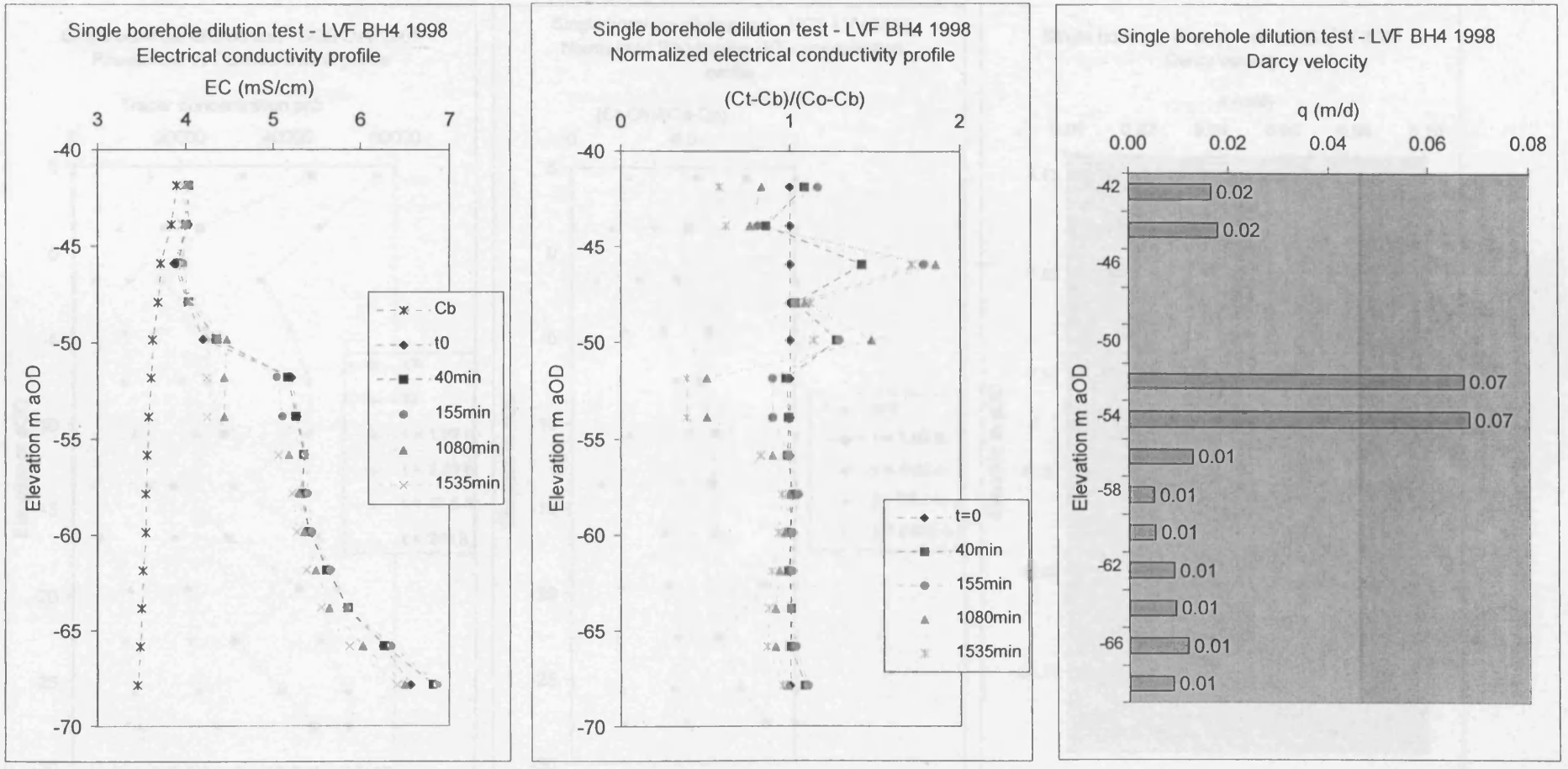

Figure 5-16 Lower Venson Farm BH4 single borehole dilution test results and analysis.

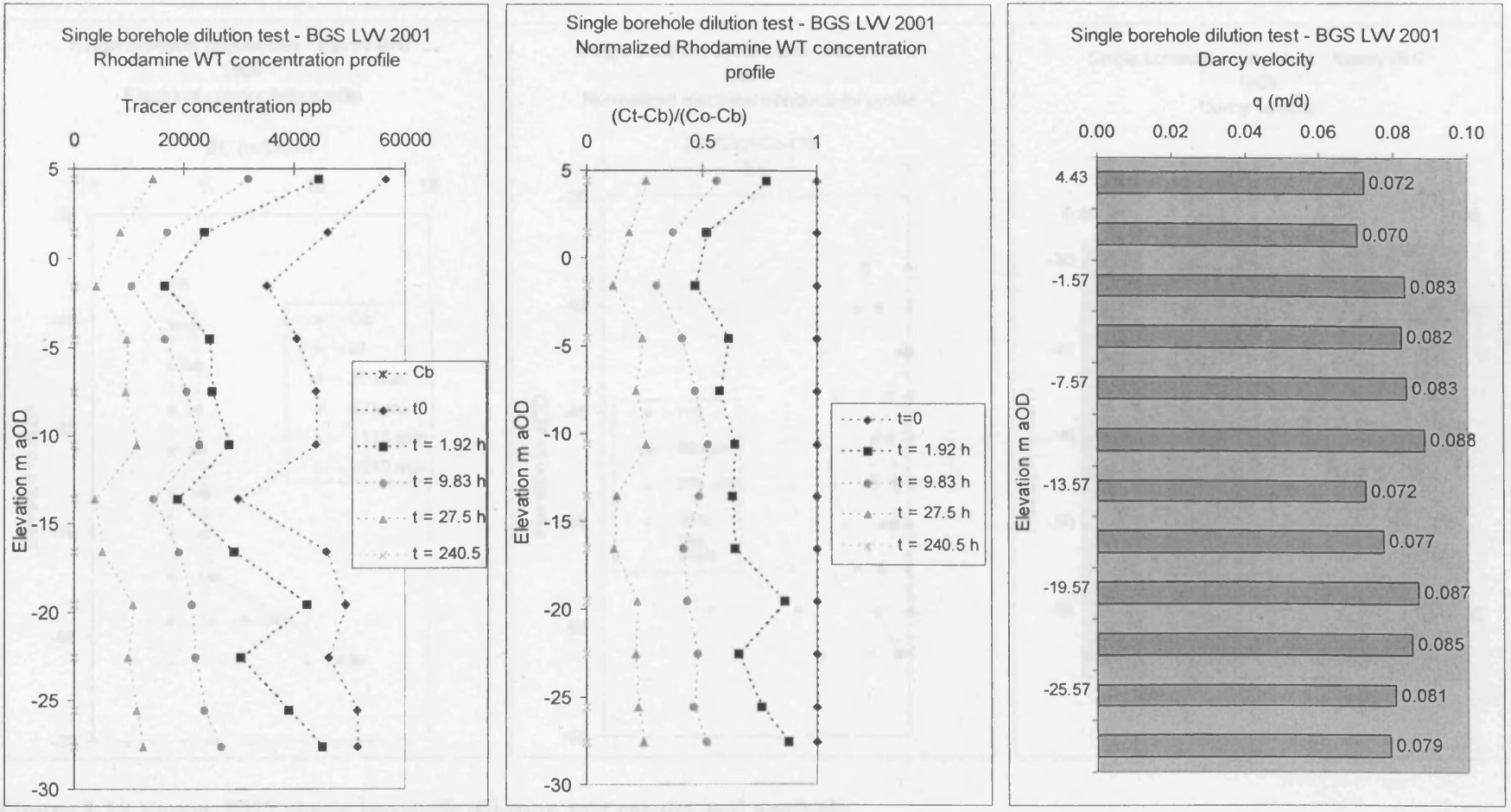

Figure 5-17 Single borehole dilution test results and analysis Lower Venson Farm BGS LVV.

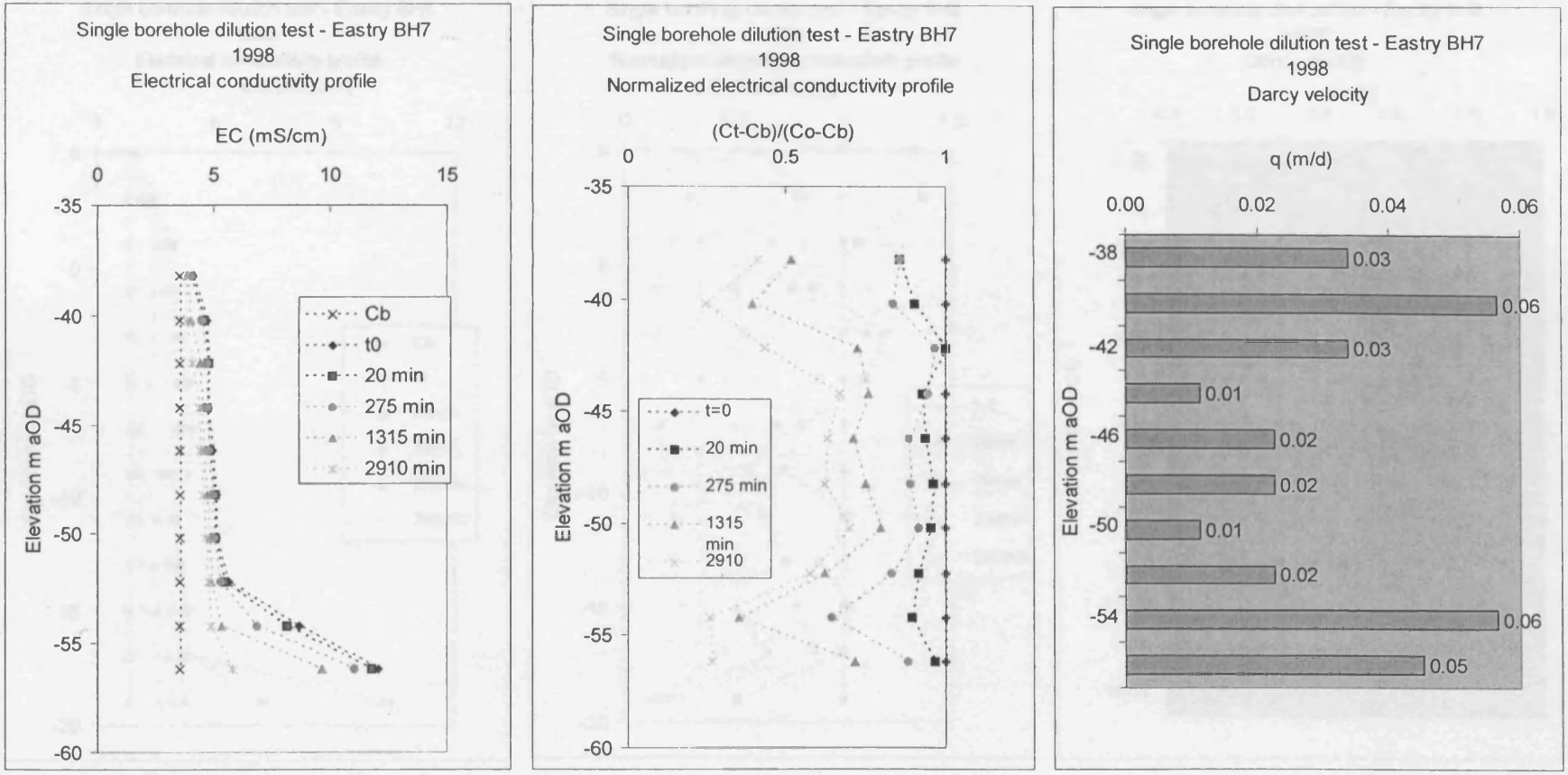

Figure 5-18 Eastry BH7 single borehole dilution test results and analysis.

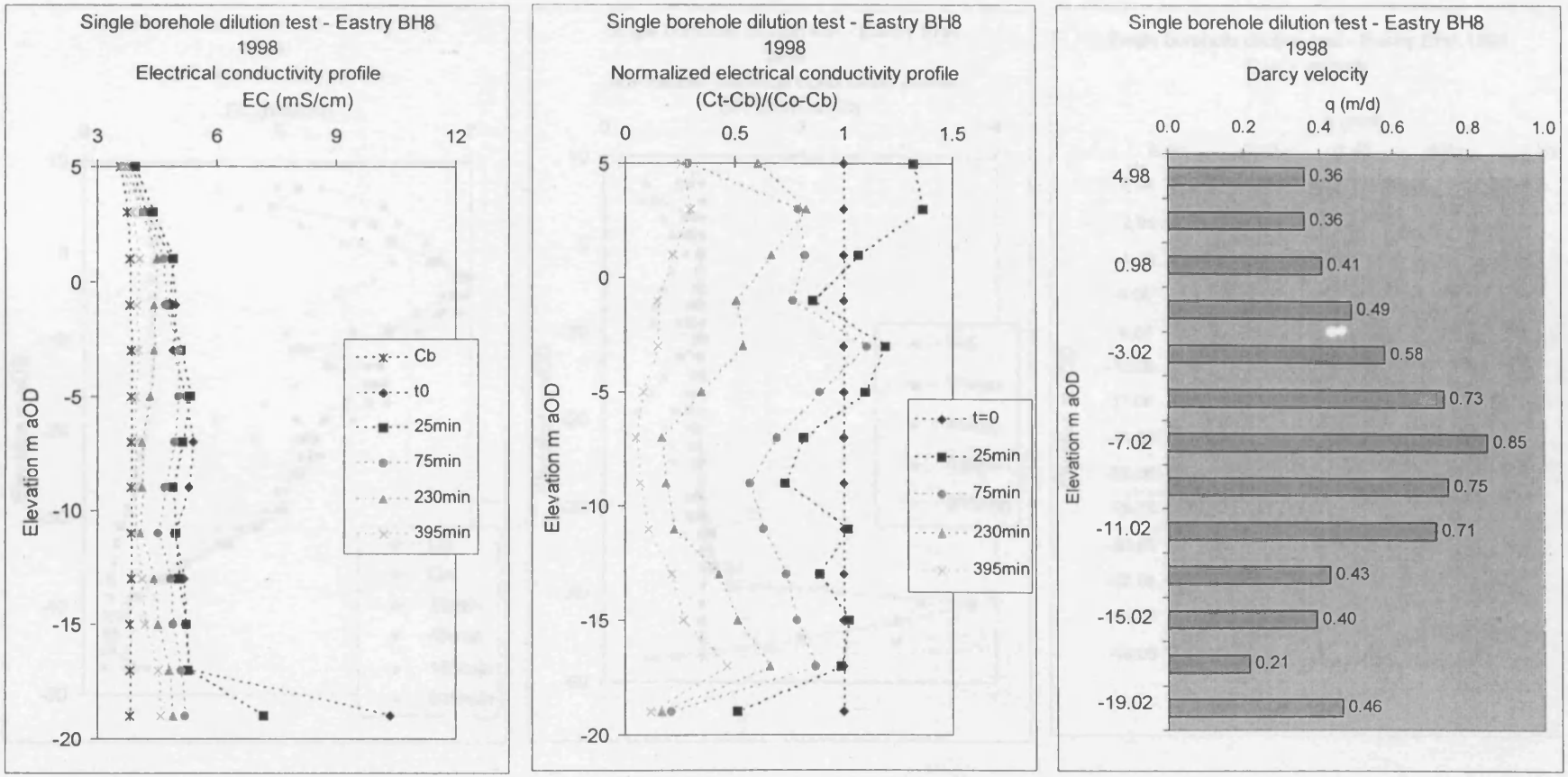

Figure 5-19 Eastry BH8 single borehole dilution test results and analysis.

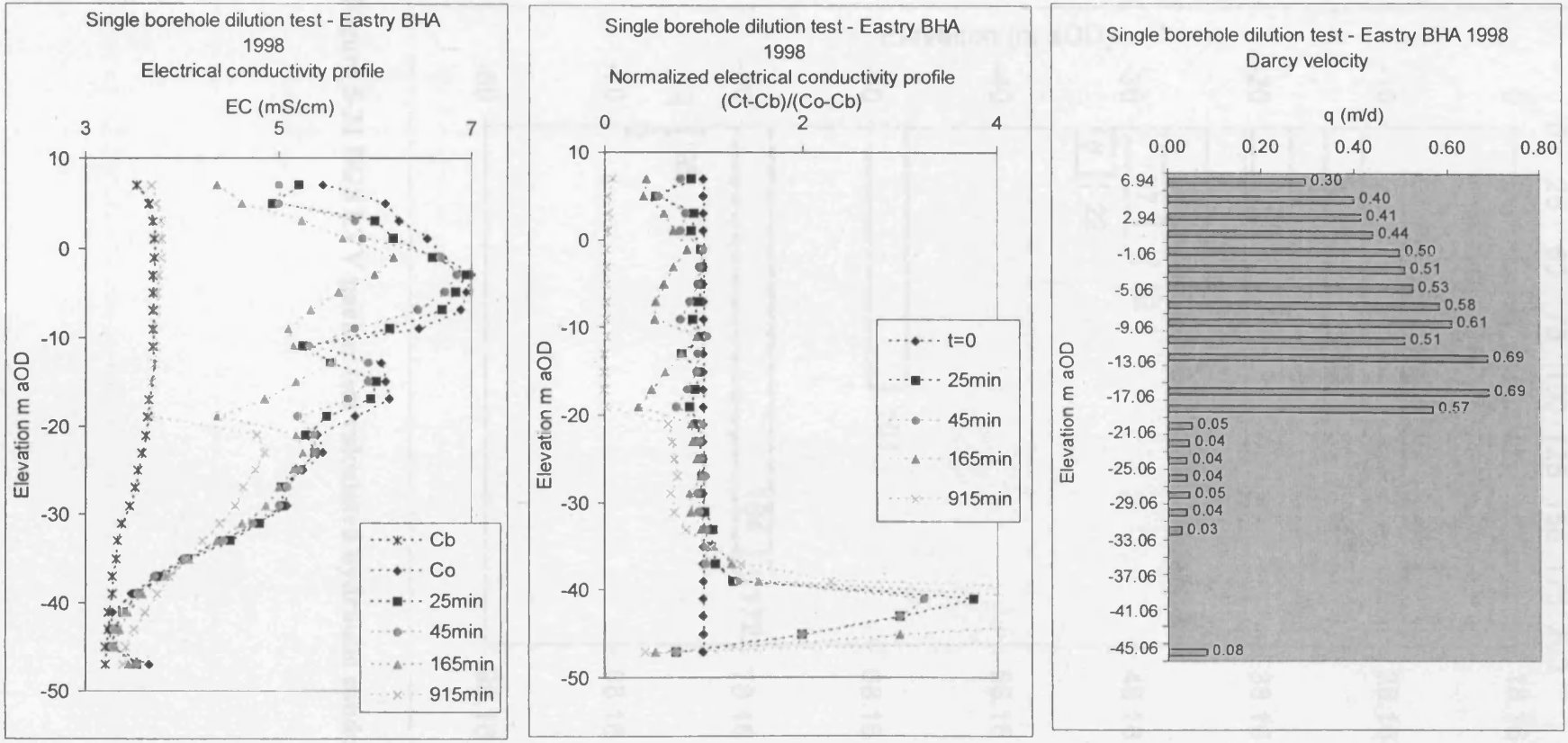

Figure 5-20 Eastry BHA single borehole dilution test results and analysis.

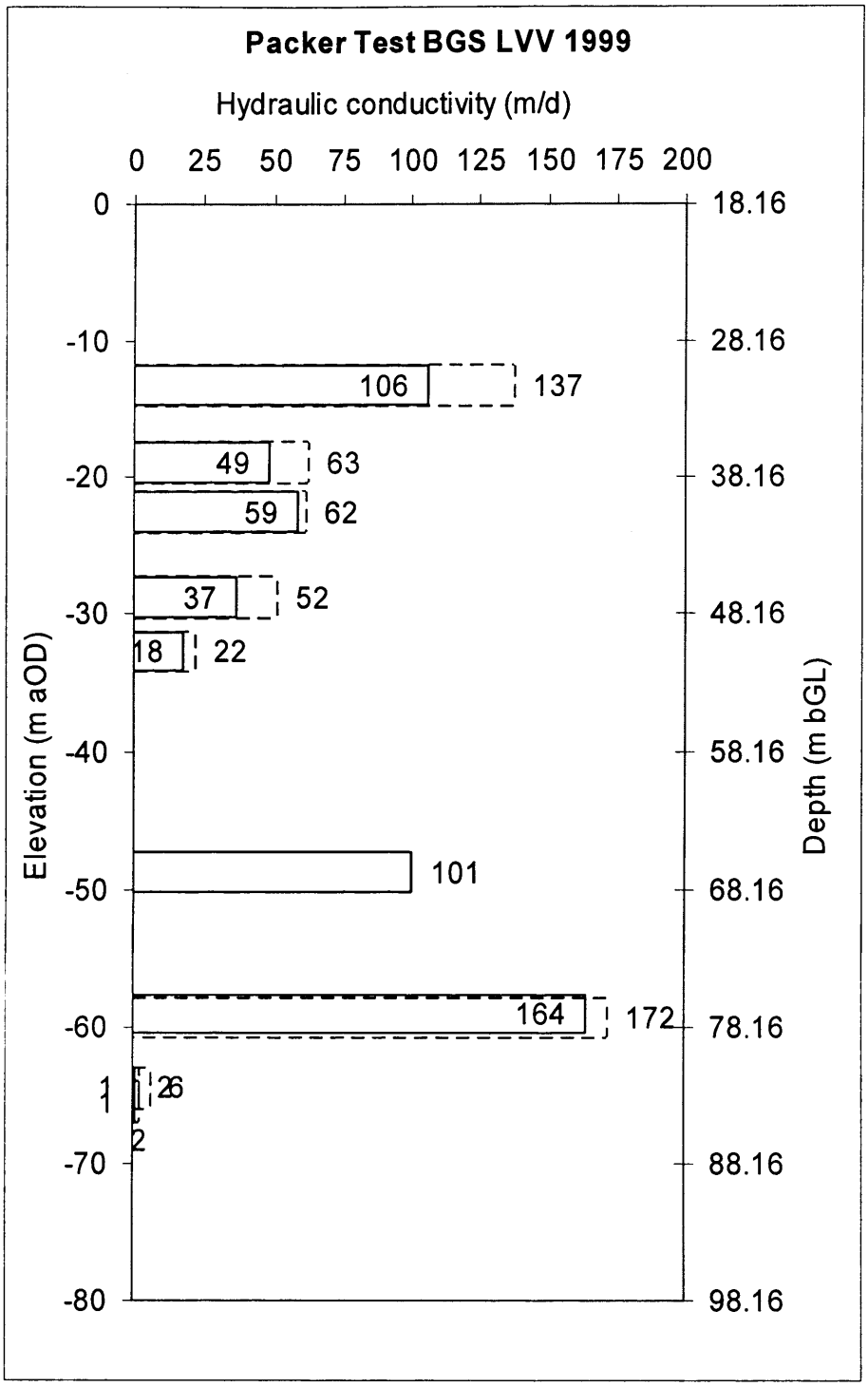

Figure 5-21 BGS LVV packer test calculated hydraulic conductivity values.

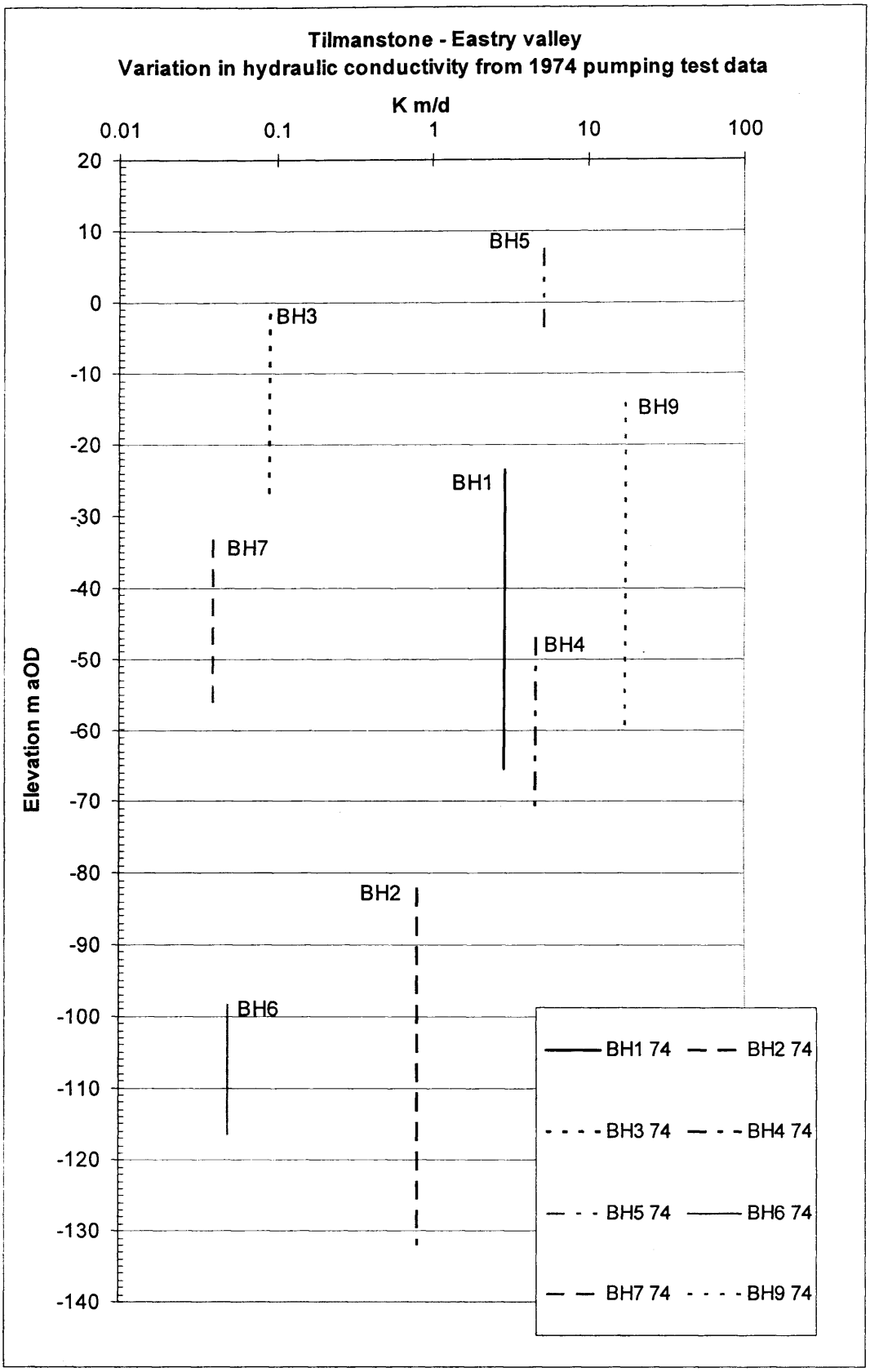

Figure 5-22 Hydraulic conductivity calculated from SWA (1976b) pumping tests.

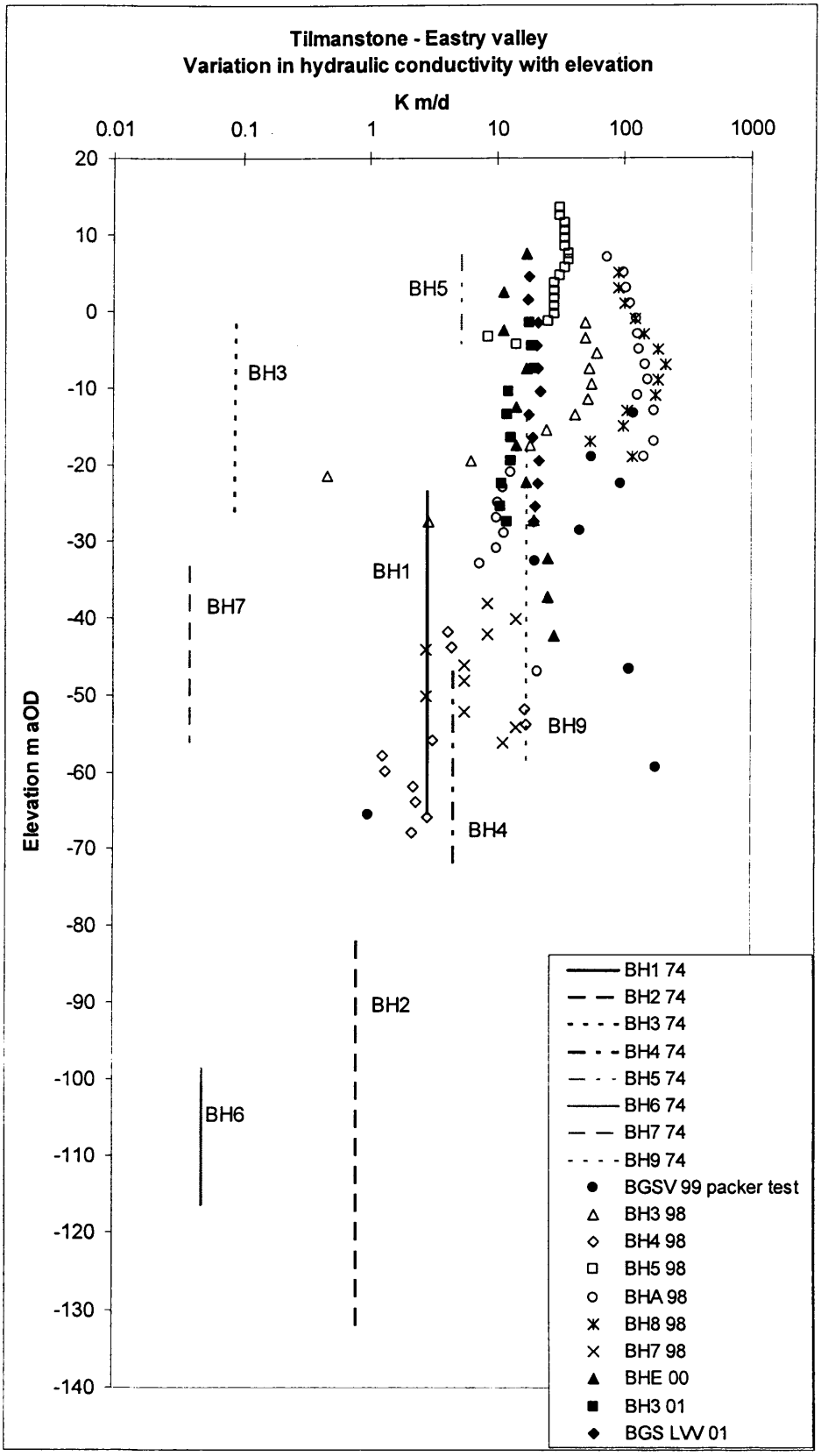

Figure 5-23 Combined plot of all hydraulic conductivity data for Tilmanstone - Eastry valley.

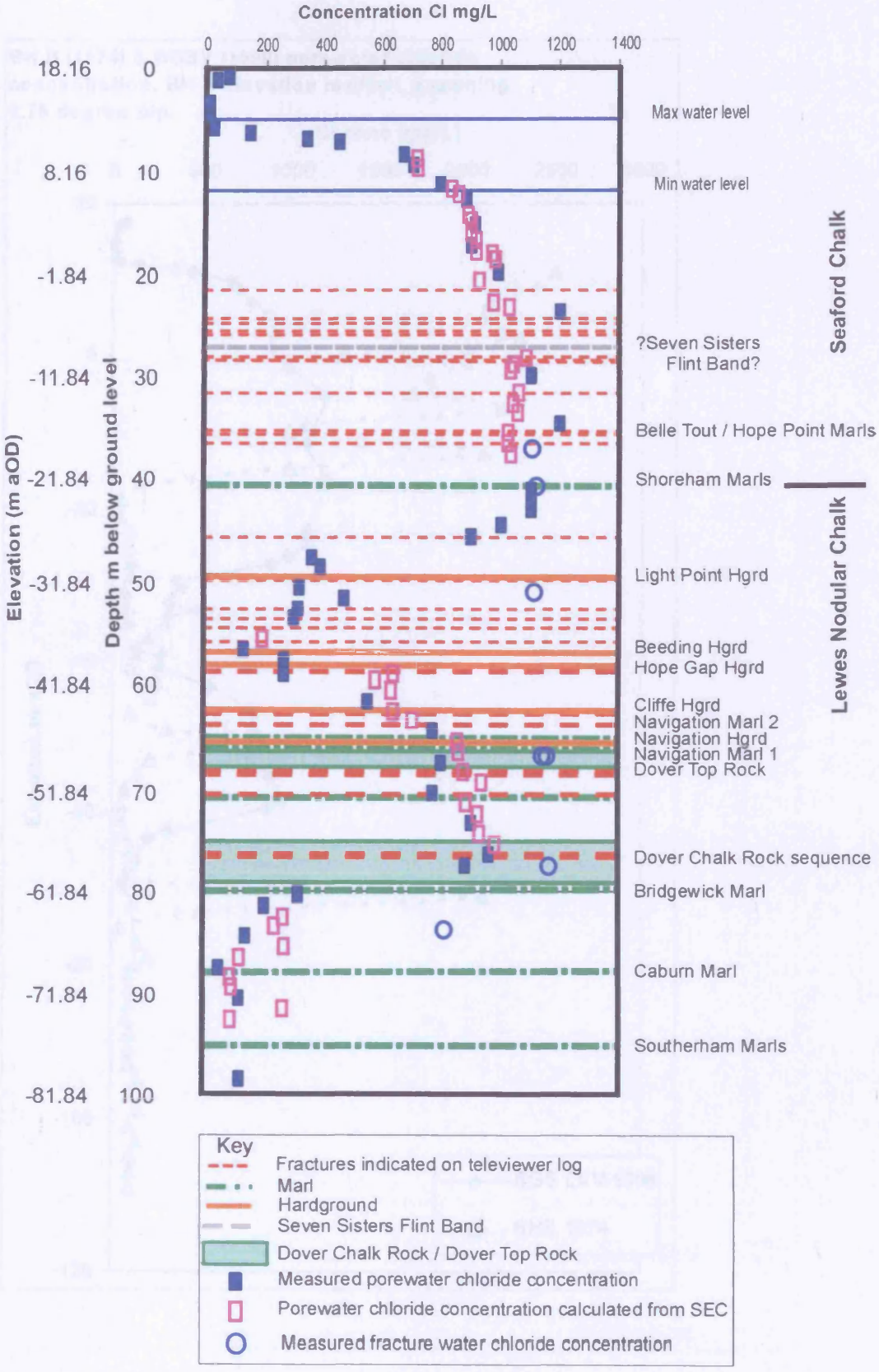

Figure 5-24 BGS LVV porewater chloride concentration overlain onto lithology and fracturing interpreted at Lower Venson Farm.

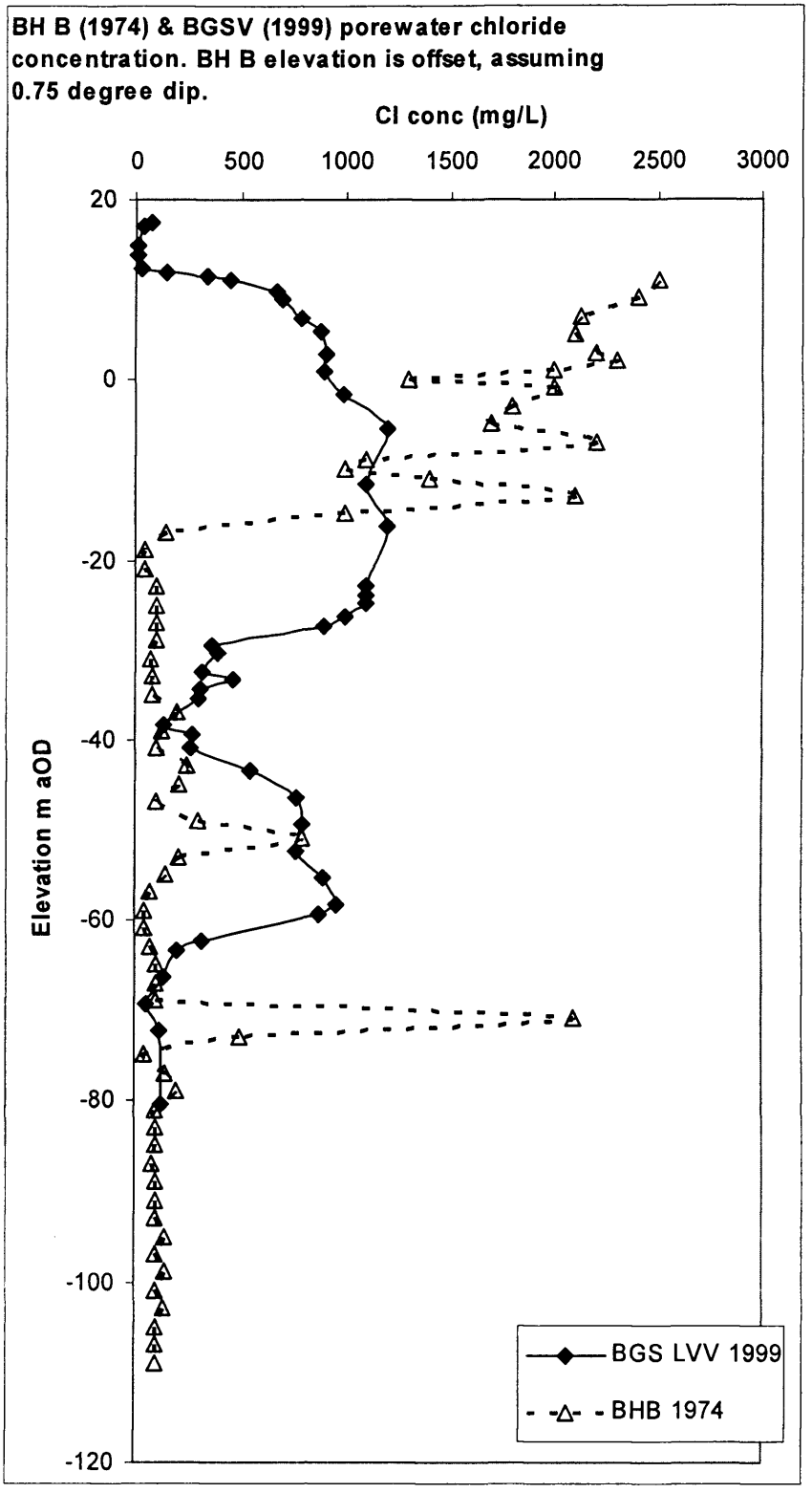

Figure 5-25 BGS LVV compared to BHB porewater chloride concentration.

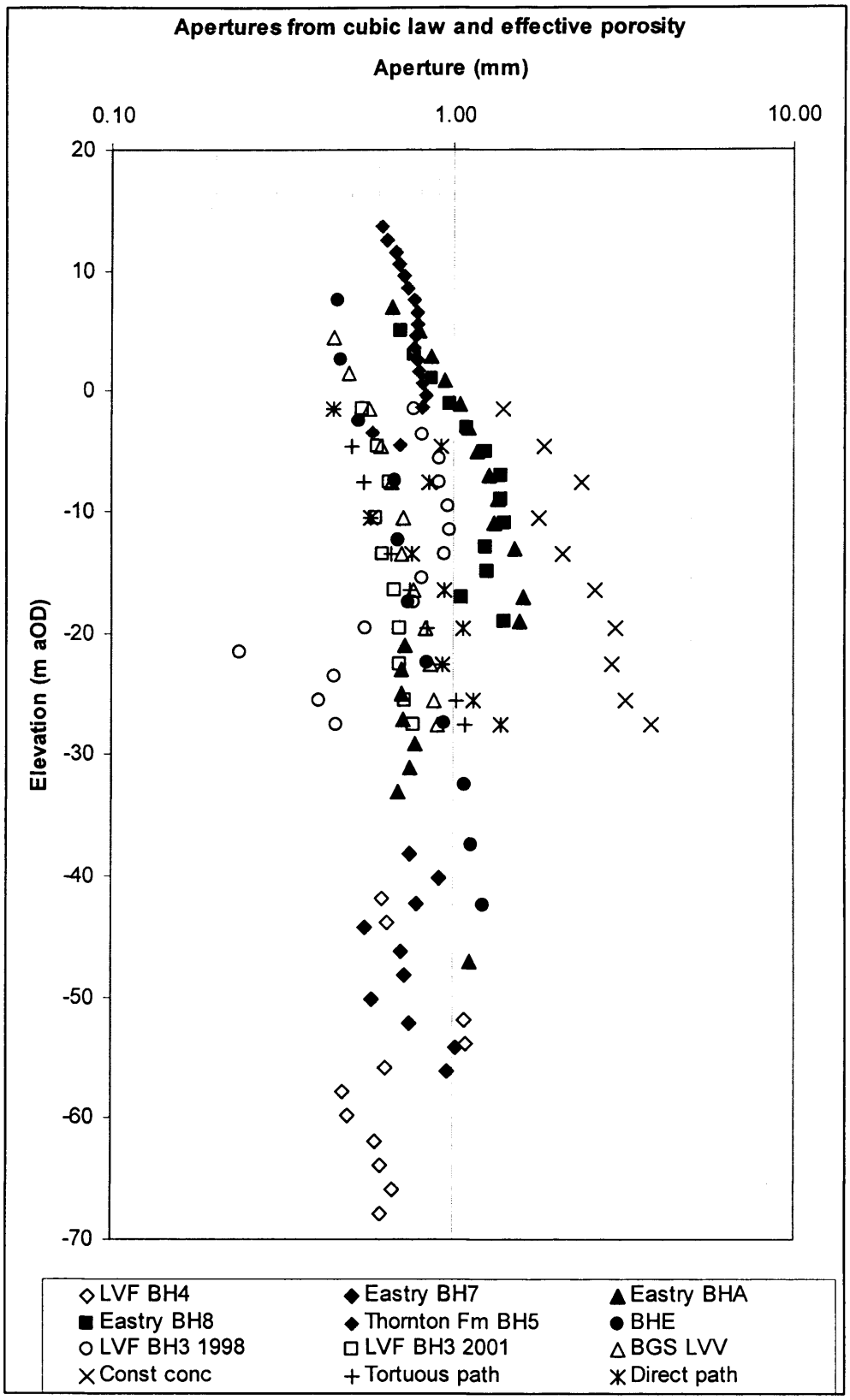

Figure 5-26 Calculated effective apertures from all boreholes.

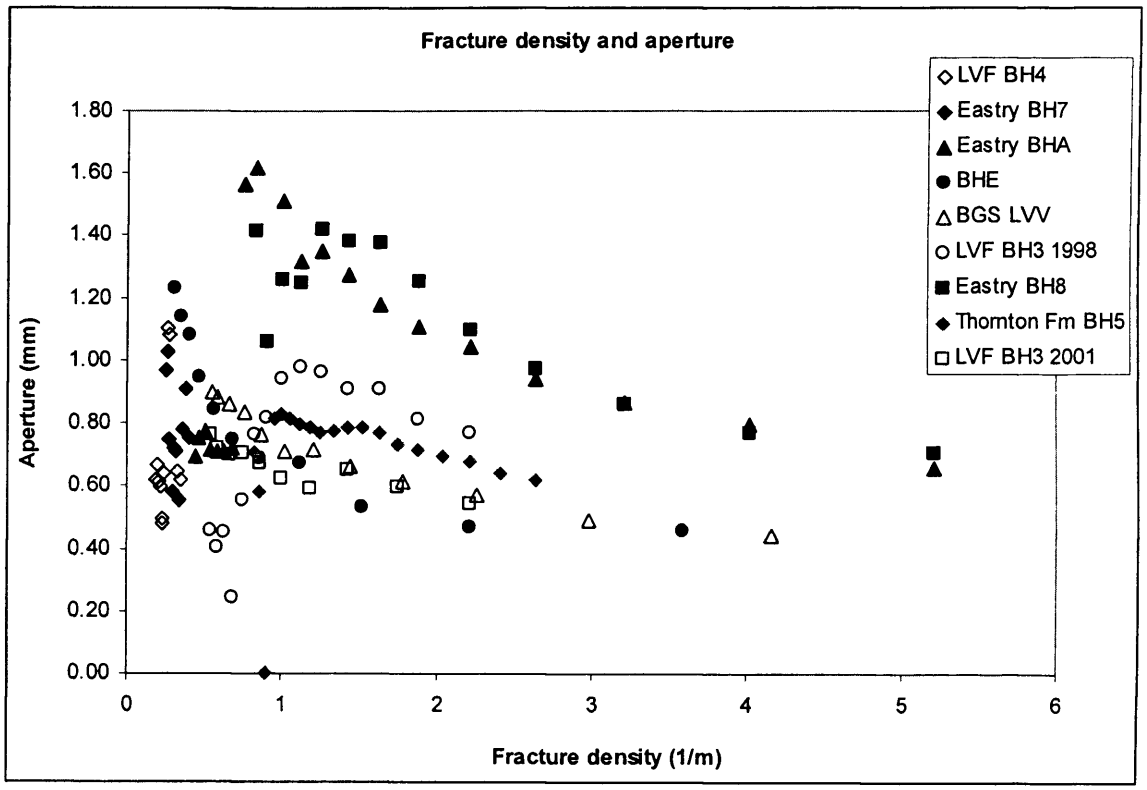

Figure 5-27 Fracture-density aperture relationship.

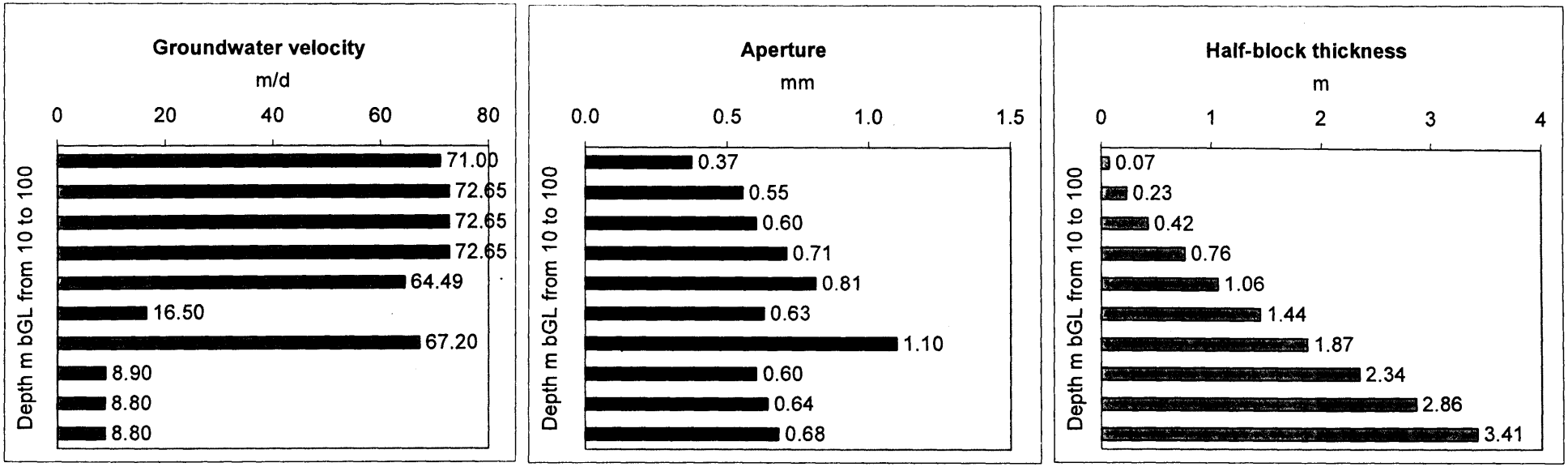

Figure 5-28 Fracture aperture, groundwater velocity and matrix-block size.

Parameter values are calculated from tracer test results, fracture-density depth relationship (Bloomfield *et al.* 2000) and an approximation of the cubic law.

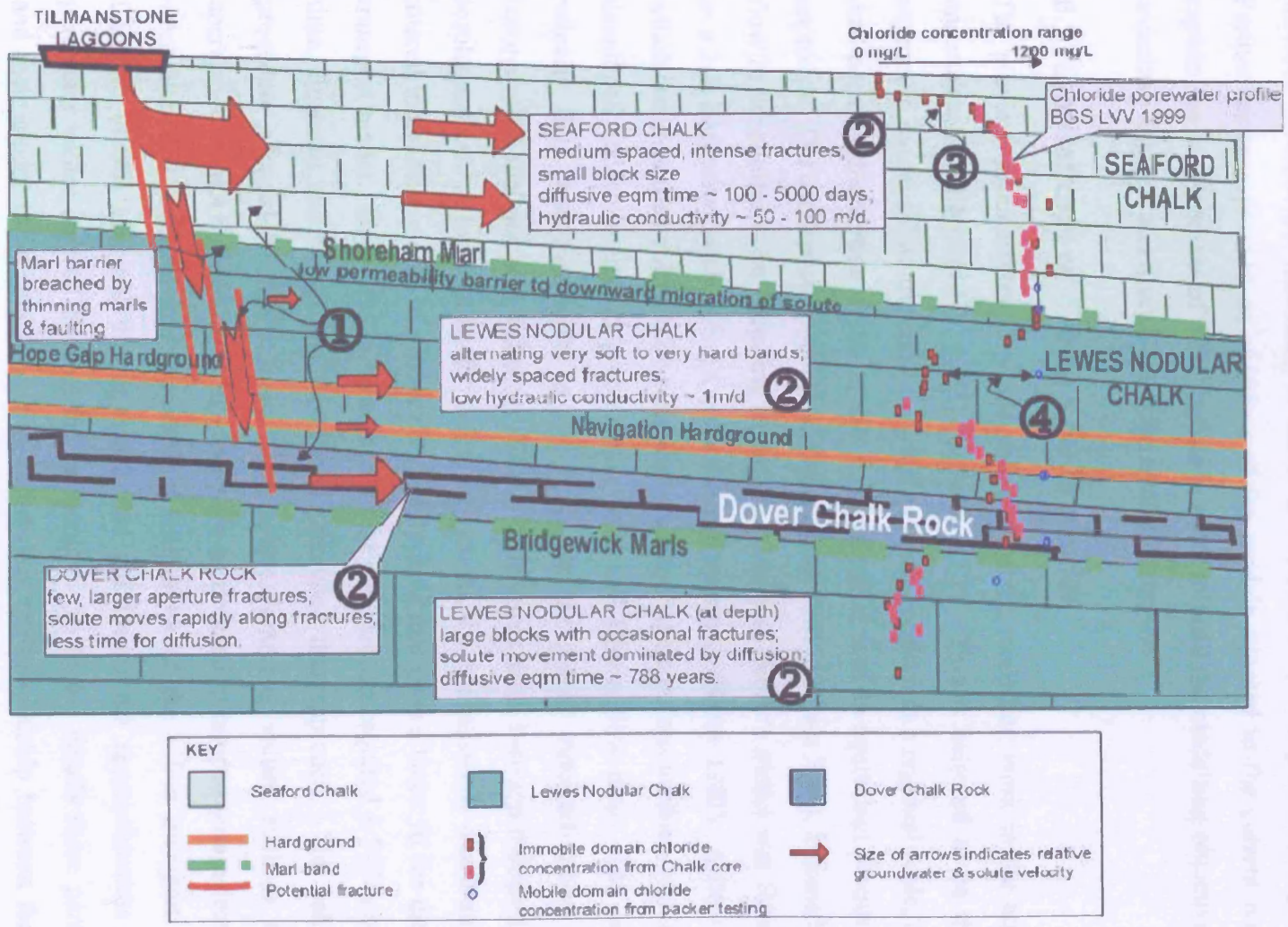

Figure 5-29 Conceptual model for solute transport from the infiltrating minewater for the Tilmanstone-Eastry valley.

6 Modelling

The conceptual understanding of the area's hydrodynamic regime and hydrogeological framework is now progressed through mathematical modelling. A brief critique of previous groundwater modelling in the area carried out by Bibby (1979) is provided. Further sections provide an overview of the models adopted in the current research, explain the development of these models in order to fulfil the modelling objectives, and undertake analysis and discussion of the modelling results.

6.1 Limitations of Bibby's 1979 model

The previous groundwater flow and solute transport modelling work in the area was undertaken by Bibby (1979, 1981) (Section 2.7.2). This is believed to be the first attempt to model solute transport in a dual porosity medium at a regional scale, using a dual porosity description of the aquifer medium rather than an equivalent porous media approach. The conceptual model (Headworth *et al.* 1980) (Figure 2-14), assumed all the flow in the aquifer to be occurring in the top 40 m, and Bibby's model was formulated as a 2-D horizontal mesh, using a finite element approach (Bibby 1981). A flow model which assumed the aquifer to be behaving as an equivalent porous medium was initially developed and calibrated to groundwater head and stream flow data. The resultant velocity field was then used as the basis for the solute transport model which incorporated dual porosity diffusion. Where differences arose between transport model results and calibration data for the solute movement, the transmissivity distribution was altered in the flow model to produce a velocity field that gave a better fit for the solute transport model. Bibby (1979) considered that the problem required a 3-D model but time, financial and computing limitations precluded this approach. The calibration procedure adopted by Bibby meant that certain parameter values, such as fracture aperture, were not defined explicitly, but were assimilated in lumped parameters which were altered to achieve improvements in calibration of the solute transport model. Carneiro (1996) assessed this approach and considered the appropriateness of the parameter values derived through the calibration. Table 6-1 details these parameters and their model values and Figure 6-1 illustrates the relationship between the block thickness and aperture.

Table 6-1 Calibration parameters used by Bibby (1979)

Calibration parameter	n_j **joint porosity**	$b.n_b$ **saturated thickness x block porosity**	α_L **longitudinal dispersivity**	α_T **transverse dispersivity**	D_d/q^2 **molecular diffusion coefficient / half block width**
Value	1%	14 m	120 m	60 m	6.3×10^{-5} d^{-1}
Component values		$n_b = 35\%$ $b = 40$ m			$D_d = 5 \times 10^{-5}$ m^2d^{-1} $2p = 9$ mm ($2p = 2q \times n_j$) $2q = 89.1$ cm

The 1% joint porosity was based on the specific yield for the Chalk perceived by Bibby. The tracer studies undertaken in this research (Section 5.3.3) indicate that this may be an order of magnitude too high for the effective porosity appropriate for solute transport in the Chalk, which is believed to occur within a restricted portion of the total fracture porosity due to the effect of channelling.

The transverse dispersivity used by Bibby is also large compared to the generally adopted ratio of 0.1:1 for transverse to longitudinal dispersivity. However the 0.1:1 ratio is generally used for porous media and no equivalent simple relationship is available for fractured rocks as the degree of dispersivity is related to the fracture network geometry (Schwartz and Smith 1988). A large value of transverse dispersivity may have been required by Bibby in order to accommodate the distribution of Chalk fractures that have subsequently been measured in the area (Section 5.2.2). The orientations of these fractures across the general direction of groundwater flow are in part responsible for the transverse spreading of the solute. Transient recharge effects may also modify the direction of groundwater flow (Fretwell 1999) and structural features, such as faults, will also modify solute distribution through acting either as barriers to or preferential routes for solute movement. The outcome of modelling undertaken for the current research also indicates that the longitudinal dispersivity values used by Bibby are large (Section 6.4.3). Molz *et al.* (1983) suggest that the dispersivity term exists to represent the heterogeneity of a system and it may be that in the simplified system modelled by Bibby the dispersivity is accounting for several processes not explicitly represented.

The component parameter $2p$ describes the width of the apertures assumed in Bibby's model, (Figure 6-1). An aperture width of 9 mm, incorporated within the lumped calibration parameter D_d/q^2 used by Bibby (Table 6-1), is considered to be large by Zuber and Motyka (1994) and is larger (by almost one order of magnitude) than the aperture widths derived from tracer testing in this research (Chapter 5 and Table 6-2, this Chapter). Measured fracture aperture widths in the Upper Chalk range from less than 0.5 mm to 23.5 mm (Bloomfield 1996) and effective aperture widths in relation to solute transport calculated from tracer tests during this research range from 0.37 to 1.1

mm (Section 5.5.2). The block width (*2q*) used by Bibby of 89.1 cm (half-block width of 44.6 cm) is reasonable, and relates well to the value for the half-block width of 42 cm at 30 m calculated from the fracture-density depth relationship established for the Tilmanstone – Eastry valley (Bloomfield *et al.* 2000) (Section 5.2.2 and Table 6-2, this Chapter).

Figure 6-2 presents Bibby's model predictions of chloride concentration in groundwater at the Eastry borehole, the observations available at that time for calibration, and the subsequent groundwater concentration observations. Bibby considers the Eastry borehole to be centrally located within the main chloride plume. Although the calibration produced a reasonable fit to the available data, over the longer-term Bibby's model underestimates the length of time required for the solute concentrations in the fractures of the aquifer to return to lower values. Considering the parameter values used for that calibration, the model's under-prediction is probably due to a combination of factors rather than any one. The large fracture aperture resulting from the calibration approach adopted by Bibby means that higher concentrations of solute moved more rapidly through the system and this also reduces the length of the concentration tail, because less solute moves into storage in the matrix pore space, or at least the depth penetrated into the matrix by the solute is less. The matrix porosity value used by Bibby is at the lower end of the range observed for Chalk at this stratigraphic level (Allen *et al.* 1997), so the pore volume available for solute storage is also underestimated.

Carneiro (1996) also considers other possible reasons for the underestimation, suggesting the effect of droughts and discrepancies between the modelled and observed direction of groundwater flow and plume dispersion. Drought has three effects that may have impacted the rate of decrease in chloride concentration:

- A decline in hydraulic gradient, reduces the groundwater discharge;
- A decline in the water table leaves chloride 'stranded' in the unsaturated zone;
- A decrease in hydraulic conductivity with depth combined with a falling water table will reduce the groundwater discharge.

Carneiro (1996) assesses the relative impacts of these effects on the chloride plume. He finds no evidence for a significant change in the hydraulic gradient since 1978, thus discounting the effect. In order for chloride trapped in the matrix porespace to have an

impact on chloride concentrations in the groundwater, the chloride would need to be diffusing from the matrix porewater to the fracture water. However Carneiro considers that for the Eastry borehole, located in the central part of the plume, the chloride concentration in the matrix porewater will be in equilibrium with the fracture water concentration such that no transfer of chloride would occur. However he recognises that since the cessation of discharge to the mine water lagoons the water table in the Tilmanstone – Eastry valley has declined by an average 2 m. He calculates a potential average mass of 5,000 tonnes of chloride becoming trapped in the Chalk matrix porewater for every metre decline in water-level, resulting in a potential 10,000 tonnes of chloride becoming trapped in the unsaturated zone. But this does not seem to provide a case for an explanation of persistence of the chloride. Rather it suggests that the initial effect of the trapped chloride would be to reduce chloride concentrations in the fracture water as the matrix porewater in the unsaturated zone acts as a sink for the chloride. In the longer term the trapped chloride will become a source of high chloride water as the chloride diffuses into lower concentration infiltrating rainwater and continues to the water table, in the way that nitrate has impacted groundwater. Carneiro does not consider the final effect of the decreasing hydraulic conductivity with depth to be significant given only an additional 4 – 5 m decline in water table during a drought. However the observations made during the current research, particularly during the packer testing (Section 5.3.3), indicate that if the water table is at a critical horizon, a 4 m decline in water level may result in the water table being located within a new lithology which has a hydraulic conductivity of half that at the higher level. So this effect may be more important than Carneiro suggests.

6.2 Modelling objectives

The modelling undertaken in this research has four objectives:

1) To apply explicitly, in a mathematical model, parameters measured during field investigations and to assess the application of these parameter values to predictions at different scales.
2) To compare the results from 3D modelling of the plume to Bibby's 2D model, to determine whether increasing the dimensionality of the problem within an improved geological framework (Section 5.2 and 5.7) gives an improved fit to the observed data.
3) To consider the treatment of the diffusive exchange in solute transport models: Fickian diffusion versus Quasi Steady State (First Order Mass Transfer).

4) To provide an improved prediction of solute movement and concentrations in fracture and porewaters over the next 75 years.

6.3 1D dual porosity model - DP1D

6.3.1 General approach

The main emphasis of this part of the mathematical modelling has been to assess whether parameters measured at the field-scale, either at the borehole from single borehole dilution tests, or over short distances of a few metres e.g. from borehole to borehole tracer tests, can be used to model and predict solute transport over larger distances. This could be used, for example, to improve the effectiveness of groundwater remediation, by understanding in more detail where best to target remediation wells or monitoring boreholes.

The modelling allows concentrations simulated by a model using parameter values derived through field investigations to be compared to observed values of matrix porewater and fracture water solute concentrations.

In order to compare the development of the fracture water and matrix porewater solute concentrations over time and with depth in the aquifer, the aquifer is conceptualized as being divided vertically into horizontal slices or slabs along a flow-line. The flow-line extends from the infiltration lagoons near the Tilmanstone colliery to the borehole BGS LVV at Lower Venson Farm and on to the North Stream springs, a total distance of approximately 4500 metres. Each horizontal slice of aquifer is assumed to have constant properties along its length, but a horizontal slice may have different properties to that above and / or below it. A constant groundwater flow regime is adopted for each slice and there is no interaction between slices, i.e. horizontal flow dominates and the hydrostratigraphy determines that vertical fluxes are negligible. The model is run for each slice and the results are compiled to produce a vertical profile of fracture water and porewater solute concentrations, at various locations along the flow-line and for different times.

6.3.2 Model concepts

The code used for this part of the modelling is called DP1D (**D**ual **P**orosity in **1**-**D**imension). The DP1D code was developed by John Barker, based on Barker (1982),

and is a semi-analytical code. It simulates one-dimensional transport through a dual porosity medium with a specified input concentration and a constant flow regime. The outputs are the solute concentration in the fractures and the average matrix porewater solute concentration for a specified set of times and distances from the input point. For the purposes of the current research, the matrix blocks are assumed to have slab geometry, as in Figure 6-3, although the code can allow for more complex block-geometries (Coy 2001).

The input concentration is piecewise constant, i.e. the input solute concentration is constant for each time period. The user creates a data file DP1D.DAT in the same directory as the executable file DP1D.EXE and the calculated fracture water and average matrix porewater solute concentrations are directed to a file called DP1D.OUT. This output file can then be processed using Excel or similar software. There is also an Excel version coded in Visual Basic which automatically generates graphical representation of results. For the purposes of the current research, the following simulated processes are of interest:

Fracture water:-

Advection at constant velocity

Diffusive exchange with matrix.

Matrix water:-

Diffusion according to Fick's second law

Transport equations and boundary conditions

The following equations describe solute transport within the fractures, diffusive exchange with the matrix porewater and solute transport across the matrix block, (*pers comm.* J. Barker).

Fracture water:

$$\frac{\partial C_f}{\partial t} + v\frac{\partial C_f}{\partial x} = -k_f C_f - \frac{2D_e}{a}\frac{\partial C_m}{\partial z}\bigg|_{z=b}$$

Equation 6-1

$$C_f(0,t) = C_0(t)$$

$$C_f(x,0) = C_i$$

Matrix water:

$$\phi\frac{\partial C_m}{\partial t}+\rho\frac{\partial S}{\partial t}=D_e\frac{\partial^2 C_m}{\partial x^2}-\phi k_m C_m+\rho P_m$$

Equation 6-2

$$C_m(x,z,0)=C_{mi}$$

$$C_m(x,0,t)=C_f(x,t)$$

$$\lim_{x\to\infty} C_m(x,z,t)=C_{mi}$$

$$\left.\frac{\partial C_m}{\partial z}\right|_{z=0}=0$$

The mean concentration in the matrix block water is:

$$\langle C_m\rangle(x,t)=\frac{1}{b}\int_0^b C_m(x,z,t)\,dz$$

Equation 6-3

The input concentration is specified by N pairs of values of concentration (C_N, t_N):

$$C_0(t)=\begin{cases}0 & t\le 0\\ C_N & t_{N-1}<t\le t_N\\ 0 & t>t_N\end{cases}$$

Characteristic parameters reported by the program:

a) The matrix/fracture porosity ratio:

$$\sigma=\frac{2b\phi}{a}$$

b) The apparent diffusion coefficient

$$D_a=\frac{D_e}{\phi}$$

c) The characteristic time for diffusion across a matrix block.

$$t_{cb}=\frac{b^2}{D_a}=\frac{\phi b^2}{D_e}$$

d) The characteristic time for diffusion from a fracture

$$t_{cf} = \frac{a^2}{4D_e\phi} = \frac{a^2}{4D_a\phi^2} = \frac{t_{cb}}{\sigma^2}$$

NOTATION

Symbol	Description	Dimension
a	Fracture aperture (full width of a single fracture)	L
b	Matrix block vol./area (e.g half slab thickness where using slab geometry)	L
$C_f(x,t)$	Concentration in fracture water	ML^{-3}
$C_{fi}(x,t)$	Initial fracture concentration	ML^{-3}
C_{mi}	Initial matrix water concentration	ML^{-3}
$C_m(x,z,t)$	Concentration in matrix water	ML^{-3}
C_N	Fracture concentration at x=0 when $t_{N-1}<t\leq t_N$	ML^{-3}
$C_0(t)$	Concentration water entering fractures at x=0	ML^{-3}
D_a	Apparent diffusion coefficient	L^2T^{-1}
D_e	Effective diffusion coefficient	L^2T^{-1}
k_f	Fissure decay constant	T^{-1}
N	Number of input periods	-
t	Time from the start	T
t_N	Time after which the input concentration changes from C_N to C_{N+1}	T
v	Velocity in fractures (can be zero)	LT^{-1}
x	Distance from input point	L
z	Distance from centre of matrix block	L
ϕ	Porosity	
ρ	Density	

6.3.3 Input parameters

DP1D has a relatively simple set of input parameters. This is an advantage at this stage as more complex parameter requirements could not be supported by the available data.

Required parameters are:

1. Initial fracture concentration
2. Fracture velocity (i.e. groundwater velocity in fractures)
3. Fracture aperture
4. Volume to surface area ratio of matrix blocks (equal to half-block thickness for slab geometry)
5. Matrix porosity
6. Initial solute concentration in matrix porewater
7. Effective diffusion coefficient

8. Input source concentration

Initial fracture water (1) and matrix porewater solute concentrations (6) are set to background levels of chloride in groundwater (30 mg/L); fracture velocity (2) is obtained from tracer testing (Section 5.5.2); fracture aperture (3) and half-block thicknesses (4) are derived from fracture-density depth relationship (Section 5.5.2) combined with results from tracer tests using the cubic law; matrix porosity (5) is obtained from laboratory testing of core material by BGS (Section 5.2.3); the effective diffusion coefficient (7) is obtained from Hill (1984) ($3x10^{-10}$ m^2s^{-1}) (Appendix 2); input solute concentrations (8) are obtained from Headworth *et al.* (1980) (Figure 2-15).

The aquifer is split into ten horizontal slices and Table 6-2 details the input parameters for each horizontal slice. The derivation of these input parameters is given in Chapter 5, Section 5.5.2.

Table 6-2 DP1D parameter values

Depth (m bGL)	Fracture velocity (m/d)	Fracture aperture (mm)	Half-block thickness (m)	Matrix porosity (%)	Equivalent elevation at Lwr Venson Fm (m aOD)
10	71	0.37	0.07	45.5	8.16
20	72.65	0.55	0.23	44.5	-1.84
30	72.65	0.60	0.42	44	-11.84
40	72.65	0.71	0.76	42.5	-21.84
50	64.49	0.81	1.06	42.4	-31.84
60	16.5	0.63	1.44	38.3	-41.84
70	67.2	1.10	1.87	43	-51.84
80	8.9	0.60	2.34	39.5	-61.84
90	8.8	0.64	2.86	43	-71.84
100	8.8	0.68	3.41	39.9	-81.84

6.3.4 Model results

Output for the horizontal slices is presented in Figure 6-4, Figure 6-5 and Figure 6-6 (the plots for 90 and 100 m depth are omitted for clarity: they display the same response as 80 m depth).

The plots show the change in fracture water and average matrix porewater solute concentrations over time at three locations in the Tilmanstone – Eastry valley: BHB, Lower Venson Farm and the northern North Stream spring (see Figure 4-1 for

locations). Plots are given for 10 m vertical intervals from 10 m to 80 m depth. The plots for the slices at 60 m, 80 m (and 90 m and 100 m) indicate that solute movement at those depths is considerably retarded. At 60 m depth the solute reaches BHB around the beginning of this century, approximately 25 years after the lagoons ceased to operate. At 80, 90 and 100 m it is approximately 75 years after the lagoons ceased to operate that any solute reaches BHB.

Notable features of the plots are the development of the lag between fracture water and matrix porewater solute concentrations. As the matrix block-size increases, i.e. generally at greater depths, the time to reach diffusive equilibrium with the fracture water solute concentration increases. Similarly as the block-size increases the available porewater storage increases and this results in a reduction in both fracture water and matrix porewater solute concentration, due to the diluting effect of the larger volume of water. The combination of reduced velocity and large matrix block-size for the slices at 80, 90 and 100 m results in the solute barely moving 700 m from the input point in the entire model run, i.e. for 100 years after the cessation of lagoon discharge. At this depth in the Chalk solute movement is dominated by diffusion. The first peak solute concentration at Lower Venson Farm breaks through at a depth of 70 m in approximately 1980. This is as a result of the relatively high velocity and large aperture calculated at this level / slice. However, due to the attenuation provided by the larger block-size at 70 m compared to shallower depths, the peak solute concentration for the fracture water only reaches approximately 890 mg/L and the peak matrix water concentration is only approximately 400 mg/L.

The overall shape of the 1974 vertical profile of modelled chloride concentration at BHB is in good general agreement with the profile for the observed data (Figure 6-7). This suggests the conceptual model that has been adopted, whereby the vertical profile has been divided into 10 m slabs each with a particular set of aquifer parameters, is able to broadly reproduce the observed chloride concentration profile.

The DP1D predicted fracture water concentrations are lower than those interpreted from the Headworth *et al.* (1980) cross-section profile (reproduced in Figure 2-14). However the matrix / immobile porewater concentrations predicted by the DP1D model are in moderately close agreement with those observed in 1974 from matrix porewater

extracted from Chalk core (U100 samples) at BHB. The difference between predicted fracture water concentrations and those given by Headworth *et al.* (1980) may be attributable to a number of factors:

- The groundwater velocity used in the model is too low. The model is restricted to a constant groundwater velocity throughout a model run. The values used in the model are derived from the natural gradient borehole tracer tests undertaken during the current research. It is possible that the groundwater velocity during lagoon operations was greater than that existing at the present time, although this is not evident from the analysis of the groundwater gradients undertaken in Section 5.3.1;

- The fracture aperture is too small, which allows more solute to diffuse into the matrix porewater, thus reducing the fracture water solute concentration;

- The Headworth *et al.* (1980) interpretation of the fracture water chloride concentration with depth is incorrect. As far as it has been possible to determine, the overall shape of the fracture water chloride profile was developed from a limited number of fracture water samples and a gradually decreasing fracture and matrix porewater concentration cross-section profile developed from these samples. However it appears, both from the BHB 1974 and BGS LVV 1999 chloride porewater profiles, that there are preferential flow horizons at depth which are contradictory to this gradual concentration decrease.

Figure 6-8 presents a composite vertical profile of the model results for the Lower Venson Farm site. The matrix porewater chloride profile observed at the site in 1999 is also included, as are available fracture water chloride concentrations.

The model results produce a profile very similar in shape to the observed matrix porewater chloride concentrations (Section 5.5.1). The lower concentrations observed in the matrix porewater sampled from -30 to -40 m aOD are well represented. The

concentrations observed in the matrix porewater for the upper part of the profile are less well reproduced.

The model predicts a peak concentration at 20 m bGL (-2 m aOD) at Lower Venson Farm of approximately 3000 mg/L in the mid 1990s for both fracture water and matrix water concentrations. The modelled concentrations at this level decrease to approximately 2100 – 2250 mg/L by 1999. However, this is still twice the concentration observed in the matrix water at the Lower Venson Farm site in 1999. There is no evidence from observed groundwater concentrations that the fracture water at this distance from the infiltration lagoons has ever reached a concentration of 2000 mg/L.

The porewater chloride concentration profile at BHB, which is modelled as experiencing the highest porewater chloride concentration of 4900 mg/L in 1974, is observed to reach only 2200 mg/L at 10 m bGL. The model results are very sensitive to aperture, both through the effect of the cubic law and due to representation of dual porosity, so a small variation in aperture will have a strong effect on the predicted solute concentrations. In order to demonstrate this sensitivity to aperture, the model was rerun for each depth interval with the aperture increased and decreased by 10%. The results of the aperture sensitivity modelling are provided in Figure 6-9.

The plot shows the original model base case results compared to a 10% increase and decrease in aperture size. The graph demonstrates the sensitivity of the results to aperture. At 20 m depth (-1.8 m aOD) the concentration of chloride has been reduced and increased by 500 mg/L due to the 10% aperture size change, an absolute change of 0.055 mm. Field observations for 1999 are also included for reference.

The plots of chloride versus time for a depth sequence at a specific site presented in Figure 6-4 to Figure 6-6 are complimented by a series of snapshots of along-valley profiles in Figure 6-10 to Figure 6-12 which show the profiles for 10, 70 and 60 m bGL. The profiles for 20, 30, 40, 50, 80, 90 and 100 m bGL are given in Appendix 6. These profiles show the predicted centre of mass of the solute plume at each depth interval. Figure 6-10 demonstrates that at 10 m bGL the main solute plume takes approximately 25 years to pass through the system as modelled. An interesting profile at 70 m is

presented in Figure 6-11 which serves to highlight the impact of the larger block-size at this depth. The large lag that develops between fracture water and matrix porewater due to the solute being stored in the matrix porewater is clearly demonstrated, and the effect this has on porewater solute concentrations along the valley length, over a long time frame, is highlighted.

Similarly Figure 6-12 for 60 m bGL (and 80, 90 and 100 m bGL in Appendix 6) demonstrates the attenuating capacity of the matrix porewater where the centre of the solute plume has moved along the valley approximately 500 m in the 25 years since minewater lagoon operations ceased. The large block-sizes, small fracture apertures and low groundwater velocities at these depths restrict solute movement to operate predominantly through diffusion, with large storage available in the matrix porewater.

The modelling presented so far provides confidence that parameter values obtained at the small scale of the fieldwork undertaken during this study (borehole to tens of metres) can be applied in models at larger scales, at least in one dimension, to produce a reasonable match with observations. The next stage of the modelling examines several effects of the impact of increasing the dimensionality to 3D from Bibby's early 2D modelling. The following section presents the modelling of the Tilmanstone – Eastry valley and surrounding groundwater system at the regional scale.

6.4 Regional modelling

6.4.1 General comments

The semi-deterministic approach to representing solute transport in numerical models at the regional scale, as proposed by Dassargues *et al.* (1996) (Section 2.5.4), is now applied here. The conceptual hydrostratigraphic model, developed through applying the lithostratigraphy developed by Bristow *et al.* (1997) and Mortimore (1997) to the Tilmanstone-Eastry valley, is combined with aquifer parameter values, derived from field testing at a local scale, and used to populate a 3-D regional numerical groundwater flow and solute transport model. Calibration of the numerical model is limited to adjustments within the initial steady-state groundwater flow model to produce an acceptable balance and overall shape to the steady-state groundwater flow field. The calibration is limited to these adjustments because the emphasis of the application is to assess the importance of the updated hydrostratigraphy to the numerical model for

predicting the development of a solute plume more similar in shape to that observed, compared to that predicted by the previous conceptual model (Bibby 1979, 1981).

MODFLOW (McDonald and Harbaugh 1984) has been used for the regional scale groundwater flow modelling and this has been coupled with MT3DMS (Zheng 2002) for the solute transport modelling at the regional scale. The pre and post-processing was carried out with GW Vistas V3 (Rumbaugh, 2001). MODFLOW has previously been used to model regional groundwater flow in the Chalk, although there are a number of limitations imposed by the assumptions of the mathematical formulation. The two major limitations that arise when applying the software to the Chalk are that it was designed for single porosity aquifers with little vertical variation in hydraulic conductivity within an aquifer unit. Considering the single porosity aspect, it is only valid to use MODFLOW when the scale of the area modelled is such that it can be considered as an equivalent porous medium (Barker 1991). For flow modelling in the Chalk at the regional scale the densely fractured nature of the Chalk aquifer meets this criterion. The second limitation is more problematical. The observed vertical variation in hydraulic conductivity in the Chalk means that it does not conform to this MODFLOW ideal. Accommodating this feature has been a major part of modelling work undertaken by others, particularly Rushton *et al* (1989) through model code written specifically for the Chalk for which hydraulic conductivity varies with depth and hence transmissivity varies with water level. The representation of this is demonstrated in Figure 6-13.

The issue has also been addressed recently by the EA who commissioned work to alter the MODFLOW code to vary the hydraulic conductivity with depth (Taylor and Hulme 2000). It has not been feasible to incorporate these modifications into the current research because the flow files are not fully transferable to the solute transport model. However, the benefits of using MODFLOW include the 3-dimensionality of the software, its compatibility with the MT3DMS solute transport code and its applicability to the Chalk at the regional scale. Analysis of the lithological log, packer test and single borehole dilution tests (Section 5.2.1, 5.3.3 and 5.5.2) demonstrate a strong correlation of hydraulic parameters with lithology. This is interpreted (Section 5.7) as the Chalk aquifer comprising quite distinct hydrostratigraphic layers, rather than the gradually varying nature more usually adopted in conceptual models (ACER 1991). This detailed,

layered conceptual model is of particular importance for solute transport modelling where the hydraulic parameters of the individual layers control the way solute moves within the aquifer (Section 5.5.1, Figure 5-29) and this is readily applied within MODFLOW. Other benefits of the MODFLOW software include its ease of use (pre and post processing software availability) and the current preference, and therefore familiarity, of the software by the EA. This latter point is of importance as the context for this research is the Water Framework Directive and the EA are proposed as the competent authority in the UK (DEFRA 2003). The EA are therefore likely to find research that uses current modelling software preferences more accessible for informing guidance and the approach adopted for groundwater body characterisation and monitoring.

6.4.2 Flow Model

Description

Grid alignment and model boundaries:

An outline of the model grid overlain on a map of east Kent is provided in Figure 6-14. The model grid is rotated through 45 degrees relative to North, such that the vertical gridlines are aligned north-east south-west. This is the alignment of the dry valleys in the area. The model grid, presented in more detail in Figure 6-15, is bounded on the right by the coast (approximately Dover to Deal); on the left by the Nailbourne and Little Stour River system; along the top by the Tertiary cover and springs of the North and South Streams and Wingham Stream; along the bottom by a fault / fracture zone as suggested by Bloomfield *et al.* (2000); and by a flow-line along the bottom right hand corner. The flow conditions imposed on these boundaries are marked on Figure 6-15. The coastal boundary is represented by constant heads and drain nodes for the dry valleys, the Nailbourne / Little Stour river system by drain nodes, the top boundary by a mixture of drain nodes and general head boundary nodes, and the bottom boundary by a mixture of no-flow and general head boundary nodes.

Layers:

The model comprises 5 layers. These dip to the north-east at approximately 0.5 degrees, as marked on the geological map of the area (Sheet 289 Canterbury (BGS 1982) and Sheet 290 Dover (BGS 1977)). The surface of layer 1 is based on the

topography taken from the OS Landranger 179 1:50 000 map Canterbury and East Kent (Figure 6-16).

The thickness of each layer is determined by combining the results from the single borehole dilution tests (Section 5.5.2) and geophysical logging interpretation (Section 5.2.1). Figure 6-17 outlines the relationship between the model layers and their associated lithological or hydrostratigraphical unit (Section 5.7).

Mesh dimensions:

The model grid is composed of 54 rows and 84 columns of cells, each of which are 250 x 250 m in dimension. Layer 1 has fewer active rows as the layer reaches outcrop to the southern boundary of the model.

Representation of surface water:

All the surface water features in the area are represented in the model using drain nodes. These allow groundwater to flow as discharge from the model domain when the water table reaches the level of the drain elevation or stage, but there is no water returned to the groundwater system if groundwater heads fall below the river bed elevation. The rate of outflow at the drain node is controlled by calculating a conductance value, based on the length and width of the drain and the hydraulic conductivity of the sediments that the water is passing through at the base of the drain. Drain nodes represent the dominant flow characteristics of the rivers in the area: essentially groundwater-fed springs and rivers. Flow only occurs in the upper reaches of the Nailbourne river during periods of exceptional rainfall, when groundwater levels rise above ground level. Flow in the North and South streams is derived from springs in the Chalk. The Wingham River also arises from springs located upgradient of the Tertiary boundary and is strongly affected by abstraction at Wingham PWS, indicating a predominantly groundwater source and strong surface water-groundwater interaction.

Abstraction:

Details of abstraction regimes at the PWS located in the area have been derived from a number of sources, including water company records and existing modelling reports (Bibby, 1979 and ACER, 1980). Well construction information, where available, has been used to determine the total depth of the well and hence the corresponding number of model layers it occurs in. Locations of the PWS in the model are shown on Figure

6-15. Table 6-3 indicates the grid cell location of the PWS and the number of layers it is set to abstract from.

Table 6-3 Public Water Supply well and location in model

PWS name	Approximate depth of well (m)	Model cell (Row, Column)	Represented in model layers
Wingham[1]	53 m	(24, 17)	1 & 2
Woodnesborough	91 m	(7, 32)	1, 2 & 3
Flemings[2]	80 m	(10, 31)	1, 2, 3, 4 & 5
St Richard's Rd Deal	40 m	(11, 66)	1, 2 & 3
Martin Mill	85 m	(28, 64)	1 & 2
Kingsdown	75 m	(19, 73)	1, 2, 3, 4 & 5
Martin Gorse	100 m	(29, 66)	1, 2, 3, 4 & 5
Sutton	80 m	(24, 60)	1, 2, 3, 4 & 5
Ringwould	100 m	(25, 72)	1, 2, 3, 4 & 5
St Margarets	91 m	(31, 76)	1, 2, 3, 4 & 5
Notes [1] Extensive adit system [2] 5 wells on this licence along valley, abstraction at 1 only			

The abstracted volumes are divided between the model layers, based approximately on the response observed during the flow logging at Lower Venson Farm (Section 4.4.2). For example, where a well is present in all 5 model layers, the abstracted volume is split as 30: 5: 10: 50: 5. At Wingham PWS the well has an extensive adit system. As shown in Figure 6-15, the adit has been represented by locating well nodes in adjacent cells. The total abstracted volume is split evenly between each location and that volume is then split 70:30 between layer 1 and layer 2.

Lagoons:

Figure 6-15 also indicates the location of the minewater discharge lagoons and ponds, as included in the model. They are represented in the model as injecting (or recharging) well nodes in layer 1. The volume of water from the plot given in Headworth *et al* (1980) (Section 3.3.4 and Figure 2-15) is divided evenly between the cells. This results in a peak discharge into the model of 1900 m^3d^{-1} at each lagoon node.

Hydraulic conductivity:

Figure 6-18 shows the distribution of hydraulic conductivity in layer 1. Two zones are represented. One zone represents the dry valley areas and the other represents the interfluves. Layers 2 to 5 have single, uniform values for hydraulic conductivity.
The values for the layers are based on results of the single borehole dilution and packer testing (Section 5.5.2 and 5.3.3). Values attributed to each model layer are given in Table 6-4.

Table 6-4 Hydraulic conductivity values applied to each model layer

Model Layer		Hydraulic Conductivity md^{-1}
1	Dry Valley	50
	Interfluve	20
2		5
3		1.5
4		8
5		0.1

Recharge:

As described in Chapter 3, recharge is distributed across the area according to elevation, which controls precipitation volume, and surficial cover type, which influences the amount of rainfall able to reach the water table. This distribution is represented in the numerical model by applying the recharge: rainfall ratios developed in Section 3.3.1 to zones across the model domain. The recharge zone distribution is shown in Figure 6-19.

A single rainfall value is used for each stress period, and this is multiplied by the zone value, see Table 6-5, to give the actual recharge for that stress period.

Table 6-5 Recharge zone multipliers

Recharge Zone		Multiplier
Zone 1: Low elevation < 70 m aOD	1a Head deposits	0.36
	1b Chalk deposits	0.37
	1c Clay deposits	0.38
Zone 2: Intermediate elevations 70 – 130 m aOD	2a Head deposits	0.38
	2b Chalk deposits	0.39
	2c Clay deposits	0.4
Zone 3:High elevations >130 m aOD	3a Head deposits	0.41
	3b Clay deposits	0.42

Model time frame and Stress Period set-up:

The transient flow model is intended to produce a flow-field that represents the history of minewater lagoon operation and continues to the present day to enable comparison to be made with recent observations. The model therefore covers the period from 1905 (when lagoon operation started) until 1999 (when the drilling and testing at Lower Venson Farm was undertaken by BGS, Section 4.4.1).

The transient model simulation is divided into stress periods (SP). Each new stress period marks a change in the flow or solute input regime. During the early part of the transient simulation these changes may be due to the minewater lagoon operating activity, a new abstraction well coming on line in the area, or a significant change in abstraction regime of an existing well. The resultant stress periods range from 3 to 13 years in duration. However, from 1978 onwards the model runs with stress periods of 6 months in length to allow seasonal variations to have an effect on water levels and the groundwater flow regime. The stress period set-up is given in Table 6-6.

Table 6-6 Model time frame and stress period set-up

Stress period (SP)	Start time	End time
1	1905	1912
2	1913	1919
3	1920	1925
4	1926	1939
5	1940	1944
6	1945	1953
7	1954	1959
8	1960	1964
9	1965	1973
10	1974	1977
11	1977	1978 (September)
12	1978 (October)	1979 (March)
13	1979 (April)	1979 (September)....etc to Stress Period 54: March 2000

Results

A steady-state model was run to obtain an initial distribution of heads as a starting point for the transient model. The accuracy with which a groundwater flow model replicates the natural system it is representing is assessed by comparing the model predictions of

groundwater head distribution and flows with those observed in the region modelled. The resulting head distribution for the steady state model is given in Figure 6-20.

The steady state groundwater head distribution compares favourably to the general directions of flow indicated by observed groundwater levels. The modelled groundwater level for model layer 1 is shown compared to median groundwater level data provided by the EA in Figure 6-21.

Modelled groundwater levels are approximately 5 m higher than median groundwater levels across much of the area modelled and particularly to the south of the area. It is not clear that this is due to a specific factor. A variety of parameters contribute to the predicted groundwater level including recharge, hydraulic conductivity and base elevation of the layer. Any and all of these can be adjusted to produce an improved fit to observed groundwater levels. However, probably of greater importance for assessing how well the steady state groundwater model is replicating the observed regional groundwater regime is through comparing the groundwater gradient and groundwater flows.

Comparison of modelled to observed gradients can be made using the contours plotted on Figure 6-21. Considering the central area of the model domain, the gradient for the modelled groundwater heads from the Tilmanstone infiltration lagoons towards the northern spring of the North and South Streams is 0.0039. The observed groundwater heads have a gradient of 0.0047 for the same line. This indicates that the numerical model of the groundwater flow system is producing a good representation of the observed groundwater gradients.

Figure 6-22 demonstrates the effect of the dry valleys on the groundwater flow regime. Velocity vectors are represented by arrows on the model grid. The relative size of the arrows indicates the larger groundwater velocities which are concentrated along the dry valleys.

Details of groundwater flows from the model are given in Table 6-7. Estimates or observations of corresponding flows are also given for comparison.

Table 6-7 Steady state model groundwater flows

Flow type & location	Steady-state model volume	Observed / estimate	Data source	Comment
North & South Streams	48196 m^3d^{-1}	23069 m^3d^{-1} 33681 m^3d^{-1} 39860 m^3d^{-1} 17000 – 55000 m^3d^{-1} 5000 - 45000 m^3d^{-1}	EA Bibby 1979 SWA 1976a ACER 1991 ACER 1991	From mean daily flow from stream gauging 1972 – 1992 1973 observations Modelled range Observed range
Nailbourne River	16118 m^3d^{-1}	11000 – 70000 m^3d^{-1}	ACER 1991	Modelled range
Wingham River	33503 m^3d^{-1}	5000 - 25000 m^3d^{-1} 4000 - 27000 m^3d^{-1} 0 - 40000 m^3d^{-1}	ACER 1991 ACER 1991 ACER 1991	Modelled range for Wingham Str. Modelled range for Well Chapel Spr. Observed range for Well Chapel Spr.
Across north-eastern boundary beyond North & South Streams	2133 m^3d^{-1} over 7.5 km			Infra-red surveys undertaken by SWA (1976c) indicate little or no outflow from the coast, as suggested by this modelled volume.
Eastern coastline	37173 m^3d^{-1} over 5 layers and 11.8 km			Groundwater seepage observed on foreshore at low-tide around St Margarets-at-Cliffe.
Springline into Dour valley	6338 m^3d^{-1}			
Recharge	170270 m^3d^{-1}	272 mm a^{-1} 288 mm a^{-1}	Kent River Authority Section 14 ACER 1991	Model recharge works out as approx. 300 mm a^{-1} Average from recharge values used in ACER model.

The purpose of the flow model is to provide a numerical representation of the flow regime for the proposed conceptual model of solute transport, incorporating the detailed hydrostratigraphic layering developed for the Tilmanstone – Eastry valley in Section 5.2.1. Given that developing a detailed regional flow model is not in itself an objective of the research and that the hydraulic and transport data gathered for this research focuses on the Tilmanstone – Eastry valley, the distribution of head and flows from the steady state model are considered to be suitable for continuing to a transient flow model.

Some results from the transient flow modelling are briefly described here to provide a context for the subsequent solute transport modelling. Figure 6-23 and Figure 6-24 demonstrate the groundwater flow regime for different stress periods from the transient model runs. Figure 6-23 is a cross-section along the Tilmanstone – Eastry valley (column 41 in the model) for Stress Period 9 (1965 – 1973) during the operation of the infiltration lagoons. Arrows represent the velocity vectors for the groundwater flow at this time. The relative size of the arrows indicates the size of the flow (on a logarithmic scale). The majority of flow occurs in layer 1, but a driving head is created by the infiltration lagoons, such that downward migration of the saline minewater can occur beneath the lagoons. Layer 4 has more flow than layers 2 and 3. This is due to its higher hydraulic conductivity and this results in preferential flow along this horizon. Figure 6-24 is a cross-section along the same column once the infiltration lagoons have ceased to operate (SP 52, winter 1998/99). The majority of groundwater flow is still occurring in layer 1 and the downward movement of groundwater due to the infiltration lagoons has stopped. Layer 4 continues to be a horizon with a greater flow rate. The results from the transient flow model provide the context for adding solute transport to assess the effect of the dual porosity nature of the Chalk.

This transient model provides the flow data necessary for the solute transport model, which is used to explore the effects of dual porosity.

6.4.3 Transport model

Description

The software used for the solute transport modelling is MT3DMS (**M**ass **T**ransport in **3**-**D**imensions **M**ulti-**S**pecies) (Zheng 2002). This is a well known solute transport code

that uses the resultant groundwater flow files from MODFLOW as the basis for solute transport calculations. The multi-species capability of the code is a relatively new facet but it is not used in the current research as only the movement of a single species, chloride, is of interest. The MS version of MT3D is used here because it has a dual porosity capability included in the code. The software takes a mobile and immobile dual-domain approach with solute transfer between the mobile and immobile domains controlled by a first order mass transfer coefficient. The statement for mass conservation in the mobile domain is:

$$\theta_{mo}\frac{\partial C_{mo}}{\partial t} = -q\frac{\partial C_{mo}}{\partial x} + \theta_{mo}D_{im}\frac{\partial^2 C_{mo}}{\partial x^2} - \zeta(C_{mo} - C_{im})$$

Equation 6-4

And for the immobile domain:

$$\theta_{im}\frac{\partial C_{im}}{\partial t} = \zeta(C_{mo} - C_{im})$$

Equation 6-5

Where

C_{mo} concentration in the mobile domain (fracture water) [ML^{-3}]

C_{im} concentration in the immobile domain (matrix porewater) [ML^{-3}]

q Darcy flux [LT^{-1}]

θ_{mo} porosity of mobile domain (fractures)

θ_{im} porosity of immobile domain (matrix blocks)

ζ first-order mass transfer coefficient [T^{-1}] (Zheng 2002)

Solute transport model set-up:

Dual porosity parameters:

The model input requires values for mobile (fracture) porosity and immobile (matrix) porosity. Three values have been used for the mobile fracture porosity. The first two values are 3% for layer 1 and 1% for layers 2 to 5. These are commonly used for fracture porosity in the Chalk and are perceived specific yield values derived from pumping tests. The third value used is 0.1%, one tenth of the usual value, and which has been derived through tracer testing at the Lower Venson Farm site (Section 5.5.2). This also links to observations (Bourke *et al.* 1985) that only approximately one tenth of

a fracture is available for the transport of solutes due to the effects of channelling, discussed previously in Section 5.3.3.

The values used for porosity of the immobile domain (in this case the matrix porosity) are derived from porosity measurements made on the core material from BGS LVV (Section 5.2.3). An average value relevant to each model layer is used, see Table 6-9.

Dispersion:

The model does not explicitly represent fractures hence the dispersivity term is used to represent the degree of spreading of the plume that the fracture pattern would be expected to produce. MT3DMS requires dispersivity values for each cell and layer for longitudinal, transverse and vertical directions. Previous modelling work by Bibby (1979) required large dispersivities (α_L – 120 m, α_T – 60 m, see Table 6-1) in order to match observed solute distributions. The approach in the current research has been to use a single value for all cells and layers and to alter it by orders of magnitude between model runs. This is to assess the sensitivity of the model results to the parameter. For most of the model runs a ratio of 1: 0.1: 0.01 has been used for α_L: α_T: α_V.

Diffusion:

An average value of the Effective Diffusion Coefficient from the range 0.53 to 3.2 m^2s^{-1} observed by Hill (1984) has been used (see Section 2.4.3 and Appendix 2).

Mass transfer coefficient:

The calculation of the mass transfer coefficient was undertaken using the approach of Barker (1985a), van Genuchten and Dalton (1986) and Sudicky (1989). These authors have shown that the first order mass transfer approach adopted by MT3DMS can be used to approximate the movement of solute between mobile and immobile domains for idealised systems at longer times. Van Genuchten and Dalton (1986) demonstrate that for idealised slab geometry:

$$\zeta = \frac{3\theta_{im} D^*_{im}}{B^2}$$

Equation 6-6

Where

ζ mass transfer coefficient [T^{-1}]

θ_{im} immobile domain porosity

D^*_{im} effective diffusion coefficient for solute in immobile domain [L^2T^{-1}]

B slab half-thickness [L]

Values used in the solute transport model are given in Table 6-8.

Table 6-8 Mass transfer coefficient values calculated for dual porosity solute transport model

Model Layer	Half-block thickness (m)	Immobile porosity (%)	Effective diffusion coefficient x 10^{-5} (m^2d^{-1})	Mass transfer coefficient (d^{-1})
1	0.36	44.7	1.61	1.65×10^{-4}
2	1.16	42.5	1.61	1.52×10^{-5}
3	1.88	40.2	1.61	5.51×10^{-6}
4	2.34	40.3	1.61	3.53×10^{-6}
5	5.83	37.2	1.61	5.28×10^{-7}

All parameter values used and runs undertaken with the solute transport model, representing a total of 8 model scenarios, are given in Table 6-9.

Table 6-9 Solute transport model runs and parameter values

Model run	Porosity		Dispersivity	Mass transfer coeff.
	θ_{mo}	θ_{im}	α_L; α_T; α_V	d^{-1}
Scenario 1 Dual porosity, low dispersivity. Fracture porosity is 'high' – based on specific yield	L1 – 3% L2-5 – 1%	L1 – 44.7% L2 – 42.5% L3 – 40.2% L4 – 40.3% L5 – 37.2%	2: 0.2; 0.02	L1 - 1.65×10^{-4} L2 - 1.52×10^{-5} L3 - 5.51×10^{-6} L4 - 3.53×10^{-6} L5 - 5.28×10^{-7}
Scenario 3 Single porosity, low dispersivity	L1 – L5 15%		2; 0.2; 0.02	n/a
Scenario 4 Single porosity, high dispersivity (in Appendix 6)	L1 – L5 15%		225; 22.5; 2.25	n/a
Scenario 5 Dual porosity, high dispersivity Fracture porosity is based on specific yield	L1 – 3% L2-5 – 1%	L1 – 44.7% L2 – 42.5% L3 – 40.2% L4 – 40.3% L5 – 37.2%	225; 22.5; 2.25	L1 - 1.65×10^{-4} L2 - 1.52×10^{-5} L3 - 5.51×10^{-6} L4 - 3.53×10^{-6} L5 - 5.28×10^{-7}
Scenario 6 Dual porosity, low dispersivity, low fracture porosity	L1-L5 – 0.1%	L1 – 44.7% L2 – 42.5% L3 – 40.2% L4 – 40.3% L5 – 37.2%	2; 0.2; 0.02	L1 - 1.65×10^{-4} L2 - 1.52×10^{-5} L3 - 5.51×10^{-6} L4 - 3.53×10^{-6} L5 - 5.28×10^{-7}
Scenario 7 Dual porosity, low dispersivity, low fracture porosity Mass Transfer Coefficient increased in all layers by one order of magnitude (in Appendix 6)	L1-L5 – 0.1%	L1 – 44.7% L2 – 42.5% L3 – 40.2% L4 – 40.3% L5 – 37.2%	2; 0.2; 0.02	L1 - 1.65×10^{-3} L2 - 1.52×10^{-4} L3 - 5.51×10^{-5} L4 - 3.53×10^{-5} L5 - 5.28×10^{-6}

Model run	Porosity		Dispersivity	Mass transfer coeff.
	θ_{mo}	θ_{im}	α_L; α_T; α_V	d^{-1}
Scenario 8 Dual porosity, low dispersivity, low fracture porosity The fracture density depth relationship is varied to reduce the block-size for layer 4	L1-L5 – 0.1%	L1 – 44.7% L2 – 42.5% L3 – 40.2% L4 – 40.3% L5 – 37.2%	2; 0.2; 0.02	L1 - 1.65×10^{-4} L2 - 1.52×10^{-5} L3 - 5.51×10^{-6} L4 – 7.77×10^{-5} L5 - 5.28×10^{-7}
Scenario 9 Dual porosity, dispersivity 2 m α_L; α_T; α_V, low fracture porosity (in Appendix 6)	L1-L5 – 0.1%	L1 – 44.7% L2 – 42.5% L3 – 40.2% L4 – 40.3% L5 – 37.2%	2; 2; 2	L1 - 1.65×10^{-4} L2 - 1.52×10^{-5} L3 - 5.51×10^{-6} L4 - 3.53×10^{-6} L5 - 5.28×10^{-7}

Solution Scheme:

The standard finite difference method with upstream weighting was used for the advection solution method with the generalized conjugate gradient solver package (Zheng 2002). This combination provided the most stable solution scheme.

Results

Plots of the modelling results from 5 of the 8 model scenarios (detailed in Table 6-9) are presented in the following section (the results from the remaining three model scenarios are provided in Appendix 6).

The aim of the model scenarios is to provide results that can be compared for different conceptual representations and parameter values. These comparative conceptual representations include dual porosity versus single porosity, changes in fracture density with depth, hence altering the value of the mass transfer coefficient. Model sensitivity to variation in parameter values such as dispersivity and fracture porosity is also explored. By comparing the results from these model scenarios it is possible to highlight, and to develop guidance on, the parameters and concepts that have the greatest control over solute transport at the scale of interest. This in turn may provide a particular direction or focus for field investigations in order to provide data for key parameters for solute transport models in the Chalk. Model results are presented for each scenario at two time periods. These times were selected for the availability of field observations for comparison: 1977 when the SWA investigation data is representative and 1999 when the most recent field research took place. Contours of predicted chloride concentration are presented in plan and cross section. The minimum contour used to delineate the outer margin of the injected solute is 150 mg/L. Generally the plan is of chloride concentration contours for layer 1, although occasionally layer 2 is used when the layer 1 concentrations have reduced such that no meaningful contours are present. For the model scenarios providing dual porosity results, all chloride concentrations are for mobile fracture water. Currently MT3DMS reports only a total immobile fraction concentration for the entire model domain. It does not report the immobile water concentrations as an average for each grid cell, for example. This is a significant disadvantage of the current code in its application to the Chalk aquifer and it is being remedied in the next version (*pers comm.* Chunmiao Zheng, author MT3DMS).

No calibration of the solute transport model was undertaken. The objective of the solute transport modelling was to observe solute transport model predictions, accepting that the flow model now provides the flow regime for an improved conceptual model. The results from runs using varying dispersivity values are compared to assess the sensitivity of the model to these parameters in comparison to its sensitivity to features such as dry valleys represented by higher hydraulic conductivity.

It is useful to compare the model predictions for the various scenarios to the fracture water concentrations measured during the field investigations, given that no calibration of the solute transport was undertaken. Rather than produce overly cluttered diagrams the chloride concentrations predicted by the MT3DMS modelling for each of the scenarios discussed below are presented in Table 6-10 with the fracture water chloride concentrations measured during the field investigations for comparison.

Table 6-10 Comparison of MT3DMS fracture water chloride concentrations to observations during packer testing at Lower Venson Farm, for 1999.

Model Layer	Scenario 1 Cl mg/L	Scenario 3 Cl mg/L	Scenario 5 Cl mg/L	Scenario 6 Cl mg/L	Scenario 8 Cl mg/L	Observed Cl mg/L
1	780	119	612	658	663	1100
2	375	1425	590	365	420	1100
3	190	1000	570	160	375	1140
4	140	1200	580	82	550	1156
5	140	15	590	44	175	800

It is important to remember that the MT3DMS fracture water chloride concentrations represent an average value for a 250 m by 250 m x layer-thickness Chalk block, whereas the samples derived from the packer testing are local to the borehole. The sensitivity of the predicted chloride concentration to the MTC is highlighted by comparing the fracture water chloride concentrations for Scenario 6 and 8. These Scenarios have the same parameter values, except that in Scenario 8 the block-size is reduced in Layer 4. This has a significant impact on the Layer 4 concentrations, as well as on the chloride concentrations predicted for the other layers. This suggests that relatively minor changes to parameter values such as the mobile porosity and the MTC may have a significant impact on the predicted concentrations. Scenario 3 has the highest predicted chloride concentrations and this is due to the Scenario using a single porosity approach. The single porosity approach does not allow any attenuation of the

chloride by diffusion into the matrix porewaters. Detailed analysis of each Scenario is provided below.

Model Scenario 1

Model scenario 1 uses MT3DMS's dual porosity capability with a low dispersivity (α_L = 2 m) and a fracture porosity value based on the Chalk specific yield (θ_{mo} layer 1 = 3%). Figure 6-25A presents the results for Stress Period (SP) 10, equivalent to 1977, as a plan view of the layer 1 chloride concentrations. This can be compared to the SWA 1977 interpretation of field observations provided in Figure 6-25B. In the MT3DMS prediction the injected solute splits vertically into two components. An upper component remains in layer 1 and travels relatively rapidly towards the North and South Stream springs. A second component moves vertically into layer 2 and deeper. This lower component is then split again. One part moves relatively rapidly along layers 3 and 4 and the other sinks into layer 5. It remains in layer 5, moving predominantly by diffusion throughout the period modelled.

The cross section for SP10 (1977) is a good representation of the trend of fracture water chloride concentrations as interpreted by Headworth *et al.* (1980) from fracture water sampling (Figure 2-14), however the absolute chloride concentration values do not match particularly well for the higher chloride concentrations closer to the disposal lagoon source.

Figure 6-26 presents the results at SP53 (1999). The fracture water chloride concentrations predicted by the model do not correspond well to those observed during packer testing and groundwater sampling in 1999 (Table 4-6). Overall, the model predicted chloride concentrations are lower than those observed. The distinct reduction in solute concentration in the porewaters observed in BGS LVV (Section 5.5.1) at a depth of 28 m aOD, *i.e.* equivalent to the top of layer 2, requires the high concentration part of the modelled plume to remain in layer 1.

This is not demonstrated by the model, where instead the plume is distributed across both layer 1 and 2. It seems likely that a greater barrier to flow, through reduced vertical conductance such as would be produced by marl horizons, is required at the layer 1 / 2 interface. However, it is still necessary to allow vertical movement of solute to deeper layers below the disposal lagoons, so a mechanism that allows this is required

within the model. This could be provided by 'high conductance windows' along the layer 1 / 2 interface which would represent thinning of lithologies or changes in properties laterally (Mortimore and Pomerol 1991), such that the hydraulic properties are more conducive to vertical movement. Vertical fractures also provide a mechanism that allows for fluid movement across several layers at intervals, rather than across the entire layer interface. Movement or reactivation along existing features in underlying strata (Mortimore and Pomerol 1991) could produce such large, cross-layer cutting fractures. This is particularly relevant in the vicinity of the disposal lagoons where features in the underlying Carboniferous strata are known (Figure 5-5).

The model simulates solute movement in an alignment further to the east of the main Tilmanstone - Eastry valley and this feature was observed during the SWA 1977 observations. This suggests that the observation boreholes in the main Tilmanstone-Eastry valley may not be situated along the main axis of the chloride plume. Lateral movement was also observed during the tracer test from BGS LVV to BH3 (Section 4.6.2). The upstream lateral spread of a secondary plume into the main South Stream valley, as suggested by observations made during the SWA 1977 investigations, is however not reproduced by the model. No movement of solute to these most southerly springs is observed in the model predictions. Unfortunately no recent field observations are available to verify the current occurrence of solute in this adjacent valley.

Model Scenario 3

This model scenario uses the same dispersivity values as model scenario 1, but is run using single porosity to investigate how well single porosity processes are able to represent the movement of solute in the Chalk. A porosity of 15% was chosen as it is much lower than would be appropriate for a porous medium. This therefore attempts to represent rapid movement through fractures yet allows for some retardation of the solute. This value has been used previously in Chalk solute transport modelling studies (Travers Morgan 1994).

The single porosity model produces greater lateral movement of the solute. The results for SP10 (1977), Figure 6-27, show a close match to the SWA observations at this time. The effect of using a single porosity with a high dispersivity is to provide a simulation of rapid flow paths along fractures, such as the orthogonal fracture sets (Section 5.2.2).

This produces transverse movement of the solute, and there is no diffusion into the matrix porewater to reduce fracture water solute concentrations.

However the single porosity means that in layer 1 the solute moves through the aquifer too rapidly with only low concentrations of solute remaining around the North and South Streams by SP53 (1999), (Figure 6-28 A and B).

In contrast, layer 2, which has a lower hydraulic conductivity than layer 1, still contains a large plume of solute. The fracture water concentrations predicted by the model are higher than those observed during packer test sampling. This is because the hydraulic properties assigned to this layer have slowed the movement of the plume compared to layer 1, producing a plume similar to that observed, but the lack of the dual porosity mechanism means that no attenuation through delayed storage of solute in the immobile matrix porewater is occurring.

This model scenario produces a vertical fracture water profile for SP10 (1977) similar in shape to that of the matrix porewater profile at BHB at a similar time (Figure 6-27 B). However, the results show a peak in layer 2 rather than at the top of the profile as observed on BHB. The model results are for the fracture water and so are not readily comparable to the BHB porewater concentrations, however the model concentrations do compare favourably to those in the interpretation of fracture water and porewater concentrations in Headworth *et al.* (1980) (Figure 2-14). The cross-section for SP10 (1977) (Figure 6-27 B) demonstrates the early distribution of the plume into two layers. This '2-layered' plume develops because the single porosity allows the rapid movement of the injected solute to deeper levels. In contrast, model scenario 1 has the dual porosity process active and restricts the downward migration by attenuating the solute through diffusion into the immobile matrix water. The results from model scenario 3 support the existence of vertical pathways to allow solute to move to the more transmissive layer 4 (representing the Dover Chalk Rock sequence, (Figure 6-17 and Table 6-4) with only limited attenuation occurring.

Model scenario 5

The purpose of this model scenario is to test the sensitivity of the model results to the dispersivity values used. The α_L value is increased by 2 orders of magnitude from 2 m to 225 m. The α_L: α_T: α_V ratio is maintained at 1: 0.1: 0.01. The increased dispersivity

value does not significantly influence the width of the plume (using the 150 mg/L contour as a guide), as shown by comparison of Figure 6-29 with Figure 6-25. This is surprising considering that the dispersivity has increased by 2 orders of magnitude, but demonstrates the ability of the immobile domain water to attenuate the solute concentration of the fracture water. The most noticeable effect of the increased dispersivity is the reduction in the solute concentrations predicted by the model in the centre of the plume at SP10 (1977).

Fracture water concentrations are approximately 250 mg/L lower than those predicted by model scenario 1. As well as the increased mass of solute transferred into the immobile domain due to the increased volume of matrix the plume comes into contact with, through the increase in α_L and α_T, the reduced concentrations in layer 1 also arise due to a greater vertical movement of solute, with the vertical dispersivity α_V = 2 m compared to 0.02 m in model scenario 1. A higher concentration solute plume develops at depth in layer 5 in model scenario 5 (Figure 6-29 B) compared to model scenario 1 (Figure 6-25 B). The solute in layer 5 is then able to disperse more rapidly than in model scenario 1. The higher dispersivities used in model scenario 5 cause the solute plume to be more evenly distributed through all the model layers. The porewater concentration profile observed at BGS LVV (Figure 4-28) would not be consistent with the fracture water solute distribution (Figure 6-30).

The results from model scenario 3 (Figure 6-27), where the single porosity allowed the plume to move vertically downwards, suggested that rapid vertical movement was an important feature allowing transport of chloride towards deeper, more transmissive layers, beneath the disposal lagoons. It seems that this is still the case, but that using a high vertical dispersivity for its representation, such as in model scenario 5, does not achieve the movement required. The dual porosity attenuation in layers 2 and 3 prevents the plume from rapidly reaching layer 4. The plume is strongly attenuated by the lower layers as the block sizes are larger and, coupled with the lower hydraulic conductivity, movement is mainly through diffusion at these greater depths. This again suggests that vertical fractures cutting across several lithologies must be present to allow the movement of solute through to the deeper, transmissive, layers beneath the disposal lagoons. The minewater infiltration lagoons provide a head to drive the flow to deeper layers during their operation.

The fracture water chloride concentrations predicted for SP 53 (1999) (Figure 6-30) are similar to those observed during groundwater sampling (Section 4.7.1). However the overall shape of the plume does not resemble that proposed from the observed fracture water and matrix water profiles and this seems to be mainly due to the smoothing effect of the high dispersivity value used and the further attenuation afforded by the diffusion into the matrix.

Model Scenario 6

Model scenario 6 is a dual porosity model run in order to assess the effect on solute movement of using lower fracture porosity. It repeats model scenario 1 but with a lower fracture (i.e. effective) porosity of 0.1%. This is the value calculated from the tracer test undertaken between BGS LVV and BH3 at the Lower Venson Farm site (Section 5.5.2). All other model parameters are the same as for model scenario 1 (α_L = 2 m). Model scenario 1 therefore provides the baseline for comparison. The lower fracture porosity produces a wider plume, with concentrations at the centre lower by approximately 200 mg/L (Figure 6-31) compared to model scenario 1 (Figure 6-25).

Decreasing the mobile porosity value has a stronger effect on the fracture water concentrations than increasing the dispersivity value. In the longer term, by SP53 (Figure 6-32), compared to model scenario 1 (Figure 6-26) the modelled concentrations still differ by approximately 150 – 200 mg/L and the plume is still wider, approximately 2750 m compared to 2250 m at its maximum width, for model scenario 1.

The cross-section for SP53 (Figure 6-32 B) shows that solute concentrations above 150 mg/L (the outer boundary limit used for contouring) are restricted to the upper 3 layers in the model. In model scenario 1 at this time layer 5 (Figure 6-26 B) still contained fracture water concentrations of 450 mg/L.

Model scenario 8

The purpose of model scenario 8 is to assess the impact of reducing the block-size in layer 4. Observations of hydraulic conductivity from single borehole dilution tests and packer testing (Section 5.3.3) combined with geophysical logging results (Section 5.3.2) indicate that this level within the aquifer is more transmissive. The lithological log (Section 5.2.1) also shows that this horizon is approximately 4 m thick and Mortimore

et al. (1990) record extensive fracturing of this unit. The observed porewater solute concentrations at BGS LVV (Section 5.5.1) suggest rapid movement of solute in this layer with less attenuation than in other layers. These observations are indicative of a well fractured transmissive unit. This is in conflict with the 4.68 m block-size calculated for this level from Bloomfield *et al.* (2000) fracture-density depth relationship which would require a single large fracture to dominate the flow, where there is no evidence of this in the fracture logs of the borehole. Model scenario 8 explores this issue by reducing the block-size to 1 m and thus increasing the mass transfer coefficient. Solute is able to move more rapidly through layer 4 and this is demonstrated by the predictions for SP10 (Figure 6-33).

The cross-section shows the plume dividing into two plumes: one in layer 1 and a second in layer 4. This division is retained through to SP53 (Figure 6-34).

Such a geometry of fracture water concentrations is necessary for consistency with the matrix porewater chloride concentration profile observed in BGS LVV (Figure 5-24), although the fracture water chloride concentrations predicted by model Scenario 8 are lower than those observed from sampling during packer testing (Table 4-6) as the predicted plume in layer 4 has not moved along the valley rapidly enough to raise fracture water concentrations, and hence porewater solute concentrations, at the Lower Venson Farm site, by SP53.

6.4.4 Discussion of regional solute transport model results

Modelled predictions versus observed solute concentrations

The development of a numerical model based on the observed, detailed, hydrostratigraphy produces a flow regime that can broadly reproduce the long term solute movement observed at the regional scale in the Tilmanstone – Eastry valley between 1977 and 1999. The results from model scenario 8 (Figure 6-33 and Figure 6-34) are particularly well matched to observations of plume geometry. It is this scenario in which the effects of dual porosity are believed to be most realistically incorporated.

Effect of infiltration from lagoons

The solute transport model results demonstrate the importance of realistic and accurate simulation of early stages of advective transport, due to the recharge mound created by the minewater lagoons, within layer 1. This effect diminishes only gradually once use of the lagoons ceases, and the plume centre (representing solute in the mobile groundwater in fractures) subsequently moves less rapidly, with transport still moved forward by advection but dominated by diffusion. This is emphasised in successive, deeper layers where the mass transfer coefficient accounts for the increased block size and therefore a greater capacity for attenuation. The large aperture size used in Bibby's model (9 mm) was unrepresentative and produced more rapid movement of the solute with insufficient diffusion into the matrix. The 2-D geometry of Bibby's model could not accommodate the development of the vertical gradients created by the recharge mounds from the lagoons and this in turn also resulted in a more rapid horizontal movement of solute than in reality.

Representation of porosity

The solute transport model results highlight the inadequacy of using models with single porosity to represent the dual porosity processes that clearly operate in the Chalk aquifer. The single porosity model scenario predictions (model scenario 3 and 4) both allow the solute to move horizontally through the upper layers of the aquifer too rapidly and there is no mechanism to represent the attenuating capacity of the Chalk matrix, in the manner attributable to matrix diffusion. However, using a single porosity approach for some model runs has been important in order to highlight the requirement for a mechanism that allows solute to move rapidly downwards beneath the disposal lagoons, with minimal attenuation, to a more transmissive layer. The possibility of the density of the infiltrating saline minewaters being responsible for this is dismissed by FRACFLOW (1999). The porosity evaluation has also emphasized the way in which different transport processes have dominated the movement of solute at different times in the history of the plume.

Dry valley and interfluve contrasts

The effect on solute movement of including dry valleys as high hydraulic conductivity cells along the valley axes is unclear. The groundwater flow model did not demonstrate any marked change in gradient due to the dry valley / interfluve contrast and this has been carried through in the solute transport simulations. Neither the dual or single

porosity scenarios predict plumes that are obviously constrained by the dry valleys, but instead the predicted plumes cut across the main valley orientation, towards the discharge points on the North and South Streams. This may be due to using too low a contrast in hydraulic conductivity between valley and interfluve areas in the model. However the lack of observation boreholes in the interfluve areas limits justification for the further calibration of the flow model in order to produce a groundwater gradient distribution that emphasises the valleys and interfluves. It is also important to note the observations made in 1977 (Figure 4-26) which indicate a wide lateral extent to the plume, with no strong influence over the lateral extent by the dry valleys. FRACFLOW (1999) observed fracture orientations which would tend to increase the transverse spread of the plume and this was also demonstrated by the movement of tracer during tests (Section 5.5.2). This illustrates the importance of understanding the influence of fracture orientation on solute movement and being able to represent fracture orientation within a model, particularly where predictions for solute transport are required. It may be that field measurements of hydraulic conductivity indicate a large contrast in value between valley and interfluve areas but fracture orientation and connectivity may have a dominating effect over solute transport.

Dispersivity

The modelling has not demonstrated a strong effect on the plume shape by varying the dispersivity over two orders of magnitude. A reduction in predicted concentrations at the centre of the plume was predicted at a higher dispersivity. Changes to the fracture porosity had a greater impact on the predicted shape of the solute plume and the fracture water concentrations than altering the dispersivity. The attenuating effect of diffusion into the matrix porewaters had a stronger influence over the solute movement than the dispersivity, as described by Barker (1993), see Section 2.4.3. Model Scenario 3 adopts a single porosity approach with a low dispersivity and this predicts a plume distribution at early times that achieves a relatively good match to observed concentrations. However at later times the match between model predictions and observations is poor due to the absence of the type of attenuation afforded by matrix diffusion. Scenario 5 investigates the effect of increasing the dispersivity by two orders of magnitude. The main impact of this is the effect of the larger vertical dispersivity which allows the solute to move more rapidly to deeper layers in the model. This effect is considered to be similar to the impact anticipated from vertical fracturing across Chalk layers.

Recharge distribution

The model was set-up with considerable attention being paid to the recharge distribution, both seasonally and spatially. However the influence of the seasonality of recharge is not clear and requires further work and analysis. This would include comparing blanket application of recharge with seasonally and spatially distributed recharge as well as detailed analysis of model predictions to determine trends arising from the recharge distribution used.

Parameter values for mass transfer coefficient calculation

The mass transfer coefficient approach of MT3DMS relies on having data suitable for inclusion in Equation 6-6. Diffusion coefficients appropriate for the Chalk (see Appendix 2) are available, and Chalk porosity data are widely available (Allen *et al.* 1997, Bloomfield 1995). The more problematical parameter is the block-size, which can have an important impact on model predictions as demonstrated in model scenario 8 (this is discussed further in Chapters 7 and 8).

Model cell drying and re-wetting

The development of the regional flow model, through its steady state and transient stages, followed by developing and running the solute transport model was very time consuming. Problems arose with the flow model due to cells drying out as the water table fell below the layer base during summer months. Observation borehole hydrographs indicate that the drying of certain horizons near the North Downs does occur in summer months, so the model is replicating field observations, but this leads to instability in the convergence of the model when the cells resaturate after winter recharge. It is difficult to suggest a way to avoid this effect if attention is being paid to a hydrostratigraphy developed through field observations. Within the context of this research moving of some model boundaries and adjusting of layer base elevation in problematical areas of the modelled domain resolved the instability difficulties. The areas affected were approximately 9 km away from the Tilmanstone – Eastry valley and over this distance there is no impact on flows in the area of interest.

Model instability and convergence

Difficulties were also encountered with instability and convergence in the solute transport model. One of the reasons for the instability arose from including a background concentration in the aquifer and in recharge of 30 mg/L chloride. The

injected solute concentrations representing the lagoon disposal are three orders of magnitude higher than these background concentrations so it was considered acceptable to ignore the background concentrations of chloride. As most of the model domain was not impacted by the lagoon disposal it was not necessary to include a background concentration across the entire model domain that caused problems with model convergence. However, this may not be an appropriate route to take if convergence problems occur when the ratio of pollutant to background concentrations is not so large as those experienced in the Tilmanstone-Eastry valley. Further improvements to model convergence and running times were made by increasing the transport time steps and using the generalised conjugate gradient solver package (Section 6.4.3).

6.4.5 Predictions of concentration to 2074

The DP1D model was used to predict future solute movement in the Tilmanstone – Eastry valley. The model time-frame was extended to 2074, 100 years after the end of operation of the minewater lagoons. Composite vertical profiles of chloride in the aquifer to this date at BHB, Lower Venson Farm and the North Stream are presented in Figure 6-35.

The plots of solute concentration over time presented in Figure 6-4, Figure 6-5 and Figure 6-6 continue to 2074 and show the predicted concentrations with depth at the three sites. Plots of along flow-line solute concentrations at 2074 are given in Figure 6-36. Figure 6-36 demonstrates that the model predicts the main source of solute emanating at the North Stream in 2074 will be derived from depths of 30, 40, 50 and 70 m bGL (fracture water chloride concentrations are approximately 1168 mg/L, 570 mg/L, 280 mg/L and 238 mg/L respectively). The chloride concentration at 30 m bGL depth at the North Stream is decreasing by this time, although at 40, 50, 60 and 70 m bGL the chloride concentration is still increasing.

6.5 Discussion of all modelling

The regional flow modelling undertaken using MODFLOW shows that the Tilmanstone - Eastry valley may not be orientated along the main direction of groundwater flow and hence of solute transport. This means that the assumption used in DP1D to locate the flow-line for the valley from the lagoons to the North stream springs may be incorrect.

The modelling indicates a requirement to represent vertical pathways within dual porosity models and fracture orientations where these have a strong effect on groundwater flow, such as in the Chalk.

The use of detailed lithological observations combined with measurements of hydraulic conductivity to guide the choice of hydrostratigraphic layers and allocation of parameter values is broadly supported by the results of the model runs. Constraint of solute movement within certain layers, as observed in the field, is reproduced in the model, with some limitations. The movement of solute to deeper more transmissive layers in the Chalk, beneath the disposal lagoons, with minimal attenuation has not been successfully replicated in the dual porosity model scenarios. This is because no rapid pathways, such as fractures that cut across several lithologies or Chalk layers, are included. Furthermore, the attenuating capacity of the matrix is high, so any downward movement of solute is constrained by diffusion into the matrix porewater. This process is enhanced because the downward velocity is slow. The single porosity Scenario 3 predicts the best plume profile in terms of producing higher chloride concentrations at depth because the diffusive process is not operating. These results indicate that it may be necessary to use a model that can explicitly represent fractures to adequately model solute transport in the Chalk.

The assumption in the DP1D model that all chloride was immediately available at each layer or level in the Chalk beneath the source region, is supported by the perceived need for vertical pathways to be available in the regional numerical model for rapid flow to deeper layers within the aquifer (Section 6.4.4, e.g. model scenario 3). By this assumption, DP1D accommodated the vertical movement that could not be so readily incorporated into the regional 3D model. However, DP1D is not able to represent variability in the flow regime, so is restricted to making predictions for a steady-state flow regime.

Run time for the DP1D model is much shorter than for the regional 3D model and the input files are considerably simpler to set up. The regional flow model took approximately 1 to 2 hours to run and the solute transport model took a further 2 hours for each scenario. The DP1D model runs take approximately 20 seconds, depending on the number of observation points and the length of time modelled.

The parameter requirements of DP1D are similar to those for the 3D model – the problematic parameters of matrix block-size and fracture aperture are necessary and a groundwater velocity is required. The latter two parameters ideally require local data from tracer tests to constrain their values.

6.5.1 Fickian diffusion versus the mass transfer coefficient or QSS approach

General comments and concepts

One of the aims of the modelling was to compare the results from a Fickian diffusion and a first order mass transfer coefficient (MTC) approach. As discussed in Chapter 2, the description of the diffusion process by a Fickian approach (the method used in DP1D) is more accurate, particularly at early and late times, than the approximation used by MT3DMS. The predictions made by the MTC approach and Fickian diffusion converge as a steady-state condition between fracture and matrix porewater solute concentrations is attained (Barker 1985a). At early times the MT3DMS approach will over-estimate solute concentrations in fracture water by underestimating the diffusive flux into the immobile matrix porewater domain. The rate of transfer from the mobile to immobile domain is too slow as it does not account for the infinitely steep concentration gradient that initially exists at the mobile / immobile interface. The MTC approach will therefore predict a solute plume to have moved further than that modelled using the Fickian exchange approach. When the concentration gradient is reversed and the movement of solute is from the immobile to the mobile domain, the reverse will be the case such that the transfer of solute back into the mobile groundwater in the fracture system will be slower than predicted by a Fickian approach. The difference in the rate of transfer between the two domains by the alternative approaches will also result in the persistence of the contamination being predicted differently.

An indication of whether the system is likely to approach a steady-state within the time frame of interest can be given by calculating the time for diffusion across a matrix block, $time = x^2/D$ (Barker 1993). If the system is likely to achieve a steady-state well within the time frame for which predictions are required then it is reasonable to model it using a MTC approach. However if accurate predictions are required for relatively early or late times, a Fickian approach is recommended.

A direct comparison of predictions by the two approaches is not possible due to the dimensional difference between the models used and the lack of porewater concentrations reported by MT3DMS. However, a comparison of fracture water chloride concentrations predicted by MT3DMS with the fracture and matrix porewater chloride concentrations predicted by DP1D has been made for two sites (BHB and Lower Venson Farm) and is presented in Figure 6-37 and Figure 6-38.

The predictions for chloride concentration in fracture water at 70 m bGL (equivalent to the Dover Chalk Rock sequence) are similar for both MT3DMS and DP1D models. The profile produced from the MT3DMS predictions is smoothed compared to the DP1D profile. This is due to the MT3DMS model only having 5 layers whereas the DP1D profile is made up of values calculated at 10 m intervals.

Considerations for the Chalk

The Tilmanstone plume is exceptional in the UK in terms of the duration of solute input and the extent of the resultant solute plume. However the mechanisms operating in the Chalk at Tilmanstone that have attenuated the concentration peak, but extended the duration of the residence time of the solute, are applicable in any Chalk aquifer and any similar dual porosity medium. The forward predictions by the DP1D modelling (Section 6.4.5) demonstrate the continued presence of chloride in the aquifer at significant concentrations over the next 75 years. It is fortunate that the concentrations that will be entering the North and South streams will be diluted and any impact on the freshwater ecosystems of these receiving waters will be minimal. An estimate of the chloride concentration of the water in the upper part of the North Stream can be made from the DP1D model output. Because the flow in the North Stream comprises a number of elements including Chalk baseflow (with the high chloride plume) and discharge from Eastry waste water treatment works (WWTW), the chloride concentration is predicted to be approximately 100 mg/L in 2074 (see Table 6-11 for an estimation of the percentage contribution to the total chloride concentration from individual DP1D model layers).

Table 6-11 Estimate of percentage contribution of each DP1D layer to the total chloride in the North Stream in 2074.

DP1D layer	Flux md^{-1}	Vol[1] m^3d^{-1}	Fracture water concentration mg/L	Mass of Chloride gd^{-1}	Contribution %
1	0.003	42.6	30	1278	1
2	0.004	65.7	34	2234	1
3	0.004	65.7	1168	76738	35
4	0.005	76.7	570	43691	20
5	0.005	76.8	280	21504	10
6	0.001	15.3	30	459	0
7	0.007	110.6	238	26311	12
All other flow[2]		1500	30	45000	21

Notes
[1] Assumes contributing width of plume of 1500 m.
[2] Estimate of flow at Hacklinge is 2100 m^3d^{-1} (NRA data) and estimate of Eastry WWTW discharge is 720 m^3d^{-1}, based on an estimated population of 4500 using 160 l/h/d.

6.6 Summary

Two questions should be addressed for the Chalk, to determine whether taking an MTC approach to modelling the movement of solute is appropriate:

- What are the Chalk block sizes encountered along the flow line taken by the solute and is the time-frame of interest large enough for steady-state to be approached for these block sizes?
- How accurate do the predictions for concentration need to be when the system is not approaching steady-state?

For a small scale or short term spill or tracer test it is unlikely that the MTC approach will provide suitable accuracy to predict the impact on groundwater quality and a Fickian diffusive approach is more appropriate. However for larger scale, longer term pollution, such as that from diffuse agricultural sources, the MTC approach may be adequate. It is reported by Barker (1993) that the MTC method is used by the Water Research Centre's (WRc) nitrate model (ANNA). In terms of the role for the MT3DMS software within the context of the WFD, it would seem to have the most potential for use in developing action plans or programme of measures and assessing the effectiveness of those programmes of measures. It will be useful for determining the likely impacts on downstream ecosystems and assessing the effectiveness of remedial or containment options in the longer term.

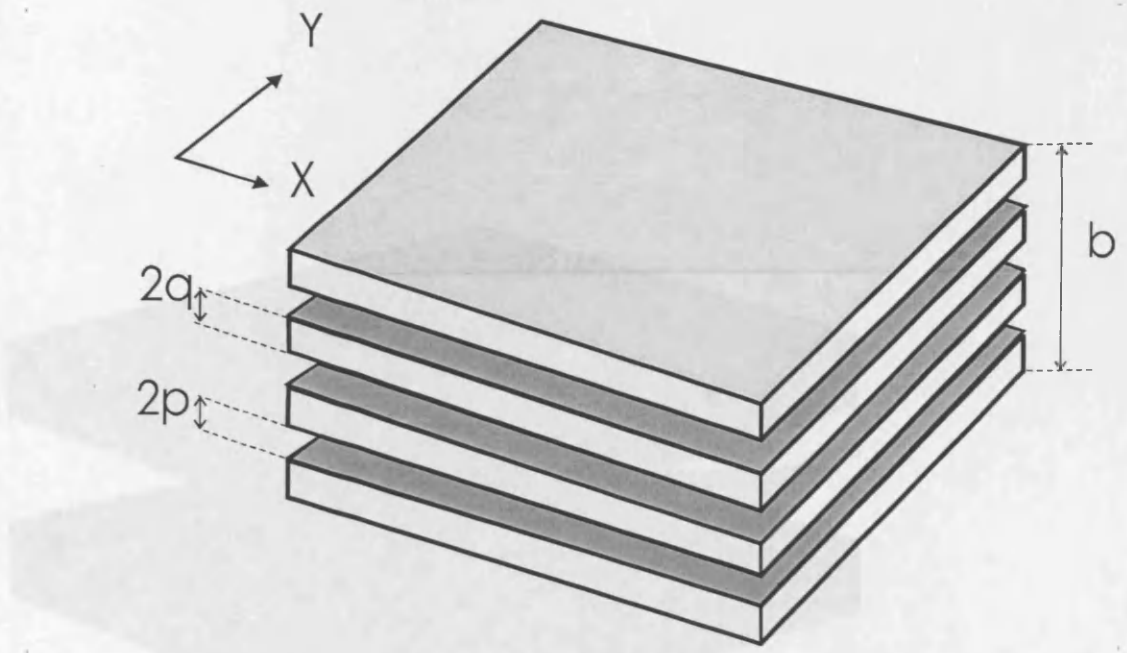

Figure 6-1 Parallel plate model used by Bibby illustrating the relationship between fracture aperture and matrix block thickness.

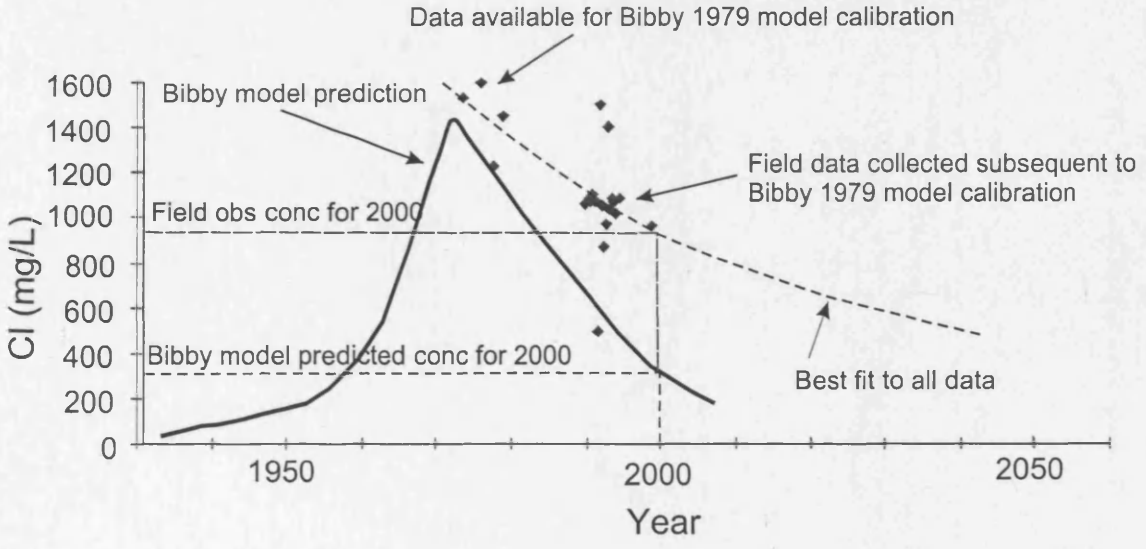

Figure 6-2 Model predictions and observations (*after* Bibby 1979).

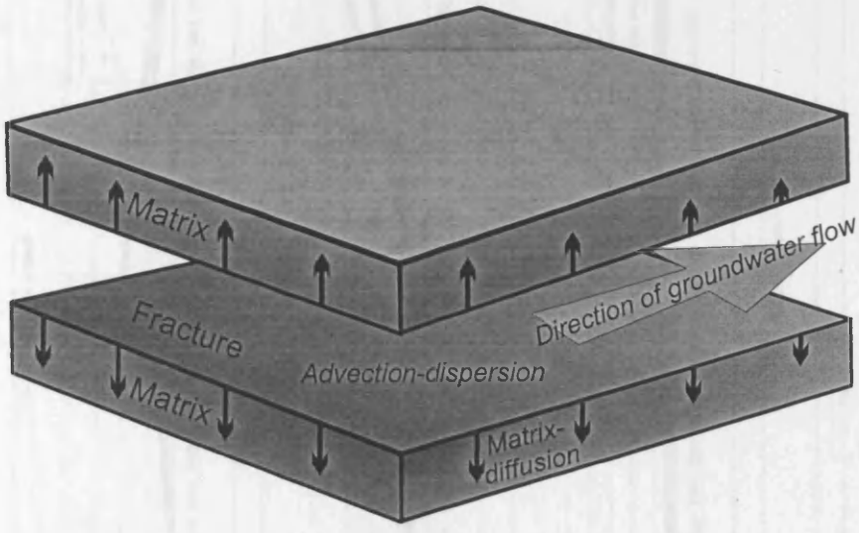

Figure 6-3 DP1D matrix block geometry.

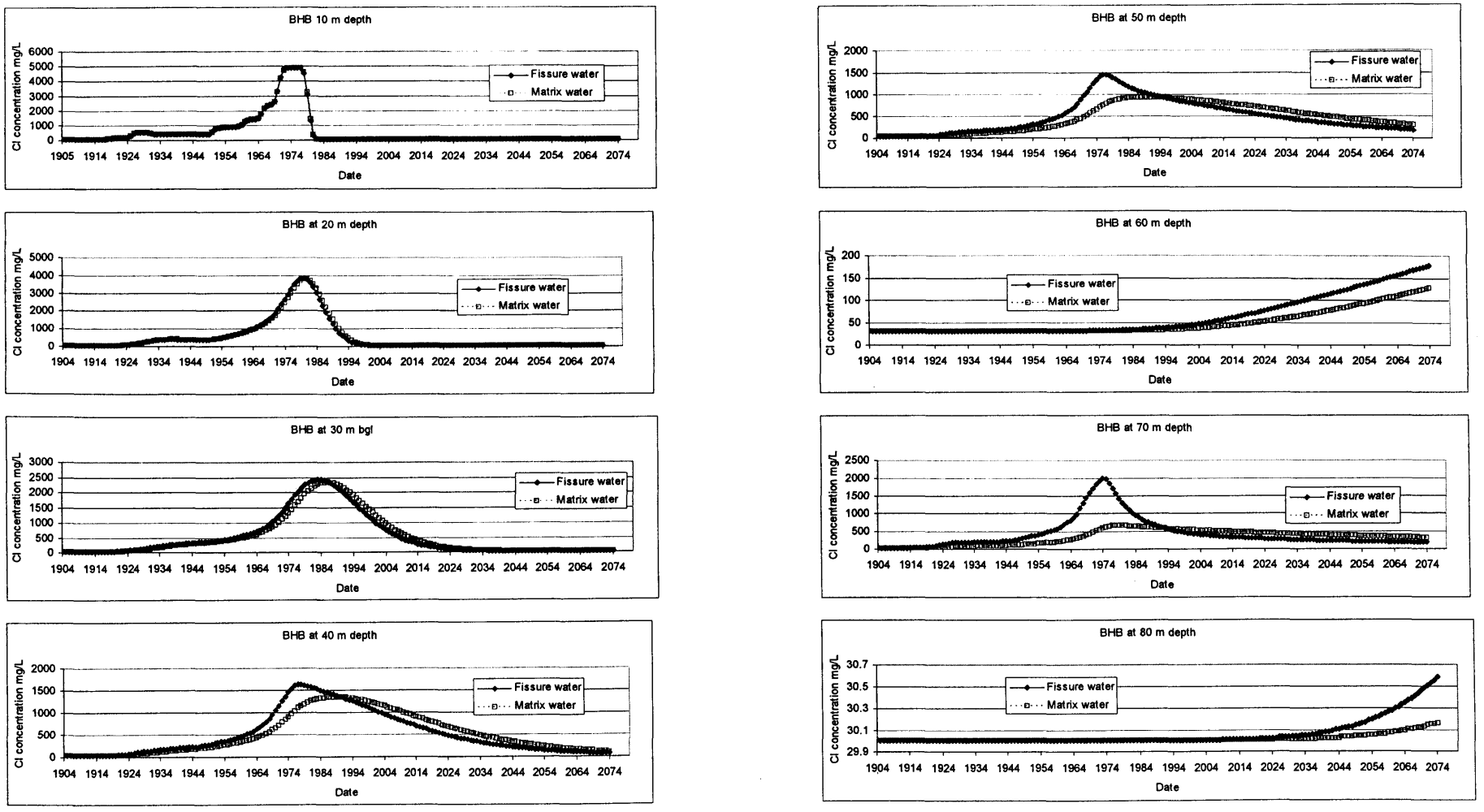

Figure 6-4 BHB DP1D modelled concentration over time

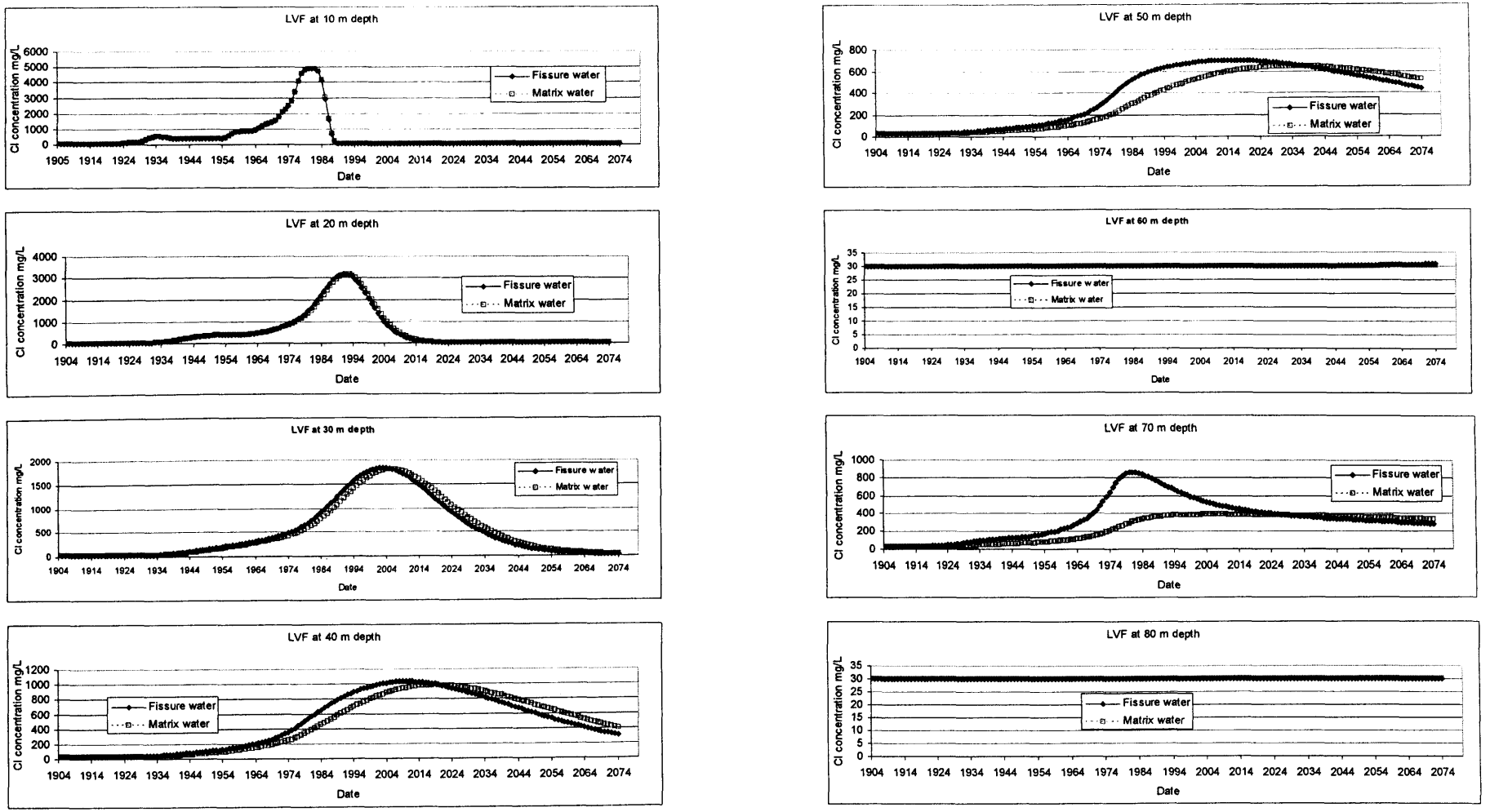

Figure 6-5 Lower Venson Farm DP1D modelled concentration over time

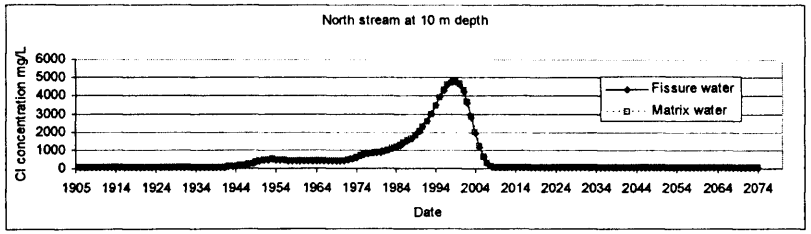

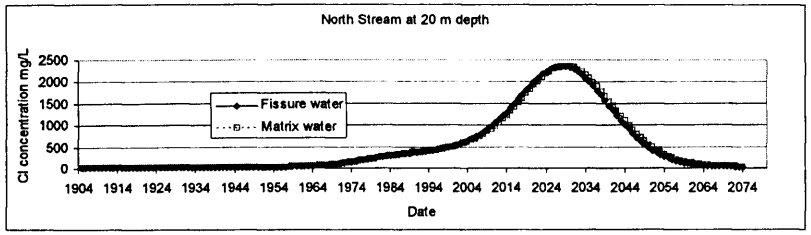

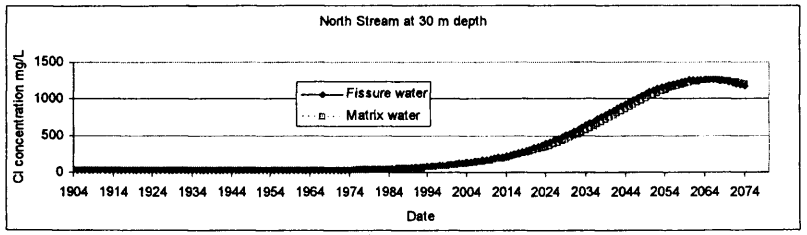

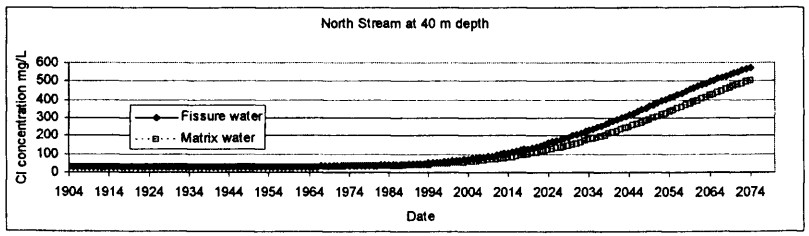

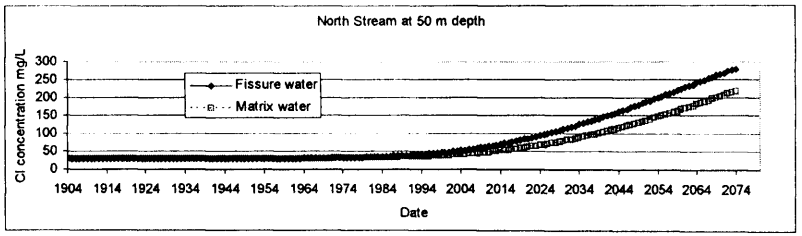

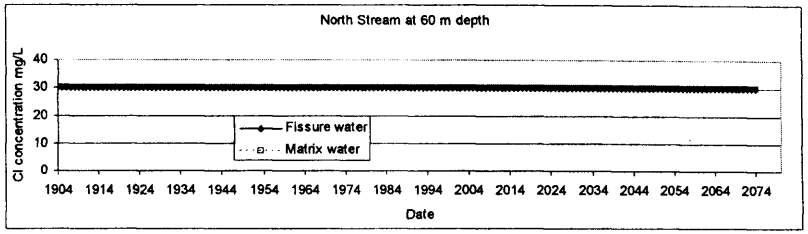

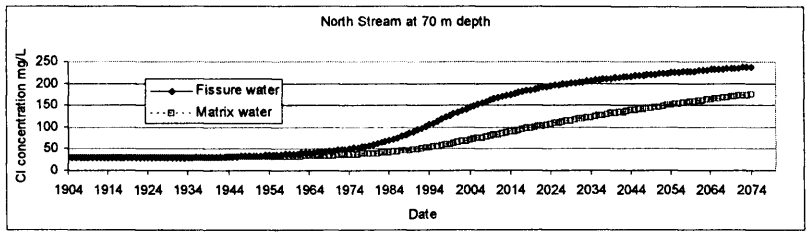

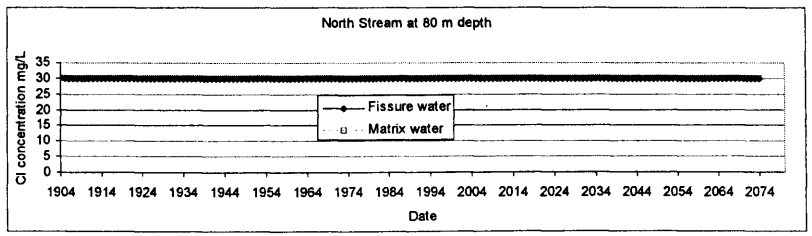

Figure 6-6 North Stream DP1D modelled concentration over time

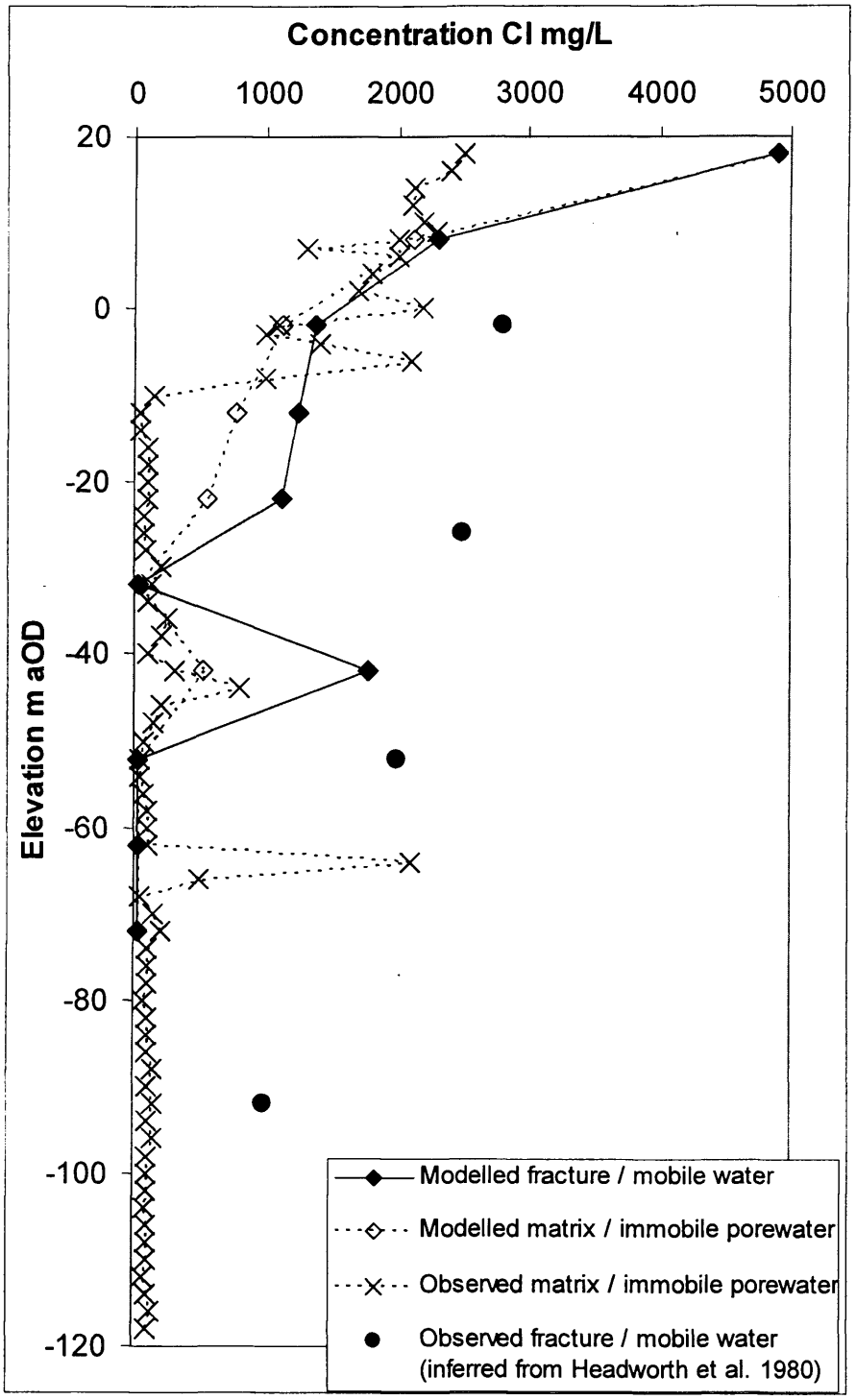

Figure 6-7 BHB 1974 DP1D model predictions compared to observed chloride concentrations.

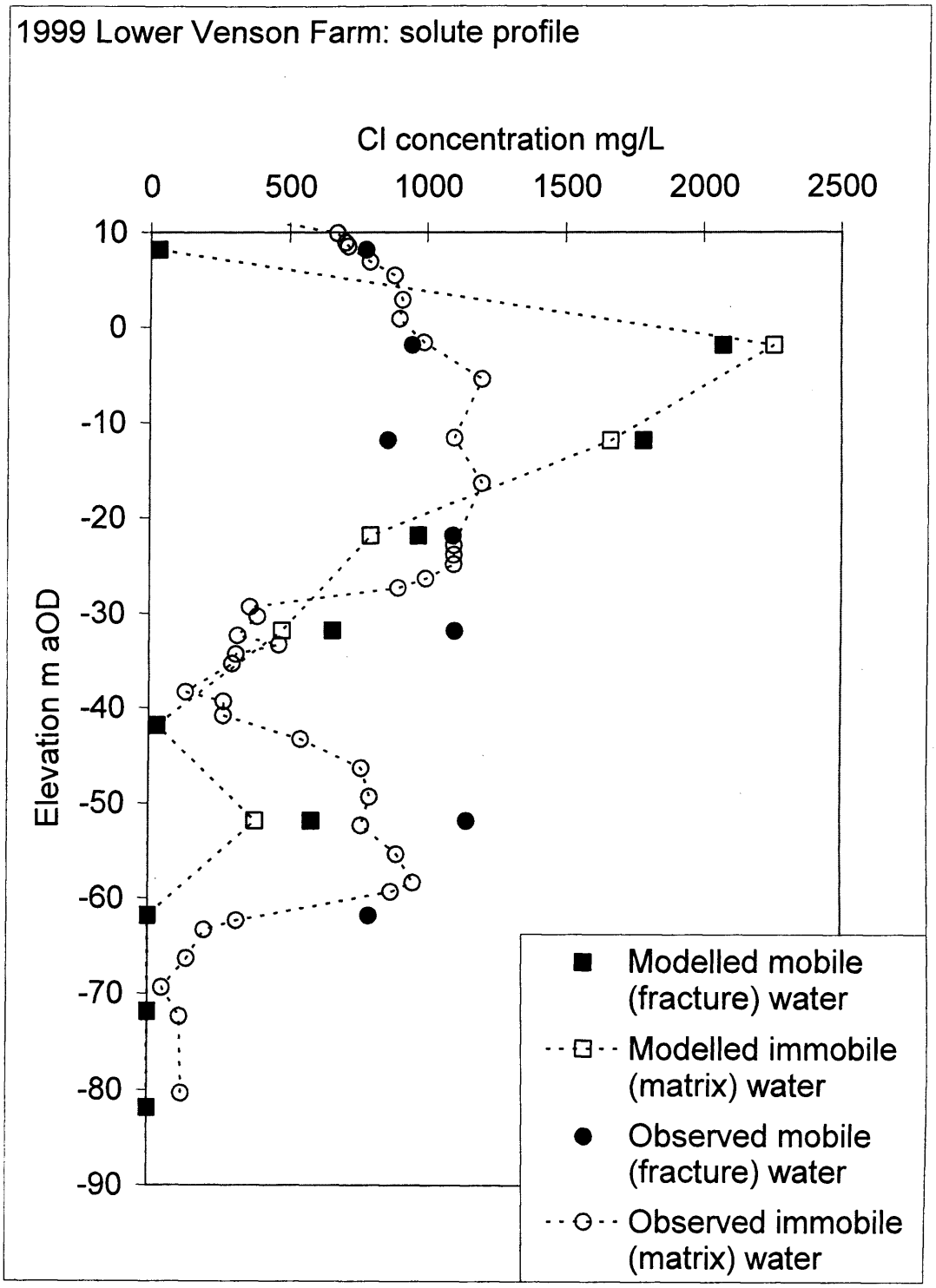

Figure 6-8 Lower Venson Farm composite profile.

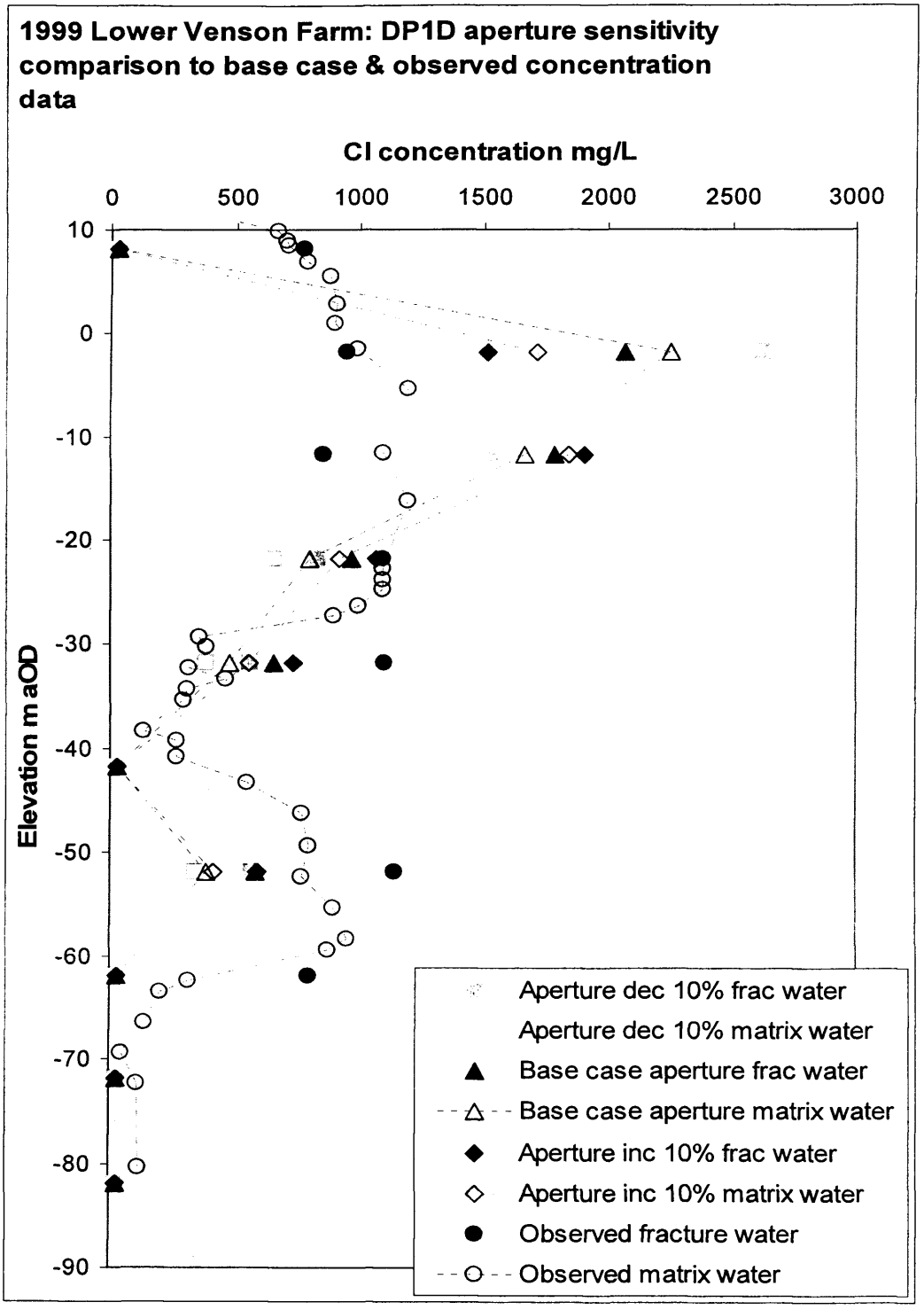

Figure 6-9 Aperture sensitivity analysis for 1999 profile at Lower Venson Farm.

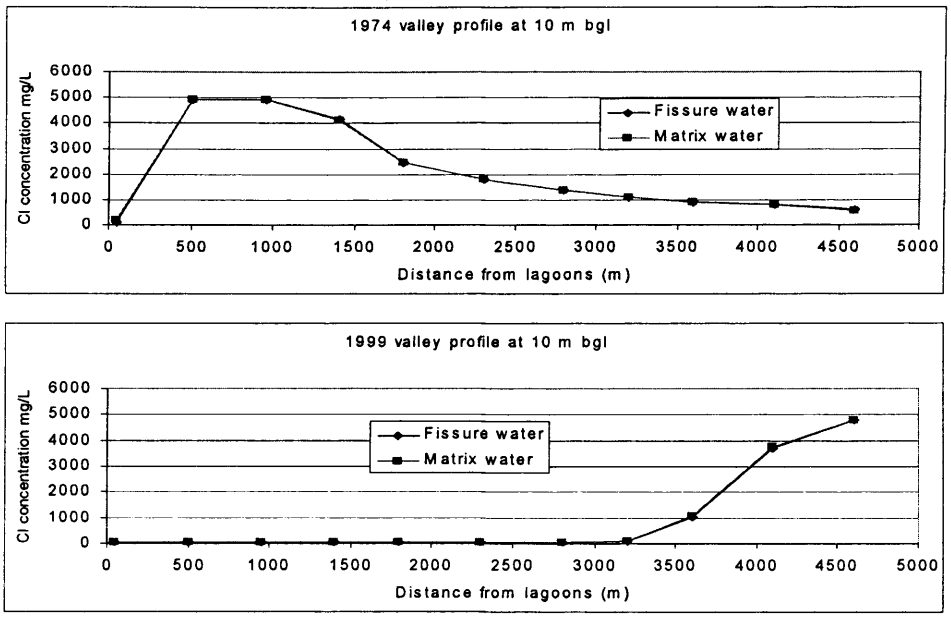

Figure 6-10 Along valley profile at 10 m below ground level.

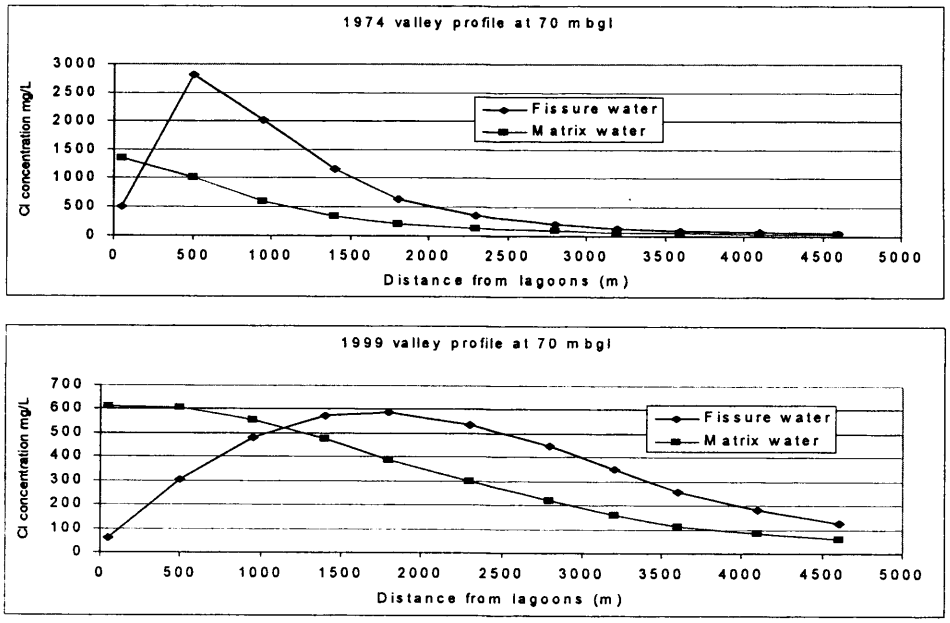

Figure 6-11 Along valley profile at 70 m below ground level.

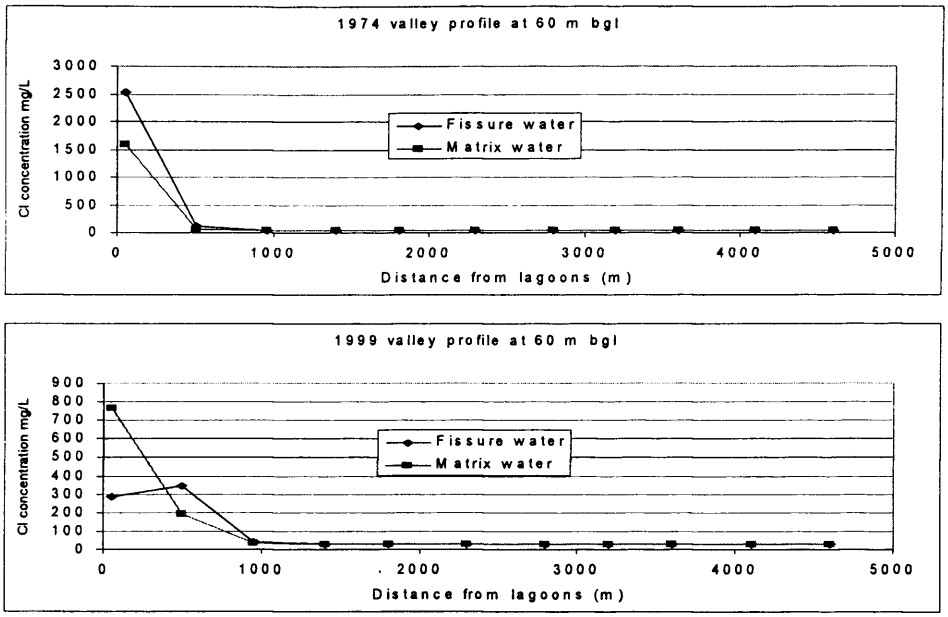

Figure 6-12 Along valley profile at 60 m below ground level.

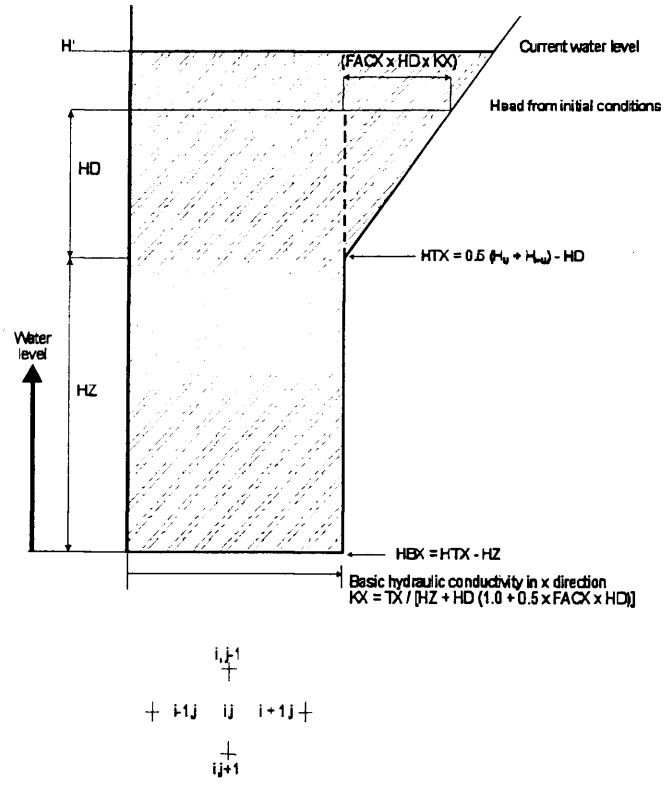

Figure 6-13 Rushton *et al.* (1989) method to simulate varying hydraulic conductivity as the saturated depth fluctuates and fracturing decreases with depth.

The transmissivity equals the area of the curve below the water table. FACX represents the slope of the line, equivalent to the rate of increase in hydraulic conductivity as fracturing increases.

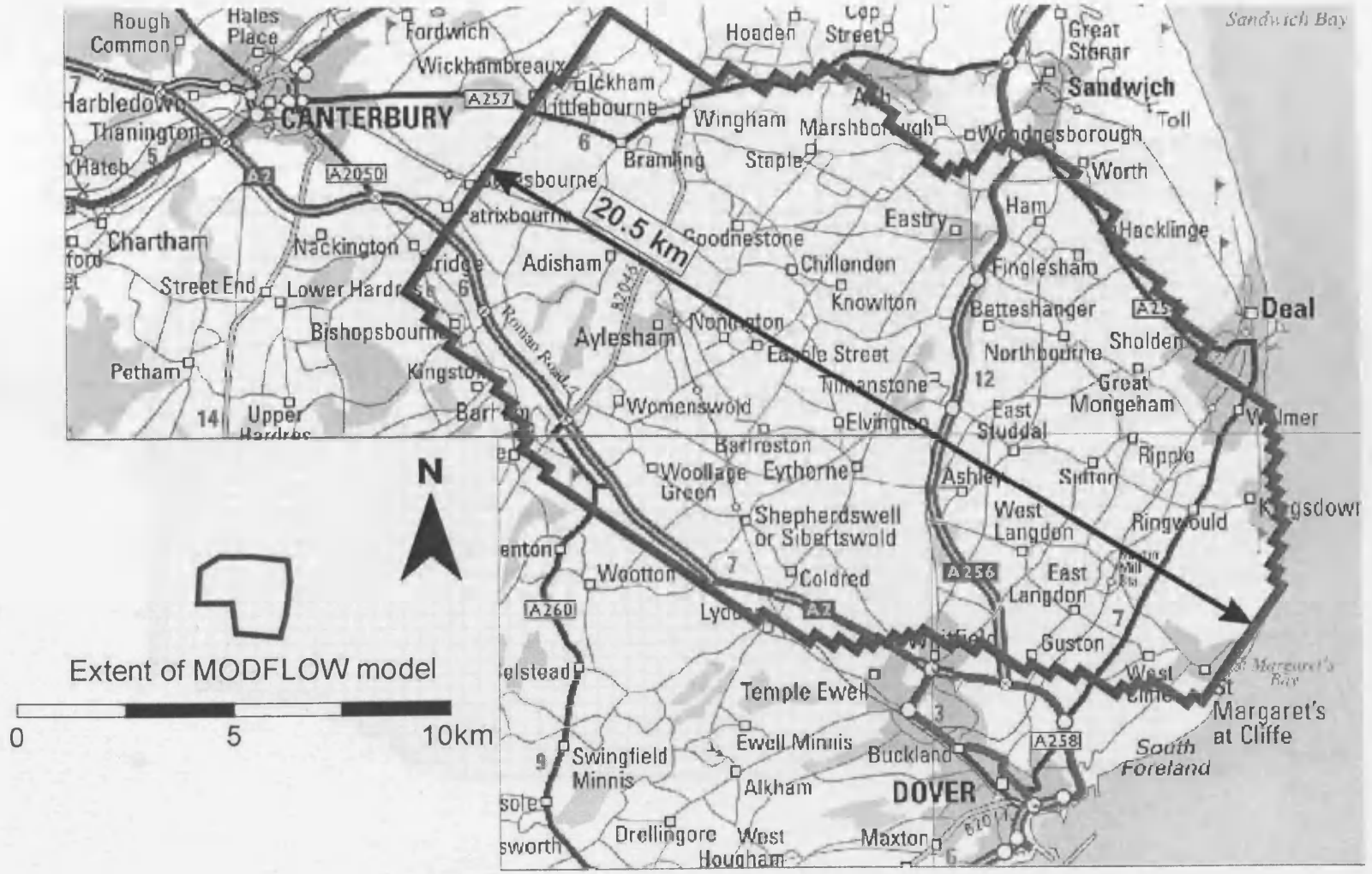

Figure 6-14 Flow model grid on map of east Kent

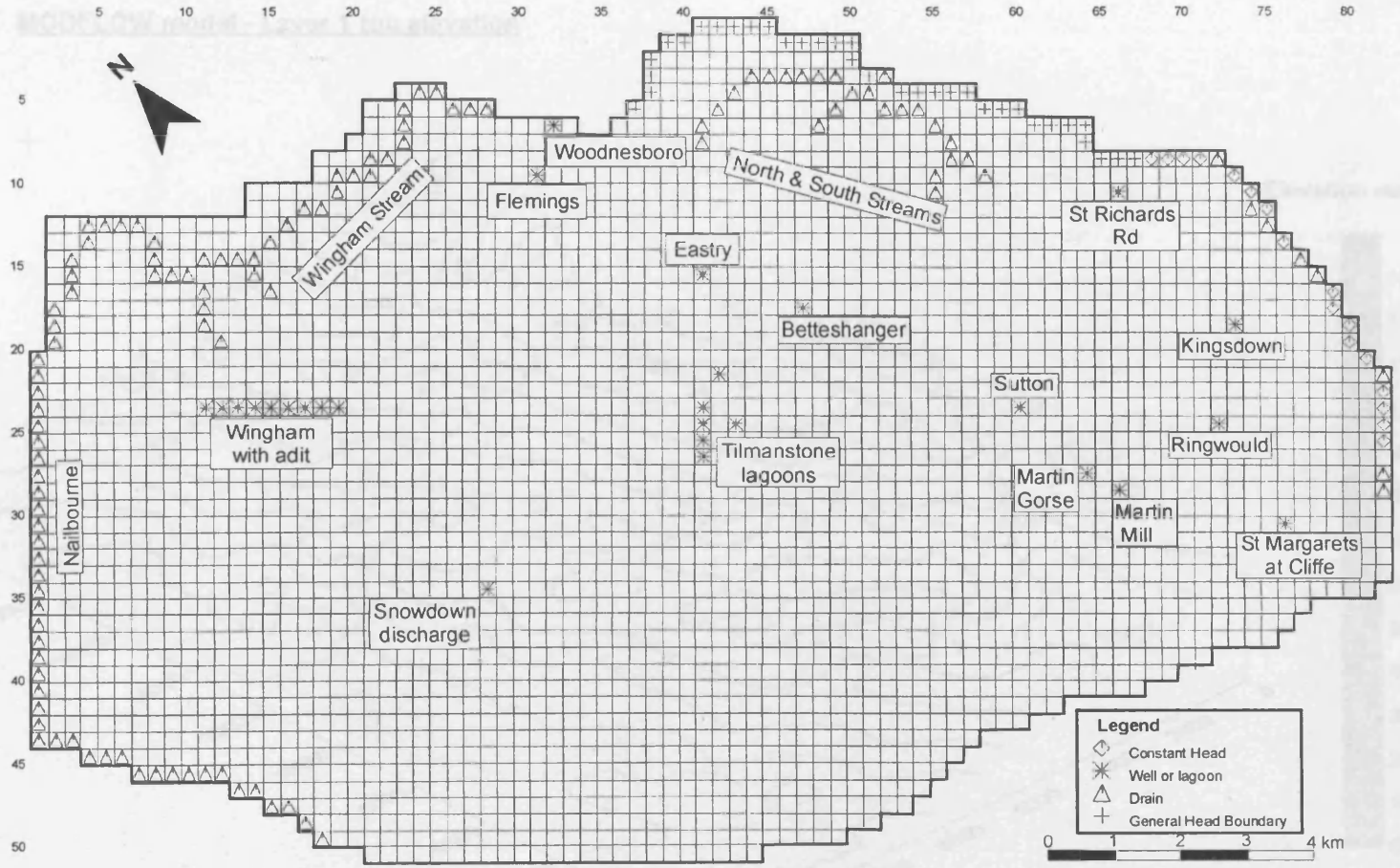

Figure 6-15 Flow model grid and boundaries.

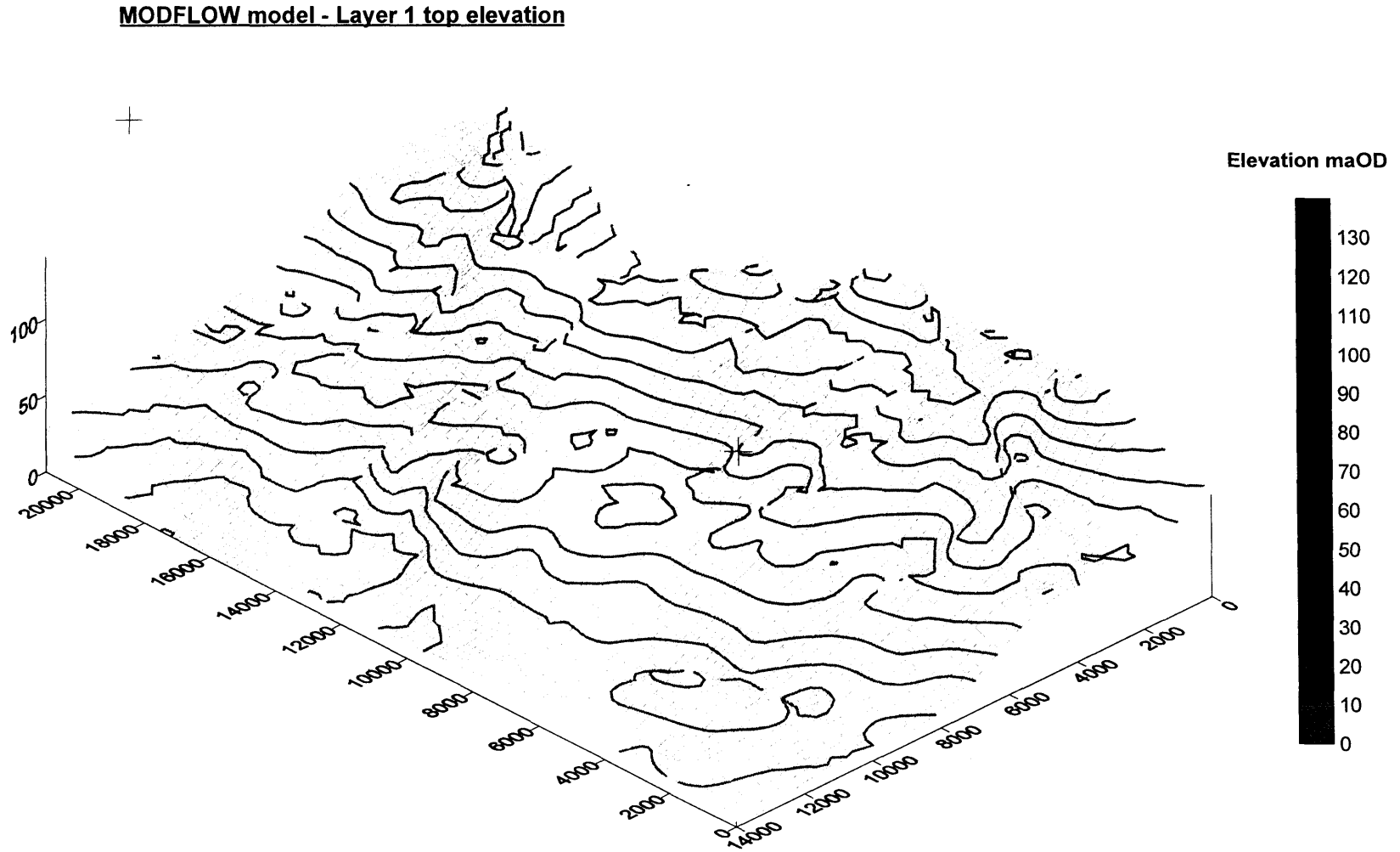

Figure 6-16 Layer 1 topography.

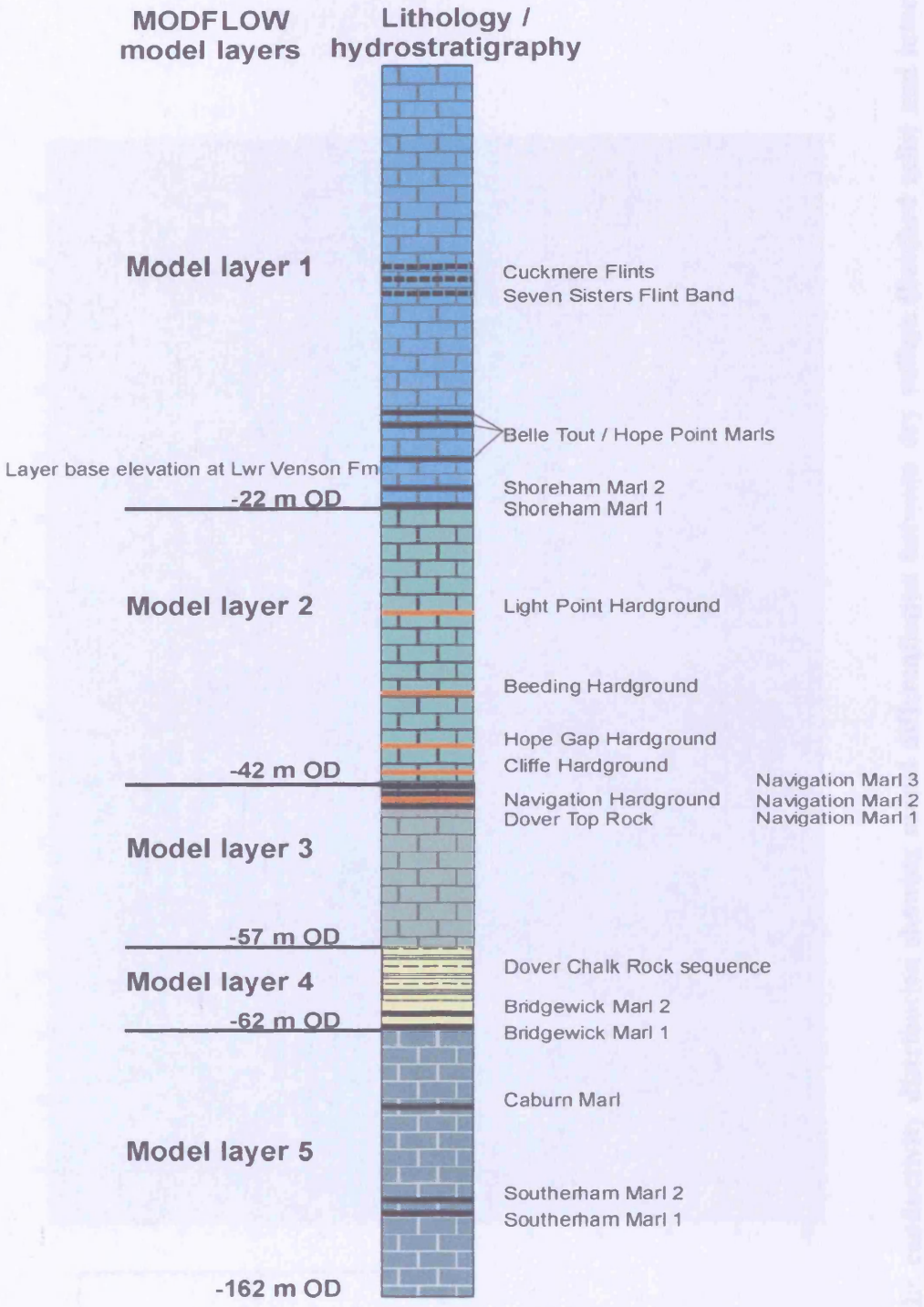

Figure 6-17 Model layers and corresponding lithology and hydrostratigraphy.

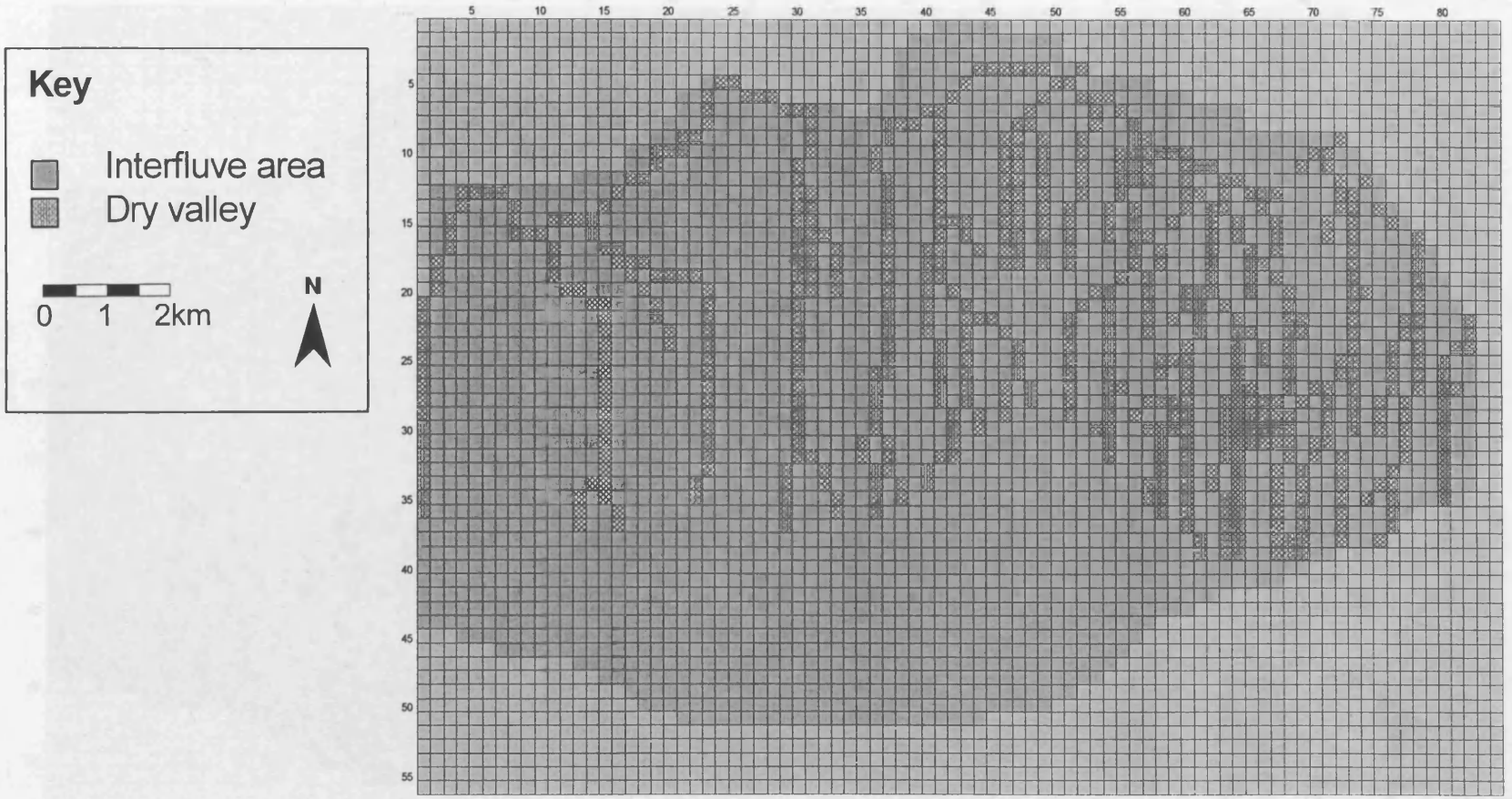

Figure 6-18 Layer 1 hydraulic conductivity distribution showing model differentiation between dry valleys (hatched cells) and interfluve areas (plain cells).

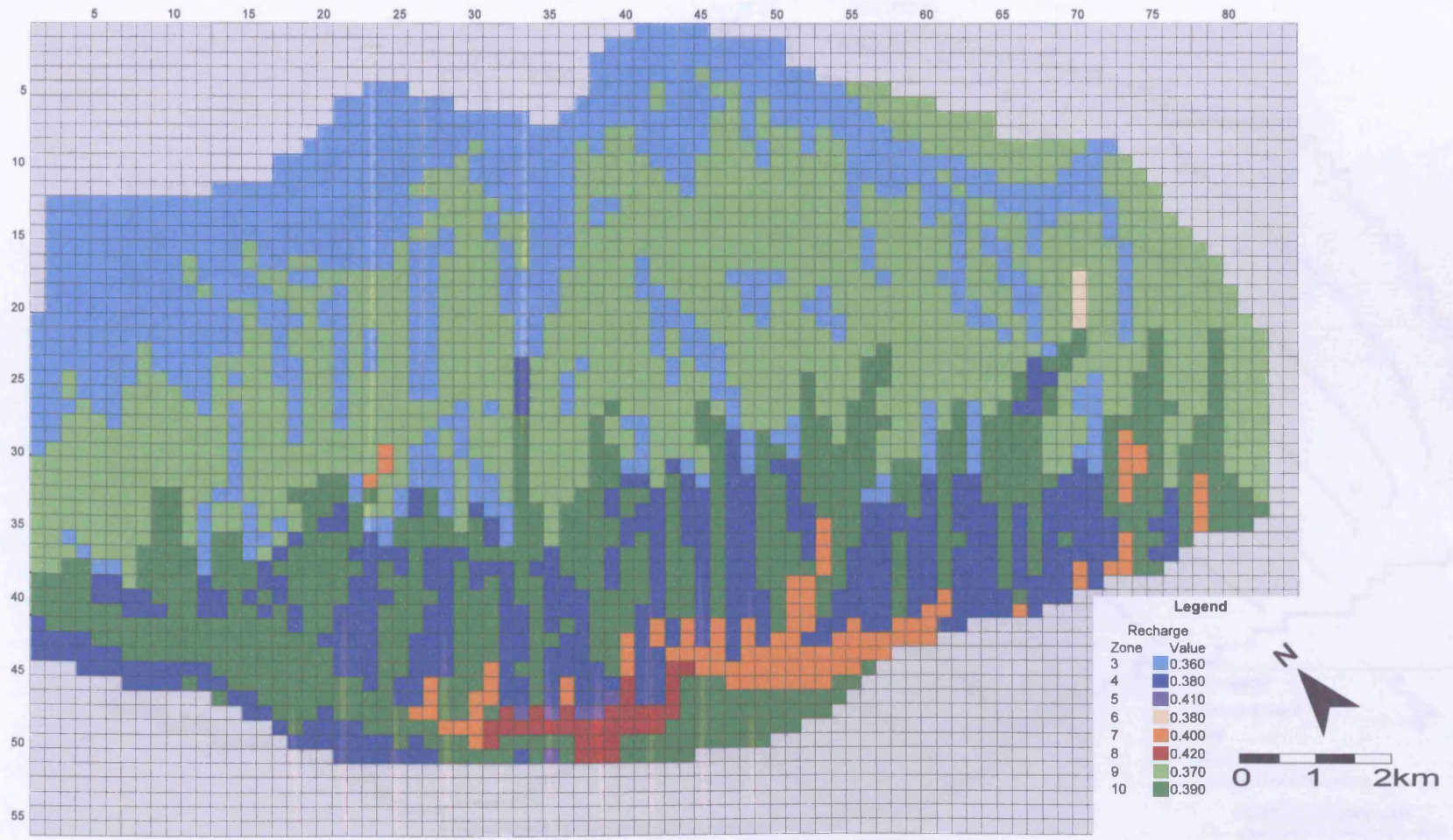

Figure 6-19 Recharge zone distribution.

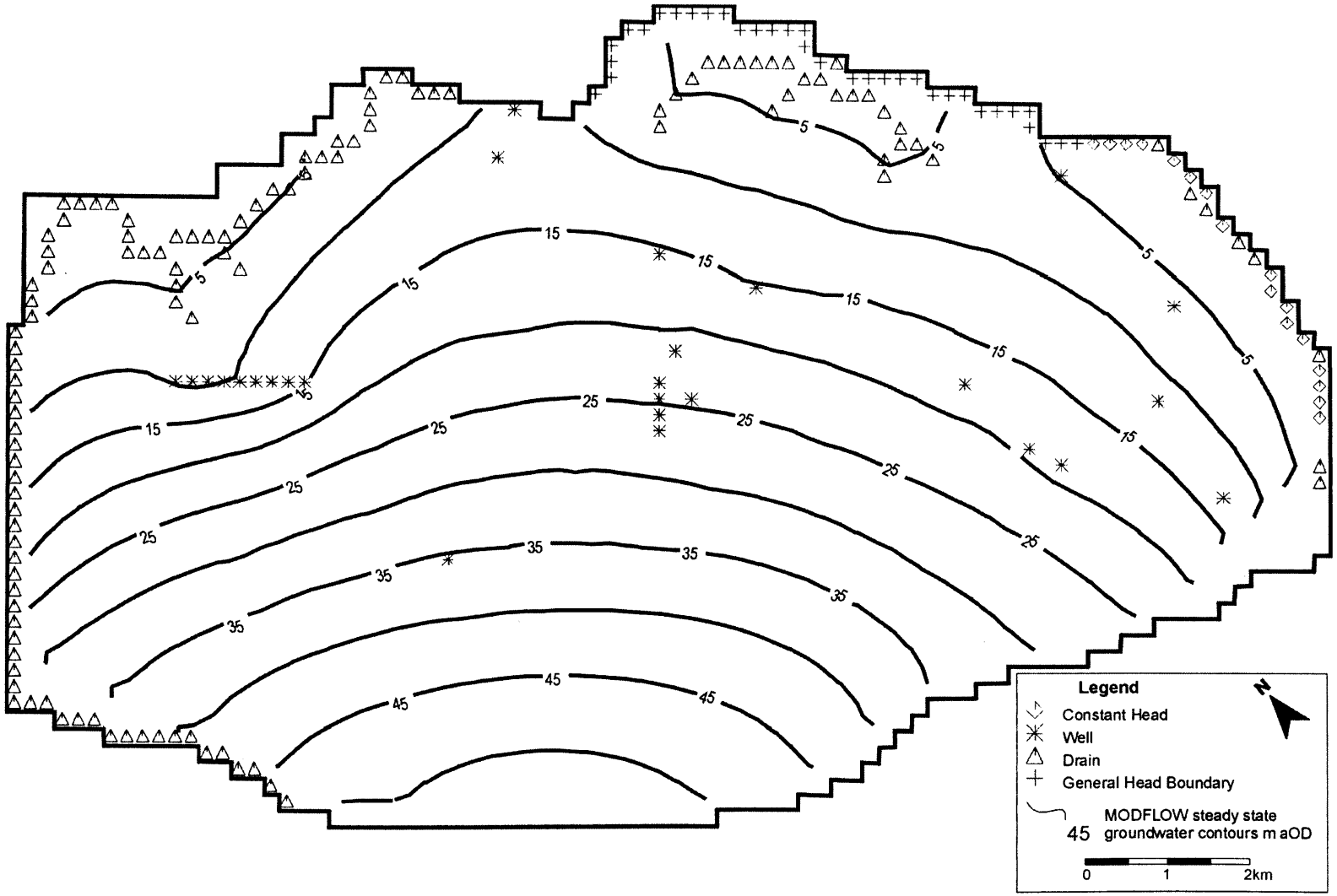

Figure 6-20 Steady state model head distribution.

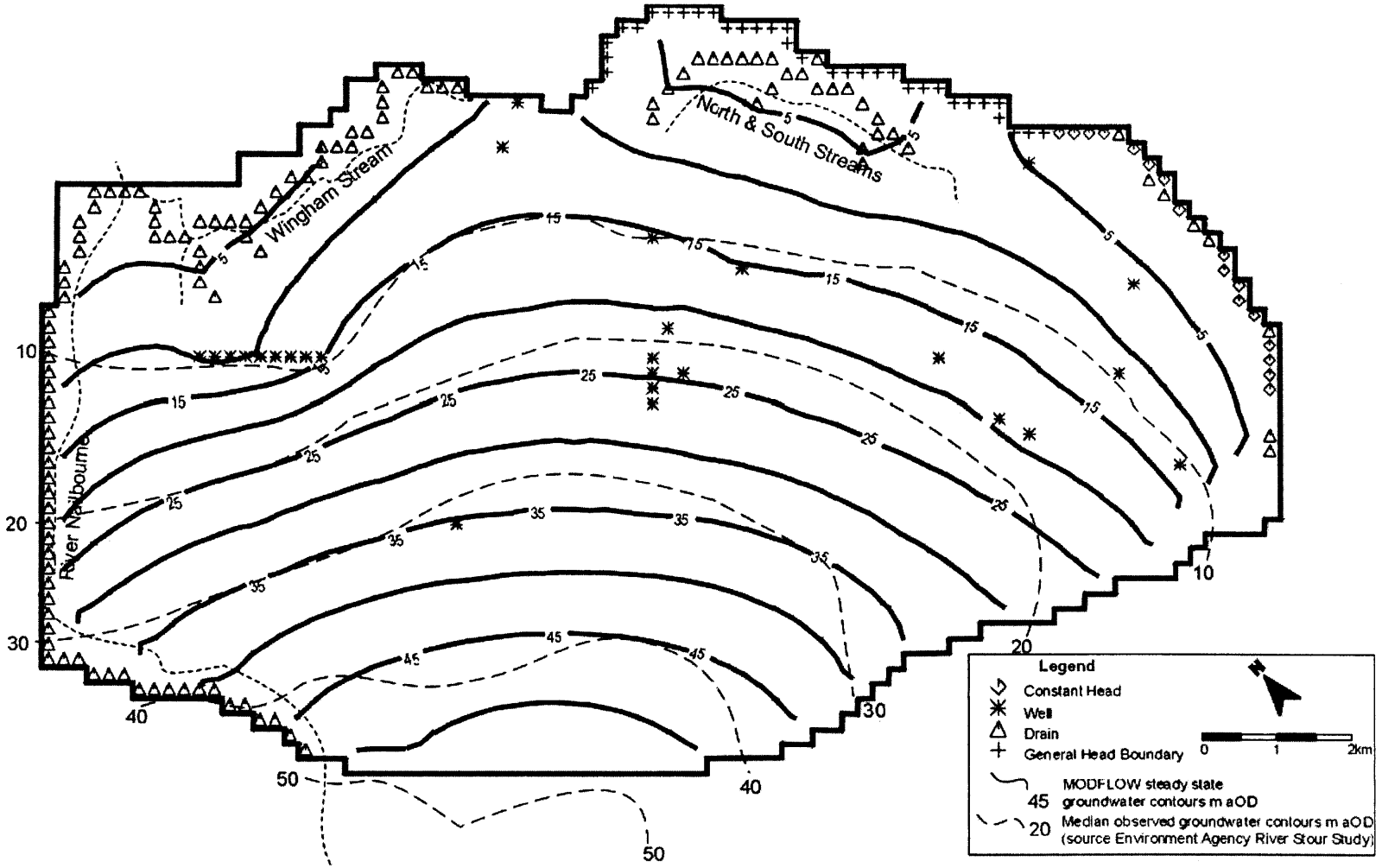

Figure 6-21 Observed groundwater contours, median groundwater level provided by EA, compared to modelled steady state groundwater level for layer 1.

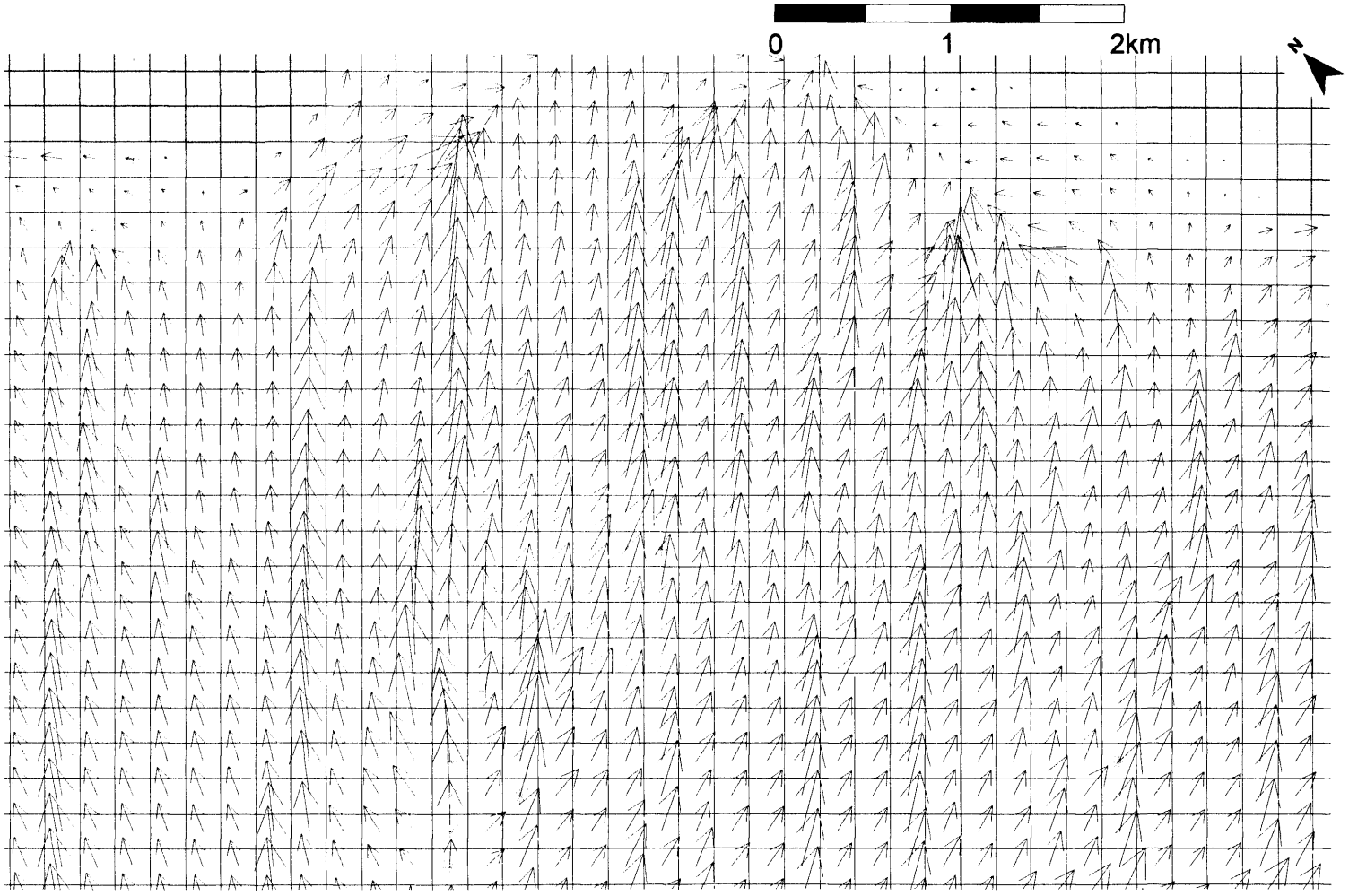

Figure 6-22 Groundwater velocity – plan of model domain to indicate constraining effect of dry valleys on groundwater flow.

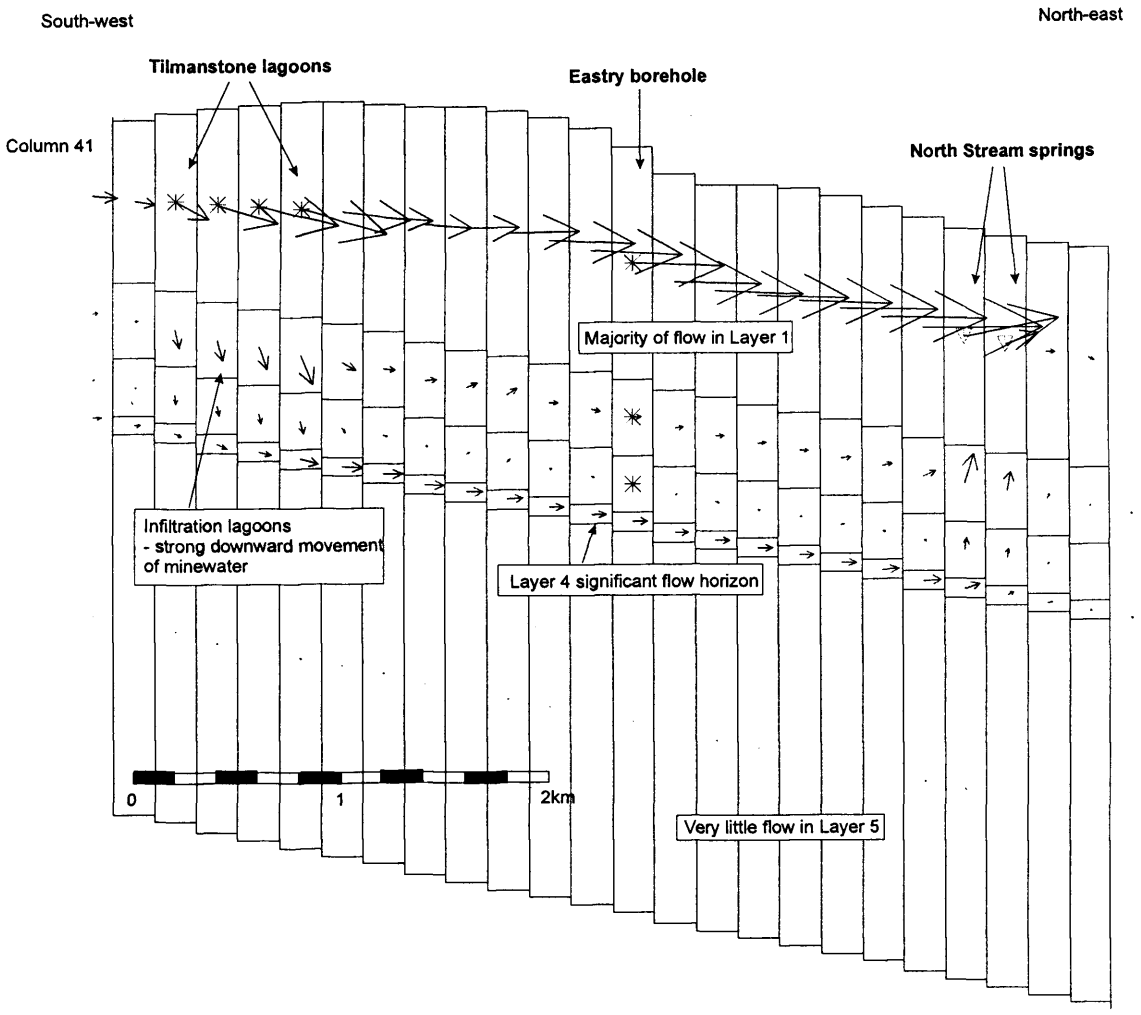

Figure 6-23 Cross section for model column 41 along the Tilmanstone – Eastry valley during lagoon operations.

Most groundwater flow is occurring in layer 1, there is a strong downward movement of water caused by the infiltration lagoons and layer 4 also has greater groundwater flow rates.

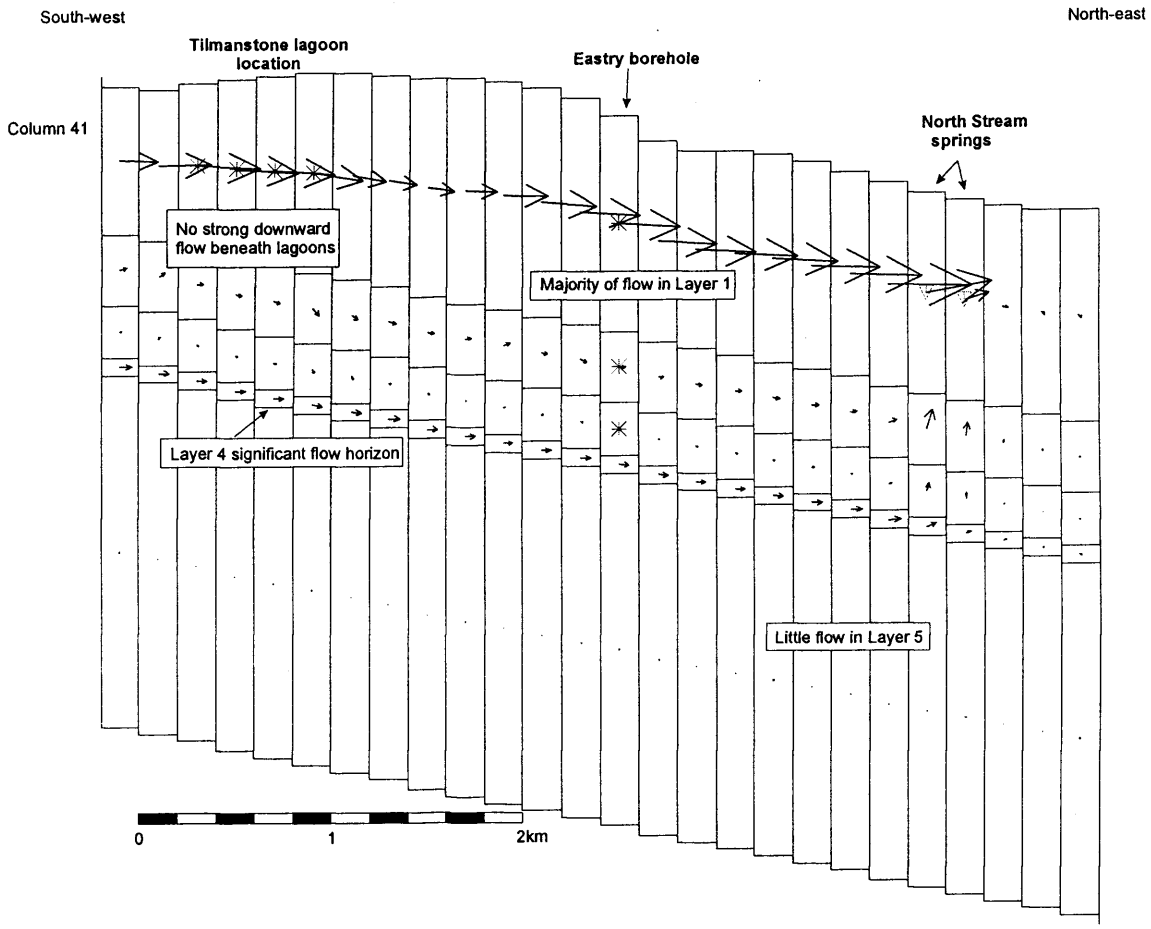

Figure 6-24 Cross section for model column 41 along the Tilmanstone – Eastry valley after lagoon operations.

Most groundwater flow is occurring in layer 1, the strong downward movement of water caused by the infiltration lagoons has ceased. Layer 4 continues to have greater groundwater flow rates compared to layer 2 and 3.

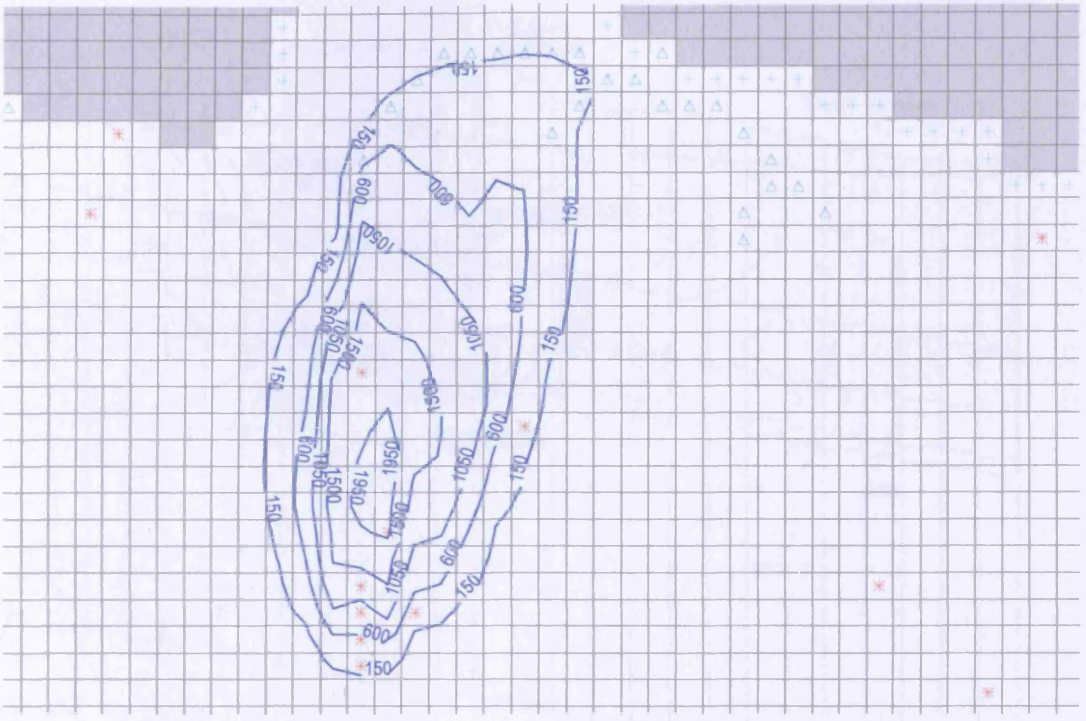
150
600
1050
1500
1950

A

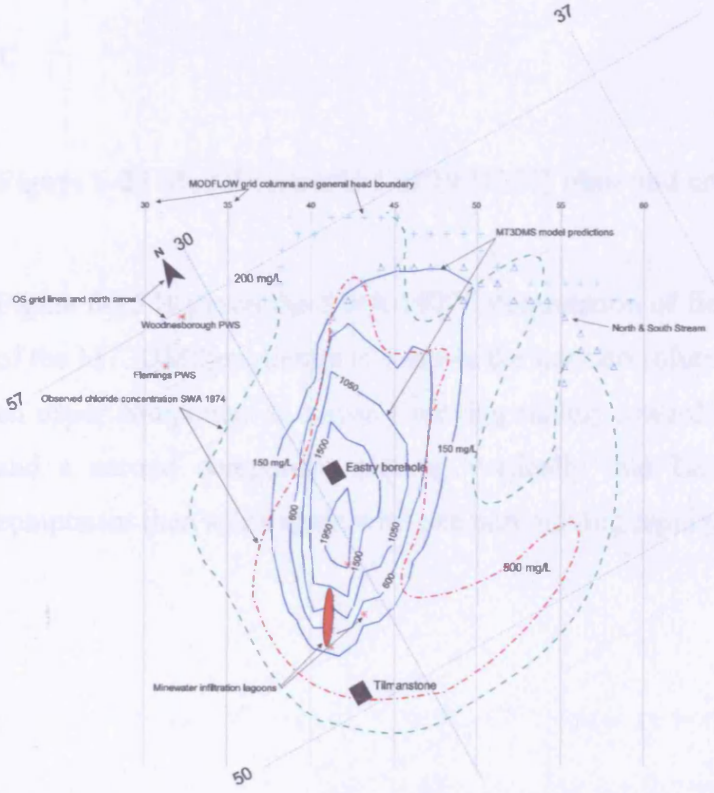
MODFLOW grid columns and general head boundary
MT3DMS model predictions
200 mg/L
OS grid lines and north arrow
Woodnesborough PWS
Flemings PWS
Observed chloride concentration SWA 1974
North & South Stream
150 mg/L
Eastry borehole
800 mg/L
Minewater infiltration lagoons
Tilmanstone
37
57
50

B

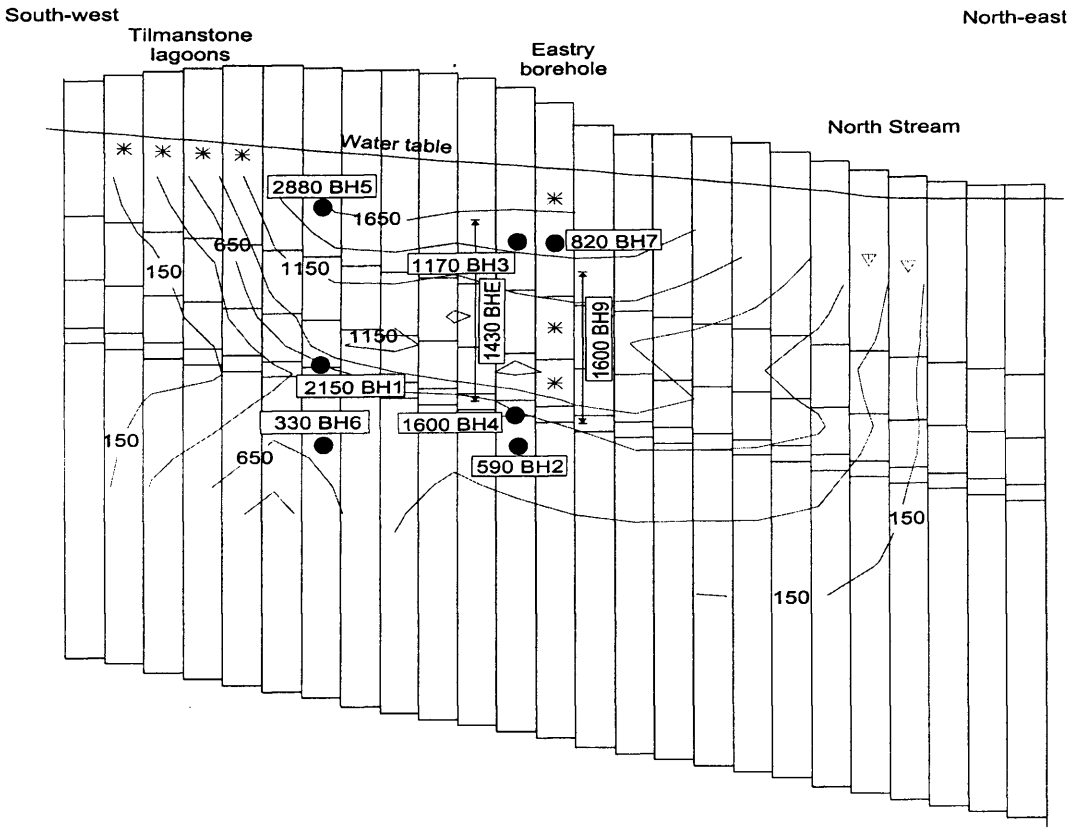

C

Figure 6-25 Model scenario 1 SP10 (1977) plan and cross-section

Figure 6-25 B shows the SWA 1977 interpretation of field sampling. The cross-section of the MT3DMS prediction (C) shows the injected solute splitting into two components: an upper component in Layer 1 moving rapidly towards the North and South Streams, and a second component moving vertically into Layer 2 and below. This lower component then splits again with one part moving rapidly along Layer 3 and layer 4.

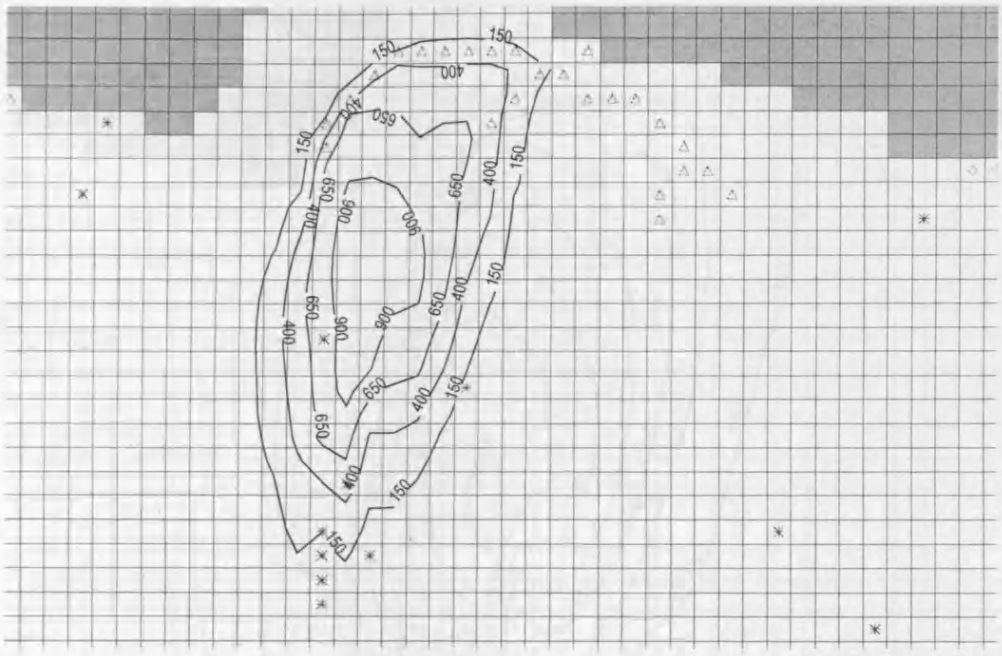

A

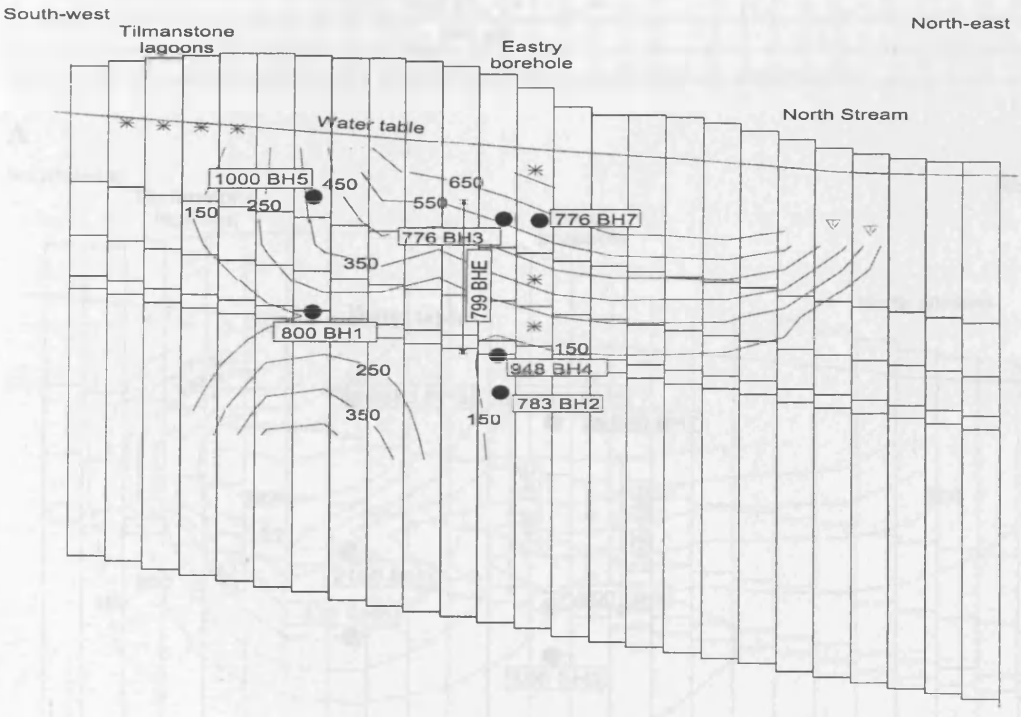

B

Figure 6-26 Model scenario 1 SP53 (1999) plan and cross-section.

Model predictions of fracture water chloride concentrations are generally lower than observations (Table 4-6). The model predicts the solute plume to spread across layer 1 and 2, which is not observed in the chloride porewater profile. This suggests that a greater barrier to flow such as may be caused by marl horizons is required, although some vertical movement is still necessary and this could be provided by vertical fracturing.

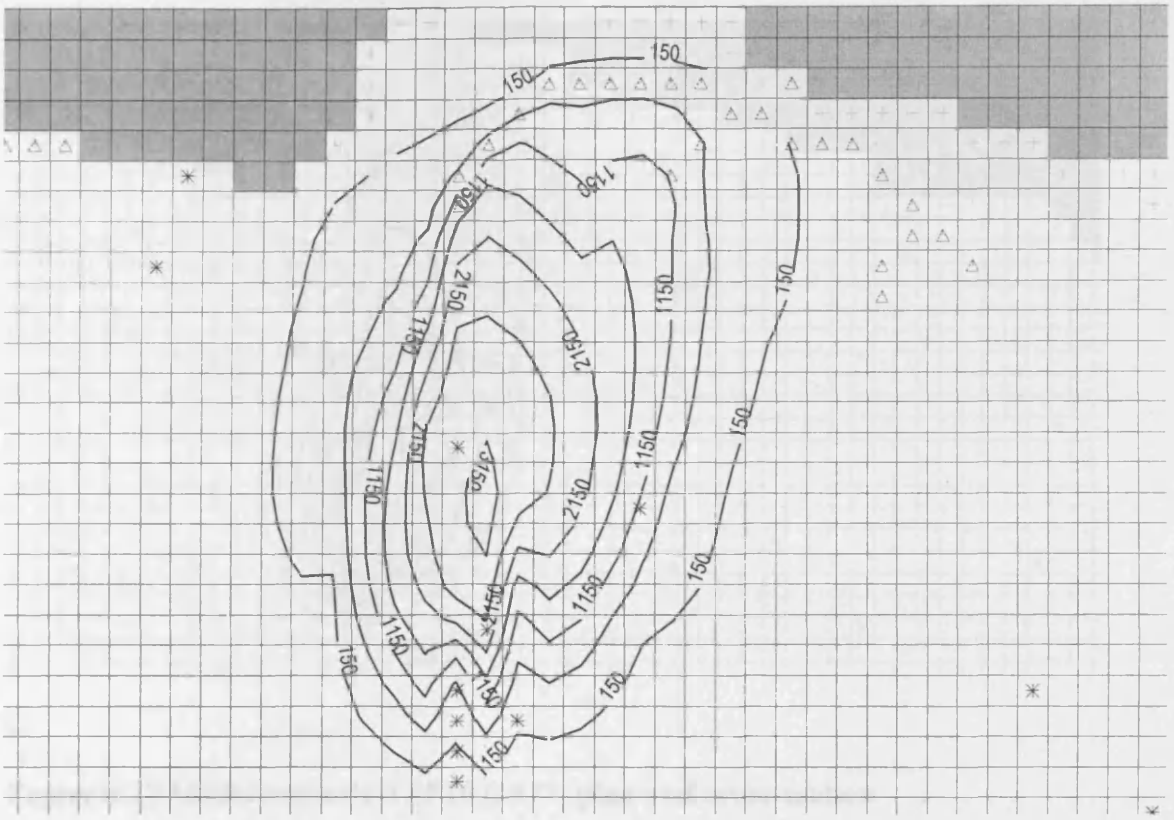
150
150
1150
2150
1150
2150
1150
2150
1150
150
150
150
150
150
150

A

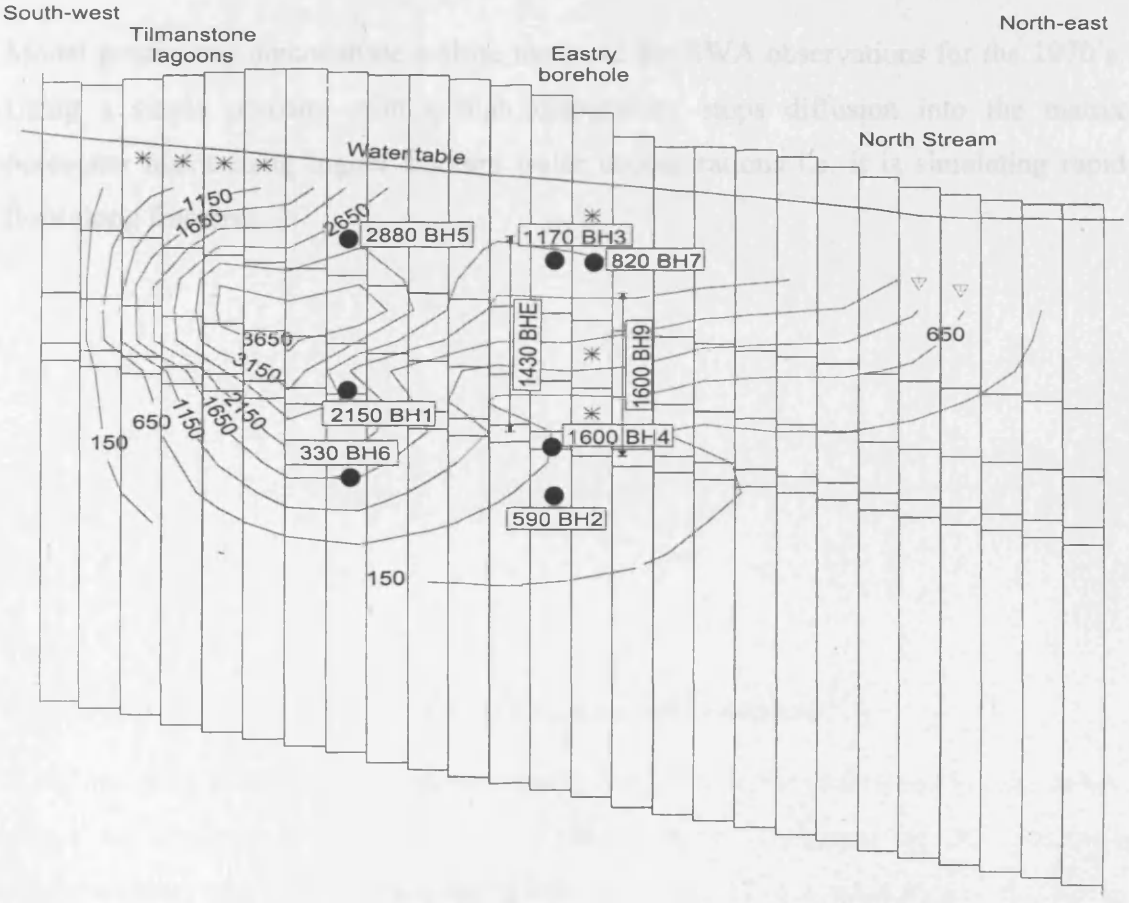
South-west
Tilmanstone lagoons
Eastry borehole
North-east
North Stream
Water table
2880 BH5
1170 BH3
820 BH7
2150 BH1
330 BH6
1600 BH4
590 BH2
1430 BHE
1600 BH9
1150
1650
2650
3650
3150
2150
1650
1150
650
150
650
150

B

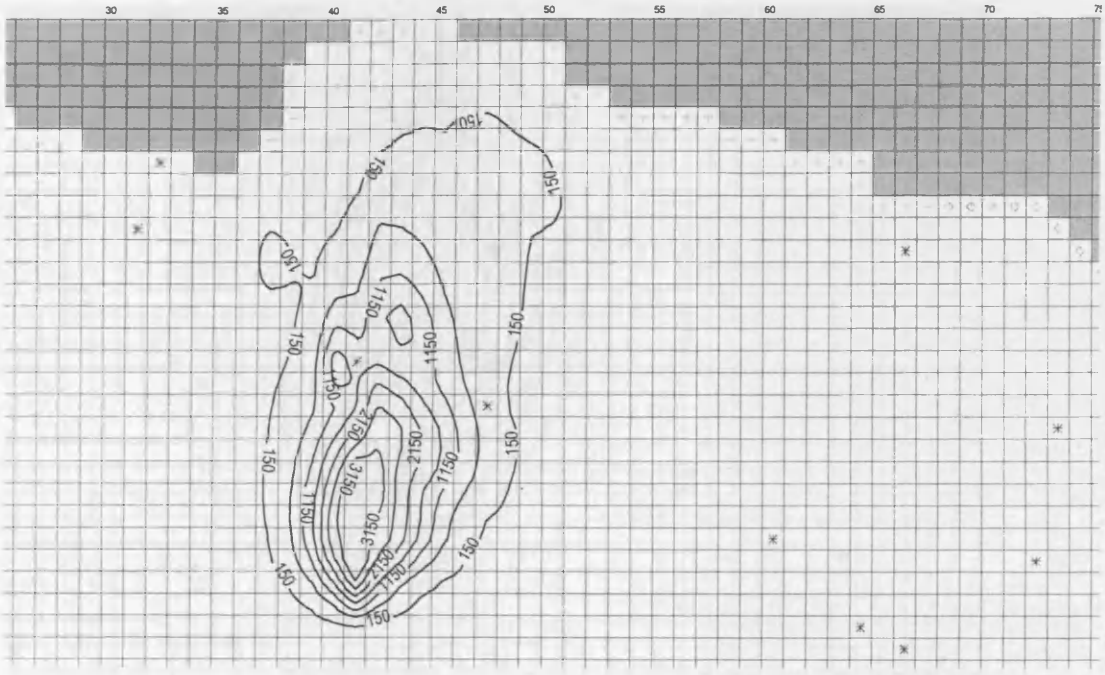

C

Figure 6-27 Model scenario 3 SP10 (1977) plan and cross-section

Model predictions demonstrate a close match to the SWA observations for the 1970's. Using a single porosity with a high dispersivity stops diffusion into the matrix porewater maintaining higher fracture water concentrations i.e. it is simulating rapid flow along fractures.

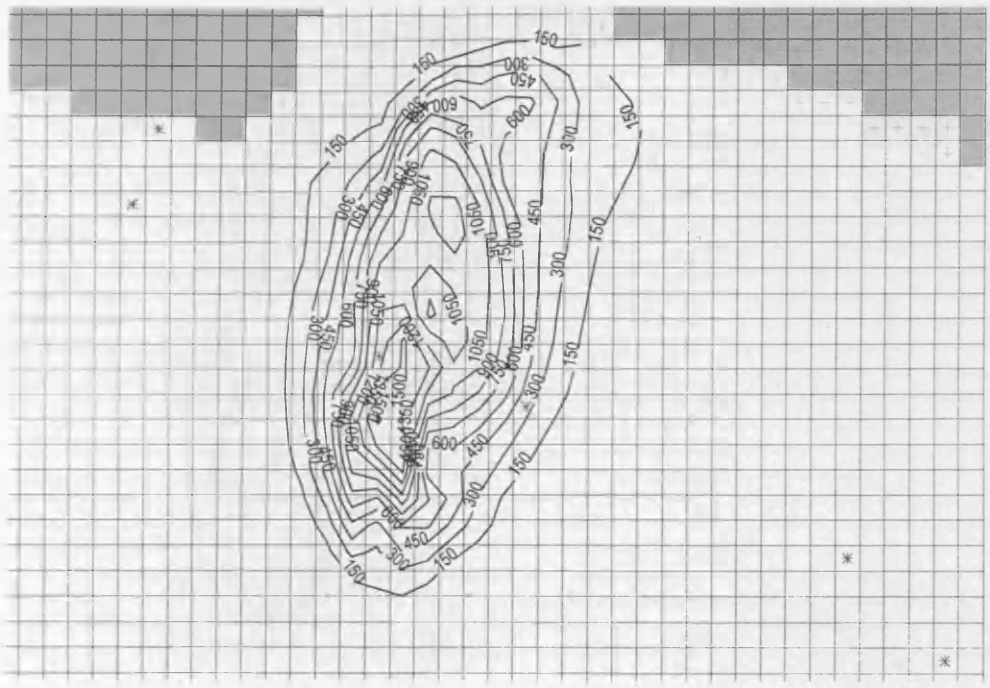

A

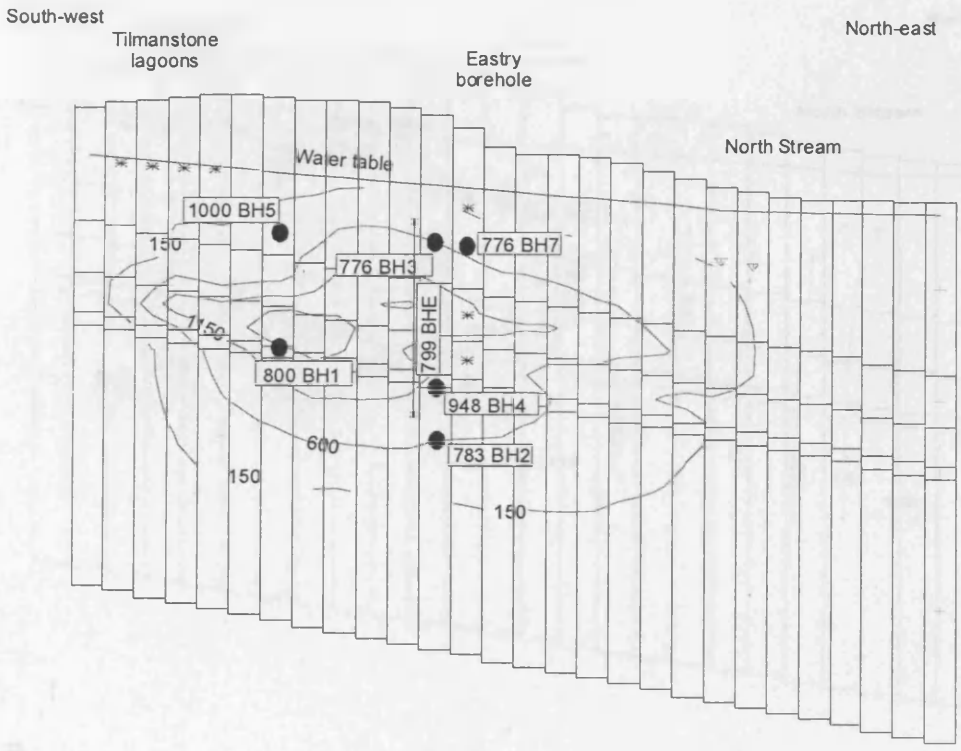

B

Figure 6-28 Model scenario 3 SP53 (1999) plan and cross-section

However using single porosity means that by the 1999 stress period (SP53) the solute plume has moved too rapidly through the aquifer, compared to the observed concentrations, and only low concentrations are predicted to remain around the North and South Streams. A large plume of solute remains in Layer 2 and the model predicts fracture water concentrations higher than those observed during packer test sampling.

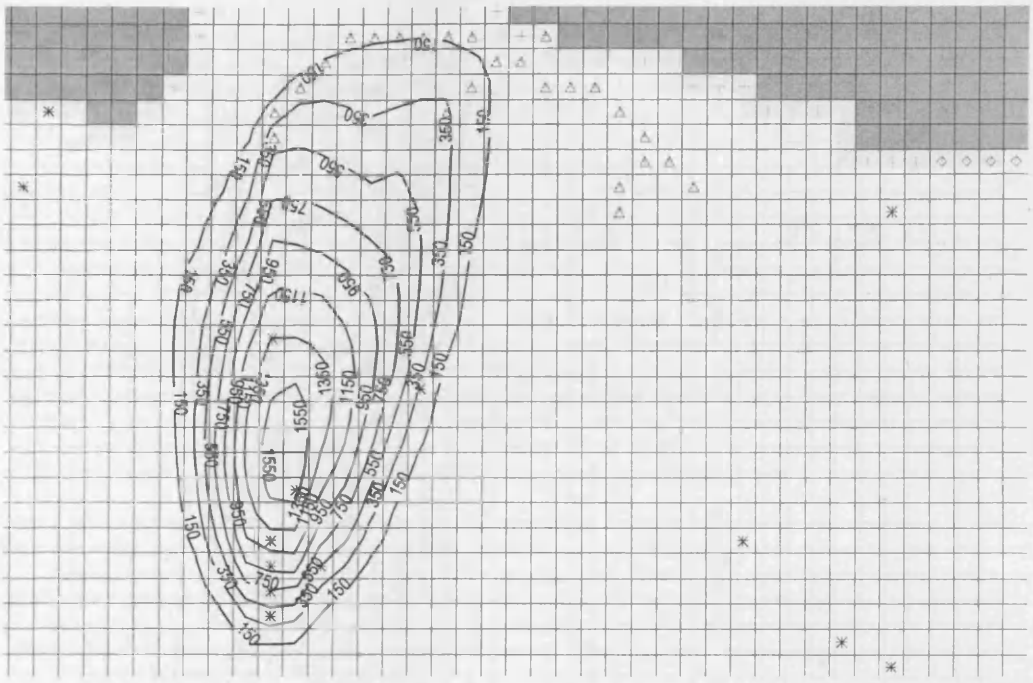

A

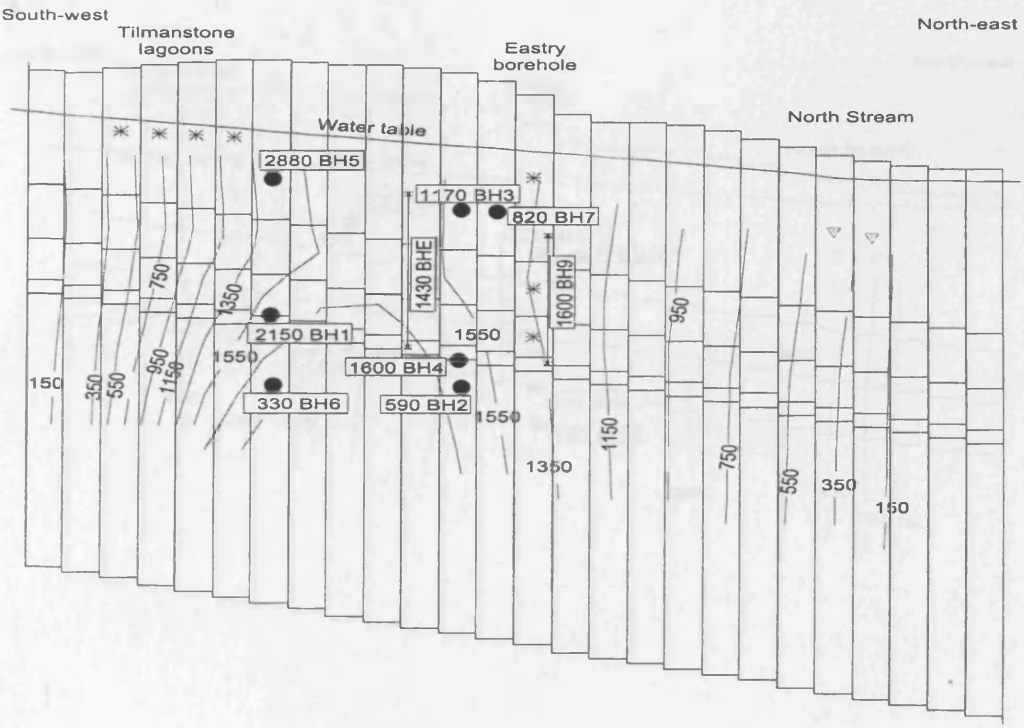

B

Figure 6-29 Model scenario 5 SP10 (1977) plan and cross-section

Model scenario 5 is used to test the effect of dispersivity on model predictions, but increasing the dispersivity parameter value from 2 to 225 m does not significantly alter the width of the plume due to the dominating effect of the immobile domain water attenuating solute concentrations. The strongest effect is to reduce the concentrations of the solute in the central part of the plume.

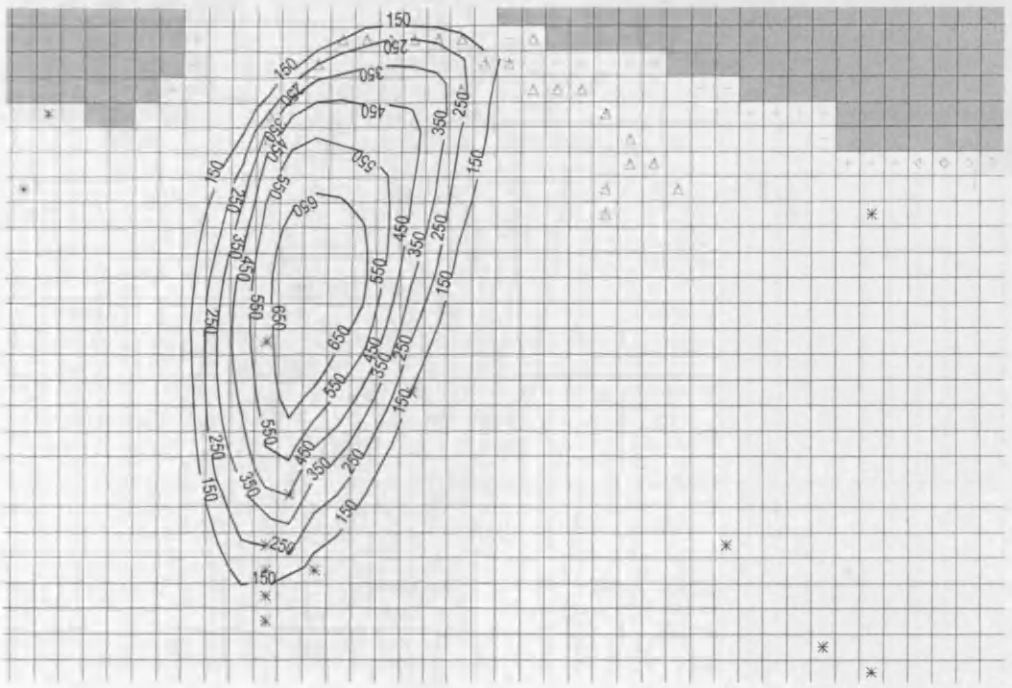

A

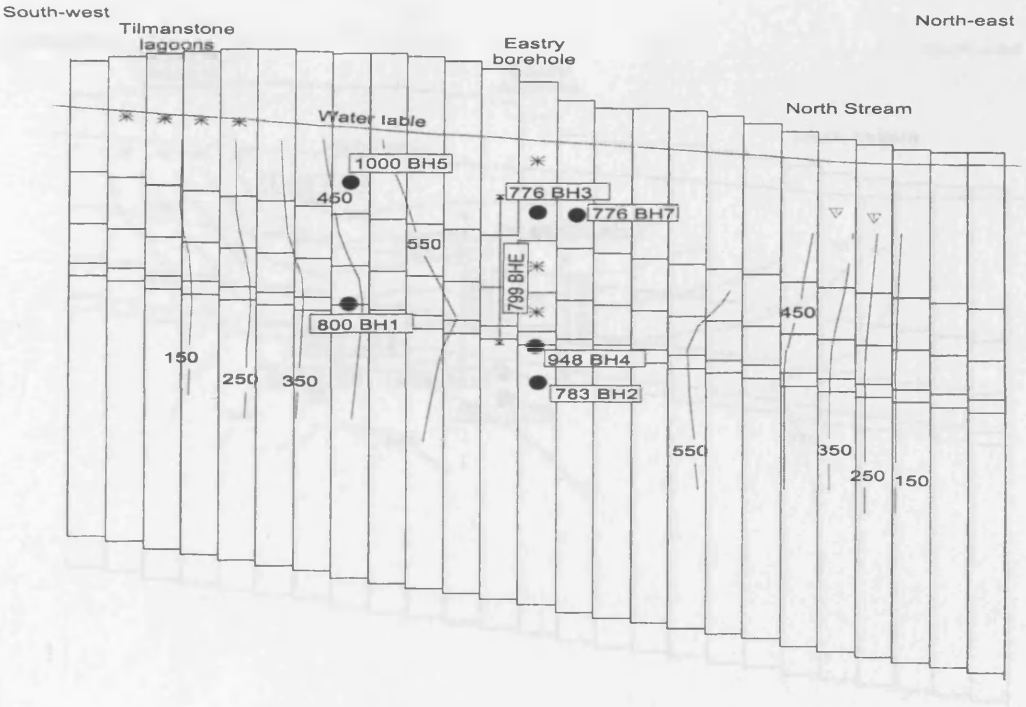

B

Figure 6-30 Model scenario 5 SP53 (1999) plan and cross-section.

A higher concentration plume develops in layer 5 which is then able to disperse more rapidly than in model scenario 1. The higher dispersivity used in model scenario 5 have the long term effect of distributing solute concentrations more evenly through the aquifer and this would not be consistent with the conditions required to produce the porewater profile observed at BGS LVV in 1999

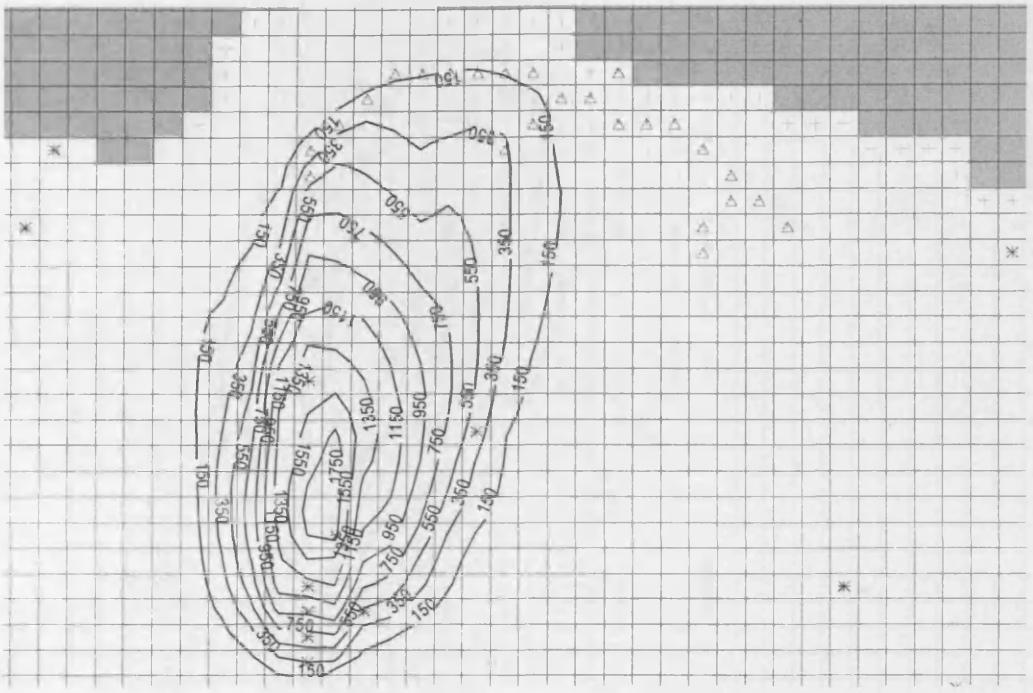

A

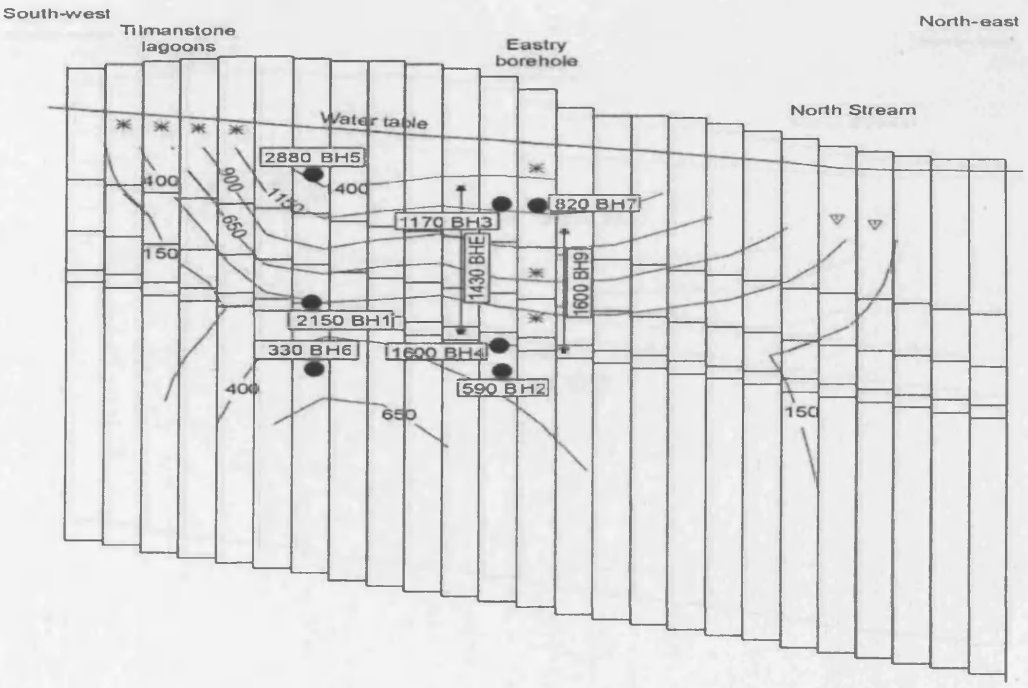

B

Figure 6-31 Model scenario 6 SP10 (1977) plan and cross-section.

A low fracture porosity of 0.1% produces a wider plume compared with model scenario 1 and concentrations of solute in the centre of the plume are lower by approximately 200 m g/L.

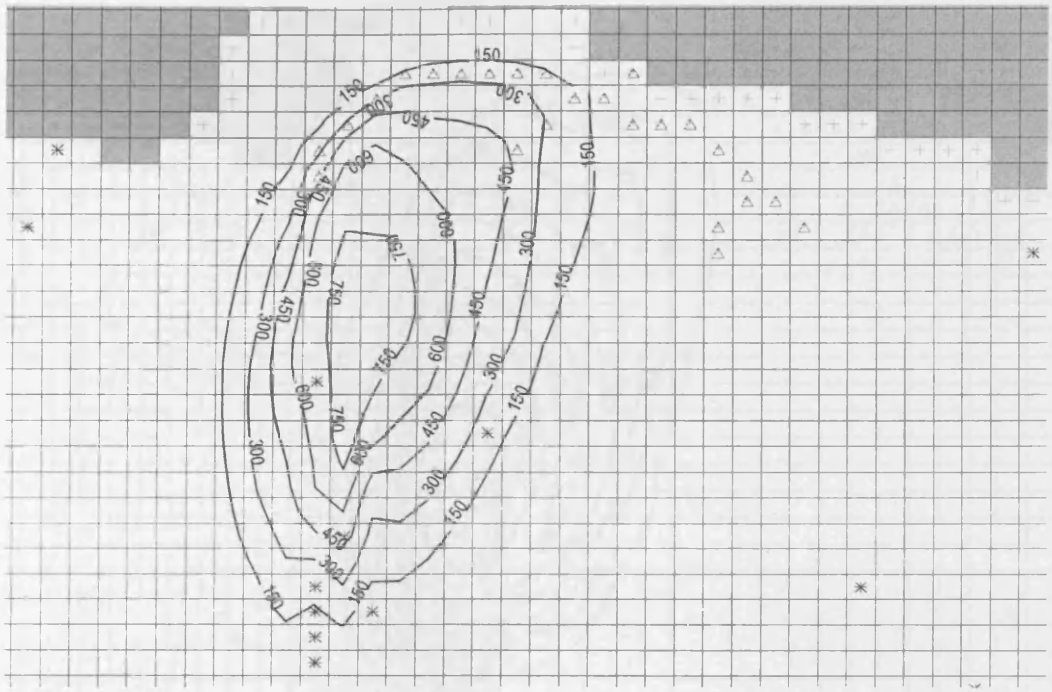

A

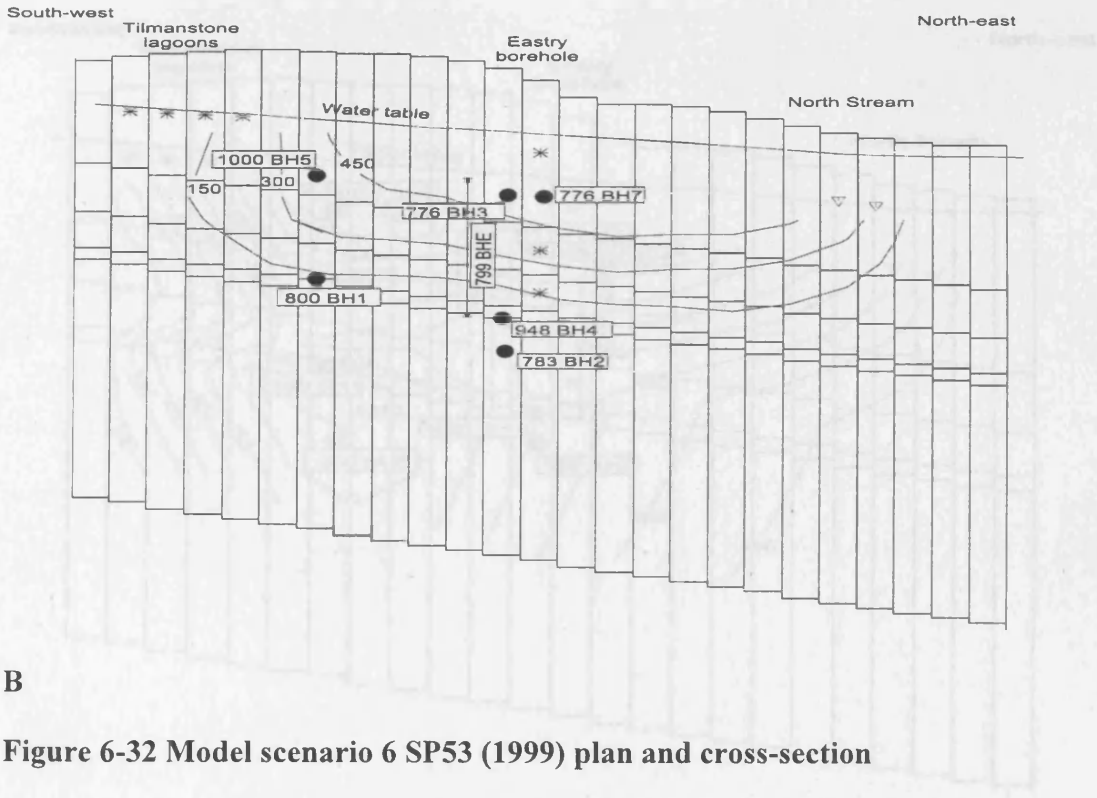

B

Figure 6-32 Model scenario 6 SP53 (1999) plan and cross-section

Decreasing the mobile porosity has a stronger effect than increasing the dispersivity value. The cross-section B shows that solute concentrations above 150 mg/L are restricted to the upper 3 layers. Compare this to model scenario 1 which had solute across all 5 layers at this time (Figure 6-26 B).

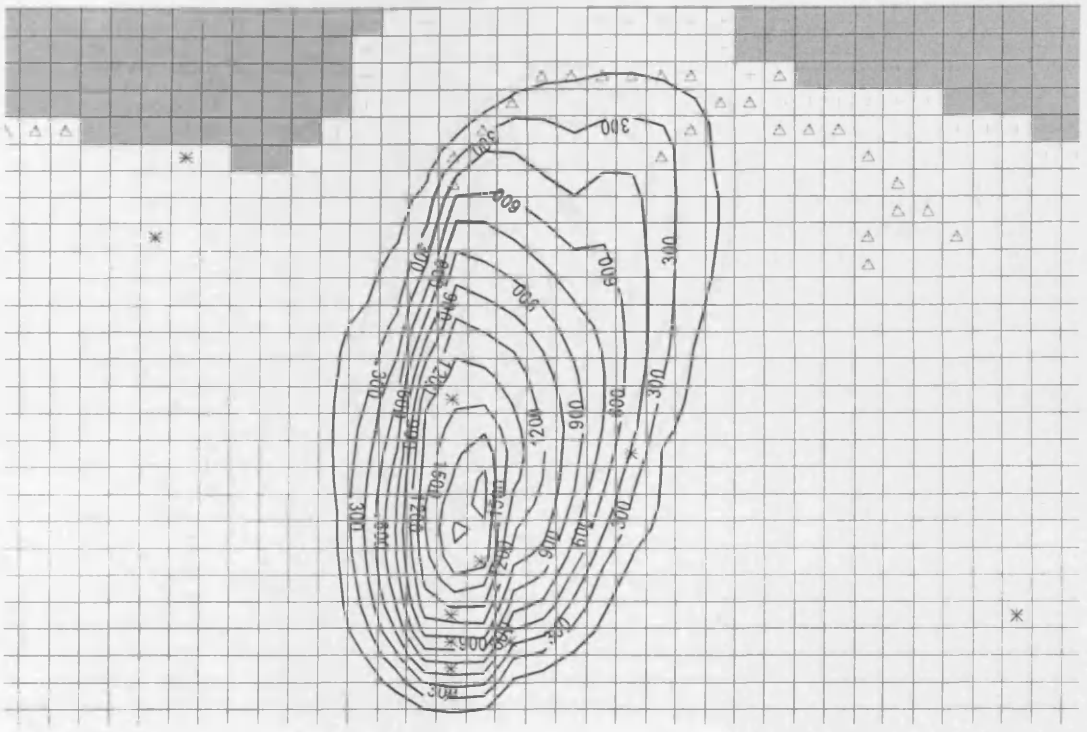

A

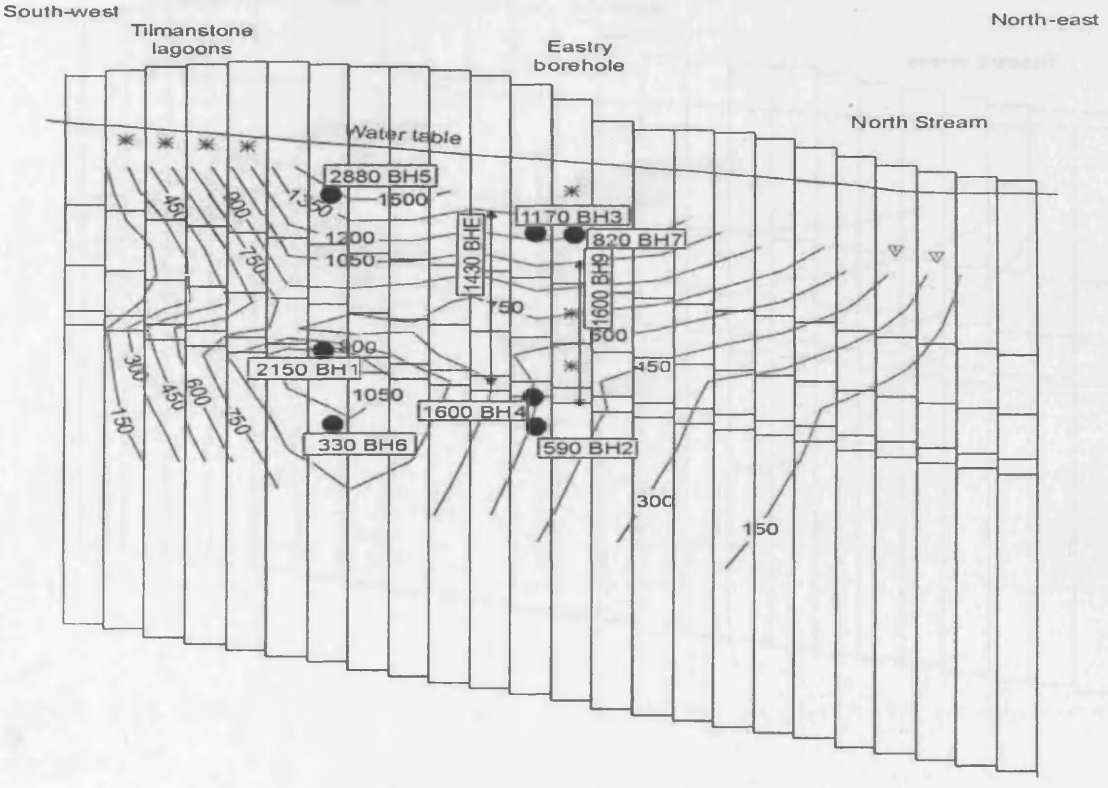

B

Figure 6-33 Model scenario 8 SP10 (1977) plan and cross-section

The introduction of a smaller block size for layer 4 predicts the solute plume splitting in two with one plume in layer 1 and a second in layer 4.

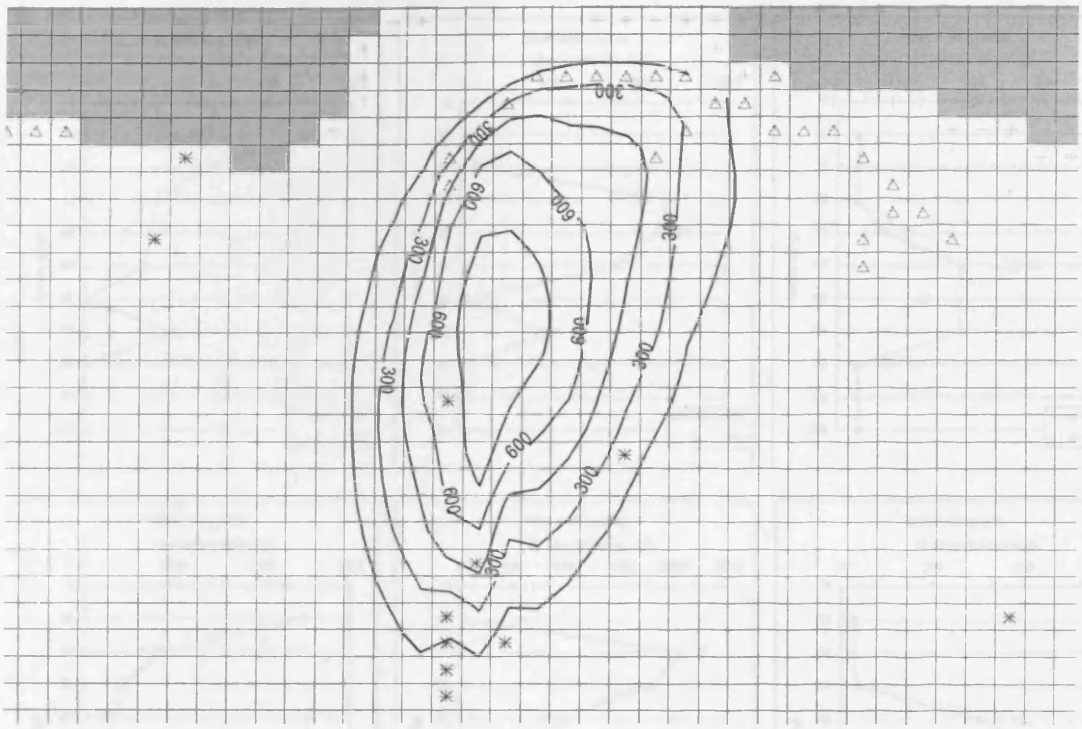

A

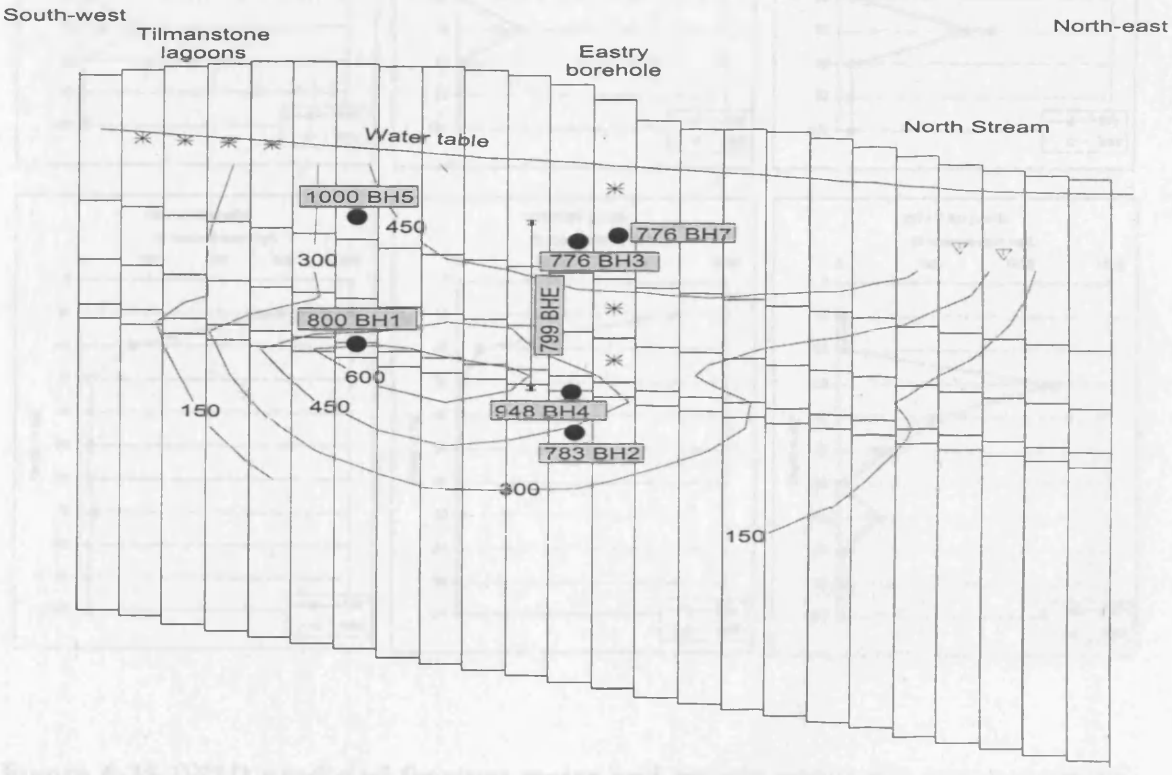

B

Figure 6-34 Model scenario 8 SP53 (1999) plan and cross-section.

The division of the plume between layers 1 and 4 is retained throughout the model stress periods. This geometry of fracture water concentrations is necessary for consistency with the matrix porewater chloride concentration profile observed in BGS LVV (Figure 5-24).

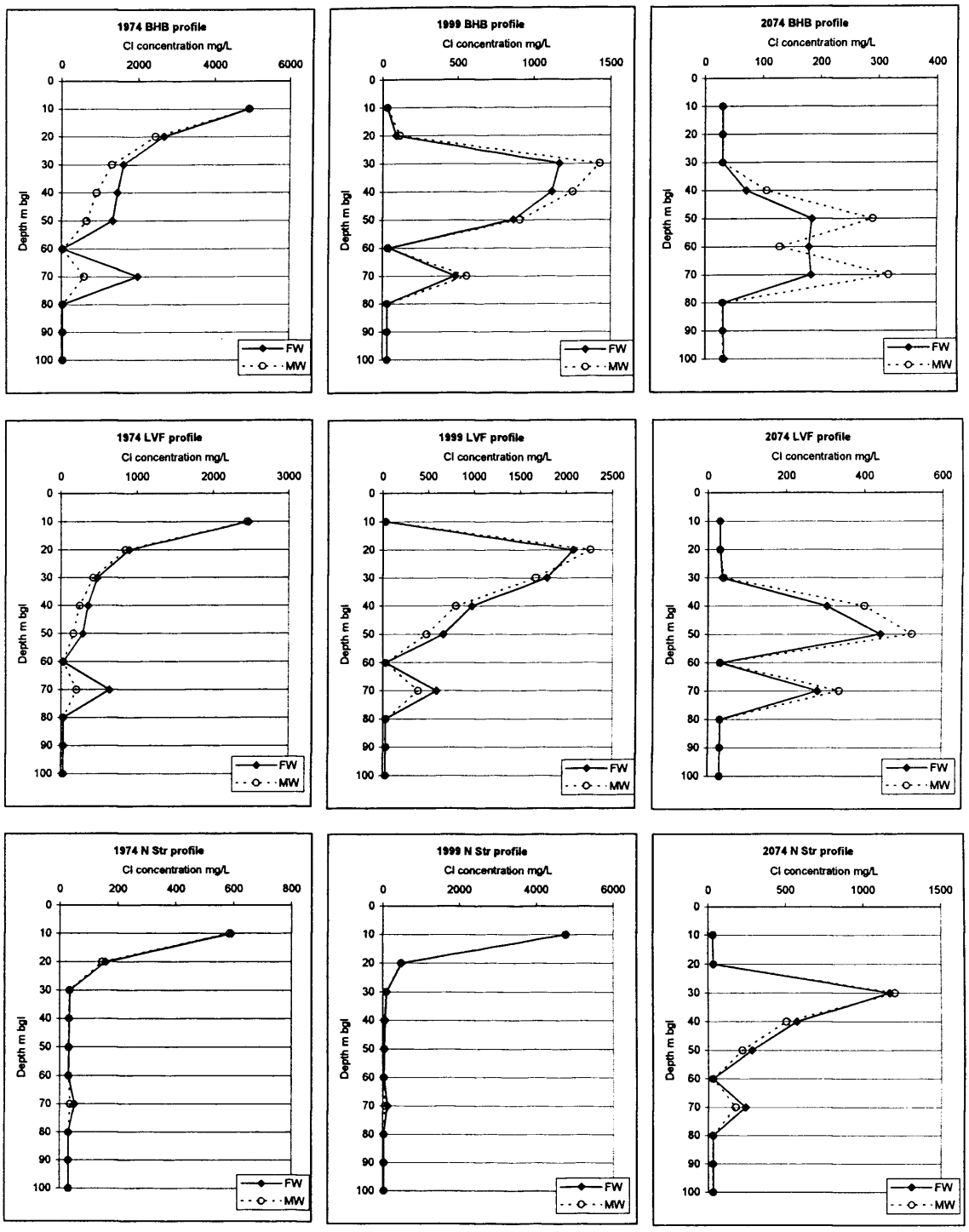

Figure 6-35 DP1D predicted fracture water and matrix porewater concentrations for 2074.

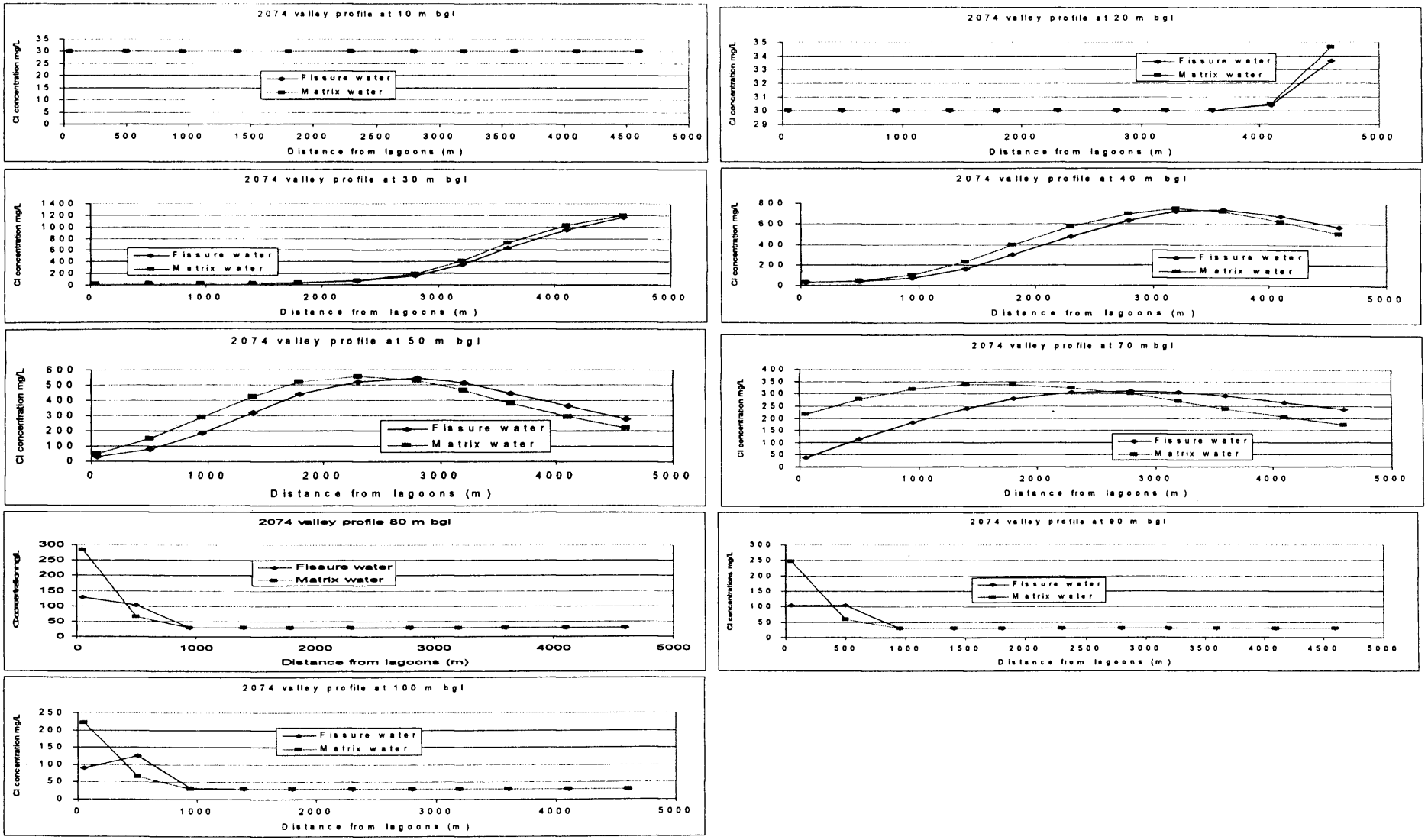

Figure 6-36 Along flow-line solute concentrations at 2074.

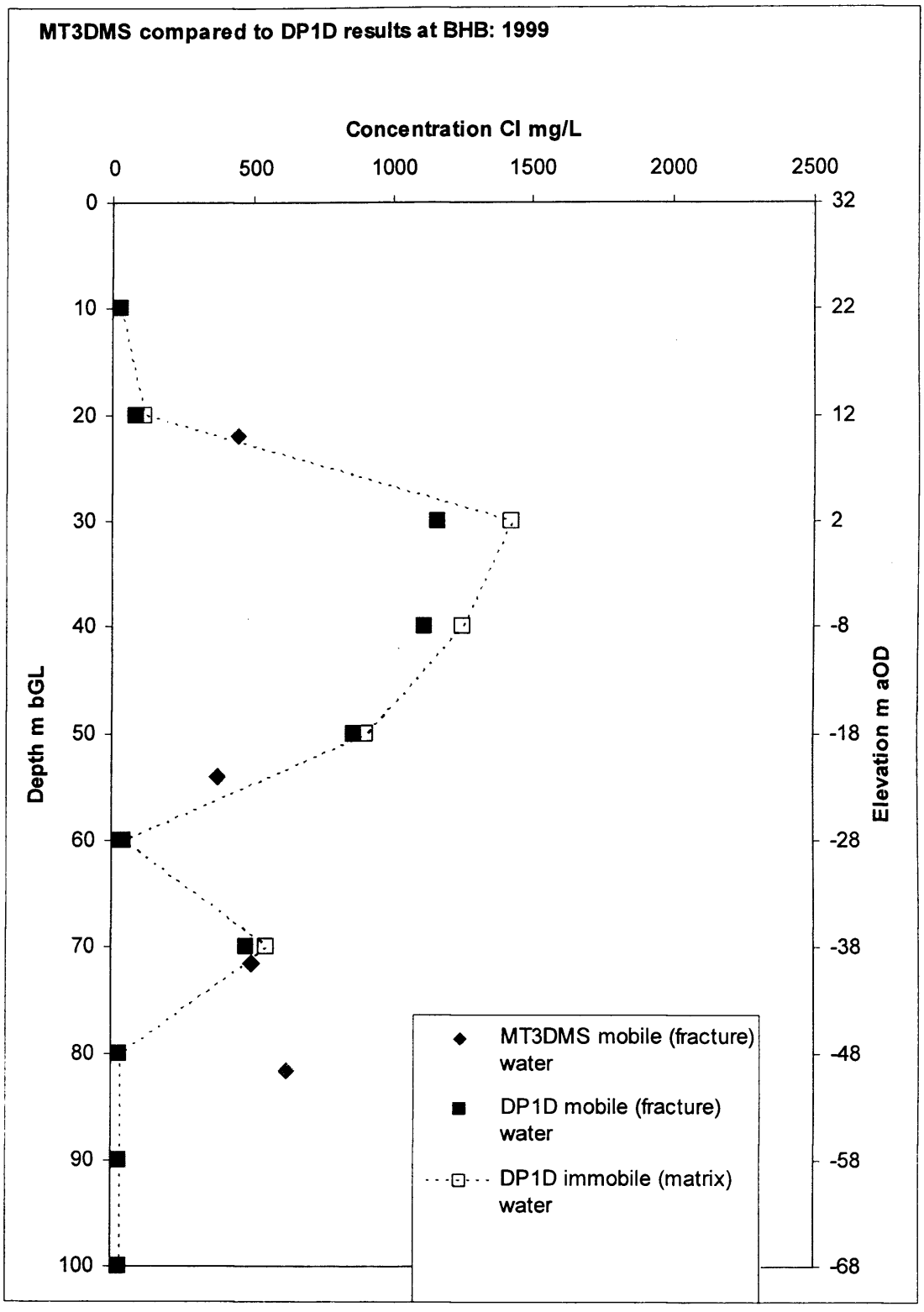

Figure 6-37 Comparison of predicted chloride concentrations at BHB for 1999.

The plot shows chloride concentrations of fracture water for MT3DMS and fracture and matrix water for DP1D.

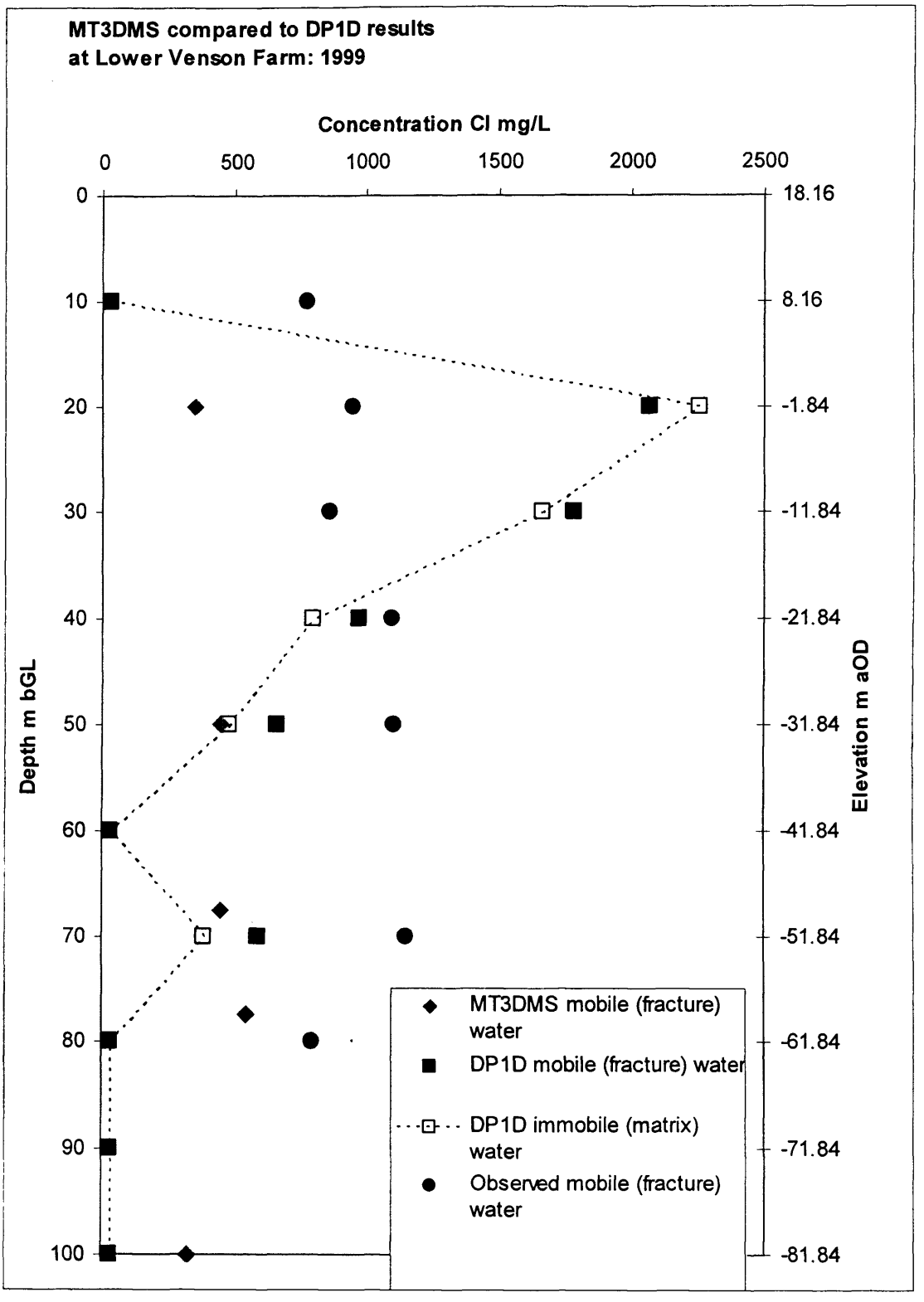

Figure 6-38 Comparison of predicted chloride concentrations at BGSLVV with observed fracture water chloride concentrations from packer testing for 1999.

The plot shows MT3DMS predicted fracture water concentrations and DP1D predicted fracture and matrix water chloride concentrations.

7 Discussion and Conclusions

This chapter provides a synthesis of the field investigations and the modelling work presented in Chapters 4, 5 and 6. It draws from their respective conclusions in order to understand solute transport in the Tilmanstone - Eastry valley in relation to requirements for characterising and monitoring the groundwater quality.

In summary, the steps described and combined in this thesis for characterising the transport characteristics of the Chalk aquifer in the Tilmanstone-Eastry valley i.e.:

- appropriate simplification of the history of the source;
- understanding the stratigraphical dependency of fracturing;
- recognising the requirements for porewater profiles;
- the use of tracer tests; and
- application of the results within a simple double-porosity model (DP1D),

constitute a coherent methodology – the Tilmanstone methodology – for addressing questions on the likely development of contaminant plumes over the long term and at large scales in the Chalk aquifer. It is proposed that the Tilmanstone methodology offers a framework for analysis of any large scale and / or long term contamination of the Chalk aquifer. The methodology emphasises the requirement for more use to be made of tracer tests; porewater profiles; fracturing related to the hydrostratigraphy, as well as the usual need for characterisation of the source term.

7.1 Research objective and specific research aims

The objective and aims of the research, as given in Chapter 1, are reiterated for clarity:
The main objective of this research is to investigate the extent to which observations of solute transport in the chalk might be linked at a variety of scales, and hence the extent to which short-term, small scale observations are related to larger-scale, longer term outcomes of interest for environmental management and assessment of groundwater contamination events.

Within this main objective, specific research aims are to:

- Evaluate the hydraulic properties of the Chalk at scales of 1 to 10 m at sites in the Tilmanstone - Eastry valley, Kent UK, using conventional field investigation techniques augmented by tracer tests;

- Re-evaluate the development of the long term pollution of groundwater by NaCl brine in the Tilmanstone - Eastry valley, at scales of 10 m to 10 km, through field studies and mathematical modelling;
- Establish the relevant application of specific data types to the prediction of solute transport in the Chalk aquifer.

The work focuses on particular features of the Chalk aquifer that may dominate solute movement at different temporal and spatial scales, for example,

- The detailed Chalk stratigraphy and associated hydrostratigraphy;
- The density, orientation and style of fracturing – at the local and regional scale;
- The significance of diffusive exchange.

7.2 Questions addressed in relation to the Chalk aquifer

In order to meet the research objective the specific research aims have been approached through a variety of field investigation methods. These field investigations were applied to investigate and characterise the framework within which solute transport in the Tilmanstone – Eastry valley is taking place, i.e. the geology, lithology and structure, and the properties of the media through which the solute has travelled, i.e. hydraulic conductivity, porosity, groundwater velocity and fracture aperture.

The approaches used to characterise the framework within which flow and solute transport have occurred and the field investigation methods adopted to quantify properties important for that flow and solute transport are discussed in the following sections.

7.2.1 The detailed Chalk stratigraphy and associated hydrostratigraphy

The detailed lithostratigraphy of the Chalk of south-east England developed by Mortimore (1986a, 1997) and Bristow *et al.* (1997) has been applied to the Chalk of the Tilmanstone – Eastry valley. Lithological detail was acquired through logging borehole core and geophysical logging. The geophysical logging was essential for extrapolating the Chalk lithology along the valley and also for identifying horizons with active groundwater flow. Widely accepted methods were employed. The digital opti-viewer, although not particularly clear at Lower Venson Farm due to the turbidity of the disturbed water column, has been used elsewhere (D. Buckley *pers. comm.*) with good

results and can provide an excellent and rapid way of determining lithology and fracturing at existing boreholes to augment core material or where core is not available.

7.2.2 Fracturing at the local and regional scale

The regional, or basin scale, structural trends identified in the area (Bloomfield *et al.* 2000) provided limits on the area modelled. Bloomfield *et al.* suggest that the regional scale structures are likely to restrict the movement of groundwater and this is supported by the success of the regional 3D groundwater flow modelling of the area.

Fracture mapping (based on the acoustic televiewer logging of BGS) and derived fracture set orientation provided insight into the BGS LVV to BH3 borehole-to-borehole tracer test (Section 5.5.2). In the tracer test tracer moved in the direction of the dominant fracture set orientation, which is approximately perpendicular to the alignment of the valley and approximately perpendicular to the direction of groundwater flow. At the scale of the Tilmanstone-Eastry valley the effect of this fracture orientation may account for the wide transverse spread of the solute.

The fracture-density depth relationship developed from field observations (Section 4.4.3 and 5.2.2) provided useful guidance for the block-size variation with depth used in the modelling. However, observations of the Dover Chalk Rock by Mortimore *et al.* (1990) provided an improved, smaller block size for use in the solute transport model (Model Scenario 8, Section 6.4.3) which resulted in an improvement to the plume geometry modelled in relation to field observations.

7.2.3 The significance of diffusive exchange

Several tracer testing techniques were employed to derive groundwater velocity, hydraulic conductivity and effective porosity values. Single borehole dilution testing was undertaken according to the methodology presented in *Groundwater Tracer Tests: a review and guidelines for their use in British aquifers* (Ward *et al.* 1998). The methodology was adapted to provide an approach suited to the Tilmanstone – Eastry valley. The solute plume in the valley is of particular value because of its long-term history and the conservative nature of chloride. The high background chloride concentration limits the standard application of single borehole dilution tests, however, which generally rely on using a simple ionic tracer and monitoring the decrease in electrical conductivity with a field EC probe. A new method for undertaking the single

borehole dilution tests, which could also be applied for natural gradient borehole to borehole tests, was investigated. The method used a string of bailers with non-return valves that allow water to flow up through the bailer as it is lowered down the borehole and then collects a sample, representative of a fixed depth, when the string is raised back up the borehole to the surface. The tracers used during the development of this method included bromide salts, Rhodamine WT, Diphenyl Brilliant Flavine 7GFF and Uranine (Sodium Fluorescein). The approach produced acceptable results; comparisons between ionic concentrations, EC measurements and bailer string and fluorescent tracer methods were good (Section 5.6). The main problem encountered was a smoothing effect on the concentration distribution in the borehole water column due to the bailer string causing more mixing in the borehole than the EC probe. This mixing effect may limit the extent to which the borehole-to-borehole BGS LVV to BH3 tracer test (Summer of 2001) can be interpreted in relation to individual fracture flow paths. Despite this, the results directly provided parameter values for DP1D model simulation of fracture and matrix porewater concentrations at the scale of the valley that provided a reasonable fit to observed data (Section 6.3.3 and 6.3.4).

The use of fluorescent dyes adds a level of complexity to undertaking tracer tests due to the sensitivity of the measuring instruments and the importance of eliminating cross contamination. All the tests using fluorescent tracers undertaken in the Tilmanstone – Eastry valley employed separate groups of helpers for injecting tracer and sampling groundwater. This produced additional burdens on personnel requirements and costs. However, these tests produced good results for Darcy velocity and hydraulic conductivity at four locations within the Tilmanstone-Eastry valley at relatively low cost, using simple equipment. In comparison to other more standard methods for determining hydraulic conductivity which were used, such as packer testing, the tracer testing was more straightforward and cheaper. The packer testing was a lengthy procedure taking approximately two days to set up and to complete six tests in one 100 m borehole. It also required a drilling rig to be on-site and the capability to dispose of pumped water. The packer test hydraulic data are representative of a larger volume of aquifer material, however, and the values obtained were more appropriate for use in the regional modelling.

The single borehole dilution testing provides evidence for a general decrease in hydraulic conductivity with depth and an increase in hydraulic conductivity down-gradient along the Tilmanstone – Eastry valley. It also revealed the existence of discrete layers or lithologies at depth with high hydraulic conductivities that proved to be important horizons for solute transport.

The results from the natural gradient tracer test produced an effective porosity value of the order of 0.1%, one order of magnitude smaller than the 1% value commonly used for solute transport calculations in the Chalk, which is based on specific yield data from pumping tests. The value of 0.1% found in this study relates well to recent suggestions that only approximately 10% of a rock fracture width is available for solute transport due to channelling effects. Further tracer testing is required to verify this value. However, if 0.1% is a reasonable representation of effective porosity for the Chalk and is demonstrated elsewhere, this will have major implications for the definition of groundwater protection zones (GPZ's) around public water supply wells in the Chalk aquifer in the UK.

The importance of using single borehole dilution tests and / or packer tests to define the hydraulic regime in the aquifer, supported by geophysical logs, is emphasised by this research. The previous work, undertaken in the 1970's, used pumping tests in order to derive hydraulic parameter values. The pumping test approach provides a homogenised view of the aquifer and the work presented in this thesis demonstrates that the solute movement in the Tilmanstone – Eastry valley has been effectively controlled by a hydrostratigraphy which has limited the vertical movement of the solute over considerable distances (at least 2000 m). This detail is not readily revealed by pumping tests unless boreholes with multiple completions are available for monitoring.

7.2.4 Summary of conclusions relating to field investigations

- Geophysical logging was essential for extrapolation of Chalk lithology along the valley and for identifying horizons with active groundwater flow;
- Regional scale geological fractures and structures act to restrict the movement of groundwater;
- Fracture set orientation may account for the wide transverse spread of the solute plume;

- The fracture-density depth relationship provided guidance for the block-size variation with depth, but direct observations of the nature of fracturing of the Dover Chalk Rock provided the best information on how to represent the block size for this formation;
- Borehole to borehole tracer tests directly provided parameter values for DP1D model simulation at the scale of the valley;
- Single borehole dilution testing identified discrete layers with high hydraulic conductivity that proved to be important horizons for solute transport;
- Tracer tests produced good results for Darcy velocity and hydraulic conductivity values along the valley at relatively low cost using simple equipment;
- The effective porosity of 0.1% derived through natural gradient tracer tests, if replicated elsewhere, may have major implications for the definition of groundwater protection zones at public water supply wells in the Chalk aquifer in the UK;
- The hydraulic conductivity values derived from packer testing proved to be more appropriate for use in the 3D regional modelling;
- Solute movement in the Tilmanstone – Eastry valley has been effectively controlled by a hydrostratigraphy which has limited the vertical movement of the solute over at least 2000 m.

7.3 Re-evaluation of the development of the long-term pollution of the Tilmanstone-Eastry valley

7.3.1 Field studies

Matrix porewater concentrations provided key data demonstrating directly that the lithology of the Chalk has a major influence over the transport of solutes in the longer-term over large distances, and that the detailed Chalk hydrostratigraphy is a necessary requirement for successful prediction of solute movement, as indicated by Mortimore (1990). Headworth (1994) also considers the porewater concentrations to have been the most useful data collected during the SWA investigations in the 1970's. It is concluded from this that wider use of matrix porewater concentration data should be adopted in order to characterise groundwater bodies (as required by the Water Framework Directive) and to strengthen the prediction of movement of contaminants in dual porosity media such as the Chalk. The 1970's SWA investigations used U100 to obtain undisturbed Chalk core and the recent 1999 investigation used wire-line rotary coring. The later technique proved problematic in the Chalk and suffered from a high level of

core loss. There is little information from the 1970's on the success of the U100 approach but it would seem that at suitable sites this method would provide core for porewater analysis relatively cheaply and would also avoid problems associated with mixing of drilling fluids and matrix porewater.

The new lithostratigraphical framework, combined with the interpretation of field investigations (geophysical logging, tracer testing, packer testing, matrix porewater profiles), required and supported the development of a new conceptual model for the hydrogeology of the Tilmanstone – Eastry valley (Section 5.7). The new conceptual model emphasises a hydrostratigraphical framework which can be tested through numerical modelling in order to make predictions about the future movement of solute in the Chalk aquifer.

7.3.2 Numerical modelling

The new conceptual model of the hydrogeology of the Tilmanstone – Eastry valley was tested through numerical modelling. The two modelling approaches presented in Chapter 6 provide interesting insights into the behaviour of solute in the Chalk aquifer. The use of a first order mass transfer coefficient approach to describe the transfer of solute between porewater and fracture water has been assessed in a 3D regional groundwater flow and transport model. The results have been considered alongside a simpler 1D semi-analytical model that describes the solute transfer according to Fickian Diffusion.

The findings from the modelling emphasise the importance of adequate determination of the 3D nature of the aquifer system but demonstrate that development of a 3D mathematical model, often a time-consuming exercise, may not be always necessary. The mathematical modelling demonstrates the requirement for the Chalk aquifer to be treated as a dual porosity medium, and the need at Tilmanstone to incorporate into the models vertical pathways for rapid solute movement which limit solute attenuation. It is not clear whether these pathways operate at all times at Tilmanstone or only under the influence of the recharge mound from the minewater infiltration lagoons, when present.

The 3D regional model was aligned parallel to the direction of the dry valleys indicated on the geological map. Higher hydraulic conductivities were ascribed to the dry valleys in the model. Although modelling reproduced a reasonable groundwater head

distribution, when the solute transport model was coupled to the flow regime it became apparent that these dry valleys act to limit the transverse movement of the contaminant in a way that is not observed in the field. This emphasises the importance of identifying fracture orientations and the impact they may have on the transverse movement of contaminant, at both a local and regional scale, and of being able adequately to represent it in a mathematical model.

The 3D solute transport modelling using MT3DMS demonstrates that using a first order mass transfer coefficient as an approximation to Fickian diffusion can provide a good representation of solute movement in the Chalk. It was not possible to compare the results from the two approaches directly, due to the difference in dimensionality between MT3DMS and DP1D. However, comparison of snapshots of predicted fracture water chloride concentrations from the MT3DMS model and the fracture and matrix water chloride concentrations predicted by the DP1D model demonstrates good agreement between the two models. The main problem that arises through using the MT3DMS approach of a first order mass transfer coefficient comes at early and late times of plume development and at the leading edge and tail of the groundwater contamination when and where the rate of mass transfer between domains is more strongly affected by the steep concentration gradients between the mobile and immobile water than the MTC approach allows. At these times and locations the solute concentrations predicted by MT3DMS will be less accurate. At early times and at the leading edges, the rate of transfer from mobile to immobile water will be underestimated by the MTC approach, so the simulated porewater concentrations will be too low, and the mobile fracture water concentrations will be too high. Contaminant will therefore be modelled as moving further and faster than if Fickian diffusion were operative. At later times, and as the remnant contamination diffuses back into the mobile groundwater from the immobile porewater, the reverse will be true: high concentration gradients occur between the mobile fracture water and the porewater, so the diffusion of solute from porewaters to fracture waters will be more rapid than is simulated using the MTC approach. MT3DMS will under-predict the fracture water solute concentrations in these situations, and the plume will be modelled as more attenuated and more persistent than by the more accurate Fickian diffusive approach. This reduction in accuracy could probably be allowed for in any risk assessment or action planning as it is predictable, and the benefits gained through being able to model

regional scale, 3D plumes may outweigh the restrictions imposed by the MTC approximation in some instances.

The transfer of field observations of groundwater velocity directly into DP1D, which was then used successfully to simulate solute movement over 2000 m, demonstrates that single borehole dilution testing and small scale (10's of m, and days) natural gradient tracer tests may be used to parameterise simple models to predict solute movement over distances and times of two orders of magnitude greater than the field tests. This is a major conclusion from the research and the more frequent use of tracer testing in the assessment of groundwater contamination is strongly recommended.

Both 3D and 1D models produce predictions that aid assessment of the risk to aquatic ecosystems from polluted groundwater. The DP1D approach is more rapid, requiring less data than required for a 3D regional groundwater flow and solute transport model. However, parameter values relating to solute transport (aperture, effective diffusion coefficient, matrix porosity etc) are required for both models. DP1D requires groundwater velocity data, and that the source and receptor are on the same flow-line. Currently only a steady state flow regime is supported, however DP1D is a powerful tool for understanding the movement of solute in a dual porosity medium. It provides excellent visualisation of the attenuation properties of the Chalk matrix, as well as the extended occurrence of the solute under elution and the changing relationship between fracture water and porewater concentrations.

7.3.3 Summary of conclusions relating to the re-evaluation of the long-term plume development

A summary of the development of the chloride plume is presented here as concluded from the field investigations and modelling work undertaken in this research. At early times of lagoon operation, chloride concentrations were low and volumes of infiltrated minewater small. Diffusive exchange with the Chalk matrix porewaters limited the extent of movement of the early plume. Increases in chloride concentration and disposal volumes infiltrating from the early 1960's produced the more significant impact on the chloride concentrations in the groundwater of the Tilmanstone – Eastry valley. The driving head produced by the (probable) saturation of the unsaturated zone beneath the infiltration lagoons caused the infiltrating chloride to move to greater depth in the Chalk. This is likely to have been aided by vertical pathways, structurally

controlled, which extend across several lithologies within the Chalk at the head of the Tilmanstone valley and may be related to tectonic features in the underlying basement rock. High groundwater velocities, due to the presence of the recharge mound under the lagoons, reduced the time for diffusive exchange with the matrix porewaters, resulting in high concentrations of chloride at greater distances from the input source than would have otherwise occurred. The high angle of fracture orientation to the general direction of the horizontal groundwater head gradient produces a large lateral dispersion of the solute plume. Particular lithologies in the Chalk at depth (notably the Dover Chalk Rock, in the Tilmanstone – Eastry valley) may in general provide important routes for more rapid transmission of solute, where hydraulic conditions are favourable. However, the porewater chloride concentrations in the Tilmanstone valley also demonstrate the capacity of the Chalk hydrostratigraphy to restrict vertical solute movement over large distances and long time-scales. The development of a fracture-density depth relationship allowed the calculation of mass transfer coefficients for use in mathematical models which provided useful insights into the significance of lithological variability.

7.4 Relevant application of specific data types to the prediction of solute transport in the Chalk aquifer

The long-term dataset of chloride measurements within the Tilmanstone – Eastry valley, held by the EA, was of limited use. It provided a guide to the extent of the movement of the solute from the minewater lagoons but, as described in Section 3.5 it does not provide information about solute stored in the matrix porewater, nor in the vertical detail required within the context of the hydrostratigraphy. The value of data on the minewater input volume and concentrations is also limited due to the absence of contemporary records of the lagoon operations. However, the predictions from the 3D regional and 1D flow-line modelling compare favourably to the observed fracture water and matrix porewater solute concentrations using the available data as the input term. As noted by Headworth (1994), it was the later volumes and concentrations from the disposal lagoons that had the greatest effect on the groundwater in the Tilmanstone - Eastry valley, and it was at this time that particular scrutiny was being paid to the lagoon operations by Southern Water. This suggests that the most important, later data are of acceptable accuracy for describing the solute input term.

From the results presented in this thesis it is evident that knowledge of the Chalk matrix porewater chloride concentrations is an essential requirement to adequately characterise the stage of development and the 3D nature of solute transport in the Chalk aquifer. The porewater chloride profiles provide evidence for lithological controls over long term movement of solutes, and also for the state of disequilibrium between mobile fracture water and immobile matrix porewater. These are essential requirements in order to characterise the groundwater body and particularly to make predictions about future trends in groundwater quality, including the quality of groundwater discharges impacting aquatic ecosystems. Chalk matrix porewater profiles would be particularly important where the history of contamination is unknown. To this end, site investigations of contaminated groundwater in the Chalk aquifer should always include collection of Chalk core for porewater analysis. This may be achieved using U100 sampling or rotary coring. In the case of rotary coring care should be taken not to introduce drilling fluid into the core sample. Removal of the outer few cm of the core or tracking drilling fluid migration by using a tracer in the drilling fluid should assist this.

7.4.1 Summary of conclusions relating to the application of specific data types to the prediction of solute transport in the Chalk aquifer

- Long-term monitoring programmes must be designed to take account of the lithologies from which groundwater is being sampled and boreholes should be constructed for sampling of specific horizons or groundwater sampling should be undertaken using packers to seal sections of borehole;
- It is important to understand the relationship and impact of fracture orientation on solute movement. The general direction of groundwater gradients may be misleading when addressing solute movement locally;
- Knowledge of the Chalk matrix porewater concentrations is an essential requirement to adequately characterise the stage of development and 3D nature of solute transport in the Chalk aquifer;
- Careful consideration needs to be given to the location of the sampling borehole within the groundwater flow field and / or the solute plume. In the case of an existing plume this means understanding whether the borehole is located centrally or is offset with respect to the plume axis. It is important to note that the borehole location relative to the main body of a plume may vary due to changes in the main

direction of groundwater movement. These changes may be due to seasonal changes in recharge or in abstraction regimes;

- Limited records of early solute disposal may not preclude the development of a source input term particularly where matrix porewater and fracture water profiles can be used to understand the stage of solute plume development or where later records indicate that later disposal quantities and concentrations were such to have had the greatest effect on groundwater concentrations.

7.5 General research conclusions

The distribution of the chloride in the groundwater of the Tilmanstone – Eastry valley has been reassessed in the light of the updated Chalk lithology presented by Mortimore (1997) and Bristow *et al.* (1997). Field investigations have been undertaken in order to develop a hydrostratigraphy for the Chalk aquifer in the Tilmanstone - Eastry valley and this has led to an updated hydrogeological conceptual model for the valley. Tracer tests have been used to determine effective solute transport parameters. Parameter values derived from tracer testing have been compared to those obtained through more conventional hydrogeological testing. Parameter values obtained through field investigations have been applied in mathematical models in order to assess the suitability of using parameters derived from small-scale tests (10's m and hours) for larger-scale (km's and decades) prediction. The results from the modelling suggest that parameter values derived from appropriate small-scale investigations can be used for larger scale prediction, but that understanding the physical framework of the aquifer is essential.

7.5.1 Implications for groundwater quality monitoring and the Water Framework Directive

One of the key purposes of the Water Framework Directive is to prevent further deterioration of, and protect and enhance the status of, aquatic ecosystems. The success of the WFD will be mainly measured by the future status of improved 'water bodies'. Water bodies should be delineated in a way that enables an appropriate description of the quantitative and chemical status of groundwater. The core porewater profile from BGS LVV (Section 5.5.1) and the modelling undertaken in Chapter 6 of this thesis demonstrate the complexity of both observing solute distribution in the Chalk aquifer and making predictions about the solute concentrations to be expected at downgradient aquatic ecosystems. The magnitude of solute concentration, as well as its duration, are

moderated by the hydraulic properties and transport characteristics of the strata through which it is moving. Predicting the risk posed to an aquatic ecosystem will have a high level of uncertainty if the hydraulic properties and transport characteristics are unknown.

The strongest influence over the movement of contaminant solutes through the Chalk aquifer is the detailed lithology and associated hydrostratigraphy, and this is demonstrated to have moderated the movement of chloride in the Tilmanstone – Eastry valley over a distance of at least 2000 m. The key to understanding this was the matrix porewater concentrations obtained from sequential Chalk core taken at BGS LVV in 1999 (Section 4.7.2) and from BHB in 1974 (Section 3.3.7). The cores also allowed the fracture-density depth relationship to be developed and these two aspects, combined with the single borehole dilution tests to describe profiles of hydraulic conductivity data for the strata, provided the necessary information to calculate the mass transfer coefficients and the required vertical stratification for use in modelling. These data, used in either the 1D or 3D modelling, considerably reduce the uncertainty attached to determining the risk posed to downstream receptors.

7.5.2 The use of the Tilmanstone-Eastry valley field site for undertaking research into solute movement in the Chalk aquifer

The Tilmanstone- Eastry valley was chosen as a field site for this research as the Chalk aquifer of the valley has experienced long-term pollution by a conservative solute and is therefore representative of a large scale, long-term tracer test in the most important aquifer in south-east England. Additionally, it has previously been the focus of experimental work and therefore has existing infrastructure and associated long-term data-sets. Access to field sites was relatively straightforward as they are covered either by Environment Agency agreements with landowners or are owned by Southern Water plc. Ownership of the Lower Venson Farm site by Southern Water plc was particularly important in gaining access for drilling of two new boreholes, BGS LVV and BGS LVI. The pollution of the groundwater in the Tilmanstone – Eastry valley means that no exploitation of the groundwater resources for public supply has occurred, and this in turn means that permissions for undertaking tracer testing is more straightforward than in areas where nearby PWS's may be affected by tracer material.

Although there is an existing borehole infrastructure in the valley, the boreholes are not ideally located for some tracer tests. The boreholes at each site (Thornton Farm, Lower Venson Farm and Eastry) were originally constructed to be open across specific, different, intervals of the active depth of the aquifer, as determined from geophysical logging, rather than being open at the same intervals. This results in each site having boreholes open at different depths which precludes borehole to borehole tracer testing except over distances of more than approximately 300 m. This was too great a distance for natural gradient tests (pumping was precluded due to the costs of disposal of abstracted water) over the lifetime of the research.

The drilling of BGS LVV and BGS LVI at the Lower Venson Farm site has resulted in 3 boreholes open over the same depth interval within 30 to 50 m of each other. This site now provides reasonable infrastructure for conducting further natural gradient borehole to borehole tracer tests as well as single borehole dilution tests. All the boreholes remain useful for sampling Chalk fracture water solute concentrations, although consideration of the size of the open interval is necessary. Pumped samples rather than bailed samples should be taken, and the use of packers to reduce the section of aquifer sampled from should be considered.

The use of boreholes for conducting larger scale tracer tests between sites (e.g. from Lower Venson Farm to Eastry) will continue to be problematic because of the effects of dilution and the uncertainty of flow paths due to fracture orientation relative to the general groundwater gradient. Pumped borehole-to-borehole tests will also be expensive due to the size of the pump required to produce an adequate cone of depression in the Chalk aquifer and the cost of disposal of the high chloride water. It may be feasible to set up a dipole test and to re-circulate abstracted water back into an injection borehole

8 Recommendations for further work

A number of recommendations for further work arise from the conclusions drawn from this thesis. These recommendations are presented below.

8.1 The importance of Chalk lithostratigraphy

The principal recommendation for further work is the application of the new Chalk stratigraphy, as determined by Mortimore (1986a, 1997) and Bristow *et al.* (1997), to other locations on the Chalk aquifer.

8.2 Further work on fractures

New boreholes drilled in the Chalk should be logged to determine fracture frequency and flow-logged to determine contribution of fractures to flow in the borehole. Fracture logging may be carried out directly on Chalk core, or indirectly through acoustic Televiewer logs and Videoscan type digital imaging. Other sources of fracture data include tunnelling and other geotechnical investigations. This could lead to the establishment of a database of fracture-density depth relationships and the relationship between fracturing, tectonic regime and specific Chalk lithologies. It is important to add to our understanding of fracture frequency with depth from deep boreholes as much of the current data is from relatively shallow or outcrop sites and this is unlikely to be representative of deeper fracturing patterns or frequency.

Further work is needed in understanding the effect of fracture orientation on solute transport in the Chalk at different scales. Appropriate ways of incorporating fracture orientation into mathematical models at different scales also needs developing.

8.3 Relationships between geomorphology and solute transport properties in the Chalk aquifer

More data are required on the differences in solute transport properties between valley and interfluve areas. Key data requirements are effective porosity, fracture-density depth relationships and groundwater flux and velocity. Acquisition of such data will continue to be problematic while observation boreholes are located away from interfluve areas. A dearth of observation boreholes located in interfluve areas results in poorly defined groundwater head gradients and, as indicated in the modelling element

of this research, it may be incorrect to assume that the main movement of solute in the groundwater will be along the axis of a valley.

8.4 The potential of groundwater tracers

Tracer tests should be more widely applied in studies of groundwater contamination. The further development of tracing methods that allow observation of borehole-to-borehole and borehole dilution in the injection borehole are required. In the Chalk aquifer the potential of fluorescent tracers and down-hole fluorometers needs to be realised in order to overcome the dilution that occurs over distances of tens of metres. Use of down-hole fluorometers may be particularly valuable in the investigation of individual fracture flow paths.

Further tracer testing should be undertaken to corroborate the effective porosity values determined during this research, both in the Tilmanstone – Eastry valley and elsewhere in the Chalk aquifer.

Tracer testing at different stages of the water-table should be undertaken to establish seasonal variability.

8.5 The requirement for porewater analysis

The findings from the research undertaken in this thesis indicate that it is essential to analyse Chalk matrix porewaters within a lithologically based hydrostratigraphic framework to describe the status of contaminant flux in a dual porosity aquifer and predict future trends in groundwater quality.

8.6 Porewater – mobile groundwater diffusive exchange

More data are required on the effect of lithology on the diffusion coefficient for Chalk, as well as the extent to which fracture skins are present and their influence on the transfer of solutes between the mobile and immobile domain.

9 References

ACER 1990a. Potential groundwater resource from a Chalk aquifer contaminated by mine water from Tilmanstone Colliery. *Unpublished report for the Folkestone and District Water Company.*

ACER 1990b. Water resources study of the East Kent aquifer; mathematical model of the Chalk aquifer – data review and mathematical model development. *Unpublished report for the Folkestone and District Water Company.*

ACER 1991. Water resources study of the East Kent aquifer; mathematical model of the Chalk aquifer – final report. *Unpublished report for the Folkestone and District Water Company.*

Allen, D. J., Brewerton, L. J., Coleby, L. M., Gibbs, B. R., Lewis, M. A., MacDonald, A. M., Wagstaff, S. J. and Williams, A. T. 1997. The physical properties of major aquifers in England and Wales. *British Geological Survey Technical Report, WD/97/34.* Environment Agency R&D Publication 8.

Anon 1953. Confidential report on the Disposal of Mine Drainage Waters in the Kent Coalfield. H.M. Geological Survey, Water Division.

Aris, R. 1956. On the dispersion of a solute flowing through a tube. *Proceedings of the Royal Society of London*, **235**, pp67-77.

Aris, R. 1975. The mathematical theory of diffusion and reaction in permeable catalysts. Vols. I and II. Clarendon, Oxford.

Atkinson, T. C. and Smith, D. I. 1974. Rapid groundwater flow in fissures in the Chalk: an example from South Hampshire. *Quarterly Journal of Engineering Geology*, **7**, pp197-205.

Banks, D., Cosgrove, T., Harker, D., Howsam, P. and Thatcher, J. P. 1993. Acidisation: borehole development and rehabilitation. *Quarterly Journal of Engineering Geology*, **26**, pp109-125.

Banks, D., Davies, C. and Davies, W. 1995. The Chalk as a karstic aquifer; the evidence from a tracer test at Stanford Dingley, Berkshire. *Quarterly Journal of Engineering Geology*, **28**, S31-38.

Barenblatt, G. E., Zheltov, I. P. and Kochina, I. N. 1960. Basic concepts in the theory of seepage of homogeneous liquids in fractured rocks. *Soviet Journal of Applied Mathematics and Mechanics*, **24(5)**, 1286-1303.

Barker, J. A. 1982. Laplace transfer solutions for solute transport in fissured aquifer. *Advances in Water Resources*, **5**, pp98-104.

Barker, J. A. 1985a. Modelling the effects of matrix diffusion on transport in densely fissured media. In: *Hydrogeology in the Service of Man.* International Association of Hydrological Sciences Publication **154**. Congress of the International Association of Hydrogeologists, Cambridge 1985.

Barker, J. A. 1985b. Block geometry functions characterising transport in densely fissured media. *Journal of Hydrology*, **77**, pp263-279.

Barker, J. A. 1991. Transport in fractured rock. In: Downing, R. A. & Wilkinson, W. B. (eds) *Applied Groundwater Hydrology*, Claridon Press, Oxford, pp199-216.

Barker, J. A. 1993. Modelling groundwater flow and transport in the Chalk, In: *The Hydrogeology of the Chalk of North-West Europe*, (Ed) Downing, R. A., Price, M. & Jones, G. P. Clarendon Press, Oxford.

Barker, J. A. and Foster, S. S. D. 1981. A diffusion exchange model for solute movement in fissured porous rock. *Quarterly Journal of Engineering Geology*, **14**, pp17-24.

Barker, J. A., Wright, T. E. and Fretwell, B. A. 2000. A pulsed-velocity method of double-porosity solute transport modelling. In: *Tracers and modelling in hydrogeology*. IAHS Publ. No. 262.

Barker, R., Lloyd, J. W. and Peach, D. W. 1984. The use of resistivity and gamma logging in lithostratigraphical studies of the Chalk in Lincolnshire and South Humberside. *Quarterly Journal of Engineering Geology*, **17(1)**, pp71-80.

Barraclough, D., Gardner, C. M. K., Wellings, S. R. and Cooper, J. D. 1994. A tracer investigation into the importance of fissure flow in the unsaturated zone of the British Upper Chalk. *Journal of Hydrology*, **156**, pp459-469.

Bear, J. 1972. Dynamics of fluids in porous media. Elsevier, New York.

Berkowitz, B. 2002. Characterising flow and transport in fractured geologic media: A review. *Advances in Water Resources*, **25**, pp861-884.

Bevan, T. G. and Hancock, P. L. 1986. A late Cenozoic regional mesofracture system in southern England and northern France. *Journal of the Geological Society*, **143**, pp355-362.

Bibby, R. 1979. A numerical model of contamination of mine drainage water of the Chalk aquifer at Tilmanstone, Kent. *Unpublished report of the Water Research Centre,* Medmenham, Berks, UK.

Bibby, R. 1981. Mass transport studies of solutes in dual porosity media. *Water Resources Research*, **17**, pp1075-81.

Biggar, J. W. and Nielsen, D. R. 1962. Miscible displacement, II. Behaviour of tracers. *Soil Science Society of America Proceedings*. **26**, pp125-128.

Bird, M. J., Bloomfield, J. P., Buckley, D. K., Gale, I. N., Griffiths, K., Williams, A. T. and Williams, P. 1999. Project FRACFLOW – Report on the drilling and installation of boreholes, Tilmanstone, Kent. British Geological Survey Technical Report WD/99/42.

Biver, P. 1994. Numerical simulation of tracer tests to quantify, at a macroscopic scale, transport processes in a multiporous aquifer, In: *Transport and Reactive Processes in Aquifers*, (Ed) T.H. Dracos and F. Stauffer. Balkema, Rotterdam.

Black, J. H. and Kipp, Jr, K. L. 1983. Movement of tracers through dual porosity media – experiments and modelling in the Cretaceous Chalk. *Journal of Hydrology*, **121**, pp293-320.

Bloomfield, J. P. 1996. Characterisation of hydrogeologically significant fracture distributions in the Chalk: an example from the Upper Chalk of southern England. *Journal of Hydrology*, **184**, pp355-379.

Bloomfield, J. P. 1999. FRACFLOW – Geological State-of-the-Art review. British Geological Survey Technical Report WD/99/13.

Bloomfield, J. P., Brewerton, L. J. and Allen, D. J. 1995. Regional trends in matrix porosity and dry density of the Chalk of England. *Quarterly Journal of Engineering Geology*, **28**, S131-S142.

Bloomfield, J. P., Gale, I., Jacobsen, P. R., Nygaard, E. and Pederson, L. 2000. Geology, In: Fracflow Third annual progress report. Contaminant transport, monitoring techniques and remediation strategies in cross European fractured chalk. European Commission Environment and Climate 1994 – 1998 Programme, contract number ENV4-CT97-0441.

Bourke, P. J., Durrance, E. M., Hodgkinson, D. P. and Heath, M. J. 1985. Fracture hydrology relevant to radionuclide transport. Report AERE-R 11414 of the Atomic Energy Research Establishment, Harwell.

Brassington, F.C. and Walthall, S. 1985. Field techniques using borehole packers in hydrogeological investigations. *Quarterly Journal of Engineering Geology*, **18**, pp181-193.

Brettmann, K. L., Hogh, J. K. and Jakobsen, R. 1993. Tracer test in fractured Chalk 2. Numerical analysis. *Nordic Hydrology* **24(4)**, pp275-296.

Brewer, R. J., Fellingham, L. R. and Jefferies, N. L. 1992. Groundwater contamination at Harwell Laboratory. *Progress Report November 1990 to April 1992,* AEA-D&R-0406, AEA Technology plc, Harwell, Didcot, Oxfordshire UK.

Bristow, R., Mortimore, R. N. and Wood, C. 1997. Lithostratigraphy for mapping the Chalk of Southern England. *Proceedings of the Geologists' Association*, **109**, pp293-315.

British Geological Survey 1977. 1:50000 Series Geological Maps, Sheet 290 Dover.

British Geological Survey 1982. 1:50000 Series Geological Maps, Sheet 289 Canterbury.

British Geological Survey 1988. Geology of the country around Ramsgate and Dover, *Her Majesty's Stationery Office, London.* ISBN 0 11 884461 X.

Brereton, R. 1973. Report on the geophysical logging of boreholes at Lower Venson Farm. *Southern Water Authority internal report.*

Brown, S. R. 1987. Fluid flow through rock joints: the effect of surface roughness. *Journal of Geophysical Research*, **92B**, pp1337-47.

Buchan, S. 1962. Disposal of drainage water from coal mines into the Chalk in Kent. *Water treatment and examination*, **11**, pp101-105.

Burgess, W. B., Dottridge, J. and Symington, R. M. 1998. Methyl tertiary butyl ether (MTBE): a groundwater contaminant of growing concern, In: *Groundwater contaminants and their migration.* (Eds) Mather, J., Banks, D., Dumpleton, S. & Fermor, M.. Geological Society, London, Special Publications, **128**, 29-34.

Carniero, J. 1996. The evolution of the Tilmanstone contaminant plume. *Unpublished MSc thesis, University College London.*

Chahinian, N. 1999. Investigating recharge mechanisms on a Chalk catchment in East Kent. *Unpublished MSc thesis, University College London.*

Chilton, P. J., Lawrence, A. R. and Barker, J. A. 1989. Chlorinated solvents in chalk aquifers: some preliminary observations on behaviour and transport, In: *Chalk, Proceedings of the International Chalk Symposium held at Brighton Polytechnic, 4-7 September 1989.* Thomas Telford, London. ISBN 0 7277 15410.

Chilton, P. J. and Milne, C. J. 1994. Groundwater quality assessment: A national strategy for the NRA. Hydrogeology Series, Technical Report WD/94/40C, British Geological Survey, Keyworth, Nottingham.

Clarke, L. 1992. Methodology for monitoring and sampling groundwater. WRc plc R&D note 126 for National Rivers Authority R&D contract 284.

Coats, K. H. and Smith, B. D. 1964. Dead-end pore volume and dispersion in porous media. *Society of Petroleum Engineers Journal*, **4**, pp73-84.

Common Implementation Strategy, 2003. Common Implementation Strategy for the Water Framework Directive (2000/60/EC): Identification of Water Bodies - Horizontal guidance document on the application of the term 'water body' in the context of the Water Framework Directive. January 2003. http://forum.europa.eu.int/Public/irc/env/wfd/library?l=/framework_directive/guidance_documents/identification_bodies&vm=detailed&sb=Title *last accessed 4th October 2003.*

Connorton, B. J. & Hanson, C. A. 1978. Regional modelling, digital and analogue approaches. *Thames Groundwater Scheme*, Institution of Civil Engineers, 61-76.

Coy, V. 2001. A study of matrix block geometry with respect to dual porosity models and tracer test analysis. *Unpublished MSc thesis, University College, London.*

Crampon, N., Roux, J. C., Bracq, P., Delay, F., Lepiller, M., Mary, G., Rasplus, L. and Alcayd, G. 1993. France. In: *The Hydrogeology of the Chalk of North-West Europe*, (Ed) Downing, R. A., Price, M. & Jones, G. P. Clarendon Press, Oxford, pp113-152.

Cross, G. A., Rushton, K. R. and Tomlinson, L. M. 1995. The east Kent chalk aquifer during the 1988-1992 drought. *Journal of the Institution of Water and Environmental Management,* **11**, pp193-199.

Dagan, G. 1979. Models of groundwater flow in statistically homogeneous porous formations. *Water Resources Research*, **15(1)**, pp47-63.

Dagan, G. 1982. Stochastic modelling of groundwater flow by unconditional and conditional probabilities, 2, Solute transport. *Water Resources Research*, **18(4)**, pp835-848.

Dassargues, A., Brouyere, S. and Derouane, J. 1996. From calibration on tracer test data to computation of protection zones: upscaling difficulties in a deterministic modelling framework. In: *Calibration and Reliability in Groundwater Modelling*, Proceedings of the ModelCARE 96 Conference held at Golden Colorado. International Association of Hydrological Sciences Publication No. **237**.

Dassargues, A., Monjoie, A., Lambert, J. and Pierlot, A. 1991. Finite element model of a regional water-table aquifer in Cretaceous chalk, Belgium. *Revue des Sciences de l'Eau*, **4(1)**, pp39-63.

Davey, I., Moxon, I. & Hybert, D. 1998. Investigation of contamination at a public supply borehole in Hertfordshire, UK, In: Groundwater contaminants and their migration. Mather, J., Banks, D., Dumpleton, S. & Fermor, M. (Eds). Geological Society, London, Special Publications, **128**, 75-92.

De Smedt, F. and Wierenga, P. J. 1984. Solute transfer through columns of glass beads. *Water Resources Research*, **20**, pp225-232.

De Smedt, F., Wierenga, P. J. and Van der Benken, A. 1981. Theoretical and experimental study of solute movement through porous media with mobile and immobile water. *VUB-Hydrology*, **6**, 219pp. Univ. Brussels, Belgium.

Deans, H. H. 1963. A mathematical model for dispersion in the direction of flow in porous media. *Society of Petroluem Engineers Journal*, **3**, pp49-52.

DEFRA 2002. Digest of Environmental Statistics, accessed from the internet. Published April 16 2002, site accessed 09/10/2002. Http://www.defra.gov.uk/environment/statistics/des/inlwater/ch034548.htm#WaterAbstractions

DEFRA 2003. Third consultation on the Water Framework Directive. Accessed via website http://www.defra.gov.uk/corporate/consult/waterframe3 last accessed 11.04.2004.

Domenico, P. A. and Schwartz, F. W. 1990. Physical and Chemical Hydrogeology. Wiley, New York.

Downing, R. A. 1956. Ground water resources of the Chalk and Eocene of North Kent. H. M. Geological Survey, Water Division.

Downing, R. A., Price, M. and Jones, G. P. 1993. The making of an aquifer, In: The Hydrogeology of the Chalk of North-West Europe, (Ed) Downing, R. A., Price, M. & Jones, G. P. Clarendon Press, Oxford. ISBN 0-19-854285-2.

Downing, R. A. and Wilkinson, W. B. (Editors) 1991. Applied Groundwater Hydrology: A British Perspective. Clarendon Press, Oxford. ISBN 0-19-852139-1.

Driscoll, F.G. 1986. Groundwater and Wells. Johnson Filtration Systems, St Paul Minnesota. ISBN 0961645601.

EEA 2003 European Environment Agency Eurowaternet Initiative http://reports.eea.eu.int/report_2003_0617_150910/en, last accessed 25/09/2003.

Environment Agency 2001. Water Resources for the Future: A Water Resources Strategy for England and Wales. Accessed via website http://www.environment-agency.gov.uk/subjects/waterres/ last accessed 09/10/2002.

European Commission 1975. Surface Water Directive 75/440/EEC, concerning the quality required of surface water intended for the abstraction of drinking water in the Member States. *Official Journal L 194,* 25.07.1975.

European Commission 1976. Dangerous Substances Directive 76/464/EC, on pollution caused by certain dangerous substances discharged into the aquatic environment of the Community. *Official Journal L129,* 18.05.1976.

European Commission 1977. Information Exchange Directive 77/795/EEC, establishing a common procedure for the exchange of information on the quality of surface freshwater in the Community. *Official Journal L334,* 24.12.1977.

European Commission 1978. Protection of Freshwater for Fish 78/659/EEC, on the quality of fresh waters needing protection or improvement in order to support fish life. *Official Journal L 222,* 14.08.1978.

European Commission 1979a. Measurement Methods Directive 79/869/EEC, concerning the methods of measurement and frequencies of sampling and analysis of surface water intended for the abstraction of drinking water in the Member States. *Official Journal L 271,* 29.10.1979.

European Commission 1979b. Quality of Shellfish Waters Directive 79/923/EEC, on the quality required of shellfish waters. *Official Journal L 281,* 10.11.1979.

European Commission 1980a. Groundwater Directive 80/68/EEC, on the protection of groundwater against pollution caused by certain dangerous substances. *Official Journal L20,* 26.01.1980.

http://europa.eu.int/eur-lex/en/consleg/main/1980/en_1980L0068_index.html last accessed 09/10/2002.

European Commission 1980b. Drinking Water Directive 80/778/EEC, relating to to the quality of water intended for human consumption. *Official Journal L229,* 30.08.1980.

European Commission 1991a. Pesticides Directive 91/414/EEC, concerning the placing of plant protection products on the market. *Official Journal L230,* 19.08.1991.

European Commission 1991b. Nitrates Directive 91/676/EEC, concerning the protection of waters against pollution caused by nitrates from agricultural sources. *Official Journal L375,* 31.12.1991.

European Commission 1992. Habitats Directive 92/43/EEC, on the conservation of natural habitats and of wild fauna and flora. *Official Journal L206,* 22.07.1992.

European Commission 2001. Priority Substances COM (2001) 17

European Commission, 1993. Communication on Ecological Water Quality COM (1993) 680.

European Commission, 1996. IPPC Directive 1996, concerning integrated pollution prevention and control. *Official Journal L 257,* 10.10.1996 P. 0026 – 0040.

European Commission, 2000. Water Framework Directive 2000/60/EC, establishing a framework for Community action in the field of water policy. *Official Journal L327,* 22.12.2000 P. 0001 – 0073. http://europa.eu.int/comm/environment/water/water-framework/index_en.html last accessed 10/10/2002

Everett, L. G. 1980. Groundwater Monitoring. Schenectady, New York. ISBN 0931690145.

Feenstra, S., Cherry, J. A., Sudicky, E. A. and Haq, Z. 1984. Matrix diffusion effects on contaminant migration from an injection well in fractured sandstone. *Groundwater* **22**, pp307-316.

Fetter, C. W. 1992. Contaminant hydrogeology, Macmillan, New York. ISBN 0-02-337135-8.

Foster S. S. D 1975. The Chalk groundwater tritium anomaly – a possible explanation. *Journal of Hydrology*, **25**, 159-165.

Foster, S. S. D. 1993. The Chalk aquifer – its vulnerability to pollution, In: The Hydrogeology of the Chalk of North-West Europe, (Ed) Downing, R.A., Price, M. & Jones, G.P. Clarendon Press, Oxford.

Foster, S. S. D., Bridge, L. R., Geake, A. K., Lawrence, A. R. & Parker, J. M. 1986. The Groundwater Nitrate Problem. Hydrogeological Report No. 86/2, British Geological Survey, Keyworth, Nottingham.

FRACFLOW 1999. Contaminant transport, monitoring techniques and remediation strategies in cross European fractured chalk. Second annual progress report. Project funded by the European Commission under the Environment and Climate 1994 – 1998 Programme. Contract No: ENV4-CT97-0441.

FRACFLOW 2000. Contaminant transport, monitoring techniques and remediation strategies in cross European fractured chalk. Third annual progress report. Project funded by the European Commission under the Environment and Climate 1994 – 1998 Programme. Contract No: ENV4-CT97-0441.

FRACFLOW 2001. Contaminant transport, monitoring techniques and remediation strategies in cross European fractured chalk. Final Report. Project funded by the European Commission under the Environment and Climate 1994 – 1998 Programme. Contract No: ENV4-CT97-0441.

Freeze, R. A. and Cherry, J. A. 1979. Groundwater, Prentice-Hall Inc, New Jersey. ISBN 0-13-365312-9.

Fretwell, B. A. 1999. Distribution of contaminants in the seasonally unsaturated zone of the Chalk aquifer. *Unpublished PhD thesis, University of London.*

Fretwell, B. A., Burgess, W. G. and Barker, J. A. 2000. Contaminant retardation within the seasonally unsaturated zone of the Chalk aquifer – the SUZ process. In: *Tracers and Modelling in Hydrogeology, Proceedings of the TraM'2000 conference*, International Association of Hydrological Sciences Publication No. 262, pp385-390.

Garnier, J. M., Crampon, N., Préaux, C., Porel, G. and Vreuix, M. 1985. Traçage par 13C, 2H, I- et uranine dans la nappe de la craie sénonienne en écoulement radial convergent (Béthune, France). *Journal of Hydrology*, **78**, pp379-392.

Gelhar, L. W. and Axness, C. L. 1983. Three dimensional stochastic analysis of macro dispersion in aquifers. *Water Resources Research*, **19(1)**, 161-180.

Gelhar, L. W., Welty, C. and Rehfeldt, K. R. 1992. A critical review of data on field-scale dispersion in aquifers. *Water Resources Research*, **28(7)**, pp1955-74.

Gershon, N. D. and Nir, A. 1969. Effect of boundary conditions of models on groundwater tracer distribution in flow through porous media. *Water Resources Research*, **5**, pp830-839.

Gillespie, P., Howard, C. B., Walsh, J. J. and Waterson, J. 1993. Measurement and charcaterisation of spatial distributions of fractures. *Tectonophysics* **226**, pp113-141.

Gooddy, D. C., Kinniburgh, D. G. and Barker, J. A. 1995. Development of a rapid method for determining apparent diffusion coefficients or chloride in Chalk. *Technical Report WD/95/66.* British Geological Survey, Keyworth, UK.

Gooddy, D. C. and Lawrence, A. R. 1994. Groundwater contamination of the Chalk by chlorinated solvents: a review of remediation techniques. Technical report WD/95/48, British Geological Survey.

Green, R. E., Rao, P. S. C. and Corey, J. C. 1972. Solute transport in aggregated soil: tracer zone shape in relation to pre-velocity distribution and adsorption. *Proceedings of the 2nd symposium on fundamentals of transport phenomena in porous media.* IAHR-ISSS, Guelph, Ontario, August 7-11, 1972, **2**, pp732-752.

Grisak, G. E. and Pickens, J. F. 1980. Solute transport through fractured media, 1: The effect of matrix diffusion. *Water Resources Research*, **16**, pp719-730.

Grisak, G. E., Pickens, J. F. and Cherry, J. A. 1980. Solute transport through fractured media, 2: Column study of fractured till. *Water Resources Research*, **20**, pp731-739.

Haggerty, R. and Gorelick, S. M. 1995. Multiple rate mass transfer for modelling diffusion and surface reactions in heterogeneous media. *Water Resources Research*, **31(10)**, pp2838-2400.

Halevy, E., Moser, H., Zellhofer, O. and Zuber, A. 1967. Borehole dilution techniques: A critical review. Isotopes in hydrology, IAEA (International Atomic Energy Agency) Vienna, pp531-564.

Hancock, J. M. 1993. The formation and diagenesis of chalk. *In*: Downing, R.A., Price, M. and Jones, G. P. (eds.) *The Hydrogeology of the Chalk of North West Europe.* Oxfrod University Press, pp14-34.

Haring, R. E. and Greenkorn, R. A. 1970. A statistical model of a porous medium with nonuniform pores. *American Institute Chemical Engineering Journal* **16**, pp477-483.

Harvey, B. 1962. Disposal of mine drainage water from Tilmanstone Colliery. H.M. Geological Survey, Water Division.

Harvey, C. F. and Gorelick, S. M. 2000. Rate-limited mass transfer or macrodispersion: which dominates plume evolution at the macrodispersion experiment (MADE) site? *Water Resources Research* **36**, pp637-650.

Hazell, S. 1998. The use of tracer tests to investigate the site of a large contamination plume. *Unpublished MSc thesis, University College London.*

Headworth H. 1994. The groundwater schemes of Southern Water 1970-1990: a golden age. Published by H. Headworth. Copy held in the library of the Geological Society of London, Burlington House, Piccadilly, London SW1.

Headworth, H. G., Puri, S. and Rampling, B. H. 1980. Contamination of a Chalk aquifer by mine drainage at Tilmanstone, East Kent, UK. *Quarterly Journal of Engineering Geology*, **13**, pp105-117.

Hess, K. M., Wolf, S. H. and Celia, M. A. 1992. Large scale natural gradient tracer test in sand and gravel, Cape Cod, Massachusetts – 3. Hydraulic conductivity variability and calculated macrodispersivities. *Water Resources Research*, **28()**, 2011-2027.

Hill, D. 1984. Diffusion coefficients of nitrate, chloride, sulphate and water in cracked and uncracked Chalk. *Journal of Soil Science*, **35**, pp27-33.

Howard, K. W. F. 1990. The role of well logging in contaminant transport studies. In: Ward, S., Geotechnical and environmental geophysics, *Society of Exploration Geophysicists*, **2**, pp289-301.

Huang, Q. and Angelier, J. 1989. Fracture spacing and its relation to bed thickness. *Geological Magazine*, **126**, pp355-362.

Hudson, J. A. and Priest, S. D. 1979. Discontinuities and rock mass geometry. *International Journal of Rock Mechanics, Mineral Science and Geomechanics Abstracts*, **16**, pp339-362.

Huyakorn, P. S. and Pinder, G. F. 1983. Computational methods in subsurface flow. Academic Press, Orlando, Florida. 473pp.

Hvorslev, M. J. 1951. Time lag and soil permeability in groundwater observations. *US Army Corps of Engineers, Waterways Experimental Station, Vicksburg, Mississippi, USA*, Bulletin No. **36**.

Ineson, J. 1962. A hydrogeological study of the permeability of the Chalk. *Journal of the Institution of Water Engineers*, **16**, 449-63.

Ineson, J. 1959. Yield depression curves of discharging wells, with particular reference to Chalk wells and their relationship to variations in transmissibility. *Journal of the Institute of Water Engineers and Scientists*, **13**, pp119-163.

Jackson, D. and Rushton, K. R. 1987. Assessment of recharge components for a Chalk aquifer unit. *Journal of Hydrology*, **15**, pp1-15.

Jakobsen, R., Hogh, J. K. and Brettman, K. L. 1993. Tracer test in fractured Chalk 1. Experimental design and results. *Nordic Hydrology*, **24(4)**, pp263-274.

Jefferies, R. P. S. 1963. The stratigraphy of the Actinocamux plenus subzone (Turonian) in the Anglo-Paris basin. *Proceedings of the Geologists Association* **74**, pp1-33.

Jones, H. K. and Robins, N. S. (Eds) 1999. The Chalk aquifer of the South Downs. Hydrogeological Report Series of the British Geological Survey, Keyworth, Nottingham. ISBN 0 852 72315 6.

Kay, B. D. and Elrick, D. E. 1967. Adsorption and movement of lindane in soils. *Soil Science,* **104**, pp314-322.

Kent County Council 1976. Kent Structure Plan: Report of Survey.

Ladeira, F. L. and Price, N. J. 1981. Relationship between fracture spacing and bed thickness. *Journal of Structural Geology*, **3**, pp179-183.

Lapidus, L. and Amundson, N. R. 1952. Mathematics of adsorption in beds, 4, The effect of longitudinal diffusion in ion exchange and chromatographic columns. *Journal of Physical Chemistry*, **56**, pp984-988.

Lawrence, A. R. and Foster, S. S. D. 1987. The pollution threat from agricultural pesticides and industrial solvents. Hydrogeological Report No. 87/2, British Geological Survey, Keyworth, Nottingham.

Lewis, D. C., Kriz, G. J. and Burgy, R. H. 1966. Tracer dilution sampling technique to determine hydraulic conductivity of fractured rock. *Water Resources Research* **2(3)** pp533-542.

Lindstrom, F. T. and Boersma, L. 1971. A theory of the mass transport of previously distributed chemicals in a water saturated sorbing porous medium. *Soil Science Society of America Proceedings*, **111**, pp192-199.

Little, R., Muller, E. and Mackay, R. 1996. Modelling of contaminant migration in a chalk aquifer. *Journal of Hydrology*, **175(4)**, pp473-509.

Lloyd, J. W. 1990. Importance of drift deposits influencing Chalk hydrogeology. In: Chalk, Thomas Telford, London, pp583-590.

Lloyd, J. W. 1993. The United Kingdom, In: The Hydrogeology fo the Chalk of north-west Europe. (Ed) Downing, R. A., Price, M. and Jones, G.P. Clarendon Press, Oxford, UK. ISBN 0-19-854285-2.

Louis, C. 1974. Introduction a l'hydraulique des roches. *Bulletin de Bureau de Recherche Geologique des Mines,* **Series 2, Section III, No. 4**.

Luckner, L. and Schestakow, W. M. 1991. Migration Processes in the Soil and Groundwater Zone. Lewis Publishers, Chelsea, Michigan.

MacDonald, A. M. and Allen, D. J. 2001. Aquifer properties of the Chalk of England. *Quarterly Journal of Engineering Geology and Hydrogeology*, **34(4)**, pp371-384.

MacDonald, A. M., Brewerton, L. J. and Allen, D. J. 1998. Evidence for rapid groundwater flow and karst-type behaviour in the Chalk of southern England. *In*: Robins, N. S. (ed.) *Groundwater Pollution, Aquifer Recharge and Vulnerability.* Geological Society, London, Special Publication, **130**, pp95-106.

Marsily, G. de 1986. Quantitative hydrogeology. Academic Press Inc. (London) Ltd., London. ISBN 0-12-208916-2.

McDonald, M. G. and Harbaugh, A. W. 1984. A modular three-dimensional finite difference ground-water flow model. United States Geological Survey, Scientific Publications Co. PO Box 23041, Washington DC 20026-3041.

McMahon, M. A. and Thomas, G. W. 1974. Chloride and tritiated water flow in disturbed and undisturbed soils. *Soil Science Society of America Proceedings*, **38**, pp727-732.

Moench, A. F. 1995. Convergent radial dispersion in a double porosity aquifer with fracture skin: Analytical solution and application to a field experiment in fractured chalk. *Water Resources Research*, **31(8)**, pp1823-1835.

Molz, F. J., Guven, O. and Melville, J. G. 1983. An examination of scale-dependant dispersion coefficients. *Groundwater*, **21(6)**, pp715-725.

Morel, E. H. 1980. The use of a numerical model in the management of the chalk aquifer in the Upper Thames Basin. *Quarterly Journal of Engineering Geology*, **13**, 153-66.

Moreno, L., Tsang, Y. W., Hale, F. V. and Neretnieks, I. 1988. Flow and tracer transport in a single fracture: a stochastic model and its relation to some field observations. *Water Resources Research*, **24**, pp2033-48.

Morris, R. E. and Fowler, C. H. 1937. The flow and bacteriology of underground water in the Lee Valley. In: Thirty-second annual report on the results of the chemical and bacteriological examination of the London waters for the twelve months ended 31st December 1937, Ed: Harold, C. H. H., Metropolitan Water Board, pp89-99.

Mortimore, R. N. 1986a. Stratigraphy of the upper Cretaceous white Chalk of Sussex. *Proceedings of the Geologists Association*, **97**, pp97-139.

Mortimore, R. N. 1986b. Controls on Upper Cretaceous sedimentation in the south Downs with particular reference to flint distribution. In: *The Scientific Study of Flint and Chert, Proceedings of the Fourth International Symposium, Brighton Polytechnic 1983*. Editors: Sieveking, G. de G. and Hart, M. B., Cambridge University Press.

Mortimore, R. N. 1987. Upper Cretaceous Chalk in the North and South Downs, England: a correlation. *Proceedings of the Geologists Association* **98**, pp77-86.

Mortimore, R. N. 1990. Chalk or chalk? In: *Chalk, Proceedings of the International Chalk Symposium, Brighton Polytechnic*. Ed: Burland, J. B., Mortimore, R. N., Roberts, L. D., Jones, D. L. and Corbett, B. O. Thomas Telford, London.

Mortimore, R. N. 1997. The Chalk of Sussex and Kent, Geologists Association Field Guide.

Mortimore, R. N. and Pomerol, B. 1987. Correlation of the Upper Cretaceous White Chalk (Turonian to Campanian) in the Anglo-Paris Basin. *Proceedings of the Geologists Association*, **98**, pp97-143.

Mortimore, R. N. and Pomerol, B. 1991. Upper Cretaceous tectonic disruptions in a placid Chalk sequence in the Anglo-Paris Basin. *Journal of the Geological Society of London*, 148, pp391-404.

Mortimore, R. N., Pomerol, B. and Foord, R. J. 1990. Engineering stratigraphy and paeleogeography for the chalk of the Anglo-Paris Basin. Proceedings of the International Chalk Symposium 1989, Thomas Telford London.

Mortimore, R. N., Pomerol, B. and Lamont-Black 1996. Examples of structural and sedimentological controls on chalk engineering behaviour. In: Engineering Geology of the Channel Tunnel. Thomas Telford, London.

Mott MacDonald 1998. Modelling report on the impact of the proposed abstraction at Eastry borehole. Confidential report for Southern Water.

Muller, E. 1987. Modelling of groundwater pollution at a site near Cambridge. *Unpublished MSc thesis, University of Newcastle upon Tyne.*

National Rivers Authority 1992. Policy and Practice for the Protection of Groundwater.

Nielsen, D. R. and Biggar, J. W. 1961. Miscible displacement, 1, Experimental information, *Soil Science Society of America Proceedings*, **25**, pp1-5.

Nkedi-Kizza, P., Biggar, J. W., Selim, H. M., Van Genuchten, M. Th., Wierenga, P. J., Davidson, J. M. and Nielsen, D. R. 1984. On the equivalence of two conceptual models for describing ion exchange during transport through an aggregated oxisol. *Water Resources Research*, **20**, pp1123-1130.

Oakes, D. B. 1977. The movement of water and solutes through the unsaturated zone of the Chalk of the United Kingdom. In: *Procedings of the 3rd Hyydrological Symposium, Fort Collins*, Colorado State University.

Oakes, D. B. and Pontin, M. J. 1976. Mathematical modelling of a Chalk aquifer. Report TR24 Water Research Centre, Medmenham.

Ogata, A. and Banks, R. B. 1961. Solution of the differential equation of longitudinal dispersion in porous media. U.S. Geological Survey Professional Paper 411-A.

Ordnance Survey. Landranger 179 Canterbury and East Kent 1:50000.

Oteri, A. U. J. 1981. Geophysical and hydrogeological investigations of contaminated aquifers in south-east England. *Unpublished PhD thesis, University College London.*

Owen, M. & Robinson, V. K. 1978. Characteristics and yield of fractured Chalk. In: Thames Groundwater Scheme. Institution of Civil Engineers, London.

Paillet, F. L. 1993. Using borehole geophysics and cross-borehole flow testing to define hydraulic coneections between fracture zones in bedrock aquifers. *Journal of Applied Geophysics*, **30(3)**, pp261-279.

Paillet, F. L. 1995. Using borehole flow logging to optimise hydraulic-test procedures in heterogeneous fractured aquifer. *Hydrogeology Journal*, **3(3)**, pp4-20.

Passioura, J. B. 1971. Hydrodynamic dispersion in aggregated media. 1. Theory. *Soil Science*, **11**, pp192-199.

Patel, R. 2001. *Unpublished MSci thesis, University College, London.*

Peedell, S. 1994. Investigation of the mine water pollution plume at Tilmanstone, East Kent. *Unpublished MSc thesis, University College, London.*

Price, M. 1987. Fluid flow in the Chalk of England. In: Fluid flow in sedimentary basins and aquifers, *Geological Society Special Publication*, **34**, pp141-156.

Price, M., Atkinson, T. C., Barker, J. A. and Monkhouse, R. A. 1992. A tracer study of the danger posed to a chalk aquifer by contaminated highway runoff. *Proceedings of the Institution of Civil Engineers Water, Maritime and Energy*, **96**, pp9-18.

Price, M., Bird, M. J. and Foster, S. S. D. Chalk pore-size measurements and their significance. *Water Services*, **80**, p596 – 600.

Price, M., Downing, R. A. and Edmunds, W. M. 1993. The Chalk as an aquifer, In: The Hydrogeology of the Chalk of North-West Europe, (Ed) Downing, R. A., Price, M. & Jones, G. P. Clarendon Press, Oxford.

Price, M., Morris, B. and Robertson, A. 1982. A study of intergranular and fissure permeability in Chalk and Permian aquifers using double packer injection testing. *Journal of Hydrology*, **54**, pp401-423.

Price, M., Robertson, A. S. and Foster, S. S. D. 1977. Chalk permeability – a study of vertical variation using water injection tests and borehole logging. *Water Services*, **81(980)**, pp603-610.

Price, M. and Williams, A. 1989. Using a double-packer system in groundwater studies. *Technical Report WD/89/55* British Geological Survey.

Priest, S. D. 1993. The collection and analysis of discontinuity orientation data for engineering design, with examples. In: *Comprehensive rock engineering*. J. A. Hudson (Ed). Vol 3, Rock testing and site characterisation. Pergammon Press Oxford.

Priest, S. D. and Hudson, J. 1976. Discontinuity spacings in rock. *International Journal of Rock Mechanics and Mineral Science*, **13**, pp135-48.

Priest, S. D. and Hudson, J. 1981. Estimation of discontinuity spacing and trace length using scanline surveys. *International Journal of Rock Mechanics and Mineral Science*, **18**, pp183-197.

Ptak, T. and Teutsch, G. 1994. Forced and natural gradient tracer tests in a highly heterogeneous porous aquifer: instrumentation and measurement. *Journal of Hydrology*, **159**, pp79-104.

Quinn, S. A. 2000. New techniques in dilution tracer testing: Examples from the Chalk aquifer, Tilmanstone, East Kent. *Unpublished MSc thesis University College London.*

Reeves, M., Ward, D. S., Johns, N. D. and Cranwell, R. M. 1986. Theory and implementation for SWIFT II, The Sandia Waste-Isolation Flow and Transport Model for Fractured Media. NUREG/CR-3162 and SAND83-0242. Sandia National Laboratories, Alberquerque, New Mexico.

Rivett, M. O., Lerner, D. N. and Lloyd, J. W. 1990. Chlorinated solvents in UK aquifers. *Journal of the Institution of Water and Environmental Management*, **4**, 242-250.

Robertson, J. B. and Barraclough, J. T. 1973. Radioactive and chemical waste transport in groundwater at National Reactor Testing Station, Idaho: 20-year case history and digital model. In: *Proceedings of a symposium on underground waste management and artificial recharge*, **1**, p291. American Association of Petroleum Geologists, New Orleans.

Robinson, J. N. 2003. Delineation of groundwater protection zones for fractured aquifers in the UK. *Unpublished PhD thesis, University of London.*

Robinson, N. D. 1986. Lithostratigraphy of the Chalk Group of the North Downs, southeast England. *Procedings of the Geologists* Association, 97, pp141-170.

Rumbaugh, J. 2001. Groundwater Vistas. ESI International, Shrewsbury, UK.

Rushton, K. R., Connorton, B. J. and Tomlinson, L. M. 1989. Estimation of the groundwater resources of the Berkshire Downs supported by mathematical modelling. *Quarterly Journal of Engineering Geology*, **22**, 329-41.

Rushton, K. R. and Ward, C. 1979. The estimation of groundwater recharge. *Journal of Hydrology*, **41**, pp345-361.

Scheidegger, A. E. 1961. General theory of dispersion in porous media. *Journal of Geophysical Research*, **66(10)**, pp3273-3278.

Schwartz, F. W. and Smith, L. 1988. A continuum approach for modelling mass transport in fractured media. *Water Resources Research* **34**, pp2515-2527.

Shapiro, A. M., 1984. Finite Element simulation of groundwater flow and contaminant migration. Lecture notes for the short course on Groundwater Flow and Pollution, University of Newcastle upon Tyne.

Skopp, J. and Warwick, A. W. 1974. A two phase model for miscible displacement of reactive solutes in soils. *Soil Science Society of America Proceedings*, **38**, pp545-550.

Smith, L. and Schwartz, F. W. 1984. An analysis of the influence of fracture geometry on mass transport in fractured media. *Water Resources Research*, **20(9)**, pp1241-52.

Snow, D. T. 1968. Rock fracture spacings, openings, and porosities. *Journal of the Soil Mechanics and Foundations Division*, Proceedings of the American Society of Civil Engineers, **94**, pp73-91.

Southern Science 1991. Report on the testing and sampling at Eastry borehole for reverse osmosis. Unpublished, internal report.

Southern Water Authority 1976a. Note on the reasons for the continued discharge of mine drainage into the Chalk, Paper B; Quantities and chloride concentration of mine discharges, Paper C; Chemical analyses of mine water and Chalk waters, Paper D. *Unpublished report of the Southern Water Authority.*

Southern Water Authority 1976b. Tilmanstone investigation: Report on the pumping test of observation boreholes, October 1975 to January 1976. *Unpublished report for the Kent Area Resource Planning Office.*

Southern Water Authority 1976c. Report on outflows along the Dover-Deal coast. *Unpublished internal report.*

Southern Water Authority 1980. Test Pumping of World's Wonder. *Unpublished internal report.*

Stephens, D. B., Hsu, K. C., Prieksat, M. A., Ankeny, M. D., Blandford, N., Roth, T. L., Kelsey, J. A. and Whitworth, J. R. 1998. A comparison of estimated and calculated effective porosity. *Hydrogeology Journal*, **6(1)**, pp156-165.

Sudicky, E. A. 1989. The Laplace transform Galerkin technique: a time continuous finite element theory and application to mass transport in groundwater. *Water Resources Research,* **28**, pp1833-1846.

Sudicky, E. A. 1986. A natural gradient experiment on solute transport in a sand aquifer: Spatial variability of hydraulic conductivity and its role in the dispersion process. *Water Resources Research*, **22,** pp2069-2082.

Sudicky, E. A. and Frind, E. M. 1981. Carbon 14 dating of groundwater in confined aquifers: Implications of aquitard diffusion. *Water Resources Research*, **17(4)**, pp1060-1064.

Sudicky, E.A. and Frind E. M. 1982. Contaminant transport in fractured porous media: Analytical solutions for a system of parallel fractures. *Water Resources Research*, **18(6)**, pp1634-1642.

Sudicky E. A. and Huyakorn, P. S. 1991. Contaminant migration in imperfectly known heterogeneous groundwater systems. *Reviews in Geophysics* **29 Supplement**, pp240-253.

Suzuki, T., Harada, M., Hammad, A. and Itoh, Y. 1996. An inverse analysis of model parameters for heterogeneous aquifer based on genetic algorithm. In: Stochastic Hydraulics, Proceedings of the Symposium, Mackay, Australia. Balkema.

Tate, T. K., Robertson, A. S. and Gray, D. A. 1970. The hydrogeological investigation of fissure flow by borehole logging techniques. *Quarterly Journal of Engineering Geology*, **2(3)**, pp195-215.

Taylor, A. & Hulme, P. 2000. Representation of variable conductivity with depth in MODFLOW. Paper given at Current Research in Hydrogeology, 14th December 2000. Geological Society, Burlington House, London.

Taylor, G. I. 1953. The dispersion of matter in solvent flowing slowly through a tube. *Proceedings of the Royal Society of London, Series A*, **219**, 189-203.

The Guardian 1996. Edition of 30 July 1996, London, pp6.

The Royal Commission on Environmental Pollution 1992. Sixteenth report: Freshwater Quality. Cmnd 1966, ISBN 9 10 119662 8.

Travers Morgan 1994. Groundwater modelling at Westwood, Lyminge. *Unpublished consultants report.*

Tsang, Y. W. 1992. Usage of equivalent apertures for rock fractures as derived and tracer tests. *Water Resources Research*, **28(5)**, pp1451-1455.

Turner, G. S. 1958. Flow structure in packed beds. *Chemical Engineering Science*, 7, pp156-165.

UK Government 1847. Cemeteries Clauses Act 1847. Published by Her Majesty's Stationary Office.

UK Government 1974. The Control of Pollution Act 1974 (c. 40). Published by Her Majesty's Stationary Office.

UK Government 1990. The Environmental Protection Act 1990 (c. 43). Accessed via website . http://www.hmso.gov.uk/acts/acts1990/UKpga_19900043_en_1.htm last accessed 11.04.2004. Published by Her Majesty's Stationary Office, ISBN 0105443905

UK Government 1991a. The Water Resources Act 1991 (c. 57). Accessed via website http://www.hmso.gov.uk/acts/acts1991/Ukpga_19910057_en_1.htm last accessed 11/04/2004. Published by Her Majesty's Stationary Office, ISBN 0105457914.

UK Government 1991b. The Control of Pollution (Silage, Slurry and Agricultural Fuel Oil) Regulations 1991. Statutory Instrument 1991 No. 324. Accessed via website http://www.hmso.gov.uk/si/si1991/Uksi_19910324_en_1.htm last accessed 11.04.2004. Published by Her Majesty's Stationary Office.

UK Government 1994. The Waste Management Licensing Regulations 1994. Statutory Instrument 1994 No. 1056. Accessed via website http://www.hmso.gov.uk/si/si1994/Uksi_19941056_en_1.htm last accessed 11.04.2004. Published by Her Majesty's Stationary Office, ISBN 0110440560.

UK Government 1995. The Environment Act 1995 (c. 25). Accessed via website http://www.hmso.gov.uk/acts/acts1995/UKpga_19950025_en_1.htm last accessed 11.04.2004. Published by Her Majesty's Stationary Office, ISBN 0105425958.

UK Government 1998. The Groundwater Regulations 1998, Statutory Instrument 1998 No. 2746. Accessed via website http://www.hmso.gov.uk/si/si1998/19982746.htm last accessed 09/10/2002. Published by Her Majesty's Stationary Office, ISBN 0 11 079799 X.

UK Government 1999. The Pollution Prevention and Control Act 1999. Accessed via website http://www.hmso.gov.uk/acts/acts1999/19990024.htm last accessed 11.04.2004. Published by Her Majesty's Stationary Office, ISBN 0105424994.

UK Government 2000. The Contaminated Land (England) Regulations 2000. Statutory Instrument No. 227. Accessed via website http://www.hmso.gov.uk/si/si2000/20000227.htm last accessed 11/04/2004. Published by Her Majesty's Stationary Office, ISBN 0110859014.

UK Government 2003. The Water Act 2003 (c. 37). Accessed via website http://www.hmso.gov.uk/acts/acts2003/20030037.htm last accessed 11.04.2004. Published by Her Majesty's Stationary Office, ISBN 0105437034.

University of Florida Institute of Food and Agricultural Sciences 1992. Water and its importance to animals http://www.idahofreedom.com/livestock/cattle/water_intake.html Article last accessed 04/09/2003.

USEPA 1992. Dense non-aqueous phase liquids, a workshop summary, Dallas Texas April 17-18 1991. EPA/600/R-92/030, Robert S Kerr Environmental Research Laboratory, Ada, Oklahoma.

van Deemter, J.J., Zuiderweg, F.J. and Klinkenberg, A. 1956. Longitudinal diffusion and resistance to mass transfer as causes of non-ideality in chromatography. *Chem. Eng. Sci.*, **5**, pp271-289.

van Genuchten, M. T. and Dalton, F. N. 1986. Models for simulating salt movement in aggregated field soils. *Geoderma*, **48**, pp165-183.

van Rooijen, P. 1993. The Netherlands, In: *The Hydrogeology of the Chalk of North-West Europe*, (Ed) Downing, R.A., Price, M. & Jones, G.P. Clarendon Press, Oxford

Vernon, J. H., Paillet, F. L., Pedlar, W. H. and Griswold, W. J. 1993. Application of boreholel geophysics in defining the wellhead protection area for a fractured crystalline bedrock aquifer. *The Log Analyst*, **35(1)**, pp41-57

Ward, R. C. and Robinson, M. 1989. Principles of hydrology. McGraw Hill Book Company, UK Ltd. ISBN 0-07-707204-9.

Ward, R. S. 1989. Artificial tracer and natural ^{222}Rn studies of the East Anglian Chalk aquifer. *Unpublished PhD thesis, School of Environmental Sciences, University of East Anglia*

Ward, R. S. and Williams, A.T. 1995. A tracer test in the Chalk near Kilham, North Yorkshire. Report of the British Geological Survey, Hydrogeology Group, WD/95/7 pp26

Ward, R. S., Williams, A. T., Barker, J. A., Brewerton, L. J. and Gale, I. N. 1998. Groundwater tracer tests: a review and guidelines for their use in British aquifers, British Geological Survey technical report WD/98/16 Hydrogeology series and Environment Agency R&D technical report W160.

Warren, J. E. and Root, P. J. 1963. The behaviour of naturally fractured reservoirs. *Journal of the Society of Petroleum Engineers*, Transactions AIME, **228**, pp245-255

Watson, S. J. 1999. Tilmanstone tracer testing Phase 2 test 1. Unpublished internal UCL report.

Witherspoon, P., Wang, J. S. Y., Iwai, K. and Gale, J. E. 1980. Validity of cubic law for fluid flow in a deformable rock fracture. *Water Resources Research*, **16(6)**, pp1016-1024.

Wray, D. S. 1995. Origin of clay-rich beds in Turonian chalks from Lower Saxony, Germany; a rare-earth element study. *Chemical Geology*, **119(4)**, pp161-173.

Yeh, T. C. J. 1992. Stochastic modelling of groundwater flow and solute transport in aquifers. *Hydrological Processes*, **6(4)**, pp369-395.

Yeh, Y. J., Lee, C. H. and Chen, S. T. 2000. A tracer method to determine hydraulic conductivity and effective porosity of saturated clays under low gradients. *Ground Water*, **38(4)**, pp522-529.

Young, C. P., Oakes, D. B. and Wilkinson, W. B. 1976. Prediction of future nitrate concentrations in groundwater. *Ground Water*, **14**, pp426-438

Younger, P. L. 1989. Devensian periglacial influences on the development of spatially variable permeability in the Chalk of south-east England. *Quarterly Journal of Engineering Geology*, **22**, 343-354.

Zemanek, J., Glenn, E. E. Norton, L. J. and Caldwell, R. L. 1970. Formation evaluation by inspection with the borehole televiewer. *Geophysics*, **35(2)**, pp254-269

Zheng, C. 2002. MT3D^{99}: A modular 3D multispecies transport simulator (Version SP-4). S.S. Papadopoulos & Associates, Inc., Bethesda, MD, USA.

Zuber, A. and Motyka, J. 1994. Matrix porosity as the most important parameter of fissured rocks for solute transport at large scales. *Journal of Hydrology*, **158**, pp19-46.

Appendix 1

Summary of EU Water Framework Directive scope and aims

EU Water Framework Directive 2000

The WFD is the most significant piece of European water legislation for over 20 years. It will overhaul the management of the water environment in the UK. The aims, practicalities and implementation of the Directive are summarised below. Embodied in the Directive is the concept of integrated river basin management. It provides a framework for environmental requirements for water status based on:

- ecological and chemical parameters;
- common monitoring and assessment strategies;
- arrangements for River Basin administration and planning; and
- a Programme of Measures in order to meet the objectives.

It will rationalise and update current water legislation, repealing a number of existing directives:

- Groundwater (80/68/EEC) for the protection of groundwater against pollution caused by certain dangerous substances (European Commission 1980a);
- Dangerous substances (76/464/EEC) for the control of pollution by dangerous substances (European Commission 1976);
- Surface water (75/440/EEC) for the protection of the quality of surface waters used for abstraction (European Commission 1975);
- Information exchange (77/795/EEC) concerning the procedure for the exchange of information on surface water quality (European Commission 1977);
- Measurement methods (79/869/EEC) on the methods of measurement and frequency of sampling of surface waters used for drinking water abstraction (European Commission 1979a);
- Protection of freshwater for fish (78/659/EEC) (European Commission 1978); and
- Quality of shellfish waters (79/923/EEC) (European Commission 1979b).

Aims

The WFD facilitates an inclusive, holistic approach to managing water as it flows through catchments from lakes, rivers and groundwater to estuaries and the sea. It aims to:

- prevent further deterioration and protect and enhance the status of aquatic ecosystems and associated wetlands;
- promote sustainable water consumption;
- progressively reduce or phase out discharges, emissions and losses of priority substances and priority hazardous substances;
- progressively reduce the pollution of groundwater; and
- contribute to mitigating the effects of floods and droughts.

Approach

The Directive will achieve this by:

- introducing the concept of River Basin Districts (river catchments or groups of catchments) and identifying and characterising water bodies within them;
- analysing the state of River Basin Districts (by assessing the status of the water bodies), and the human and ecological needs and impacts within them;
- establishing monitoring programmes using biological and chemical parameters;
- developing management plans for River Basin Districts; and
- establishing a Programme of Measures that will set out the actions to achieve the environmental objectives of the Directive.

Specific requirements of the WFD with regard to the chemical status of groundwater bodies

Surveillance monitoring

Surveillance monitoring will be undertaken as a supplementary exercise to risk assessment and characterisation of groundwater bodies. The collected data will provide a core set of parameters which can be used to define a baseline for the chemical status of the groundwater body and the results can be used to inform requirements for additional operational monitoring.

Operational monitoring

Operational monitoring is required where a groundwater body has been identified as at risk of failing to achieve good status (by 2015) following the risk assessment and surveillance monitoring exercises. Operational monitoring will be used to establish the chemical status of the groundwater body and identify anthropogenically induced trends in deterioration of the status. The data concerned will need to be representative of the whole groundwater body.

Appendix 2

Matrix diffusion

The diffusive laws used to describe diffusion into immobile water are Fick's first and second laws and the process is represented by a diffusion coefficient. Several different diffusion coefficients are necessary to describe the diffusive process and this seems to have led to some confusion in the literature. For clarity, the relationship between the three diffusion coefficients used in tracer studies in porous media is given here.

Fick's first law, applied to the diffusion of a solute in water (or any solvent), relates the diffusive flux, J_{Diff}, directly to the gradient of the concentration, c. For 1-dimensional transport in the x-direction:

$$J_{Diff} = -D_T \frac{dc}{dx}$$

Equation A7

D_T is the tracer or free-water diffusion coefficient. Equation A7 also applies to a saturated porous medium, but the matrix will impede transport of the solute, so a smaller diffusion coefficient, D_E, is used. This is termed the effective or intrinsic diffusion coefficient.

$$J_m = -D_E \frac{\partial c}{\partial x}$$

Equation A8

J_m is the mass flux per unit area of water and rock in the x-direction in saturated rock.

Fick's second law is used to describe **time-dependant** diffusion in a porous medium. Here the apparent diffusion coefficient, D_A, is used:

$$\frac{\partial c}{\partial t} = D_A \frac{\partial^2 c}{\partial x^2}$$

Equation A9

These three diffusion coefficients are related through:

$$D_E = \alpha D_A = \psi D_T$$

Equation A10

where:

α = ϕR, the 'rock capacity factor' or 'fictitious porosity'

ϕ = total connected porosity

R = the retardation coefficient

ψ = $\phi_D \delta / \tau^2$, the diffusibility

ϕ_D = the through-diffusion porosity

δ = constrictivity

τ = tortuosity

Dead-end pores that contribute to storage but not to diffusion have been ignored. Diffusibility is taken to be an intrinsic property of the porous medium (similar to permeability) and tortuosity is taken to be the ratio of path length in the porous medium to distance in the direction of flow. For an isotropic material the porosities ϕ and ϕ_D are identical (Gooddy *et. al.* 1995).

Diffusion coefficients for chloride in the Chalk of southern England have been determined experimentally by Oakes (1977); Hill (1984); Brewer *et al.* (1992); Gooddy *et al.*(1995); Fretwell (1999); and FRACFLOW (2000). Values range from 5.2×10^{-11} to 1.3×10^{-9} m^2/s. Data relevant to the current study are given in Table A2-1. Reported values show no consistent differences between the Lower, Middle and Upper Chalk.

Table A2-1

Solute	Diffusion coefficient	Value 10^{-10} m^2s^{-1}	Rock type	Porosity %	Temp Deg. C	Source
Na^+	Tracer	13	N/A	100	20	L&S[1]
Cl^-	Tracer	20	N/A	100	20	L&S[1]
NaCl	Tracer	12	N/A	100	18	L&S[1]
Cl^-	Effective[4]	0.5	Till	30-35	-	GP&C[2]
SO_4^{2-}	Effective[4]	0.28-1.48	Chalk	24-46	20	Hill[3]
Cl^-	Effective[4]	0.53-3.2	Chalk	24-46	20	Hill[3]
NO_3^-	Effective[4]	0.52-3.23	Chalk	24-46	20	Hill[3]
^3H	Effective[4]	0.6-3.51	Chalk	24-46	20	Hill[3]
Cl^-	Apparent	0.034-0.32	Sandstone	9	23-25	Feenstra[5]
Cl^-	Apparent	5.5-6 (Ave 5.75)	Upper Chalk (63.99 m	48.4		Gooddy[6]

Solute	Diffusion coefficient	Value 10^{-10} m^2s^{-1}	Rock type	Porosity %	Temp Deg. C	Source
			bGL)			
Cl^-	Apparent	4.4-4.5 (Ave 4.45)	Middle Chalk (133.3 m bGL)	40		Gooddy[6]
Cl^-	Apparent	7-8.4 (Ave 7.7)	Middle Chalk (156.63 m bGL)	40.4		Gooddy[6]
Cl^-	Apparent	2.5-3.7 (Ave 3.1)	Lower Chalk (188.77 m bGL)	31.9		Gooddy[6]
Cl^-	Apparent	2.9-3.8 (Ave 3.35)	Lower Chalk (205.62 m bGL)	32.6		Gooddy[6]
Cl^-	Apparent	8.6-8.8 (Ave 8.7)	Upper Chalk	38		Gooddy[6]
Cl^-	Apparent	2.5	Lower Chalk			Fretwell[7]
Cl^-	Apparent	1.7-2.9	Lower Chalk			Brewer[8]

Notes: [1]Luckner and Schestakow 1991;[2]Grisak, Pickens and Cherry 1980;[3]Hill 1984;[4]Incorrectly referred to as D_A in paper, should be divided by the porosity to give a diffusivity that can be used in Fick's second law (Barker 1993);[5] Feenstra *et al.* 1984;[6]Goody *et al.* 1996; [7] Fretwell 1999; [8] Brewer *et al.* 1992.

Luckner and Schestakow, (1991) suggest that D_E, can be estimated from D_T through the relationship:

$$D_E / D_T = \psi = \tau\eta\phi_D$$

Equation 11

where τ is tortuosity, η is the electromolecular retardation factor and ϕ_D is the through diffusion porosity. Table A2-2 gives parameter values.

Table A2-2

Parameter	Values	Rock
χ	0.25-0.5	Consolidated
	0.5-0.7	Unconsolidated
η	0.2	Clay
	0.4-0.5	Silt
	0.9-1	Sands and gravels

Muller (1987) suggests using a value of 0.25 for diffusibility, ψ, for Chalk matrix.

Appendix 4

Geophysical logs:

Well Name: Lower Venson Farm inclined borehole
File Name: C:\VLW\RGL\VENFARMI\ALL.HDR
Location: TR

Geophysical logs run by BGS 28/6/99.Log datum is GL. SWL:9.52mbd
Borehole is inclined 30 deg from vertical. Caliper log suspect, arms not touching wall in casing.Caliper values incorrect scale
Log display is distance

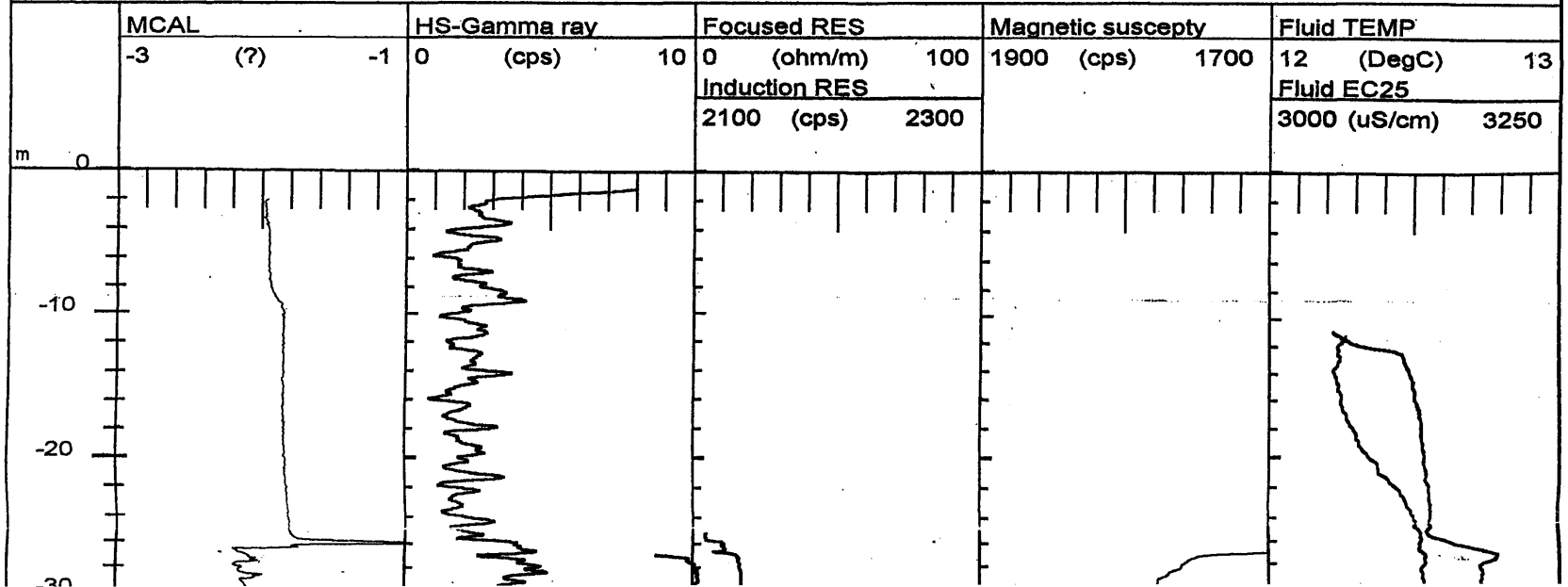

Lower Venson Farm inclined: BGS LVI

Well Name: Lower Venson Farm inclined borehole
File Name: C:\VLW\RGL\VENFARMI\ALL1.HDR
Location: TR

Geophysical logs run by BGS 28/6/99.Log datum is GL. SWL:9.52mbd
Borehole is inclined 30 deg from vertical. Caliper log suspect, arms not touching wall in casing.Caliper values incorrect scale
Log displayed as true vertical depth

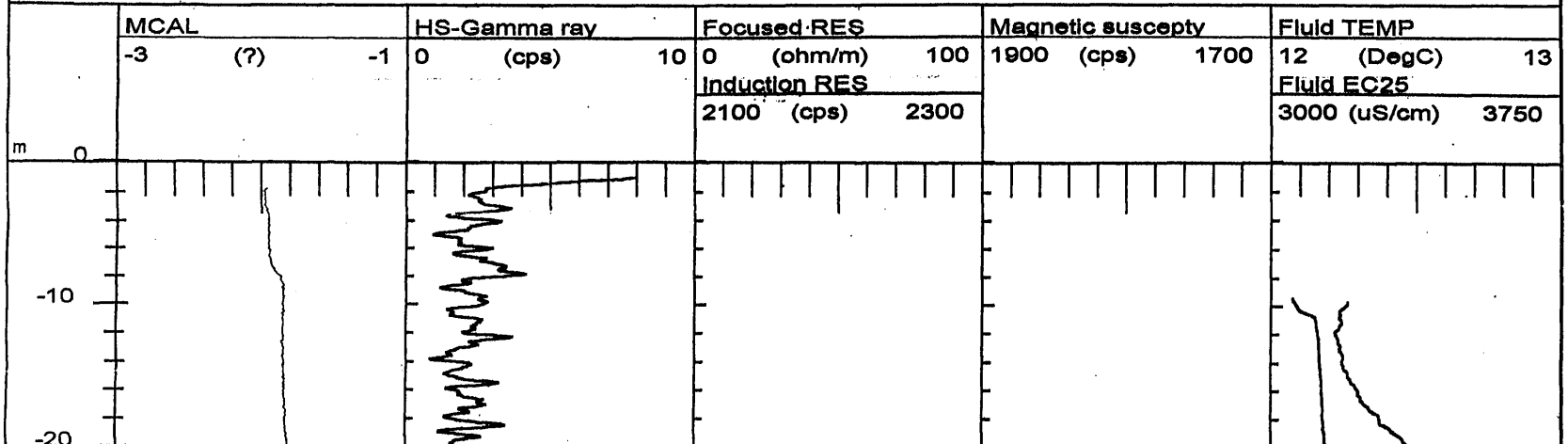

Well Name: Lower Venson Farm 2
File Name: C:\VLW\RGL\VENFARM2\ALL.HDR
Location: TR 3026 5311

Geophysical logs run by BGS 29/6/99.Log datum is concrete plinth.SWL: 8.90mbd
Borehole has 4in diameter GRP (fibreglass) blank casing to 96mbd, backfilled with sand. Fluid EC/TEMP run with high range (HR) probe.
Gamma ray influenced by sand fill behind casing.

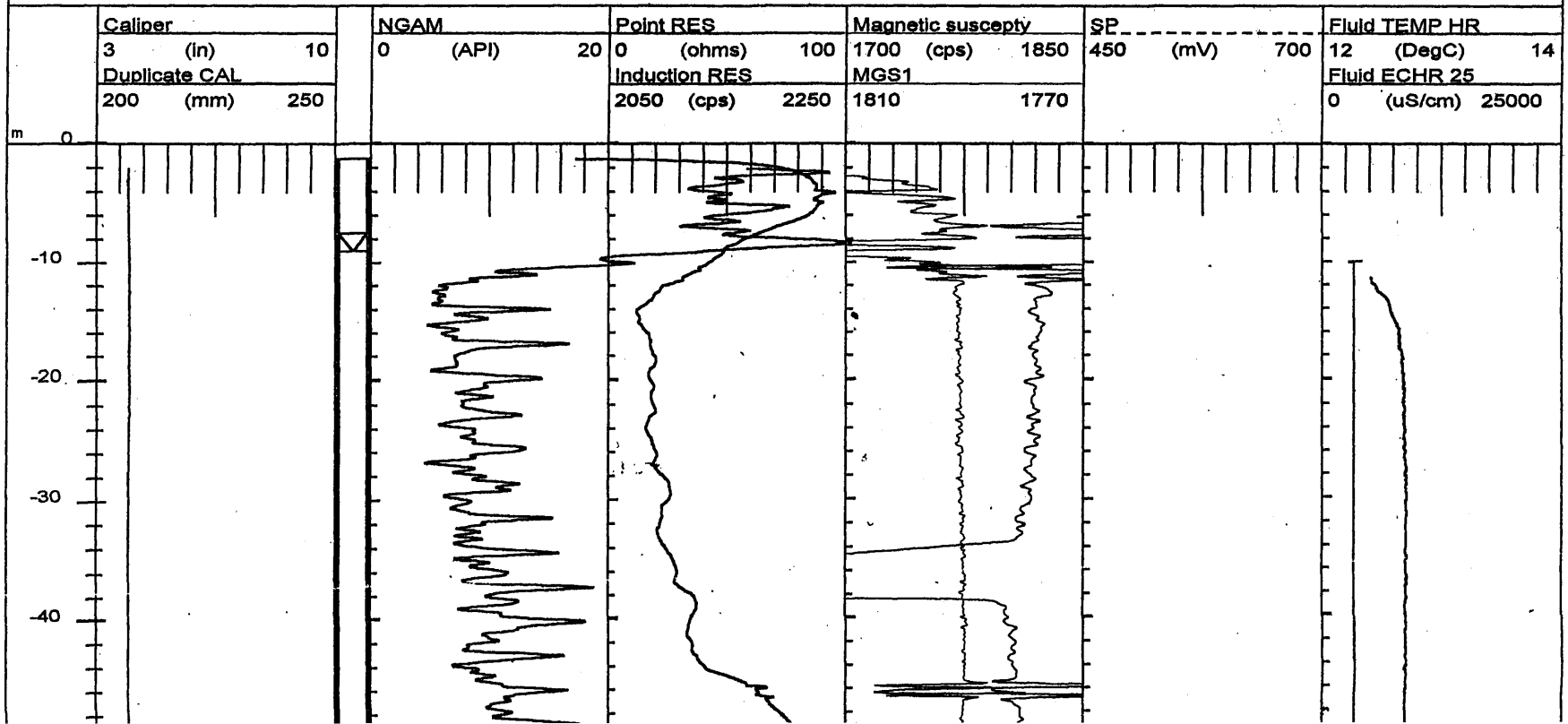

Well Name: Lower Venson Farm borehole 3
File Name: C:\VLW\RGL\VENFARM3\ALL.HDR
Location: TR 3027 5308

Geophysical logs run by BGS 30/6/99.Log datum is concrete plinth (=GL).SWL: 8.865mbd. Borehole has 4in diameter GRP (fibreglass) blank casing to 20mbd. Borehole has black sand

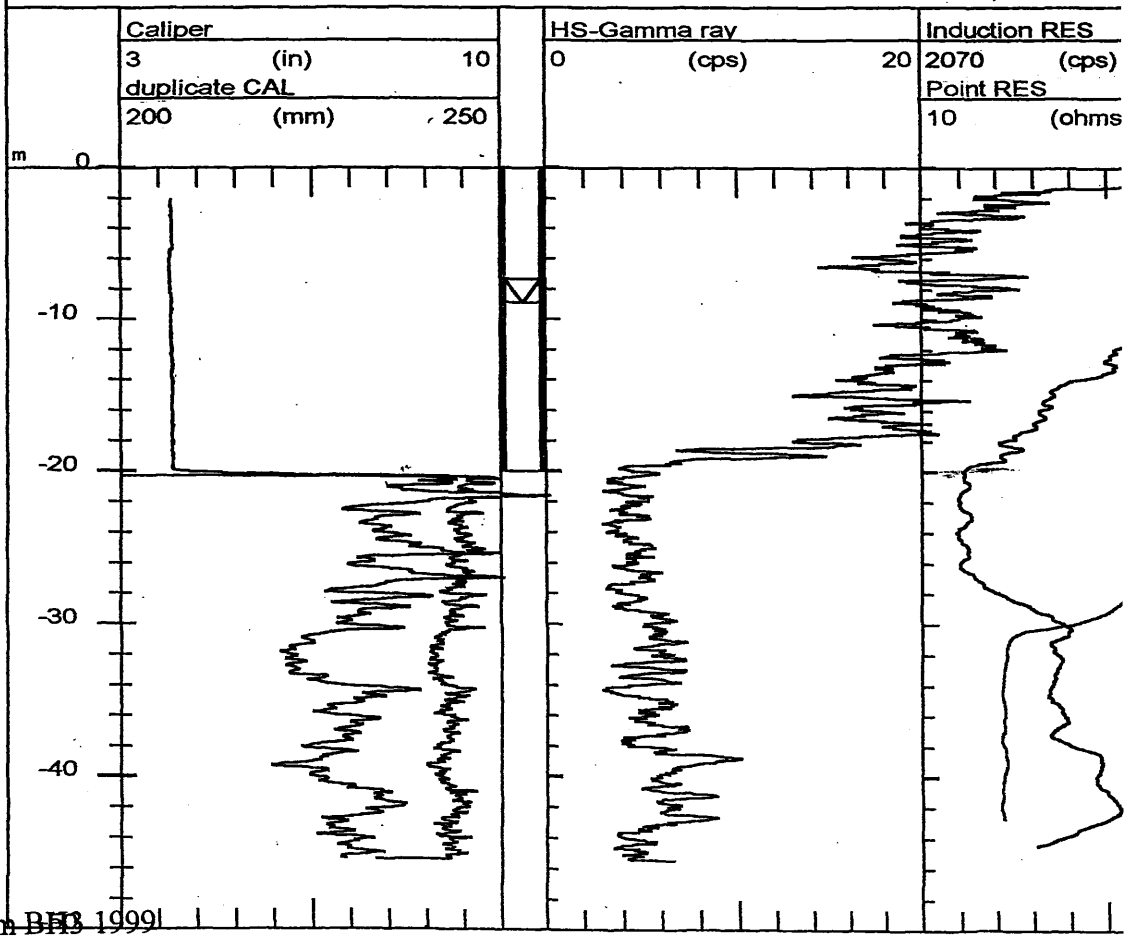

Lower Venson Farm BH3 1999

Well Name: Lower Venson Farm Borehole 4
File Name: C:\VLW\RGL\VENFARM4\ALL.HDR
Location: TR 3025 5308

Geophysical logs run by BGS 30/6/99. Log datum is concrete plinth (GL).SWL:8.21mbd
Borehole has 4in diameter GRP (fibreglass) casing to 64m depth

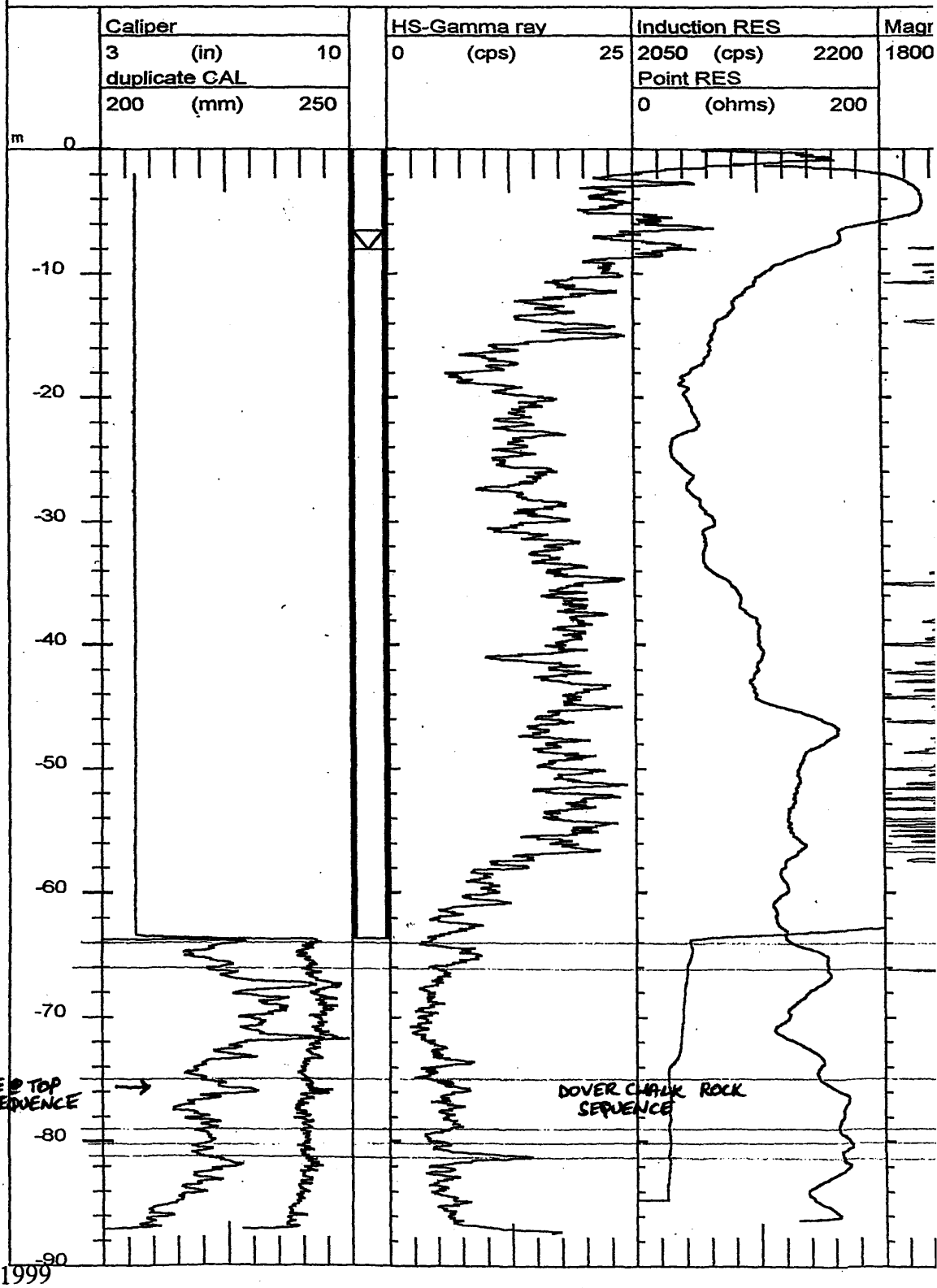

Lower Venson Farm BH4 1999

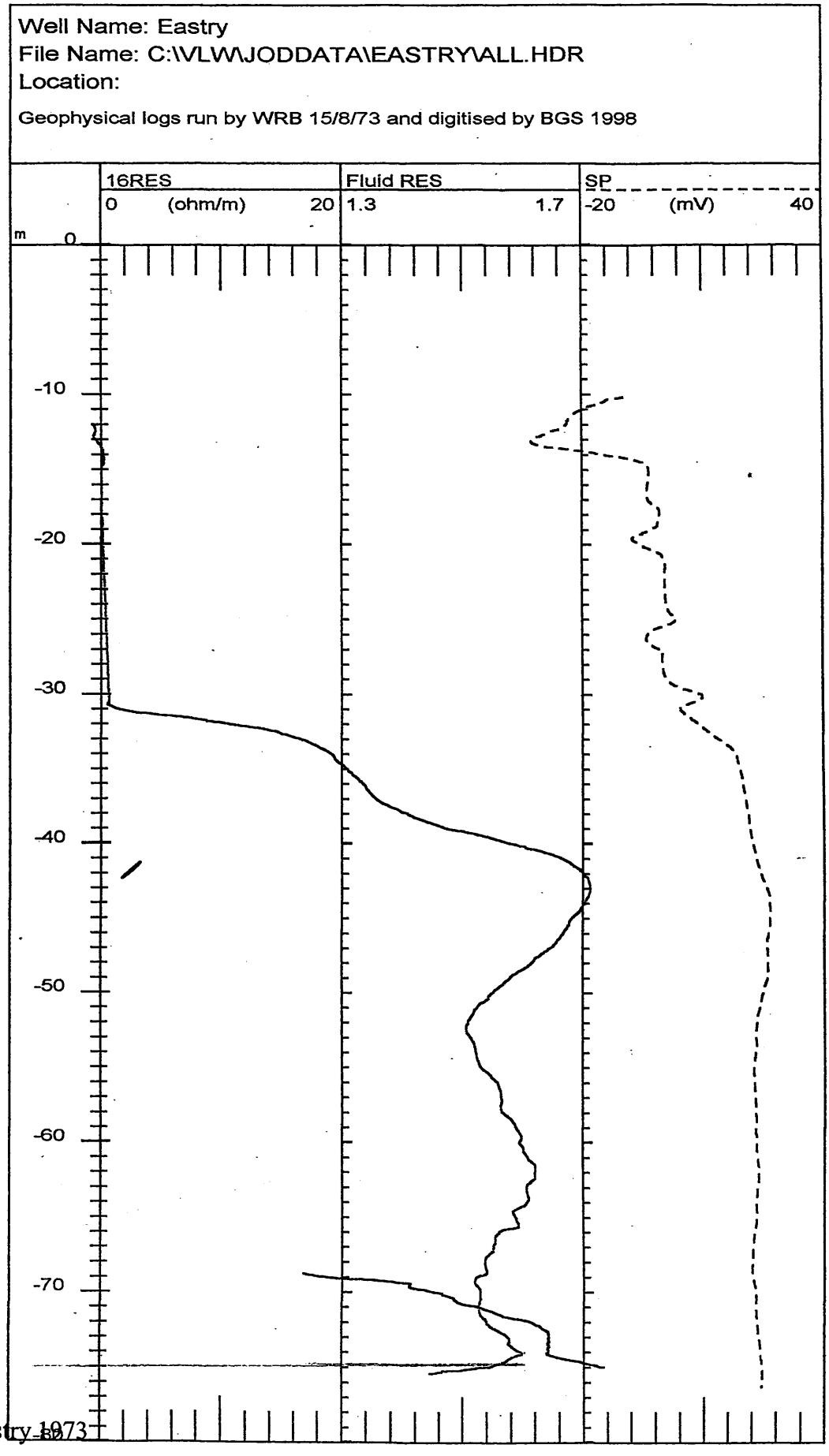

Eastry 1973

Eastry 1973

Thornton Farm BH 1974

Well Name: Thornton Farm 100m Bh
File Name: C:\VLW\JODDATA\THORNF10\ALL.HDR
Location: Tilmanstone

Geophysical logs by WRB 27/3/74 digitised at BGS 1998

Datum = 31 m OD

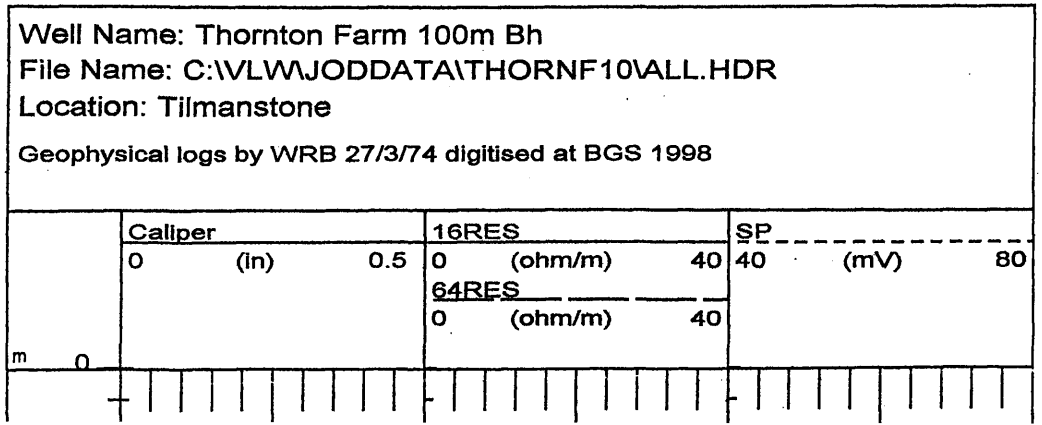

ThF BH6
Now cased to 130m
Datum = 31.52 m OD

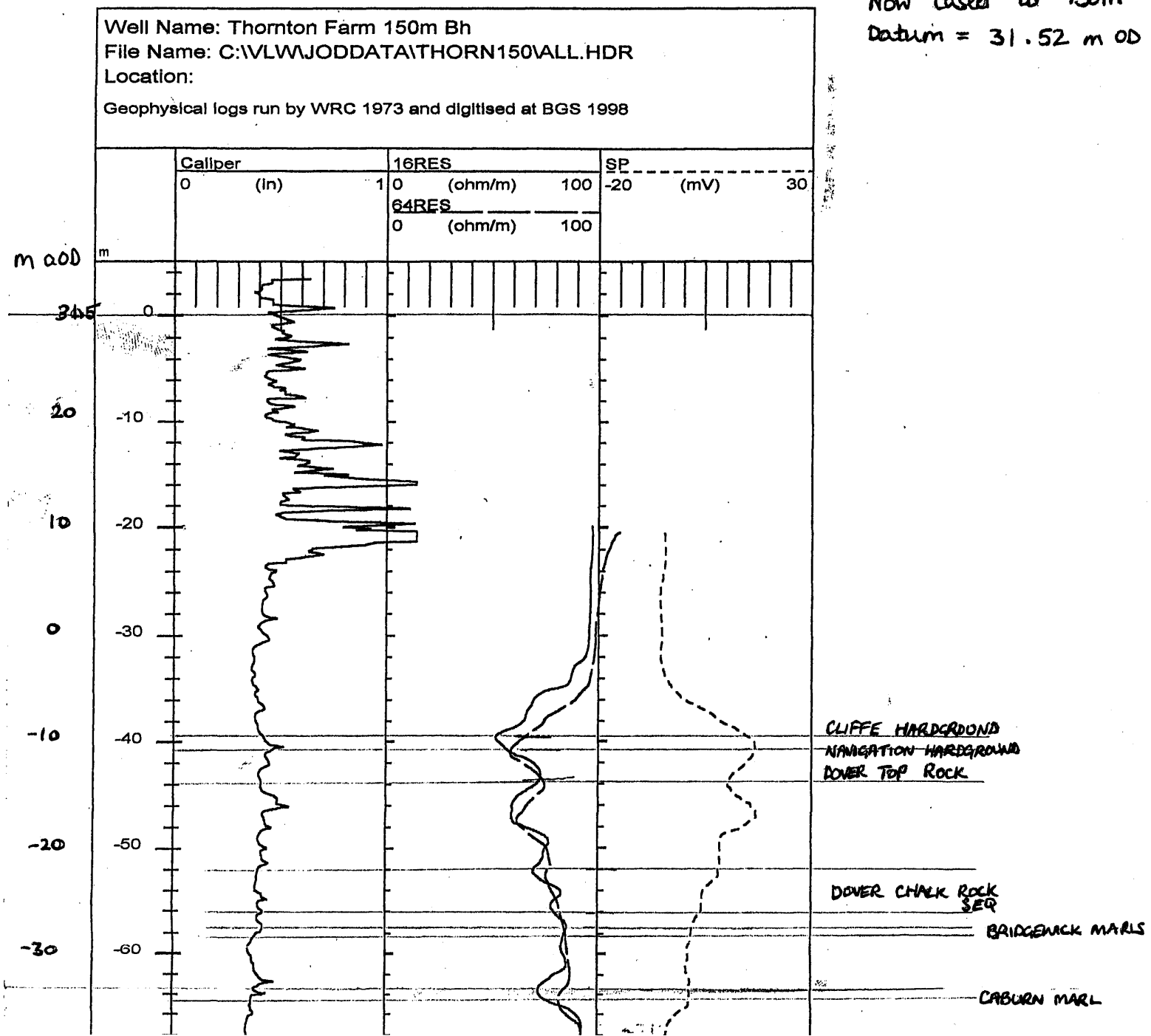

Single Borehole Dilution Tests
Theory & Results Analysis

Assumptions:

1. The concentration in the borehole remains uniform and equal to the concentration leaving it
2. The concentration at time zero is instantaneously raised to Ci
3. Water enters the borehole from an aquifer thickness that is the same as the screened length of the borehole - i.e. there is no vertical flow
4. Water upstream of the borehole is at a uniform concentration Cb
5. The flow is steady state

Source: BGS Tracer Test Manual 1998

So the change of tracer mass in the borehole in time dt will equal the difference between the mass fluxes into and out of the borehole:

Eqn 1 $$\pi R^2 L_{sat} \Delta C = q L_{scrn} \alpha D (C_b - C) \Delta t$$ if this is integrated, we get

Eqn 2 $$\pi R^2 L_{sat} \int_{C_i}^{C} \frac{\partial C'}{C_b - C'} = q L_{scrn} \alpha D \int_{0}^{t} \partial t'$$

R = borehole radius
Lsat = saturated depth of the borehole
delta C = change in BH conc
q = Darcy vel
Lscrn = open length of the BH
alpha = ratio of the width of the aquifer contributing flow
D = BH diameter (2R)
Cb = background conc of tracer

alpha can have a value anywhere in the range 0 to 8 (Klotz et al 1972). Where there is no gravel pack alpha = 2 is usually sufficient.

Performing the integrals on this we get:

Eqn 3 $$\pi R^2 L_{sat} Ln\left(\frac{C_b - C}{C_b - C_i}\right) = q L_{scrn} \alpha D t$$

This can be rearranged to give the Darcy velocity, q, and thence the true velocity, v:

Eqn 4 $$v = \frac{q}{n_e} = \frac{\pi R L_{sat}}{2 n_e L_{scrn} \alpha t} Ln\left(\frac{C - C_b}{C_i - C_b}\right)$$

ne is the porosity

For the purpose of field analysis, data is often plotted on semi-log paper, so it is preferable to write the equation:

Eqn 5 $$\log\left(\frac{C - C_b}{C_i - C_b}\right) = At + B$$

the slope, A, of the plot log[(C-Cb)/(Ci-Cb)] vs t is given by:

Eqn 6 $$A = \frac{2 n_e L_{scrn} \alpha v}{Ln(10) \pi R L_{sat}}$$

This leads to the aquifer flow velocity in terms of A:

Eqn 7 $$v = \frac{Ln(10) \pi R L_{sat} A}{2 n_e L_{scrn} \alpha} \approx \frac{3.6 R L_{sat} A}{n_e L_{scrn} \alpha}$$

which is what we are after.

For a dil test carried out in an open-hole, where Lsat=Lscrn, when alpha is taken as 2,
the true vel can be calc'd by plotting a graph of (C-Cb)/(Ci-Cb) on the log scale of semi-log paper against t on the linear scale
A straight line of slope A is drawn through the data and the vel is calc'd using the simple formula:

Eqn 8 $$\upsilon = \frac{1.8R}{n_e} A$$

Alternatively
The integrated Eqn 3 can also be rearranged to give q directly:

Eqn 9 $$q = \frac{\pi R^2 L_{sat}}{\alpha 2RtL_{scrn}} Ln\left(\frac{C_b - C}{C_b - C_i}\right)$$

If we take Lsat = Lscrn, and alpha = 2 again, this becomes:

Eqn 10 $$q = \frac{\pi R}{4T} Ln\left(\frac{C_b - C}{C_b - C_i}\right)$$

or, in terms of $Ln\left(\frac{C_b - C}{C_b - C_i}\right)$,

Eqn 11 $$Ln\left(\frac{C_b - C}{C_b - C_i}\right) = \frac{4qt}{\pi R}$$

BUT, we have plotted our graph in terms of Ln[(C-Cb)/(Ci-Cb)], and not Ln[(Cb-C)/(Ci-Cb)]
SO we must multiply both sides of Eqn 11 by -1 to complete the analysis giving:

Eqn 12

$$Ln\left(\frac{C - C_b}{C_i - C_b}\right) = -\frac{4qt}{\pi R}$$

Again, the slope of the line is A, so:

$$A = \frac{4\ q}{\pi\ R}$$

$$thus$$

$$q = \frac{\pi\ RA}{4}\ or$$

$$0\ .\ 7\ 8\ 5\quad RA$$

(N.B. The slope of A is negative, but so is q (q=-Ki))

LOWER VENSON BOREHOLE 3
Single borehole dilution test run using salt in 1998. By S Watson & S Hazell
Depth:46m Cased to:20m

Depth(m)	Cb (mS/cm	Temp (°C)	Co / Ct 0	25	45	70	135	190	262	330	405	485	1325	1775	Elevation m OD
10	3.6		3.99	3.9	3.85		3.71	3.8	3.97	4.06	4.05	4.06	4.08	4.04	8.433
12	3.59		3.96	3.88	3.81	3.91	3.81	3.95	4.01	4.08	4.09	4.08	4.12	4.09	6.433
14	3.6		4.23	4.01	4.09	4.26	4.06	4.18	4.32	4.4	4.45	4.45	4.26	4.07	4.433
16	3.61	5.6	5.87	5.2	5.4	5.85	5.23	5.38	5.57	5.36	5.09	4.87	4.2	3.99	2.433
18	3.59	5.7	8.68	8.08	7.38	6.6	5.96	5.55	5.3	5.18	4.87	4.67	4.04	3.88	0.433
20	3.62	5.4	7.08	5.86	5.5	5.29	4.69	4.56	4.48	4.39	4.23	4.15	3.8	3.71	-1.567
22	3.59	5.6	5.62	5.47	5.34	5.12	4.86	4.74	4.6	4.51	4.33	4.19	3.76	3.67	-3.567
24	3.61	5.4	5.26	5.14	5.11	4.85	4.65	4.5	4.45	4.39	4.25	4.09	3.72	3.64	-5.567
26	3.56	5.6	5.29	4.93	4.87	4.82	4.52	4.45	4.34	4.27	4.13	4.04	3.68	3.61	-7.567
28	3.56	5.5	5.35	5.13	5.07	4.95	4.77	4.72	4.63	4.54	4.36	4.21	3.69	3.61	-9.567
30	3.55	5.6	5.48	5.25	5.2	5.14	4.99	5.01	4.94	4.9	4.68	4.54	3.73	3.62	-11.567
32	3.56	5.5	5.58	5.38	5.33	5.22	5.16	5.22	5.25	5.27	5.17	5.05	3.91	3.69	-13.567
34	3.54	5.6	5.66	5.43	5.38	5.22	5.21	5.2	5.27	5.31	5.25	5.18	4.35	3.89	-15.567
36	3.55	5.6	5.62	5.43	5.35	5.18	5.16	5.22	5.25	5.31	5.24	5.19	4.52	4.08	-17.567
38	3.54	5.7	5.46	5.29	5.19	5	5.09	5.15	5.18	5.28	5.24	5.21	4.93	4.61	-19.567
40	3.56	5.5	5.21	5.02	5	4.87	4.95	5.1	5.12	5.22	5.19	5.18	5.11	5.05	-21.567
42	3.68	5.5	4.95	4.87	4.84	4.76	4.83	4.99	5.05	5.16	5.16	5.15	5.12	5.07	-23.567
44	3.7	5.4	5.19	4.95	4.88	4.94	4.83	4.99	5	5.12	5.13	5.14	5.14	5.09	-25.567
46	4.14	4.7	6.63	6.31	6.22	6.04	6.03	6.17	6.16	6.41	6.28	6.32	5.85	6.06	-27.567
Average	3.618421	5.49375	5.532105	5.238421	5.147895	5.112222	4.868947	4.888421	4.888947	4.903158	4.799474	4.724737	4.316316	4.182632	

Ln values

Depth(m)	Cb (mS/cm)	time mins	0	25	45	70	135	190	262	330	405	485	1325	1775
		time hrs	0	0.42	0.75	1.17	2.25	3.17	4.37	5.50	6.75	8.08	22.08	29.58
10	3.6		0	-0.262364	-0.444686		-1.265666	-0.667829	-0.052644	0.16508	0.143101	0.16508	0.207639	0.120628
12	3.59		0	-0.243622	-0.519875	-0.145182	-0.519875	-0.027399	0.126752	0.280902	0.301105	0.280902	0.359374	0.301105
14	3.6		0	-0.429563	-0.251314	0.04652	-0.314493	-0.082692	0.133531	0.238892	0.299517	0.299517	0.04652	-0.292987
16	3.61		0	-0.351631	-0.233149	-0.008889	-0.332939	-0.244385	-0.14242	-0.255749	-0.423323	-0.584253	-1.342998	-1.782949
18	3.59		0	-0.125425	-0.294912	-0.525338	-0.764388	-0.954333	-1.090784	-1.163544	-1.380418	-1.550317	-2.425786	-2.865152
20	3.62		0	-0.434793	-0.609997	-0.728445	-1.17361	-1.303144	-1.392091	-1.502633	-1.735565	-1.876147	-2.956067	-3.649214
22	3.59		0	-0.076764	-0.14842	-0.282768	-0.469019	-0.568274	-0.698085	-0.791417	-1.009141	-1.218861	-2.479993	-3.233764
24	3.61		0	-0.075508	-0.09531	-0.285664	-0.461555	-0.617309	-0.675129	-0.749237	-0.947062	-1.234744	-2.70805	-4.007333
26	3.56		0	-0.233311	-0.278094	-0.31701	-0.588943	-0.664655	-0.796583	-0.890612	-1.11024	-1.282091	-2.668385	-3.543854
28	3.56		0	-0.13114	-0.170106	-0.252912	-0.391595	-0.433796	-0.514557	-0.602418	-0.805359	-1.012999	-2.622436	-3.577948
30	3.55		0	-0.126892	-0.156745	-0.193786	-0.292877	-0.279084	-0.328216	-0.357415	-0.535302	-0.66757	-2.372318	-3.31678
32	3.56		0	-0.104261	-0.132118	-0.19628	-0.233094	-0.19628	-0.178369	-0.166604	-0.226863	-0.304321	-1.75292	-2.743318
34	3.54		0	-0.114839	-0.141651	-0.232622	-0.238592	-0.244598	-0.203295	-0.180437	-0.214923	-0.25672	-0.962137	-1.801238
36	3.55		0	-0.096277	-0.139762	-0.238969	-0.251314	-0.214725	-0.19692	-0.162235	-0.20282	-0.232852	-0.758008	-1.362427
38	3.54		0	-0.092709	-0.15155	-0.273889	-0.21407	-0.176091	-0.157629	-0.09844	-0.121697	-0.139502	-0.323021	-0.584667
40	3.56		0	-0.122339	-0.136132	-0.230748	-0.171472	-0.068993	-0.056089	0.006042	-0.012195	-0.018349	-0.06252	-0.101999
42	3.68		0	-0.065064	-0.090597	-0.162056	-0.099255	0.03101	0.075794	0.153025	0.153025	0.146246	0.125626	0.090287
44	3.7		0	-0.175633	-0.233262	-0.183665	-0.276558	-0.144134	-0.136412	-0.048119	-0.041102	-0.034133	-0.034133	-0.069472
46	4.14		0	-0.137556	-0.179915	-0.270429	-0.275706	-0.204247	-0.209185	-0.092503	-0.151477	-0.132958	-0.375789	-0.259958

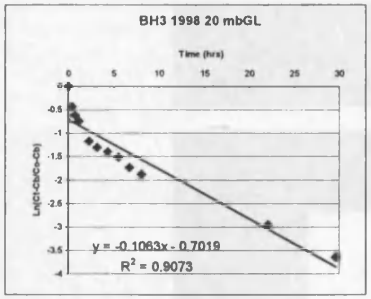

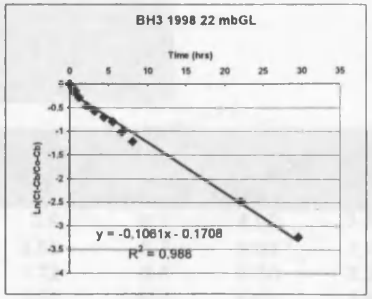

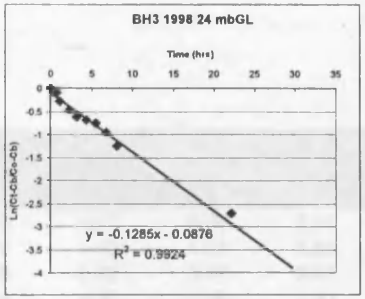

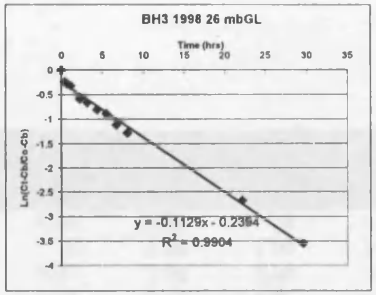

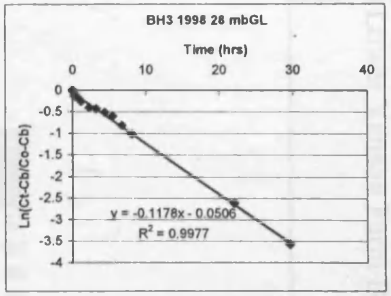

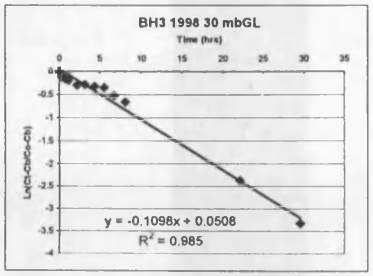

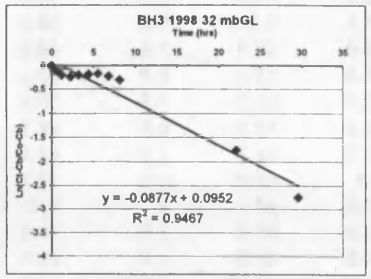

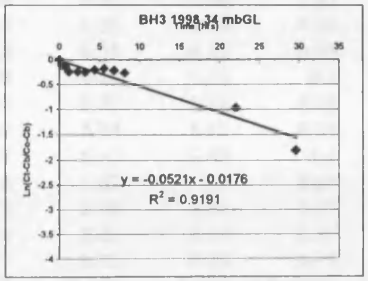

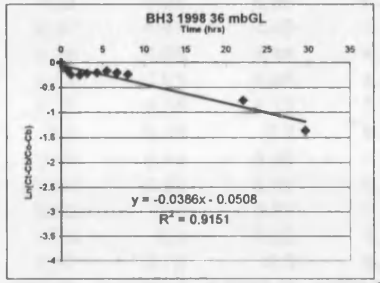

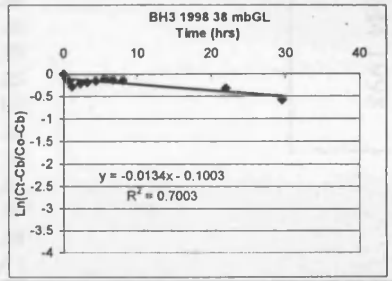

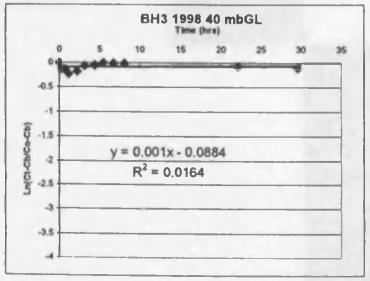

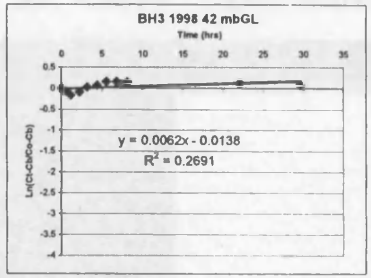

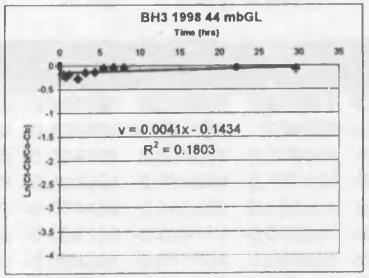

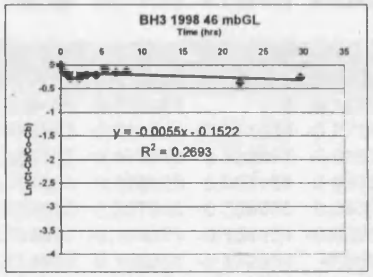

Elevation	q=0.785rA Depth	A	r=100mm q (m/hr)	q (m/d)
-1.567	20	0.1063	0.00834455	0.20
-3.567	22	0.1061	0.00832885	0.20
-5.567	24	0.1285	0.01008725	0.24
-7.567	26	0.1129	0.00886265	0.21
-9.567	28	0.1178	0.0092473	0.22
-11.567	30	0.1098	0.0086193	0.21
-13.567	32	0.0877	0.00688445	0.17
-15.567	34	0.0521	0.00408985	0.10
-17.567	36	0.0386	0.0030301	0.07
-19.567	38	0.0134	0.0010519	0.03
-21.567	40	0.001	0.0000785	0.00
-23.567	42	0.0062	0.0004867	0.01
-25.567	44	0.0041	0.00032185	0.01
-27.567	46	0.0055	0.00043175	0.01

LOWER VENSON BOREHOLE 4
Single BH dilution test 1998
Depth:88m
Cased to:65m

Depth(m)	Cb (mS/cm)	Temp (°C)	Co 0	15	40	70	105	155	235	1080	1535
60	3.9	6.7	4.02	3.93	4.03	4.08	3.98	4.04	4.02	4	3.97
62	3.83	6.7	4.04	3.97	4.01	4.05	3.96	4	3.99	3.99	3.96
64	3.72	6.8	3.86	3.85	3.92	3.97	3.91	3.97	3.96	3.98	3.96
66	3.68	6.6	4.02	3.94	4.03	4.09	3.97	4.03	4.04	4.05	4.06
68	3.62	6.7	4.2	4.16	4.36	4.42	4.25	4.37	4.41	4.48	4.28
70	3.61	6.4	5.22	5.12	5.18	5.21	5.06	5.06	4.99	4.44	4.25
72	3.58	6.5	5.28	5.19	5.26	5.29	5.1	5.11	5.01	4.45	4.25
74	3.57	6.2	5.38	5.32	5.35	5.41	5.32	5.37	5.35	5.19	5.07
76	3.54	6.4	5.31	5.32	5.34	5.41	5.35	5.4	5.39	5.3	5.22
78	3.54	6.1	5.42	5.37	5.42	5.49	5.4	5.45	5.44	5.36	5.28
80	3.51	6.2	5.63	5.6	5.62	5.7	5.61	5.66	5.63	5.49	5.39
82	3.5	6	5.85	5.75	5.86	5.94	5.77	5.85	5.8	5.65	5.56
84	3.48	6.1	6.26	6.24	6.27	6.36	6.27	6.35	6.3	6.03	5.88
86	3.46	6.1	6.56	6.77	6.82	6.89	6.73	6.87	6.75	6.5	6.41
Average:	3.61	6.392857	5.075	5.037857	5.105	5.165	5.048571	5.109286	5.077143	4.922143	4.824286

Ln values

Depth(m)	Cb (mS/cm	time mins	0	15	40	70	105	155	235	1080	1535
		time hrs	0	0.25	0.67	1.17	1.75	2.58	3.92	18.00	25.58
60	3.9		0	-1.386294	0.080043	0.405465	-0.405465	0.154151	0	-0.182322	-0.538997
62	3.83		0	-0.405465	-0.154151	0.04652	-0.479573	-0.211309	-0.271934	-0.271934	-0.479573
64	3.72		0	-0.074108	0.356675	0.579818	0.305382	0.579818	0.538997	0.619039	0.5389965
66	3.68		0	-0.268264	0.028988	0.187212	-0.159065	0.028988	0.057158	0.084557	0.1112256
68	3.62		0	-0.071459	0.243622	0.321584	0.082692	0.257045	0.309005	0.393904	0.1292117
70	3.61		0	-0.064125	-0.025159	-0.006231	-0.104671	-0.104671	-0.154151	-0.662564	-0.922521
72	3.58		0	-0.054394	-0.011834	0.005865	-0.111918	-0.105361	-0.172954	-0.66989	-0.931106
74	3.57		0	-0.033711	-0.016713	0.016439	-0.033711	-0.00554	-0.016713	-0.110901	-0.187862
76	3.54		0	0.005634	0.016807	0.054959	0.022347	0.049597	0.044206	-0.005666	-0.052186
78	3.54		0	-0.026956	0	0.036558	-0.010695	0.015831	0.010582	-0.032435	-0.077387
80	3.51		0	-0.014252	-0.004728	0.032485	-0.009479	0.014052	0	-0.068319	-0.120144
82	3.5		0	-0.043485	0.004246	0.037583	-0.034635	0	-0.021506	-0.088947	-0.131709
84	3.48		0	-0.00722	0.003591	0.035339	0.003591	0.031861	0.014286	-0.086358	-0.146982
86	3.46		0	0.065546	0.080539	0.101158	0.053388	0.09531	0.059485	-0.019545	-0.049597

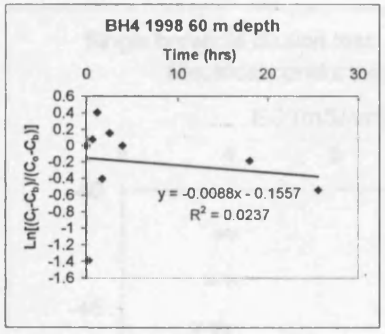

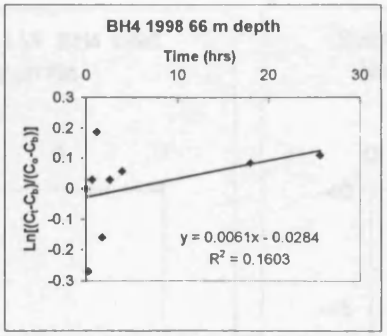

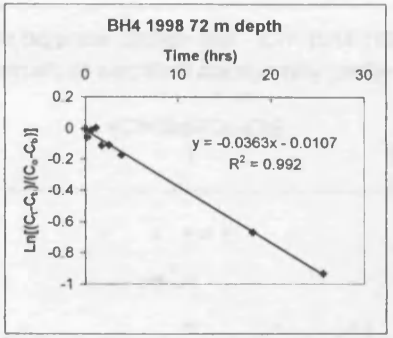

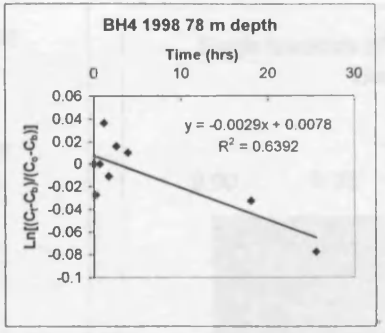

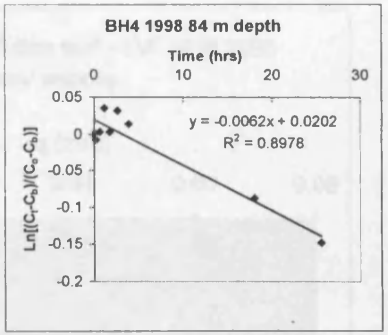

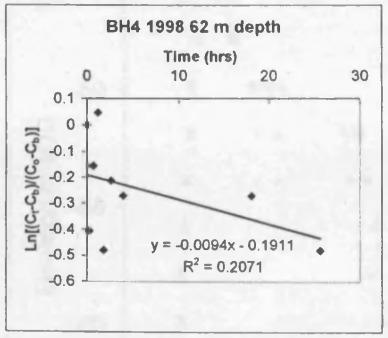

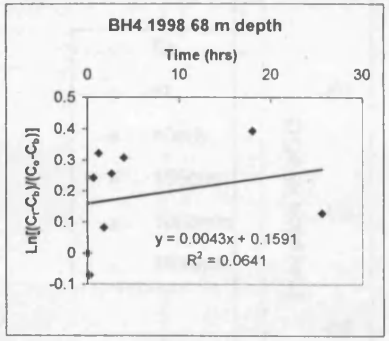

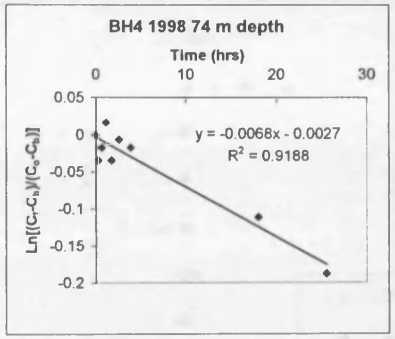

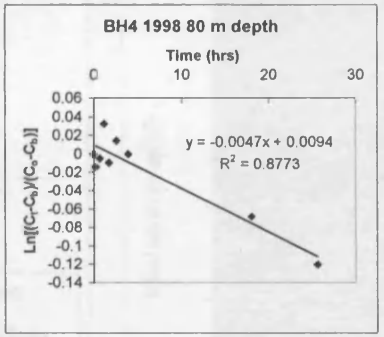

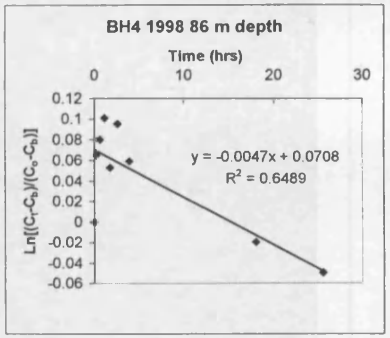

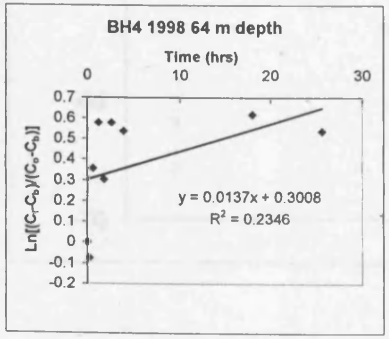

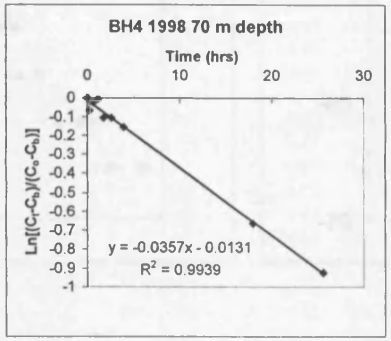

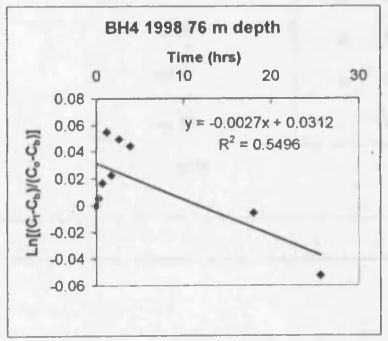

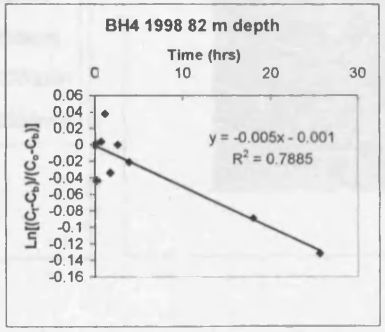

Depth (m)	Elevation rA	r=100mm		
			q [m/hr]	q (m/d)
60	-41.866	0.0088	0.000691	0.017
62	-43.866	0.0094	0.000738	0.018
64	-45.866			
66	-47.866			
68	-49.866			
70	-51.866	0.0357	0.002802	0.067
72	-53.866	0.0363	0.00285	0.068
74	-55.866	0.0068	0.000534	0.013
76	-57.866	0.0027	0.000212	0.005
78	-59.866	0.0029	0.000228	0.005
80	-61.866	0.0047	0.000369	0.009
82	-63.866	0.005	0.000393	0.009
84	-65.866	0.0062	0.000487	0.012
86	-67.866	0.0047	0.000369	0.009

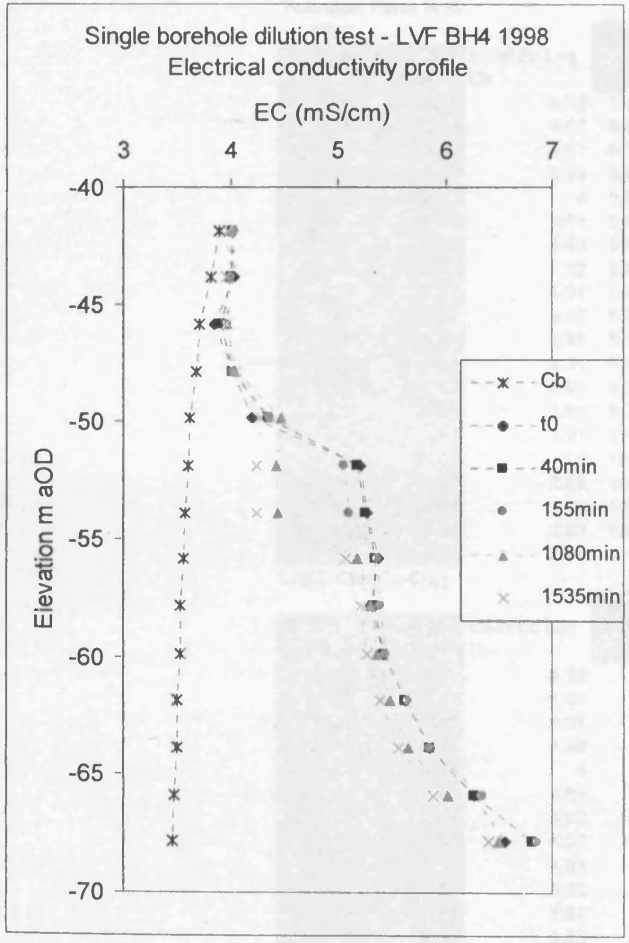
Single borehole dilution test - LVF BH4 1998
Electrical conductivity profile
EC (mS/cm)
3
4
5
6
7
-40
-45
-50
-55
-60
-65
-70
Elevation m aOD
Cb
t0
40min
155min
1080min
1535min

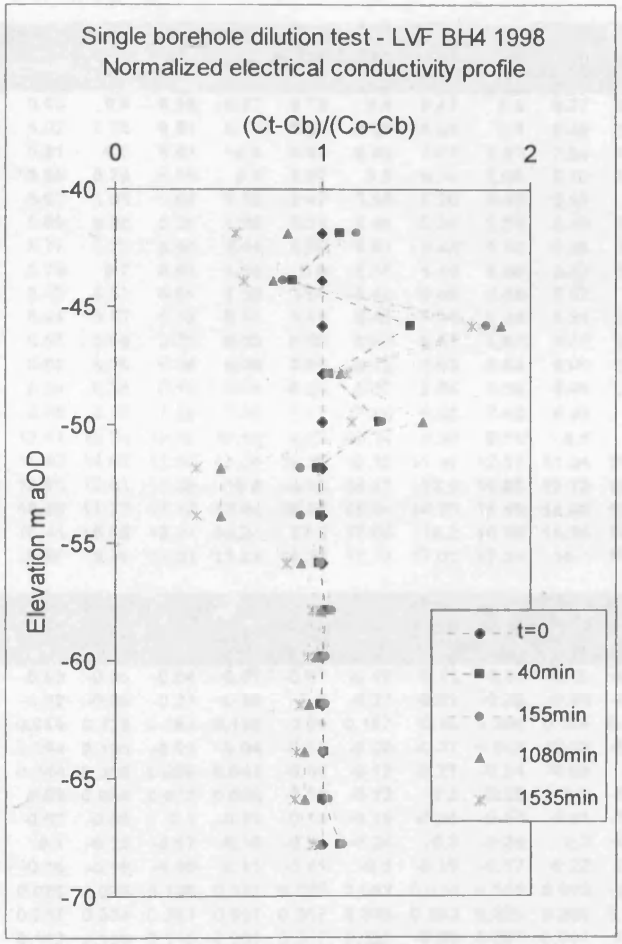
Single borehole dilution test - LVF BH4 1998
Normalized electrical conductivity profile
(Ct-Cb)/(Co-Cb)
0
1
2
-40
-45
-50
-55
-60
-65
-70
Elevation m aOD
t=0
40min
155min
1080min
1535min

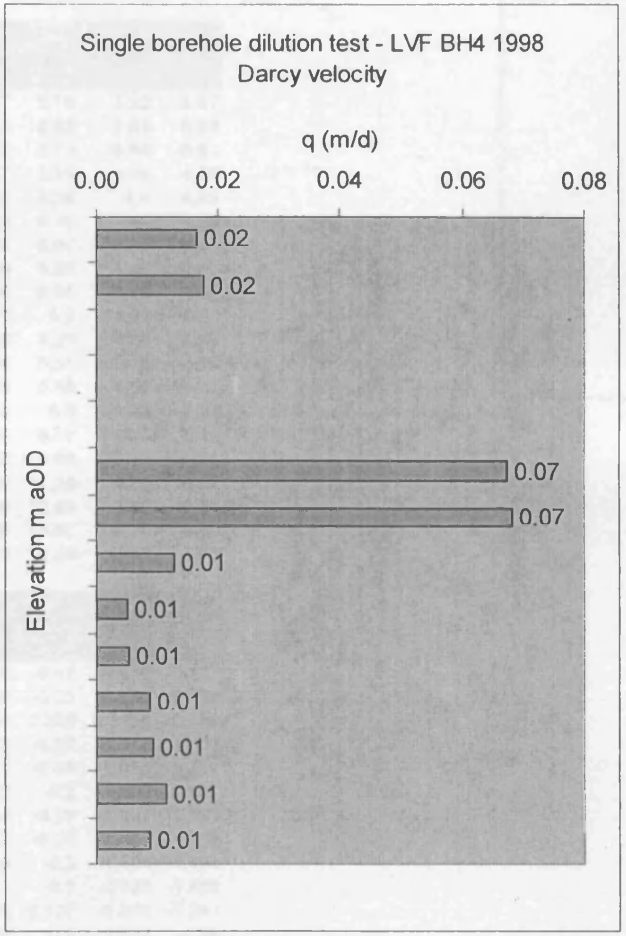
Single borehole dilution test - LVF BH4 1998
Darcy velocity
q (m/d)
0.00
0.02
0.04
0.06
0.08
Elevation m aOD
0.02
0.02
0.07
0.07
0.01
0.01
0.01
0.01
0.01
0.01
0.01

Thornton Farm BH5
1998

Depth (m)	Elevation (mAOD)	Initial Ec Log Cb	Time after tracer input (mins) 30 Co	30 Ct	45	60	75	90	120	160	185	270	310	340	395	1185	1585
36	-4.43	4.12	10.1	9.95	9.8	9.86	9.67	9.72	9.4	9.47	9.5	9.27	9.27	9.18	7.22	6.87	
35	-3.43	4.02	9.55	8.02	8.28	8.51	8.14	8.56	8.25	8.52	8.3	8.32	8.32	8.33	7.03	6.69	
34	-2.43	4.01	6.18	6.21	6.5	6.61	6.5	6.91	6.55	7.09	6.67	7.04	7.07	7.18	6.98	6.61	
33	-1.43	3.96	5.57	5.66	5.75	5.55	5.5	5.37	5.2	5.19	5.65	5.53	5.37	5.25	4.49	4.39	
32	-0.43	4	5.55	5.62	5.66	5.64	5.62	5.47	5.38	5.26	5.49	5.48	5.4	5.28	4.4	4.43	
31	0.57	4.01	5.64	5.69	5.68	5.66	5.65	5.55	5.46	5.34	5.51	5.49	5.46	5.35	4.44	4.45	
30	1.57	4.02	5.83	5.77	5.73	5.66	5.64	5.59	5.51	5.42	5.54	5.48	5.45	5.37	4.45	4.47	
29	2.57	4.02	5.97	5.79	5.7	5.67	5.65	5.6	5.55	5.46	5.56	5.47	5.44	5.38	4.46	4.47	
28	3.57	4.01	5.76	5.52	5.51	5.61	5.52	5.58	5.44	5.45	5.48	5.42	5.4	5.31	4.44	4.44	
27	4.57	3.92	5.33	5.44	5.47	5.52	5.56	5.47	5.45	5.35	5.48	5.39	5.31	5.2	4.29	4.26	
26	5.57	3.92	5.18	5.55	5.68	5.71	5.72	5.65	5.63	5.51	5.67	5.52	5.45	5.35	4.28	4.27	
25	6.57	3.91	5.67	5.98	5.96	5.88	6.08	5.81	5.72	5.62	5.83	5.69	5.64	5.51	4.3	4.28	
24	7.57	3.92	6.55	6.34	6.38	6.16	6.21	6.05	6.07	5.86	6.08	5.88	5.79	5.66	4.38	4.3	
23	8.57	3.91	8.79	9.08	8.47	7.28	7.85	7.17	7.36	6.66	7.42	6.93	6.5	6.6	4.63	4.71	
22	9.57	3.91	15.1	12.61	12.04	10.45	10.93	9.75	10.14	8.92	9.96	9.6	8.5	8.18	5.4	5.13	
21	10.57	3.9	16.7	15.42	14.61	12.67	13.23	12.26	12.18	11.32	12.07	11.04	10.23	9.89	6.19	5.6	
20	11.57	3.88	16.6	16.95	16.51	15.22	15.5	14.35	14.17	13.5	13.93	12.72	12.29	11.24	6.85	6.02	
19	12.57	3.85	17.6	18.23	17.73	17.12	17.04	15.94	15.84	14.73	15.49	14.08	13.66	12.64	7.32	6.36	
18	13.57	3.82	19.4	19.34	18.68	18.21	18.21	17.5	17.09	16.2	16.56	15.26	14.65	13.67	7.79	6.65	
17	14.57	3.76		19.86	19.39	19.01	19.09	18.28	17.77	17.02	17.25	16.1	15.42	14.39	8.8	6.78	

Ln[(C-Cb)/(Co-Cb)]

Depth (m)	Elevation (m AOD)	Initial Ec Log Cb	Time after tracer input (mins) 30	45	60	75	90	120	160	185	270	310	340	395	1185	1585
36	-4.43	4.12	1	-0.03	-0.05	-0.04	-0.07	-0.07	-0.12	-0.11	-0.11	-0.15	-0.15	-0.17	-0.657	-0.777
35	-3.43	4.02	1	-0.32	-0.26	-0.21	-0.29	-0.2	-0.27	-0.21	-0.26	-0.25	-0.25	-0.25	-0.608	-0.728
34	-2.43	4.01	1	0.014	0.138	0.181	0.138	0.29	0.157	0.35	0.204	0.334	0.344	0.379	0.3138	0.181
33	-1.43	3.96	1	0.054	0.106	-0.01	-0.04	-0.13	-0.26	-0.27	0.048	-0.03	-0.13	-0.22	-1.111	-1.32
32	-0.43	4	1	0.044	0.069	0.056	0.044	-0.05	-0.12	-0.21	-0.04	-0.05	-0.1	-0.19	-1.355	-1.282
31	0.57	4.01	1	0.03	0.024	0.012	0.006	-0.06	-0.12	-0.2	-0.08	-0.1	-0.12	-0.2	-1.333	-1.31
30	1.57	4.02	1	-0.03	-0.06	-0.1	-0.11	-0.14	-0.19	-0.26	-0.17	-0.21	-0.24	-0.29	-1.437	-1.392
29	2.57	4.02	1	-0.1	-0.15	-0.17	-0.18	-0.21	-0.24	-0.3	-0.24	-0.3	-0.32	-0.36	-1.489	-1.466
28	3.57	4.01	1	-0.15	-0.15	-0.09	-0.15	-0.11	-0.2	-0.19	-0.17	-0.22	-0.23	-0.3	-1.404	-1.404
27	4.57	3.92	1	0.075	0.095	0.126	0.151	0.095	0.082	0.014	0.101	0.042	-0.01	-0.1	-1.338	-1.422
26	5.57	3.92	1	0.257	0.334	0.351	0.357	0.317	0.305	0.233	0.329	0.239	0.194	0.127	-1.253	-1.281
25	6.57	3.91	1	0.162	0.153	0.113	0.209	0.077	0.028	-0.03	0.087	0.011	-0.02	-0.1	-1.507	-1.56
24	7.57	3.92	1	-0.08	-0.07	-0.16	-0.14	-0.21	-0.2	-0.3	-0.2	-0.29	-0.34	-0.41	-1.744	-1.935
23	8.57	3.91	1	0.058	-0.07	-0.37	-0.21	-0.4	-0.35	-0.57	-0.33	-0.48	-0.63	-0.6	-1.914	-1.808
22	9.57	3.91	1	-0.25	-0.32	-0.54	-0.46	-0.65	-0.58	-0.8	-0.61	-0.67	-0.89	-0.96	-2.014	-2.214
21	10.57	3.9	1	-0.11	-0.18	-0.38	-0.32	-0.43	-0.44	-0.55	-0.45	-0.59	-0.71	-0.76	-1.723	-2.021
20	11.57	3.88	1	0.026	-0.01	-0.12	-0.09	-0.2	-0.21	-0.28	-0.24	-0.36	-0.41	-0.55	-1.455	-1.783
19	12.57	3.85	1	0.046	0.011	-0.03	-0.04	-0.13	-0.14	-0.23	-0.17	-0.29	-0.34	-0.45	-1.375	-1.699
18	13.57	3.82	1	-0	-0.05	-0.08	-0.08	-0.13	-0.16	-0.23	-0.2	-0.31	-0.36	-0.46	-1.367	-1.706

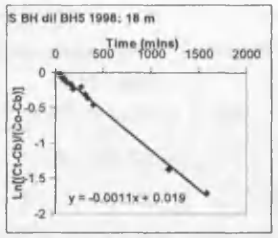

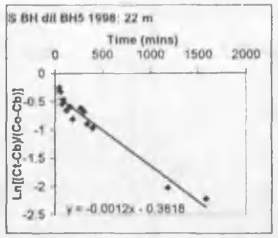

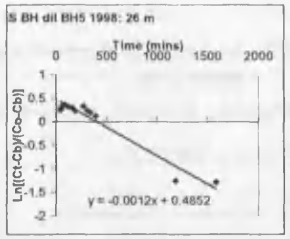

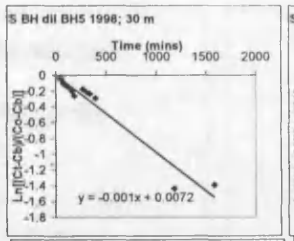

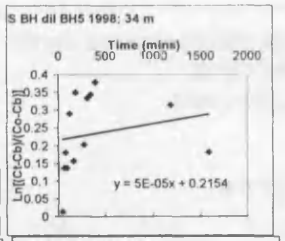

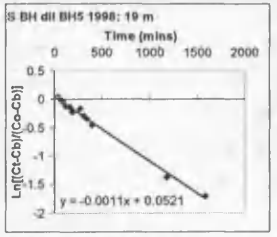

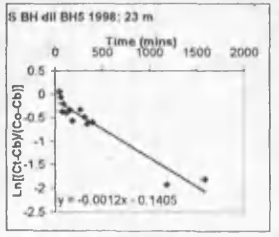

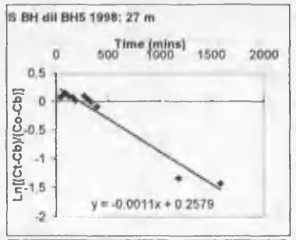

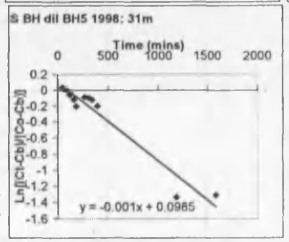

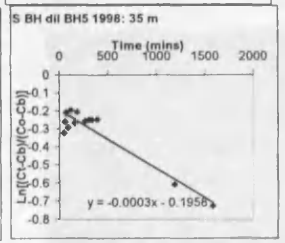

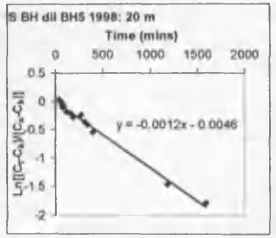

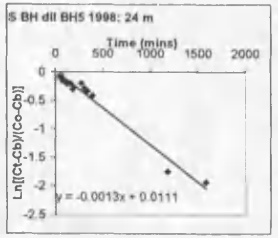

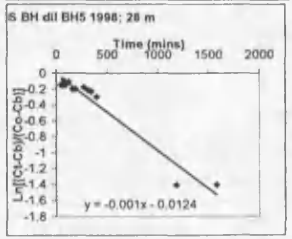

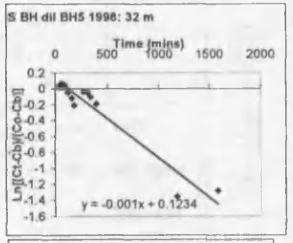

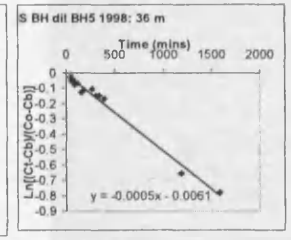

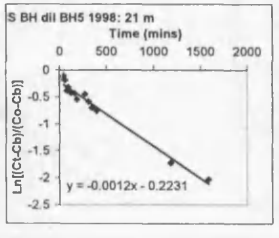

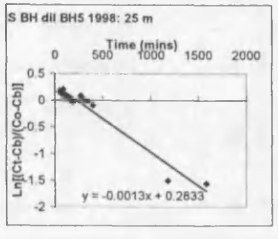

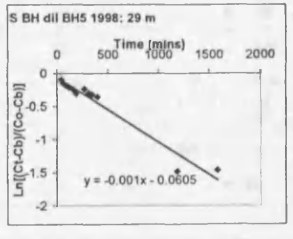

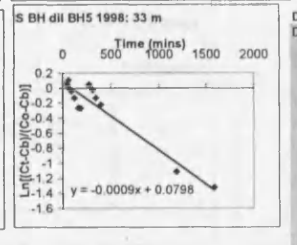

Darcy velocity

Depth (m)	Elevation (n A		q (m/d)
18	13.57	0.0011	0.124
19	12.57	0.0011	0.124
20	11.57	0.0012	0.136
21	10.57	0.0012	0.136
22	9.57	0.0012	0.136
23	8.57	0.0012	0.136
24	7.57	0.0013	0.147
25	6.57	0.0013	0.147
26	5.57	0.0012	0.136
27	4.57	0.0011	0.124
28	3.57	0.001	0.113
29	2.57	0.001	0.113
30	1.57	0.001	0.113
31	0.57	0.001	0.113
32	-0.43	0.001	0.113
33	-1.43	0.0009	0.102
34	-2.43		
35	-3.43	0.0003	0.034
36	-4.43	0.0005	0.057

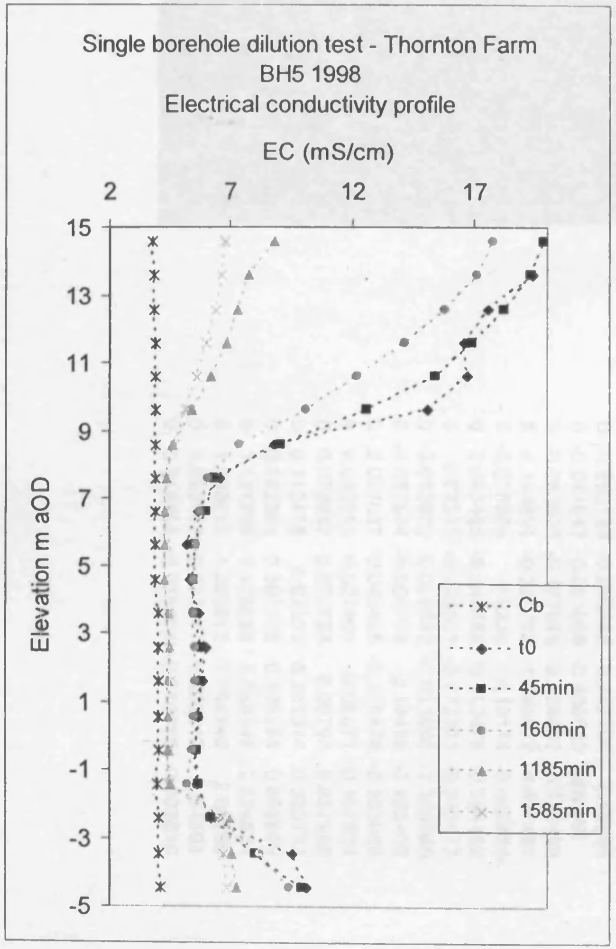
Single borehole dilution test - Thornton Farm
BH5 1998
Electrical conductivity profile
EC (mS/cm)
2
7
12
17
15
13
11
9
7
5
3
1
-1
-3
-5
Elevation m aOD
Cb
t0
45min
160min
1185min
1585min

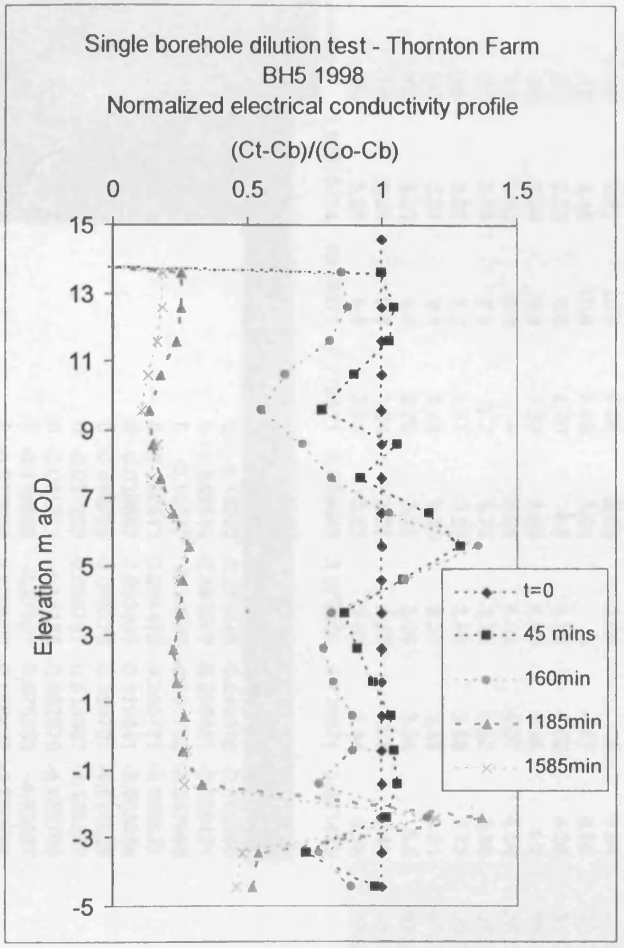
Single borehole dilution test - Thornton Farm
BH5 1998
Normalized electrical conductivity profile
(Ct-Cb)/(Co-Cb)
0
0.5
1
1.5
15
13
11
9
7
5
3
1
-1
-3
-5
Elevation m aOD
t=0
45 mins
160min
1185min
1585min

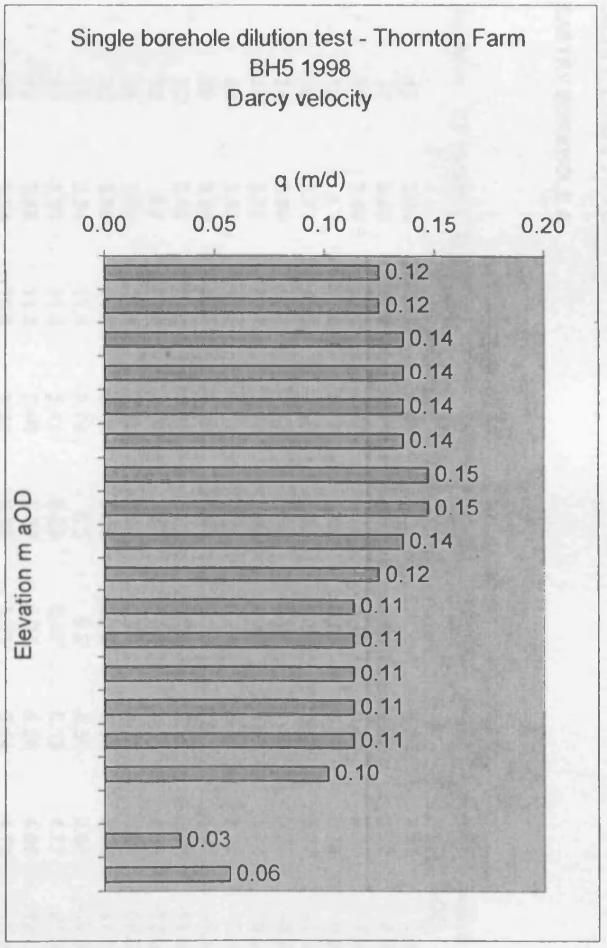
Single borehole dilution test - Thornton Farm
BH5 1998
Darcy velocity
q (m/d)
0.00
0.05
0.10
0.15
0.20
0.12
0.12
0.14
0.14
0.14
0.14
0.15
0.15
0.14
0.12
0.11
0.11
0.11
0.11
0.11
0.10
0.03
0.06
Elevation m aOD

Eastry BHA 1998

EASTRY BOREHOLE A

			Co					
Depth(m)	Cb (mS/cm)	Temp (°C)	0	25	45	165	915	Elevation m aOD
12	3.52	13.2	5.46	5.22	5	4.35	3.68	6.94
14	3.65	12.2	6.11	4.94	5.01	4.62	3.72	4.94
16	3.69	11.8	6.25	6	5.79	5.24	3.78	2.94
18	3.7	11.4	6.54	6.2	5.88	5.67	3.78	0.94
20	3.71	11.5	6.69	6.6	6.68	6.2	3.77	-1.06
22	3.69	11.4	7	6.94	6.85	6	3.75	-3.06
24	3.69	11.5	6.94	6.84	6.73	5.63	3.74	-5.06
26	3.69	11.3	6.89	6.7	6.44	5.34	3.72	-7.06
28	3.69	11.4	6.46	6.15	5.79	5.1	3.71	-9.06
30	3.69	11.3	5.28	5.26	5.33	5.16	3.72	-11.06
32	3.7	11.4	6.07	5.54	5.93	5.55	3.71	-13.06
34	3.68	11.4	6.12	6.02	5.93	5.18	3.68	-15.06
36	3.65	11.5	6.16	5.96	5.73	4.86	3.66	-17.06
38	3.64	11.4	5.79	5.5	5.2	4.36	3.66	-19.06
40	3.62	11.5	5.41	5.28	5.37	5.19	4.77	-21.06
42	3.58	11.3	5.46	5.38	5.38	5.26	4.86	-23.06
44	3.54	10.8	5.26	5.22	5.21	5.14	4.76	-25.06
46	3.51	10.7	5.05	5.03	5.09	5	4.64	-27.06
48	3.46	10.6	5.09	5.03	5	4.87	4.55	-29.06
50	3.38	8.6	4.79	4.8	4.73	4.62	4.39	-31.06
52	3.33	8.8	4.39	4.49	4.42	4.36	4.2	-33.06
54	3.32	8.8	4	4.05	4.02	4.07	4.04	-35.06
56	3.28	9.5	3.7	3.75	3.71	3.82	3.86	-37.06
58	3.27	9.2	3.47	3.53	3.54	3.58	3.73	-39.06
60	3.24	9.4	3.28	3.39	3.37	3.43	3.61	-41.06
62	3.23	9.5	3.25	3.29	3.29	3.34	3.5	-43.06
64	3.21	9.6	3.24	3.27	3.27	3.3	3.42	-45.06
66	3.21	9.6	3.65	3.53	3.53	3.44	3.39	-47.06
Average	3.52035714	10.73571	5.278571	5.139643	5.079286	4.738571	3.921429	

Ln values							
Depth(m)	Cb (mS/cm)	time mins	0	25	45	165	915
		time hrs	0	0.42	0.75	2.75	15.25
12	3.52		0	-0.13206	-0.270646	-0.849018	-2.495269
14	3.65		0	-0.645519	-0.592677	-0.930621	-3.559421
16	3.69		0	-0.10276	-0.19807	-0.501752	-3.347953
18	3.7		0	-0.127513	-0.264479	-0.365771	-3.569533
20	3.71		0	-0.030667	-0.003361	-0.179641	-3.905334
22	3.69		0	-0.018293	-0.046376	-0.359701	-4.010359
24	3.69		0	-0.031253	-0.066797	-0.515967	-4.174387
26	3.69		0	-0.061211	-0.15155	-0.662376	-4.669709
28	3.69		0	-0.118686	-0.27691	-0.675258	-4.93087
30	3.69		0	-0.012658	0.030962	-0.078472	-3.970292
32	3.7		0	-0.253124	-0.060888	-0.247704	-5.46806
34	3.68		0	-0.041847	-0.081068	-0.486533	#NUM!
36	3.65		0	-0.083035	-0.187915	-0.729662	-5.525453
38	3.64		0	-0.144891	-0.320782	-1.093972	-4.677491
40	3.62		0	-0.075398	-0.0226	-0.13114	-0.442454
42	3.58		0	-0.043485	-0.043485	-0.112478	-0.384412
44	3.54		0	-0.02353	-0.029501	-0.072321	-0.343473
46	3.51		0	-0.013072	0.025642	-0.033006	-0.309565
48	3.46		0	-0.037504	-0.056798	-0.14499	-0.402402
50	3.38		0	0.007067	-0.043485	-0.128478	-0.333639
52	3.33		0	0.090151	0.027909	-0.02871	-0.197531
54	3.32		0	0.070952	0.028988	0.09798	0.057158
56	3.28		0	0.112478	0.02353	0.251314	0.322773
58	3.27		0	0.262364	0.300105	0.438255	0.832909
60	3.24		0	1.321756	1.178655	1.558145	2.224624
62	3.23		0	1.098612	1.098612	1.704748	2.60269
64	3.21		0	0.693147	0.693147	1.098612	1.94591
66	3.21		0	-0.318454	-0.318454	-0.648695	-0.893818

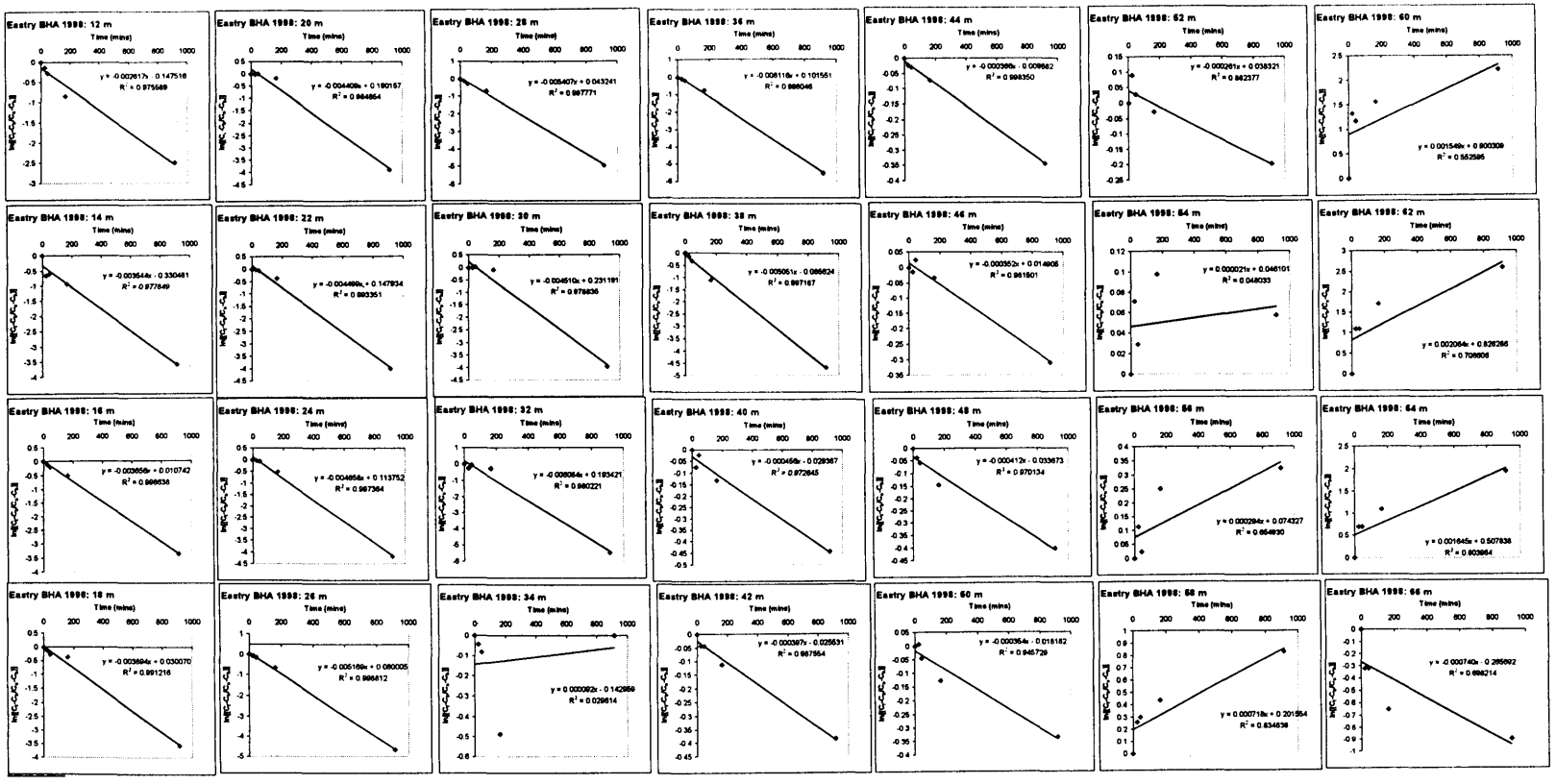

Darcy velocity summary

Depth	Elevation	A	q m/s	q m/d
12	6.94	0.002617	0.000205	0.296
14	4.94	0.003544	0.000278	0.401
16	2.94	0.003856	0.000287	0.413
18	0.94	0.003894	0.000306	0.440
20	-1.06	0.004409	0.000348	0.498
22	-3.06	0.004499	0.000353	0.509
24	-5.06	0.004658	0.000366	0.527
26	-7.06	0.005169	0.000406	0.584
28	-9.06	0.005407	0.000424	0.611
30	-11.06	0.00451	0.000354	0.510
32	-13.06	0.006084	0.000478	0.688
34	-15.06			
36	-17.06	0.006116	0.00048	0.691
38	-19.06	0.005051	0.000397	0.571
40	-21.06	0.000456	3.58E-05	0.052
42	-23.06	0.000397	3.12E-05	0.045
44	-25.06	0.000366	2.87E-05	0.041
46	-27.06	0.000352	2.76E-05	0.040
48	-29.06	0.000412	3.23E-05	0.047
50	-31.06	0.000354	2.78E-05	0.040
52	-33.06	0.000261	2.05E-05	0.030
54	-35.06			
56	-37.06			
58	-39.06			
60	-41.06			
62	-43.06			
64	-45.06			
66	-47.06	0.00074	5.81E-05	0.084

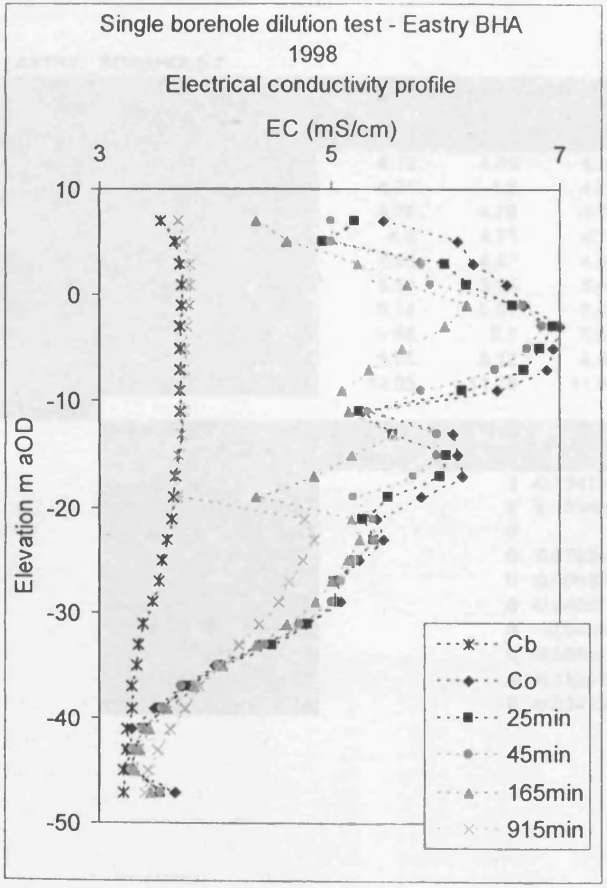
Single borehole dilution test - Eastry BHA
1998
Electrical conductivity profile
EC (mS/cm)
3
5
7
10
0
-10
-20
-30
-40
-50
Elevation m aOD
Cb
Co
25min
45min
165min
915min

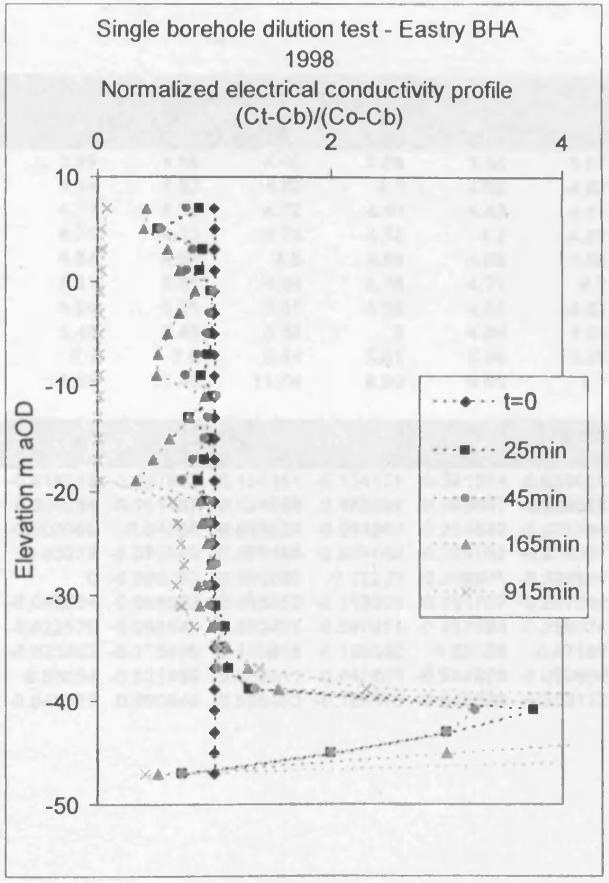
Single borehole dilution test - Eastry BHA
1998
Normalized electrical conductivity profile
(Ct-Cb)/(Co-Cb)
0
2
4
10
0
-10
-20
-30
-40
-50
Elevation m aOD
t=0
25min
45min
165min
915min

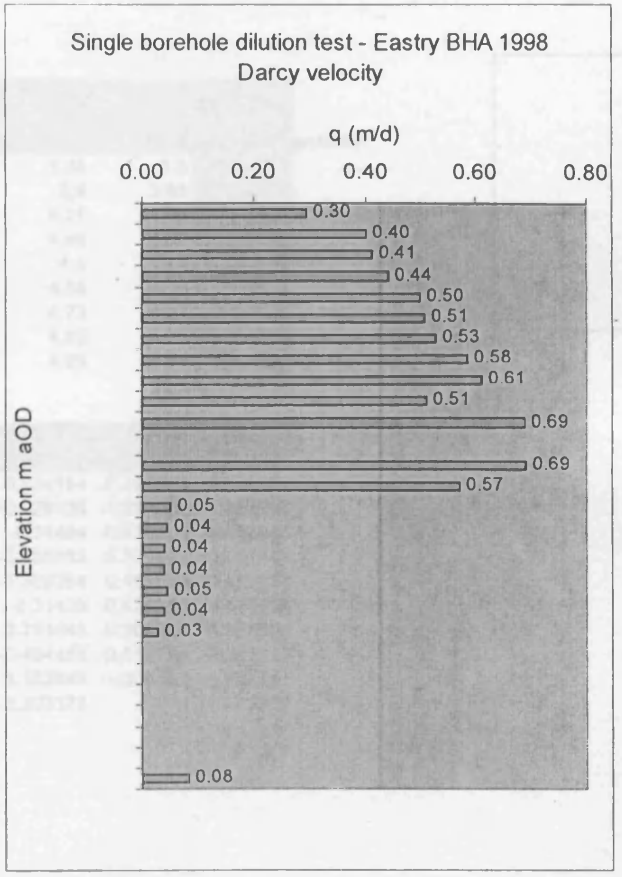
Single borehole dilution test - Eastry BHA 1998
Darcy velocity
q (m/d)
0.00
0.20
0.40
0.60
0.80
Elevation m aOD
0.30
0.40
0.41
0.44
0.50
0.51
0.53
0.58
0.61
0.51
0.69
0.69
0.57
0.05
0.04
0.04
0.04
0.05
0.04
0.03
0.08

Eastry BH7 1998

EASTRY: BOREHOLE 7

1998			Time minutes since start of test											
			Co											
Depth(m)	Cb (mS/cm	Temp (°C)	0	20	50	80	115	275	1030	1315	1540	2465	2910	Elevation (mAOD)
55	3.57	12.3	4.13	4.05	4.12	3.99	4.05	4.05	3.88	3.86	3.87	3.88	3.8	-38.2
57	3.57	12.3	4.71	4.6	4.72	4.54	4.57	4.52	4.1	4.02	4.02	3.9	3.85	-40.2
59	3.56	12.4	4.76	4.76	4.75	4.71	4.72	4.72	4.49	4.43	4.41	4.21	4.08	-42.2
61	3.56	12.4	4.8	4.71	4.76	4.71	4.73	4.73	4.55	4.5	4.52	4.46	4.39	-44.2
63	3.57	9.8	4.96	4.87	4.96	4.84	4.84	4.8	4.59	4.56	4.56	4.5	4.45	-46.2
65	3.59	10.1	5.11	5.05	5.05	5.01	5.01	4.94	4.76	4.73	4.7	4.58	4.54	-48.2
67	3.58	10.5	5.14	5.07	5.09	5.04	5.05	5.01	4.86	4.82	4.83	4.73	4.67	-50.2
69	3.58	10.6	5.68	5.5	5.61	5.45	5.46	5.32	5	4.89	4.94	4.83	4.79	-52.2
71	3.57	10.5	8.66	8.12	8.86	8.5	7.6	6.84	5.61	5.35	5.26	4.95	4.88	-54.2
73	3.58	10.6	12.05	11.76	11.65	11.55	11.49	11.04	8.03	9.65	8.7		5.83	-56.2

Ln values

Depth(m)	Cb (mS/cm)	time mins	0	20	50	80	115	275	1030	1315	1540	2465	2910
		time hrs	0	0.33	0.83	1.33	1.92	4.58	17.17	21.92	25.67	41.08	48.50
55	3.57		0	-0.154151	-0.018019	-0.287682	-0.154151	-0.154151	-0.591364	-0.658056	-0.624154	-0.591364	-0.889857
57	3.57		0	-0.101469	0.008734	-0.161487	-0.131028	-0.182322	-0.765907	-0.929536	-0.929536	-1.239691	-1.403994
59	3.56		0	0	-0.008368	-0.04256	-0.033902	-0.033902	-0.254892	-0.321584	-0.34484	-0.613104	-0.836248
61	3.56		0	-0.075349	-0.03279	-0.075349	-0.058108	-0.058108	-0.225162	-0.276987	-0.255933	-0.320472	-0.401441
63	3.57		0	-0.066939	0	-0.090287	-0.090287	-0.12229	-0.309501	-0.339354	-0.339354	-0.401874	-0.457137
65	3.59		0	-0.040274	-0.040274	-0.068053	-0.068053	-0.118606	-0.261707	-0.287682	-0.31435	-0.428761	-0.470004
67	3.58		0	-0.04591	-0.032576	-0.066249	-0.059423	-0.087011	-0.197826	-0.229574	-0.221542	-0.304924	-0.358508
69	3.58		0	-0.089612	-0.033902	-0.115999	-0.110666	-0.188052	-0.39128	-0.47191	-0.434453	-0.518794	-0.551317
71	3.57		0	-0.112151	0.03854	-0.031939	-0.233511	-0.442488	-0.914328	-1.050664	-1.102549	-1.305194	-1.357251
73	3.58		0	-0.034838	-0.048377	-0.060846	-0.068403	-0.126975	-0.643626	-0.333172	-0.503376		-1.3256

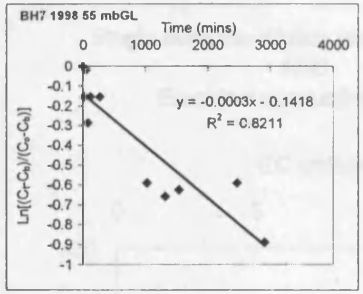

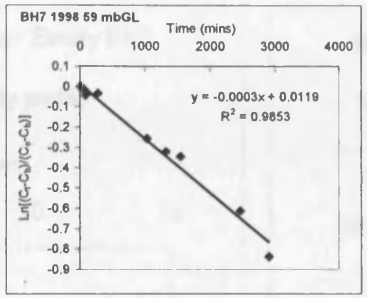

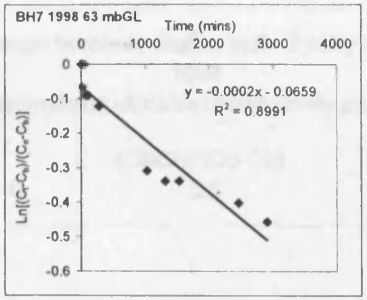

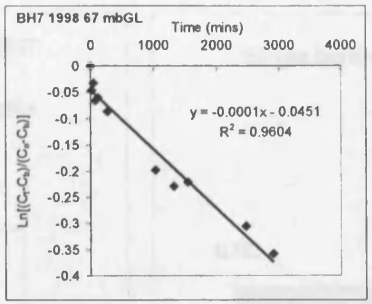

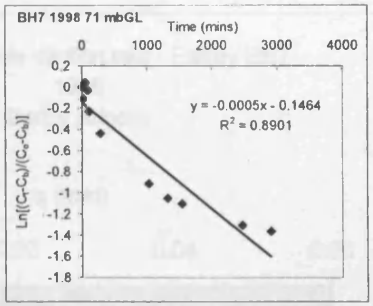

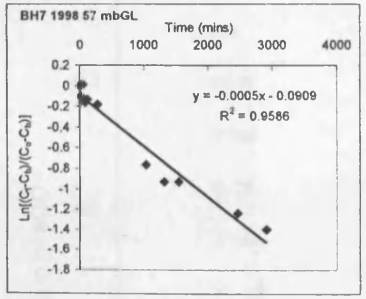

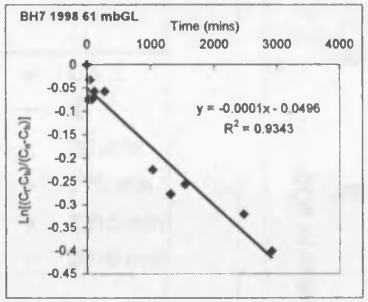

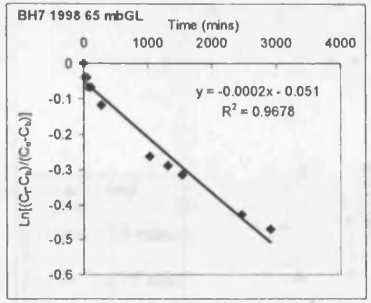

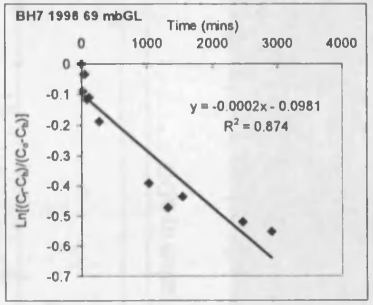

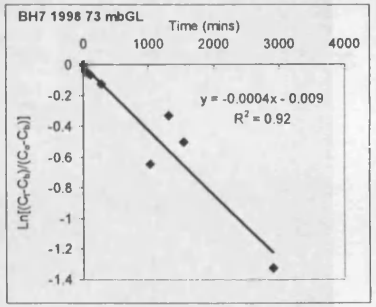

Darcy Velocity

Elevation	q=0.785rA Depth	A	r=100mm q (m/min)	q (m/d)
-38.2	55	0.0003	2.36E-05	0.03
-40.2	57	0.0005	3.93E-05	0.06
-42.2	59	0.0003	2.36E-05	0.03
-44.2	61	0.0001	7.85E-06	0.01
-46.2	63	0.0002	1.57E-05	0.02
-48.2	65	0.0002	1.57E-05	0.02
-50.2	67	0.0001	7.85E-06	0.01
-52.2	69	0.0002	1.57E-05	0.02
-54.2	71	0.0005	3.93E-05	0.06
-56.2	73	0.0004	3.14E-05	0.05

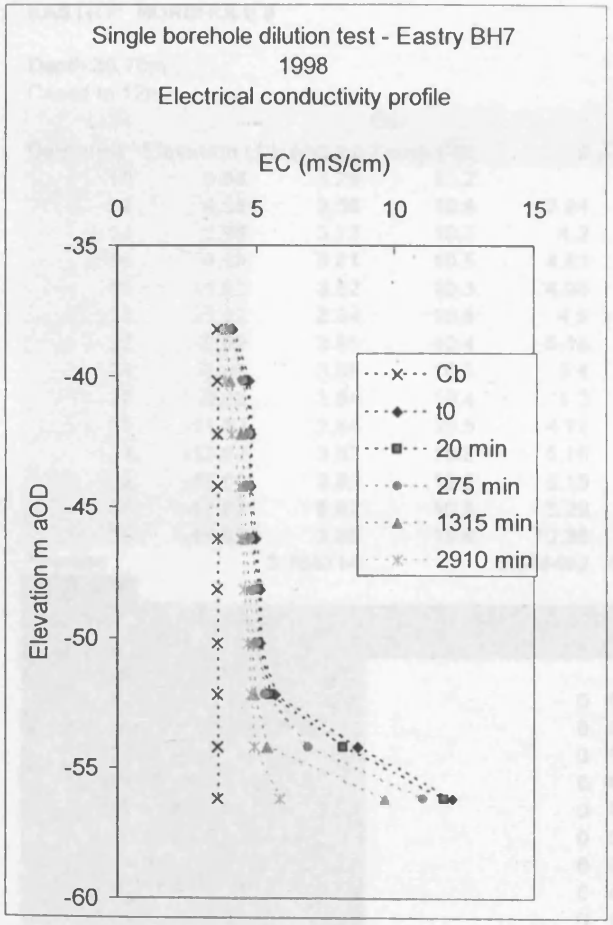
Single borehole dilution test - Eastry BH7
1998
Electrical conductivity profile
EC (mS/cm)
0
5
10
15
-35
-40
-45
-50
-55
-60
Elevation m aOD
Cb
t0
20 min
275 min
1315 min
2910 min

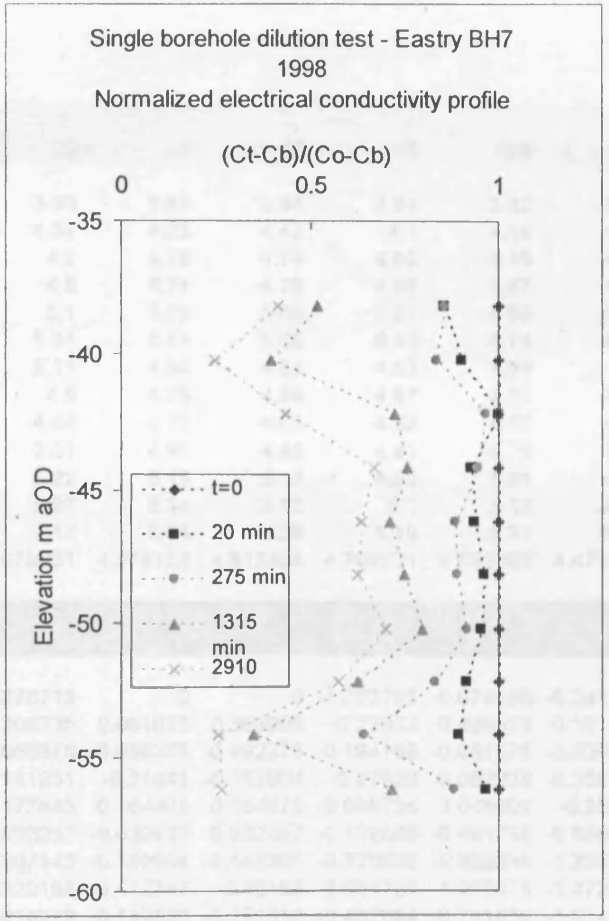
Single borehole dilution test - Eastry BH7
1998
Normalized electrical conductivity profile
(Ct-Cb)/(Co-Cb)
0
0.5
1
-35
-40
-45
-50
-55
-60
Elevation m aOD
t=0
20 min
275 min
1315 min
2910

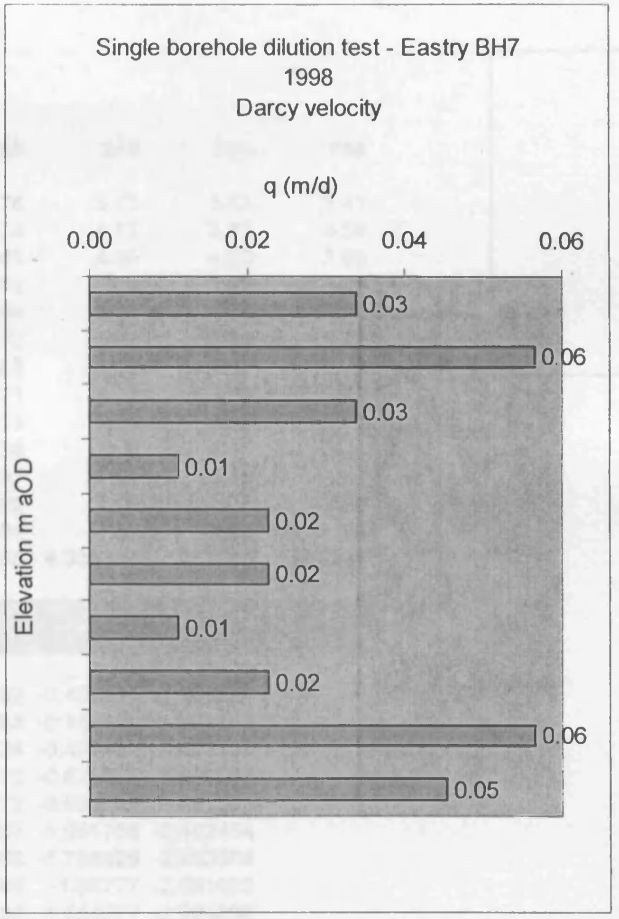
Single borehole dilution test - Eastry BH7
1998
Darcy velocity
q (m/d)
0.00
0.02
0.04
0.06
Elevation m aOD
0.03
0.06
0.03
0.01
0.02
0.02
0.01
0.02
0.06
0.05

Eastry BH8 1998

EASTRY: BOREHOLE 8

Depth:36.70m
Cased to 12m

Depth(m)	Elevation r	Cb (mS/cn	Temp (°C)	0	25	40	55	75	120	165	230	395	750
10	6.98	3.29	10.2										
12	4.98	3.56	10.4	3.84	3.93	3.84	3.84	3.64	3.82	3.78	3.73	3.63	3.41
14	2.98	3.73	10.3	4.2	4.37	4.23	4.42	4.1	4.45	4.13	4.12	3.87	3.59
16	0.98	3.81	10.5	4.83	4.9	4.78	4.74	4.65	4.75	4.62	4.49	4.03	3.68
18	-1.02	3.82	10.3	4.96	4.8	4.74	4.76	4.69	4.87	4.62	4.4	3.99	3.69
20	-3.02	3.84	10.5	4.9	5.1	5.09	5.09	5.01	4.95	4.66	4.41	4	3.72
22	-5.02	3.85	10.4	5.18	5.31	5.14	5.05	5.03	4.74	4.52	4.31	3.96	3.72
24	-7.02	3.85	10.5	5.4	5.11	4.89	4.84	4.92	4.54	4.3	4.11	3.93	3.72
26	-9.02	3.84	10.4	5.3	4.9	4.75	4.64	4.67	4.37	4.21	4.11	3.94	3.72
28	-11.02	3.84	10.5	4.92	4.94	4.77	4.68	4.52	4.37	4.13	4.08	3.95	3.72
30	-13.02	3.83	10.5	5.16	5.01	4.93	4.85	4.81	4.76	4.56	4.4	4.11	3.71
32	-15.02	3.82	10.5	5.19	5.22	5.15	5.13	4.89	5.01	4.67	4.52	4.18	3.7
34	-17.02	3.82	10.5	5.29	5.27	5.14	5.13	5.1	5.13	4.92	4.79	4.5	3.78
36	-19.02	3.82	10.6	10.36	7.17	5.94	5.39	5.19	5.24	5.01	4.89	4.59	3.8
Average		3.765714		5.348462	5.079231	4.876154	4.812308	4.709231	4.692308	4.471538	4.335385	4.052308	3.689231

Ln values

Depth(m)	Elevation r	Cb (mS/cn	time mins	0	25	40	55	75	120	165	230	395	750
			time hrs	0	0.42	0.67	0.92	1.25	2.00	2.75	3.83	6.58	12.50
10	6.98	3.29											
12	4.98	3.56		0	0.278713	0	0	-1.252763	-0.074108	-0.241162	-0.498991	-1.386294	
14	2.98	3.73		0	0.308735	0.061875	0.383959	-0.23923	0.426519	-0.161268	-0.186586	-1.21109	
16	0.98	3.81		0	0.066375	-0.050262	-0.092373	-0.194156	-0.081678	-0.230524	-0.405465	-1.53393	
18	-1.02	3.82		0	-0.151231	-0.21441	-0.192904	-0.27029	-0.082238	-0.354172	-0.675755	-1.902985	
20	-3.02	3.84		0	0.172843	0.164875	0.164875	0.098735	0.046091	-0.25672	-0.620388	-1.89085	
22	-5.02	3.85		0	0.093257	-0.030537	-0.102857	-0.119665	-0.401713	-0.685657	-1.061708	-2.492454	
24	-7.02	3.85		0	-0.207143	-0.399034	-0.448305	-0.370596	-0.809319	-1.236763	-1.785329	-2.963984	
26	-9.02	3.84		0	-0.320168	-0.472747	-0.60158	-0.564766	-1.013315	-1.372689	-1.68777	-2.681022	
28	-11.02	3.84		0	0.018349	-0.149532	-0.251314	-0.462624	-0.711839	-1.314835	-1.504077	-2.284236	
30	-13.02	3.83		0	-0.119665	-0.189869	-0.265376	-0.305382	-0.35775	-0.59989	-0.847298	-1.558145	
32	-15.02	3.82		0	0.021661	-0.029632	-0.044784	-0.247152	-0.140857	-0.47733	-0.671486	-1.336462	
34	-17.02	3.82		0	-0.013699	-0.107631	-0.115235	-0.138402	-0.115235	-0.289952	-0.415722	-0.770925	
36	-19.02	3.82		0	-0.668977	-1.126521	-1.426862	-1.563126	-1.52728	-1.703984	-1.810279	-2.139302	

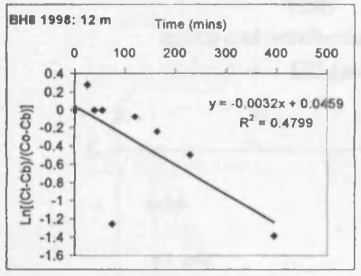

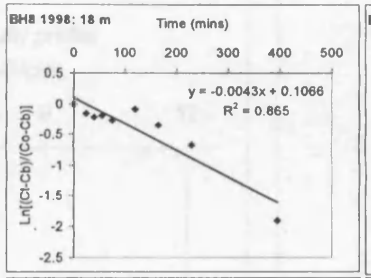

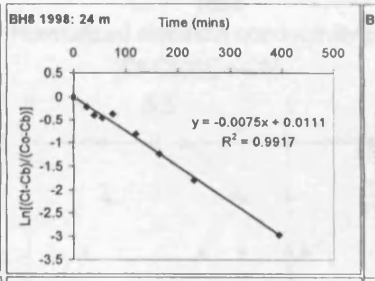

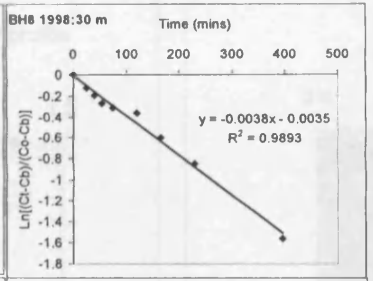

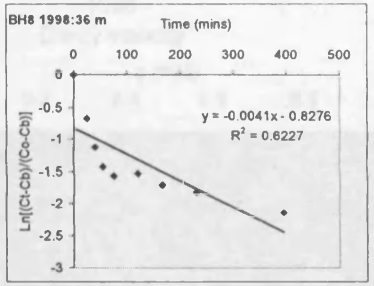

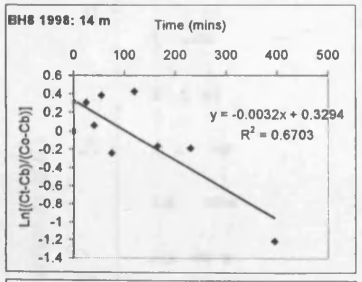

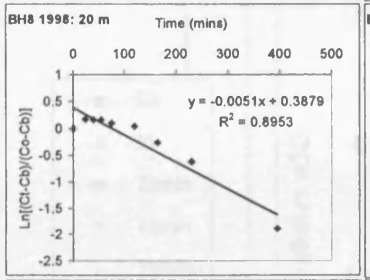

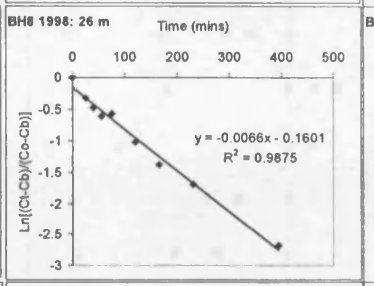

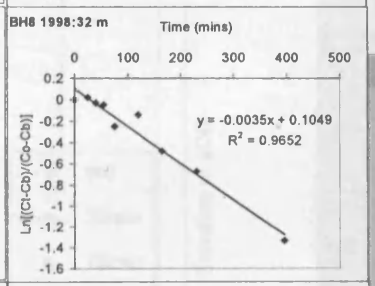

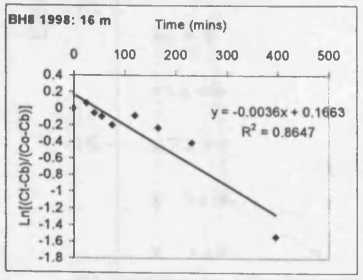

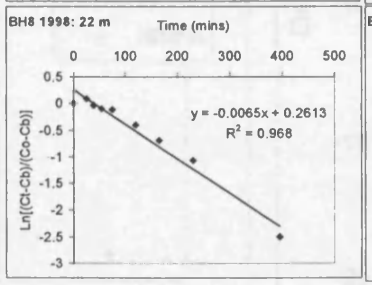

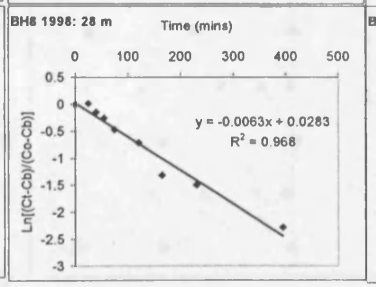

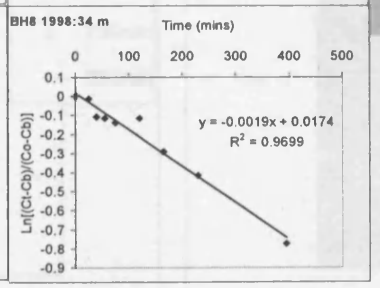

Depth	Elevation	q=0.785rA A	r=100mm q (min)	q (m/d)
12	4.98	0.0032	0.000251	0.36
14	2.98	0.0032	0.000251	0.36
16	0.98	0.0036	0.000283	0.41
18	-1.02	0.0043	0.000338	0.49
20	-3.02	0.0051	0.0004	0.58
22	-5.02	0.0065	0.00051	0.73
24	-7.02	0.0075	0.000589	0.85
26	-9.02	0.0066	0.000518	0.75
28	-11.02	0.0063	0.000495	0.71
30	-13.02	0.0038	0.000298	0.43
32	-15.02	0.0035	0.000275	0.40
34	-17.02	0.0019	0.000149	0.21
36	-19.02	0.0041	0.000322	0.46

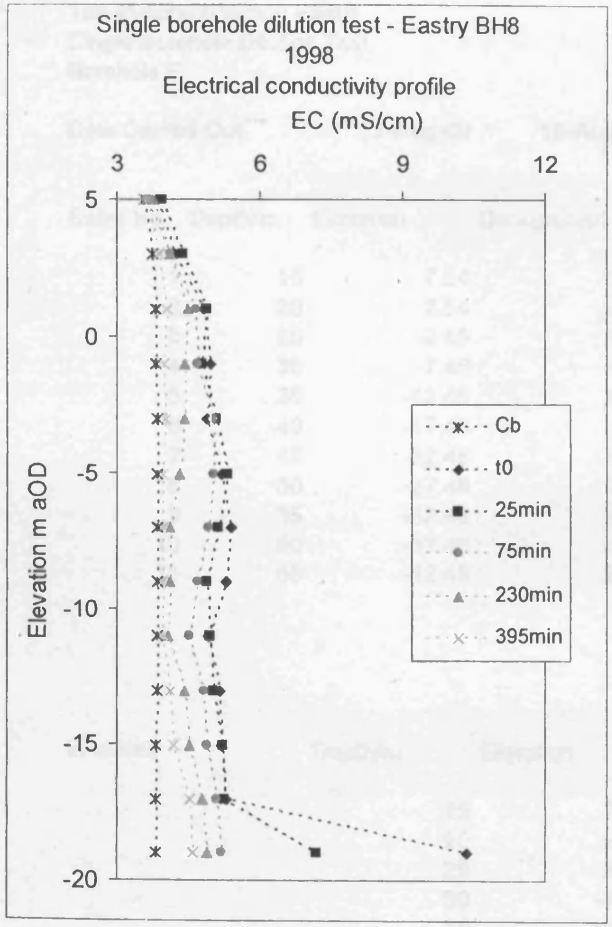
Single borehole dilution test - Eastry BH8
1998
Electrical conductivity profile
EC (mS/cm)
3
6
9
12
5
0
-5
-10
-15
-20
Elevation m aOD
Cb
t0
25min
75min
230min
395min

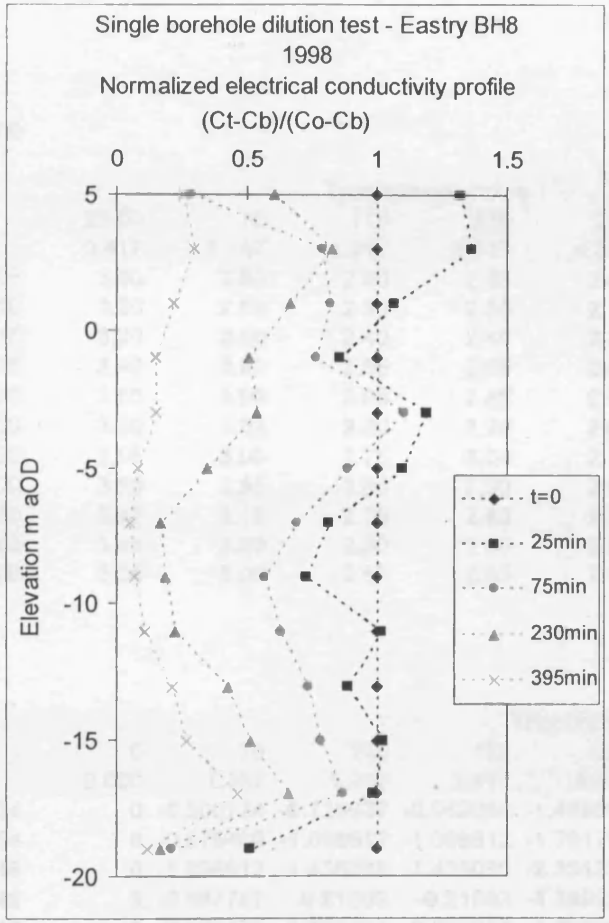
Single borehole dilution test - Eastry BH8
1998
Normalized electrical conductivity profile
(Ct-Cb)/(Co-Cb)
0
0.5
1
1.5
5
0
-5
-10
-15
-20
Elevation m aOD
t=0
25min
75min
230min
395min

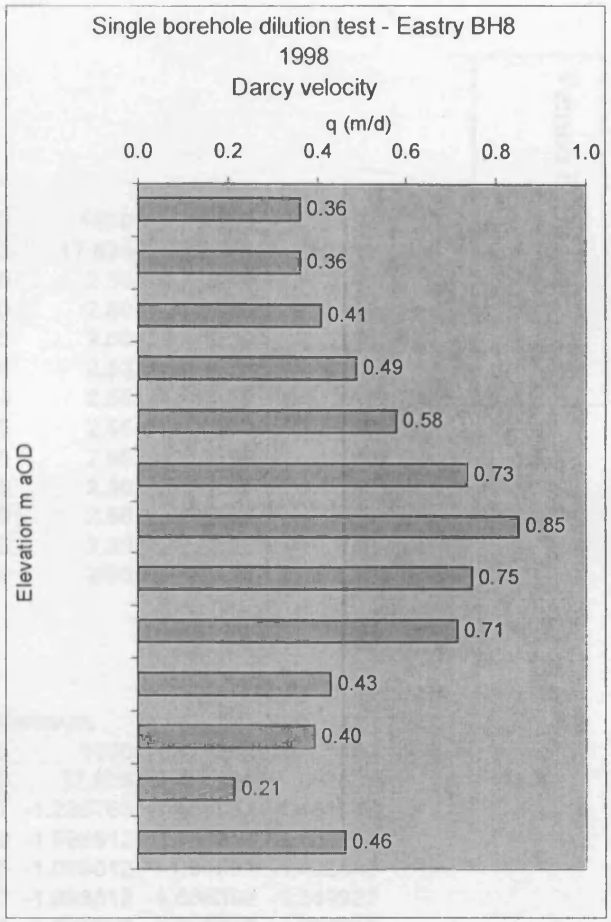
Single borehole dilution test - Eastry BH8
1998
Darcy velocity
q (m/d)
0.0
0.2
0.4
0.6
0.8
1.0
Elevation m aOD
0.36
0.36
0.41
0.49
0.58
0.73
0.85
0.75
0.71
0.43
0.40
0.21
0.46

Tilmanstone (Venson Farm)
Single Borehole Dilution Test
Borehole E

Venson Farm BHE 2000

Date Carried Out 17-Aug-00 18-Aug-00

				Time/minutes/hours							
Bailer No.	Depth/m	Elevation	Background	25.00	70	115	175	290	1070	1365	1490
				0.417	1.167	1.917	2.917	4.833	17.833	22.750	24.833
1	15	7.54	2.05	3.60	2.90	2.80	2.65	2.40	2.50	2.40	2.40
2	20	2.54	2.10	3.30	2.60	2.50	2.50	2.30	2.50	2.35	2.40
3	25	-2.46	2.15	3.20	2.50	2.40	2.40	2.25	2.50	2.30	2.40
4	30	-7.46	2.05	3.40	2.80	2.65	2.65	2.40	2.50	2.30	2.40
5	35	-12.46	2.00	3.50	3.00	2.85	2.85	2.50	2.55	2.50	2.50
6	40	-17.46	2.00	3.60	3.00	2.80	2.90	2.65	2.55	2.50	2.50
7	45	-22.46	2.00	3.55	3.00	2.75	3.00	2.70	2.65	2.50	2.45
8	50	-27.46	2.00	3.50	2.95	2.60	2.90	2.80	2.50	2.35	2.40
9	55	-32.46	2.00	3.45	3.10	2.75	2.80	2.70	2.50	2.25	2.30
10	60	-37.46	2.00	3.45	3.00	2.90	2.80	2.60	2.30	2.30	2.30
11	65	-42.46	2.00	3.55	3.00	2.85	2.85	2.60	2.30	2.30	2.30

			Time/minutes/hours							
ln values	Depth/m	Elevation	0	70	115	175	290	1070	1365	1490
			0.000	1.167	1.917	2.917	4.833	17.833	22.750	24.833
	15	7.54	0	-0.600774	-0.725937	-0.949081	-1.488077	-1.236763	-1.488077	-1.488077
	20	2.54	0	-0.875469	-1.098612	-1.098612	-1.791759	-1.098612	-1.568616	-1.386294
	25	-2.46	0	-1.098612	-1.435085	-1.435085	-2.351375	-1.098612	-1.94591	-1.435085
	30	-7.46	0	-0.587787	-0.81093	-0.81093	-1.349927	-1.098612	-1.686399	-1.349927
	35	-12.46	0	-0.405465	-0.567984	-0.567984	-1.098612	-1.003302	-1.098612	-1.098612
	40	-17.46	0	-0.470004	-0.693147	-0.575364	-0.900787	-1.067841	-1.163151	-1.163151
	45	-22.46	0	-0.438255	-0.725937	-0.438255	-0.79493	-0.869038	-1.131402	-1.236763
	50	-27.46	0	-0.456758	-0.916291	-0.510826	-0.628609	-1.098612	-1.455287	-1.321756
	55	-32.46	0	-0.276253	-0.659246	-0.594707	-0.728239	-1.064711	-1.757858	-1.575536
	60	-37.46	0	-0.371564	-0.476924	-0.594707	-0.882389	-1.575536	-1.575536	-1.575536
	65	-42.46	0	-0.438255	-0.600774	-0.600774	-0.949081	-1.642228	-1.642228	-1.642228

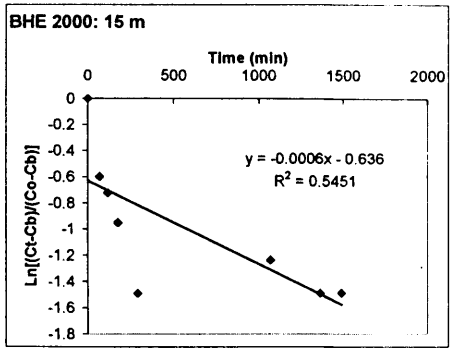

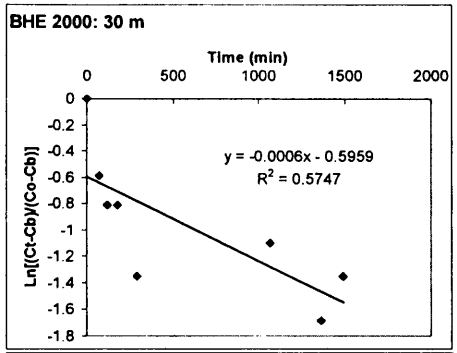

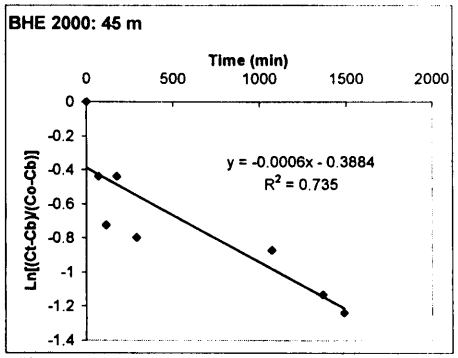

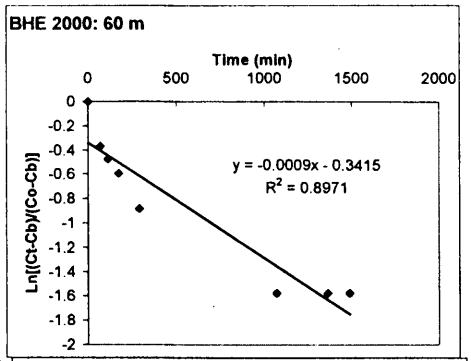

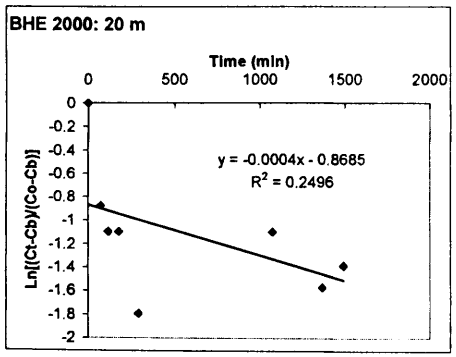

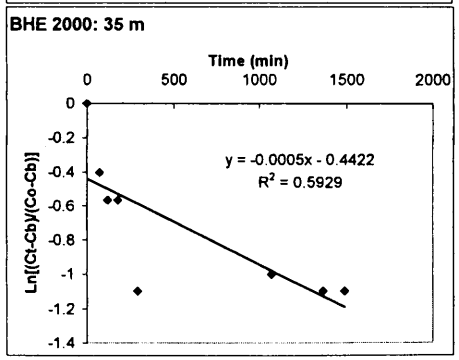

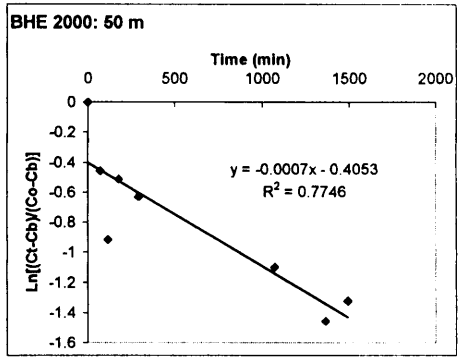

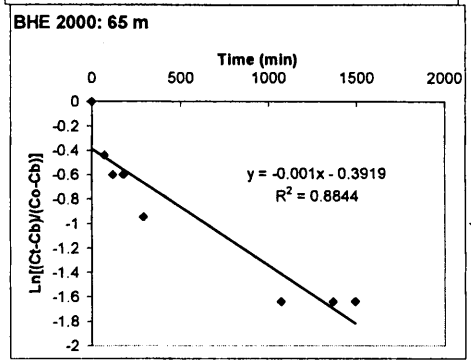

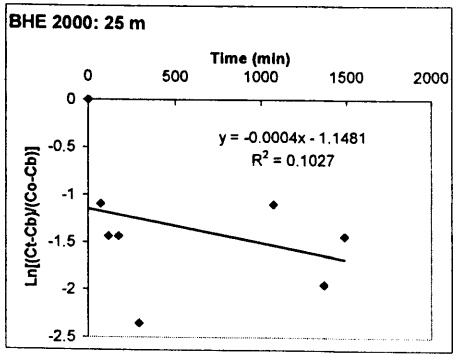

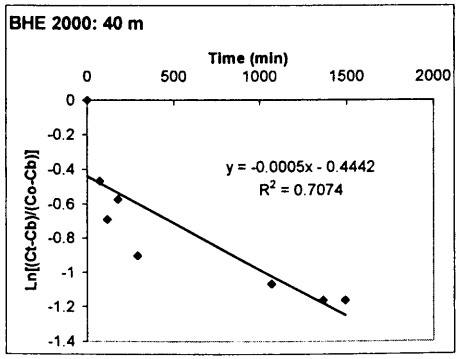

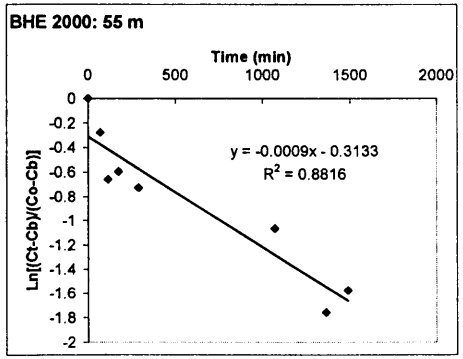

	All data			
Depth	Elevation	A	q (m/min)	q (m/d)
15	7.54	0.0006	4.71E-05	0.068
20	2.54	0.0004	3.14E-05	0.045
25	-2.46	0.0004	3.14E-05	0.045
30	-7.46	0.0006	4.71E-05	0.068
35	-12.46	0.0005	3.93E-05	0.057
40	-17.46	0.0005	3.93E-05	0.057
45	-22.46	0.0006	4.71E-05	0.068
50	-27.46	0.0007	5.5E-05	0.079
55	-32.46	0.0009	7.07E-05	0.102
60	-37.46	0.0009	7.07E-05	0.102
65	-42.46	0.001	7.85E-05	0.113

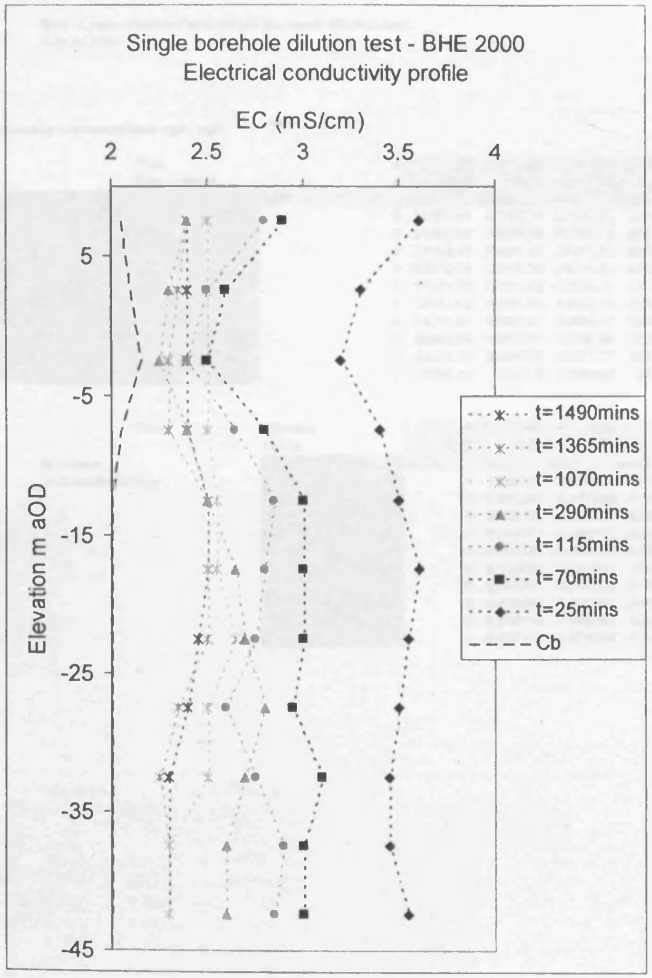
Single borehole dilution test - BHE 2000
Electrical conductivity profile
EC (mS/cm)
2
2.5
3
3.5
4
5
-5
-15
-25
-35
-45
Elevation m aOD
t=1490mins
t=1365mins
t=1070mins
t=290mins
t=115mins
t=70mins
t=25mins
Cb

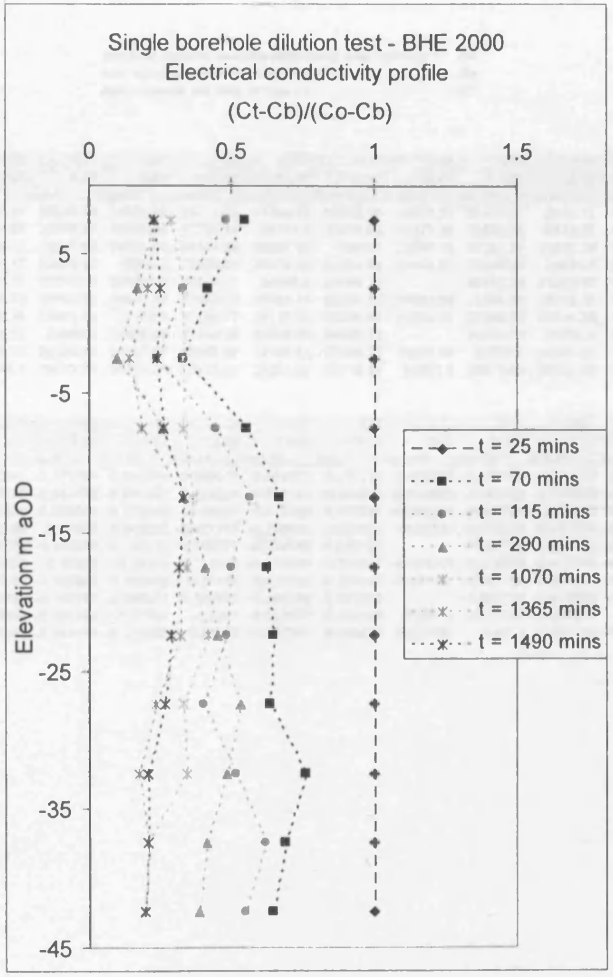
Single borehole dilution test - BHE 2000
Electrical conductivity profile
(Ct-Cb)/(Co-Cb)
0
0.5
1
1.5
5
-5
-15
-25
-35
-45
Elevation m aOD
t = 25 mins
t = 70 mins
t = 115 mins
t = 290 mins
t = 1070 mins
t = 1365 mins
t = 1490 mins

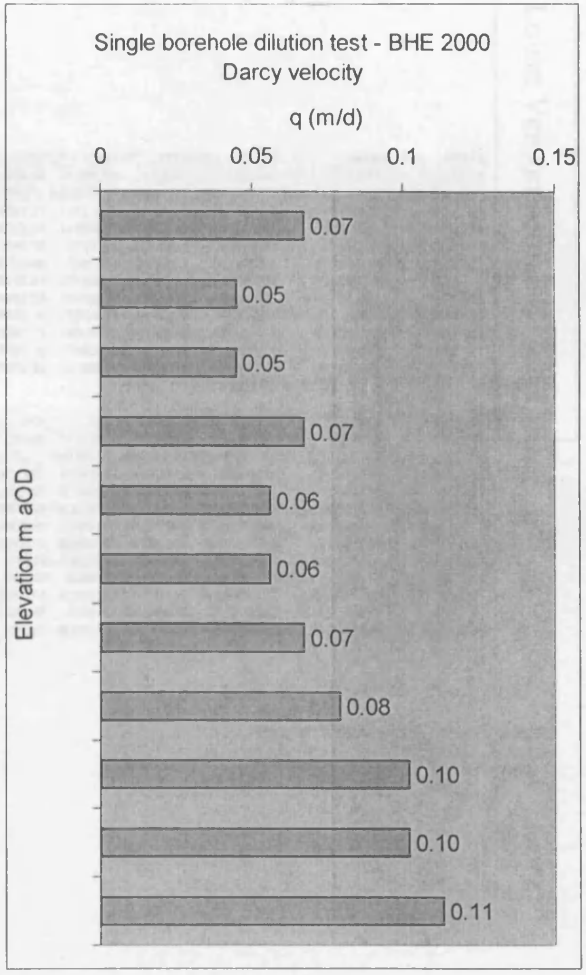
Single borehole dilution test - BHE 2000
Darcy velocity
q (m/d)
0
0.05
0.1
0.15
Elevation m aOD
0.07
0.05
0.05
0.07
0.06
0.06
0.07
0.08
0.10
0.10
0.11

BH3 - Lower Venson Farm Single Borehole dilution test
July 24 2001

use run2 samples as immediate concs after injection = Co
run1 samples are background concs = Cb
run3 onwards are conc at time t = Ct

Measured concentrations ppb: ug/L

		Time		0	15	45	105	225	530	590	725	845	970	1085	1205	1330	1455	1565	1775	10385	14510	40390
		time (hours)		0	0.25	0.75	1.75	3.75	8.83	9.83	12.08	14.08	16.17	18.08	20.08	22.17	24.25	26.08	29.58	173.08	241.83	673.17
Baller	Depth mbgl	Elevation m AOD	run1	run2	run3	run4	run5	run9	run11	run13	run15	run17	run19	run21	run23	run25	run27	run29	run30	run31	run32	
1	20	-1.57	0	33501.91	33707.75	30624.51	29940.57	28233.76	24528.92	22771.82	17588.23	20872.39	21873.27	22479.32	9654.72	14792.35	13721.88	10530	12343.353	6266.825	8612.552	
2	23	-4.57	0	31405.64	34548.76	31954.74	30275.88	30036.47	28635.03	27734.14	16372.5	21074.83	21377.16	23522.66	18175.57	18142.24	14982.28	5765.799	11932.848	5633.291	3800.754	
3	26	-7.57	0	29168.45	33390.57	29011.85	30589.78	26917.69	26027.44	24346.24	12947.18	10866.7	21983.79	22361.67	15872.18	13669.25	17275.5	5092.734	10479.59	9717.173	267.019	
4	29	-10.57	0	32012.98	33455.36	29530.54	31594.17	30050.27	19923.9	26693.61	25879.38	21389.79	24195.37	23264.43	20585.5	16750.85	15821.3	13733.57	13510.193	12764.618	7970.363	
5	32	-13.57	0	33374.78	33261.45	32576.34	31532.19	28776.07	29302.83	28174.82	24607.4	25168.77		23175.19	21253.07	15613.36	17783.19	16043.05	14267.464	12809.411		
6	35	-16.57	0	33683.65	34886.87	32629.32	32203.73	29760.82	29252.42	27994.12	28838.41	25250.99	24232.56	23044.32	20952.73	19691.63	18068.44	12243.12	13864.795	12766.021	10838.168	
7	38	-19.57	0	34219.88	34265.61	32664.17	32306.53	29961.16	29143.3	27706.77	25116.49	25258.94	24362.26	23360.56	20316.39	19048.15	17830.09	13017	14919.36	11528.892	10931.613	
8	41	-22.57	0	33442.03	34000.71	32250.98	32280.92	29964.9	24803.88	27460.23	26646.82	24502.72		23266.65	20790.4	18587.71	18139.43	16801.72	13753.807	12421.127	8608.225	
9	44	-25.57	0	32002.22	33859.55	29877.77	32658.56	29090.56	24427.87	22968.07	19165.81	22926.78	24279.58	22075.6	20420.25	17396.78	17893.83	16786.4	14636.1	13372.891		
10	46	-27.57	0	35995.23	33995.8	33396.42	32945.1	29641.99	28875.36	27513.21	25331.22	25115.21	24092.8	22375.93	20782.22	17639.92	18136.84	17029.78	13442.828	13099.571	7341.507	

	Time	Minutes		15	45	105	225	530	590	725	845	970	1085	1205	1330	1455	1565	1775	10385	14510	40390
		hours		0.25	0.75	1.75	3.75	8.83	9.83	12.08	14.08	16.17	18.08	20.08	22.17	24.25	26.08	29.58	173.08	241.83	673.17
ln values		Elevation m AOD	run2	run3	run4	run5	run9	run11	run13	run15	run17	run19	run21	run23	run25	run27	run29	run30	run31	run32	
JAB methodology		-1.57	0	0.006125	-0.089802	-0.112388	-0.171084	-0.311749	-0.386079	-0.644373	-0.473175	-0.426337	-0.399007	-1.244155	-0.817492	-0.892611	-1.157374	-0.99848469	-1.676332546	-1.358381718	
		-4.57	0	0.095384	0.017333	-0.036636	-0.044575	-0.092357	-0.124324	-0.651384	-0.398908	-0.384665	-0.289023	-0.546909	-0.548745	-0.740119	-1.695044	-0.96769262	-1.71829374	-2.11178809	
		-7.57	0	0.135186	-0.005383	0.047578	-0.080304	-0.113936	-0.18071	-0.812209	-0.987384	-0.282782	-0.265739	-0.60852	-0.757939	-0.523798	-1.745273	-1.02365802	-1.099192845	-4.693523039	
		-10.57	0	0.044071	-0.080717	-0.013169	-0.06327	-0.474222	-0.181717	-0.212695	-0.403228	-0.27998	-0.319216	-0.441554	-0.647693	-0.704784	-0.846298	-0.86269698	-0.91946429	-1.390411377	
		-13.57	0	-0.003401	-0.024214	-0.056792	-0.148256	-0.130117	-0.169372	-0.304753	-0.282197		-0.364718	-0.451299	-0.759674	-0.629547	-0.732525	-0.84981882	-0.95762039		
		-16.57	0	0.035098	-0.031801	-0.04493	-0.12382	-0.14105	-0.185018	-0.155305	-0.288147	-0.329315	-0.379593	-0.474744	-0.536819	-0.622846	-1.012048	-0.88765975	-0.970225614	-1.133938667	
		-19.57	0	0.001335	-0.046528	-0.057537	-0.132905	-0.160582	-0.21113	-0.309282	-0.303627	-0.339771	-0.381758	-0.521379	-0.585837	-0.65192	-0.96655	-0.83014715	-1.087950617	-1.141147983	
		-22.57	0	0.016568	-0.036265	-0.035337	-0.109787	-0.298813	-0.197075	-0.227143	-0.311029		-0.362793	-0.475322	-0.587313	-0.611726	-0.688332	-0.88849777	-0.990416619	-1.357095291	
		-25.57	0	0.056416	-0.068691	0.020302	-0.095392	-0.27008	-0.3317	-0.512677	-0.333499	-0.27617	-0.371332	-0.449278	-0.60952	-0.58135	-0.645236	-0.7823142	-0.872575677		
		-27.57	0	-0.057149	-0.074938	-0.088544	-0.194194	-0.220398	-0.26872	-0.351349	-0.359913	-0.401473	-0.4754	-0.549289	-0.713222	-0.685331	-0.748423	-0.9849407	-1.010806948	-1.589842295	

All data - runs 2 - 32 Analysis same as S. Hazell 1998, JAB methodology

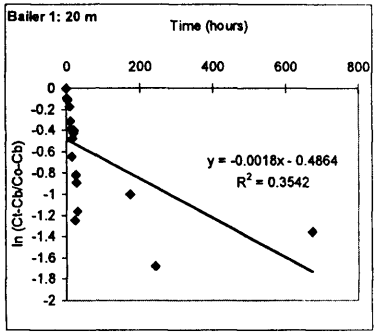

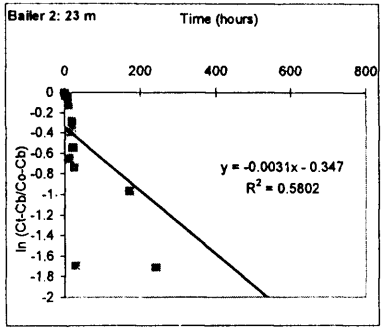

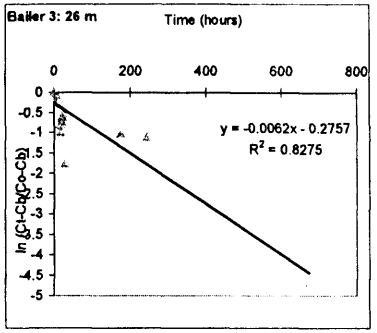

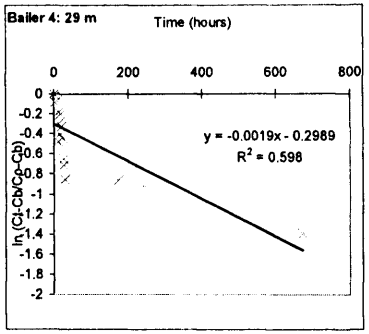

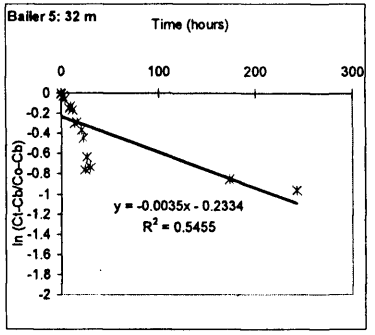

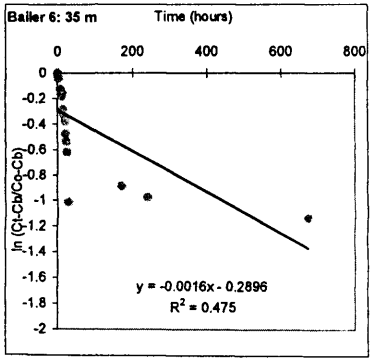

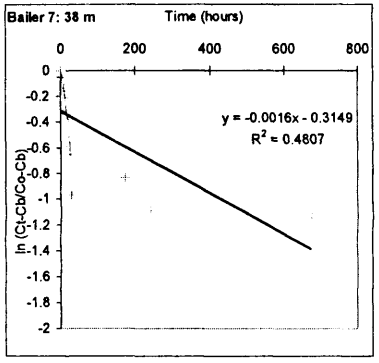

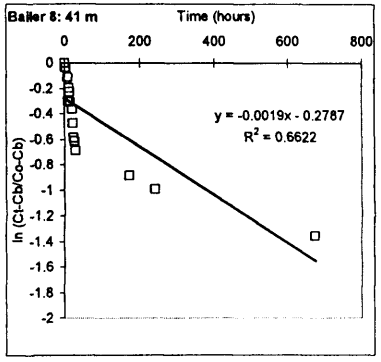

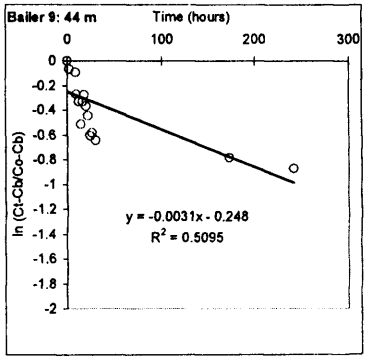

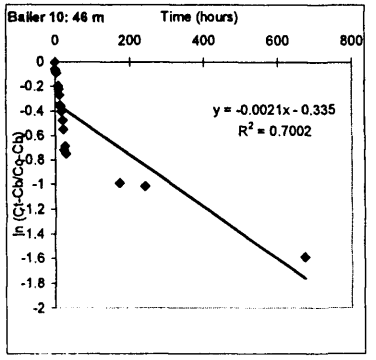

q = 0.785RA **R = 100mm**

Bailer	A	q (m/d)	Depth	Elevation m AOD
1	0.0018	0.003391	20	-1.57
2	0.0031	0.00584	23	-4.57
3	0.0062	0.011681	26	-7.57
4	0.0019	0.00358	29	-10.57
5	0.0035	0.006594	32	-13.57
6	0.0016	0.003014	35	-16.57
7	0.0016	0.003014	38	-19.57
8	0.0019	0.00358	41	-22.57
9	0.0031	0.00584	44	-25.57
10	0.0021	0.003956	46	-27.57

Early data - runs 2 - 29 Analysis same as S. Hazell 1999, JAB methodology

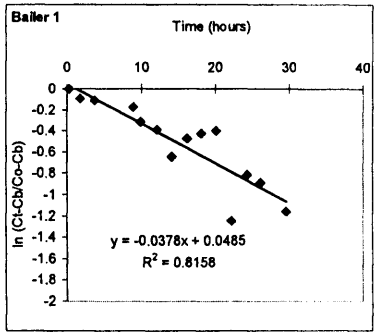

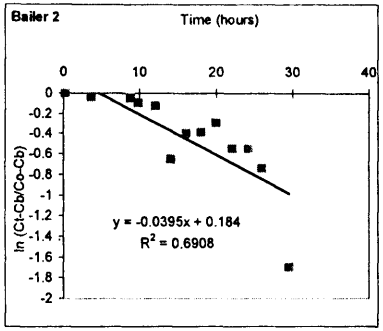

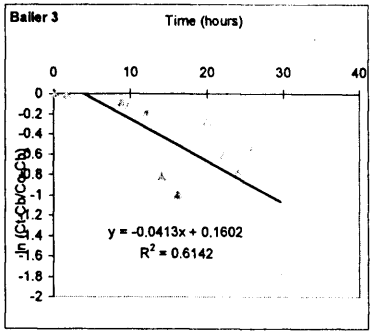

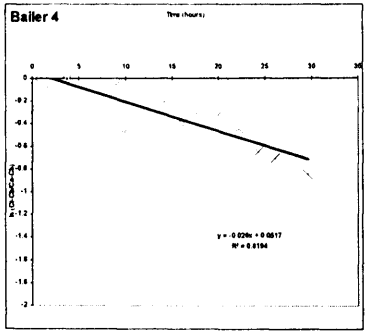

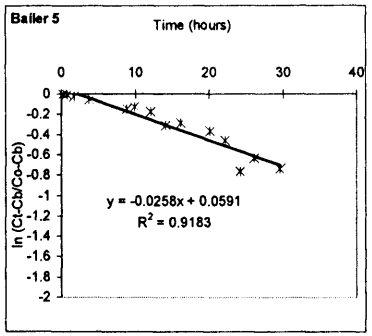

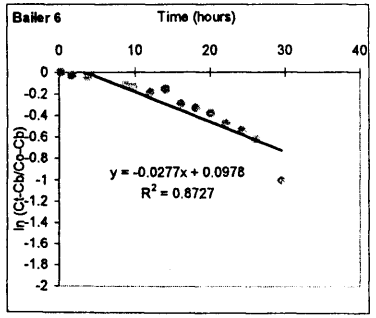

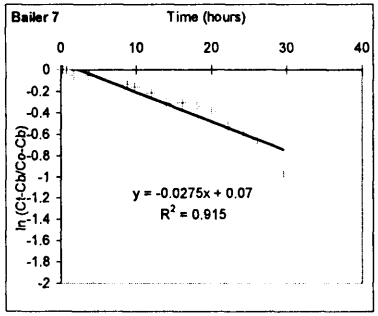

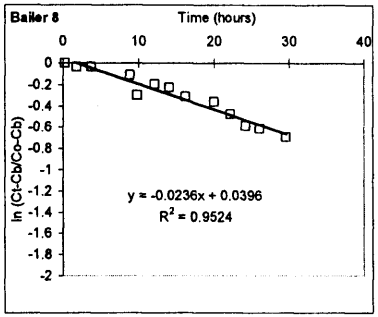

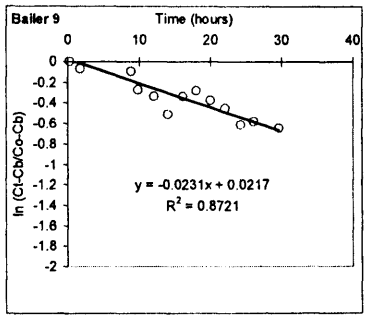

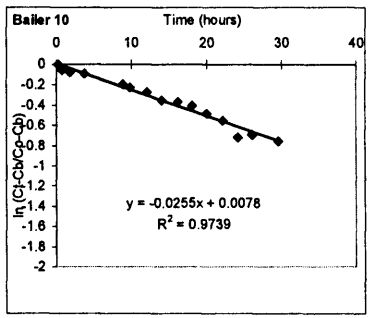

q = 0.785RA **R = 100mm**

Bailer	A	q (m/d)	Depth	Elevation m AOD
1	0.0378	0.07	20	**-1.57**
2	0.0395	0.07	23	**-4.57**
3	0.0413	0.08	26	**-7.57**
4	0.026	0.05	29	**-10.57**
5	0.0258	0.05	32	**-13.57**
6	0.0277	0.05	35	**-16.57**
7	0.0275	0.05	38	**-19.57**
8	0.0236	0.04	41	**-22.57**
9	0.0231	0.04	44	**-25.57**
10	0.0255	0.05	46	**-27.57**

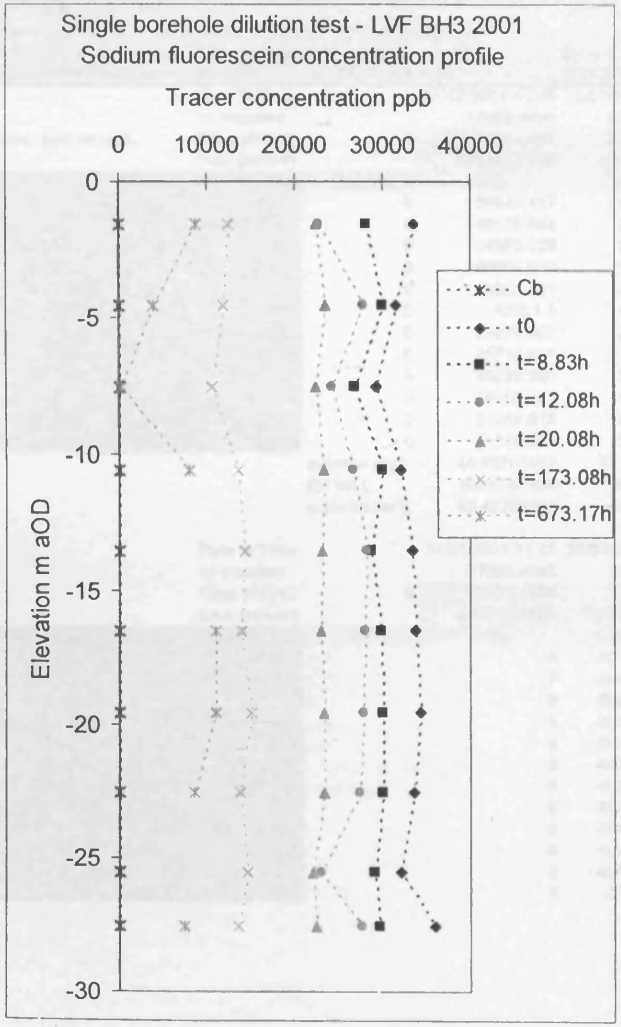
Single borehole dilution test - LVF BH3 2001
Sodium fluorescein concentration profile
Tracer concentration ppb
0
10000
20000
30000
40000
Elevation m aOD
0
-5
-10
-15
-20
-25
-30
Cb
t0
t=8.83h
t=12.08h
t=20.08h
t=173.08h
t=673.17h

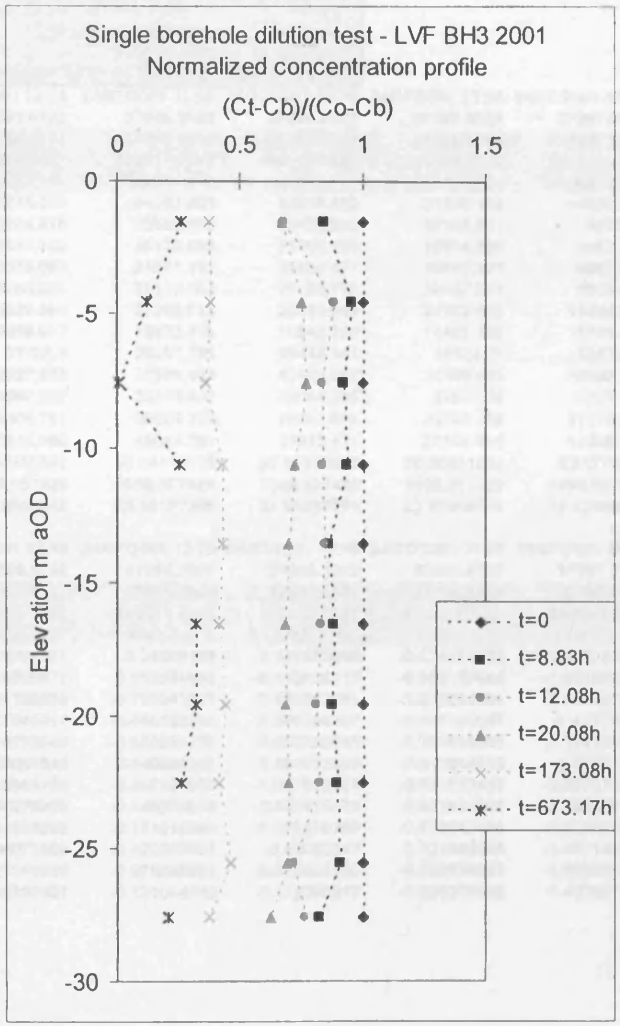
Single borehole dilution test - LVF BH3 2001
Normalized concentration profile
(Ct-Cb)/(Co-Cb)
0
0.5
1
1.5
Elevation m aOD
0
-5
-10
-15
-20
-25
-30
t=0
t=8.83h
t=12.08h
t=20.08h
t=173.08h
t=673.17h

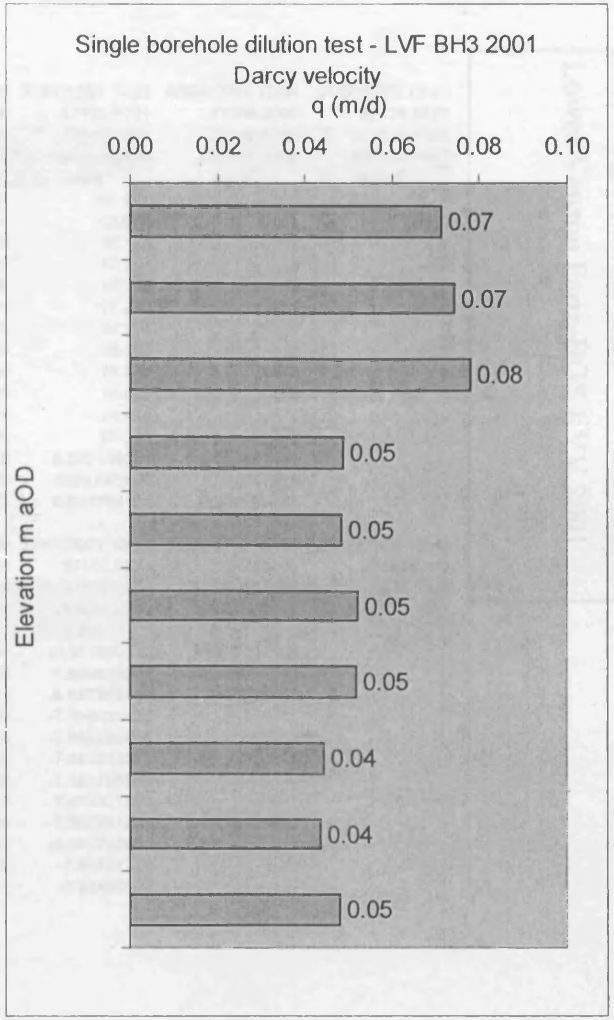
Single borehole dilution test - LVF BH3 2001
Darcy velocity
q (m/d)
0.00
0.02
0.04
0.06
0.08
0.10
Elevation m aOD
0.07
0.07
0.08
0.05
0.05
0.05
0.05
0.04
0.04
0.05

24-Jul-01 BGS LVV					24/07/2001 11:30 start time - t0								
injection of 4 litres of tracer containing 195g Rhodamine WT =					40.95 g active ingredient								
hose withdrawal starts at 10:50, completed at 11:14					BH vol L = 1099.557429								
original attempted concentration = 37.24225668 mg/L					BUT SOME GOT LEFT IN THE CASED SECTION								
		Date & Time as number			24/07/2001 11:45	24/07/2001 12:19	24/07/2001 13:25	24/07/2001 15:19	24/07/2001 21:20	25/07/2001 15:00	31/07/2001 16:15	03/08/2001 12:00	21/08/2001 12:40
Conc: ppb or ug/L		Time (days)		0	37096.4896	37096.5132	37096.5590	37096.6382	37096.8889	37097.6250	37103.6771	37106.5000	37124.5278
		time (hours)			890315.7500	890316.3167	890317.4167	890319.3167	890325.3333	890343.0000	890488.2500	890556.0000	890988.6667
Bailer	Depth mbgl	Elevation m	run1		run2	run3	run4	run5	run6	run7	run8	run9	run10
1	13.73	4.434		0	56541.417	50218.287	44307.403	44018.866	31842.134	14392.804	81.511	4.358	0
2	16.73	1.434		0	46009.663	29684.516	23838.868	30426.533	17109.841	8475.34	68.506	2.683	0
3	19.73	-1.566		0	34988.058	21611.102	16473.695	21865.793	10514.439	3927.329	37.148	0.2	0
4	22.73	-4.566		0	40391.022	39313.093	24841.135	31464.477	16667.597	9667.895	17.304	0	0
5	25.73	-7.566		0	43801.103	38993.051	25117.787	25188.722	20462.841	9258.639	15.289	0	0
6	28.73	-10.566		0	43981.8	43628.398	28298.012	26815.044	22982.455	11424.504	17.257	0.351	0
7	31.73	-13.566		0	29979.502	23488.917	18972.413	10842.798	14497.793	3791.806	24.216	0	0
8	34.73	-16.566		0	45712.671	31756.5	29257.793	29413.841	19120.26	5247.624	25.683	0	0
9	37.73	-19.566		0	49239.395	32627.472	42329.463	41423.892	21456.907	10696.248	25.572	0.416	0
10	40.73	-22.566		0	46159.781	41597.292	30318.902	29144.185	22077.95	9727.525	14.837	0	0
11	43.73	-25.566		0	51264.015	45406.181	38889.729	26681.004	23763.484	11374.974	24.446	0	0
12	45.73	-27.566		0	51355.869	50159.098	45048.261	43210.478	26800.495	12568.225	33.511	0	0
			average mg/L		44.95202467	37.37365892	30.64112175	30.04130275	20.60801633	9.21274275	0.032106667	0.000667333	
			BH vol L		1099.557429	1099.557429	1099.557429	1099.557429	1099.557429	1099.557429	1099.557429	1099.557429	
			mass tracer g		49.42733266	41.0944843	33.69167305	33.03213761	22.65969745	10.12993973	0.035303124	0.000733771	

		Date & Time as number			24/07/2001 11:45	24/07/2001 12:19	24/07/2001 13:25	24/07/2001 15:19	24/07/2001 21:20	25/07/2001 15:00	31/07/2001 16:15	03/08/2001 12:00	21/08/2001 12:40
		Time (days)		0	37096.4896	37096.5132	37096.5590	37096.6382	37096.8889	37097.6250	37103.6771	37106.5000	37124.5278
		time (hours)			890315.7500	890316.3167	890317.4167	890319.3167	890325.3333	890343.0000	890488.2500	890556.0000	890988.6667
Bailer	Depth mbgl	Elevation m	run1		run2	run3	run4	run5	run6	run7	run8	run9	run10
1	13.73	4.434			0	-0.118594171	-0.24382164	-0.250355099	-0.574183033	-1.368245054	-6.541990712	-9.470715456	
2	16.73	1.434			0	-0.438225877	-0.657534082	-0.413536416	-0.989197645	-1.691690669	-6.509685386	-9.749671147	
3	19.73	-1.566			0	-0.481799639	-0.753241937	-0.470083351	-1.202257348	-2.187047252	-6.847852148	-12.07219999	
4	22.73	-4.566			0	-0.027049914	-0.486106584	-0.249748337	-0.885140997	-1.42979693	-7.755425123		
5	25.73	-7.566			0	-0.116275549	-0.556082759	-0.553262645	-0.761048393	-1.554101938	-7.960280663		
6	28.73	-10.566			0	-0.008067643	-0.440984357	-0.494812839	-0.649044813	-1.34801539	-7.843313333	-11.73850025	
7	31.73	-13.566			0	-0.243985189	-0.457527905	-1.017012801	-0.726517451	-2.067671459	-7.121255589		
8	34.73	-16.566			0	-0.364278095	-0.446229559	-0.440910178	-0.871627018	-2.164600122	-7.484301509		
9	37.73	-19.566			0	-0.411539382	-0.151210646	-0.172836199	-0.830647416	-1.526800989	-7.562951291	-11.68151931	
10	40.73	-22.566			0	-0.104073809	-0.420337531	-0.45985347	-0.737529505	-1.557149382	-8.042740096		
11	43.73	-25.566			0	-0.121340803	-0.276258864	-0.653037193	-0.768838927	-1.505573365	-7.64827772		
12	45.73	-27.566			0	-0.02357931	-0.131044842	-0.172696212	-0.650358866	-1.407607421	-7.33466076		

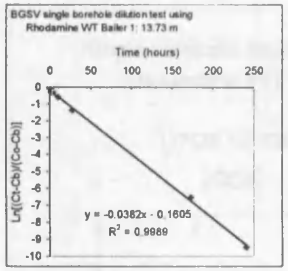

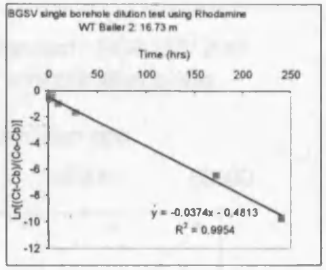

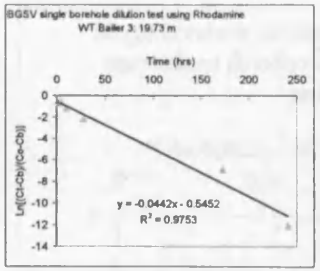

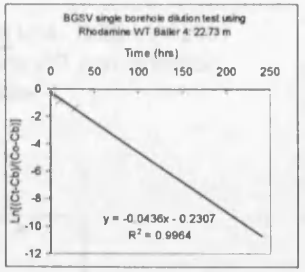

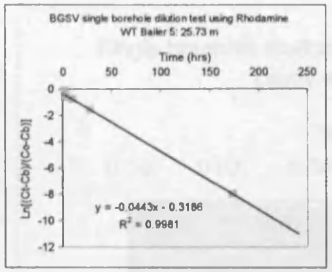

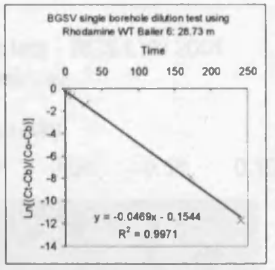

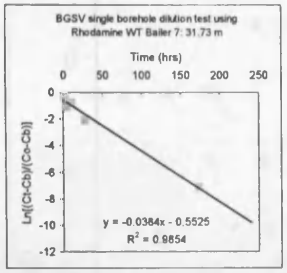

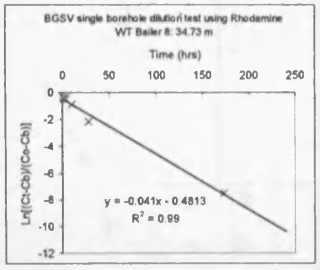

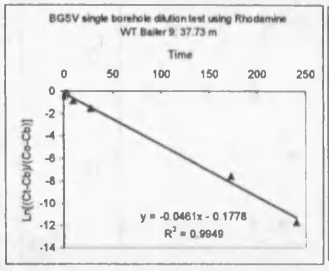

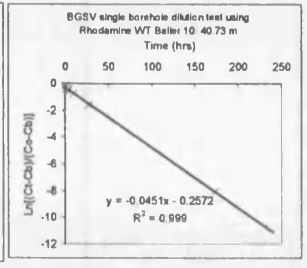

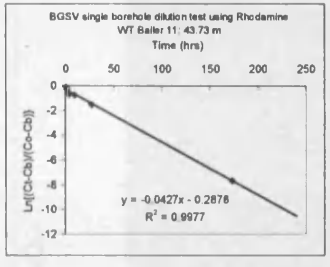

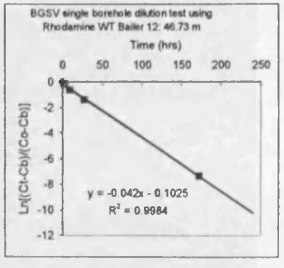

q=0.785 r A q= seepage velocity

Bailer	A	q (m/d)	Depth mbgl	Elevation m AOD
1	0.0382	0.072	13.73	4.434
2	0.0374	0.070	16.73	1.434
3	0.0442	0.083	19.73	-1.566
4	0.0436	0.082	22.73	-4.566
5	0.0443	0.083	25.73	-7.566
6	0.0469	0.088	28.73	-10.566
7	0.0384	0.072	31.73	-13.566
8	0.041	0.077	34.73	-16.566
9	0.0461	0.087	37.73	-19.566
10	0.0451	0.085	40.73	-22.566
11	0.04275	0.081	43.73	-25.566
12	0.042	0.079	46.73	-27.566

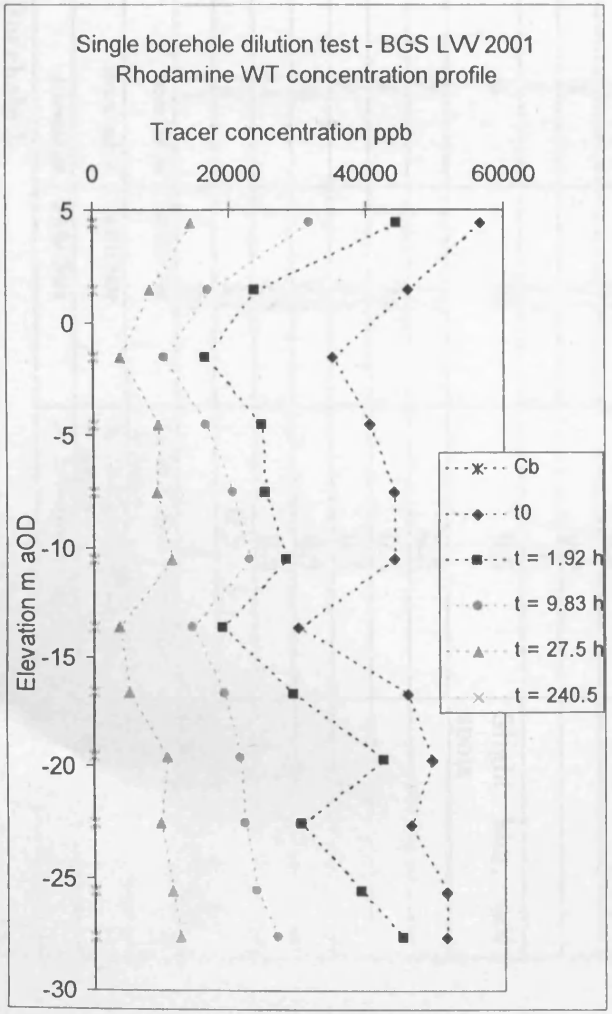
Single borehole dilution test - BGS LVV 2001
Rhodamine WT concentration profile
Tracer concentration ppb
0
20000
40000
60000
5
0
-5
-10
-15
-20
-25
-30
Elevation m aOD
Cb
t0
t = 1.92 h
t = 9.83 h
t = 27.5 h
t = 240.5

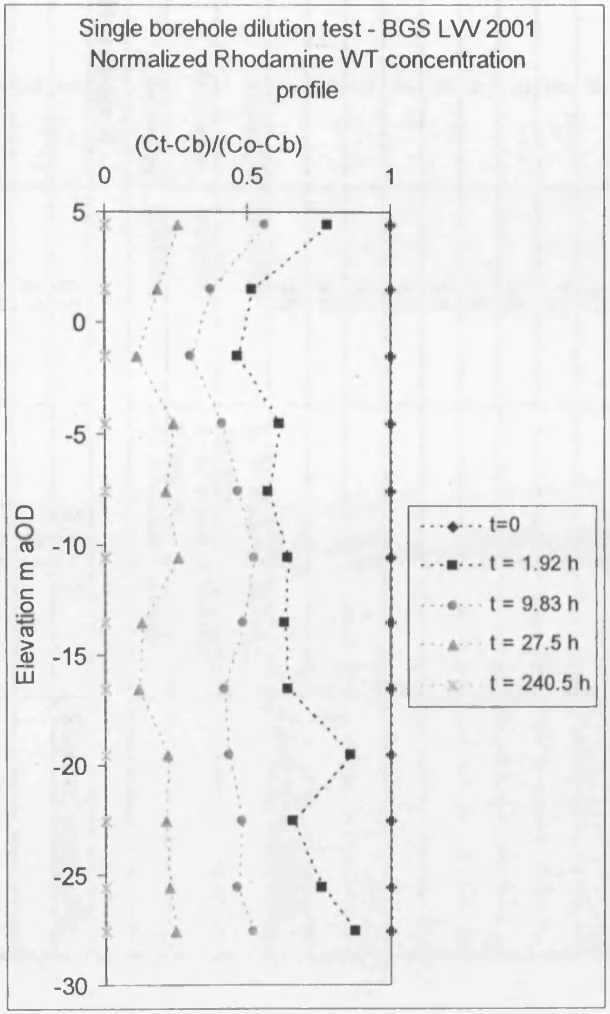
Single borehole dilution test - BGS LVV 2001
Normalized Rhodamine WT concentration profile
(Ct-Cb)/(Co-Cb)
0
0.5
1
5
0
-5
-10
-15
-20
-25
-30
Elevation m aOD
t=0
t = 1.92 h
t = 9.83 h
t = 27.5 h
t = 240.5 h

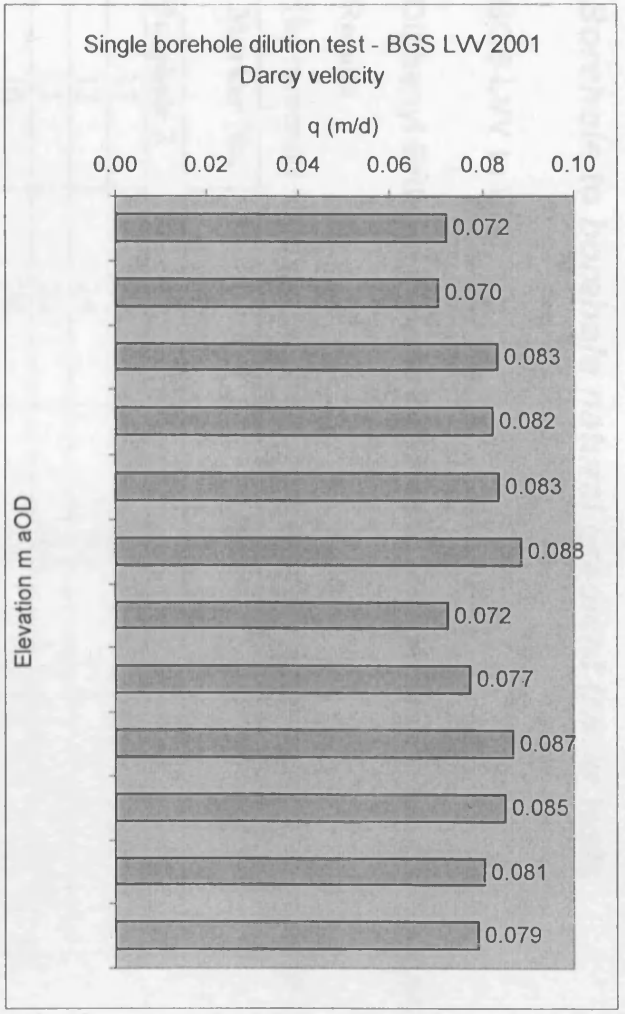
Single borehole dilution test - BGS LVV 2001
Darcy velocity
q (m/d)
0.00
0.02
0.04
0.06
0.08
0.10
Elevation m aOD
0.072
0.070
0.083
0.082
0.083
0.088
0.072
0.077
0.087
0.085
0.081
0.079

Borehole to borehole natural gradient tracer tests

BGS LVV to BH3

Diphenyl Brilliant Flavine 7GFF 1999 – 2000 natural gradient tracer test

Results

The responses observed for all the detectors collected from BH2, 3 & 4 are given below.

Marker No.	Depth mbgl (approx.)	Score	Comments
Borehole 3			
13	22	0.5	Start of openhole
12	24	0.5	
11	26	0.5	
10	28	2	
9	30	2.5	
8	32	2.5	
7	34	2.5	
6	36	2.5	
5	38	3	
4	40	2	
3	42	2.5	
2	44	3	
1	46	2.5	Base of borehole
Installed on	*20/12/1999*	*By: SJ Watson; T Atkinson; M Betson*	
Retrieved on	*14/01/2000*	*By: SJ Watson; N Robinson; W Burgess*	
Assessed on	*20/01/2000*	*By: SJ Watson; T Atkinson*	
Borehole 4			
1	65	0.5 – 1	Start of openhole
2	67	0.5	
3	69	0.5	
4	71	0.5	
5	73	0	
6	75	0.5	Slight blur, not spots
7	77	0.5	
8	79	0.5	
9	81	0.5	
10	83	0.5	
11	85	0.5	
12	87	0.5 – 1	
13	89	0	Base of borehole
Installed on	*20/12/1999*	*By: SJ Watson; T Atkinson; M Betson*	
Retrieved on	*14/01/2000*	*By: SJ Watson; N Robinson; W Burgess*	
Assessed on	*20/01/2000*	*By: SJ Watson; T Atkinson*	
Borehole 2			

Marker No.	Depth mbgl (approx.)	Score	Comments
26	102	0.5	Start of openhole
25	104	0	
24	106	0.5	Many tiny spots
23	108	0	
22	110	0.5	
21	112	0	
20	114	0.5	
19	116	0.5	
18	118	0.5	
17	120	0.5	
16	122	0	
15	124	0	)Visible yellow on
14	126	0	)detectors, seems
13	128	0	)to be staining,)not dye
12	130	0	
11	132	1	
10	134	1	
9	136	0	
8	138	0	
7	140	0	
6	142	0	
5	144	0	
4	146	0.5	Negative
3	148	0	
2	150	0	
1	152	Missing detector	Base of borehole
Installed on	*20/12/1999*	*By: SJ Watson; T Atkinson; M Betson*	
Retrieved on	*14/01/2000*	*By: SJ Watson; N Robinson; W Burgess*	
Assessed on	*20/01/2000*	*By: SJ Watson; T Atkinson*	

Hydrochemical results 1998

Name	Grid Ref.	Datum (m a OD)	SWL (m b dat)	SWL (m a OD)	Temp (^{0}C)	pH	DO_2 (%)	Cond. (mS/cm)	HCO_3^- mg/l	Cl^- mg/l	Br^- mg/l	NO_3^- mg/l	PO_4 mg/l	SO_4^{2-} mg/l	Ca^{2+} mg/l	Na^+ mg/l	K^+ mg/l
Venson BHE	3000 5267	28.37	11.25	17.12	13	7.03	77	3300	242.78	798.97	3.129	32.040	0.000	170.729	154.90	514.20	8.80
L.Venson Fm BH 2	3026 5311	18.04	9	9.04	13	7.03	62	3050	244.00	783.33	3.164	21.408	0.000	141.643	161.10	527.30	8.00
L.Venson Fm BH 3	3027 5308	18.47	8.26	10.21	13	7.33	37	3100	224.48	775.77	3.211	21.431	0.000	140.982	155.80	512.90	8.70
L.Venson Fm BH 4	3025 5308	18.17	8.92	9.25	12.9	7.02	69	3500	253.76	947.52	3.541	24.735	0.000	169.987	158.00	600.00	10.40
Th'ton Fm BH 1	2927 5203	31.52	15.55	15.97	15.5	7.18	65	3350	278.16	812.86	3.168	26.289	0.000	188.594	142.40	540.10	10.20
Th'ton Fm BH 5 @ 16m	2926 5205									1005.39	3.953	24.654	0.000	218.071	143.20	652.30	12.20
Th'ton Fm BH 5 @ 25m	2926 5205									988.76	3.854	24.020	0.000	213.967	143.30	659.90	12.00
Th'ton Fm BH 5 @ 37m	2926 5205									1093.19	4.028	19.359	0.779	206.386	150.30	692.20	11.90
Th'ton Fm BH 5	2926 5205	31.57	15.43	16.14	13.7	7.16	65	3900	278.16	997.67	3.745	24.040	0.000	212.117	144.20	645.80	12.30
Th'ton Fm BH 6 @ 21m	2925 5206	31.57	15.015	16.555						52.69	0.658	0.000	0.000	6.138	48.40	20.90	44.50
Eastry BHC	3061 5358	15.66	8.63	7.03	12.6	7.05	85.5	2800	373.32	776.51	3.283	31.703	0.000	157.911	154.30	525.70	9.50
Rowling Cottages	2770 5443	21.23	10.25	10.98	12.9	7.11	87.5	685	248.88	71.08	0.000	33.000	0.000	34.080	129.40	40.70	3.50
Shingleton Farm Cottages	2850 5230	????	16.63		13.5	7.23		1750	387.96	308.73	1.338	28.616	0.000	109.076	132.60	222.90	4.20
Pixwell Farm Cottages	3460 5100	22.54	17.69	4.85	13.2	7.26	78	1050	353.80	150.23	0.594	34.400	0.000	49.431	127.70	101.80	2.90
Statenborough (pumping well)	3140 5580	13.74			13	6.99	85	1300	331.84	154.95	0.689	56.009	0.000	94.115	190.40	94.10	6.20
Delf Nurseries (pumping well)	3315 5724	2.94			12.7	6.89		1350	358.68	85.94	3.422	64.535	0.000	177.555	168.60	93.90	5.00

Name -	Mg^{2+}	Fe^{2+}	Al^{3+}	B^{3+}	Ba^{2+}	Cd^{2+}	Co^{2+}	Cr^{2+}	Cu^{+}	Li^{+}	Mn^{2+}	Ni^{2+}	Pb^{2+}	S	Sr^{2+}	Ti	V	Y	Zn^{2+}
	mg/l	mg/l	mg/l	mg/l	mg/l	mg/l	mg/l	mg/l	mg/l	mg/l	mg/l	mg/l	mg/l	mg/l	mg/l	mg/l	mg/l	mg/l	mg/l
Venson BHE	21.850	-0.030	0.030	0.900	0.080	0.020	0.040	0.010	0.000	0.240	0.000	0.070	-0.080	58.210	1.960	0.000	0.010	0.000	0.040
L.Venson Fm BH 2	16.460	-0.020	0.030	0.990	0.110	0.010	0.040	0.010	0.000	0.220	0.010	0.060	-0.130	49.220	1.320	0.000	0.000	0.000	0.040
L.Venson Fm BH 3	16.710	-0.010	0.030	0.970	0.100	0.020	0.040	0.010	0.000	0.220	0.010	0.080	-0.080	48.920	1.350	0.000	0.000	0.000	0.070
L.Venson Fm BH 4	21.160	-0.030	0.020	1.080	0.090	0.010	0.030	0.010	0.000	0.260	0.000	0.060	-0.080	59.030	1.720	0.000	0.000	0.000	0.040
Th'ton Fm BH 1	23.420	-0.030	0.020	0.920	0.080	0.010	0.030	0.010	0.000	0.280	0.000	0.040	-0.040	65.850	2.450	0.000	0.000	0.000	0.040
Th'ton Fm BH 5 @ 16m	27.660	-0.020	0.020	1.070	0.080	0.020	0.030	0.010	0.000	0.330	0.000	0.060	-0.080	75.280	3.160	0.000	0.000	0.000	0.050
Th'ton Fm BH 5 @ 25m	27.800	-0.030	0.020	1.090	0.080	0.010	0.030	0.010	0.000	0.340	0.000	0.050	-0.050	75.380	3.150	0.000	0.000	0.000	0.040
Th'ton Fm BH 5 @ 37m	24.940	0.160	0.030	1.190	0.090	0.020	0.030	0.010	0.000	0.330	0.020	0.040	-0.080	71.290	2.670	0.000	0.000	0.000	0.030
Th'ton Fm BH 5	27.530	-0.030	0.030	1.060	0.080	0.010	0.030	0.010	0.000	0.330	0.010	0.060	-0.080	74.470	3.130	0.000	0.010	0.000	0.050
Th'ton Fm BH 6 @ 21m	4.030	0.300	0.030	0.120	0.020	0.010	0.010	0.000	0.000	0.020	0.400	0.020	0.000	2.360	0.410	0.000	0.000	0.000	0.030
Eastry BHC	20.300	0.100	0.020	0.940	0.080	0.020	0.030	0.010	0.000	0.230	0.010	0.060	-0.100	55.780	1.770	0.000	0.000	0.000	0.040
Rowling Cottages	3.840	-0.030	0.030	0.060	0.050	0.010	0.030	0.010	0.010	0.030	0.000	0.040	-0.070	12.940	0.320	0.000	0.000	0.000	0.050
Shingleton Farm Cottages	13.950	-0.030	0.020	0.420	0.050	0.010	0.030	0.000	0.000	0.100	0.000	0.050	-0.070	39.880	1.120	0.000	0.000	0.000	0.030
Pixwell Farm Cottages	5.980	-0.030	0.030	0.190	0.040	0.010	0.030	0.010	0.000	0.060	0.000	0.050	-0.060	17.980	0.450	0.000	0.000	0.000	0.040
Statenborough (pumping well)	9.880	0.010	0.060	0.250	0.100	0.020	0.040	0.010	0.000	0.060	0.010	0.060	-0.110	33.710	0.640	0.000	0.000	0.000	0.090
Delf Nurseries (pumping well)	17.550	0.090	0.030	0.120	0.050	0.020	0.050	0.010	0.000	0.050	0.140	0.080	-0.080	60.200	0.870	0.000	0.010	0.000	0.040

	Anions																
	HCO_3^-	Cl	Br	NO3	PO4	SO4	Anion Sum										
	meq	meq	meq	meq	meq	meq											
Venson E	3.979	22.538	0.039	0.517	0.000	3.554	30.628										
L.Venson bh 2	3.999	22.097	0.040	0.345	0.000	2.949	29.430										
L Venson bh 3	3.679	21.883	0.040	0.346	0.000	2.935	28.884										
L Venson bh 4	4.159	26.728	0.044	0.399	0.000	3.539	34.870										
Thornton Farm bh 1	4.559	22.930	0.040	0.424	0.000	3.926	31.879										
Thornton Farm bh 5 @ 16m	0.000	28.361	0.049	0.398	0.000	4.540	33.348										
Thornton Farm bh 5 @ 25m	0.000	27.892	0.048	0.387	0.000	4.455	32.782										
Thornton Farm bh 5 @ 37m	0.000	30.838	0.050	0.312	0.008	4.297	35.505										
Thornton Farm bh 5	4.559	28.143	0.047	0.388	0.000	4.416	37.553										
Thornton Farm bh 6 @ 21m	0.000	1.486	0.008	0.000	0.000	0.128	1.622										
Eastry C	6.119	21.904	0.041	0.511	0.000	3.288	31.863										
Rowling Cottages	4.079	2.005	0.000	0.532	0.000	0.710	7.326										
Shingleton Farm Cottages	6.359	8.709	0.017	0.462	0.000	2.271	17.817										
Pixwell Farm Cottages	5.799	4.238	0.007	0.555	0.000	1.029	11.628										
Statenborough (pumping well)	5.439	4.371	0.009	0.903	0.000	1.959	12.681										
Delf Nurseries (pumping well)	5.879	2.424	0.043	1.041	0.000	3.697	13.083										
	Cations																
	Ca	Na	K	Mg	Fe	Al	B	Ba	Co	Li	Mn	Ni	Sr	Zn	Cation Sum	Anion Sum	Ionic balance
	meq	meq	meq	meq	meq	meq	meq	meq	meq	meq	meq	meq	meq	meq			
Venson E	7.730	22.367	0.225	1.798	0.000	0.003	0.250	0.001	0.001	0.035	0.000	0.002	0.045	0.001	32.458	30.628	5.804
L.Venson bh 2	8.039	22.937	0.205	1.354	0.000	0.003	0.275	0.002	0.001	0.032	0.000	0.002	0.030	0.001	32.882	29.430	11.079
L Venson bh 3	7.774	22.311	0.223	1.375	0.000	0.003	0.269	0.001	0.001	0.032	0.000	0.003	0.031	0.002	32.026	28.884	10.317
L Venson bh 4	7.884	26.099	0.266	1.741	0.000	0.002	0.300	0.001	0.001	0.037	0.000	0.002	0.039	0.001	36.375	34.870	4.226
Thornton Farm bh 1	7.106	23.494	0.261	1.927	0.000	0.002	0.255	0.001	0.001	0.040	0.000	0.001	0.056	0.001	33.146	31.879	3.898
Thornton Farm bh 5 @ 16m	7.146	28.374	0.312	2.276	0.000	0.002	0.297	0.001	0.001	0.048	0.000	0.002	0.072	0.002	38.533	33.348	14.427
Thornton Farm bh 5 @ 25m	7.151	28.705	0.307	2.288	0.000	0.002	0.302	0.001	0.001	0.049	0.000	0.002	0.072	0.001	38.881	32.782	17.022
Thornton Farm bh 5 @ 37m	7.500	30.110	0.304	2.052	0.006	0.003	0.330	0.001	0.001	0.048	0.001	0.001	0.061	0.001	40.420	35.505	12.946
Thornton Farm bh 5	7.196	28.092	0.315	2.265	0.000	0.003	0.294	0.001	0.001	0.048	0.000	0.002	0.071	0.002	38.290	37.553	1.943
Thornton Farm bh 6 @ 21m	2.415	0.909	1.138	0.332	0.011	0.003	0.033	0.000	0.000	0.003	0.015	0.001	0.009	0.001	4.870	1.622	100.054
Eastry C	7.700	22.867	0.243	1.670	0.004	0.002	0.261	0.001	0.001	0.033	0.000	0.002	0.040	0.001	32.826	31.863	2.978
Rowling Cottages	6.457	1.770	0.090	0.316	0.000	0.003	0.017	0.001	0.001	0.004	0.000	0.001	0.007	0.002	8.669	7.326	16.794
Shingleton Farm Cottages	6.617	9.696	0.107	1.148	0.000	0.002	0.117	0.001	0.001	0.014	0.000	0.002	0.026	0.001	17.731	17.817	-0.483
Pixwell Farm Cottages	6.372	4.428	0.074	0.492	0.000	0.003	0.053	0.001	0.001	0.009	0.000	0.002	0.010	0.001	11.446	11.628	-1.577
Statenborough (pumping well)	9.501	4.093	0.159	0.813	0.000	0.007	0.069	0.001	0.001	0.009	0.000	0.002	0.015	0.003	14.673	12.681	14.565
Delf Nurseries (pumping well)	8.413	4.085	0.128	1.444	0.003	0.003	0.033	0.001	0.002	0.007	0.005	0.003	0.020	0.001	14.148	13.083	7.820

Hydrochemical results: BGS LVV porewater samples.

Analysis undertaken by BGS 1999.

Analysis of porewater samples and fracture water. Undertaken by BGS 1999																	
Sample Number	**Top depth** (m)	**Bottom depth** (m)	**MC** g/Kg dry	**mid point** (m)	**T** °C	**pH**	**pH (lab)**	**SEC** µS cm^{-1}	**d2H** l	**d18O** l	**d13C** l	**Cl** mg l^{-1}	**Br** mg l^{-1}	**NO3** mg l^{-1}	**NH4-N** mg l^{-1}	**HCO3** mg l^{-1}	**HCO3 lab** mg l^{-1}
990698	0.5	0.8	19.37	0.65			7.95	374				75.9	0.166	3.9	0.01		112
990699	0.8	1.3	29.26	1.05			8.32	311				36.9	0.07	0.2	0.01		171
990700	3.0	3.5	31.47	3.25			8.10	230				9.3		0.5	-0.01		166
990701	3.5	4.0	29.13	3.75			8.20	231									156
990702	4.0	4.5	32.29	4.25			8.26	239				10.0	0.04	0.4	-0.01		158
990703	5.0	5.5	30.20	5.25			8.04	229									132
990704	5.5	6.0	30.59	5.75			8.13	257				26.4	0.073	0.5	0.01		134
990705	6.0	6.5	29.09	6.25			8.03	668				147	0.544	3.5	0.03		153
990706	6.5	7.0	30.63	6.75			7.98	1180				339	1.32	6.2	0.01		124
990707	7.0	7.2	31.56	7.10			8.03	1390				450	1.57	7.7	0.01		127
990708	8.0	8.5	31.92	8.25			7.95	2020				670	2.57	8.3	-0.01		131
990709	8.5	9.0	31.43	8.75			8.10	2180									140
990710	9.0	9.5	32.53	9.25			8.11	2130				700	2.58	8.3	0.01		147
990711	9.5	9.8	29.64	9.65			8.05	2190									126
990712	11.0	11.5	31.42	11.25			7.93	2360				790	2.87	7.7	0.01		109
990713	11.5	12.0	32.51	11.75			8.10	2500									199
990714	12.0	12.5	30.09	12.25			8.20	2560									208
990715	12.5	12.9	31.02	12.70			8.08	2720				880	3.33	6.9	0.02		154
990716	14.0	14.5	32.71	14.25			8.25	2650									177
990717	14.5	15.0	33.47	14.75			8.15	2680									198
990718	15.0	15.5	33.51	15.25			8.13	2600				910	3.42	6.4	-0.01		173
990719	15.5	16.0	32.42	15.75			8.12	2670									131
990720	16.0	16.5	32.83	16.25			8.20	2680									191
990721	16.5	17.0	34.75	16.75			8.21	2720									190
990722	17.0	17.5	31.81	17.25			8.13	2730				900	3.47	6.2	0.01		149
990723	17.5	18.0	32.55	17.75			8.24	2720									156
990724	18.0	18.2	31.50	18.10			8.05	2870									146
990725	18.5	18.8	33.27	18.65			8.05	2900									154
990726	19.5	20.0	31.35	19.75			8.14	3020				990	3.86	5.6	0.01		212
990727	20.5	21.0	33.59	20.75			8.07	2750									166

Sample Number	F mg l^{-1}	Sr mg l^{-1}	Cd µg l^{-1}	Ba mg l^{-1}	Si mg l^{-1}	Mn mg l^{-1}	Fe mg l^{-1}	P mg l^{-1}	SO4 mg l^{-1}	B mg l^{-1}	Mg mg l^{-1}	V µg l^{-1}	Na mg l^{-1}	Mo µg l^{-1}	Al µg l^{-1}	Be µg l^{-1}	Ca mg l^{-1}	Zn µg l^{-1}	Cu µg l^{-1}	Pb µg l^{-1}	Li µg l^{-1}	Zr µg l^{-1}	Co µg l^{-1}
990698		0.31	<6	0.89	4.53	0.004	<0.006	<0.045	18.1	1.03	5.30	<10	24.2	<8	<28	<0.3	71.3	88.2	6	<35	<3	<4	<11
990699		0.28	<6	0.10	2.87	0.002	<0.006	<0.045	15.2	0.43	5.01	<10	18.2	<8	<28	<0.3	57.1	72.4	<5	<35	6	<4	<11
990700		0.28	<6	0.10	2.68	<0.001	<0.006	<0.045	16.2	0.40	4.52	<10	15.3	<8	<28	<0.3	43.9	28.0	<5	<35	6	<4	<11
990701																							
990702		0.42	<6	0.09	2.66	0.001	<0.006	<0.045	22.3	0.45	4.31	<10	17.9	<8	<28	<0.3	42.7	55.9	<5	<35	13	<4	<11
990703																							
990704		0.44	<6	0.10	3.07	<0.001	<0.006	<0.045	20.6	0.47	3.87	<10	25.7	<8	<28	<0.3	36.8	25.1	<5	<35	34	<4	<11
990705		0.56	<6	0.11	4.35	0.003	<0.006	0.053	69.0	0.50	4.90	<10	118	<8	<28	<0.3	46.3	56.1	15	<35	54	<4	<11
990706		0.85	<6	0.13	3.08	0.001	<0.006	<0.045	86.0	0.54	7.95	<10	209	<8	<28	<0.3	70.0	43.0	<5	<35	66	<4	<11
990707		1.05	<6	0.15	3.64	0.002	<0.006	0.048	99.7	0.58	9.56	<10	258	<8	<28	<0.3	77.7	50.8	<5	<35	89	<4	<11
990708		1.40	<6	0.13	3.89	0.003	<0.006	<0.045	150	0.81	13.9	<10	410	<8	<28	<0.3	91.6	59.4	<5	<35	140	<4	<11
990709																							
990710		1.46	<6	0.13	4.03	0.002	<0.006	<0.045	153	0.88	14.6	<10	424	<8	<28	<0.3	93.0	60.6	7	<35	150	<4	<11
990711																							
990712		1.46	<6	0.14	3.86	0.002	<0.006	0.052	165	0.94	14.8	<10	469	<8	<28	<0.3	89.1	54.9	5	<35	164	<4	<11
990713																							
990714																							
990715		1.66	<6	0.13	4.38	0.002	<0.006	0.054	175	1.08	17.1	<10	540	<8	<28	<0.3	104	58.3	<5	<35	191	<4	<11
990716																							
990717																							
990718		1.60	<6	0.15	4.78	0.004	<0.006	0.063	176	1.11	17.4	<10	546	<8	<28	<0.3	104	68.6	<5	<35	199	<4	<11
990719																							
990720																							
990721																							
990722		1.60	<6	0.15	4.67	0.002	<0.006	<0.045	177	1.12	16.9	<10	563	<8	<28	<0.3	102	58.4	6	<35	192	<4	<11
990723																							
990724																							
990725																							
990726		1.59	<6	0.18	4.83	0.002	<0.006	0.050	184	1.27	19.1	<10	618	<8	<28	<0.3	122	75.3	6	<35	210	<4	<11
990727																							

Sample Number	Ni $\mu g\ l^{-1}$	Y $\mu g\ l^{-1}$	La $\mu g\ l^{-1}$	K $mg\ l^{-1}$	Cr $\mu g\ l^{-1}$
990698	12	<1	<7	0.93	<19
990699	<8	<1	<7	0.82	<19
990700	<8	<1	<7	0.82	<19
990701					
990702	<8	<1	<7	1.50	<19
990703					
990704	<8	<1	<7	2.43	<19
990705	<8	<1	<7	4.53	<19
990706	<8	<1	<7	4.57	<19
990707	<8	<1	<7	5.39	<19
990708	<8	<1	<7	7.04	<19
990709					
990710	<8	<1	<7	7.14	<19
990711					
990712	<8	<1	<7	7.33	<19
990713					
990714					
990715	<8	<1	<7	8.44	<19
990716					
990717					
990718	<8	<1	8	8.11	<19
990719					
990720					
990721					
990722	<8	<1	<7	8.35	<19
990723					
990724					
990725					
990726	<8	<1	<7	8.82	<19
990727					

Sample	Top depth	Bottom depth	MC	mid point	T	pH	pH (lab)	SEC	d2H	d18O	d13C	Cl	Br	NO3	NH4-N	HCO3	HCO3 lab
Number	(m)	(m)	g/Kg dry	(m)	°C			µS cm^{-1}	l	l	l	mg l^{-1}	mg l^{-1}	mg l^{-1}	mg l^{-1}	mg l^{-1}	mg l^{-1}
990728	22.5	23.0	32.28	22.75			8.18	2880									191
990729	23.0	23.4	29.58	23.20			8.10	3020									200
990730	23.4	23.8	28.36	23.60			8.07	3050				1200	4.00	5.5	0.01		121
990731	28.0	28.5	27.76	28.25			8.00	3180									130
990732	28.5	29.0	30.70	28.75			8.09	3060									120
990733	29.0	29.5	30.84	29.25			7.96	3040									91
990734	29.5	30.0	30.56	29.75			7.90	3080				1100	4.10	5.2	0.01		96.8
990735	31.0	32.0	31.38	31.50			8.18	3110									253
990736	32.0	33.0	31.03	32.50				3060									
990737	33.0	34.0	31.03	33.50				3100									
990738	34.0	35.0	31.95	34.50			8.15	3070				1200	4.14	5.0	0.01		158
990739	35.0	36.0	26.74	35.50				3010									
990740	36.0	37.0	26.44	36.50				3010									
990741	37.0	38.0	31.84	37.50				3040									
990742	40.5	41.5	28.54	41.00			8.05	2930				1100	3.75	4.7	0.01		116
990743	41.5	42.5	29.72	42.00			8.07	3160				1100	4.29	4.3	0.01		156
990744	42.5	43.5	30.63	43.00			8.20	3210				1100	4.18	4.3	0.05		152
990745	44.0	45.0	29.83	44.50			8.24	3100				1000	3.83	4.8	-0.01		230
990746	45.0	46.0	29.89	45.50			8.19	2780				900	3.56	4.3	-0.01		187
990747	47.0	48.0	30.79	47.50			8.26	1340				364	1.40	3.8	0.01		196
990748	48.0	49.0	31.80	48.50			8.21	1370				391	1.48	4.0	0.03		159
990749	50.0	51.0	29.73	50.50			8.18	1110				320	1.19	4.1	0.01		148
990750	51.0	52.0	19.95	51.50			8.09	1632				470	1.84	4.0	0.01		180
990751	52.0	53.0	32.66	52.50			8.22	1160				315	1.17	4.3	0.02		135
990752	53.0	54.0	30.32	53.50			8.21	1170				301	1.10	4.3	0.02		192
990753	55.0	56.0	32.16	55.50				793									
990754	56.0	57.0	27.41	56.50			8.17	619				134	0.500	4.2	0.03		140
990755	57.0	58.0	19.38	57.50			8.23	1040				271	1.01	3.7	0.15		165
990756	59.0	59.0	30.23	59.00			8.15	1980				270	1.01	3.9	0.04		123
990757	59.0	60.0	29.92	59.50				1818									
990758	60.0	61.0	26.55	60.50				1960									
990759	61.0	62.0	29.39	61.50			8.08	1850				550	2.14	3.8	0.03		100
990760	62.0	63.0	28.78	62.50				1980									
990761	63.0	64.0	30.40	63.50				2150									

Sample	F	Sr	Cd	Ba	Si	Mn	Fe	P	SO4	B	Mg	V	Na	Mo	Al	Be	Ca	Zn	Cu	Pb	Li	Zr	Co
Number	mg l^{-1}	mg l^{-1}	µg l^{-1}	mg l^{-1}	mg l^{-1}	mg l^{-1}	mg l^{-1}	mg l^{-1}	mg l^{-1}	mg l^{-1}	mg l^{-1}	µg l^{-1}	mg l^{-1}	µg l^{-1}	µg l^{-1}	µg l^{-1}	mg l^{-1}	µg l^{-1}	µg l^{-1}	µg l^{-1}	µg l^{-1}	µg l^{-1}	µg l^{-1}
990728																							
990729																							
990730		1.30	<6	0.14	4.05	0.002	<0.006	0.053	186	1.22	16.6	<10	616	<8	<28	<0.3	104	42.1	5	<35	204	<4	<11
990731																							
990732																							
990733																							
990734		1.13	<6	0.13	3.93	0.002	<0.006	<0.045	187	1.25	15.1	<10	624	<8	<28	<0.3	104	46.8	<5	<35	209	<4	<11
990735																							
990736																							
990737																							
990738		1.08	<6	0.16	5.48	0.002	<0.006	<0.045	177	1.32	15.3	<10	628	<8	<28	<0.3	117	56.0	<5	<35	199	<4	<11
990739																							
990740																							
990741																							
990742		0.81	<6	0.19	4.11	0.002	<0.006	<0.045	140	1.19	10.4	<10	573	<8	<28	<0.3	116	52.3	<5	<35	171	<4	<11
990743		0.63	<6	0.21	4.66	0.002	<0.006	<0.045	96.4	1.27	7.08	<10	588	<8	<28	<0.3	143	52.3	7	<35	156	<4	<11
990744		0.73	<6	0.20	4.74	0.003	<0.006	0.049	120	1.31	8.99	<10	626	<8	<28	<0.3	133	59.0	<5	<35	172	<4	<11
990745		1.19	<6	0.20	5.07	0.002	<0.006	0.061	163	1.30	16.6	<10	601	<8	<28	<0.3	131	74.2	8	<35	201	<4	<11
990746		0.69	<6	0.19	4.98	0.002	<0.006	<0.045	97.4	1.20	8.17	<10	529	<8	<28	<0.3	126	66.0	5	<35	145	<4	<11
990747		0.50	<6	0.24	4.98	0.001	<0.006	<0.045	16.1	0.41	3.90	<10	185	<8	<28	<0.3	109	50.2	<5	<35	35	<4	<11
990748		0.51	<6	0.17	4.94	<0.001	<0.006	<0.045	26.9	0.49	4.33	<10	202	<8	<28	<0.3	96.2	36.0	<5	<35	44	<4	<11
990749		0.49	<6	0.24	4.98	<0.001	<0.006	<0.045	10.5	0.38	3.32	<10	148	<8	<28	<0.3	93.8	43.2	<5	<35	26	<4	<11
990750		0.66	<6	0.19	5.44	<0.001	<0.006	<0.045	33.9	0.58	5.11	<10	254	<8	<28	<0.3	112	34.6	<5	<35	96	<4	<11
990751		0.44	<6	0.24	4.95	0.001	<0.006	<0.045	20.8	0.46	3.43	<10	168	<8	<28	<0.3	81.5	35.0	<5	<35	39	<4	<11
990752		0.53	<6	0.23	5.27	0.001	<0.006	<0.045	23.9	0.47	3.98	<10	163	<8	<28	<0.3	92.0	52.0	<5	<35	39	<4	<11
990753																							
990754		0.36	<6	0.17	4.85	<0.001	<0.006	<0.045	10.0	0.31	2.35	<10	71.3	<8	<28	<0.3	61.3	40.8	<5	<35	4	<4	<11
990755		0.41	<6	0.24	4.49	0.001	<0.006	<0.045	19.3	0.54	3.07	<10	153	<8	<28	<0.3	73.9	30.6	6	<35	30	<4	<11
990756		0.41	<6	0.21	4.71	0.007	0.027	<0.045	19.3	0.53	2.83	<10	152	<8	<28	<0.3	72.2	33.0	5	<35	20	<4	<11
990757																							
990758																							
990759		0.49	<6	0.20	4.31	0.001	<0.006	<0.045	49.0	0.89	4.01	<10	325	<8	<28	<0.3	77.9	37.3	<5	<35	66	<4	<11
990760																							
990761																							

Sample	Ni	Y	La	K	Cr
Number	$\mu g\ l^{-1}$	$\mu g\ l^{-1}$	$\mu g\ l^{-1}$	$mg\ l^{-1}$	$\mu g\ l^{-1}$
990728					
990729					
990730	<8	<1	<7	8.57	<19
990731					
990732					
990733					
990734	<8	<1	<7	8.07	<19
990735					
990736					
990737					
990738	<8	<1	<7	8.48	<19
990739					
990740					
990741					
990742	<8	1	<7	7.49	<19
990743	<8	1	7	6.69	<19
990744	<8	<1	<7	7.48	<19
990745	<8	1	<7	8.03	<19
990746	<8	<1	<7	6.15	<19
990747	<8	<1	<7	3.81	<19
990748	<8	<1	<7	3.53	<19
990749	<8	<1	<7	3.24	<19
990750	<8	<1	<7	4.22	<19
990751	<8	<1	<7	3.49	<19
990752	<8	<1	<7	4.06	<19
990753					
990754	<8	<1	<7	2.96	<19
990755	<8	<1	<7	3.82	<19
990756	<8	<1	<7	4.03	<19
990757					
990758					
990759	<8	<1	<7	4.99	<19
990760					
990761					

Sample	Top depth	Bottom depth	MC	mid point	T	pH	pH (lab)	SEC	d2H	d18O	d13C	Cl	Br	NO3	NH4-N	HCO3	HCO3 lab
Number	(m)	(m)	g/Kg dry	(m)	°C			µS cm^{-1}	l	l	l	mg l^{-1}	mg l^{-1}	mg l^{-1}	mg l^{-1}	mg l^{-1}	mg l^{-1}
990762	64.0	65.0	27.18	64.50			8.07	2340				770	2.84	4.0	0.01		131
990763	65.0	66.0	20.34	65.50				2560									
990764	66.0	67.0	25.01	66.50				2570									
990765	67.0	68.0	25.68	67.50			8.20	2600				800	3.09	4.5	-0.01		154
990766	68.0	69.0	28.51	68.50				2620									
990767	69.0	70.0	27.58	69.50				2780									
990768	70.0	71.0	31.05	70.50			8.17	2530				770	2.94	4.5	-0.01		176
990769	71.0	72.0	30.80	71.50				2640									
990770	72.0	73.0	30.71	72.50				2740									
990771	73.0	74.0	25.41	73.50			8.22	2760				900	3.45	4.0	0.02		164
990772	74.0	75.0	27.55	74.50				2760									
990773	75.0	76.0	32.85	75.50				2900									
990774	76.0	77.0	25.10	76.50			8.12	3000				960	3.72	4.3	0.01		144
990775	77.0	78.0	15.64	77.50			8.06	2790				880	3.37	5.2	0.01		105
990776	80.0	81.0	27.62	80.50			8.16	1155				322	1.21	4.2	0.01		120
990777	81.0	82.0	19.11	81.50			8.10	821				206	0.772	2.0	0.02		236
990778	82.0	83.0	18.64	82.50				984									
990779	83.0	84.0	25.93	83.50				915									
990780	84.0	85.0	25.69	84.50			8.15	626				142	0.53	2.1	0.03		111
990781	85.0	86.0	27.58	85.50				993									
990782	86.0	87.0	23.72	86.50				588									
990783	87.0	88.0	22.72	87.50			8.16	391				51.7	0.209	1.0	0.01		121
990784	88.0	89.0	24.27	88.50				508									
990785	89.0	90.0	23.77	89.50				527									
990786	90.0	91.0	23.50	90.50			8.22	559				117	0.455	1.7	0.01		100
990787	91.0	92.0	27.94	91.50				991									
990788	92.0	93.0	26.21	92.50				519									
990789	98.0	99.0	25.89	98.50			8.21	580				124	0.489	1.5	-0.01		113

Sample	F	Sr	Cd	Ba	Si	Mn	Fe	P	SO4	B	Mg	V	Na	Mo	Al	Be	Ca	Zn	Cu	Pb	Li	Zr	Co
Number	mg l^{-1}	mg l^{-1}	µg l^{-1}	mg l^{-1}	mg l^{-1}	mg l^{-1}	mg l^{-1}	mg l^{-1}	mg l^{-1}	mg l^{-1}	mg l^{-1}	µg l^{-1}	mg l^{-1}	µg l^{-1}	µg l^{-1}	µg l^{-1}	mg l^{-1}	µg l^{-1}	µg l^{-1}	µg l^{-1}	µg l^{-1}	µg l^{-1}	µg l^{-1}
990762		0.60	<6	0.29	4.72	0.001	<0.006	<0.045	90.4	1.01	5.78	<10	436	<8	<28	<0.3	100	38.7	6	<35	111	<4	<11
990763																							
990764																							
990765		0.72	<6	0.22	4.64	0.002	0.039	<0.045	128	1.05	9.31	<10	482	<8	<28	<0.3	111	32.3	<5	<35	135	<4	<11
990766																							
990767																							
990768		0.76	<6	0.23	4.61	0.001	<0.006	<0.045	99.1	0.98	8.94	<10	463	<8	<28	<0.3	108	37.2	<5	<35	121	<4	<11
990769																							
990770																							
990771		0.71	<6	0.24	4.73	0.002	<0.006	0.046	95.0	1.22	6.62	<10	522	<8	<28	<0.3	116	28.0	6	<35	119	<4	<11
990772																							
990773																							
990774		0.73	<6	0.16	4.27	0.002	<0.006	0.048	150	1.21	8.77	<10	584	<8	<28	<0.3	117	38.6	6	<35	175	<4	<11
990775		1.22	<6	0.21	4.07	0.001	0.025	0.057	155	1.07	13.0	<10	530	<8	<28	<0.3	97.2	28.6	<5	<35	159	<4	<11
990776		0.68	<6	0.20	4.70	0.001	<0.006	<0.045	34.7	0.33	4.45	<10	165	<8	<28	<0.3	84.2	21.1	<5	<35	29	<4	<11
990777		0.78	<6	0.23	5.41	0.001	<0.006	<0.045	26.5	0.25	4.27	<10	97.0	<8	<28	<0.3	76.0	23.9	<5	<35	24	<4	<11
990778		0.55	<6	0.18	4.53	<0.001	<0.006	<0.045	21.0	0.20	3.42	<10	63.0	<8	<28	<0.3	66.5	17.8	<5	<35	12	<4	<11
990779																							
990780																							
990781																							
990782																							
990783		0.80	<6	0.17	11.2	0.001	<0.006	<0.045	32.6	0.16	3.78	<10	27.2	<8	<28	<0.3	51.7	28.9	<5	<35	49	<4	<11
990784																							
990785																							
990786		0.88	<6	0.28	10.0	0.001	<0.006	0.194	31.3	0.26	3.94	<10	56.3	<8	<28	<0.3	54.9	31.5	<5	<35	39	<4	<11
990787																							
990788																							
990789		0.86	<6	0.16	8.61	<0.001	<0.006	0.051	26.1	0.16	4.30	<10	48.9	<8	<28	<0.3	65.3	32.7	<5	<35	78	<4	<11

Sample	Ni	Y	La	K	Cr
Number	µg l^{-1}	µg l^{-1}	µg l^{-1}	mg l^{-1}	µg l^{-1}
990762	<8	<1	<7	5.78	<19
990763					
990764					
990765	<8	<1	<7	6.36	<19
990766					
990767					
990768	<8	<1	<7	6.71	<19
990769					
990770					
990771	<8	<1	<7	6.88	<19
990772					
990773					
990774	<8	<1	<7	6.90	<19
990775	<8	<1	<7	7.24	<19
990776	<8	<1	<7	3.49	<19
990777	<8	<1	<7	2.62	<19
990778	<8	<1	<7	2.37	<19
990779					
990780					
990781					
990782					
990783	<8	<1	<7	5.28	<19
990784					
990785					
990786	<8	<1	<7	5.93	<19
990787					
990788					
990789	<8	<1	<7	3.89	<19

Hydrochemical results: Fracture water samples.

Analysis undertaken by BGS 1999

Sample	Top depth	Bottom depth	MC	mid point	T	pH	pH (lab)	SEC	d2H	d18O	d13C	Cl	Br	NO3	NH4-N	HCO3	HCO3 lab
Number	(m)	(m)	g/Kg dry	(m)	°C			µS cm^{-1}	l	l	l	mg l^{-1}	mg l^{-1}	mg l^{-1}	mg l^{-1}	mg l^{-1}	mg l^{-1}
Depth Sample	**Collected during geophysical logging on 28 June 1999.**																
990790	106			106			8.30	3230	-47	-7.2	-12.7	820	3.187	5.0			330
990791	120			120			8.03	680	-44	-7	-10.1	270	0.930	1.1			314
990792	140			140			7.93	17800	-48	-6.9	-5.6	5100	1.962	0.2			424
Packer samples LVFV																	
	toppacker	**bottompacker**															
	(m)	**(m)**															
Tests performed on 13 and 14 July 1999																	
990793	30.18	33.05		31.615			8.01	1317	-46	-7.2	too smal	860	3.407	5.2			329
990794	45.5	48.37		46.935			8.09	1317	-48	-7.2	too smal	860	3.654	5.2			305
990795	75.8	78.67		77.235			8.03	1417	-46	-7.3	too smal	840	3.424	5.3			391
Tests performed on 16 to 19 August 1999																	
991013	35.7	38.575		37.1375	13.8	7.24	8.12	3230	-47	-7.3	-12.7	880	3.415	5.8		296	202
991014	39.225	42.13		40.6775	13.5	7.22	8.06	3260	-47	-7.3	-12.6	850	3.359	5.5		294	257
991015	49.455	52.33		50.8925	13.5	6.86	8.08	3250	-47	-7.4	-12.6	900	3.368	5.5		294	134
991016	65.5	68.375		66.9375	14.1	7.20	8.09	3375	-46	-7	-12.6	850	3.434	5.4		303	282
991017	65.5	68.375		66.9375	13.3	6.87	8.05	3330	-46	-7.1	-13.3	860	3.553	5.5		301	151
991018	76.085	78.96		77.5225	13.6	7.07	8.14	3390	-46	-7.2	-13.0	830	3.462	5.5		276	247
991019	82.275	85.15		83.7125	16.5	7.15	7.97	2440	-45	-7.2	-12.2	540	2.173	4.1			163

Sample	F	Sr	Cd	Ba	Si	Mn	Fe	P	SO4	B	Mg	V	Na	Mo	Al	Be	Ca	Zn	Cu	Pb	Li	Zr	Co
Number	mg l^{-1}	mg l^{-1}	µg l^{-1}	mg l^{-1}	mg l^{-1}	mg l^{-1}	mg l^{-1}	mg l^{-1}	mg l^{-1}	mg l^{-1}	mg l^{-1}	µg l^{-1}	mg l^{-1}	µg l^{-1}	µg l^{-1}	µg l^{-1}	mg l^{-1}	µg l^{-1}	µg l^{-1}	µg l^{-1}	µg l^{-1}	µg l^{-1}	µg l^{-1}
Depth Samples BH2																							
990790	0.31	1.22	<6	0.09	4.82	0.015	0.056	<0.045	144	1.00	16.7	<10	492	<8	<28	<0.3	150	102	<5	<35	213	<4	<11
990791	0.44	1.18	<6	0.14	4.90	0.010	0.021	<0.045	41.8	0.24	8.14	<10	102	<8	<28	<0.3	109	52.8	<5	<35	1856	<4	<11
990792	1.78	6.43	<30	0.28	5.23	0.040	0.135	0.235	82.3	1.12	48.8	<50	228	<40	<140	<1.5	117	58.4	<25	<175	1105000	29	<55
Packer samples LVFV																							
Tests performed on 13 and 14 July 1999																							
990793	0.30	1.36	14	0.08	4.69	0.005	<0.006	<0.045	155	1.04	17.9	<10	532	<8	<28	<0.3	147	86.4	<5	<35	165	<4	<11
990794	0.33	1.37	<6	0.08	4.67	0.005	0.016	<0.045	156	1.04	17.9	<10	530	<8	<28	<0.3	146	59.6	<5	<35	166	<4	<11
990795	0.32	1.37	<6	0.08	4.66	0.009	0.039	<0.045	157	1.06	18.0	<10	533	<8	<28	<0.3	148	32.3	<5	<35	169	<4	<11
Tests performed on 16 to 19 August 1999																							
991013	0.32	1.36	17	0.08	4.66	0.004	0.073	0.055	157	1.05	17.8	<10	526	<8	<28	<0.3	148	65.3	<5	<35	168	<4	<11
991014	0.33	1.36	23	0.07	4.65	0.002	0.044	<0.045	157	1.05	17.7	<10	530	<8	<28	<0.3	146	91.5	<5	<35	164	<4	<11
991015	0.36	1.36	13	0.08	4.66	0.003	0.059	<0.045	156	1.06	17.9	<10	529	<8	<28	<0.3	148	55.0	<5	<35	166	<4	<11
991016	0.34	1.37	60	0.07	4.63	0.014	0.113	<0.045	157	1.04	17.9	<10	533	<8	<28	<0.3	147	177	8	<35	166	<4	<11
991017	0.31	1.34	12	0.07	4.65	0.004	0.062	<0.045	153	1.03	17.6	<10	523	<8	<28	<0.3	146	65.4	<5	<35	160	<4	<11
991018	0.28	1.37	<6	0.08	4.68	0.006	0.126	<0.045	157	1.05	18.0	<10	535	<8	<28	<0.3	149	78.8	17	<35	167	<4	<11
991019	0.27	1.08	11	0.10	4.75	0.012	0.035	<0.045	101	0.70	12.3	<10	331	<8	<28	<0.3	136	148	13	<35	100	<4	<11

Sample	Ni	Y	La	K	Cr	
Number	µg l^{-1}	µg l^{-1}	µg l^{-1}	mg l^{-1}	µg l^{-1}	
Depth Samples BH2						
990790	<8	<1	<7	6.72	<19	
990791	<8	<1	<7	2.59	<19	
990792	50	11	146	9.16	<95	
Packer samples LVFV						
Tests performed on 13 and 14 July 1999						
990793	<8	<1	<7	7.22	<19	
990794	<8	<1	<7	7.18	<19	
990795	39	<1	<7	7.36	<19	
Tests performed on 16 to 19 August 1999						
991013	<8	2	9	7.28	<19	
991014	<8	<1	<7	7.18	<19	
991015	<8	1	<7	7.32	<19	
991016	<8	<1	<7	7.35	<19	
991017	<8	<1	<7	7.14	<19	
991018	<8	<1	<7	10.7	<19	
991019	<8	<1	<7	5.29	<19	

Appendix 6

DP1D along valley profiles

At 20 m depth

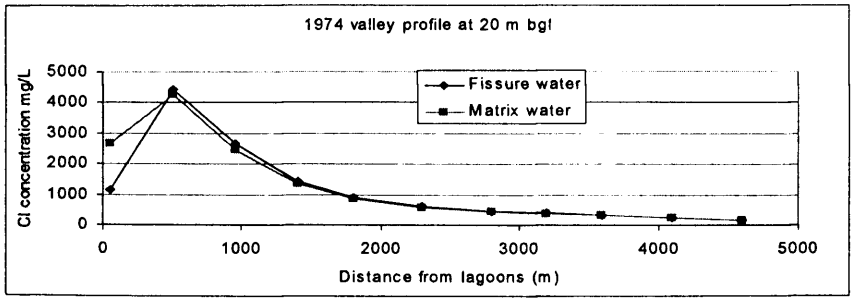

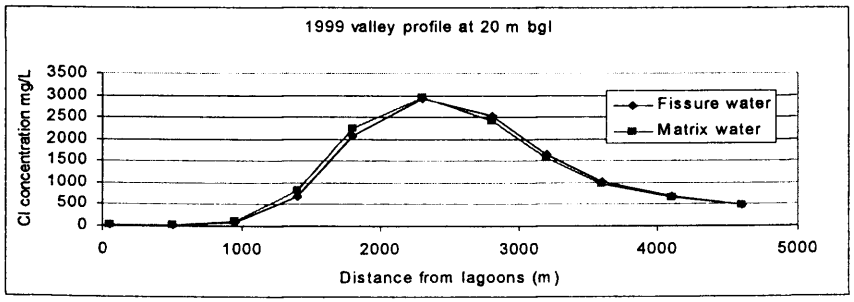

At 30 m depth

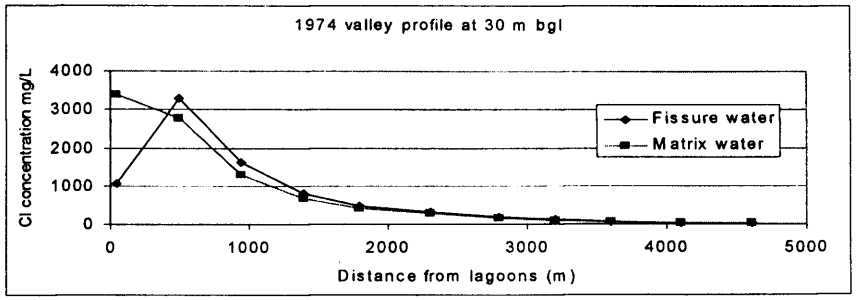

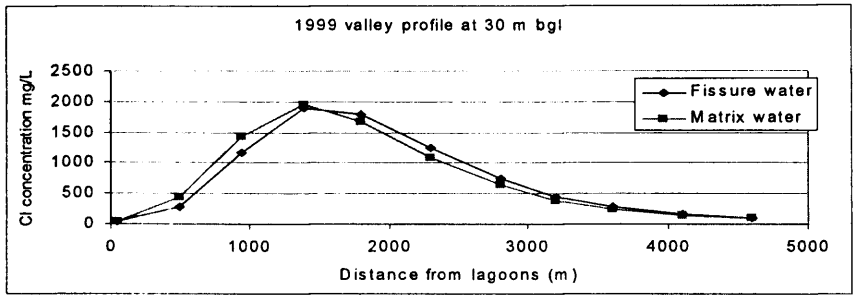

At 40 m depth

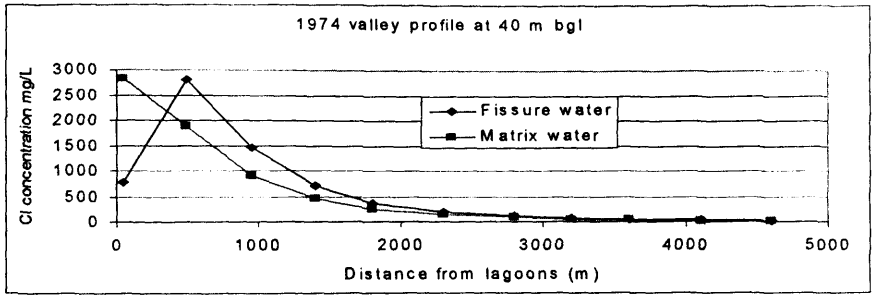

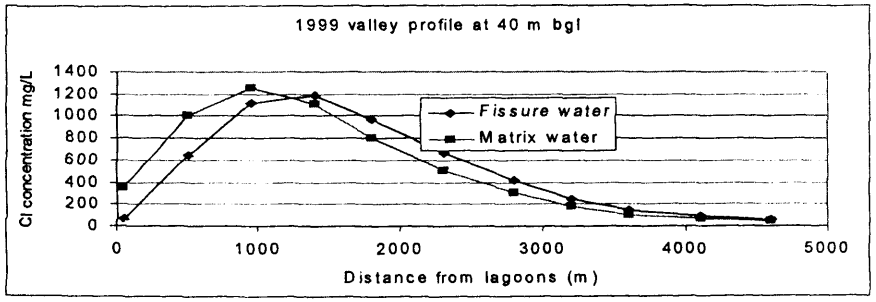

At 50 m depth

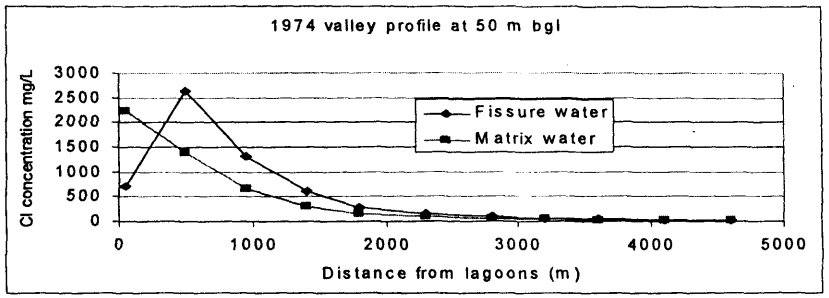

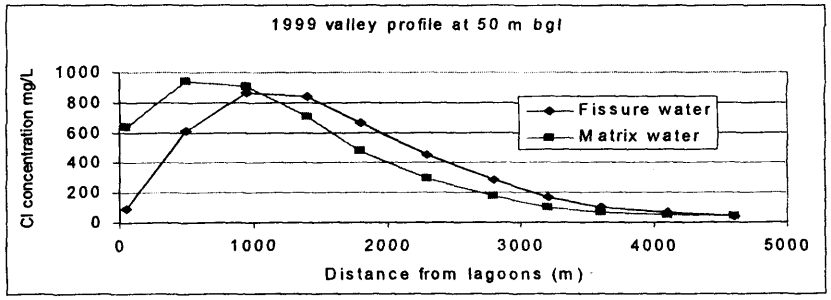

At 80 m depth

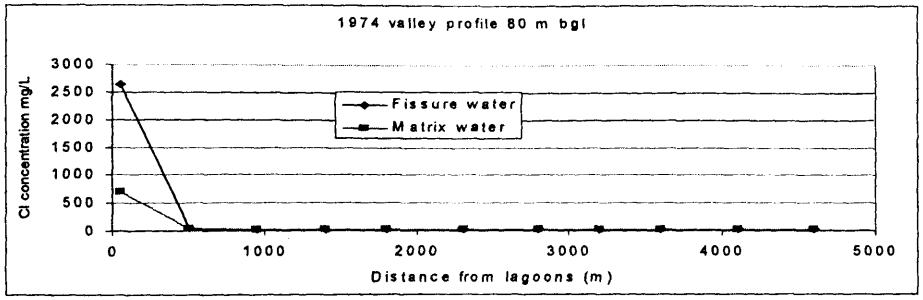

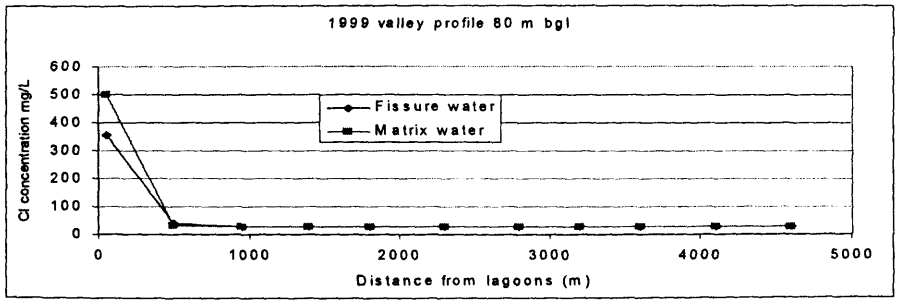

At 90 m depth

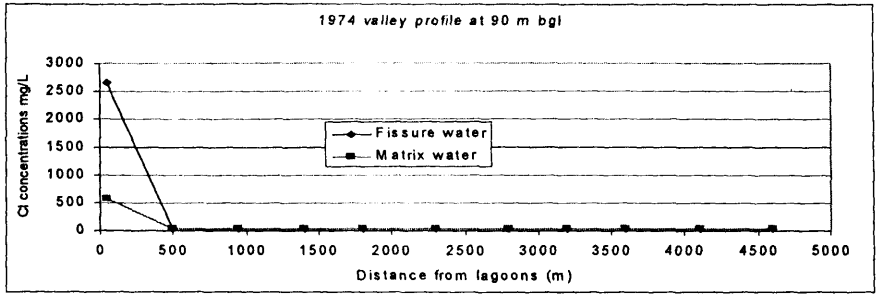

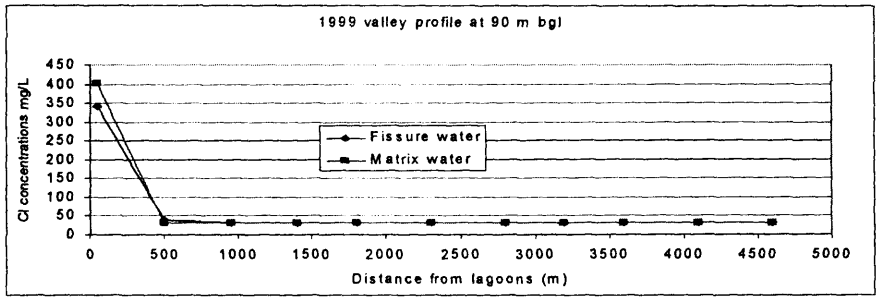

At 100 m depth

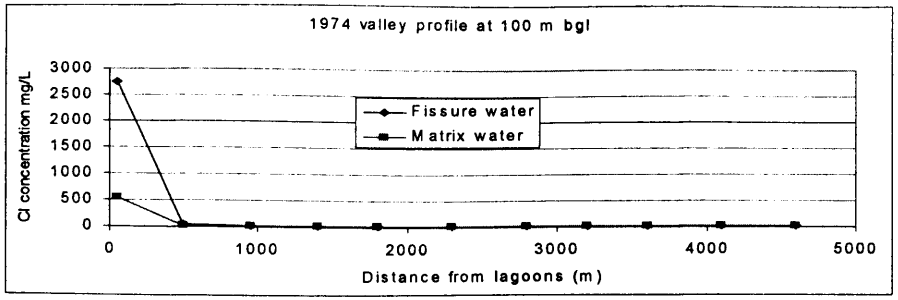

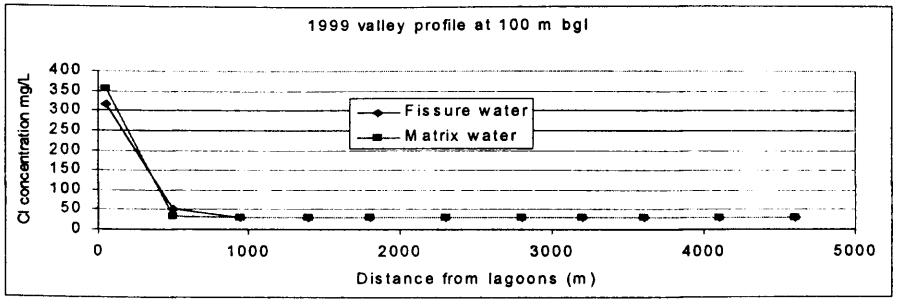

Additional 3D solute transport modelling results.

Model scenario 4

Model scenario 4 has the same parameter set-up as model scenario 3, but with a larger longitudinal dispersivity, α_L = 225 m (as used in model scenario 5). The SP10 plan view, Figure A6-1, shows a wide solute plume, more similar to the SWA 1974 (SWA 1976a) observations than produced by the dual porosity assumptions of model scenario's 1 and 5.

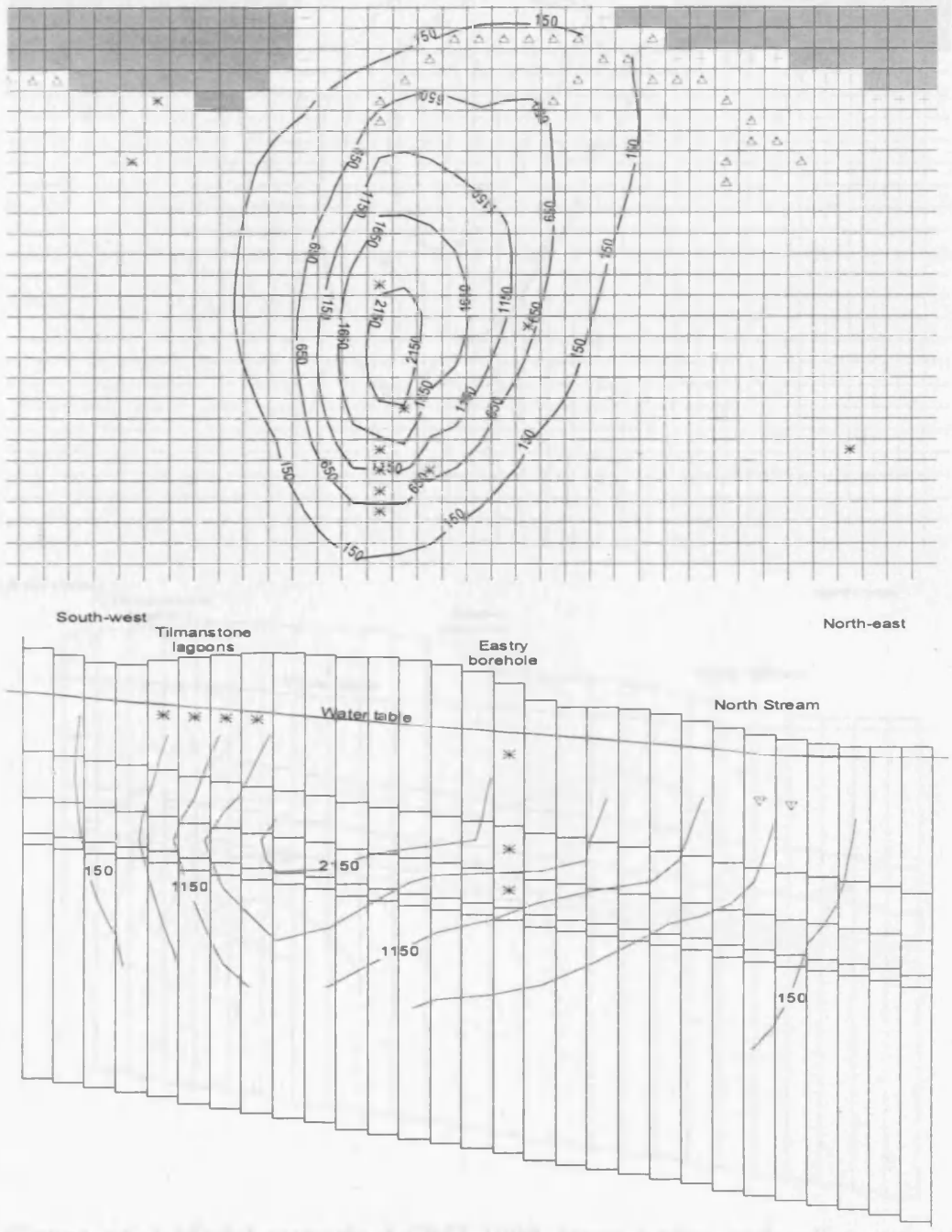

Figure A6-1 Model scenario 4 SP10 1977 Model scenario 4 SP10 1977; layer 1 plan and valley cross-section of chloride contours.

The main influence of the increased dispersivity is to reduce the solute concentrations predicted at the centre of the plume and to extend the outer boundary (marked by the 150 mg/L concentration contour). One difference to the outer boundary occurs immediately up gradient of the input lagoons where the contour moves approximately 750 m up gradient by SP10. By SP53 (Figure A6-2) the plume in model scenario 4 is much larger than model scenario 3. At its widest part it extends to approximately 2750 m compared to approximately 1500 m in model scenario 3 at the same time.

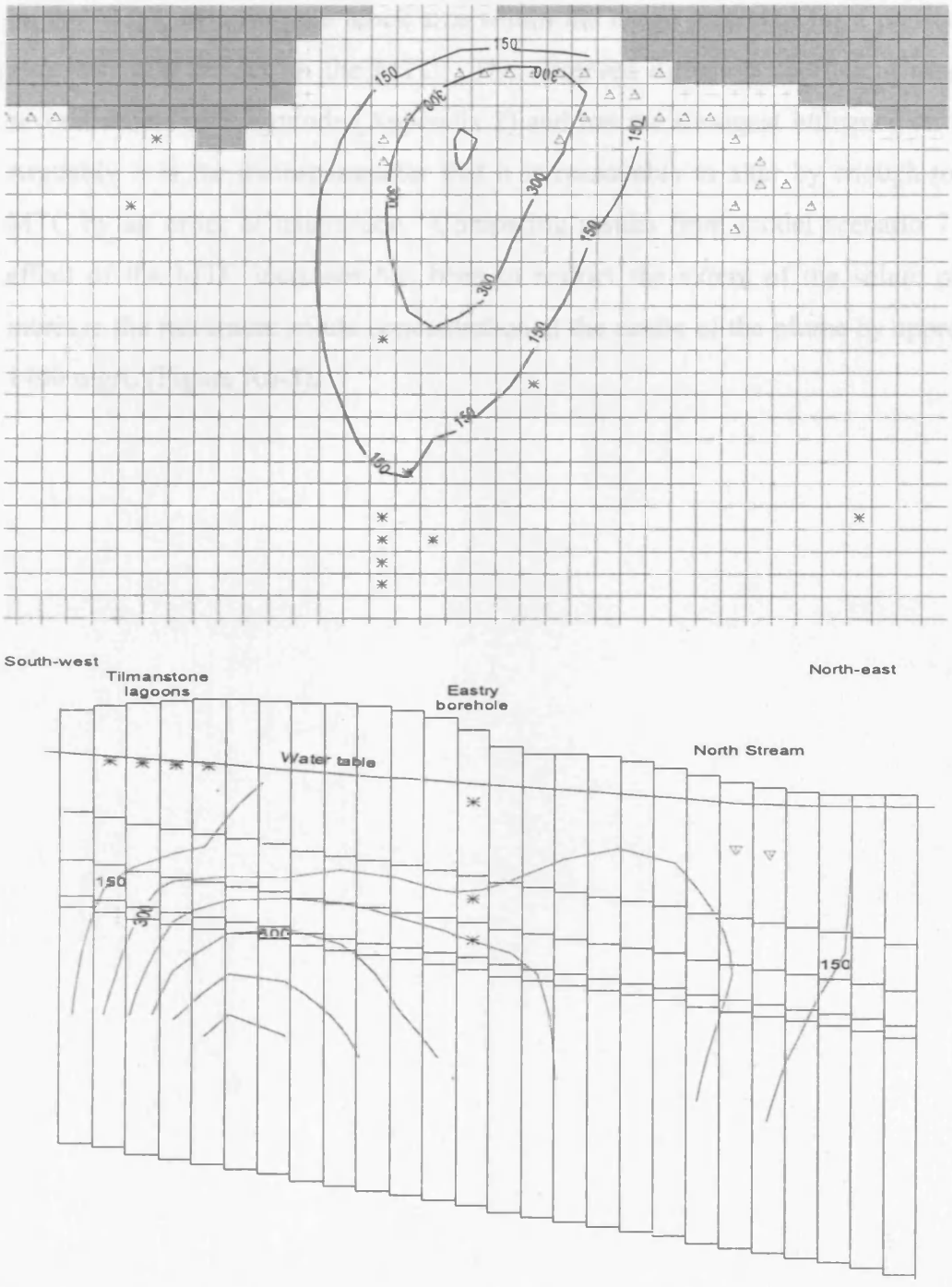

Figure A6-2 Model scenario 4 SP53 1999, layer 1 plan and valley cross-section of chloride contours.

Model scenario 7

Model scenario 7 addresses the sensitivity of the model predictions to the mass transfer coefficient (MTC). Model scenario 7 continues to use the mobile porosity value of 0.1% and α_L = 2 m, as in Model scenario 6. The MTC's were increased by one order of magnitude (Table 6-8). Increasing the MTC can be considered as reflecting a decrease in the matrix block size, increasing the diffusion coefficient or increasing the immobile porosity. Increasing immobile porosity within the observed range has very little impact on the MTC. Altering the block size within the range predicted for a particular depth also has little impact on the MTC. The observed diffusion coefficient range covers several orders of magnitude (Appendix 2) and has the strongest influence on the MTC. Arguably it is the main parameter that it is reasonable to alter by enough to vary the MTC by an order of magnitude. Comparing results from model scenario 7 to 6, the effect of the MTC increases has been to restrict the extent of the solute plume and increase the maximum solute concentration at the centre of the plume by approximately 1400 mg/L (Figure A6-3).

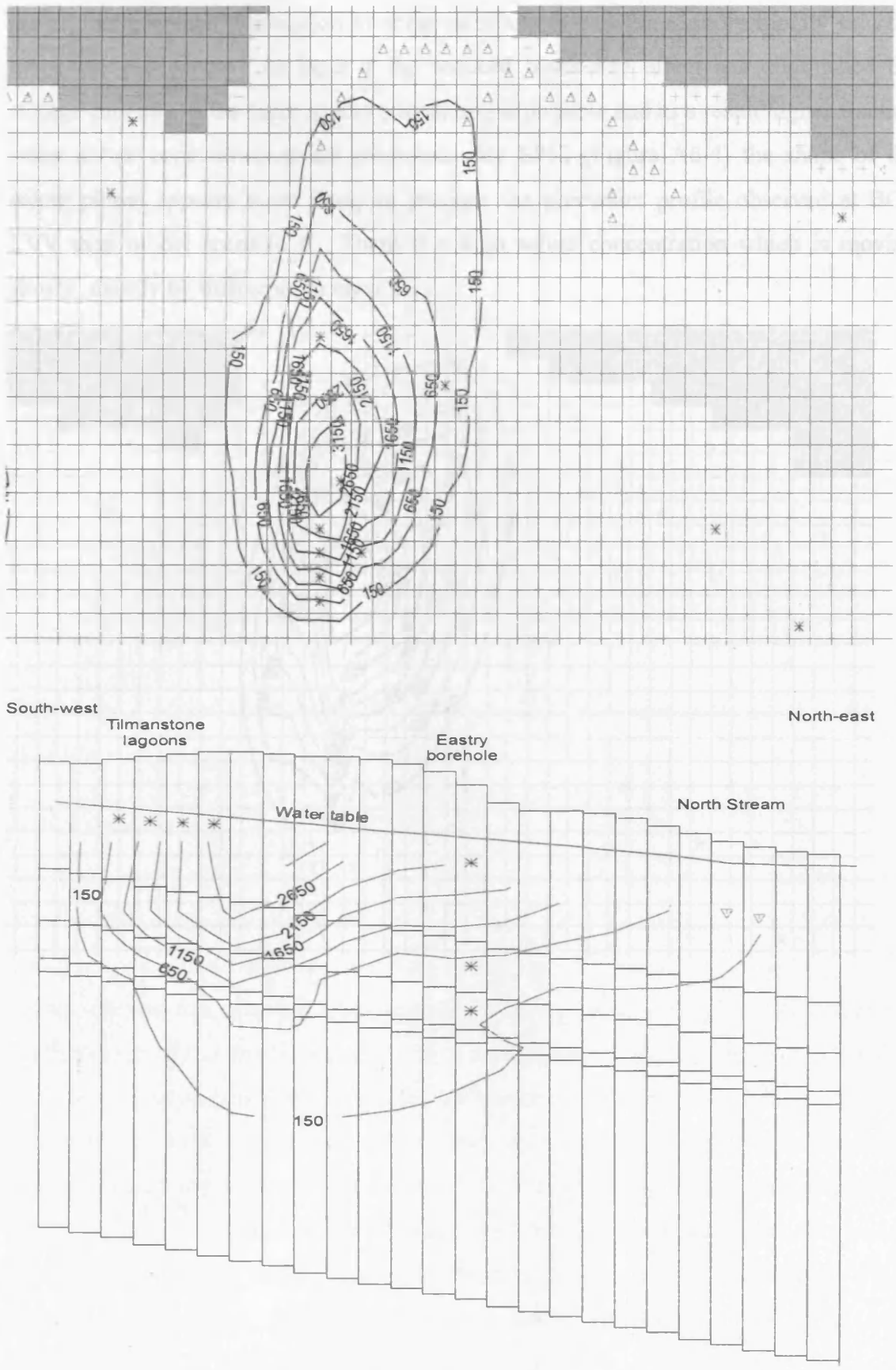

Figure A6-3 Model scenario 7 SP10 1977; layer 1 plan and valley cross-section of chloride contours.

The vertical extent of the solute is also reduced. This suggests that the higher MTC's are allowing greater attenuation to occur as solute is transferred more rapidly into the immobile porewaters. In layer 1 the reduced block-size effect has diminished the storage capacity of the layer so less attenuation is possible and as a result higher fracture water solute concentrations are predicted. By SP53 (Figure A6-4) the shape of the solute plume appears more likely to produce the porewater profile observed at BGS LVV than model scenario 6. There is a high solute concentration which is moving slowly, mainly by diffusion, in layer 2.

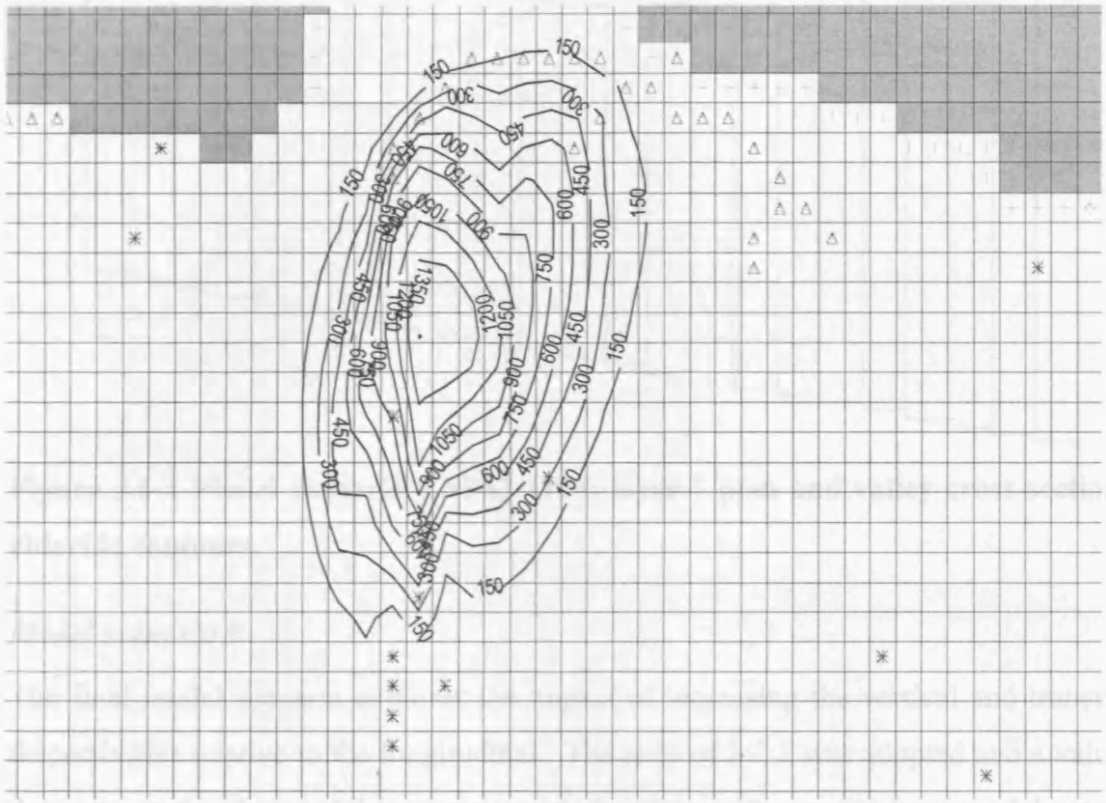

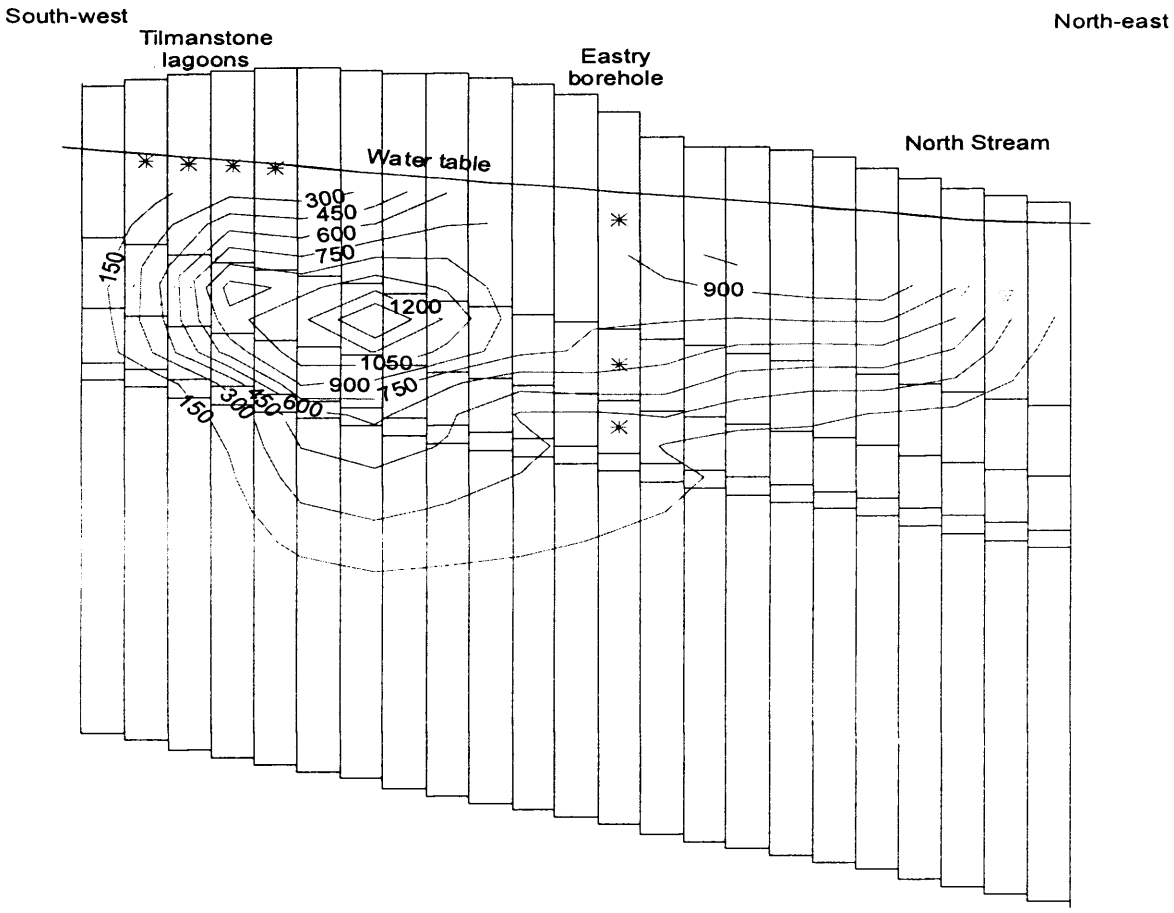

Figure A6-4 Model scenario 7 SP53 1999; layer 1 plan and valley cross-section of chloride contours.

Model scenario 9

The final model scenario explores the impact of increasing the vertical and transverse dispersivities relative to the longitudinal. The ratio of 1:1:1 was adopted and a value of 2 m was used. This model scenario was undertaken as the results from model scenario 3 demonstrated that allowing rapid vertical movement of higher concentration solute to depth supported the development of the second plume in layer 4 which is needed to produce the matrix porewater solute profile observed in BGS LVV (Section 5.5.1). The value for the block-size in layer 4 was calculated using the Bloomfield *et al.* (2000) fracture-density depth relationship, so the MTC for this layer is reduced compared to model scenario 8. The results for SP10 (Figure A6-5) show that the higher dispersivity ratio causes solute to move rapidly into layer 5 and the plume is relatively evenly distributed across the layers compared to model scenario 6 (dispersivity ratio 1:0.1:0.01).

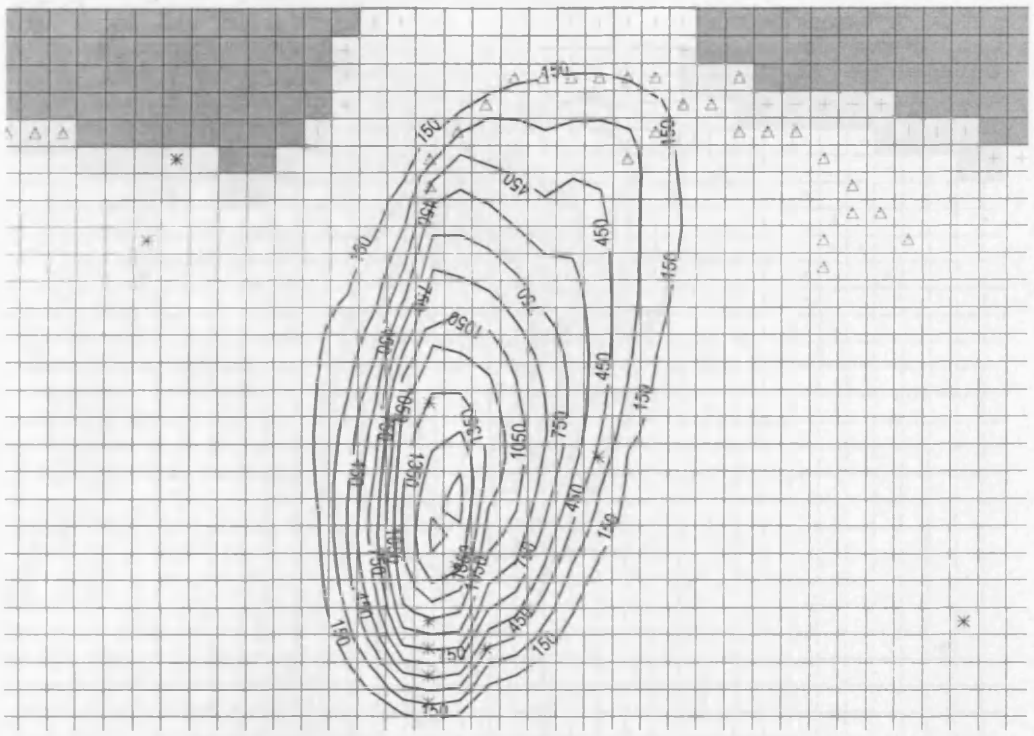

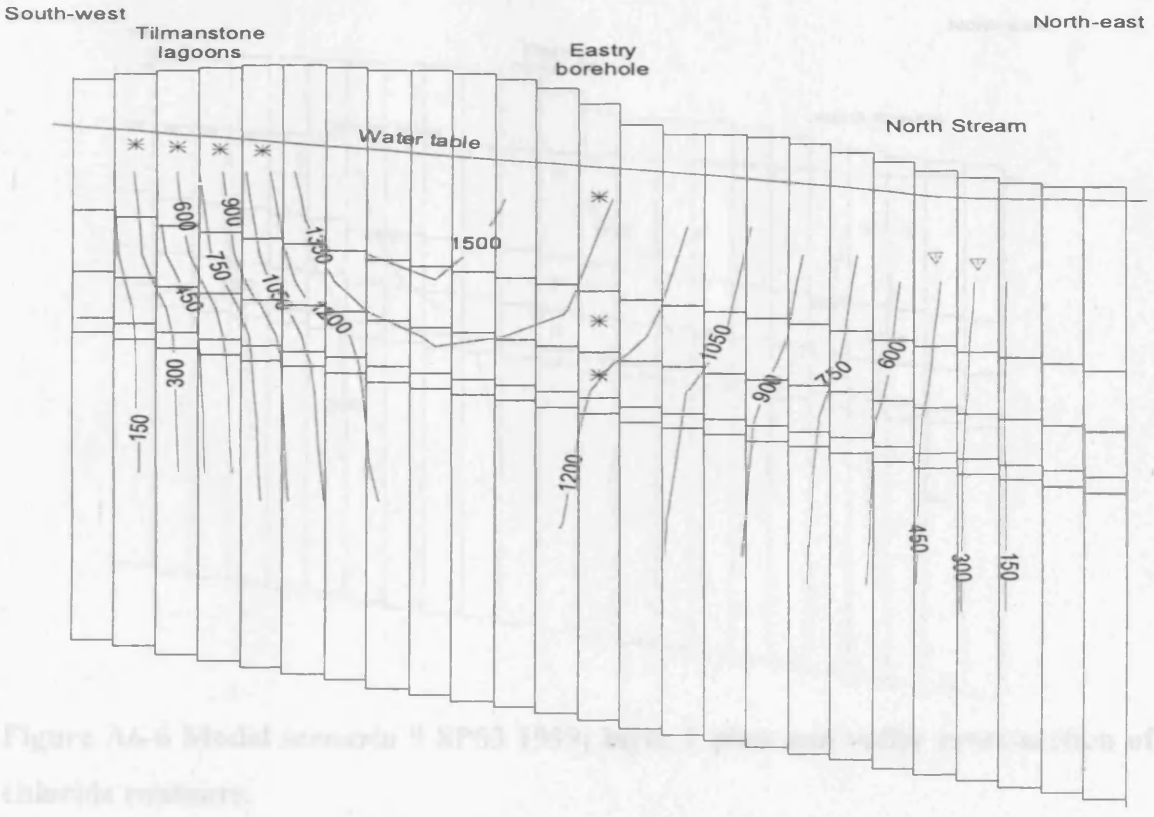

Figure A6-5 Model scenario 9 SP10 1977; layer 1 plan and valley cross-section of chloride contours.

The long term impact of this is demonstrated in the model predictions for SP53 (Figure A6-6).

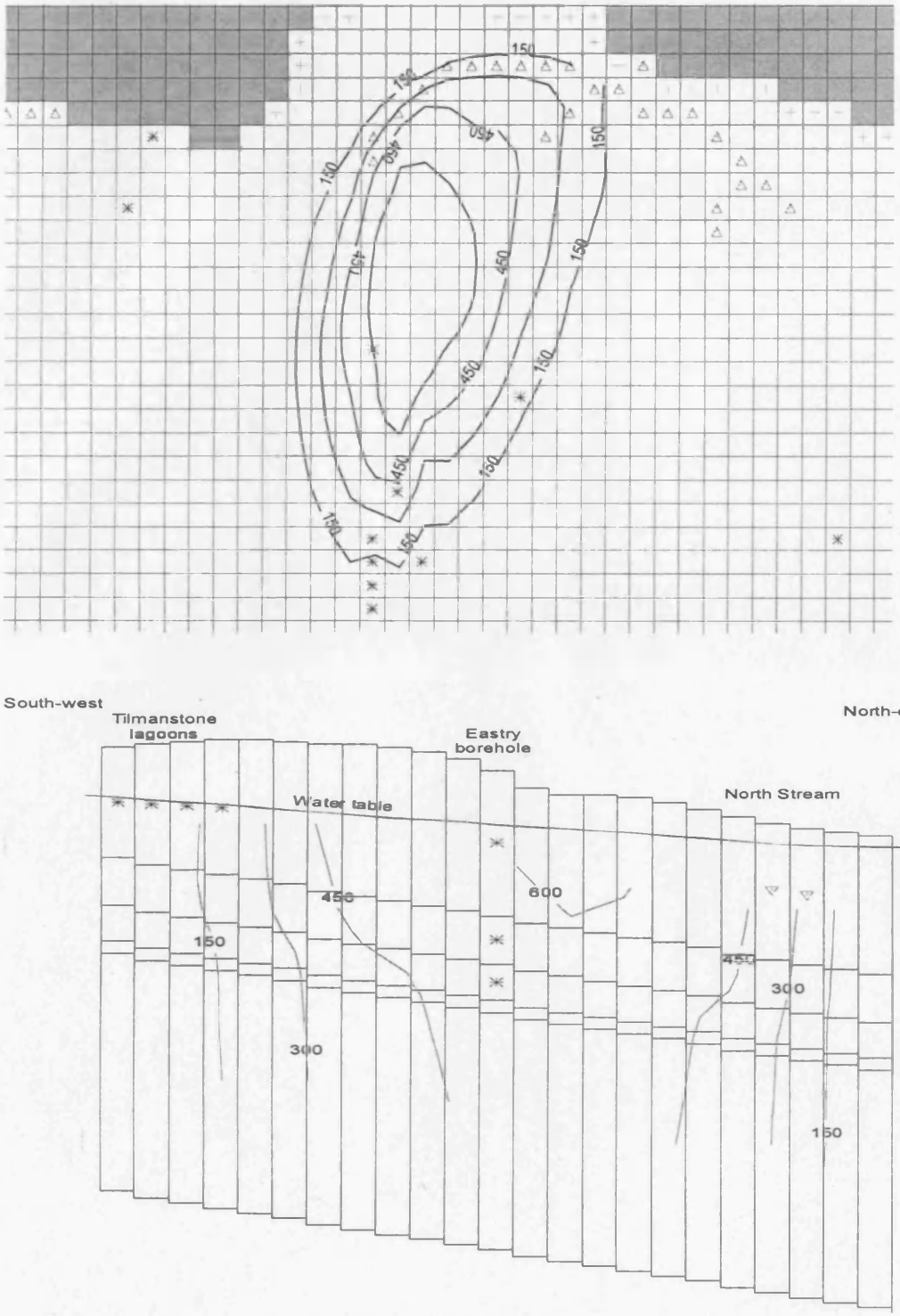

Figure A6-6 Model scenario 9 SP53 1999; layer 1 plan and valley cross-section of chloride contours.

The higher concentrations remain in the fracture water at depth due to solute eluting from the matrix / immobile domain compared to model scenario 6 at this time. The use of the higher dispersivity ratio does not aid the development of the plume geometry required to produce the solute profile observed in BGS LVV.